Universidad Autónoma de Madrid

Programa de doctorado en Biociencias Moleculares

Role of tetraspanin CD9 in murine experimental colitis

Doctoral Thesis

María Laura Saiz Álvarez

Madrid, 2018

Departamento de Bioquímica

Facultad de Medicina

Universidad Autónoma de Madrid

Programa de Doctorado en Biociencias Moleculares

Role of tetraspanin CD9 in murine experimental colitis

Memoria presentada por la licenciada en Bioquímica:

María Laura Saiz Álvarez

Para optar al título de Doctor por la Universidad Autónoma de Madrid

Doctorado en Biociencias Moleculares

Director de tesis:

Dr. Francisco Sánchez-Madrid

Doctor en Ciencias Biológicas y Catedrático de Inmunología de la Universidad Autónoma de Madrid

Este trabajo se realizó en el Centro Nacional de Investigaciones Cardiovasculares (CNIC)

Madrid, 2018

Francisco Sánchez Madrid, Doctor en Ciencias Biológicas y Catedrático de Inmunología de la Universidad Autónoma de Madrid,

CERTIFICA:

Que María Laura Saiz Álvarez, Licenciada en Bioquímica por la Universidad de Oviedo, ha realizado bajo su dirección el trabajo de investigación correspondiente a su Tesis Doctoral con el título:

Role of tetraspanin CD9 in murine experimental colitis

Revisado este trabajo, el que suscribe lo considera satisfactorio y autoriza su presentación para ser evaluado por el tribunal correspondiente.

Y para que así conste y a los efectos oportunos, firma el presente certificado en Madrid a 22 de mayo de 2018.

Fdo.: Prof. Francisco Sánchez-Madrid

A mis padres, a Rocío y Luis,

A mi abuela Carmen,

A Pablo.

"Hay una fuerza motriz más poderosa que el vapor, la electricidad y la energía atómica: la voluntad"

Albert Einstein (1879-1955)

Agradecimientos

Agradecimientos

En primer lugar, me gustaría darle las gracias a Paco por su apoyo y por haber sido un jefe excepcional tanto el ámbito profesional como personal. Gracias por haberme permitido aprender tanto en tu laboratorio, siempre formado por gente muy entusiasta e inteligente. Siempre recordaré las apasionadas discusiones en los seminarios. Gracias también por transmitirme esa perspectiva de sabio y por siempre sacar lo positivo de cada experimento. También gracias por compartir con tus estudiantes tus experiencias tan valiosas.

En segundo lugar, a Danay, sin ella nada de este trabajo hubiera sido posible. Gracias por tu apoyo desde el día uno, por ser tan buena profesora y transmitir todos tus conocimientos y razonamientos conmigo. Gracias por tu paciencia con mi genética entropía, por enseñarme a razonar y por transmitirme tu rigor científico y la valía del esfuerzo. Un privilegio haber aprendido de tan gran científica, luchadora, apasionada e inconformista, de conocimiento insaciable. Gracias por tu franqueza, por intentar siempre sacar lo mejor de mí y enseñarme que en este mundo hay que hacerse valer. Y por supuesto gracias por las risas y por nuestros momentos "chocoboms", ¡cuanto los echaré de menos!

Gracias a Olga, mi compañera de tesis todos estos años. Gracias por tu apoyo durante todo este complicado proceso y por tranquilizarme y comprenderme en los momentos más delicados. Gracias por preocuparte tanto por mí y sacarme de casa esos fines de semana de soledad en Madrid lejos de mi familia y amigos. Gracias por tu dulzura y cariño y por darme la fuerza que necesitaba para terminar esta dura etapa. Cuánto echaré de menos esas meriendas pre-tésicas de risas y desahogo. Gracias Marta por esas largas y meditativas charlas donde siempre me hacías ver el lado positivo de las cosas y a estar agradecida con la vida. Gracias por hablar siempre con esa franqueza que te caracteriza y tus valiosos consejos siempre acompañados de esa dosis de realidad que tanta falta nos hace a algunos de vez en cuando. Gracias también por las risas y por toda la ayuda con el proyecto. Me acordaré de ti cada vez que escuché la tabla de multiplicar del 4, y lo sabes jajaja. Gracias a Dani por las risas y esos momentos de desahogo existencial. Gracias a Raquelilla por su apoyo incondicional y preocupación el tiempo que hemos coincidido en el laboratorio, que, aunque corto, ha sido intenso. Qué gran compañera ha ganado el laboratorio de Paco con tu llegada, siempre con esa infinita disposición a ayudar a los demás y esa preocupación por que los experimentos salgan lo mejor posible. Gracias Anita por tu apoyo y tus sesiones de psicología. Gracias por escucharme en cualquier momento que necesitara. Poca gente se pone en el lugar del otro como tú lo haces, gracias por tu sensibilidad y familiaridad. Gracias a Irene también tu sensibilidad, en eso Ana y tú os parecéis un rato, gracias también por tu apoyo y por sacarme del colapso cuando tenía que hacer algo relativo a la autónoma jaja. Gracias a Nieves, Lola, Noa y Eugenio por vuestro cariño y también apoyo. Gracias también a la gente que ya se ha ido. Gracias a Vera por sus consejos zen. Gracias a Noelia, Cris, Fran, Carol, Giulia, Dieguito y Jaso, con los que he compartido tantas experiencias y tantas charlas durante las comidas en el CNIC. Gracias a Rafa por ser tan buen amigo. Echaré de menos nuestros viajes matutinos hacia el CNIC. Gracias a Bárbara por tu apoyo desde que llegué a Madrid

y acogerme con tanto cariño. Gracias por motivarme y animarme a continuar. Gracias también a Sheila y Myriam. Gracias a Helena por tu empatía, apoyo y comprensión durante toda la tesis. Gracias por esos fines de semana tan divertidos donde nos relajábamos y arreglábamos el mundo un poquito. Gracias por estar siempre pendiente de mí y de mi estado emocional, has sido un gran apoyo. Haber conocido a personas como tú hacen que la tesis haya merecido aún más la pena. Gracias también a los "Jacobs" en especial a Carlos, Esmeralda y Paula. Sois geniales. Gracias también a Mitchel. Gracias a Raquel Toribio. Gracias a José Pintor por los ánimos y por su apoyo. Esas conversaciones en el coche volviendo del CNIC a las tantas de la noche eran mejor que cualquier terapia jaja. Gracias Eva (María) por tu apoyo y por contagiarme tu alegría. Gracias por esas cenas en Bravo Murillo que tanto echaré de menos. Si hay algo bueno en haber alargado la tesis unos meses ha sido haber coincidido contigo y habernos visto tanto, como en los viejos tiempos. Gracias a Jesús también. Gracias a Coral, Marta y Bea. Aunque nuestra relación sea en la distancia sé que puedo contar con vosotras en cualquier momento. No faltaré a ninguna cena Navideña, lo prometo. Gracias a Coris, por todos estos años de amistad, por preocuparte tanto por mí y estar siempre ahí. Me llevo una joya de Madrid. Sin ti esta etapa no hubiera sido lo mismo y haces que mis recuerdos sean buenos y me olvide de los malos. Te admiro muchísimo. Gracias a Alberto también, ha sido todo un consuelo (a la par que un placer) compartir nuestras hipocondrías y dudas existenciales. Ya sabes, mal de muchos….

Gracias a las de siempre, mis amigas desde que tengo uso de razón de como dice Paco, mi "amada Salinas". Gracias Lourdes, Estela, Ana, Cova, Zoraida, Paula, Belén y Candela. Aprovecho para pediros perdón si estos años no he estado tan pendiente de vosotras como me hubiera gustado, y gracias por entenderme cuando sabíais que tenía muy poco tiempo para cultivar nuestra amistad como se merece.

En especial quiero darle las gracias a mi familia y mi pareja. Su apoyo ha sido imprescindible. Gracias papá y mamá, por estar siempre ahí, por darme ánimos continuamente y el apoyo incondicional, por ayudarme también económicamente y entender mi situación y sobre todo por enseñarme la valía del esfuerzo. Sé que habéis sufrido conmigo esta etapa y un cachito de esta tesis os pertenece. Gracias a mis hermanos, Rocío y Luis, no se puede tener unos hermanos mejores. Gracias Rochi porque sé que a pesar de la distancia siempre has estado ahí. Gracias por las aliviantes charlas por skype o llamadas de whats ap en momentos de crisis. Gracias por motivarme y empujarme hasta el final. Gracias a mi abuela Carmen, una mujer luchadora como ninguna, te admiro muchísimo. Gracias a mi prima Bárbara, que me contagia siempre esa energía que tiene y gracias a mis tíos Jesús y Patricia y también a mis primos Román y María, sois geniales. Gracias a Pablo, mi amigo y compañero de viaje, por cuidarme cada día, por animarme en cada paso que he dado y por soportar 7 años de relación en la distancia. Sin tu apoyo esto hubiera sido un imposible. Gracias por tu optimismo irrefrenable, tu motivación y cariño diarios. Por tu sentido del humor y por sacarme una sonrisa cada día después de un duro día en el laboratorio. Gracias por hacerme ver las cosas con la perspectiva que merecen y llevarme de la mano a tu nido de paz. Otro trocito de esta tesis también te pertenece a ti. Gracias también a Marisa y a Jose, por vuestro apoyo y acogimiento, para mi sois parte de mi familia.

Summary

Summary

Inflammatory bowel diseases (IBD), mainly consisting of Crohn's disease (CD) and ulcerative colitis (UC) are chronic relapsing and remitting diseases resulting in uncontrolled inflammation of the gastrointestinal (GI) tract. The etiology of these diseases is unknown, but accumulating evidence suggests that it results from an inappropriate inflammatory response to intestinal microbes in a genetically susceptible host. The prevalence of IBD has increased during the last decades, overall in newly industrialized countries and is increasingly considered an emerging global disease. Unfortunately, IBD remains incurable due to its complex etiopathogenesis, and current treatments available only ameliorate symptoms. Current knowledge of these disorders are based on a combination of gene association studies, clinical investigations, and laboratory experiments in mice. The last ones have been very valuable tools to understand the pathogenesis of IBD.

In this thesis work, we investigated the role of CD9, a tetraspanin that regulates major biological processes such as cell migration and immunological responses, in two mouse models of colitis that have been used to study the pathogenesis of IBD. Tetraspanins are a family of proteins with four transmembrane domains that associate between themselves and cluster with other partner proteins, conforming a distinct class of membrane domains, the tetraspanin-enriched microdomains (TEMs). These TEMs constitute macromolecular signaling platforms that regulate key processes in several cellular settings controlling signaling thresholds and avidity of receptors. Previous *in vitro* studies revealed an important role for CD9 in the interaction of leukocytes with inflamed endothelium, but *in vivo* evidence of the involvement of this tetraspanin in inflammatory diseases is scarce. Here, we studied the role of CD9 in the pathogenesis of colitis *in vivo*. Colitis was induced by administration of dextran sodium sulfate (DSS), a chemical colitogen that causes epithelial disruption and intestinal inflammation. $CD9^{-/-}$ mice showed less severe colitis than wild-type counterparts upon exposure to DSS (2% solution) and enhanced survival in response to a lethal DSS dose (4%). Decreased neutrophil and macrophage cell infiltration was observed in colonic tissue from $CD9^{-/-}$ animals, in accordance with their lower serum levels of TNF-α, IL-6, and other proinflammatory cytokines in the colon. The specific role of CD9 in IBD was further dissected by transfer of $CD4^{+}$ $CD45RB^{hi}$ naive T cells into the $Rag1^{-/-}$ mouse colitis model. However, no significant differences were observed in these settings between both groups, ruling out a role for CD9 in IBD in the lymphoid compartment. Experiments with bone marrow chimeras revealed that CD9 in the non-hematopoietic compartment is involved in colon injury by limiting the proliferation of epithelial cells. Future strategies to repress CD9 expression may be of therapeutic benefit in the treatment of IBD.

Resumen

Resumen

La enfermedad inflamatoria intestinal (EII) engloba dos patologías, la colitis ulcerosa (CU) y la enfermedad de Crohn (EC), las cuales se caracterizan por una inflamación crónica intermitente de diferentes partes del tracto gastrointestinal. La etiología de la EII es desconocida, pero las evidencias obtenidas hasta ahora sugieren que son el resultado de una respuesta inflamatoria exacerbada desencadenada contra los microbios intestinales en sujetos con susceptibilidad genética. La prevalencia de la EII ha ido incrementando durante las últimas décadas, sobre todo en países recientemente industrializados alcanzando un carácter global. Desafortunadamente, debido a la compleja etiopatogenia que subyace a la EII, ésta permanece incurable y los tratamientos actuales únicamente atenúan los síntomas. Los conocimientos que se tienen hoy en día acerca de estas enfermedades se basan en la combinación de estudios de asociación genética, estudios clínicos y experimentos con ratones en los laboratorios de investigación.

En este trabajo de tesis doctoral, hemos investigado el papel de CD9, una tetraspanina que regula importantes procesos biológicos tales como la migración celular o la respuesta inmunológica, en dos modelos murinos de colitis utilizados para estudiar la patogénesis de la EII. Las tetraspaninas son una familia de proteínas con cuatro dominios transmembrana que interaccionan entre sí y se agrupan con otras proteínas asociadas, conformando unos dominios de membrana, llamados microdominios enriquecidos en tetraspaninas o TEMs (del inglés, *tetraspanin-enriched microdomains*). Estos TEMs constituyen plataformas macromoleculares de señalización que regulan importantes procesos en diversos escenarios celulares controlando umbrales de señalización y avidez de receptores. Estudios previos *in vitro* han revelado un papel importante de CD9 en la interacción de los leucocitos con el endotelio inflamado, pero no existen prácticamente estudios *in vivo* relacionados con la implicación de esta tetraspanina en enfermedades inflamatorias. En este trabajo, estudiamos el papel de CD9 en la patogénesis de la colitis *in vivo*. La inducción de la colitis se realizó mediante la administración del químico colitogénico dextrano sulfato de sodio (DSS), el cual causa una disrupción de la barrera epitelial e inflamación intestinal. Los ratones $CD9^{-/-}$ mostraron menos colitis en comparación con los ratones de cepa salvaje tras la administración de una solución de DSS al 2% y una mayor supervivencia en respuesta a una dosis letal del químico al 4%. De manera concordante, se detectó una menor infiltración de neutrófilos y macrófagos en el colon de los ratones $CD9^{-/-}$, así como una disminución de los niveles séricos de TNF-α, IL-6 y otras citoquinas pro-inflamatorias en el colon. El papel específico de CD9 en EII se investigó también en el modelo de transferencia de células T naïve $CD4^{+}CD45RB^{hi}$ en animales $Rag1^{-/-}$. Sin embargo, no se observaron diferencias entre ratones inyectados con linfocitos que expresaban CD9 o no. Los experimentos realizados en ratones quiméricos mediante trasplante de médula ósea demostraron que la no expresión de CD9 en el compartimento no hematopoyético era la responsable de mediar la protección frente a la colitis inducida por DSS. En estos animales se detectó una mayor proliferación del epitelio intestinal. Por ello, CD9 podría llegar a ser en un futuro una posible diana terapéutica para el tratamiento de la EII.

Index

INDEX

List of abbreviations

LIST OF ABBREVIATIONS

5-ASA: 5-aminosalicylic acid

6-MP : 6-mercaptopurine

ADAM: A Disintegrin and metalloproteinase domain-containing protein

AJ: Adherens junction

AJC: Apical junctional complex

ALCAM: Activated leukocyte cell adhesion molecule

AMPs: Antimicrobial peptides

AOM: Azoxymethane

APCs: Antigen presenting cells

AZA: Azathioprine

BMDCs: Bone marrow-derived dendritic cells

BMP: Bone morphogenetic protein

CD: Crohn's disease

CRC: Colorectal carcinoma

DRAP: Diphtheria toxin receptor-associated protein

DSS: Dextran sodium sulfate

EC: Extracellular

ECM: Extracellular matrix

EGF: Epidermal growth factor

EGFR: Epidermal growth factor receptor

EIM: Extraintestinal manifestation

EO-IBD: Early-onset inflammatory bowel disease

EpCAM: Epithelial cell adhesion molecule

ER: Endoplasmic reticulum

ERK: Extracellular signal-regulated kinase

ERM: Ezrin/radixin/moesin

FAK: Focal adhesion kinase

FDA: Food and drug administration

FITC: Fluorescein isothiocyanate

FLIM: Fluorescence-lifetime imaging

FRET: Fluorescence Resonance Energy Transfer

GH: Growth hormone

GI: Gastrointestinal

GM-CSF: Granulocyte-macrophage colony-stimulating factor

GPCR: G-protein-coupled receptor

GPI: Glycophosphatidylinositol

GST: Glutathione S-transferase

GWAS: Genome wide association studies

HB-EGF: Heparin-binding EGF-like growth factor

HLA-DM: Human leukocyte antigen DM

HNF4A: Hepatocyte nuclear factor 4 alpha

HUVEC: Human endothelial umbilical cells

IBD: Inflammatory bowel disease

IBS: Irritable bowel syndrome

IC: Intracellular

ICAM-1: Intercellular adhesion molecule-1

IEC: Intestinal epithelial cell

IFN-γ: Interferon gamma

IGF: Insulin-like growth factor

IRAK-M: Interleukin-1 receptor-associated kinase M

JAK: Janus kinase

JAM: Junctional adhesion molecule

KGF: Keratinocyte growth factor

KO: Knockout

LEL: Large extracellular loop

LFA-1: Lymphocyte function-associated antigen 1

LP: Lamina propria

LPA: Lysophosphatidic acid

Mac-1: Macrophage-1 antigen

MAdCAM-1: Mucosal addresin cell adhesion molecule-1

MAPK: Mitogen activated protein kinase

MCP-1: Monocyte chemoattractant protein-1

MH: Mucosal healing

MHC-II: Major histocompatibility complex-II

MIP-1α/β: Macrophage inflammatory protein-1 alpha/beta

MMP: Matrix metalloproteinase

MRP-1: Motility related protein-1

MTX: Methotrexate

NASH: Nonalcoholic fatty liver disease

NETs: Neutrophil extracellular traps

NF-kB: Nuclear factor kappa B

NK: Natural killer

NLRP3: Nod-like receptor protein-3

NOD2: Nucleotide-binding oligomerization domain-containing protein 2

NSAIDs: Non-stereoidal anti-inflammatory drugs

PCD: Programmed cell death

PDE-4: Phosphodiesterase-4

PI4-K: Phosphatidylinositol 4-kinase

PKC: Protein kinase C

PMN: Polymorphonuclear

PRR: Pattern recognition receptor

RA: Retinoic Acid

RNAi: Interfering RNA

SCFAs: Short chain fatty acids

SEL: Short extracellular loop

SNPs: Single nucleotide polymorphisms

TA: Transit amplifying

TCR: T-cell receptor

TEM: Tetraspanin enriched microdomain

TFF: Trefoil factor

TGF-α: Transforming growth factor alpha

TGF-β: Transforming growth factor beta

TJ: Tight junction

TLR: Toll-like receptor

TM: Transmembrane

TNF-α: Tumor necrosis factor alpha

TRAF6: TNF receptor associated factor 6

TREM2: Triggering receptor expressed on myeloid cells 2

TRIF: TIR-domain-containing adapter-inducing interferon-β

Tspan: Tetraspanin

UC: Ulcerative colitis

VCAM-1: Vascular cell Adhesion molecule-1

VEO-IBD: Very-early-onset inflammatory bowel disease

VLA-4: Very late antigen-4

WAVE: Wiskott-Aldrich syndrome protein family verprolin-homologous protein

WGO: World gastroenterology organisation

WT: Wild type

Introduction

1. INTRODUCTION

1.1. INFLAMMATORY BOWEL DISEASE

1.1.1. Introduction

Inflammatory bowel disease (IBD) defines a group of complex and multifactorial intestinal disorders, principally, ulcerative colitis (UC) and Crohn's disease (CD). Both diseases are characterized by chronic inflammation of the gastrointestinal tract interspersed with relapsing phases [429]. UC and CD disorders have distinct pathological and clinical characteristics. CD affects any component of the gastrointestinal tract from the oral cavity to the annus (although it mostly associates with the terminal ileum and colon) in a non-continuous fashion, as opposed to a colon-limited disease in the case of UC (**Figure 1.1**). Transmural inflammation leading to a thickened colon wall and a typical "cobblestone" appearance are observed in CD, corresponding to longitudinal and circumferential fissures and ulcers that separate islands of mucosa (**Figure 1.2**) [298].

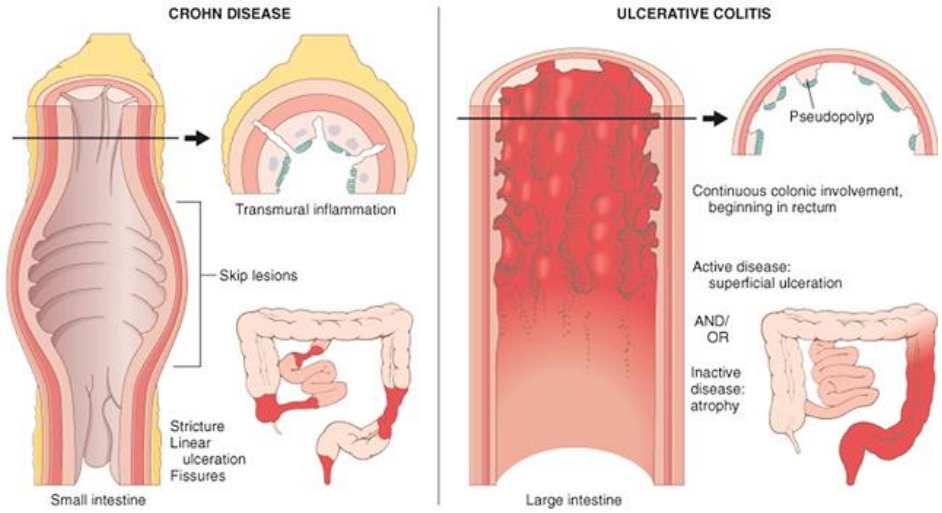

Figure 1.1. **Basic hallmarks and distribution of IBD disorders found in colon of patients with active disease**. Left CD, right UC. Taken from MBBS medicine webpage.

Moreover, CD can be associated with intestinal granulomas, strictures (narrowing of the intestinal lumen due to the scar tissue produced by the repair process after inflammation), and fistulas, but these are not typical findings in UC. On the other hand, UC involves superficial inflammatory changes, affecting mainly the mucosa and a thinner colon wall shows continuous inflammation with no patches of healthy tissue [3,560] (**Figure 1.1**), pseudopolyps (non-neoplastic lesions originating from the mucosa) (**Figure 1.2**), cryptitis and/or crypt abscesses. In both diseases, patients could experience diarrhea, fever and fatigue, abdominal pain and cramping, blood in stools, reduced appetite and weight loss [135]. The natural course of IBD alternates periods of remission and relapse, meaning that often IBD symptoms can be stable (low or absent) but suddenly worsen during a flare [429]. IBD diseases remain incurable and existing treatments only pale sympthoms and have a

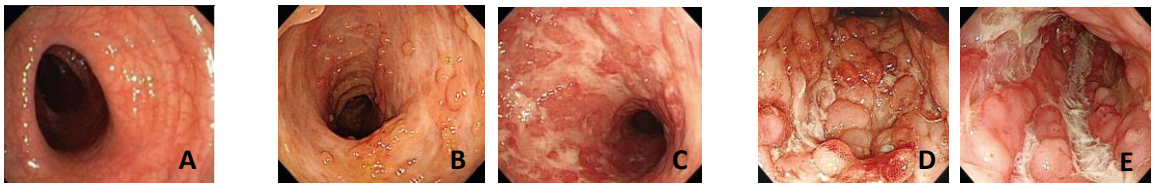

Figure 1.2. Typical endoscopic features of UC (B and C) and CD (D and E). (A) Normal looking mucosa in the descending colon (B) pseudopolyps (C) ulcers (D) cobblestone appearance (E) linear ulceration. Modified from: Lee JM. *et al*, 2016 [298].

limited efficiency [554]. Additionally, around 20-30% of UC and 30-40% of CD patients require surgical intervention at some point in their lifes to remove the affected region of the bowel [147]. Some of them may also require temporary or permanent colostomy or ileostomy. Nevertheless, in many cases, surgical resection or stomas do not achieve a permanent cure, and patients suffer relapses later in time [219]. On top of that, IBD patients display an elevated risk for colorectal carcinoma (CRC). In both cases, UC and CD, the risk of CRC is related to disease duration as well as the length of colon involved [125,126,232]. Thus, IBD constitutes an incurable, chronic, lifelong disease which entails detrimental consequences on patient's quality of life [165] and causes a major impact on health care resources [246,579].

1.1.2. Epidemiology

IBD could be diagnosed at any age, but the majority of new cases turn up in adolescence and early adulthood, being its peak onset in persons from 15 to 30 years of age [235]. Pediatric IBD (before 20 years old) accounts for approximately 25% of patients, with the peak onset in adolescence [466]. Nowadays, IBD affects around 5 million people worldwide, although the highest incidence and prevalence are found in westernized countries of Northern Europe and Northern America [9] (**Table 1.1.**)

Table 1.1. Highest annual incidence rates and reported prevalence rates for IBD. Taken from World Gastroenterology Organisation (WGO)

	Highest annual incidence (per 100,000 person-years)		Highest reported prevalence values (per 100,000 persons)	
	UC	CD	UC	CD
Europe	24.3	12.7	505	322
Asia/Middle East	6.3	5.0	114	29
North America	19.2	20.2	249	319
Australasia	11.2	17.4	145	155

However, during the last decades, both prevalence and incidence of IBD have increased in newly industrialized countries whose societies have become more westernized, evolving into a global disease [386,597]. Besides, economic advances inherent to industrialization increased health-care access and case reports. Importantly, Asia, South America and Middle East countries have documented the rise of IBD cases [388,454,474,528,563,586,638]. These cases report the same complications, morbidity, and mortality as in already settled patient populations in high-income countries [387,438]. Intriguingly, if epidemiological forecasts are correct, the global prevalence of IBD will affect tens of millions of people worldwide within a

few decades [243,244]. Along with industrialization, people from developing countries faced a series of changes in lifestyle behaviors that have been reported to correlate with IBD pathogenesis: 1) dietary changes from home-grown to processed foods which contain chemical food additives [98], reduction in fiber intake and breast-feeding [411]; 2) augmented antibiotic use [509]; 3) pollution exposure [35,404]; and 4) chronic stress [340], among others. Moreover, the rise in migratory rates to occidental countries impulsed by natural population increase, would also contribute to increase IBD incidence [37,306]. However, the exact causative relationships with IBD are yet to be unraveled and further research is needed to precisely elucidate the associated molecular alterations.

1.1.3. Etiology: factors contributing to the development of intestinal inflammation

Although much progress has been made in understanding IBD, the exact etiopathogenesis remains unknown. Recent studies have implicated an interaction between genetics, immunology, environment, and microbiome [9].

Genetic factors

Accumulating evidence points out that IBD results from an inappropriate and continuing inflammatory response to intestinal microbes in a genetically susceptible individual [3], and a heritable component to the disease has been recognized [256]. Epidemiological evidence for a genetic contribution support this hypothesis [315]. Early epidemiological observations showed clear familial clustering in IBD, translated in higher risk ratios among first-degree relatives, especially siblings, and a positive family history [138,313,417]. Indeed, a positive family history is reported in around 8 to 12% of IBD patients [486]. Moreover, twin concordance rates are significantly greater in monozygotic than dizygotic twins for both CD (50-58% versus 0-12%) and UC (6-14% versus 0-5%) [44,57,406,569], providing additional evidence for genetic contribution in IBD. Likewise, an increased burden of IBD has been observed in certain ethnic groups like Ashkenazi Jews, who present a significantly higher risk of developing CD irrespective of their geographical location [467,252]. As a complex multifactorial disorder, IBD possess the added difficulty that a susceptibility allele often requires other genetic and non-genetic cues to manifest its symptoms [256]. Thus, the genetic predisposition to develop IBD does not follow Mendelian inheritance patterns for a single locus, being instead polygenic in nature [86]. Only rare early-onset (EO-IBD) (before 5 years) and very-early-onset (VEO-IBD) (before 2 years) forms of IBD or IBD-like diseases (it is sometimes difficult to clearly ascribe the diseases to CD or UC), rely on monogenic defects [43,573]. Therefore, the advent of Genome Wide Association Studies (GWAS) at the beginning of the 21st century, constituted a crucial step towards the understanding of complex disorders like IBD. Importantly, the recent advances during the past two decades in sequencing techniques and the creation of large consortia assembling thousands of patients with IBD, allow for the discovery of many genetic risk loci, experiencing an exponential increase since GWAS development from 2005 onwards [110,614]. By now, around 200 genetic variants have been specifically found to be associated with CD, UC or both [81,345]. In fact, irrespective of their distinct clinical features, nearly 30% of IBD-related genetic loci are shared between CD and UC [256] (**Figure 1.3.**). Analyses of the genetic risk loci implicated in IBD elucidated numerous pathways that are

crucial for intestinal homeostasis. Genetic variations that disturb any stage of immune homeostasis, inflammation, or resolution can result in the exaggerated inflammatory response found in IBD [171]. Some of these genes are involved in epithelial barrier function, epithelial restitution, microbial defense, innate immune regulation, antigen sampling, antigen presentation or T cell differentiation, among others. At the cellular level,

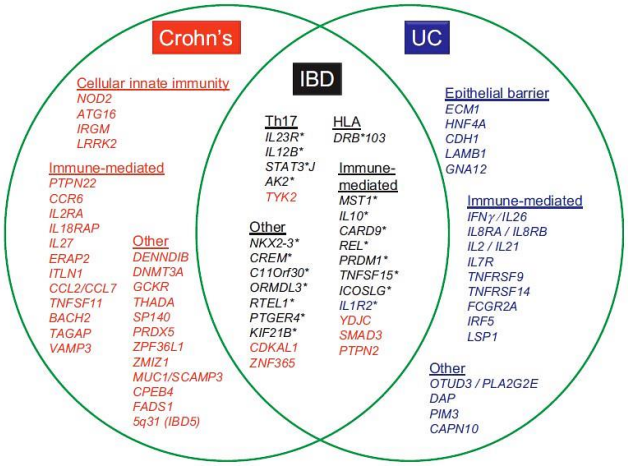

Figure 1.3. **Inflammatory bowel disease susceptibility loci.** The loci are depicted by lead gene name, according to pathway. Loci attaining genome-wide significance ($P<5x10^{-8}$) are shown for CD (red), UC (blue) and IBD (black). This last includes the shared loci that confer susceptibility to both CD and UC (approximately one-third of loci). From Lees CW. *et al*., 2011[299].

processes like autophagy, endoplasmic reticulum (ER) stress, apoptosis, cell migration or oxidative stress could be also affected in IBD [256]. Genetic studies are already used to predict sensitivity to IBD therapies [55]. Combining these studies with different aspects of IBD pathophysiology will promote advances in translating genetic knowledge into predictive biomarkers and new treatments.

Environmental factors

Genetics alone cannot explain IBD. Allele variants found in genetic analyses can only explain about 20-25% of all IBD cases [315], and a lack of a 100% concordance rate in monozygotic twins is noticed. Thus, this is indicating microbiota and other environmental cues might be interacting with genetic susceptibility in the pathogenesis of the disease. In order to validate GWAS data, a number of genetically modified mice have been developed. However, a direct link of gene targeting to pathogenesis has not always been straight forward [77,108] supporting that additional environmental triggers are required for developing of the disease. The changing epidemiology of IBD across time and geography further supports environmental factors influence [9,245]. The more recent emergence of IBD in developing countries over the last two decades points to westernization of lifestyle and industrialization as the responsibles of introducing higher incidence numbers through environmental changes [597]. Some of these changes have been revised above, under "Epidemiology" section. Mainly, drugs and antibiotics intake, infection, stress, smoking, pollution and changes in diet and intestinal microbial milieu (also affected through the use of antibiotics and infections) have all been implicated in the development of intestinal inflammation in cohorts of patients [10,291,339,455]. Besides, migratory data have been quite valuable and informative in this matter. Many migrant populations from developing low incidence countries acquire higher incidence rates than their country of origin and similar to the country they migrated to, mainly in the second generation [74,439].

Gut microbiota in IBD

The human GI tract harbors a complex microbial community containing over 10^{14} microorganisms of greater than 1000 different species, which occupy a vast mucosal interface (250-400m^2) of the human body [22]. As a result of many years of co-evolution, the host immune system has been shaped to tolerate commensals as a means to maintain a symbiotic relationship within the human body [20,104]. Some of the gut microbiota benefits include nutrient metabolism, xenobiotic and drug metabolism, maintenance of structural integrity of the gut mucosal barrier, immunomodulation, and protection against colonization of pathogenic microorganisms [229]. Tolerance mechanisms exerted by microbial species include inhibition of proinflammatory cytokines [325,50] and NF-κB induction [616], compartmentalization of mucosal IgA secretion [326], promotion of regulatory T cells (Tregs) generation [158,446,468,367], secretion of anti-inflammatory cytokines like IL-10 [185,51] and generation of metabolic substrates that stimulate mucosal barrier functions, like butyrate [459]. In IBD, microbiota can act as a double edged-sword, as it is important in both maintaining health and mediating disease [324]. On one hand, it is indispensable for colitis development [174,488,103,536] and, for instance, IL10KO mice housed in germ-free facilities do not develop colitis at all, as opposed to their counterparts raised under conventional conditions [284]. The clinical observation that IBD can respond to antibiotic treatment substantiate that gut microbiota is an essential factor in driving the inflammatory response [593,254,75]. Moreover, the detection of more inflammation associated to certain anatomical regions like the terminal ileum and rectum with faecal stasis [270], together with inflammatory remission observed in the excluded intestinal segment after faecal diversion (by means of an ileostomy or colostomy) [230], and reactivation after reinfusion of intestinal contents [105], support this notion. On the other hand, certain immunoregulatory bacterial subpopulations help to maintain intestinal homeostasis [240]. On top of this, we have to take into account that several aspects may complex the study of the relationship between microbiota and IBD. First, there is a huge interindividual variability (even among monozygotic twins only the 40% of faecal phylotypes are shared) [567], secondly, the vast majority of studies are performed in mice whose microbiota composition can be finely tuned and not always a correlation with humans occurs [389], and lastly, it is sometimes difficult to ascribe whether the changes detected on microbial populations are cause or consequence of enterocolitis [390].

1.1.4. Mediators of intestinal inflammation

The intestinal mucosa is constantly exposed to commensal bacteria and dietary antigens. The first line of defense is constituted by the intestinal epithelial cell line, which provides a physical barrier to pathogens but also acts as a frontline sensor that translates information to underneath mucosal immune cells. Thus, epithelial barrier disruption accounts for IBD pathogenesis, and alterations in these cells functions have been found in IBD patients [420]. In a normal situation, after pathogen clearance, resolution of the inflammatory process is required to fully achieve the restoration of tissue integrity and function [407]. Unfortunately, may the host have a genetic susceptibility trait and/or failure to accurately trigger tolerance mechanisms, an acute

inflammatory response that should be dampened could derive in chronic inflammation, leading to IBD [464,487].

Disruption of the epithelial cell barrier

Intestinal epithelial cells (IECs) have a dual role, regulating water and nutrients uptake while at the same time acting as a barrier to the permeation of luminal pathogens and potentially harmful substances. The GI columnar epithelium is covered by a single-cell-thick layer, composed of different subtypes of specialized IECs, including absorptive cells (the most abundant, up to 80% of all epithelial cells), goblet cells, enteroendocrine cells, Paneth cells (only found in small intestine), M cells and Tuft cells [420], all of which differentiate from epithelial stem cells [392]. Of note, mucus production by globet cells is of vital importance for keeping at bay luminal microbes [233,234], emphasized by observations in active enterocolitis of an altered thickness, continuity [442] and composition [58,88] of the intestinal mucus layer, as well as an altered mucin structure [293,79]. Moreover, globet cell and mucus depletion is characteristic of UC [231] and Muc2 knockout mice develop spontaneous colitis [578]. Paneth cells are specialized for the secretion of many antimicrobial peptides (AMPs), including defensins (cryptdins in mice), cathelicidins and lysozyme; representing key players in innate immunity in the gut. Indeed, a reduced expression of α-defensin mRNA has been detected in ileal biopsies from CD patients [596] and Paneth cell abnormalities were found to be associated with mucosal dysbiosis in the context of CD [314].

An effective sealing and proper paracellular permeability is achieved thanks to the apical junctional complex (AJC), located at the enterocyte apical pole, and composed by tight junction (TJ) and subjacent adherens junction (AJ) protein complexes. Both TJ and AJ are reinforced by a dense perijunctional ring of actin and myosin [568]. TJs consist of the transmembrane proteins occludin, the claudin family of proteins and junctional adhesion molecules (JAMs), and its cytoplasmic plaque involves mainly the scaffolding zonula occludens family of proteins and cingulin [566]. AJs together with desmosomes, provide the adhesive strength required for maintenance of cell-cell interactions, whereas TJs are the responsible for sealing the paracellular space and also act as fence to prevent the mixing of membrane proteins between the apical and basolateral membranes, thus contributing to epithelial cell polarization [397]. In the setting of IBD, a compromised integrity of the epithelial barrier and an increased permeability have been recognized since the eighties, in both ulcerated and non-ulcerated epithelia [574,415,200] and in first-degree relatives [525,501,202]. Latter studies revealed altered TJ function, ultrastructure and protein composition in IBD patients [437,499] and reduced expression of occludin [281] as well as the AJ molecules E-cadherin and α-catenin in both CD and UC [120,247]. However, it is not known for certain whether impaired barrier function is secondary to gut inflammation and tissue damage, or if it is a self-determining event. Evidence suggesting prior barrier defects contributing to IBD come from reports documenting changes in intestinal permeability 8 years before onset of CD [224], increased intestinal permeability in 10-54% of first-degree relatives in the absence of clinical symptoms [416,341,201] and animal models of IBD that documented increased epithelial permeability prior to the inflammatory process [192]. In this regard, intestinal permeability has been reported to be a trustable

prognostic indicator of relapse to active disease in patients with CD during clinical remission [106,610]. In favor of a consequence rather than a cause, proinflammatory cytokines produced in excess in IBD like IFN-γ, TNF-α, and IL-13 can lead to cytoskeletal rearrangements that disrupt TJ and increase the epithelial permeability further aggravating inflammation in active disease [478,333,329,46]. Moreover, some experiments in transgenic mice with genetic defects in TJ associated proteins suggest that disruption of barrier function alone is not always enough to trigger disease [538,257]. Overall, intestinal barrier loss can be considered as one component that contributes to a multifactorial mechanism of IBD pathogenesis [398].

Mucosal immune response dysregulation

IECs do not regulate intestinal homeostasis by their own, but instead establish a dynamic crosstalk with intestinal microbes and local immune cell populations. Microbial cells in the intestinal lumen are estimated to outnumber our own somatic and germ cells by one order of magnitude (~10^{14}) [444]. Thus, a sophisticated immune system in our GI tract, shaped after millions of years of co-evolution, is tasked to remain tolerant to this huge quantity of beneficial commensal microorganisms, while accurately prevents the invasion of occasionally incoming pathogens.

Innate immune responses

Innate immune cells from the intestinal mucosa can monitor microbial ligands using PRRs, and microbial metabolites using G-protein-coupled receptors (GPCRs) and solute carriers. Unlike other tissues, in the gut, incoming monocytes are continuously replenishing the macrophage pool in the intestine [23]. Interestingly, depending on the context, the same Ly6C^{hi} monocyte precursors can give rise to hyporesponsive macrophages in homeostasis or proinflammatory macrophages in an inflammatory context [24]. In a resting healthy epithelium, gut-resident macrophages have a limited capacity to respond to bacterial adjuvants, despite they express a full repertoire of TLR receptors. In this sense, downregulation of its downstream mediators including MyD88, TRAF6, TRIF and CD14 [524,523,522] and/or increased expression of molecules that impair TLR signalling like IRAK-M and IkBNS [198], are responsible for their hyporesponsiveness. Similarly, IECs typically have low levels of TLRs, and some of these are exclusively located in the basolateral membrane of the cell, which allow epithelial cells to reside in the high bacterial concentration of the distal ileum and colon and respond only when the epithelial cell line is broken [629]. In intestinal DCs, the hyporesponsiveness is thought to be restricted to TLR4 [78]. Importantly, intestinal CD103^{+} DCs have the unique ability to induce the differentiation of peripheral Foxp3^{+} T regulatory (Treg) cells from naïve T cells in a process dependent on retinoic acid (RA) and active transforming growth factor (TGF)-β [540,85], thus playing a key role in the development of intestinal tolerance. In an inflammatory context, macrophages and DCs in the lamina propria (LP) are increased in absolute numbers and have an activated phenotype in both forms of IBD [487], mainly derived from incoming inflammatory monocytes that migrate to the inflammatory focus. These monocytes conserved normal TLR levels, as polymorphonuclear cells do. Thus, an extensive array of proinflammatory cytokines mainly IL1-β, TNF-α, IL-6, IL-8, members of the IL-12 family [382] and chemokines like MCP-1, MIP-1α, MIP-1β, RANTES, CXCL5 and fractalkine (CX3CL1), were all described to be augmented in IBD [483,572,173]. The selective inhibition of all these proinflammatory mediators has been proved to attenuate

the onset of experimental colitis [487]. On the other hand, accumulating evidence claims for deficient innate immune responses in CD. Increased CD susceptibility associated with NOD2 polymorphisms [218] (which encodes the receptor of the muramyl dipeptide bacterial wall molecule) and the therapeutic activity of granulocyte-macrophage colony-stimulating factor (GM-CSF) [273] support the hypothesis that CD is the result of defective bacterial killing. In this regard, several studies have reported neutrophil and/or macrophage dysfunction in CD patients [520,582,184,503] that would imply a deficient removal of bacterial antigens leading to the subsequent chronic inflammatory status [150]. However, in UC, neutrophil over-activation may imply collateral tissue damage as the extent of neutrophil infiltration correlates with the severity of the disease [60] and neutrophil chemotaxis and ROS production are both increased [502,449].

Adaptive immune responses

The traditional concept over the past decade that in CD Th1 and Th17 responses are selectively upregulated but not in UC, which was thought to represent a Th2-driven disease, has been challenged [112]. Mucosal levels of typical Th1 cytokines like IL-12, IL-18, IL-2, TNF-α and IFNγ are increased in CD patients [393,59,359,360] whereas numerous reports describe an atypical Th2 response in UC, mediated by natural killer (NK) T cells that secrete IL-13 [187,159], although the upregulation of IL-4 and IL-5 Th2 cytokines is variable in UC tissues [160]. On the other hand, an upregulation of prototypic Th2 cytokines like IL-5 and IL-13, was observed in an animal model of human CD [27] and also of IL-4 and IL-5 in lesions of patients with CD [27]. Moreover, the efficacy of anti TNF-α treatment in dampening Th1 responses on UC patients [472], suggests that this T helper subset also plays an important role in UC. The production of IL-17 is stimulated by the production of IL-6, TGF-β and IL-23 by innate immune cells and APCs, especially dendritic cells. Levels of both IL-23 and IL-17 are increased in CD tissues and several types of experimental colitis [626,497,154]. Despite of that, administration of anti-IL-17A monoclonal antibody to patients with moderate to severe CD had no therapeutic effect and in some cases exacerbated the disease [217]. Moreover, anti-IL23p19 therapy failed to meet clinical remission end points [482]. Tregs are crucially involved in the maintenance of gut mucosal homeostasis by suppressing abnormal immune responses against commensal flora or dietary antigens. They have a potent anti-inflammatory role in experimental colitis [515,136], and also are depleted in peripheral blood of patients with active IBD [92].

Leukocyte extravasation

The steps of the leukocyte extravasation cascade comprise the sequential adhesion steps known as tethering, rolling, tight adhesion and transmigration [394]. Inflammatory cytokines upregulate local endothelial expression of adhesion molecules that cause circulating leukocytes to adhere to the inflamed endothelium [30]. Tethering and rolling are mediated by selectins and their carbohydrate ligands [304]. The selectins are a family of transmembrane mammalian lectins expressed on the surface of leukocytes (L-selectin), endothelial cells (P-, E-selectins), and platelets (P-selectin) [242]. The importance of each selectin varies between organs and the inflammatory stimuli [304]. In animal models with intestinal inflammation, conflicting results were obtained as double deficient mice for E and P-selectins showed enhanced leukocyte recruitment and more severe disease [342], and no protection was observed after blocking neither E-selectin nor P-selectin or L-selectin [484];

whereas others observed colitis severity attenuation by P-selectin blocking antibodies or in P-selectin deficient mice [627,588,168]. Nevertheless, more robust effects were observed with the blockade of tight adhesion molecules like Intercellular adhesion molecule-1 (ICAM-1) or CD54, Vascular Cell Adhesion Molecule-1 (VCAM-1) or CD106, and Mucosal Addressin Cell Adhesion Molecule-1 (MAdCAM-1), all playing important roles in the dysregulated trafficking of leukocytes that occurs during IBD [83,62,107,237] and in mice models of intestinal inflammation [250,249,541]. Circulating T cells that bear the gut-homing α4β7 integrin bind to the MAdCAM expressing colonic endothelium [42], which increases its expression levels upon inflammation [83]. Likewise, VCAM-1 and ICAM-1 protein levels are rapidly upregulated in an inflammatory onset [124,72]. VCAM-1 is the ligand for α4β1 (VLA-4) [132] and can also bind α4β7 albeit with lower affinity [465]. ICAM-1 is the ligand for LFA-1 (αLβ2) [336] and Mac-1 (αMβ2) [114]. Thus, blockade of these adhesion molecules have proven efficacy in acute colitis models in mice and rats [38,182,553,608,137,627] and in human clinical trials [580]. On the leukocyte side, targeted blockade of a combinatorial epitope on the α4β7 integrins in cotton-top tamarins [193], in mice [422] and humans [140], and of β2 integrin (CD18) in rats [346] were successful in attenuating colitis. The selective expression of CCL25 by colonic endothelium mediates the gut-specific recruitment of T cells that express the chemokine receptor CCR9 [208]. However, during intestinal inflammation, CCR2 expressing $CD4^+$ T lymphocytes are preferentially recruited to the inflamed ileum [84], and an amelioration of colitis was observed in monocytopenic CCR2-deficient mice [427] and in mice depleted of CCR2-expressing cells [643].

1.1.5. Intestinal epithelial cell damage and mucosal repair

Cell death is an integral part of tissue homeostasis. Elimination of damage or aged cells through programmed cell death (PCD) by apoptosis or autophagy processes is of particular importance for the GI tract, which is continuously exposed to environmental harmful agents [380]. However, in some settings, immune-cell-derived triggers, cytotoxic drugs and physical stressors can lead to excessive IEC apoptosis and undiscriminating necrosis, causing extensive tissue damage. Upon infection, intracellular virus and bacteria induce host cell death through several distinct modalities, including apoptosis, necrosis, and inflammasome-mediated pyroptosis [300,19]. Besides, activation of macrophages and T cells leads to TNF and FasL expression, which promotes apoptosis in mature epithelial cells and crypt cells [348,177,302]. Other proinflammatory cytokines like IFN-γ [471,177] or IL-12 [177] can also trigger epithelial apoptosis. Of note, the intestinal epithelium is much more sensitive to the apoptosis-inducing activity of TNF-α than other tissues [238,424] and apart of inducing apoptosis leads to the disruption of TJ [625], further fueling inflammation and tissue destruction. Neutrophil serine proteases such as elastase, proteinase-3 and cathepsin G, and matrix metalloproteinases like MMP-9, also contribute to further amplify tissue damage due to the relatively indiscriminate range of action of these molecules in terms of their target [280]. Apart from infections, other environmental agents can cause a disruption of the epithelial cell barrier. Ionizing radiation [221] and a variety of drugs like non-stereoidal anti-inflammatory drugs (NSAIDs) [606] or chemotherapy agents [433], provoke apoptosis of IECs. Indeed, many of these molecules are causative agents of IBD development or relapses

[271,550]. After epithelial injury and barrier breakdown, signals from nearby IECs, underlying stromal cells and immune cells promote rapid resealing of the epithelial cell lining to reestablish homeostasis. In a simplified way, epithelial repair is achieved by three distinct mechanisms: restitution, proliferation and differentiation [117].

Epithelial restitution

Despite the need for an impenetrable defence, the intestinal epithelium is only one cell thick to allow for the exchange of nutrients and solutes. Thus, the integrity of the intestinal barrier can be easily compromised, and mechanisms or rapid gap sealing are required. To accomplish this, the first step in mucosal healing consist on a quick migration to the denuded area of cells surrounding the wound, which is called epithelial restitution. This process starts within minutes to hours of injury and is independent of proliferation [555,119]. During restitution, epithelial cells lose their columnar polarity and experience and extensive actin cytoskeletal rearrangement, mediated by Rho family of GTPases [485,204]. Cells lose their microvilli and apical/basolateral orientation, flatten, and extend their lamellipodia into the denudated area [63,287]. New focal attachments are formed at the leading edge mediated by integrins engagement [539,320,319] with clustering of focal adhesion kinase (FAK) [544,628] and where extracellular matrix (ECM) proteins play a key role [458,169,33]. GI restitution is modulated by several factors including: 1) growth factors [100,183,391,489,148,571,119,601,430]; 2) cytokines such as IL-2, IFN-γ and IL-1β [70,119]; 3) chemokines CXCL12 and CCL20 [587,521]; 4) prostaglandins [648] and 5) other luminal factors like short chain fatty acids (SCFAs) [600], bile acids [290], polyamines [453,591], lysophosphatidic acid (LPA) [197] and trefoil factors (TFF) [199].

Epithelial proliferation

After restitution, cell proliferation is triggered to increase the pool of enterocytes available to resurface the denudated area, generally beginning hours to days after injury [310]. Stem cells located at the base of the crypts experience asymmetric cell division, generating one rapidly cycling daughter cell, while the other daughter cell replaces the parent stem cell. The more rapidly proliferating daughter cells, also called transit-amplifying (TA) cells, are the responsible for building tissue mass, and undergo a limited number of cell divisions before terminally differentiating into the functional cells of the tissue [29]. The proliferation phase is temporally and spatially distinct from migration, and at the molecular level these processes depend on excluding patterns of kinase activation and gene expression. For instance, EGF promotes p38 mitogen-activated protein kinase (MAPK) migration or ERK-dependent proliferation, which oppose one another's function [152]. TGF-β [264], LPA [537] and adenine nucleotides [118] stimulate migration, but blunt proliferation. *In vivo*, rapid and immediate migration of injured epithelia is followed by a surge of proliferation much later in time, supporting temporal disassociation of migration and proliferation [287,144,143]. Several molecules modulating intestinal epithelial proliferation are peptide growth factors, such as EGF, TGF-α, and insulin-like growth factor 1 (IGF-1) [323]; peptide hormones like neurotensin, cholecystokinin, bombesin, peptide YY [556,170] and glucagon-like peptide 2 [121]; prostaglandins [557]; cytokines like IL-6 [283], IL-22 [423] and IL-10 [447] and TLR agonists, among the most important ones. TLRs activation in IECs promotes

the proliferation of epithelial stem cells by inducing the production of ligands for EGFR, such as amphiregulin and prostaglandin E2 [211,155]. Also, changes in ECM elasticity after intestinal damage promote the new formation of FAK-integrin complexes, cyclin D1 upregulation and progression through the cell cycle [412]. Importantly, type 2 immunity responses promote epithelial cell proliferation, in a way to favor worm expulsion and initiate the repair process of the damaged barrier [441]. In this sense, type 2 cytokine IL-4 [344] promotes proliferation acting directly on the IEC and indirectly, together with IL-13, induce the expression of the cell surface receptor Trem2 (with as yet undetermined ligand) on M2 macrophages, which have a critical role in the proliferative, but not in the migratory phase, of intestinal wound repair [506].

Epithelial maturation and differentiation.

Once the gap has been filled, epithelial maturation and differentiation is required to restore villus architecture as well as digestive, absorptive and defensive functions. The signaling pathways and transcription factors implicated in the regulation of cell fate determination and lineage specific differentiation in the intestine are becoming increasingly well understood. Among these molecular pathways we can find Wnt-β-catenin-TCF [334,272], Notch and its downstream effectors HES1 and Math1 [620], BMP-TGF-β-SMAD [186,34] and hedgehog signaling [576]. Moreover, E-cadherin-mediated cell-cell [500] and integrin-mediated cell-ECM adhesion [330], and an array of cytokines, hormones and growth factors, are also involved in ruling IECs maturation [251]. Noteworthy, imbalances in these processes ranging from death mechanisms of IECs to the recovery mechanisms including epithelial restitution, proliferation and maturation have been involved in IBD pathogenesis.

1.1.7. Mice models of intestinal inflammation

The development of murine models of acute and chronic intestinal inflammation have provided valuable insights into the complex mechanisms behind IBD pathogenesis. Mice models of IBD can be classified as spontaneous or inducible through chemicals, bacterial infection, immune cells adoptive transfer, transgenesis and gene depletion (**Table 1.2.**).

Table 1.2. Mice models of intestinal inflammation

Spontaneous	Chemically induced	Infection	Adoptive transfer	Transgenic	Knockout
C3H/HeJBir [562] Samp1/Yit[282]	DSS [415] TNBS/DNBS[398,188] Oxazolone[51] Acetic acid[338] Carrageenan[141] Indomethacin [638] Peptidoglycan-polysaccharide[471]	Salmonella-induced[185] *Citrobacter rodentium*[200] Adherent invasive *E.coli*[331]	CD45RBhi → Rag1$^{-/-}$ /SCID[377,451] BM → Cd3εTg26[207] Hsp60 CD8+ → TCRβ$^{-/-}$[551]	STAT-4[628] dn-N-cadherin[195] IL-7[617]	IL-2[490] MUC2[600] IL-10[42] STAT3[569] XBP1[254] CRF2-4[550] TGF-β[531] Giα2[487] TCR-α[372] A20[308] NEMO[394] MDR1A[428] TNFΔARE [279]

DSS colitis model

Dextran sodium sulfate (DSS)-induced colitis has become a widely used model for studying IBD in the mouse [87,401] and among the chemically induced colitis models, is one of the most used due to its rapid development, highly reproducibility and easy way of administration (by water intake). Moreover, acute or chronic models of intestinal inflammation can be achieved by modifying the concentration of DSS and the frequency of administration. Acute colitis is usually induced by continuous administration of 2-5% DSS for short period (5-9 days), whereas chronic colitis may be generated by continuous treatment of low concentrations of DSS or cyclical administration of higher concentrations of DSS intercalated with water intake [131]. Each version is used to study innate vs adaptive immune responses, respectively. This model is suitable for studying events triggered by temporary failure of mucosal homeostasis after epithelial cell shedding and loss of barrier integrity, and can also provide insight into the mechanisms that lead to mucosal healing after initial injury [258]. DSS is an anionic surfactant that disrupts the epithelial cell monolayer lining, leading to the entry of luminal bacteria and associated antigens and stimulating local inflammation [97]. Several mechanisms have been postulated about DSS-induced colonic mucosal inflammation. Recent results indicate that sulfate groups of the DSS molecules destabilize the mucus layers and make them more permeable to bacteria [421]. Moreover, it also exerts a direct toxic effect on the epithelial cells due to its surfactant properties and fusion with colonocyte membranes through the formation of nano-lipocomplexes with medium-chain-length fatty acids (MCFAs) in the colon [292].

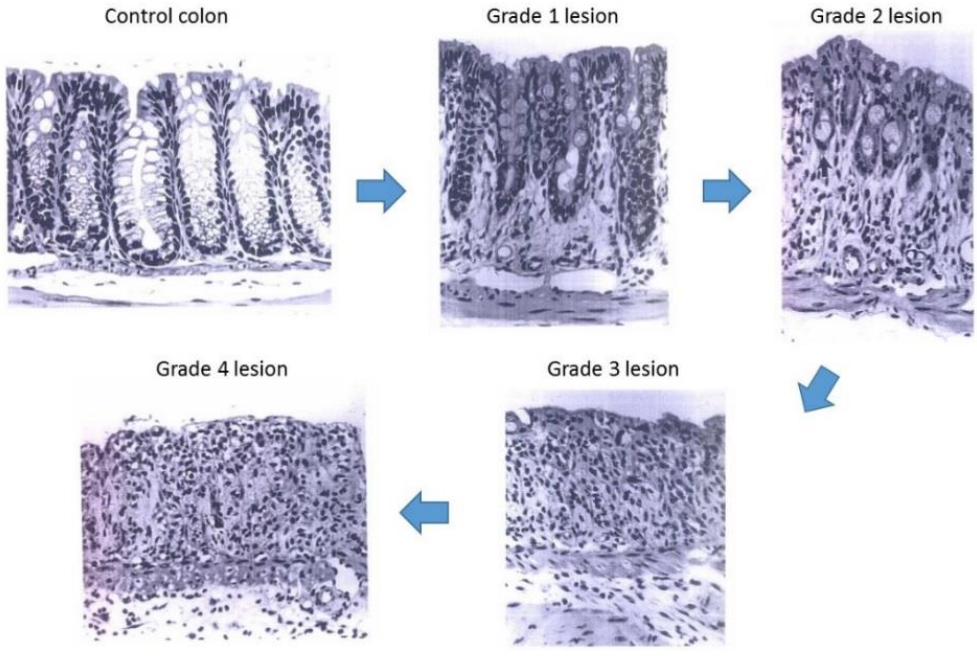

Figure 1.4. **Schematic progression of DSS-induced colonic damage**. Control colon shows straight healthy crypts with their base sitting on the muscularis mucosae and plenty of big globet cells. As the damage goes on, globet cell depletion and crypts shortening are detected. Grade 1 lesion: loss of the basal one-third of the crypts, which fails to sit on the muscularis mucosae. No inflammation can be appreciated yet. Grade 2 lesion: loss of the basal two-thirds and focal thinning of the epithelium. Some inflammation in the lamina propria is beginning to be appreciated. Grade 3 lesion: Loss of the entire crypt with retainment of the surface epithelium. LP and submucosa show broader inflammatory infiltrate. Grade 4 lesion: Total disappearance of the epithelial cell lining and huge inflammatory infiltrate. Modified from Cooper HS. *et al*, 1993 [87].

Interestingly, DSS-induced extensive pathology is mainly confined to the large intestine, specifically the distal colon, where an enormous number of microorganisms live and where the absorption of MCFAs takes place [97]. DSS administration induces changes in the expression of tight junction proteins [432] and increased expression of proinflammatory cytokines [617] as soon as day 1 after treatment. These modest initial effects are followed by increasingly drastic symptoms. During DSS administration, mice can exhibit pronounced weight loss, increased intestinal permeability, diarrhea, severe bleeding, hunched back, piloerection, anaemia and eventually death. The typical histological changes induced by acute DSS include mucin and globet cell depletion, epithelial erosion, ulceration, submucosa swelling and a mixed inflammatory infiltrate of neutrophils and macrophages in the LP and submucosa [419] (**Figure 1.4**) . Importantly, DSS-induced colitis model responds to typical treatments of human disease [347], thus represents a relevant model for the translation of data from mice to humans.

Adoptive transfer colitis model

Transfer of naïve ($CD45RB^{hi}$) $CD4^+$ T cells into syngeneic immunodeficient (lymphopenic) SCID or $Rag1^{-/-}$ recipients leads to wasting disease and colitis [436,364]. Intestinal inflammation develops after 5 to 10 weeks after treatment. As lymphopenic recipient mice do not have any T cell population, nor Treg cells, they cannot dampen the expansion of naïve T cells into the Th1 and Th17 proinflammatory T cell populations that differentiate after several weeks in the intestine due to commensal microbiota stimulation. In this line, the transfer of mature $CD4^+CD45RB^{low}$ (which include Tregs) [435] or directly the transfer $CD4^+CD25^+$ Tregs [366] inhibits the induction of the disease. Macroscopically, mice inflamed colons are thickened and shortened compared to non-transferred control mice. Histopathological inspection of distal colon obtained from mice with active disease reveals a typical transmural inflammation, epithelial cell hyperplasia, polymorphonuclear leukocyte (PMN) and mononuclear leukocyte infiltration, crypt abscesses, and epithelial cell erosions [409] (**Figure 1.5**). This model is very useful for studying the mechanisms that govern Th1 and Th17 T-cell differentiation, the role by Tregs in suppressing or limiting intestinal inflammation, as other immunoregulatory promoters like some bacterial species [258]. Thus, this model helped to define and establish the basis of mucosal homeostasis dependence on a balance between proinflammatory effector and anti-inflammatory regulatory functions.

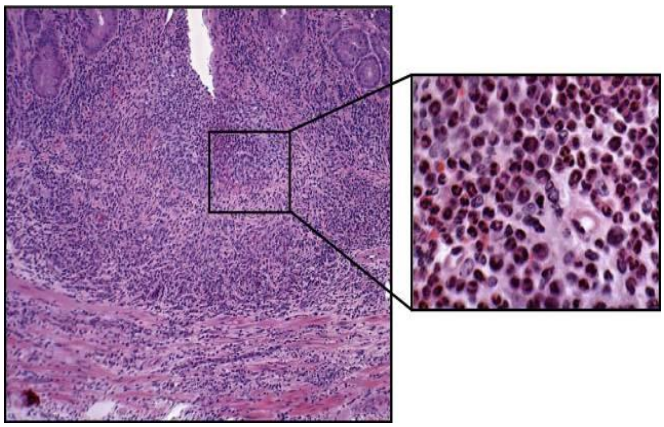

Figure 1.5. Histological magnification of colon obtained from $RAG^{-/-}$ at 8 weeks following adoptive transfer with $CD4^+CD45RB^{high}$ T cells. A large mixed leukocyte infiltrate composed primarily of granulocytes, T cells, and monocytes (*inset*) can be detected. Increased bowel thickness and transmural injury affecting all layers of the colon including loss of globet cells, epithelial disruption and erosion and even muscularis mucosae distortion are observed. From Ostantin DV. *et al*, 2008 [409].

1.2. TETRASPANINS

1.2.1. Introduction

Tetraspanins belong to a family of small glycoproteins (20-30kDa) that contain four transmembrane (TM) regions spanning the plasma membrane. Tetraspanins have been found in all metazoans, plants and some protozoans and multicellular fungi [216]. The structure of tetraspanins is widely conserved across several species, and the expression of several tetraspanins in invertebrates (*Drosophila, Schistosoma, Caenorhabditis Elegans*) [559,191,558] indicates that these molecules appeared early during evolution. Tetraspanins uniform architecture and conserved motifs may suggest these molecules arise from a common ancestor through sequence divergence [161,216]. In humans and mice, 33 tetraspanin members have been identified. These proteins are widely distributed in cells and tissues and every mammal cells express some tetraspanins which are often expressed at 30,000–100,000 or more copies per cell [54]. Some of them are ubiquitous (CD81, CD82, CD9 or CD63), whereas others have a tissue-restricted expression (CD37 or CD53 in immune cells) [188]. Throughout many years, tetraspanins have been overlooked because of their small size, protruding only ~3.5-5 nm above the plasma membrane [353,262] and hidden by their tall glycoprotein neighbours. Consequently, tetraspanins often elude biochemical and immunological detection and it was not until the nineties when these molecules started to be studied [190]. Interestingly, many tetraspanin proteins were originally identified as human tumour antigens. The first description of a tetraspanin protein occurred in 1981 on preB and leukemic cells by Kersey et al. [253]. However, the first characterization of a tetraspanin protein (ME491/CD63) at the sequence level did not appear until 1988 and was identified as a melanoma-associated antigen [209]. After these discoveries, the existence of a family of related structures was finally unveiled in 1990 and tetraspanins were detected apart from in cancer cells [356,405], in leukocytes [13,80] and human parasites [163,609].

1.2.2. Structure

The four TM domains of tetraspanins are linked by one intracellular (IL) and two extracellular (EC1-2) loops and have short intracellular N- and C- termini containing 8-21 amino acids, with a few exceptions [189,95,190,54] (**Figure 1.6**). The smallest EC domain, so-called SEL (Short Extracellular Loop) or EC1 (Extracellular domain 1), possesses between 13 and 31 amino acids [190] and despite its high sequence divergence among the different tetraspanins has a conserved secondary structure in form of a β-strand enriched in hydrophobic residues [504]. The largest EC domain, LEL (Large Extracellular Loop) or EC2 (Extracelullar domain 2) is the most studied part of tetraspanins and also the only part whose structure was determined from crystal X-ray diffraction [263]. LEL possesses between 69-132 amino acids, and can be further subdivided into a constant region, containing conserved three α-helices (A, B and E), and a variable region containing helices C and D [534,190]. The constant region provides a putative dimerization interface [262], whereas the variable region contains various protein-protein interaction sites, specific for each tetraspanin and which

mediates most of tetraspanin interactions with their protein partners [505] (**Figure 1.6**). Although several classes of proteins contain four TM domains, they are not members of the tetraspanin family unless they contain distinctive structural features, including 4-6 conserved cysteine residues and a CCG motif which form critical disulphide bonds within the LEL, as well as some polar residues within the first, third and fourth TM domains [534]. These polar TM residues are involved in the association with other proteins and in the formation of strong hydrogen bonds between themselves, allowing the stabilization of the protein [504,275,641,172]. In addition, TM domain interactions can stabilize the conformation of the EC2 domain [68]. The cytoplasmic tails are short, containing generally less than 20 residues.

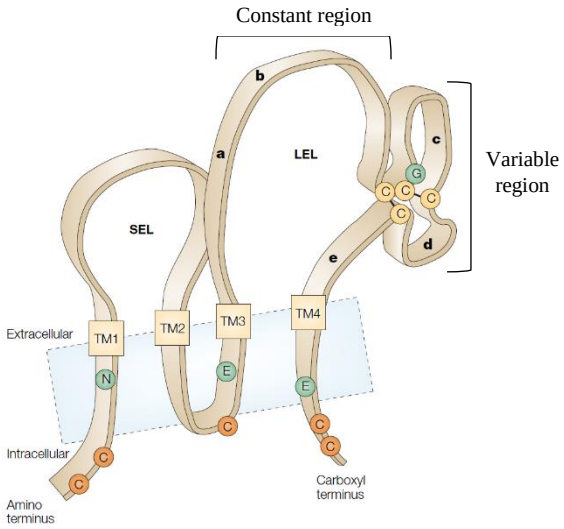

Figure 1.6. Prototypical tetraspanin structure. The four transmembrane (TM) domains contain conserved polar residues (green circles), and they flank the small and large extracellular loops (SEL and LEL, respectively). The LEL is subdivided into a constant region conserved among the tetraspanins (containing helices a, b and e), and a variable region composed by helices c and d, which are flanked by a CCG motif and further conserved cysteine residues (yellow circles). This region is folded as a result of disulphide bridges (black lines). Modified from Levy *et al*, 2005 [303].

Tetraspanins can be subjected to three major post-translational modifications: palmitoylation, N-glycosylation and ubiquitination. Palmitoylation takes place at several cysteine residues in the cytoplasmic tails near the membrane/cytoplasmic interface, which was demonstrated to regulate protein-protein interactions [640,96,40]. N-linked glycosylation occurs mainly at the LEL, which has up to three predicted sites [54], and whose role is less clearly understood although it has been demonstrated to be implicated in some protein interactions [335,403]. Finally, tetraspanins may also be ubiquitinated at cytoplasmic sites, entailing their degradation and consequent down-regulation [594,565,309].

1.2.3. Tetraspanin enriched microdomains (TEMs).

Tetraspanins do not have the characteristics of prototype membrane receptors. They have small cytoplasmic tails that lack known motifs involved in signal transduction [54], and there are only a few reports claiming tetraspanin ligands [239,443,595]. Instead, tetraspanins function as molecular facilitators (termed coined by Maecker et al. in 1997 [327] and organizers of multimolecular membrane complexes, which facilitate signal transduction processes [190]. Through the association with proteins and lipids, they organize specific membrane microdomains with a particular composition and detergent-solubilization properties, conforming the so-called tetraspanin-enriched microdomains or TEMs [618,189] also referred to as "tetraspanin web" [470]. TEMs are distinct from other well-known membrane domains, like lipid rafts (although TEMs involved also cholesterol as a major lipid component), caveolae and GPI-linked protein

nanodomains [618]. The first proofs of the existence of TEMs came from biochemical and proteomic approaches concerning membrane solubilization by a wide range of detergents [296], followed by structural elucidation of tetraspanin dimerization [122] and by fluorescence and electron microscopy images of fixed cells [1,39]. Later on, cutting edge fluorescence microscopy techniques, as single-molecule tracking, phasorFLIM-FRET, and super-resolution microscopy, have more recently demonstrated that TEM organization and composition is highly dynamic [646,463,134,32]. These studies shed light into TEMs behaviour across the plasma membrane, where it is shown that TEMs platforms are dynamic, slowly diffuse throughout the membrane and show a continuous exchange of components characterized by their transience. In this line, some small tetraspanins ensembles move in an aleatory way through Brownian motion which intersperse with confined movements corresponding to their coalescence into enriched tetraspanins areas, conforming the TEMs. It could also happen that TEMs cluster into bigger immobilized platforms induced by the binding of tetraspanin partners to ligands and cytoskeleton constraints. Apart from this high dynamism, the composition of TEMs could differ between cells and in the same cell could exist different TEMs. Thus, this heterogeneous and dynamic composition allows tetraspanins to finely tune a breadth of biological processes [618]. Biochemical approaches have shown that TEMs follow a hierarchical network of associations based on the stoichiometry and strength of the interactions [189,54], where at least three levels have been proposed. The first level, comprises the direct and specific interaction of a tetraspanin and its tetraspanin partner, and are resistant to strong detergent conditions. The second level is characterized by interactions between tetraspanins, that are at the same time associated with their respective partners. These interactions are more labile, resistant to mild detergents and regulated by palmitoylation. Lastly, the third level consists on interactions between tetraspanins from second level complexes and which are very weak and only resistant to very mild detergents such as CHAPS. The inclusion into the tetraspanin microenvironment of their partner proteins confers these an adequate molecular density and local enrichment to efficiently exert their physiological functions, but also, tetraspanins could act as negative regulators by the sequestration of molecules far from other proteins required for signalling transmission or by altering their membrane representation for instance by inducing endocytosis or promoting protease cleavage. The first identification of tetraspanin-tetraspanin interactions was demonstrated by three laboratories, which also described that MHC-II and certain integrins associated with several tetraspanins [470,41,12]. Some years later, mass-spectrometry analyses elucidated an extensive number of tetraspanin-interacting proteins [297,276,93,11].

1.2.4. Tetraspanin CD9

Tetraspanin CD9, also known as motility-related protein 1 (MRP-1), DRAP27 or Tspan29, is one of the most studied tetraspanin members. This 24-25kDa tetraspanin contains two disulphide bridges in the LEL and a putative glycosylation site in the SEL [54]. CD9 was the first identified tetraspanin, originally described as a 24kDa protein expressed on B-lineage-derived acute lymphoblastic leukaemia cells and developing pre-B lymphocytes, hence its original name, p24 [253]. However, it is now known that CD9 displays a much wider expression including many malignant tumour cells, as well as normal hematopoietic, endothelial, and epithelial

cells [618,54]. CD9 was cloned in 1991 [53] which helped to determine the primary structure of the molecule but also was useful to look for similarities with other known surface proteins to characterize the new tetraspanin family of proteins. CD9 was found to associate with several membrane proteins and a few intracellular signalling molecules including phosphatidylinositol 4-kinase (PI4-kinase) and several forms of protein kinase C (PKC) (see **Table 1.3**). However, CD9 can associate with other protein partners through indirect interactions in TEMs. All these interactions confer CD9 ability to contribute to various cellular activities.

Table 1.3. **CD9-interacting proteins.**

Integrins	Adhesion molecules	Immune system	Growth factors	Metalloproteinases	Intracellular proteins	Other proteins
α1β1[321] α2β1[65,495,236] α3β1[41,495,236] α4β1[469,470] α5β1[469,495] α6β1[470,41] α6β4[236] αIIbβ3[317,222] αLβ2[457]	ICAM-1 [31] EpCAM[498] Claudin-1[276] CD47[317] CD42[317,519] CD44[498,296,236] Syndecan[236] Fibronectin[316]	MHC-II[133,575] FcγRI/II[241] FcεRI[418] CD3[562] CD4[562] CD5[562] CD19[207] CD46[321]	ProTGF-α[511] ProHB-EGF[377] EGFR[374]	ADAM-10[17] ADAM-17[176]	PI4K[623] PKC[636]	GPCR[311] c-kit[15] CD36[350] EWI-2[532] EWI-F[535,94] ERMs[477]

Numerous studies have analyzed the changes in CD9 mRNA and/or protein levels in cancer and its relationship to patient prognosis [645]. CD9 was found downregulated in many tumours where its expression inversely correlated with metastasis promotion. Indeed, CD9 was also called Motility Related Protein 1 (MRP -1), because it resulted to be the target of an antibody capable of inhibiting tumour cell migration and invasion [356].The reduced CD9 expression is associated with poor prognosis and/or metastasis in melanoma [514], non-small-cell lung cancer [195], and breast [358,213,357], colon [363], pancreatic [513], oesophageal [570], ovarian [210] and prostate [590] cancers. Decreased levels of CD9 in cancer cells may be achieved by promoter hypermethylation (Drucker et al., 2006). Additionally, CD9 expression have been described to be proapoptotic [403,371,476] and to inhibit proliferation of several tumour cell lines [639,410]. In this line, a plausible underlying mechanism for inhibiting proliferation might be the negatively regulation of cell surface EGFR expression levels by CD9 [552,589,374]. CD9 interacts with the membrane forms of the EGF ligands heparin-binding EGF (pro-HB-EGF) [377,227], transforming growth factor alfa (pro-TGF-a) [511] and amphiregulin (pro-amphiregulin) [223] and enhances their juxtacrine proliferative effect [196,223]. On the contrary, CD9 membrane expression is required for an efficient EGFR internalization, thus, deficiency or decreased expression of CD9 resulted in increased levels of EGFR and its phosphorylation and consequently, augmented proliferation [374,552,589]. Of note, CD9 associates with the metalloproteases ADAM10 [17] and ADAM-17 [176], which are required for the efficient proteolytic release of a number EGFR ligands [48]. Thus, through all these mechanisms CD9 constitutes a key regulator of proliferation. CD9 also plays a role in metastasis and transendothelial invasion, where its expression is locally relocated at site of migration [490,318]. Anti-CD9 monoclonal antibodies were found to specifically inhibit the transendothelial migration of melanoma cells, an inhibitory effect likely caused by a strengthening of CD9-mediated heterotypic interactions of tumour cells to the endothelial monolayer [318]. These evidences suggest that CD9 may play a role of tumour suppressor.

This is supported by *in vivo* trials of adenoviral CD9 gene delivery into tumours [548,355] or ectopic expression of CD9 by transfection of tumour cell lines prior their injection into nude mice [639]. In all the cases, mice injected with CD9 gene lived longer and developed less metastasis. However, this is not always the case. Some reports claim that CD9 expression positively correlates with progression and poor prognosis in some gastric cancers [530,205], chemoresistance in small lung cancer specimens and cell lines [266] and increased trans-endothelial invasion of multiple myeloma [109]. Thus, in summary, the role of CD9 in cancer progression might be disparate in different tumour cell types and stages of tumour development (e.g. the establishment of the primary tumour vs metastasis progression). In relation to this role of CD9 in tumour transendothelial invasion, this tetraspanin has been also reported to regulate the endothelial nanoscopic organization and expression levels of ICAM-1 and VCAM-1 upon TNF-α activation together with CD151, enabling the formation of the docking structure required for leukocyte extravasation [31,32]. Thanks to tetraspanin-induced generation of this docking structure, also known as transmigratory cup [73], it was first demonstrated that endothelial cells do play an active role during the diapedesis process embracing the leukocytes. Moreover, FLIM-FRET studies revealed that the interaction strength between CD9 and ICAM-1, between CD151 and VCAM-1, and between the two tetraspanins was similar [32]. Consequently, soluble CD9-LEL-GST peptides or tetraspanin specific siRNA inhibit leukocyte transmigration and enhance their detachment by shear stress, supporting the functional role of CD9 in transendothelial migration [31].

CD9 can exert pro- or anti-migratory effects [434]. The regulatory effects of CD9 on cell migration may be mediated by integrin-dependent signalling such as phosphorylation of FAK [494] and activation of PI3K, Akt, and p38 kinases [101,274]. In addition to modulating integrin function, CD9 has the potential to regulate motility through the control of other transmembrane proteins and actin cytoskeleton rearrangement. In this regard, CD9 expression downregulates Wiskott-Aldrich syndrome protein family verprolin-homologous protein (WAVE) 2. WAVE2 is known to act as scaffolds that link upstream signals to the activation of the ARP2/3 complex, leading to nucleation of actin polymerization. However, the mechanism by which CD9 regulates WAVE2 expression is not yet elucidated, but it is known to take place in a Wnt-independent way [215]. This is important because the same group demonstrated some years before that CD9 expression induced the downregulation of Wnt1, Wnt2b and Wnt5a proteins [214]. Again, the mechanism how CD9 exerts this downregulation is unknown. However, Wnt5a acts through Wnt-Ca^{2+} pathway which leads to actin reorganization and might modulate cell adhesion and motility. Additionally, CD9 associates with members of EWI family [532] and both CD9 and CD81 co-immunoprecipitate with ezrin-radixin-moesin (ERMs) family of proteins [477], which act as linkers of membrane components like the foregoing EWI proteins, among others, and the underlying cytoskeleton [142]. Interestingly, EWI proteins may also regulate clustering of integrins at the plasma membrane, where tetraspanins play a crucial role as intermediaries through TEMs formation [533,269]. Type IV collagen induces cell migration through a DDR1 and CD9-dependent pathway, and knockdown of either DDR1 or CD9 inhibits migration of breast cancer cells on this substrate [76]. Finally, CD9 has been described to directly interact with fibronectin through its LEL domain, which has been

demonstrated to be required for the proper haptotactic migration of CHO (Chinese-hamster ovary) cells overexpressing this tetraspanin [316].

CD9 in the immune system

The immune roles of CD9 are diverse due to its broad expression in several hematopoietic cell types, including myeloid and lymphoid subsets. In myeloid cells, CD9 restricts LPS-induced macrophage activation and TNF-α production by preventing the TLR-4 co-receptor CD14 localization into lipid rafts. Through this mechanism, CD9 deficiency in mice enhances macrophage infiltration and lung inflammation after in vivo intranasal LPS administration [543]. Some Fc receptors seem to be included in TEMs in phagocytic cells. CD9 antibody cross-linking stimulates intracellular signalling dependent on FcγRIIB and FcγRIII, thus promoting mouse macrophage activation [241]. FcεRI (Fc receptor for IgE), was also found to be a molecular partner of CD9 (and CD81) in human monocytes and skin-derived DCs [418] participating in FcεRI signalosome [181].

MHC-II is expressed on professional APCs and associates with several tetraspanins, including CD9 [133]. CD9 co-immunoprecipitates with I-A MHC-II molecules in mouse BM-derived DCs and B blasts, and I-A/I-E heterologous multimerization is reduced in CD9-deficient BM-derived DCs [575]. Another study has also suggested that MHC-II, together with HLA-DM and CD86, were included in TEMs containing tetraspanins CD9, CD63, CD81 and CD82 [279]. However, deficiency in CD9 does not affect MHC-II clustering at the surface of mouse BM-derived DCs, while surface cholesterol content is essential for multimerization [52,255]. Besides, downregulation of CD9 in human cell lines does not affect surface expression of peptide-bound MHC-II [203] and CD9 deficiency in BMDCs does not affect antigen proteolysis [462]. Recently, it has been reported that tetraspanin CD9 is important for MHC-II egress to the surface of mouse immature MoDCs and that surface expression of MHC-II is decreased in the absence of CD9. Indeed, mouse $CD9^{-/-}$ MoDCs induce less T-cell activation and proliferation than wild-type MoDCs, due to reduced surface expression of MHC-II [462]. This tetraspanin directly interacts with MHC-II, and CD9 engagement with antibodies promotes the formation of antigen-dependent conjugates between human $CD14^{+}$ monocytes and T cells [644]. CD9 is differentially expressed on conventional and plasmacytoid DCs [647,354]. Interestingly, $CD141^{+}$ human and $CD8\alpha^{+}$ mouse cDCs show high expression of CD9, together with CD53 and CD81 and CD82 [647]. However, further studies are necessary to ascertain whether specific tetraspanin expression profiles can be used as markers of cDC subsets and/or define APC functions. CD9 expression allows the recognition of immature and mature mouse pDCs subsets. $CD9^{+}$Siglec-H^{low} pDCs have an immature phenotype, producing high levels of type I IFN and other pro-inflammatory cytokines. These cells are mainly present in mouse bone marrow and spleen, and when stimulated can induce strong $CD4^{+}$ and $CD8^{+}$ T cell responses in vitro and *in vivo*. In contrast, tissue resident pDCs are negative for CD9, do not produce IFN-γ, and have a tolerogenic phenotype, increasing the numbers of $Foxp3^{+}CD4^{+}$ Treg cells in tumour-draining lymph nodes [45].

CD9 has also been implicated in immune cell migration. Human MoDC in vitro migration towards MIP-5 and MIP-1α chemokines was enhanced by 50% after treatment with anti-CD9 mAb [332]. However, monocyte transmigration across brain endothelial cell monolayers was significantly inhibited by the same anti-CD9 mAb,

in human *in vitro* models [493]. Bone marrow-derived macrophages (BMDM) from CD9 and CD81 double deficient mice show reduced motility, through a mechanism dependent on the regulation of MMP-2 and MMP-9 expression and activity. Interestingly, these double deficient mice spontaneously develop pulmonary emphysema, with elevated numbers of alveolar macrophages and increased MMP activity [549]. A similar decrease in macrophage motility and increase in macrophage infiltration was observed in CD9-deficient mice after intranasal administration of LPS. An increase in MMP-2 and MMP-9 production and activity was also observed in BMDMs in the absence of CD9 [543]. In addition, CD9 was shown to regulate migration of B1 cells from the peritoneal cavity to the spleen. LPS stimulation reduces the expression of integrins and CD9 on B1 cell surface, and both CD9 mAb pre-treatment or CD9 deficiency in B1 cells increase migration, by a mechanism dependent on α4 integrin [178]. In this line, increased CD9 expression enhanced the integrin dependent cell motility of B cells involving β1 integrins and the activation of protein tyrosine kinases [508]. On the contrary, CD9 have been found to negatively regulate LFA-1-mediated adhesion under shear flow, due to the alteration of its state of aggregation [457]. Thus, this tetraspanin may have a dual role at regulating β1 or β2 integrin function.

CD9 is highly expressed in marginal zone (MZ) B cells, antibody producing plasma cells and in the B1 subset, but not in splenic follicular (FO) B cells [607]. Nevertheless, $CD9^{-/-}$ mice do not display any impairment in B cell numbers and only a slight increase in IgM secreting cells was detected in steady-state animals, though B cell response to immunization was perfectly normal [69]. In T cells, CD9 has been described to act as a potent costimulatory molecule [547] that synergizes with CD28 [561] and facilitates the insertion of CD3 into lipid rafts [621]. However, engaging CD9 on T cells leads to costimulation by a mechanism distinct from the classic CD28 pathway and independent of NF-κB signalling pathway which fails to sustain IL-2 production [642]. Indeed, unlike CD28 costimulation, CD9 costimulation results in apoptosis of previous TCR-triggered T cells, rather than complete activation [414,546,622]. By immunoprecipitation studies, CD9 was found to interact with CD3, CD4, CD5, CD2, CD29 and CD44 on the T cell surface, being the most prominent one with CD5 [562]. In humans, CD9 was detected to be preferentially expressed on the $CD4^{+}CD45RA^{+}$ naïve T cell population, and to favour both the self-antigen and recall antigen-induced T cell activation [265]. At the immune synapse, CD9 (together with CD151) modulates VLA-4 relocalization and supports high-affinity β1 integrin accumulation, being crucial for FAK and ERK1/2 phosphorylation and IL-2 production [461]. Moreover, CD9 is required to support ALCAM-CD6 (APC-T cell) heterophilic interaction to properly induce T cell activation after conjugate formation [166].

In summary, IBD is a complex multifactorial disorder whose etiology is not fully understood and which remains incurable. Thus, further research is of high relevance to develop new therapeutic approaches. Due to the role of tetraspanin CD9 in several biological processes which might be relevant for IBD development such as regulation of the immune response as well as cell migration and proliferation, we decided to explore CD9 role in the pathogenesis of two mouse models of intestinal inflammation.

Objectives

2. OBJECTIVES

Due to the relevant role of tetraspanin CD9 in key processes such as cell proliferation, migration and leukocyte biology and extravasation, we postulate that CD9 could be implicated in inflammatory bowel disease (IBD) development.

In order to challenge our hypothesis, our main aims were:

1) Assess $CD9^{-/-}$ mice susceptibility to the DSS colitis model compared to WT mice

2) Determine in which cellular compartment CD9 might be exerting its functions

3) Study the role of CD9 in a second model of murine experimental colitis mediated by T cells and T cell differentiation *in vitro*

Objetivos

3. OBJETIVOS

Debido al importante papel de la tetraspanina CD9 en procesos como la proliferación y migración celulares, así como la biología y extravasación leucocitarias, postulamos que CD9 podría estar implicada en el desarrollo de la enfermedad inflamatoria intestinal (EII).

Para abordar nuestra hipótesis, nuestros objetivos principales fueron:

1) Evaluar la susceptibilidad de los ratones $CD9^{-/-}$ en el modelo de colitis inducida por DSS en comparación con animales de cepa salvaje

2) Determinar en qué compartimento celular CD9 está mediando su función

3) Analizar el papel de CD9 en un segundo modelo de colitis mediado por células T y en la diferenciación de células T *in vitro*.

Materials and Methods

4. MATERIALS AND METHODS

4.1. Mice

Experiments were performed with sex and age matched (8-12-week-old) $CD9^{-/-}$ and WT mice on the C57BL/6 background. $CD9^{-/-}$ mice have been described previously (Le Naour F., 2000). $Rag1^{-/-}$ mice (Mombaerts P., 1992) used in the adoptive transfer colitis model were kindly provided by Dr. J. Mª González-Granado (Centro Nacional de Investigaciones Cardiovasculares, CNIC). For chimeric reconstitution experiments, B6SJL CD45.1 mice (Jackson Laboratories) were used. All animals were housed in pathogen-free conditions at the CNIC animal facility. Experimental procedures were approved by the local research ethics committee and conformed to EU Directive 2010/63EU and Recommendation 2007/526/EC, enforced in Spanish law under Real Decreto 53/2013.

4.2. Genotyping of mice

In order to genotype the mice and check the homozygosity of the deletion of CD9, a PCR was performed with the two pairs of primers of the **Table 3.1**

Tabla 4.1. Genotyping primers. Table of primers used to genotype mice disclosed by gene name, sequence 5´-3´ and size of the amplification product. (bp: base pair).

Specificity	Primer	Sequence (5´-3´)	Amplification product
WT allele	CD9Fw	TGCAGGCATGGAGGCGCAGC	354bp
	CD9Rv	TGCCGGCCTCGCCTTTCCC	
Mutant allele	CD9KOFw	CTGGTCACACCCCCTAACGGAGC	550 bp
	CD9neoRv	AGAGCTTGGCGGCGAATGGGCTGA	

The pair of primers CD9Fw/CD9Rv amplifies the WT allele (354 bp), whereas the pair of primers CD9KOfw/CD9neoRv amplifies the mutant allele (550 bp). These two pairs of primers were employed in PCR reactions using the genomic DNA from mouse tails as template DNA. Genomic DNA was obtained from mouse tails using the protocol of the reactive REDExtractc-N-Amp tissue PCR kit (Sigma). As controls, genomic DNA from WT, heterozygous and homozygous mice were used. The amplification protocol is showed in the **Table 3.2**.

Table 4.2. PCR amplification protocol. Table of PCR cycles for genotyping mice disclosed by phase, temperature, time and number of cycles.

Phase	Temperature (°C)	Time	Cycles
1	95	5 min	1x
2	95	1 min	30x
	64	40 sec	
	72	2 min	
3	72	5 min	1x

4.3. Induction and assessment of DSS-induced colitis

Dextran sulfate sodium salt (DSS, MP Biomedicals; MW=36,000-50,000) was dissolved at 2% or 4% (w/v) in sterile drinking water provided to mice ad libitum. Mice were checked daily for development of colitis by monitoring body weight, fecal occult blood (Hemoccult II Sensa; Beckman Coulter) or gross rectal bleeding, and stool consistency. Overall disease severity was assessed by a clinical scoring system defined as follows: weight loss: 0 (no loss), 1 (1-5%), 2 (5-10%), 3 (10-20%), and 4 (>20%); stool consistency: 0 (normal), 2 (loose stool), and 4 (diarrhea); and bleeding: 0 (no blood), 1 (Hemoccult positive), 2 (Hemoccult positive and visual pellet bleeding), and 4 (gross bleeding, blood around anus). At the end of the experiment, tissues were fixed in 10% neutral buffered formalin (Bio Optica) for 24h and transferred to 70% ethanol. After embedding in paraffin, transverse sections (4-5 µm) of proximal and distal colon were stained with H&E for histological studies. Images were digitized using Hamamatsu Nanozoomer 2.0 RS scan and NDP.scan 2.5 digitization software. Three images of 2 serial sections cut at a separation of 100µm (6 sections in total) were evaluated for each mouse for each part of the colon (proximal and distal). Histological scoring evaluated inflammation severity, crypt damage, and ulceration. Inflammation severity was scored as follows: 0, rare inflammatory cells in the lamina propria; 1, increased numbers of granulocytes in the lamina propria; 2, confluence of inflammatory cells extending into the submucosa; 3, transmural extension of the inflammatory infiltrate. Crypt damage was scored as follows: 0, intact crypts; 1, loss of the basal one-third; 2, loss of the basal two-thirds; 3, entire crypt loss; 4, change of epithelial surface with erosion; 5, confluent erosion. Ulceration was scored as follows: 0, absence of ulcers; 1, 1 to 2 ulceration foci; 2, 3 to 4 ulceration foci; 3, confluent or extensive ulceration. Scores for each parameter were summed to give a maximum histological score of 11.

4.4. T cell-mediated colitis

Naive $CD4^+$ T cells were sorted (FACSaria sorter, BD) from single-cell spleen suspensions of $CD9^{-/-}$ or WT mice. Live cells were isolated after labeling with antibodies to CD4, CD62, CD25, and CD45RB (**Table 4.3**) and hoechst 33258 (Sigma-Aldrich). Cells were transferred to recipient $Rag1^{-/-}$ mice (4-5 x 10^5 cells per mouse) by intraperitoneal injection.

4.5. Bone marrow chimeras

Bone marrow transfer was used to create chimeric mice in which genetic deficiency for CD9 was confined to either circulating cells ($CD9^{-/-}$ >WT) or nonhematopoietic tissue (WT > $CD9^{-/-}$). Briefly, bone marrows were collected from femur and tibia of congenic WT donor mice (expressing CD45.1 leukocyte antigen) or $CD9^{-/-}$ and WT donor mice (expressing CD45.2 leukocyte antigen) by flushing with PBS. Erythrocytes were lysed (ACK lysis buffer, Lonza) for 1 minute on ice. After a washing step, cells were resuspended in PBS at 1 x 108/ml. This cell suspension (100 µl) was injected intravenously into 13 Gy-irradiated recipient mice 48h post-irradiation. Four chimera groups were generated: WT > WT (WT cells expressing CD45.1 into WT mice expressing CD45.2); WT > $CD9^{-/-}$ (WT cells expressing CD45.1 into $CD9^{-/-}$ mice expressing CD45.2); WT >

WT (WT cells expressing CD45.2 into WT mice expressing CD45.1); $CD9^{-/-}$ > WT ($CD9^{-/-}$ cells expressing CD45.2 into WT mice expressing CD45.1). Bone marrow reconstitution was verified after 8 weeks by staining for CD45.1 or CD45.2 in blood cells with anti-CD45.1 or anti-CD45.2 specific antibodies (**Table 4.3**).

4.6. *In vivo* permeability assay

Food was withdrawn overnight and mice were gavaged with the permeability tracer FITC-dextran (Mw 4000; Sigma-Aldrich) at 60 mg/100 g body weight. After 4h, blood was collected by heart puncture and serum FITC-dextran was measured with a fluorescence spectrophotometer (Fluoroskan Ascent; Thermo Labsystems) using emission and excitation wavelengths of 490 nm and 520 nm, respectively. FITC-dextran concentration was determined from a standard curve generated by serial dilution.

4.7. Isolation and flow cytometry analysis of colonic leukocytes

Colons were dissected longitudinally, washed several times with PBS to remove feces, and cut into small pieces. Samples were digested with 0.25 mg/ml Liberase TM (Roche), 50µg/ml DNAseI (Roche), and 1mM DTT diluted in Hank's Balanced Solution (HBSS) for 30 min at 37ºC. At the end of the incubation period, enzyme activity was blocked by adding 50 ml PBS supplemented with 0.5% BSA and 0.05mM EDTA (PBS-BSA-EDTA), and the sample was mechanically disrupted by passing through a 70-micron cell strainer to obtain a cell suspension. When only epithelial cells were required, samples were incubated in 5mM EDTA, 1mM DTT for 20 minutes before enzyme digestion. Before all staining procedures, colon cell suspensions were incubated with anti-mouse CD16/CD32 (Fc block) for 10 min at 4ºC in PBS-BSA-EDTA. For intracellular staining, cells were fixed and permeabilized using the CytoFix/Cytoperm kit (BD Biosciences). The antibodies used are listed in **Table 4.3** Absolute cell numbers were obtained using TruCount Tubes (BD Biosciences). Cell samples were acquired in a FACSCanto Flow Cytometer (BD Biosciences), and the data were analyzed with FlowJo (Tree Star) or FACSDiva (BD Biosciences) software

4.8. Flow cytometric bead array (CBA)

Serum TNF-α, IL-6 and IFNγ were determined using the mouse Th1/Th2/Th17 BD cytometric bead array (CBA).

4.9. RNA extraction and real-time quantitative PCR

RNA was isolated by disrupting colon tissue samples with TRIzol Reagent (1ml per 50-100mg tissue, Qiagen) and homogenizing in a tissue disruptor (Ika ultra-turrax T10 homogenizer). DSS traces were removed by the LiCl method (Ambion). Residual DNA contamination was eliminated with the Turbo DNA-free Kit (Ambion). Total RNA (1µg) was reverse transcribed to cDNA with a Reverse Trancription Kit (Applied Biosystems). Quantitative PCR was then performed in an AB7900_384 (Applied Biosystem) using SYBR Green (Applied Biosystems) as the reporter. Gene-specific primers used are listed in the

Table 4.3. List of antibodies for flow cytometry (FC). Table of antibodies used in FC experimental procedures disclosed by reference, brand, host and dilution

Antibody	Reference	Brand	Host	Dilution
CD45.2-v450	560697	BD Pharmingen	mouse	1:200
CD45.2-PeCy7	560696	BD Pharmingen	mouse	1:200
CD45.1-PercPCy5.5	560580	BD Pharmingen	mouse	1:200
CD45RB-FITC	553099	BD biosciences	rat	1:200
EpCAM-FITC	118207	Biolegend	rat	1:200
EpCAM-PeCy7	118215	Biolegend	rat	1:200
CD31-APC	551262	BD Pharmingen	rat	1:200
Ki67-Alexa647	558615	BD Pharmingen	mouse	1:200
CD9-PE	12009181	eBioscience	rat	1:200
CD9-APC	17009182	eBioscience	rat	1:200
CD64-Alexa647	558539	BD Pharmingen	mouse	1:200
CD11b-FITC	553310	BD Pharmingen	rat	1:200
CD11c-PeCy7	558079	BD Pharmingen	hamster	1:200
CD16/32 Fc-block	70-0161	TONBO Biosciences	rat	1:200
CD3-FITC	555274	BD Pharmingen	rat	1:200
CD8-APC	558079	BD Pharmingen	rat	1:200
CD4-PeCy7	600042	TONBO Biosciences	rat	1:200
CD62L-PE	553151	BD biosciences	rat	1:200
CD25-APC	102011	Biolegend	rat	1:200
Ly6C-PerCP-Cy5.5	560525	Becton Dickinson	rat	1:200
Ly6G-PeCy7	605931	TONBO Biosciences	rat	1:200
MHC-II I-A/I-E-FITC	553623	BD Pharmingen	rat	1:300

Table 4.4. List of qPCR primers. Table of primers used in qPCR disclosed by gene name and forward and reverse sequences.

Gene	Forward Primer (5´- 3´)	Reverse Primer (5´- 3´)
Zo1	GAGCGGGCTACCTTACTGAAC	GTCATCTCTTTCCGAGGCATTAG
Tricellulin	TTCCGAAGCCTATCGTGATGC	GAACACAGCCTTATAGCGTTCT
Claudin-5	TATGAATCTGTGCTGGCGCT	GTGCTACCCGTGCCTTAACT
Claudin-7	CAGGCCACTCGAGCCTTAAT	GCAAGACCTGCCACAATGAAA
Claudin-8	GCAACCTACGCTCTTCAAATGG	TTCCCAGCGGTTCTCAAACAC
Claudin-10	AATCGTCGCCTTCGTAGTCTC	GTTGGCAAAATAAGTGGCTGTG
Muc1	GGCATTCGGGCTCCTTTCTT	TGGAGTGGTAGTCGATGCTAAG
Muc2	TGACTGCCGAGACTCCTACA	CCAGCTTGTGGGTGAGGTAG
Tff3c	GATTACGTTGGCCTGTCTCC	TGAAGCACCAGGGCACATTT
Il6	TAGTCCTTCCTACCCCAATTTCC	TTGGTCCTTAGCCACTCCTTC
Nlrp3	CGAGACCTCTGGGAAAAAGCT	GCATACCATAGAGGAATGTGATGTACA
Il1b	GCAACTGTTCCTGAACTCAACT	ATCTTTTGGGGTCCGTCAACT
Il12p35	TACTAGAGAGACTTCTTCCACAACAAGAG	CTGGTACATCTTCAAGTCCTCATAGA
Il12p40	GGAAGCACGGCAGCAGAAT	AACTTGAGGGAGAAGTAGGAATGG
inos	CAGGAAGTAGGTGAGGGCT	AATCTTGGAGCGAGTTGTGG
Ifng	CGGCACAGTCATTGAAAGCC	TGCATCCTTTTTCGCCTTGC
Il17	TTTAACTCCCTTGGCGCAAAA	CTTTCCCTCCGCATTGACAC
Il22	ATGAGTTTTTCCCTTATGGGGAC	GCTGGAAGTTGGACACCTCAA
Il10	ATAACTGCACCCACTTCCCA	GGGCATCACTTCTACCAGGT
Il2	TTGTGCTCCTTGTCAACAGC	CTGGGGAGTTTCAGGTTCCT
TNFa	CAGGCGGTGCCTATGTCTC	CGATCACCCCGAAGTTCAGTAG
Tgfb	CCTGCAAGACCATCGACATG	TGTTGTACAAAGCGAGCACC
Gapdh	AGCTTGTCATCAACGGGAAG	TTTGATGTTAGTGGGGTCTCG
c-myb	GAGCACCCAACTGTTCTCG	CACCAGGGGCCTGTTCTTAG
c-fos	CGGGTTTCAACGCCGACTA	TTGGCACTAGAGACGGACAGA
Ccdn1	GCGTACCCTGACACCAATCTC	CTCCTCTTCGCACTTCTGCTC

4.10. *In vitro* T cell differentiation

Naive $CD4^+$ T cells were obtained by incubating single-cell suspensions of spleen and lymph nodes with biotinylated antibodies to CD8, CD16, CD19, F4/80, Gr-1, MHC class II (I-Ab), CD11b, CD11c, and DX5 followed by incubation with Streptavidin Microbeads (MACS, Miltenyi Biotec). $CD4^+$ T cells were isolated by negative selection in an auto-MACSTM Pro Separator (Miltenyi Biotec). Next, cells were activated with plate-bound anti-CD3 (5μg/ml) and anti-CD28 (2μg/ml) in RPMI 1640 medium (Sigma-Aldrich) supplemented with 10% FCS, $2x\ 10^{-3}$ M L-glutamine, 100 U/ml penicillin, 100 μg/ml streptomycin, 50 μM 2-mercaptoethanol, and the corresponding cytokine cocktail: for Th0, anti-IFNγ (4 μg/ml), anti-IL-4 (4 μg/ml), and IL-2 (10ng/ml); for Th1 anti-IL-4 (4 μg/ml), IL-12 (10ng/ml), and IL-2 (10ng/ml); for Th17 anti-IFNγ (4 μg/ml), anti-IL-4 (4 μg/ml), IL-6 (20 ng/ml), IL-23 (10 ng/ml), and TGF-β1 (5ng/ml); and for Treg anti-IFNγ (4 μg/ml), anti-IL-4 (4 μg/ml), and TGF-β1 (10ng/ml). after 72h of culture IFNγ, IL-17, or IL-10 in the supernatant were measured by ELISA (Ready-SET-Go, eBiosciences). For FACS analysis, intracellular cytokine staining was preceded by restimulation for 4h with 50 ng/ml phorbol dibutyrate (PMA) and 500 ng/ml ionomycin in the presence of brefeldin A (1μg/ml) (BD Biosciences).

4.11. Immunohistochemical analysis

For IHC staining, colon sections were deparaffinized, boiled in antigen retrieval solution (10 mM Tris Base, 1 mM EDTA Solution, 0.05% Tween 20, pH 9.0 for Ki67 and 10 mM sodium citrate, 0.05% Tween 20, pH = 6 for caspase-3), and incubated with the rabbit monoclonal anti-mouse Ki67 primary antibody (Master Diagnostica, clon SP6) or anti active caspase-3 rabbit polyclonal antibody (R&D system, catalog AF835). Bound antibodies were detected with anti-rabbit EnVision FLEX-HRP detection system (Agilent). Staining was developed with DAB substrate (Dako K3468), and slides were counterstained with Mayers Hematoxylin. Ki67 staining in epithelial cells was quantified in at least 4 fields (20X magnification) from each DSS-treated mouse (6-7 mice per group). Active caspase-3 staining in epithelial cells were quantified in the whole colon sections from each DSS-treated mouse (4-5 mice per group). Image J (1.46r) was used to measure intensities relative to the total area corresponding to the complete epithelial layer in each image.

4.12. Statistical analysis

Data are presented as mean ± SD. Normal data distribution was assessed with the Kolmogorov Smirnov test, and the statistical significance of between-group differences was assessed by one-tailed unpaired Student t test, one-way ANOVA with Newman Keuls multiple comparison t-test, or two-way ANOVA with Bonferroni multiple comparison as required. All statistical analyses were performed with GraphPad Prism (GraphPad Software Inc.).

Results

5. RESULTS

5.1. CD9$^{-/-}$ mice are protected against DSS-induced colonic injury

To explore the function of CD9 in colitis development, we challenged CD9$^{-/-}$ and WT mice with the toxic compound DSS (2% solution) in drinking water for 7 days. Due to the colitogenic properties of DSS, animals experience progressive weight loss, severe diarrhea and intestinal bleeding. CD9$^{-/-}$ mice lost less than 10% of their initial body weight, whereas WT counterparts lost around 20% at the end of the treatment (**Figure 5.1a**). In addition, to monitor disease activity, we recorded a daily disease activity index (DAI) combining weight loss, stool consistency, and bleeding. From day 4, DAI values were lower in CD9$^{-/-}$ mice than in WT counterparts (**Figure 5.1b**).

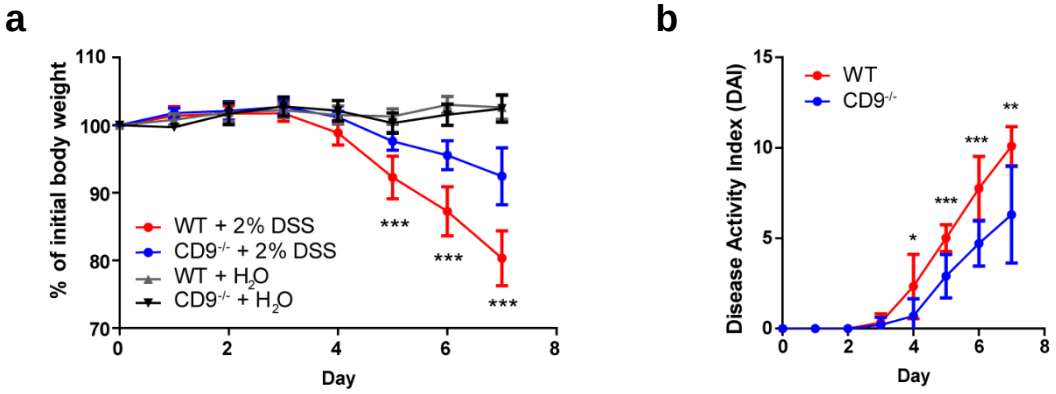

Figure 5.1. CD9-deficiency reduces sensitivity to dextran sodium sulfate (DSS)-induced colitis. (a) Body-weight loss in WT and CD9$^{-/-}$ mice after administration of 2% DSS in drinking water for 7 days. Controls for each genotype were administered with unadulterated drinking water. **(b)** Disease activity index (DAI) score in WT and CD9$^{-/-}$ mice after administration of 2% DSS for 7 days. *n* = 10–12 per group. Data represent means ± SD; **P* < 0.05; ***P* < 0.005; ****P* < 0.001.

Due to tissue destruction, colon shortening in DSS-treated animals can be observed. Autopsy revealed that DSS-treated CD9$^{-/-}$ mice had significantly larger colons than WT counterparts (**Figure 5.2.**), in accordance to the differences observed in body weight drop and DAI scores between both groups**.**

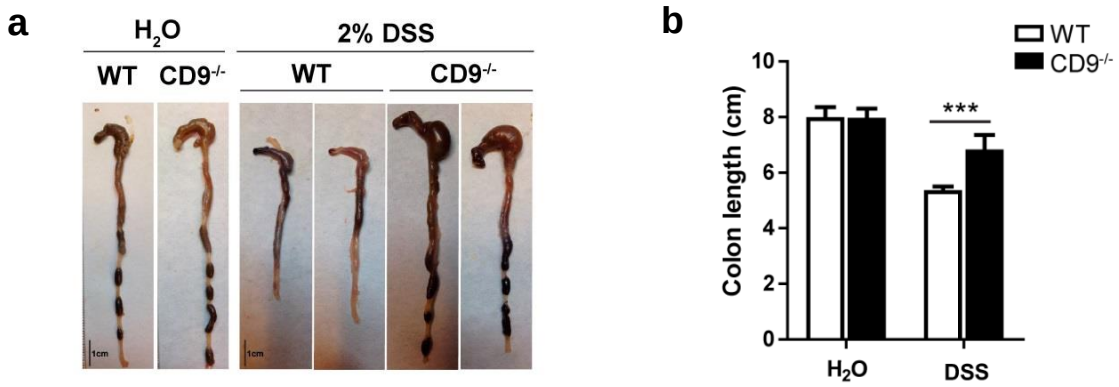

Figure 5.2. Macroscopic colon damage in DSS-treated WT and CD9$^{-/-}$ mice. (a) Representative images of colon shrinkage. **(b)** Quantification of the changes in colon length. *n* = 10–12 mice per group.

Histology revealed a better preservation of tissue architecture in CD9$^{-/-}$ mice, in both the proximal and the distal colon. DSS-treated WT animals showed more pronounced epithelial denudation, crypt distortion, leukocyte infiltration of the lamina propria, and submucosal swelling (**Figure 5.3a**). Histological sections were scored for the severity of DSS-induced inflammation as described in Materials & Methods. DSS-induced extensive pathology is practically confined to the large intestine, specifically the distal colon where an enormous number of microorganisms live. In both proximal and distal colon, histological scores were lower in CD9$^{-/-}$ mice than in WT mice, with the difference more pronounced in the distal colon (**Figure 5.3b**).

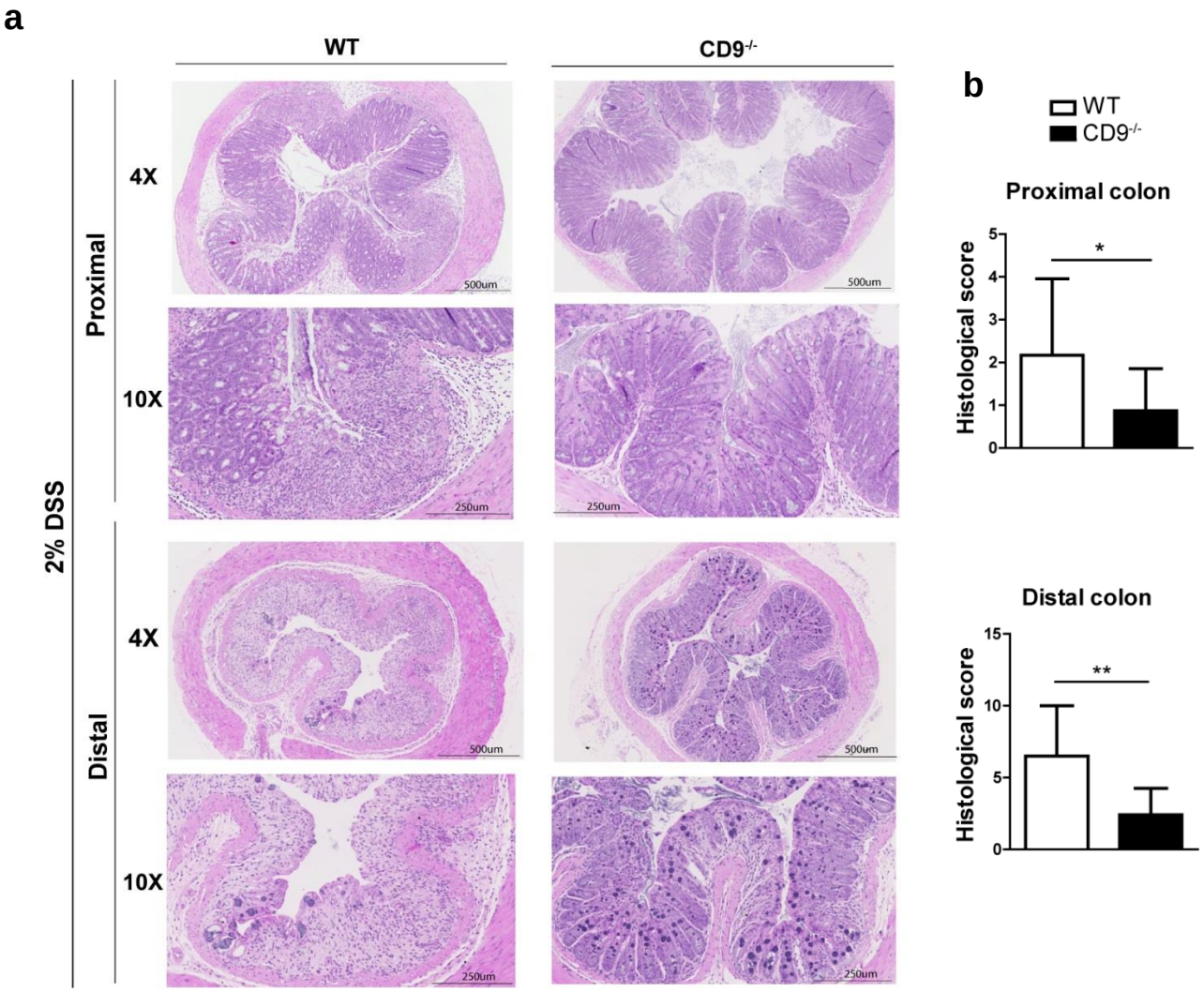

Figure 5.3. Colon histopathological examination. (a) Representative photomicrographs of proximal colon (near the cecum) and distal colon (near the anus) from WT and CD9$^{-/-}$ mice at day 7 of DSS administration (H&E; magnifications: 4X and 10X). **(b)** Histological scores obtained from H&E-stained proximal and distal colon tissue sections from DSS-treated WT and CD9$^{-/-}$ mice. Data are pooled from two independent experiments (n = 4). Values represent mean ± SD of the mean: *P < 0.05; **P < 0.005; ***P < 0.001, unpaired t-test.

5.2. CD9 exacerbates tissue injury and decreases mouse survival after a lethal DSS dose

Intestinal epithelial integrity is necessary for efficient defence against intraluminal toxins, antigens, and enteric bacteria. Cells are tightly joined in a healthy epithelium, and transepithelial permeability can thus be determined as an index of epithelial integrity. To monitor gut barrier function in vivo, we treated CD9$^{-/-}$ and WT animals with 2% DSS for 7 days and then orally administered 4KDa FITC-Dextran. Fluorescence spectrophotometry detection of serum FITC after 4h revealed markedly lower gastrointestinal permeability in CD9-/- mice than in WT mice (**Figure 5.4**). Serum FITC levels in non-treated animals showed no significant between-genotype differences and remained below 5ug/ml, consistent with an intact intestinal barrier function in the steady state (**Figure 5.4**).

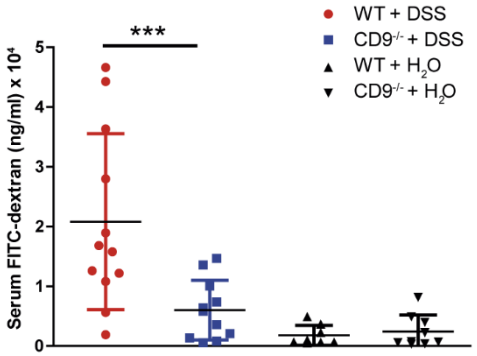

Figure 5.4. Enhanced epithelial barrier integrity in CD9$^{-/-}$ mice after DSS challenge. In vivo colon permeability, indexed from the serum level of 4 kDa FITC-dextran 4 h after feeding by gavage. Data are pooled from two independent experiments, n = 5–6 animals per group. Data were analyzed by one-way ANOVA and the Newman–Keuls multiple comparison test; ***P < 0.001.

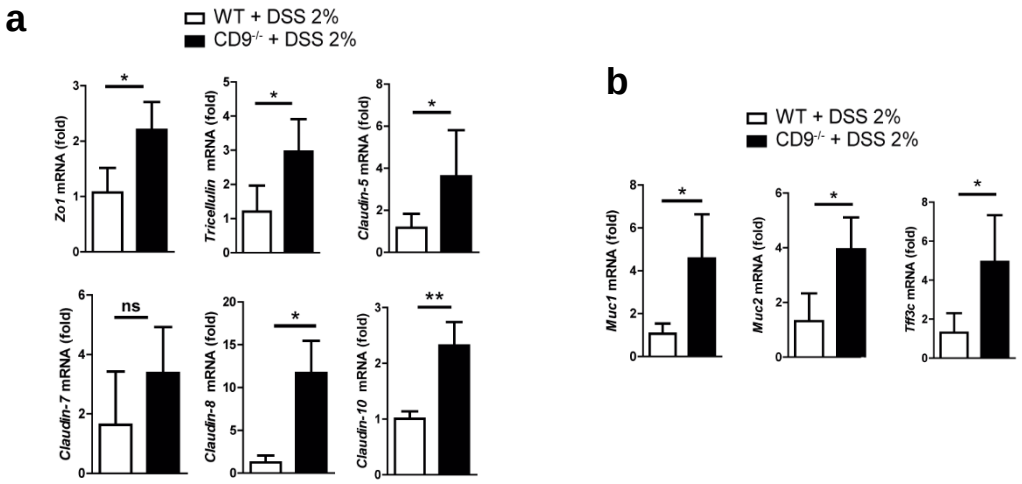

Figure 5.5. Enhanced preservation of the epithelial barrier in CD9$^{-/-}$ mice after DSS treatment. (a) qPCR analysis of tight junction and **(b)** mucin gene expression in colon samples after 7 days of DSS exposure. Data are from one experiment repeated two times with similar results. unpaired t-test. ns= non-significant, *P < 0.05; **P < 0.005.

Consistent with the FITC-Dextran data, qPCR of colon samples from DSS-treated CD9$^{-/-}$ mice revealed elevated expression of genes encoding epithelial tight junction proteins, such as ZO-1, tricellulin, and claudin

family members (**Figure 5.5a**). CD9$^{-/-}$ colon also showed elevated expression of genes encoding epithelial globet cell proteins, such as the secretory mucin glycoproteins MUC1, MUC2, and trefoil factor 3 (TFF3), indicating normal intestinal function (**Figure 5.5b**).

In a further approach, we exposed mice to a lethal DSS dose (4%) for 7 days followed by unadulterated drinking water for a further 8 days. At the end of the experiment all WT mice had died, whereas only 45% of the CD9$^{-/-}$ group were dead (**Figure 5.6a**). Moreover, the surviving CD9$^{-/-}$ mice showed a recovery in body weight (**Figure 5.6b**). These results show that CD9 impedes epithelial repair and contributes to colon injury at both sublethal and lethal DSS doses.

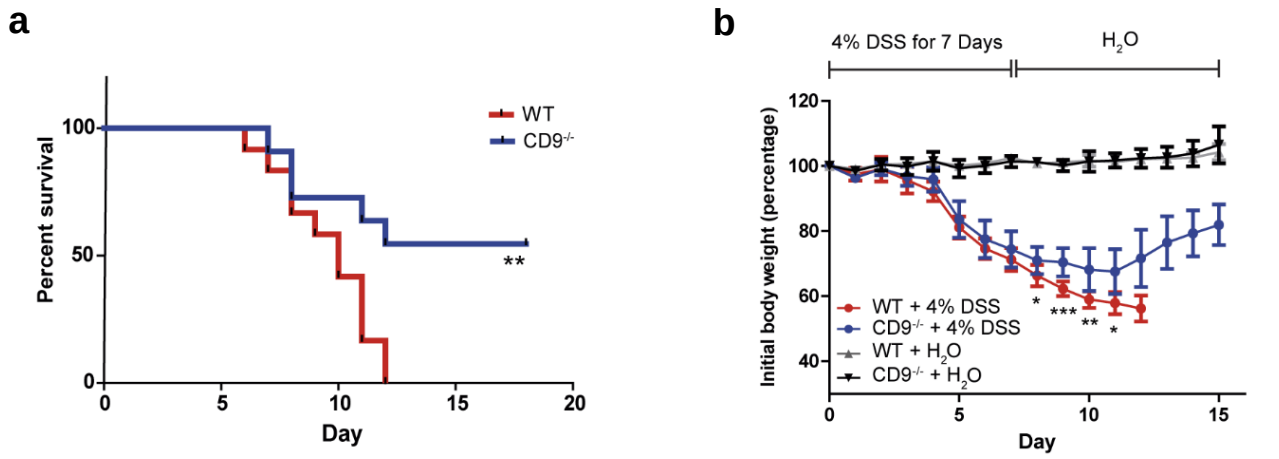

Figure 5.6. Increased survival and recovery of CD9$^{-/-}$ mice after lethal 4% DSS dose administration. (a) Kaplan–Meier survival for WT and CD9$^{-/-}$ mice given 4% DSS in drinking water. $^{**}P < 0.01$, Log-rank (Mantel–Cox) test. **(b)** Percentage of initial body weight of WT and CD9$^{-/-}$ mice after 7-day intake of 4% DSS chased by unadulterated water. $n = 11–12$ per group: $^{*}P < 0.05$; $^{**}P < 0.005$; $^{***}P < 0.001$; unpaired t-test for WT and CD9$^{-/-}$ groups.

5.3. Reduced myeloid cell infiltration and proinflammatory cytokine expression in the colon of CD9$^{-/-}$ mice

To characterize the immune mechanisms of colonic mucosa damage, we analyzed CD9$^{-/-}$ and WT colon cells by flow cytometry. After 7-day exposure to 2% DSS, CD9$^{-/-}$ colon showed markedly lower neutrophil and macrophage infiltration than WT colon (**Figure 5.7a and b**). In contrast, in non-treated mice, gut populations of these immune cell subsets were comparable between genotypes (**Figure 5.7a and b**), as were lamina propria (LP) (**Figure 5.8a and b**), intraepithelial lymphocyte (IELs) (**Figure 5.8c**), and mesenteric lymph nodes (MLNs) populations **(Figure 5.8d**).

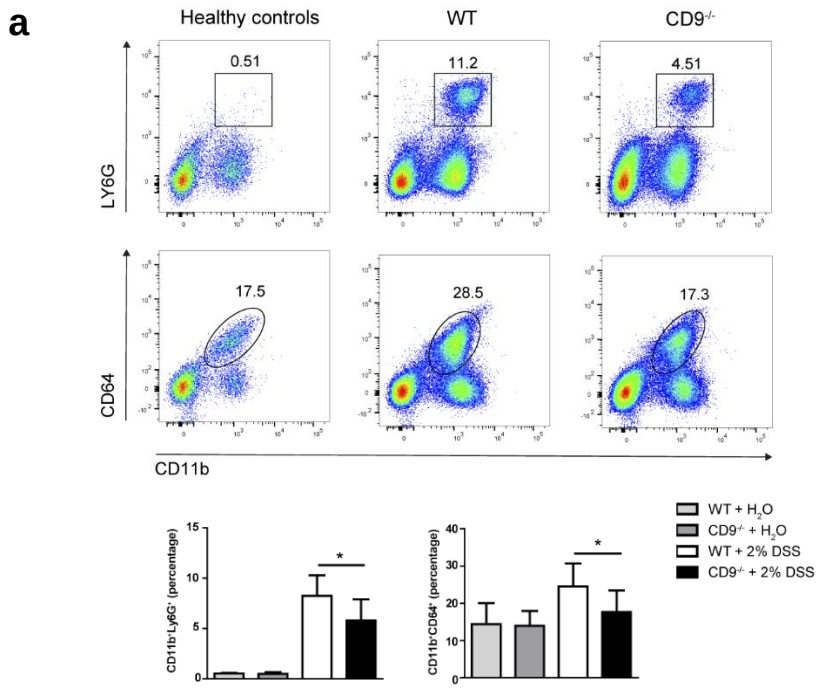

Figure 5.7. CD9$^{-/-}$ mice exhibit lower leukocyte infiltration in the colon after 2% DSS administration. (a) Flow cytometry analysis of whole colon from WT and CD9$^{-/-}$ mice after 7-day 2% DSS intake. Representative dot plots and percentage quantification of neutrophils (Ly6G^{+}) and macrophages (CD64^{+}) populations gated in CD45^{+} cells. **(b)** Total neutrophil and macrophage numbers in the CD45^{+}-gated population. Data are pooled from two independent experiments. n = 6-7 mice per group with two repeats and analysis by one-way ANOVA and the Newman–Keuls multiple comparison test. *P < 0.05; **P < 0.005.

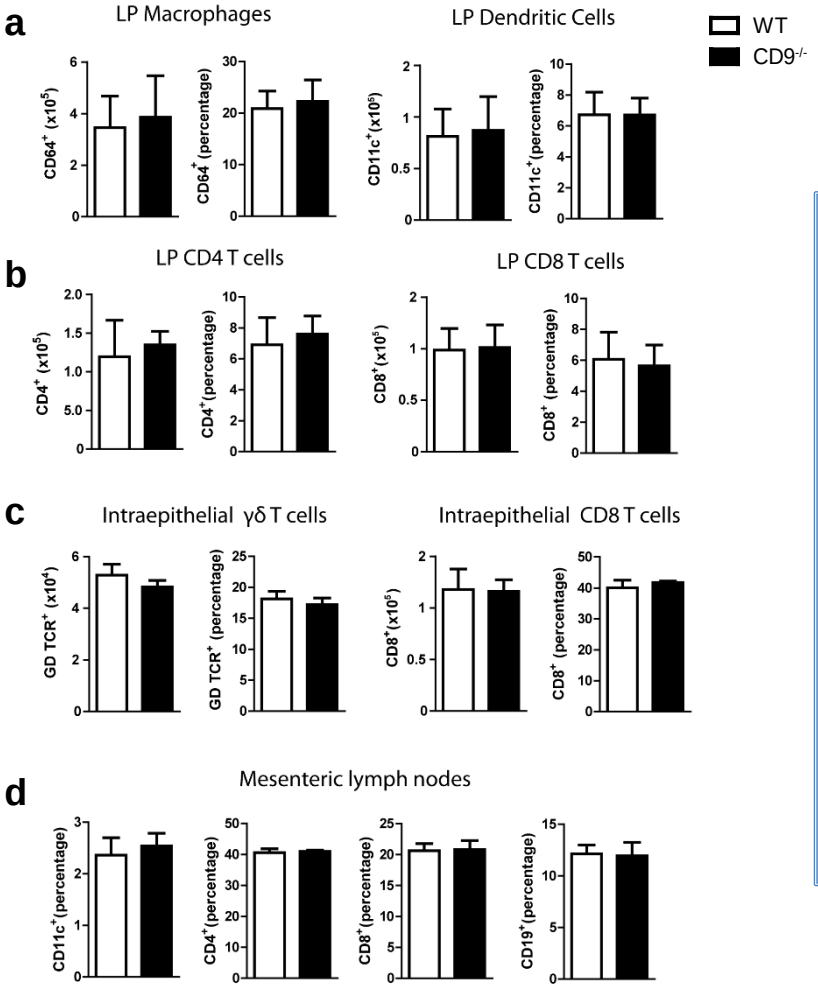

Figure 5.8. Immune cell populations in the colon and MLNs do not differ between CD9$^{-/-}$ and WT mice in steady state. Flow cytometry analysis of immune cell populations from untreated mice revealed no between-genotype differences in **(a)** lamina propria (LP) macrophages (CD11b^{+}CD64^{+}), DCs (gated on MHCII^{+}CD11c^{+}CD64^{-}) and lymphoid CD4^{+} and CD8^{+} T cell; **(b)** intraepithelial lymphocytes (IELs), γδ and CD8^{+} T cells and **(c)** mesenteric lymph nodes (MLNs) DCs, T and B cells. Total numbers and percentages from the CD45^{+}-gated population. Data are representative of three independent experiments. n = 5 mice per group; unpaired t-test.

DSS-treated CD9$^{-/-}$ mice also had lower serum levels of IL-6 and TNFα than WT mice, whereas IFNγ was similarly increased in response to DSS in both genotypes (**Figure 5.9a**). Analysis of colon samples by qPCR revealed lower DSS-induced levels of IL-6, IL-1β, NLPR3, iNOS, IL12p35, and IL12p40 mRNA in CD9$^{-/-}$ animals (**Figure 5.9b**), whereas IFNγ, IL-22, IL-17, IL-10, IL-2 and TGF-β showed no significant between-genotype differences (**Figure 5.9c**).

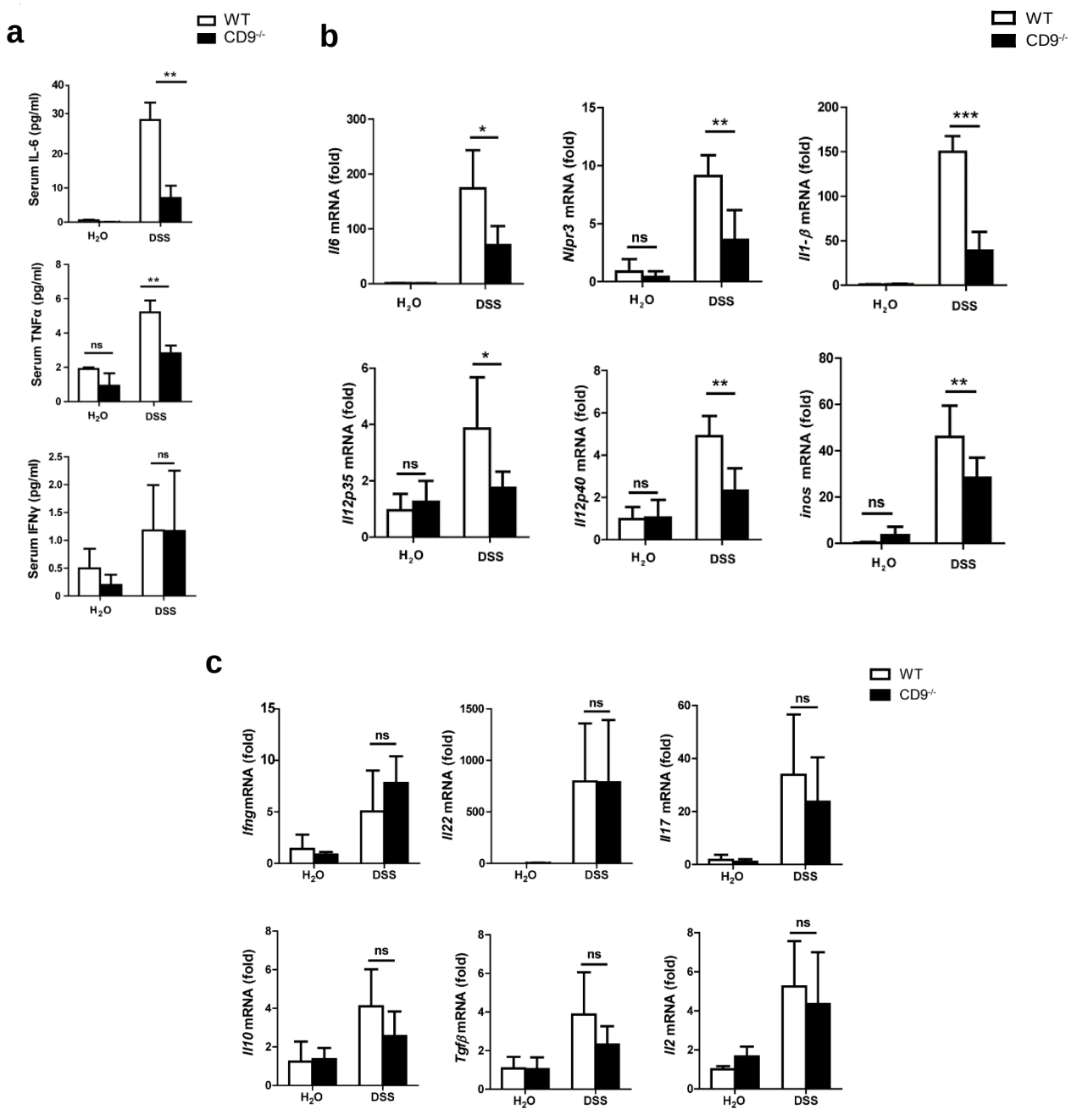

Figure 5.7. CD9$^{-/-}$ mice display decreased proinflammatory cytokines in serum and colon after 2% DSS administration. **(a)** Serum levels of TNFα, IL-6, and IFNγ **(b,c)** qPCR analysis of colonic proinflammatory cytokine mRNA expression. Bars denote the mean ± SD of *n* = 4–5 mice per genotype. Data were analyzed by two-way ANOVA and the Bonferroni multiple comparison test.

5.4. CD9$^{-/-}$ bone marrow cells transplanted into WT mice do not provide protection against colonic injury

As tetraspanin CD9 is expressed in leukocytes, but also in non-hematopoietic cells like endothelial and epithelial cells, we next investigated in each compartment the possible implication of the absence of CD9 in mediating colitis protection. For that, two groups of chimeric mice were generated using the CD45.1 and CD45.2 haplotypes. Reconstitution experiments were carried out with WT CD45.1 mice and CD9$^{-/-}$ or WT CD45.2 mice, with irradiation and transplantation in either direction. Reconstitution levels were checked by flow cytometry of the blood cell populations, showing levels of 95 to 99 percent **(Figure 5.10a**). Moreover, CD9 expression was checked. Between 34 to 40 percent of blood cells were positive for CD9 in the corresponding groups in which donor WT mice were used, and negative in the group were donor CD9$^{-/-}$ mice were employed (**Figure 5.10b**).

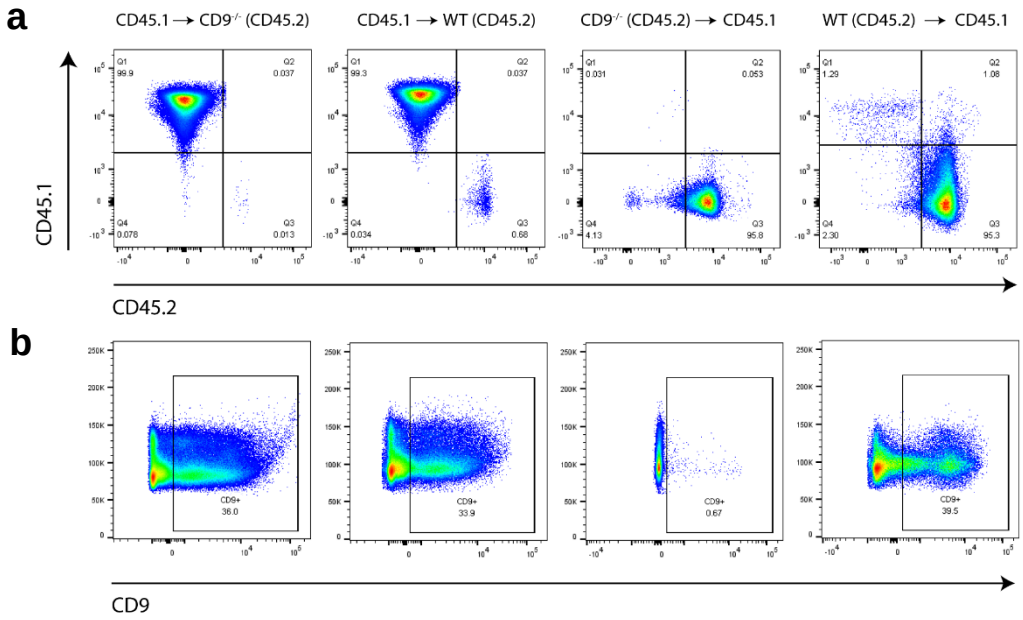

Figure 5.8. FACS analysis of chimeric mice blood samples. (a) CD45 haplotypes were used to discriminate between donor and receptor mice cell populations. **(b)** Confirmation of CD9 expression or abscence in the donor compartment.

After checking reconstitution levels, chimeric mice were administered with 2% DSS for 6 days. Protection against DSS-induced colitis was observed only when irradiated CD9$^{-/-}$ mice were used as recipients of WT bone marrow, as these mice display reduced weight loss (**Figure 5.11a**), DAI scores (**Figure 5.11b**), and colon shortening than their chimeric counterparts (**Figure 5.11c**). Histology revealed typical DSS-induced changes in the distal and proximal colon of WT recipients and less pronounced alterations in CD9$^{-/-}$ recipients reconstituted with CD45.1 WT bone marrow (**Figure 5.12a and b**).

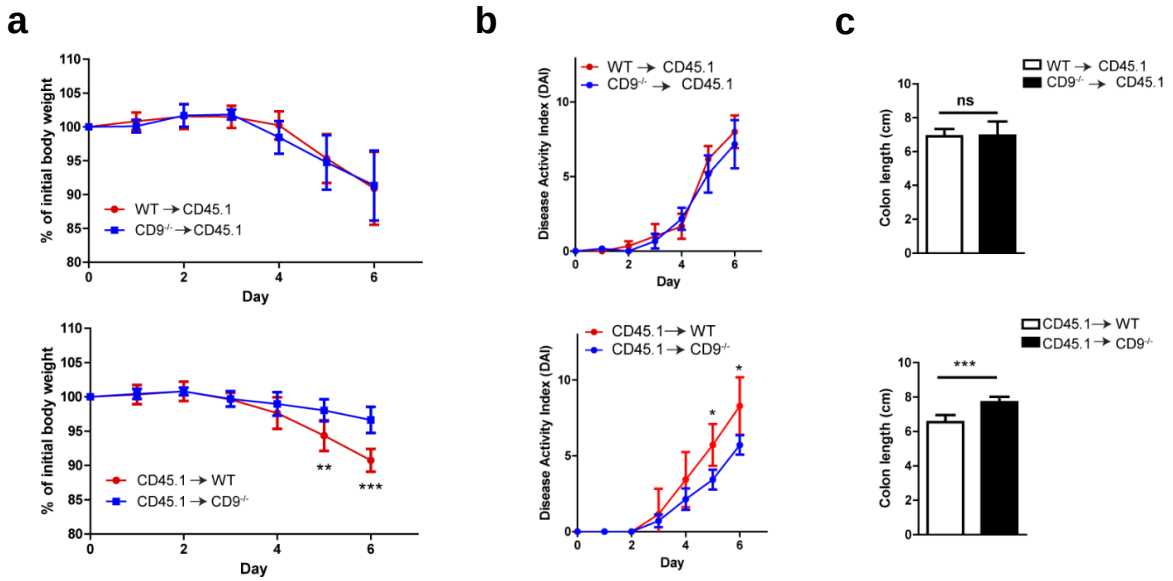

Figure 5.9. **Lack of CD9 in the resident non-hematopoietic compartment confers the reduced susceptibility to DSS-mediated colitis.** Lethally irradiated WT CD45.1 mice were rescued with WT or CD9$^{-/-}$ CD45.2 bone marrow, whereas lethally irradiated WT and CD9$^{-/-}$ CD45.2 mice were rescued with WT CD45.1 bone marrow. Three months post-transplantation mice were treated with 2% DSS. **(a)** Body weight evolution, **(b)** disease activity index and **(c)** colon shortening. Representative experiment repeated twice, n = 6–7 per group. All between-group comparisons were analyzed by unpaired t-test; *P < 0.05; **P < 0.005; ***P < 0.001.

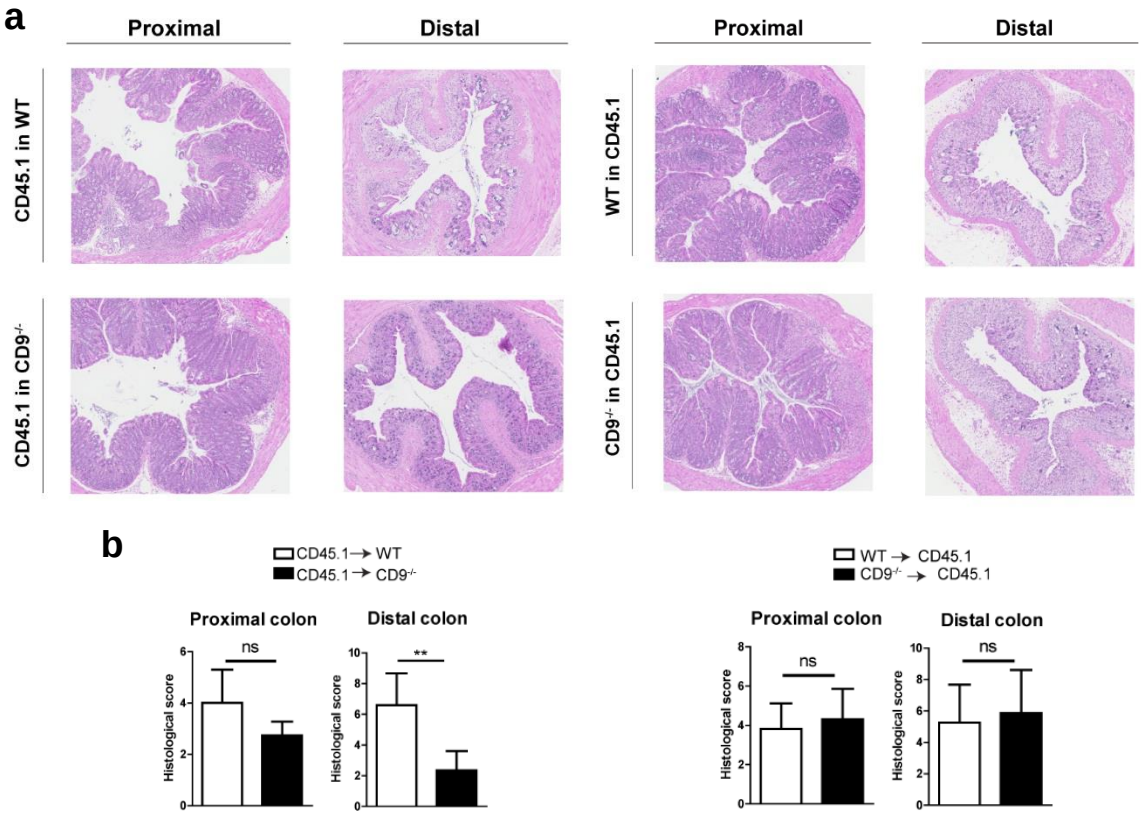

Figure 5.10. Reduced histological damage in chimeric CD9$^{-/-}$ recipients after DSS treatment. (a) H&E stained proximal and distal colon sections. **(b)** Histological injury scores. Representative experiment repeated twice, n = 6–7 per group. Data were analyzed by unpaired t-test; ns = non-significant, **P < 0.005.

CD9$^{-/-}$ recipients had lower DSS-induced levels of serum IL-6 measured by ELISA (**Figure 5.13a**), and colon samples from CD9$^{-/-}$ recipients also had lower induced transcript expression of proinflammatory cytokines IL-6, TNF-α, IL-1β, IL12p35 and IL12p40, and inflammatory mediators such as NLPR3 measured by qPCR (**Figure 5.13b**). These results underscore the conclusion that susceptibility to DSS-induced colitis is increased by CD9 expression in the non-hematopoietic compartment.

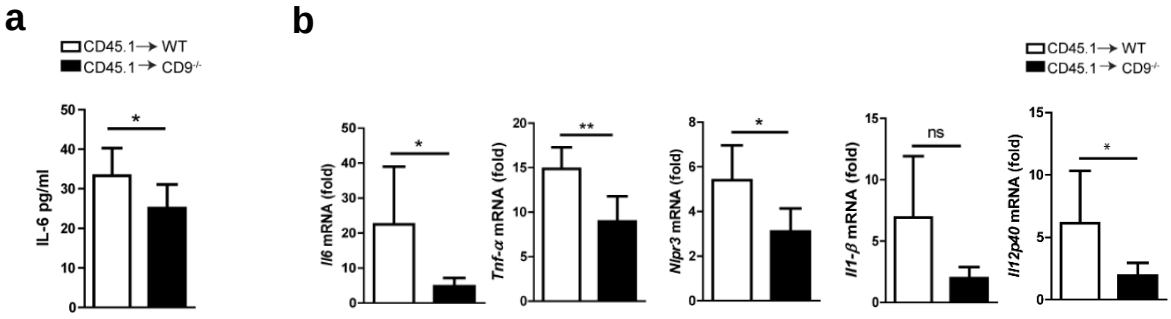

Figure 5.11. CD9$^{-/-}$ recipients display a reduced proinflammatory status upon DSS challenge (a) Serum IL-6 measured by ELISA. **(b)** qPCR analysis of proinflammatory cytokine expression in the colon of WT or CD9$^{-/-}$ CD45.2 recipients. Experiments were perfomed twice, giving similar results. *n* = 6–7 per group. Data were analyzed by unpaired t-test; ns = non-significant. **P* < 0.05; ***P* < 0.005.

The main two non-hematopoietic compartments are endothelial and epithelial cells. Thus, we wonder how CD9 expression levels behave during the advance of DSS treatment in these two cell types. CD9 membrane expression increases in endothelial cells (CD31^{+}) since day 3 of treatment and sustains until day 6 (**Figure 5.14a**). On the contrary, in epithelial cells (EpCAM^{+}), a drop in CD9 membrane levels is detected at the end of the treatment on day 6 (**Figure 5.14b**). Of note, CD9 expression levels are higher at all-time points in endothelial cells than in epithelial cells.

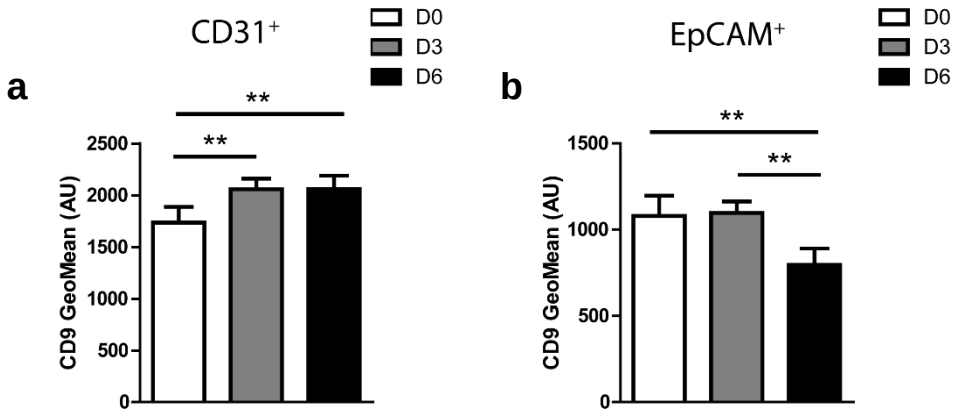

Figure 5.12. FACS analysis of CD9 expression levels in the resident compartment in colon tissue at days 0 (D0), 3 (D3) and 6 (D6) of DSS treatment. (a) Geometric mean (GeoMean) levels of membrane CD9 in live endothelial cells gated as CD45^{-} CD31^{+} and in **(b)** live epithelial cells gated as CD45^{-} EpCAM^{+}. AU: arbitrary units. Experiments were perfomed three times, giving similar results. Bars denote the mean ± SD of *n* = 5 mice per genotype. Data were analyzed by one-way ANOVA and the Newman-Keuls multiple comparison test.

5.5. CD9 expression does not sensitize IECs to DSS-induced apoptosis

To investigate the molecular mechanism underlying the protective effect of CD9 loss on DSS-induced colitis, we determined the apoptotic levels in WT and CD9$^{-/-}$ recipient mice IECs after DSS treatment. For that, we analyse the levels of active caspase-3, a biochemical marker of apoptosis. Caspase-3 staining showed that both WT and CD9$^{-/-}$ mice epithelia had very low levels of apoptosis, and no differences were found between both groups of mice (**Figure 5.15a and b**).

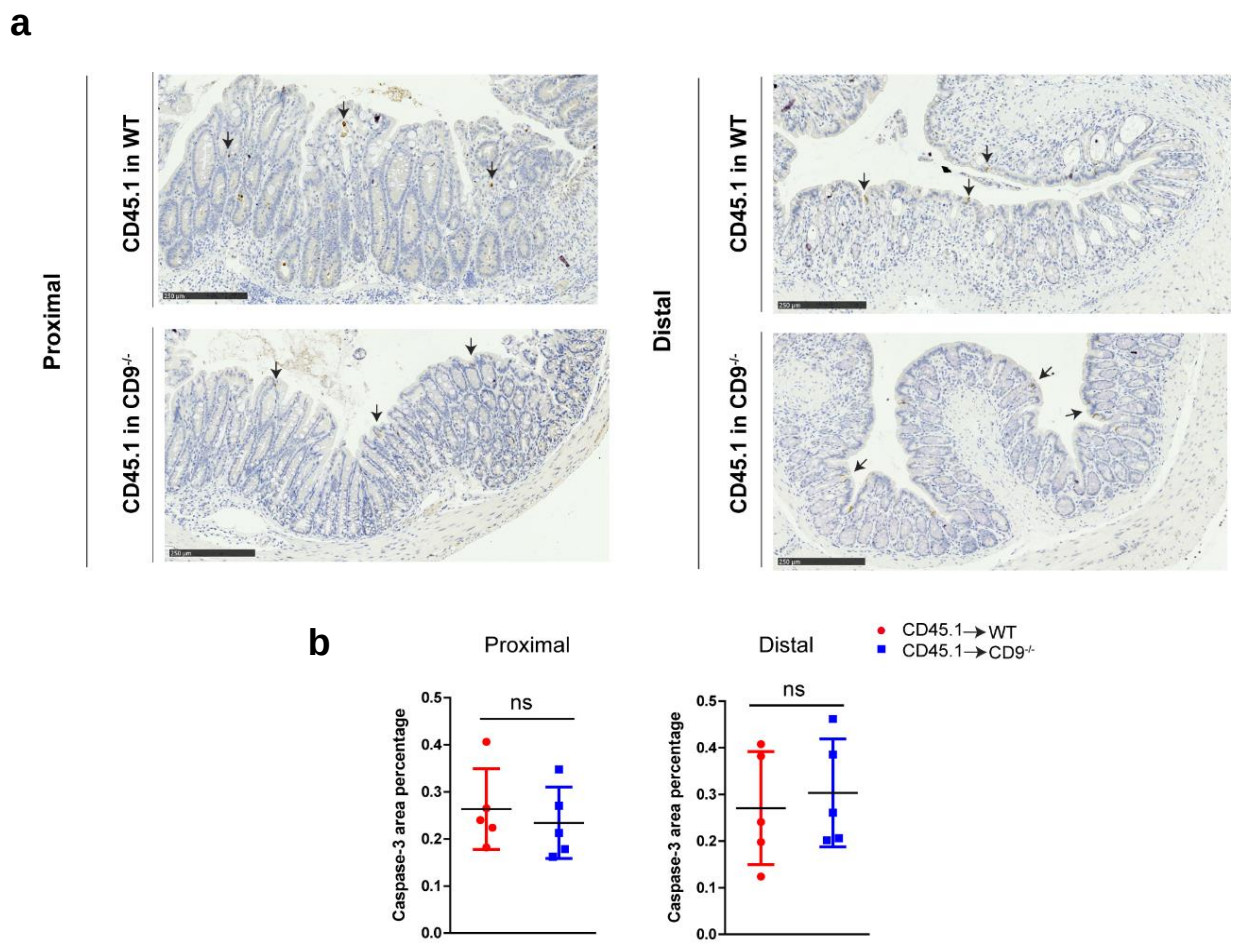

Figure 5.13. **Apoptosis analysis after DSS exposure in chimeric mice show no differences between WT and CD9$^{-/-}$ recipients. (a)** Representative activated caspase-3 immunohistochemistry staining images (10x) after 6 days of 2% DSS treatment. Positive cells are pointed by arrows. **(b)** Quantification of activated caspase-3 staining (*n*=5 mice per genotype). Each dot corresponds to the percentage of positive area relative to the total epithelial layer. Between group comparisons were analyzed by unpaired t-test. ns, non significant.

5.6. Enhanced colonocyte proliferation after DSS-induced injury in CD9$^{-/-}$ mice

We next investigated proliferative capacity of IECs in the presence or absence of CD9. After DSS-induced epithelial cell damage, the colonic epithelium actively proliferates to restore intestinal barrier integrity. Flow cytometry analysis of the proliferation marker Ki67 in colonic EpCAM^{+} intestinal epithelial cells (IECs) from mice revealed that CD9 deficiency supports elevated colonic epithelial cell proliferation after DSS exposure (**Figure 5.16a**). Remarkably, although the percentage of Ki67^{+} cells was slightly higher in CD9$^{-/-}$

colon after 2 and 4 days of DSS exposure, the significant difference was observed at day 6. This is coincident with significant lower body weight loss (**Figure 5.16b**) and higher colon length in CD9$^{-/-}$ mice (**Figure 5.16c**).

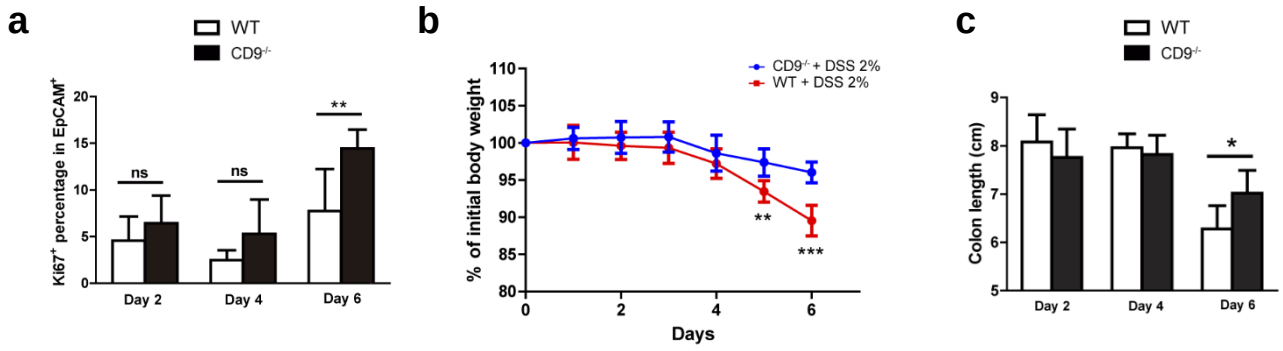

Figure 5.14. CD9 limits epithelial cell proliferation upon dextran sodium sulfate (DSS) challenge. **(a)** FACS analysis of Ki67^{+} cells in the EpCAM^{+}CD45^{-} gated population after days 2, 4, and 6 days 2% DSS exposure. **(b)** Body weight loss and **(c)** colon shortening, n = 5–6 mice per group. Between-group comparisons were analyzed by unpaired t-test; *P < 0.05; **P < 0.005; ***P < 0.001.

Moreover, CD9$^{-/-}$ colon showed higher mRNA expression of the cell cycle genes c-myb, cyclin D1 and c-fos (**Figure 5.17**), which supports an enhanced proliferation in the absence of CD9.

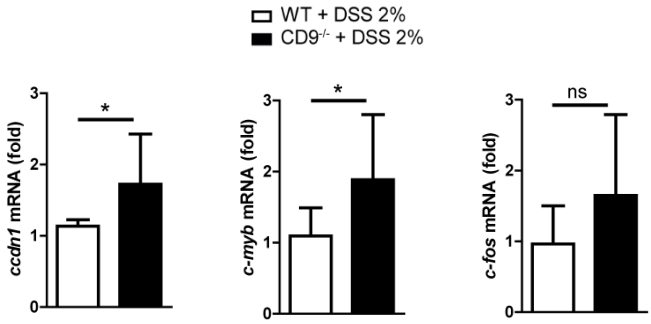

Figure 5.15. CD9$^{-/-}$ colon expresses higher levels of cell cycle genes mRNA after DSS-induced damage. qPCR analysis of colonic mRNA expression of the cell-cycle genes, *ccdn1*, *c-myb* and *c-fos*. Data are pooled from two independent experiments, n = 4-6 mice per group. Data were analyzed by unpaired t-test; ns = non-significant. *P < 0.05.

Proliferation in DSS-exposed colon of mouse chimeras was determined by counting immunostained Ki67^{+} cells in colon crypts on histological sections (**Figure 5.18a**). The percentage of Ki67^{+} colonic cells was higher after DSS exposure in CD9$^{-/-}$ recipients than in WT recipients (**Figure 5.18b**). Taken together, these results demonstrate that CD9 limits epithelial cell proliferation in response to injury.

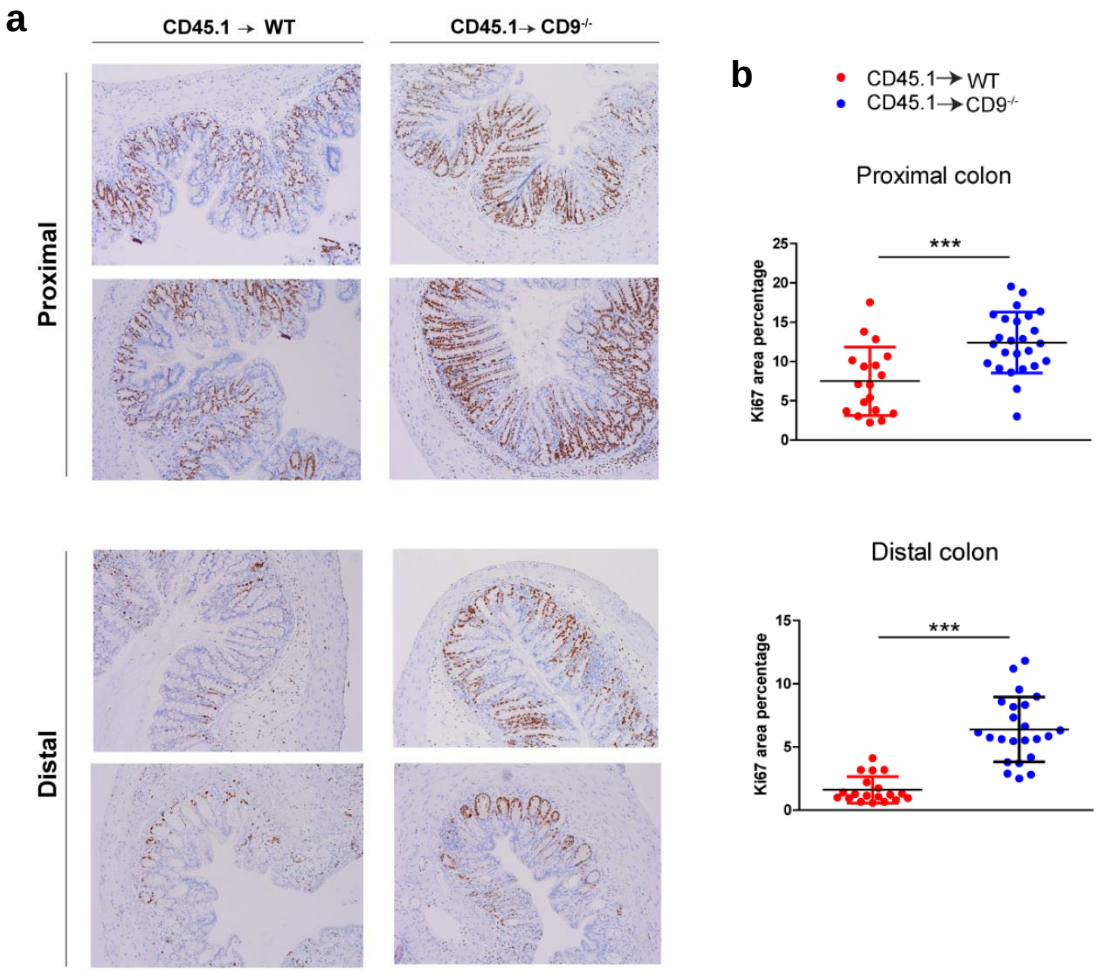

Figure 5.16. CD9$^{-/-}$ IECs proliferate more than WT IECs after DSS exposure. (a) Ki67 immunohistochemical staining on proximal and distal colon sections from 6-day DSS-treated chimeric mice. Two independent 10X images are shown per section. **(b)** Quantification of Ki67^{+} cells in the epithelial layer of colons from 6-day DSS-fed chimeric mice. Each dot corresponds to one analyzed image; 5-6 images were analyzed per mouse, *n*=5 mice per genotype. All between-group comparisons were analyzed by unpaired t-test;

Due to the described interaction of CD9 with EpCAM [498], we analyzed membrane expression levels of this molecule in IECs upon DSS damage. However, no differences were detected, and EpCAM decreases after 4 and 6 days of DSS treatment in WT and CD9$^{-/-}$ mice colon epithelial cells (**Figure 5.19**).

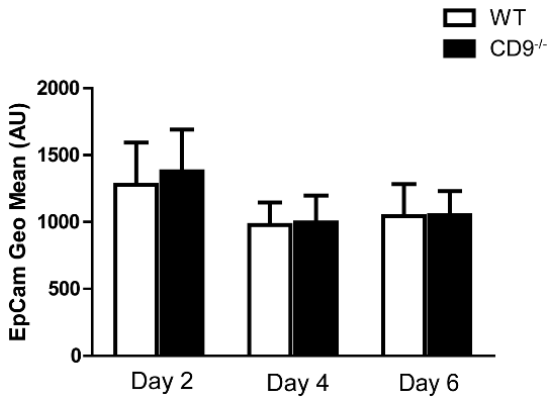

Figure 5.17. IECs EpCAM levels do not differ between CD9$^{-/-}$ and WT mice. Mice were administered a 2% DSS solution and EpCAM membrane expression levels in colon IECs were analyzed by flow cytometry. A marked reduction is observed at days 4 and 6 of DSS exposure compared to day 2 in both groups of mice. Bars denote the mean ± SD of *n* = 5-6 mice per genotype. Geo Mean: geometric mean; AU: arbitrary units.

5.7. Differential microbiota is not the cause of the decreased DSS susceptibility in CD9$^{-/-}$mice

Due to the known relevance that differences in mice microbiota composition might exert in DSS susceptibility, cohousing experiments were performed in which the mice were caged together for several weeks in order to share their microbiota constituents. However, cohoused WT and CD9$^{-/-}$ mice display the same susceptibility to DSS as their non-cohoused counterparts showing similar weight loss (**Figure 5.18a**), colon shortening (**Figure 5.18b**) and neutrophils and macrophages infiltration into the colon (**Figure 5.18c**). Thus, this result discards a possible role of a differential microbiota in the protection detected in CD9$^{-/-}$ mice.

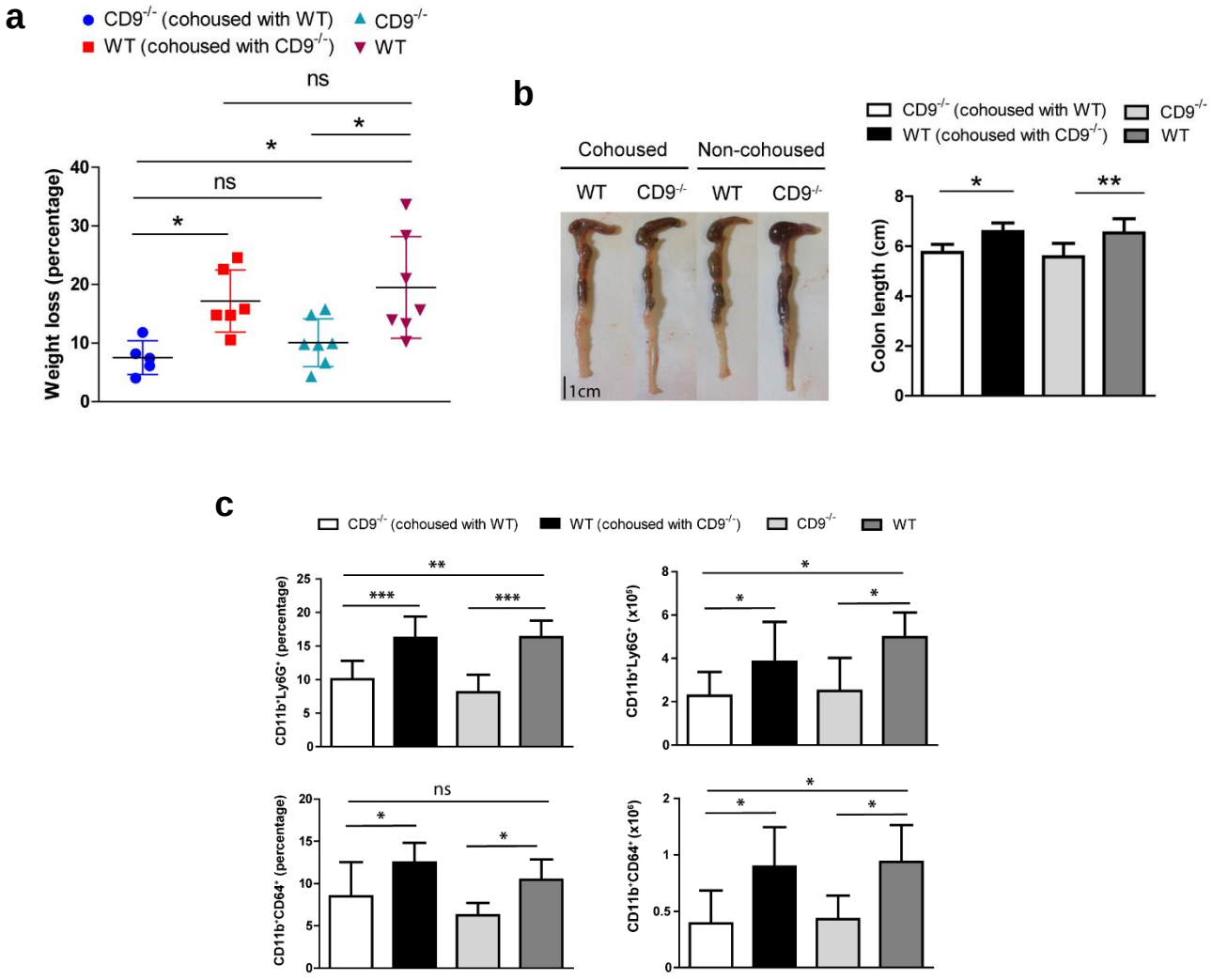

Figure 5.18. Cohoused WT and CD9$^{-/-}$ mice experience the same susceptibility to 2% DSS damage than their non-cohoused counterparts. Female CD9$^{-/-}$ and WT mice were cohoused after weaning for 8 weeks. **(a)** Body weight change. **(b)** Representative colon pictures and colon length measurements. **(c)** Quantification of neutrophils (Ly6G^{+}) and macrophages (CD64^{+}) populations gated in CD45^{+} CD11b^{+} cells in mice colon tissue. Percentage from CD45^{+} cells (left) and total numbers normalized using TruCount beads (right) are shown. Statistical analysis was performed by one-way ANOVA and the Newman–Keuls multiple comparison test. *P < 0.05; **P < 0.005; ***P < 0.001; ns = non-significant, n = 6-7 mice per group.

5.8 CD9 expressed on CD4$^+$ T cells does not contribute to immune-cell adoptive transfer-mediated colitis.

Colitis can be initiated by adoptive transfer of syngeneic splenic CD4$^+$CD62L$^+$CD25$^-$CD45RB^{hi} naïve T cells into T and B cell-deficient recipient Rag1$^{-/-}$ mice which cause a disruption in T cell homeostasis. Due to the important role of CD9 in T-lymphocytes physiology, we decided to further explore possible CD9-mediated immune mechanisms in IBD by using this alternative model of colitis through the intraperitoneal transfer into Rag1$^{-/-}$ mice of naïve T cells sorted from WT or CD9$^{-/-}$ mice. Body weight was recorded over 2 months, showing no between-group differences (**Figure 5.21a**). Colon shortening was also similar in both genotypes (**Figure 5.21b and c**). Consistent with these findings, histological inspection revealed a similar extent of transmural inflammation in injected animals (**Figure 5.21d**).

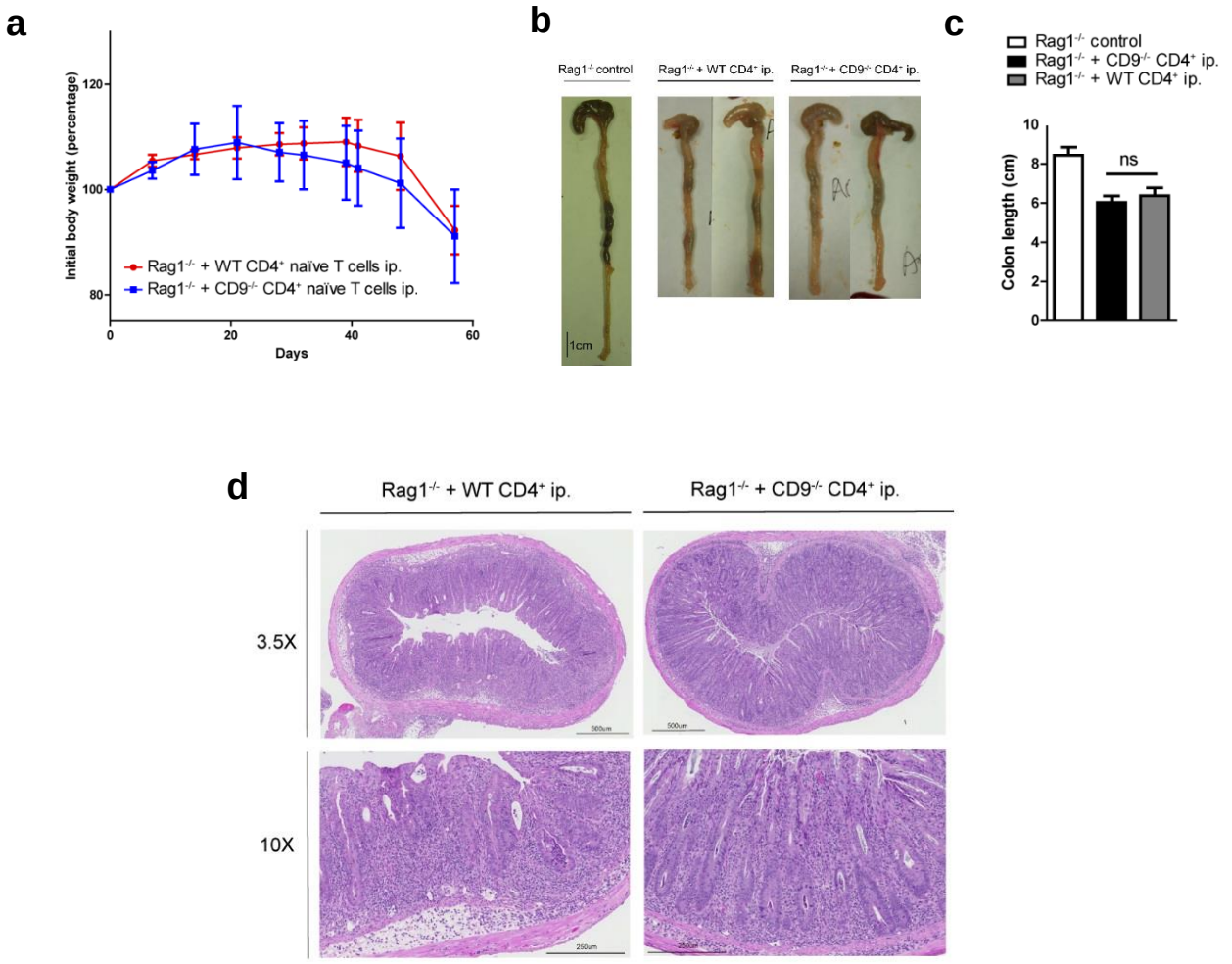

Figure 5.19. CD4$^+$ T cell-expressed CD9 does not contribute to adoptive transfer-mediated colitis. (a) Body weight after intraperitoneal adoptive transfer of CD4$^+$CD45RB^{hi} CD62L$^+$CD25$^-$ T cells from WT and CD9$^{-/-}$ donors into Rag1$^{-/-}$ recipients. **(b,c)** Colon length at sacrifice on day 57. **(d)** Representative 3.5x and 10x magnification H&E-stained colonic sections from Rag1$^{-/-}$ mice injected with WT and CD9$^{-/-}$ CD4$^+$ cells, showing transmural infiltration affecting all colon layers in both settings. Data are from a representative experiment repeated three times with similar results. *n* = 5-6 mice per group; unpaired t-test. ns, non significant.

Several weeks after the transfer, a mixed immune cellular infiltration can be detected in the mice lamina propria (**Figure 5.21d**) composed by polymorphonuclear cells, macrophages and mononuclear cells corresponding to the expanded $CD4^+$ T cell population that now became proinflammatory Th1 and Th17 cells. By flow cytometry similar increases in neutrophil and macrophage infiltration were detected independently of the expression of CD9 in $CD4^+$ T cells (**Figure 5.22a**). Additionally, restimulation of mesenteric lymph node $CD4^+$ cells with CD3/CD28 revealed no significant differences in Th1 and Th17 effector cell populations or cytokine production (**Figure 5.22b**).

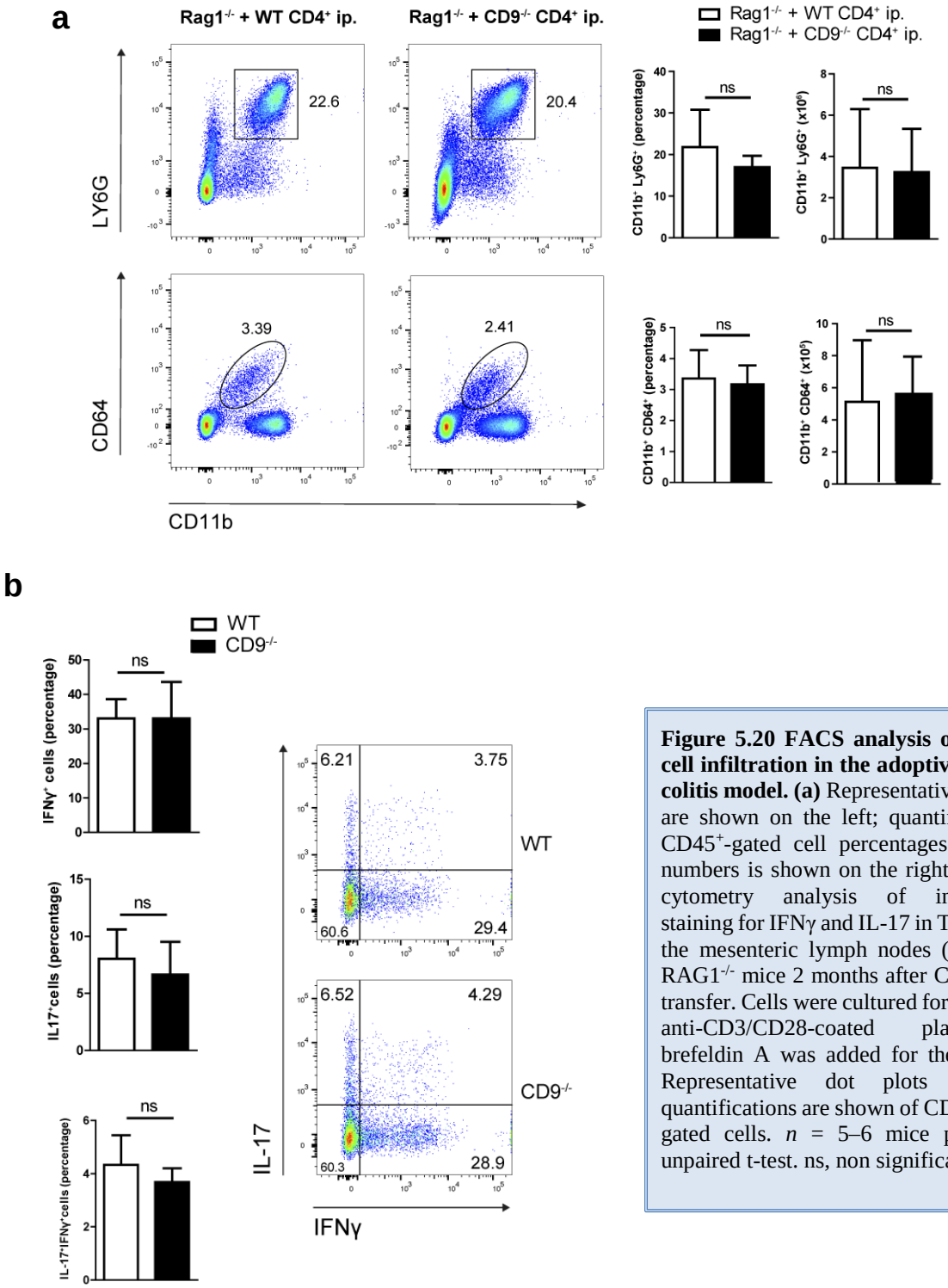

Figure 5.20 FACS analysis of myeloid cell infiltration in the adoptive transfer colitis model. (a) Representative dot plots are shown on the left; quantification of $CD45^+$-gated cell percentages and total numbers is shown on the right. **(b)** Flow cytometry analysis of intracellular staining for IFNγ and IL-17 in T cells from the mesenteric lymph nodes (MLNs) of $RAG1^{-/-}$ mice 2 months after $CD4^+$ T cell transfer. Cells were cultured for 72 h on an anti-CD3/CD28-coated plate and brefeldin A was added for the last 4 h. Representative dot plots and bar quantifications are shown of $CD4^+CD25^+$-gated cells. *n* = 5–6 mice per group; unpaired t-test. ns, non significant.

5.9 T cell differential subset skewing *in vitro* shows no differences with CD9 expression

In parallel, naïve CD4$^+$ T cells from CD9$^{-/-}$ and WT mice were skewed *in vitro* using recombinant cytokines and polyclonal stimulus to in-deep explore CD9 role in T cells. However, like in the *in vivo* model of colitis described under section 4.8, no between-genotype differences were observed in the percentages of Th1, Th17, and Treg cells (**Figure 5.23a and b**) nor cytokine production (**Figure 5.23c**).

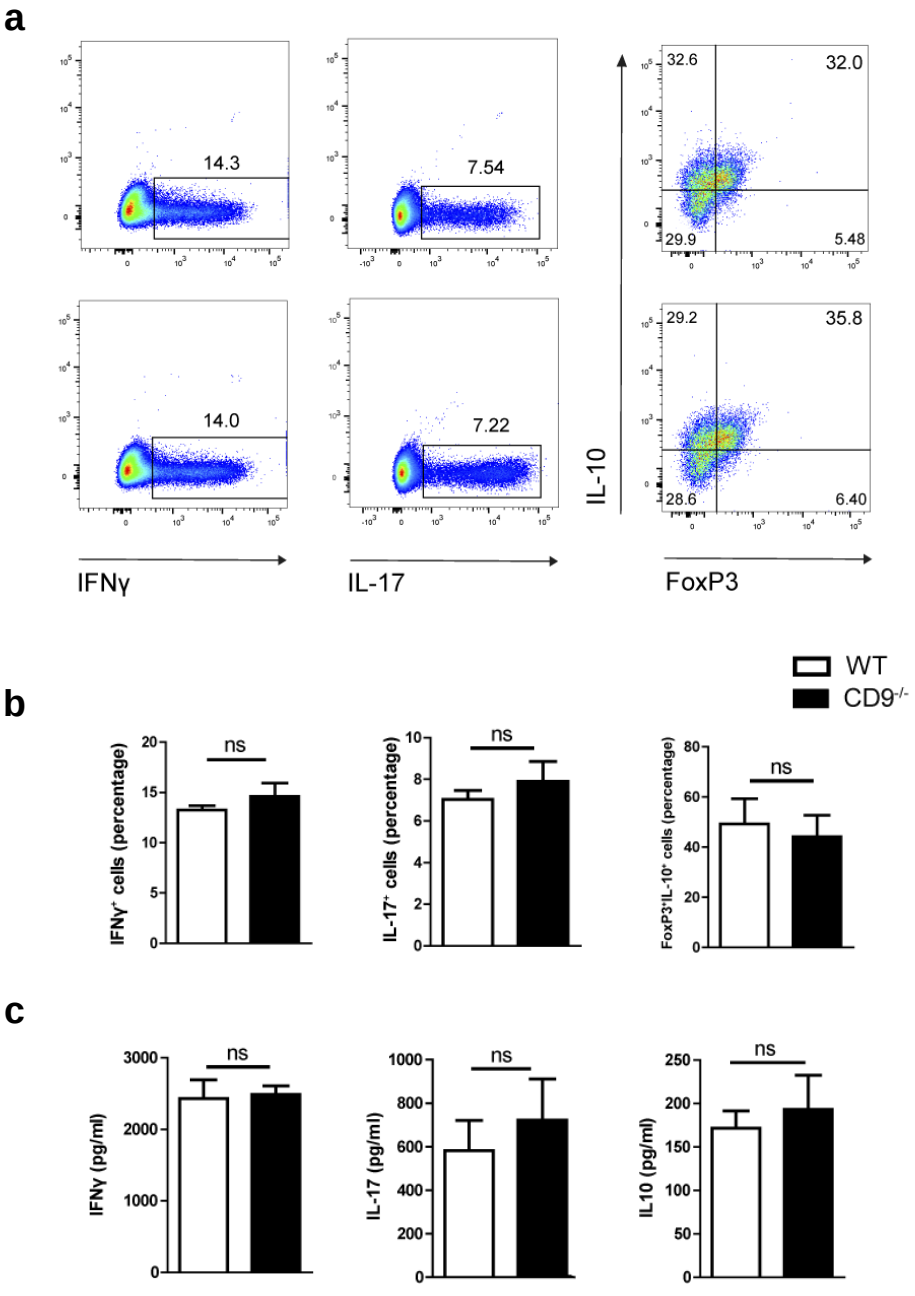

Figure 5.21. *In vitro* T cell differentiation towards Th1, Th17, and Treg CD4$^+$ T cell subsets. **(a)** Representative dots plots are shown of intracellular IFNγ, IL-17, and IL-10 in sorted populations, with quantification on **(b)**. **(c)** Cytokine release was quantified by ELISA. Data are from a representative independent experiment of three performed and are presented as mean ± SD. *n* = 5 per genotype; unpaired t-test. ns, non significant.

Discussion

5. DISCUSSION

Inflammatory bowel disease (IBD) arises through close interaction between genetics, immunology, environment, and microbiome. The development and progression of this multifactorial disorder is affected by several factors, including diet, lifestyle, and behaviour. DSS-induced colitis has become a widely used model for studying IBD in the mouse [87,401]. DSS is a chemical colitogen toxic to gut epithelial cells, interfering with intestinal barrier function and stimulating local inflammation. This model is suitable for studying events triggered by temporary failure of mucosal homeostasis after epithelial cell shedding and loss of barrier integrity, and can also provide insight into the mechanisms that lead to mucosal healing (MH) after initial injury [258]. In this thesis work we report protection against DSS-induced colonic mucosal damage in CD9-deficient ($CD9^{-/-}$) mice. These mice show lower DAI scores throughout treatment, larger colons, and have a less severe histological injury. The protection conferred by CD9 absence was confirmed by the increased survival of $CD9^{-/-}$ mice upon administration of a lethal 4% DSS dose.

5.1. CD9 and epithelial permeability

Epithelial preservation *in vivo* was demonstrated by lower colonic transepithelial FITC-dextran leakage in $CD9^{-/-}$ mice, and the importance of CD9 in the control of intestinal epithelial barrier function and integrity was further demonstrated by preserved expression of tight junction and other barrier-related genes in $CD9^{-/-}$ mice. Reduced intestinal epithelial barrier function is associated with a variety of gastrointestinal diseases, including irritable bowel syndrome (IBS) [337,67], steatohepatitis (NASH) [491] and IBD [228,14,329]. IBD patients have shown several defects in the key players of the intestinal epithelial barrier function, ranging from defensins, mucus layer components to the adhesion molecules that regulate paracellular permeability [164,478] and increased intestinal permeability has been correlated with IBD [598,610,106]. Nevertheless, it is difficult to elucidate whether the loss of barrier function is a cause or just a consequence of intestinal inflammation. Supporting the first, many genetic risk loci in IBD have been found in genes related to epithelial barrier function [256]. However, some studies report that the expression pattern of TJ proteins are unaltered in patients with inactive IBD [633], and suggest that TJ disturbances are more likely to be a consequence rather than a cause. In any case, experimental evidence using mouse models with genetic defects in tight-junction-associated proteins demonstrate that these defects usually are insufficient to cause disease in the absence of other insults [257,538,294]. This notion is supported by findings of increased permeability in a subset of unaffected first-degree relatives with CD [416,248] and in healthy mucosa of the proper IBD patients [526,527]. In mice studies, increased paracellular permeability accelerates experimental colitis and preservation of tight junction barrier function delays disease progression. In clinical practice, several studies have documented that changes in intestinal permeability can predict IBD relapse during clinical remission [610,18]. Although there are no currently available FDA-approved agents that target specifically the epithelial barrier, many promising approaches have been proposed and are being investigated. Currently, anti-TNF-α therapy is capable of reduce mucosal inflammation and restore intestinal permeability in IBD patients. In

addition, some probiotics, certain fatty acids like butyrate, or zinc element also mitigate mucosal barrier dysfunction [352]. However, further research is required before therapeutically manipulating intestinal permeability. CD9 directly interacts with tight junction protein claudin-1, which has been detected by chemical cross-linking followed by mass spectrometry analysis, and to claudins-2, 3 and 7 to a much lower extent and only detected by co-immunoprecipitation in mild detergent conditions [276]. However, CD9 stabilizes the expression of claudins when they are not in tight junctions, and concordantly, depletion of CD9 by small interfering RNA had no effect on paracellular permeability [276]. Functional experiments assessed by *in vivo* FITC-dextran leakage analysis, demonstrated that there were no differences between both genotypes in the paracelullar permeability in steady state. Thus, *a priori*, there are no epithelial barrier differences in non inflammatory conditions, that could predispose or protect beforehand one group of animals versus the other one. Conversely, great differences were observed after DSS challenge, in which $CD9^{-/-}$ mice display an enhanced barrier integrity. Apart from a direct toxic effect of DSS to colonocytes, the increase amount of proinflammatory cytokines detected in WT mice, including TNF-α and IL-1β, may also account for tight junction proteins downregulation [6,5]. Other works observed a decreased expression in ZO-1 in mice [432], and sealing claudins 3,5,7 and 8 in mice and rats [631,611] after DSS treatment, which is in concordance with our results. Of note, IBD patients also display these reductions [408,633]. Interestingly, it has been reported that tetraspanin CD9 is mainly localized at lateral cell-cell junctions in polarized epithelial cells in association with integrins, but the localization of these complexes takes place independently of the cadherin-catenin molecular system [376,619] which have been described to be necessary for the correct assembly of tight junctions [175]. Thus, CD9 regulation of intercellular epithelial cell adhesion may not influence junctional adhesions and paracellular sealing. Regarding other non-classical junction proteins, CD9 has also been described to interact with epithelial cell adhesion molecule (EpCAM) [297,498]. EpCAM is a transmembrane glycoprotein which mediates homotypic cell-cell adhesion in normal epithelia [312] but it is also considered a cancer marker because its expression is markedly increased in various carcinomas [577,564] and it has been described to participate in epithelial cell proliferation, migration, and transduction of mitogenic signals [370,369]. EpCAM inclusion in TEMs (CD9 and D6.1A) forms a complex together with a specific CD44 variant isoform (CD44v), which is required to support tumour apoptosis resistance [498]. Claudin-7 interacts with EpCAM [288] and recruits it into TEMs [395], and the complex composed of CD44, claudin-7, EpCAM, and Tspan8 promotes cancer progression while the individual molecules do not have this effect [285]. However, in relation to IBD, contradictory reports exist on the role of this molecule. On one hand, EpCAM colon tissue expression is significantly decreased in UC [157], and on the other hand, no differences are detected in neither CD nor UC and EpCAM and its diminished expression is just considered a specific marker of congenital tuft enterophaty (CTE) disorder [368]. Though it has been reported by using EpCAM-deficient mice that this molecule contributes to formation of functional tight junctions in the intestinal epithelium by recruiting claudin proteins [301], no DSS colitis, or any other experimental colitis model has been performed in EpCAM-deficient mice. In our kinetic experiment in DSS treated mice, a decreased was noticed in the levels of this molecule at days 4 and 6, in accordance with other reports [157]. However, no differences were observed between $CD9^{-/-}$ and WT mice at any time point.

5.2 CD9 and inflammatory cell recruitment

CD9 is quite ubiquitously expressed, and we therefore performed chimeric reconstitution experiments to determine which cell compartment is responsible for mediating DSS-induced toxicity. Our data clearly demonstrated that protection in $CD9^{-/-}$ animals was not dependent on the hematopoietic cell compartment. In $CD9^{-/-}$colon, crypt and villous distortion is minimal and surface epithelium is more preserved; this keeps luminal pathogens outside the lamina propria, and therefore proinflammatory cytokine and chemokine release is lower and there is less inflammatory cell recruitment. Specifically, the myeloid-derived cytokines involved in the inflammatory response in DSS acute colitis iNOs, TNF-α, IL-6, IL-12, and the inflammasome drivers NLRP3 and IL-1β were enhanced in WT mice versus $CD9^{-/-}$ mice, but no differences were observed in either IFNγ, IL-17, or IL-22 cytokines which are mainly produced by lymphoid cells. Accordingly, increased neutrophil and macrophage infiltration was observed in WT versus $CD9^{-/-}$ mice. In this regard, several studies have underscored the role that innate cells such as neutrophils and macrophages play in DSS-induced intestinal inflammation. Large neutrophil and macrophage infiltration is observed upon DSS administration, and inhibitors or promoters of these cells recruitment dampen or enhance DSS damage, respectively [261,139,617,481]. Likewise, the acute version of DSS colitis takes place also in immunodeficient SCID [116], $Rag1^{-/-}$ [259] and $Rag2^{-/-}$ [277] mice, meaning that neither T nor B cells are required for the induction of the disease. However, the role of T cells in DSS-induced colitis should not be obviated. Though comparable results were obtained at a high dose of DSS (5%), colitis progression was much more tolerable in $Rag1^{-/-}$ mice than in WT BL6 mice when a lower dose was used (1,5%), accompanied by improved symptomatic and histological parameters [259]. Moreover, multiple works report that a Treg/Th1-Th17 dysbalance worsens disease outcome in DSS-induced colitis, even in the acute version of the model [425,612,212,25,49,634,99,592]. Thus, we analysed by qPCR, apart from IFNγ, IL-17 and IL-22 the levels of IL-10, TGF-β and IL-2 in the colon of DSS-treated mice, however, no between-genotype differences were detected.

DSS colitis can be exacerbated by both granulocyte [261,91,603,378,481] and monocyte/macrophage [496,277,261,481] recruitment. After the breakdown of mucosal homeostasis provoked by DSS, neutrophils arrive to eliminate extracellular microorganisms through phagocytosis, degranulation, production of ROS, and release of DNA neutrophil extracellular traps or NETs [267]. Unfortunately, the activity of many enzymes and chemicals produced by neutrophils is not specific to pathogens, so they can damage host tissues when released extracellularly, contributing to the aggravation of mucosal inflammation. Thus, in an innate model such as DSS acute colitis, neutrophils are detrimental. However, in other colitis models such as the T cell adoptive transfer colitis model, in which disease is induced by transfer of $CD45RB^{high}$ T cells lacking regulatory T cells into T-cell-deficient $RAG\text{-}1^{-/-}$ recipients, depletion of neutrophils by a monoclonal antibody given at the time of T-cell transfer into the $RAG\text{-}1^{-/-}$ recipients resulted in greater severity of colitis and earlier death. Increased mortality was also observed when neutrophil depletion was delayed until day 14, around the time that the initial symptoms of colitis developed [282]. Interestingly, these results resemble what happens in human disease. In UC, unrestricted neutrophil activation may cause significant tissue damage that further leads to chronic pathology and the extent of neutrophil infiltration correlates with the severity of the disease [60],

whereas in CD, defective neutrophils may not be able to limit invasion by microorganisms, leading to subsequent uncontrolled inflammatory reaction. Additionally, the proinflammatory and antimicrobicidal activities of macrophages may participate in the inflammation-associated tissue damage as well. For example, in $Ccr2^{-/-}$ mice, which have a paucity of monocyte derived cells in circulation and tissues due to a failure in classical monocyte release from the bone marrow [507], or animals depleted of CCR2-expressing cells [643], there is an amelioration of DSS-driven colitic inflammation. The same happens when monocyte recruitment is impaired by $\alpha_1\beta_1$ or β_7 integrin treatments [277,496]. Importantly, though CD9 is expressed in both neutrophils and monocyte/macrophage cell populations, the reconstitution experiments ruled out a contribution to colon protection from CD9 deficiency in innate immune cells. Whether CD9 expression in leukocytes may have a role in extravasation, one may expect the opposite effect that the one observed in the $CD9^{-/-}$ DSS-treated mice, that is, $CD9^{-/-}$ cells might migrate more, based on previous reports performed in other cell types like B1 innate-like B cells, eosinophils but also in macrophages. In B1 peritoneal cells, CD9 expression diminishes upon TLR4 stimulation and allows for B1 cell egress from the peritoneum to the spleen. Experiments performed using $CD9^{-/-}$ B1 cells, corroborate the previous observation and demonstrate that a higher number of $CD9^{-/-}$ cells reached to the spleen. However this effect was not due to CD9 downregulation of surface integrins, as no differences in those were observed after anti-CD9 antibody induced-downregulation, but most likely to increased cell motility [178]. Compared with peripheral blood eosinophils, transmigrated eosinophils in allergen-challenged chambers exhibit reduced CD9 expression levels, and their adhesion properties are inhibited by antibodies against CD9 [145,146]. Furthermore, $CD9^{-/-}$ mice display an enhanced macrophage infiltration after lung intranasal administration of LPS, when compared to WT mice, due to enhanced MMP-2 and MMP-9 production and activity [543]. In this line, CD81 and CD9 double deficient mice spontaneously develop pulmonary emphysema, and also exhibit elevated numbers of alveolar macrophages and increased MMP activity [549]. Although the decreased expression of CD9 in inflammatory cells could promote their migratory capacities, the early maintenance of the epithelial barrier integrity that we observed in $CD9^{-/-}$ mice would prevent for the massive bacterial invasion to the lamina propria and, consequently, inflammatory cells recruitment. On the other hand, endothelial expression of CD9 is required for an efficient leukocyte extravasation through its regulation of the endothelial adhesive platforms (EAPs) [31]. In favour of the phenotype observed in this work, CD9 downregulation by the use of siRNA or CD9 TEMs alteration by CD9-large extracelullar loop (LEL)-glutation S-transferase (GST) peptides in human umbilical vein endothelial cells (HUVECs), interfered with ICAM-1 and VCAM-1 function and prevented lymphocyte transendothelial migration in shear flow chamber experiments *ex vivo* [31]. Indeed, blockade of these adhesion molecules have proven efficacy in acute colitis models in mice and rats [38,182,553,608,137,627]. Thus, the role of endothelial CD9 could not be completely ruled out, and additional research with endothelium-specific deletion of CD9 would be required to solve this issue.

5.3. CD9 and epithelial proliferation and apoptosis

Flow cytometry and immunohistochemistry analysis revealed a higher percentage of Ki67 IECs in DSS-exposed $CD9^{-/-}$ colon. In the distal colon, the percentage $Ki67^{+}$ cells is lower than in the proximal colon which likely reflects the more severe colitis in the middle and distal third of the colon described for DSS-exposed mice [419]. Though DSS may also induce some damage in the small intestine [624], it is mostly confined to the large intestine, and mainly the distal part of it, where an enormous number of microorganisms live [97]. On the other hand, DSS toxicity provokes a decreased proliferation in the first days of treatment (days 2-4) followed by an increase in proliferation generated as a regenerative response aimed to restore the epithelial barrier (days 6-8) [379,456]. Notably, the difference in proliferation among WT and $CD9^{-/-}$ mice was observed after 6 days of DSS exposure, suggesting that it is related to mechanisms of post-injury epithelial recovery. Several other works exemplify how augmenting epithelial cell proliferation leads to DSS-induced colitis protection. Some of the mechanisms involve growth factors [102,512,351,604,338,130], cytokines such as IL-22 [423] or IL-18 [399], TLR signaling [211,56,450,156], NLRP3 inflammasome [632], focal adhesion kinase (FAK) activation [412], cell cycle transcription factors such as KLF5 [343], or the NF-κB pathway in epithelial cells [396,127]. After DSS treatment, the intestinal epithelium undergoes a wound healing process. First, IECs rapidly cover the denudated ulcers by a process known as epithelial restitution, that is independent of proliferation but induces it afterwards to recover the pool of enterocytes [220]. The exposure of the Toll-like receptors of the basolateral surface of the IEC triggers proliferation that contributes to mucosal repair after injury and mice with gene deletions affecting TLR signaling such as $Tlr2^{-/-}$, $Tlr4^{-/-}$ and $Myd88^{-/-}$ mice exhibit exacerbation of DSS colitis [71,156,450]. It has been described that CD9 sequesters CD14 from lipid rafts, preventing the formation of the LPS receptor complex. Thereby, in the absence of CD9, TLR4 signaling after LPS triggering is enhanced [543]. Thus, the enhanced proliferation observed in the CD9 deficient mice may be promoted by increased TLR4 signaling in IECs. Besides, and also interconnected with TLR signaling [211,56], activation of EGFR has been shown to be necessary to maintain intestinal homeostasis in the setting of acute mucosal damage [428,36]. EGFR signaling has been described to be of particular relevance in IBD, where it has been observed a decrease in the signaling by this receptor [400,206,21,7]. Importantly, EGF was effective in a double-blind clinical trial in UC [517]. Supporting this notion, numerous studies in mice have demonstrated a protective role of EGFR in intestinal inflammation. Mice with impaired EGFR activity [123,128] or devoid of the EGFR ligand TGF-α [130] are more susceptible to experimental colitis, whereas mice overexpressing TGF-α [129] or rats treated with exogenous EGF [440] are resistant. Moreover, probiotic bacteria-derived soluble protein p40, from *Lactobacillus rhamnosus* GG, ameliorates DSS colitis in mice by an EGFR- and Akt-dependent mechanism [615]. In this setting, CD9 could be playing several roles. EGFR signaling is increased in CD9-deficient cell lines [374,552,589]. On one hand, expression of CD9 specifically attenuates EGFR signalling through the downregulation of surface expression of the receptor by dynamin-2 mediated endocytosis [552]. However, other reports claim that CD9 decreases the phosphorylation of EGFR at tyrosines Y1173 and Y1086 and attenuates EGFR induced PI3K/Akt and MAPK/Erk signaling and proliferation, but without affecting EGFR expression levels at the cell surface [589]. Nonetheless, regardless

the mechanism, all the reports coincide in the antiproliferative effects of CD9 through EGFR signaling dampening. In the intestinal mucosa, there are several members of the family of EGF-related growth factors that can activate EGFR signalling and many of them such as TGF-α, HB-EGF, amphiregulin (AR) and epiregulin (EPR) are released after tumour necrosis factor α-converting enzyme (TACE/ADAM17) shedding [375,542,475]. Accordingly, ADAM17$^{-/-}$ [512] or TLR4$^{-/-}$ [450,156] mice display an increased susceptibility to DSS-induce colitis, due to reduced EGFR ligands generation and decrease IECs proliferation. In this regard, CD9 has been described to negatively regulate ADAM17 [176] and thereby, in CD9$^{-/-}$ IECs, an increase activity of this metalloproteinase would entail an increase in EGFR ligands release. Moreover, EpCAM extracellular and intracellular domains are sequentially cleaved by ADAM17 and presenilin-2 (PSEN2), respectively [328]. The released intracellular EpCAM domain interacts with the transcriptional regulators FHL2, β-catenin and Lef-1 to form a nuclear complex that stimulates transcription of proliferative and oncogenic genes including c-Myc and cyclins [328,370]. However, increased ADAM17 cleavage of EpCAM in these reports entails reduced levels of EpCAM surface expression, and in CD9$^{-/-}$ mice no differences were observed in EpCAM levels measured by flow cytometry (geo mean levels). Thus, the increment in proliferation detected in CD9$^{-/-}$ mice might not be explained by this mechanism. Other regenerative mediators such as TGF-β, IL-22 and IL-10 have been measured in mice colon, but no differences were observed compared with WT mice.

On the other hand, CD9 absence does not increase IEC proliferation per se and only supports MH after injury. Indeed, dysplasia was not observed in any healthy CD9$^{-/-}$ animal nor after DSS exposure. However, this model is acute and very short in time, so to accurately evaluate if CD9 deficiency could lead to tumour progression after damage, a longer experiment should be performed like the chronic version of the DSS model where the animals are given repeated cycles of the chemical interspersed with water intake [286,402]. Additionally, an inducible mouse model of colon carcinogenesis through the use of the mutagenic agent azoxymethane (AOM), alone or combined with DSS, could be use to explore CD9 pro-neoplastic role [381]. The absence of CD9 have been extensively studied in gastrointestinal cancers, where its reduced expression is associated with a poor prognosis and entails an increased risk of metastasis [363,66,373]. The amount of CD9 is inversely correlated to the lymph node status in gastric cancers and in esophageal squamous cell carcinomas [372,570]. Moreover, the reduced CD9 expression is related to a poor prognosis in patients with pancreatic cancers [513]. On the contrary, there is only one report that claims that CD9 expression promotes cancerous cell proliferation and consequent metastasis generation due to the enhanced mitogenic activity of HB–EGF [205]. Thus, clarifying the consequences of CD9 depletion in mouse models *in vivo* would be critical before developing an anti-CD9 therapy for the treatment of IBD.

Besides a direct control of proliferation, CD9 might regulate epithelial restitution. CD9 absence could be favouring the rapid reseal of the intestinal epithelial barrier and promote IECs migration through several mechanisms. CD9 deficiency leads to impaired localization of talin1 to focal adhesions [434] and decreases both stress fiber formation and integrin clustering [162,494], which correlates with increased motility. Accordingly, increased integrin-mediated affinity between the enterocyte and the underlying ECM may impair epithelial restitution [448]. Moreover, lack of CD9 in IECs might increase p-EGFR induced restitution (apart

from proliferation) through p38 MAPK signalling [151]. In addition, CD9 expression has been demonstrated to downregulate pro-migratory Wnt5a and its target genes, which modulate cell adhesion and motility. Thus, in the absence of the tetraspanin, an increased cell motility through this mechanism could be plausible. Finally, CD9 regulates actin cytoskeleton rearrangements through its interaction with EWI-2 [532,93,477]. EWI-2 inhibits cell migration on both fibronectin and laminin [637] and contributes to CD9-dependent inhibition of gliobastoma cells migration [268]. In this sense, the absence of the tetraspanin might enhance the migratory capabilities of the cell.

A tight balance between proliferation and apoptosis is crucial for homeostasis maintenance in the gut [111,380]. The development of many infectious and immune-mediated diseases, such as gastritis, coeliac disease and IBD, may be triggered by the prevalence of pro-apoptotic signals [451,413,365], whereas prolonged cell survival, due to apoptosis inhibition, may give rise to neoplastic clones [349]. In IBD, high levels of apoptosis in the epithelium have been reported in both UC and CD [529,113,226,179], but the precise nature and role of IECs death in the pathogenesis of IBD has not been elucidated to date. Whether a causative relationship exists or it is secondary to the chronic inflammatory state of these patients, is not certainly known [47]. Regarding DSS mice colitis model, the exact mechanism of epithelial damage is unknown, but an increment in apoptosis [16,585] and necrosis [97,167] is detected upon administration of the chemical. Moreover, augmented levels of apoptosis due to cell-intrinsic defects [90,445,452] or provoked by pro-inflammatory cytokines [602,613] exacerbates the disease. Though the foregoing works report an exacerbation of DSS-induced colitis in the case of increased apoptotic levels, there are some others which describe a protection of mice with reduced apoptotic levels [630,551,599]. On the other hand, CD9 ligation with the activating antibody ALB6 in a gastric cancer line (MKN-28), induces apoptosis through the specific activation of c-Jun N-terminal kinase/stress-activated protein kinase (JNK/SAPK) and p38 mitogen-activated protein kinase (MAPK) pathway, as well as caspase-3 and the p46 Shc isoform [371]. Thus, we analyse the levels of cleaved caspase-3 in the epithelial layer of chimeric mice, but found no differences between $CD9^{-/-}$ and WT epithelium, ruling out a possible implication of this mechanism in the protection of $CD9^{-/-}$ mice upon DSS exposure.

Several reports support a role for the microbiota in DSS-induced experimental colitis. Interestingly, not only microbiota composition can shift upon DSS treatment [180,401] but initial gut microbiota structure might affect DSS sensitivity and some bacterial species can reduce DSS susceptibility or increase it [305,61]. Cage sharing (cohousing) of mice reduces natural microbiota variation via coprophagy and direct animal to animal contact, and is now a widely accepted method for normalising microbiota communities before trial treatments being applied [362]. Therefore, as $CD9^{-/-}$ and WT mice lines were carried out in a separate way due to the inability to work with littermates, cohousing of $CD9^{-/-}$ and WT mice was performed for several weeks and then DSS treatment susceptibility was evaluated. However, no differences were observed between both genotypes, meaning that an intrinsic but not an environmental component was the responsible for the differences detected among both groups of mice.

5.4. CD9 and T cells

CD9 plays an important role in T cell activation. T cell co-stimulation by engagement of CD9 with monoclonal antibodies was as potent as that induced by engagement of CD28 [547]. Interestingly, the tetraspanin triggers T cell co-stimulation by a different pathway from CD28 and NF-kB [642], though both co-stimulatory molecules can work synergistically. The combination of anti-CD9 and anti-CD28 co-stimulation, induced the production of higher levels of IL-2 and IFN-γ accompanied by higher proliferative rates compared with the individual co-stimulation by engaging separately only one of the molecules [561]. Other groups confirmed this observation and detected higher levels of IL-2 production in Jurkatt T cells after anti-CD9 engagement [289]. Unlike the effects of CD28, which suppresses apoptosis and promotes cell proliferation, CD9 crosslinking promotes apoptosis after T cell activation and fails to sustain a T cell proliferative response [414,622,546]. These actions might be due to CD9 interaction with CD3 itself and other co-stimulatory molecules like CD4, CD5, CD2, CD29 (β1 integrin) and CD44 [562]. For instance, CD9 co-stimulatory capabilities have been linked to the co-localisation of this tetraspanin with lipid rafts [621]. Moreover, downregulation of CD9 by shRNA in primary T lymphoblasts entail a marked reduction in T cell activation and IL-2 secretion due to impaired β1 integrin recruitment to the immune synapse [461]. However, despite all these works document a role for CD9 in T cell biology, no in depth analysis of the $CD9^{-/-}$ mice immune system has been performed. There is only one work regarding B cell responses where CD9 absence does not affect neither B cell development nor B cell response to immunization [69]. Naïve T cell proliferation is the first step after the efficient interaction of the TCR and CD4 co-receptor to the antigen-MHCII complex exposed by professional antigen presenting cells (APCs). Subsequent microenvironmental cues involving the cytokine milieu together with antigen dose (strength and/or duration of TCR signalling) and costimulatory molecules further drive T cell differentiation into specific effector T cells [322]. For instance, IL-2 production, which is markedly decreased in CD9-downregulated T cells or strongly increased after anti-CD9 engagement, has been described to be involved in promoting the differentiation of Th1 [510,307] and Th2 cells [308,89], while inhibiting Th17 [295] and T follicular helper (Tfh) cell [26] development, though promoting Th17 cell expansion once cells develop [8]. Moreover, IL-2 is crucial for Treg homeostasis and suppressive activity [492]. On the other hand, deficiency of the co-stimulatory molecules CD28, which works synergistically with CD9 [561], or CD5, to which CD9 binds more strongly [562], provoke alterations in effector T cell generation. CD28 deficiency entails impaired Th2 [260] and Treg responses [635,4]. $CD5^{-/-}$ mice display increased numbers of $CD4^{+}CD25^{+}FoxP3^{+}$ thymocytes and peripheral natural Tregs, and reduced Th17 cell expansion. Moreover, CD5 co-stimulation induces Th17 development by promoting the expression of the interleukin IL-23R and sustained STAT3 activation [545]. Thus, due to the potential influence that CD9 might exert in the foregoing events during T cell responses, we decided to explore whether CD9 deficiency had any transcendence in T cell differentiation and expansion *in vitro* and *in vivo*. However, we did not detect any differences between $CD9^{-/-}$ and WT $CD4^{+}$ T cells neither in polyclonal differentiation experiments nor in the adoptive transfer colitis model, which is mediated by a strong Th1/Th17 expansion [258]. On the other hand, it has been recently demonstrated in our group an impairment in the T cell stimulatory capacity of $CD9^{-/-}$

monocyte-derived DCs (moDCs), but not conventional DCs (cDCs), due to compromised MHC-II targeting to the plasma membrane [462]. During intestinal inflammation, $Ly6C^{hi}$ monocytes give rise to migratory antigen-presenting cells which can induce $CD4^+$ T cell activation at day 7 of DSS-induced colitis [643]. In accordance, other reports describe how the same $Ly6^{hi}$ monocyte precursor can give rise to anti-inflammatory macrophages in homeostasis but inflammatory dendritic cells during colitis development [24,460]. However, chimeric mice with WT or $CD9^{-/-}$ DCs in CD45.1 WT recipients, behave the same way upon DSS exposure. Nonetheless, to further evaluate the role of CD9 in antigen presentation by colitic DCs, other experimental approaches such as DSS chronic colitis or injecting CD9-deficient DCs along with $CD4^+$ naïve WT T cells in the adoptive transfer colitis model, are more suitable.

5.5. Future perspectives: IBD and CD9

There is no cure for IBD. Current IBD treatments have the goal to induce and maintain remission, or achieve extended periods of time when patients do not experience symptoms [384]. On top of that, many therapeutic agents are only effective transiently, while in some patients they fail to work at all. IBD is a chronic condition, and affected people will typically need treatment throughout their lives. The actual treatment of IBD consists of 1) anti-inflammatory drugs 5-aminosalicylic acid (5-ASA) and corticosteroids, 2) immunosuppresive drugs azathioprine (AZA), 6-mercaptopurine (6-MP), methotrexate (MTX) and calcineurin inhibitors (cyclosporin-A and tacrolimus), and 3) anti-TNF-α antibodies (infliximab, adalimumab, certolizumab). Treatment's choice depends on the clinical goal (induction or maintenance of remission), extent and severity of disease, response to current or previous medication and the occurrence of complications [2]. However, due to the lack of a 100% effectiveness and the differences in patients' responsiveness accounting for a complex multifactorial disorder, new drugs are being developed and many of them success to induce an improvement in IBD symptoms. New therapies explore blocking immune effector cells activation, blocking biologic activity of proinflammatory cytokines and their receptors, inhibiting T cell–APC interactions, selectively blocking effector cell extravasation, inducing apoptosis of activated effector cells or enhancing regulatory cell activity. Indeed, the gut-specific integrin blocker Vedolizumab (anti α4β7 heterodimer) [82,516] have been recently introduced for clinical IBD therapy. On the basis of the success of Vedolizumab, further strategies targeting gut T-cell homing are currently being tested in clinical trials, like anti-MadCAM-1 [115] anti-β7 antibodies [583]. Apart from anti-TNF-α, other anti-cytokine therapies against IL-6 [225], IL-12 [331] and IL-23 [141] have been successful. Indeed, Ustekinumab, a monoclonal antibody directed against the p40 common subunit of IL-12 and IL-23 was recently approved for CD therapy in the USA and in Europe [141]. Moreover, blockade of cytokine signalling pathways through targeting of intracellular JAK kinases [584,479], phosphodiesterase (PDE)4 [531], or SMAD7 (TGF-β signalling inhibitor) [361] are currently under evaluation in clinical trials, with promising results. Other potential strategies which have been already validated in mice models of colitis are directed against transcription factors controlling cytokine gene transcription like RORγt [605] or GATA3 [431], and no longer may be evaluated in human patients [149]. Additionally, non-immune therapy has also been investigated. The use of growth factors to achieve epithelial barrier restitution and healing have entered early clinical trials, like EGF [517], KGF [480], GH [194,518] and

glucagon-like peptide 2 analogues [64], whereas others are currently in preclinical evaluation. However, these early clinical trials are small and short in time. Thus, due to the risk that the use of growth factors might imply in carcinogenesis and fibrosis, larger and longer in time studies are still required [278,28]. Importantly, recent clinical studies have revealed mucosal healing as the major prognostic predictor of long-term remission in IBD patients [385,153], suggesting that epithelial regeneration is critical to improving IBD therapy [426]. Thus, the goals of treating IBD patients have evolved over the past few years to include mucosal healing in addition to clinical remission [581]. However, pharmacological anti-inflammatory agents such as glucocorticosteroids or 5-aminosalicylic acid do not heal the bowel mucosa [473], and the efficacy of growth factors such as GH and EGF has yet to be established [383]. There is thus a clear need to identify new therapeutic targets for MH. Our results indicate that CD9 depletion enhances IEC proliferation, resulting in a high regenerative response and reduced susceptibility to DSS-induced colitis. Our findings thus reveal a critical role for the tetraspanin CD9 in colon inflammation and suggest a novel therapeutic opportunity. Growing recent evidence suggests that targeting tetraspanins by an array of tools including monoclonal antibodies, soluble large-loop proteins, and RNAi technology may be used to improve the course of IBDs. Of note, animal models of IBD provide valuable information about *in vivo* mechanistic insights on the role that single pathways have in IBD pathogenesis, and allow for the testing of novel therapies at the preclinical level. Nevertheless, it should be noted that none of the existing models truly recapitulates the complex and waving nature of the human disease. Therefore, the limitations of each model must always be taken into account before directly applying experimental findings to the human condition.

Conclusions

6. CONCLUSIONS

The findings presented herein support the following conclusions:

1) The absence of CD9 protects against DSS-induced colonic injury *in vivo*. $CD9^{-/-}$ mice display a reduced myeloid cell infiltration and proinflammatory cytokine expression in the colon after DSS challenge, along with decreased epithelial cell barrier damage and permeability compared to WT mice.

2) The CD9-deficient non-hematopoietic component is the one involved in conferring the protection in DSS-induced colitis.

3) CD9-deficient intestinal epithelial cells do not have decreased apoptotic levels but increased proliferative rates than CD9 expressing intestinal epithelial cells.

4) CD9 deficiency on $CD4^+$ T cells does not alter $CD4^+$ effector T cell generation neither *in vivo* nor *in vitro*.

Conclusiones

7. CONCLUSIONES

Los resultados presentados en este trabajo permiten concluir:

1) La ausencia de CD9 protege frente al daño intestinal provocado por la administración de DSS *in vivo*. Los animales $CD9^{-/-}$ muestran una reducción en los niveles de infiltración de células mieloides y de expresión de citoquinas pro-inflamatorias en el colon tras el tratamiento con DSS, junto con un menor daño de la barrera epitelial y menor permeabilidad en comparación con los animales de cepa salvaje.

2) La deficiencia de CD9 en el compartimento no hematopoyético es la responsable de conferir la protección a los animales en el modelo de colitis inducida por DSS.

3) Las células epiteliales intestinales deficientes de CD9 no experimentan una menor apoptosis, pero si un incremento de su capacidad proliferativa en comparación con las células epiteliales intestinales de ratones de cepa salvaje tras el daño ejercido por la administración de DSS.

4) La deficiencia de CD9 en células T $CD4^{+}$ no altera la generación de células T efectoras *in vivo* ni *in vitro.*

References

8. REFERENCES

1. Abitorabi MA, Pachynski RK, Ferrando RE, Tidswell M, Erle DJ (1997) Presentation of integrins on leukocyte microvilli: a role for the extracellular domain in determining membrane localization. J Cell Biol 139:563-571

2. Abraham BP, Ahmed T, Ali T (2017) Inflammatory Bowel Disease: Pathophysiology and Current Therapeutic Approaches. Handb Exp Pharmacol 239:115-146. doi:10.1007/164_2016_122

3. Abraham C, Cho JH (2009) Inflammatory bowel disease. N Engl J Med 361:2066-2078. doi:10.1056/NEJMra0804647

4. Akieda Y, Wakamatsu E, Nakamura T, Ishida Y, Ogawa S, Abe R (2015) Defects in regulatory T cells due to CD28 deficiency induce a qualitative change of allogeneic immune response in chronic graft-versus-host disease. J Immunol 194:4162-4174. doi:10.4049/jimmunol.1402591

5. Al-Sadi R, Guo S, Ye D, Dokladny K, Alhmoud T, Ereifej L, Said HM, Ma TY (2013) Mechanism of IL-1beta modulation of intestinal epithelial barrier involves p38 kinase and activating transcription factor-2 activation. J Immunol 190:6596-6606. doi:10.4049/jimmunol.1201876

6. Al-Sadi R, Guo S, Ye D, Ma TY (2013) TNF-alpha modulation of intestinal epithelial tight junction barrier is regulated by ERK1/2 activation of Elk-1. Am J Pathol 183:1871-1884. doi:10.1016/j.ajpath.2013.09.001

7. Alexander RJ, Panja A, Kaplan-Liss E, Mayer L, Raicht RF (1995) Expression of growth factor receptor-encoded mRNA by colonic epithelial cells is altered in inflammatory bowel disease. Dig Dis Sci 40:485-494

8. Amadi-Obi A, Yu CR, Liu X, Mahdi RM, Clarke GL, Nussenblatt RB, Gery I, Lee YS, Egwuagu CE (2007) TH17 cells contribute to uveitis and scleritis and are expanded by IL-2 and inhibited by IL-27/STAT1. Nat Med 13:711-718. doi:10.1038/nm1585

9. Ananthakrishnan AN (2015) Epidemiology and risk factors for IBD. Nat Rev Gastroenterol Hepatol 12:205-217. doi:10.1038/nrgastro.2015.34

10. Ananthakrishnan AN, Bernstein CN, Iliopoulos D, Macpherson A, Neurath MF, Ali RAR, Vavricka SR, Fiocchi C (2018) Environmental triggers in IBD: a review of progress and evidence. Nat Rev Gastroenterol Hepatol 15:39-49. doi:10.1038/nrgastro.2017.136

11. Andre M, Le Caer JP, Greco C, Planchon S, El Nemer W, Boucheix C, Rubinstein E, Chamot-Rooke J, Le Naour F (2006) Proteomic analysis of the tetraspanin web using LC-ESI-MS/MS and MALDI-FTICR-MS. Proteomics 6:1437-1449. doi:10.1002/pmic.200500180

12. Angelisova P, Hilgert I, Horejsi V (1994) Association of four antigens of the tetraspans family (CD37, CD53, TAPA-1, and R2/C33) with MHC class II glycoproteins. Immunogenetics 39:249-256

13. Angelisova P, Vlcek C, Stefanova I, Lipoldova M, Horejsi V (1990) The human leucocyte surface antigen CD53 is a protein structurally similar to the CD37 and MRC OX-44 antigens. Immunogenetics 32:281-285

14. Antoni L, Nuding S, Wehkamp J, Stange EF (2014) Intestinal barrier in inflammatory bowel disease. World J Gastroenterol 20:1165-1179. doi:10.3748/wjg.v20.i5.1165

15. Anzai N, Lee Y, Youn BS, Fukuda S, Kim YJ, Mantel C, Akashi M, Broxmeyer HE (2002) C-kit associated with the transmembrane 4 superfamily proteins constitutes a functionally distinct subunit in human hematopoietic progenitors. Blood 99:4413-4421

16. Araki Y, Mukaisyo K, Sugihara H, Fujiyama Y, Hattori T (2010) Increased apoptosis and decreased proliferation of colonic epithelium in dextran sulfate sodium-induced colitis in mice. Oncol Rep 24:869-874

17. Arduise C, Abache T, Li L, Billard M, Chabanon A, Ludwig A, Mauduit P, Boucheix C, Rubinstein E, Le Naour F (2008) Tetraspanins regulate ADAM10-mediated cleavage of TNF-alpha and epidermal growth factor. J Immunol 181:7002-7013.

18. Arnott ID, Kingstone K, Ghosh S (2000) Abnormal intestinal permeability predicts relapse in inactive Crohn disease. Scand J Gastroenterol 35:1163-1169

19. Ashida H, Ogawa M, Kim M, Mimuro H, Sasakawa C (2011) Bacteria and host interactions in the gut epithelial barrier. Nat Chem Biol 8:36-45. doi:10.1038/nchembio.741

20. Ayres JS (2016) Cooperative Microbial Tolerance Behaviors in Host-Microbiota Mutualism. Cell 165:1323-1331. doi:10.1016/j.cell.2016.05.049

21. Babyatsky MW, Rossiter G, Podolsky DK (1996) Expression of transforming growth factors alpha and beta in colonic mucosa in inflammatory bowel disease. Gastroenterology 110:975-984.

22. Backhed F, Ley RE, Sonnenburg JL, Peterson DA, Gordon JI (2005) Host-bacterial mutualism in the human intestine. Science 307:1915-1920. doi:10.1126/science.1104816

23. Bain CC, Bravo-Blas A, Scott CL, Perdiguero EG, Geissmann F, Henri S, Malissen B, Osborne LC, Artis D, Mowat AM (2014) Constant replenishment from circulating monocytes maintains the macrophage pool in the intestine of adult mice. Nat Immunol 15:929-937. doi:10.1038/ni.2967

24. Bain CC, Scott CL, Uronen-Hansson H, Gudjonsson S, Jansson O, Grip O, Guilliams M, Malissen B, Agace WW, Mowat AM (2013) Resident and pro-inflammatory macrophages in the colon represent alternative context-dependent fates of the same Ly6Chi monocyte precursors. Mucosal Immunol 6:498-510. doi:10.1038/mi.2012.89

25. Baixauli F, Acin-Perez R, Villarroya-Beltri C, Mazzeo C, Nunez-Andrade N, Gabande-Rodriguez E, Ledesma MD, Blazquez A, Martin MA, Falcon-Perez JM, Redondo JM, Enriquez JA, Mittelbrunn M (2015) Mitochondrial Respiration Controls Lysosomal Function during Inflammatory T Cell Responses. Cell Metab 22:485-498. doi:10.1016/j.cmet.2015.07.020

26. Ballesteros-Tato A, Leon B, Graf BA, Moquin A, Adams PS, Lund FE, Randall TD (2012) Interleukin-2 inhibits germinal center formation by limiting T follicular helper cell differentiation. Immunity 36:847-856. doi:10.1016/j.immuni.2012.02.012

27. Bamias G, Martin C, Mishina M, Ross WG, Rivera-Nieves J, Marini M, Cominelli F (2005) Proinflammatory effects of TH2 cytokines in a murine model of chronic small intestinal inflammation. Gastroenterology 128:654-666.

28. Barahona-Garrido J, Hernandez-Calleros J, Garcia-Juarez I, Yamamoto-Furusho JK (2009) Growth factors as treatment for inflammatory bowel disease: a concise review of the evidence toward their potential clinical utility. Saudi J Gastroenterol 15:208-212. doi:10.4103/1319-3767.54742

29. Barker N, van de Wetering M, Clevers H (2008) The intestinal stem cell. Genes Dev 22:1856-1864. doi:10.1101/gad.1674008

30. Barreiro O, Martin P, Gonzalez-Amaro R, Sanchez-Madrid F (2010) Molecular cues guiding inflammatory responses. Cardiovasc Res 86:174-182. doi:10.1093/cvr/cvq001

31. Barreiro O, Yanez-Mo M, Sala-Valdes M, Gutierrez-Lopez MD, Ovalle S, Higginbottom A, Monk PN, Cabanas C, Sanchez-Madrid F (2005) Endothelial tetraspanin microdomains regulate leukocyte firm adhesion during extravasation. Blood 105:2852-2861. doi:10.1182/blood-2004-09-3606

32. Barreiro O, Zamai M, Yanez-Mo M, Tejera E, Lopez-Romero P, Monk PN, Gratton E, Caiolfa VR, Sanchez-Madrid F (2008) Endothelial adhesion receptors are recruited to adherent leukocytes by inclusion in preformed tetraspanin nanoplatforms. J Cell Biol 183:527-542. doi:10.1083/jcb.200805076

33. Basson MD, Sanders MA, Gomez R, Hatfield J, Vanderheide R, Thamilselvan V, Zhang J, Walsh MF (2006) Focal adhesion kinase protein levels in gut epithelial motility. Am J Physiol Gastrointest Liver Physiol 291:G491-499. doi:10.1152/ajpgi.00292.2005

34. Batts LE, Polk DB, Dubois RN, Kulessa H (2006) Bmp signaling is required for intestinal growth and morphogenesis. Dev Dyn 235:1563-1570. doi:10.1002/dvdy.20741

35. Beamish LA, Osornio-Vargas AR, Wine E (2011) Air pollution: An environmental factor contributing to intestinal disease. J Crohns Colitis 5:279-286. doi:10.1016/j.crohns.2011.02.017

36. Beck PL, Podolsky DK (1999) Growth factors in inflammatory bowel disease. Inflamm Bowel Dis 5:44-60

37. Benchimol EI, Mack DR, Guttmann A, Nguyen GC, To T, Mojaverian N, Quach P, Manuel DG (2015) Inflammatory bowel disease in immigrants to Canada and their children: a population-based cohort study. Am J Gastroenterol 110:553-563. doi:10.1038/ajg.2015.52

38. Bennett CF, Kornbrust D, Henry S, Stecker K, Howard R, Cooper S, Dutson S, Hall W, Jacoby HI (1997) An ICAM-1 antisense oligonucleotide prevents and reverses dextran sulfate sodium-induced colitis in mice. J Pharmacol Exp Ther 280:988-1000

39. Berditchevski F, Odintsova E (1999) Characterization of integrin-tetraspanin adhesion complexes: role of tetraspanins in integrin signaling. J Cell Biol 146:477-492

40. Berditchevski F, Odintsova E, Sawada S, Gilbert E (2002) Expression of the palmitoylation-deficient CD151 weakens the association of alpha 3 beta 1 integrin with the tetraspanin-enriched microdomains and affects integrin-dependent signaling. J Biol Chem 277:36991-37000. doi:10.1074/jbc.M205265200

41. Berditchevski F, Zutter MM, Hemler ME (1996) Characterization of novel complexes on the cell surface between integrins and proteins with 4 transmembrane domains (TM4 proteins). Mol Biol Cell 7:193-207

42. Berlin C, Berg EL, Briskin MJ, Andrew DP, Kilshaw PJ, Holzmann B, Weissman IL, Hamann A, Butcher EC (1993) Alpha 4 beta 7 integrin mediates lymphocyte binding to the mucosal vascular addressin MAdCAM-1. Cell 74:185-195. doi:0092-8674(93)90305-A [pii]

43. Bianco AM, Girardelli M, Tommasini A (2015) Genetics of inflammatory bowel disease from multifactorial to monogenic forms. World J Gastroenterol 21:12296-12310. doi:10.3748/wjg.v21.i43.12296

44. Binder V (1998) Genetic epidemiology in inflammatory bowel disease. Dig Dis 16:351-355. doi:10.1159/000016891

45. Bjorck P, Leong HX, Engleman EG (2011) Plasmacytoid dendritic cell dichotomy: identification of IFN-alpha producing cells as a phenotypically and functionally distinct subset. J Immunol 186:1477-1485. doi:10.4049/jimmunol.1000454

46. Blair SA, Kane SV, Clayburgh DR, Turner JR (2006) Epithelial myosin light chain kinase expression and activity are upregulated in inflammatory bowel disease. Lab Invest 86:191-201. doi:10.1038/labinvest.3700373

47. Blander JM (2016) Death in the intestinal epithelium-basic biology and implications for inflammatory bowel disease. FEBS J 283:2720-2730. doi:10.1111/febs.13771

48. Blobel CP (2005) ADAMs: key components in EGFR signalling and development. Nat Rev Mol Cell Biol 6:32-43. doi:10.1038/nrm1548

49. Boehm F, Martin M, Kesselring R, Schiechl G, Geissler EK, Schlitt HJ, Fichtner-Feigl S (2012) Deletion of Foxp3+ regulatory T cells in genetically targeted mice supports development of intestinal inflammation. BMC Gastroenterol 12:97. doi:10.1186/1471-230X-12-97

50. Borruel N, Carol M, Casellas F, Antolin M, de Lara F, Espin E, Naval J, Guarner F, Malagelada JR (2002) Increased mucosal tumour necrosis factor alpha production in Crohn's disease can be downregulated ex vivo by probiotic bacteria. Gut 51:659-664

51. Borruel N, Casellas F, Antolin M, Llopis M, Carol M, Espiin E, Naval J, Guarner F, Malagelada JR (2003) Effects of nonpathogenic bacteria on cytokine secretion by human intestinal mucosa. Am J Gastroenterol 98:865-870. doi:10.1111/j.1572-0241.2003.07384.x

52. Bosch B, Heipertz EL, Drake JR, Roche PA (2013) Major histocompatibility complex (MHC) class II-peptide complexes arrive at the plasma membrane in cholesterol-rich microclusters. J Biol Chem 288:13236-13242. doi:10.1074/jbc.M112.442640

53. Boucheix C, Benoit P, Frachet P, Billard M, Worthington RE, Gagnon J, Uzan G (1991) Molecular cloning of the CD9 antigen. A new family of cell surface proteins. J Biol Chem 266:117-122

54. Boucheix C, Rubinstein E (2001) Tetraspanins. Cell Mol Life Sci 58:1189-1205. doi:10.1007/PL00000933

55. Bradford K, Shih DQ (2011) Optimizing 6-mercaptopurine and azathioprine therapy in the management of inflammatory bowel disease. World J Gastroenterol 17:4166-4173. doi:10.3748/wjg.v17.i37.4166

56. Brandl K, Sun L, Neppl C, Siggs OM, Le Gall SM, Tomisato W, Li X, Du X, Maennel DN, Blobel CP, Beutler B (2010) MyD88 signaling in nonhematopoietic cells protects mice against induced colitis by regulating specific EGF receptor ligands. Proc Natl Acad Sci U S A 107:19967-19972. doi:10.1073/pnas.1014669107

57. Brant SR (2011) Update on the heritability of inflammatory bowel disease: the importance of twin studies. Inflamm Bowel Dis 17:1-5. doi:10.1002/ibd.21385

58. Braun A, Treede I, Gotthardt D, Tietje A, Zahn A, Ruhwald R, Schoenfeld U, Welsch T, Kienle P, Erben G, Lehmann WD, Fuellekrug J, Stremmel W, Ehehalt R (2009) Alterations of phospholipid concentration and species composition of the intestinal mucus barrier in ulcerative colitis: a clue to pathogenesis. Inflamm Bowel Dis 15:1705-1720. doi:10.1002/ibd.20993

59. Breese E, Braegger CP, Corrigan CJ, Walker-Smith JA, MacDonald TT (1993) Interleukin-2- and interferon-gamma-secreting T cells in normal and diseased human intestinal mucosa. Immunology 78:127-131

60. Bressenot A, Salleron J, Bastien C, Danese S, Boulagnon-Rombi C, Peyrin-Biroulet L (2015) Comparing histological activity indexes in UC. Gut 64:1412-1418. doi:10.1136/gutjnl-2014-307477

61. Brinkman BM, Becker A, Ayiseh RB, Hildebrand F, Raes J, Huys G, Vandenabeele P (2013) Gut microbiota affects sensitivity to acute DSS-induced colitis independently of host genotype. Inflamm Bowel Dis 19:2560-2567. doi:10.1097/MIB.0b013e3182a8759a

62. Briskin M, Winsor-Hines D, Shyjan A, Cochran N, Bloom S, Wilson J, McEvoy LM, Butcher EC, Kassam N, Mackay CR, Newman W, Ringler DJ (1997) Human mucosal addressin cell adhesion molecule-1 is preferentially expressed in intestinal tract and associated lymphoid tissue. Am J Pathol 151:97-110

63. Buck RC (1986) Ultrastructural features of rectal epithelium of the mouse during the early phases of migration to repair a defect. Virchows Arch B Cell Pathol Incl Mol Pathol 51:331-340

64. Buchman AL, Katz S, Fang JC, Bernstein CN, Abou-Assi SG (2010) Teduglutide, a novel mucosally active analog of glucagon-like peptide-2 (GLP-2) for the treatment of moderate to severe Crohn's disease. Inflamm Bowel Dis 16:962-973. doi:10.1002/ibd.21117

65. Cailleteau L, Estrach S, Thyss R, Boyer L, Doye A, Domange B, Johnsson N, Rubinstein E, Boucheix C, Ebrahimian T, Silvestre JS, Lemichez E, Meneguzzi G, Mettouchi A (2010) alpha2beta1 integrin controls association of Rac with the membrane and triggers quiescence of endothelial cells. J Cell Sci 123:2491-2501. doi:10.1242/jcs.058875

66. Cajot JF, Sordat I, Silvestre T, Sordat B (1997) Differential display cloning identifies motility-related protein (MRP1/CD9) as highly expressed in primary compared to metastatic human colon carcinoma cells. Cancer Res 57:2593-2597

67. Camilleri M, Lasch K, Zhou W (2012) Irritable bowel syndrome: methods, mechanisms, and pathophysiology. The confluence of increased permeability, inflammation, and pain in irritable bowel syndrome. Am J Physiol Gastrointest Liver Physiol 303:G775-785. doi:10.1152/ajpgi.00155.2012

68. Cannon KS, Cresswell P (2001) Quality control of transmembrane domain assembly in the tetraspanin CD82. EMBO J 20:2443-2453. doi:10.1093/emboj/20.10.2443

69. Cariappa A, Shoham T, Liu H, Levy S, Boucheix C, Pillai S (2005) The CD9 tetraspanin is not required for the development of peripheral B cells or for humoral immunity. J Immunol 175:2925-2930.

70. Cario E, Becker A, Sturm A, Goebell H, Dignass AU (1999) Peripheral blood mononuclear cells promote intestinal epithelial restitution in vitro through an interleukin-2/interferon-gamma-dependent pathway. Scand J Gastroenterol 34:1132-1138

71. Cario E, Gerken G, Podolsky DK (2007) Toll-like receptor 2 controls mucosal inflammation by regulating epithelial barrier function. Gastroenterology 132:1359-1374. doi:10.1053/j.gastro.2007.02.056

72. Carlos TM, Schwartz BR, Kovach NL, Yee E, Rosa M, Osborn L, Chi-Rosso G, Newman B, Lobb R, et al. (1990) Vascular cell adhesion molecule-1 mediates lymphocyte adherence to cytokine-activated cultured human endothelial cells. Blood 76:965-970

73. Carman CV, Springer TA (2004) A transmigratory cup in leukocyte diapedesis both through individual vascular endothelial cells and between them. J Cell Biol 167:377-388. doi:10.1083/jcb.200404129

74. Carr I, Mayberry JF (1999) The effects of migration on ulcerative colitis: a three-year prospective study among Europeans and first- and second- generation South Asians in Leicester (1991-1994). Am J Gastroenterol 94:2918-2922. doi:10.1111/j.1572-0241.1999.01438.x

75. Casellas F, Borruel N, Papo M, Guarner F, Antolin M, Videla S, Malagelada JR (1998) Antiinflammatory effects of enterically coated amoxicillin-clavulanic acid in active ulcerative colitis. Inflamm Bowel Dis 4:1-5

76. Castro-Sanchez L, Soto-Guzman A, Navarro-Tito N, Martinez-Orozco R, Salazar EP (2010) Native type IV collagen induces cell migration through a CD9 and DDR1-dependent pathway in MDA-MB-231 breast cancer cells. Eur J Cell Biol 89:843-852. doi:10.1016/j.ejcb.2010.07.004

77. Cattin AL, Le Beyec J, Barreau F, Saint-Just S, Houllier A, Gonzalez FJ, Robine S, Pincon-Raymond M, Cardot P, Lacasa M, Ribeiro A (2009) Hepatocyte nuclear factor 4alpha, a key factor for homeostasis,

cell architecture, and barrier function of the adult intestinal epithelium. Mol Cell Biol 29:6294-6308. doi:10.1128/MCB.00939-09

78. Cerovic V, Jenkins CD, Barnes AG, Milling SW, MacPherson GG, Klavinskis LS (2009) Hyporesponsiveness of intestinal dendritic cells to TLR stimulation is limited to TLR4. J Immunol 182:2405-2415. doi:10.4049/jimmunol.0802318

79. Clamp JR, Fraser G, Read AE (1981) Study of the carbohydrate content of mucus glycoproteins from normal and diseased colons. Clin Sci (Lond) 61:229-234

80. Classon BJ, Williams AF, Willis AC, Seed B, Stamenkovic I (1990) The primary structure of the human leukocyte antigen CD37, a species homologue of the rat MRC OX-44 antigen. J Exp Med 172:1007

81. Cleynen I, Vermeire S (2015) The genetic architecture of inflammatory bowel disease: past, present and future. Curr Opin Gastroenterol 31:456-463. doi:10.1097/MOG.0000000000000215

82. Colombel JF, Sands BE, Rutgeerts P, Sandborn W, Danese S, D'Haens G, Panaccione R, Loftus EV, Jr., Sankoh S, Fox I, Parikh A, Milch C, Abhyankar B, Feagan BG (2017) The safety of vedolizumab for ulcerative colitis and Crohn's disease. Gut 66:839-851. doi:10.1136/gutjnl-2015-311079

83. Connor EM, Eppihimer MJ, Morise Z, Granger DN, Grisham MB (1999) Expression of mucosal addressin cell adhesion molecule-1 (MAdCAM-1) in acute and chronic inflammation. J Leukoc Biol 65:349-355

84. Connor SJ, Paraskevopoulos N, Newman R, Cuan N, Hampartzoumian T, Lloyd AR, Grimm MC (2004) CCR2 expressing CD4+ T lymphocytes are preferentially recruited to the ileum in Crohn's disease. Gut 53:1287-1294. doi:10.1136/gut.2003.028225

85. Coombes JL, Siddiqui KR, Arancibia-Carcamo CV, Hall J, Sun CM, Belkaid Y, Powrie F (2007) A functionally specialized population of mucosal CD103+ DCs induces Foxp3+ regulatory T cells via a TGF-beta and retinoic acid-dependent mechanism. J Exp Med 204:1757-1764. doi:10.1084/jem.20070590

86. Cooney R, Jewell D (2009) The genetic basis of inflammatory bowel disease. Dig Dis 27:428-442. doi:10.1159/000234909

87. Cooper HS, Murthy SN, Shah RS, Sedergran DJ (1993) Clinicopathologic study of dextran sulfate sodium experimental murine colitis. Lab Invest 69:238-249

88. Corfield AP, Myerscough N, Bradfield N, Corfield Cdo A, Gough M, Clamp JR, Durdey P, Warren BF, Bartolo DC, King KR, Williams JM (1996) Colonic mucins in ulcerative colitis: evidence for loss of sulfation. Glycoconj J 13:809-822

89. Cote-Sierra J, Foucras G, Guo L, Chiodetti L, Young HA, Hu-Li J, Zhu J, Paul WE (2004) Interleukin 2 plays a central role in Th2 differentiation. Proc Natl Acad Sci U S A 101:3880-3885. doi:10.1073/pnas.0400339101

90. Cha H, Lee S, Hwan Kim S, Kim H, Lee DS, Lee HS, Lee JH, Park JW (2017) Increased susceptibility of IDH2-deficient mice to dextran sodium sulfate-induced colitis. Redox Biol 13:32-38. doi:10.1016/j.redox.2017.05.009

91. Chami B, Yeung AW, van Vreden C, King NJ, Bao S (2014) The role of CXCR3 in DSS-induced colitis. PLoS One 9:e101622. doi:10.1371/journal.pone.0101622

92. Chamouard P, Monneaux F, Richert Z, Voegeli AC, Lavaux T, Gaub MP, Baumann R, Oudet P, Muller S (2009) Diminution of Circulating CD4+CD25 high T cells in naive Crohn's disease. Dig Dis Sci 54:2084-2093. doi:10.1007/s10620-008-0590-6

93. Charrin S, Le Naour F, Labas V, Billard M, Le Caer JP, Emile JF, Petit MA, Boucheix C, Rubinstein E (2003) EWI-2 is a new component of the tetraspanin web in hepatocytes and lymphoid cells. Biochem J 373:409-421. doi:10.1042/BJ20030343

94. Charrin S, Le Naour F, Oualid M, Billard M, Faure G, Hanash SM, Boucheix C, Rubinstein E (2001) The major CD9 and CD81 molecular partner. Identification and characterization of the complexes. J Biol Chem 276:14329-14337. doi:10.1074/jbc.M011297200

95. Charrin S, le Naour F, Silvie O, Milhiet PE, Boucheix C, Rubinstein E (2009) Lateral organization of membrane proteins: tetraspanins spin their web. Biochem J 420:133-154. doi:10.1042/BJ20082422

96. Charrin S, Manie S, Oualid M, Billard M, Boucheix C, Rubinstein E (2002) Differential stability of tetraspanin/tetraspanin interactions: role of palmitoylation. FEBS Lett 516:139-144.

97. Chassaing B, Aitken JD, Malleshappa M, Vijay-Kumar M (2014) Dextran sulfate sodium (DSS)-induced colitis in mice. Curr Protoc Immunol 104:Unit 15 25. doi:10.1002/0471142735.im1525s104

98. Chassaing B, Koren O, Goodrich JK, Poole AC, Srinivasan S, Ley RE, Gewirtz AT (2015) Dietary emulsifiers impact the mouse gut microbiota promoting colitis and metabolic syndrome. Nature 519:92-96. doi:10.1038/nature14232

99. Chen J, Xie L, Toyama S, Hunig T, Takahara S, Li XK, Zhong L (2011) The effects of Foxp3-expressing regulatory T cells expanded with CD28 superagonist antibody in DSS-induced mice colitis. Int Immunopharmacol 11:610-617. doi:10.1016/j.intimp.2010.11.034

100. Chen K, Nezu R, Wasa M, Sando K, Kamata S, Takagi Y, Okada A (1999) Insulin-like growth factor-1 modulation of intestinal epithelial cell restitution. JPEN J Parenter Enteral Nutr 23:S89-92

101. Chen S, Sun Y, Jin Z, Jing X (2011) Functional and biochemical studies of CD9 in fibrosarcoma cell line. Mol Cell Biochem 350:89-99. doi:10.1007/s11010-010-0685-1

102. Chen Y, Chou K, Fuchs E, Havran WL, Boismenu R (2002) Protection of the intestinal mucosa by intraepithelial gamma delta T cells. Proc Natl Acad Sci U S A 99:14338-14343. doi:10.1073/pnas.212290499

103. Chichlowski M, Hale LP (2008) Bacterial-mucosal interactions in inflammatory bowel disease: an alliance gone bad. Am J Physiol Gastrointest Liver Physiol 295:G1139-1149. doi:10.1152/ajpgi.90516.2008

104. Chistiakov DA, Bobryshev YV, Kozarov E, Sobenin IA, Orekhov AN (2014) Intestinal mucosal tolerance and impact of gut microbiota to mucosal tolerance. Front Microbiol 5:781. doi:10.3389/fmicb.2014.00781

105. D'Haens GR, Geboes K, Peeters M, Baert F, Penninckx F, Rutgeerts P (1998) Early lesions of recurrent Crohn's disease caused by infusion of intestinal contents in excluded ileum. Gastroenterology 114:262-267.

106. D'Inca R, Di Leo V, Corrao G, Martines D, D'Odorico A, Mestriner C, Venturi C, Longo G, Sturniolo GC (1999) Intestinal permeability test as a predictor of clinical course in Crohn's disease. Am J Gastroenterol 94:2956-2960. doi:10.1111/j.1572-0241.1999.01444.x

107. Danese S, Semeraro S, Marini M, Roberto I, Armuzzi A, Papa A, Gasbarrini A (2005) Adhesion molecules in inflammatory bowel disease: therapeutic implications for gut inflammation. Dig Liver Dis 37:811-818. doi:10.1016/j.dld.2005.03.013

108. Darsigny M, Babeu JP, Dupuis AA, Furth EE, Seidman EG, Levy E, Verdu EF, Gendron FP, Boudreau F (2009) Loss of hepatocyte-nuclear-factor-4alpha affects colonic ion transport and causes chronic

inflammation resembling inflammatory bowel disease in mice. PLoS One 4:e7609. doi:10.1371/journal.pone.0007609

109. De Bruyne E, Andersen TL, De Raeve H, Van Valckenborgh E, Caers J, Van Camp B, Delaisse JM, Van Riet I, Vanderkerken K (2006) Endothelial cell-driven regulation of CD9 or motility-related protein-1 expression in multiple myeloma cells within the murine 5T33MM model and myeloma patients. Leukemia 20:1870-1879. doi:10.1038/sj.leu.2404343

110. de Lange KM, Barrett JC (2015) Understanding inflammatory bowel disease via immunogenetics. J Autoimmun 64:91-100. doi:10.1016/j.jaut.2015.07.013

111. Delgado ME, Grabinger T, Brunner T (2016) Cell death at the intestinal epithelial front line. FEBS J 283:2701-2719. doi:10.1111/febs.13575

112. Di Sabatino A, Biancheri P, Rovedatti L, MacDonald TT, Corazza GR (2012) New pathogenic paradigms in inflammatory bowel disease. Inflamm Bowel Dis 18:368-371. doi:10.1002/ibd.21735

113. Di Sabatino A, Ciccocioppo R, Luinetti O, Ricevuti L, Morera R, Cifone MG, Solcia E, Corazza GR (2003) Increased enterocyte apoptosis in inflamed areas of Crohn's disease. Dis Colon Rectum 46:1498-1507. doi:10.1097/01.DCR.0000089118.20964.12

114. Diamond MS, Staunton DE, Marlin SD, Springer TA (1991) Binding of the integrin Mac-1 (CD11b/CD18) to the third immunoglobulin-like domain of ICAM-1 (CD54) and its regulation by glycosylation. Cell 65:961-971.

115. Dickson I (2017) IBD: Phase II trial success for anti-MADCAM1 antibody. Nat Rev Gastroenterol Hepatol 14:386. doi:10.1038/nrgastro.2017.82

116. Dieleman LA, Ridwan BU, Tennyson GS, Beagley KW, Bucy RP, Elson CO (1994) Dextran sulfate sodium-induced colitis occurs in severe combined immunodeficient mice. Gastroenterology 107:1643-1652.

117. Dignass AU (2001) Mechanisms and modulation of intestinal epithelial repair. Inflamm Bowel Dis 7:68-77

118. Dignass AU, Becker A, Spiegler S, Goebell H (1998) Adenine nucleotides modulate epithelial wound healing in vitro. Eur J Clin Invest 28:554-561

119. Dignass AU, Podolsky DK (1993) Cytokine modulation of intestinal epithelial cell restitution: central role of transforming growth factor beta. Gastroenterology 105:1323-1332.

120. Dogan A, Wang ZD, Spencer J (1995) E-cadherin expression in intestinal epithelium. J Clin Pathol 48:143-146

121. Drucker DJ, Erlich P, Asa SL, Brubaker PL (1996) Induction of intestinal epithelial proliferation by glucagon-like peptide 2. Proc Natl Acad Sci U S A 93:7911-7916

122. Drummer HE, Wilson KA, Poumbourios P (2005) Determinants of CD81 dimerization and interaction with hepatitis C virus glycoprotein E2. Biochem Biophys Res Commun 328:251-257. doi: 10.1016/j.bbrc.2004.12.160

123. Dube PE, Yan F, Punit S, Girish N, McElroy SJ, Washington MK, Polk DB (2012) Epidermal growth factor receptor inhibits colitis-associated cancer in mice. J Clin Invest 122:2780-2792. doi:10.1172/JCI62888

124. Dustin ML, Rothlein R, Bhan AK, Dinarello CA, Springer TA (1986) Induction by IL 1 and interferon-gamma: tissue distribution, biochemistry, and function of a natural adherence molecule (ICAM-1). J Immunol 137:245-254

125. Eaden J (2004) Review article: colorectal carcinoma and inflammatory bowel disease. Aliment Pharmacol Ther 20 Suppl 4:24-30. doi:10.1111/j.1365-2036.2004.02046.x

126. Eaden JA, Abrams KR, Mayberry JF (2001) The risk of colorectal cancer in ulcerative colitis: a meta-analysis. Gut 48:526-535

127. Edelblum KL, Washington MK, Koyama T, Robine S, Baccarini M, Polk DB (2008) Raf protects against colitis by promoting mouse colon epithelial cell survival through NF-kappaB. Gastroenterology 135:539-551. doi:10.1053/j.gastro.2008.04.025

128. Egger B, Buchler MW, Lakshmanan J, Moore P, Eysselein VE (2000) Mice harboring a defective epidermal growth factor receptor (waved-2) have an increased susceptibility to acute dextran sulfate-induced colitis. Scand J Gastroenterol 35:1181-1187

129. Egger B, Carey HV, Procaccino F, Chai NN, Sandgren EP, Lakshmanan J, Buslon VS, French SW, Buchler MW, Eysselein VE (1998) Reduced susceptibility of mice overexpressing transforming growth factor alpha to dextran sodium sulphate induced colitis. Gut 43:64-70

130. Egger B, Procaccino F, Lakshmanan J, Reinshagen M, Hoffmann P, Patel A, Reuben W, Gnanakkan S, Liu L, Barajas L, Eysselein VE (1997) Mice lacking transforming growth factor alpha have an increased susceptibility to dextran sulfate-induced colitis. Gastroenterology 113:825-832.

131. Eichele DD, Kharbanda KK (2017) Dextran sodium sulfate colitis murine model: An indispensable tool for advancing our understanding of inflammatory bowel diseases pathogenesis. World J Gastroenterol 23:6016-6029. doi:10.3748/wjg.v23.i33.6016

132. Elices MJ, Osborn L, Takada Y, Crouse C, Luhowskyj S, Hemler ME, Lobb RR (1990) VCAM-1 on activated endothelium interacts with the leukocyte integrin VLA-4 at a site distinct from the VLA-4/fibronectin binding site. Cell 60:577-584.

133. Engering A, Pieters J (2001) Association of distinct tetraspanins with MHC class II molecules at different subcellular locations in human immature dendritic cells. Int Immunol 13:127-134

134. Espenel C, Margeat E, Dosset P, Arduise C, Le Grimellec C, Royer CA, Boucheix C, Rubinstein E, Milhiet PE (2008) Single-molecule analysis of CD9 dynamics and partitioning reveals multiple modes of interaction in the tetraspanin web. J Cell Biol 182:765-776. doi:10.1083/jcb.200803010

135. Fakhoury M, Negrulj R, Mooranian A, Al-Salami H (2014) Inflammatory bowel disease: clinical aspects and treatments. J Inflamm Res 7:113-120. doi:10.2147/JIR.S65979

136. Fantini MC, Becker C, Tubbe I, Nikolaev A, Lehr HA, Galle P, Neurath MF (2006) Transforming growth factor beta induced FoxP3+ regulatory T cells suppress Th1 mediated experimental colitis. Gut 55:671-680. doi:10.1136/gut.2005.072801

137. Farkas S, Hornung M, Sattler C, Edtinger K, Steinbauer M, Anthuber M, Schlitt HJ, Herfarth H, Geissler EK (2006) Blocking MAdCAM-1 in vivo reduces leukocyte extravasation and reverses chronic inflammation in experimental colitis. Int J Colorectal Dis 21:71-78. doi:10.1007/s00384-004-0709-y

138. Farmer RG, Michener WM, Mortimer EA (1980) Studies of family history among patients with inflammatory bowel disease. Clin Gastroenterol 9:271-277

139. Farooq SM, Stillie R, Svensson M, Svanborg C, Strieter RM, Stadnyk AW (2009) Therapeutic effect of blocking CXCR2 on neutrophil recruitment and dextran sodium sulfate-induced colitis. J Pharmacol Exp Ther 329:123-129. doi:10.1124/jpet.108.145862

140. Feagan BG, Greenberg GR, Wild G, Fedorak RN, Pare P, McDonald JW, Dube R, Cohen A, Steinhart AH, Landau S, Aguzzi RA, Fox IH, Vandervoort MK (2005) Treatment of ulcerative colitis with a humanized antibody to the alpha4beta7 integrin. N Engl J Med 352:2499-2507. doi:10.1056/NEJMoa042982

141. Feagan BG, Sandborn WJ, D'Haens G, Panes J, Kaser A, Ferrante M, Louis E, Franchimont D, Dewit O, Seidler U, Kim KJ, Neurath MF, Schreiber S, Scholl P, Pamulapati C, Lalovic B, Visvanathan S, Padula SJ, Herichova I, Soaita A, Hall DB, Bocher WO (2017) Induction therapy with the selective interleukin-23 inhibitor risankizumab in patients with moderate-to-severe Crohn's disease: a randomised, double-blind, placebo-controlled phase 2 study. Lancet 389:1699-1709. doi:10.1016/S0140-6736(17)30570-6

142. Fehon RG, McClatchey AI, Bretscher A (2010) Organizing the cell cortex: the role of ERM proteins. Nat Rev Mol Cell Biol 11:276-287. doi:10.1038/nrm2866

143. Feil W, Lacy ER, Wong YM, Burger D, Wenzl E, Starlinger M, Schiessel R (1989) Rapid epithelial restitution of human and rabbit colonic mucosa. Gastroenterology 97:685-701.

144. Feil W, Wenzl E, Vattay P, Starlinger M, Sogukoglu T, Schiessel R (1987) Repair of rabbit duodenal mucosa after acid injury in vivo and in vitro. Gastroenterology 92:1973-1986.

145. Fernvik E, Lundahl J, Hallden G (2000) The impact of eotaxin- and IL-5-induced adhesion and transmigration on eosinophil activity markers. Inflammation 24:73-87

146. Fernvik E, Lundahl J, Magnusson CG, Hallden G (1999) The effect of in vitro activation and platelet interaction on the CD9 distribution and adhesion properties of human eosinophils. Inflamm Res 48:28-35. doi:10.1007/s000110050383

147. Ferrari L, Krane MK, Fichera A (2016) Inflammatory bowel disease surgery in the biologic era. World J Gastrointest Surg 8:363-370. doi:10.4240/wjgs.v8.i5.363

148. Finch PW, Rubin JS (2004) Keratinocyte growth factor/fibroblast growth factor 7, a homeostatic factor with therapeutic potential for epithelial protection and repair. Adv Cancer Res 91:69-136. doi:10.1016/S0065-230X(04)91003-2

149. Fitzpatrick LR (2013) Inhibition of IL-17 as a pharmacological approach for IBD. Int Rev Immunol 32:544-555. doi:10.3109/08830185.2013.821118

150. Fournier BM, Parkos CA (2012) The role of neutrophils during intestinal inflammation. Mucosal Immunol 5:354-366. doi:10.1038/mi.2012.24

151. Frey MR, Dise RS, Edelblum KL, Polk DB (2006) p38 kinase regulates epidermal growth factor receptor downregulation and cellular migration. EMBO J 25:5683-5692. doi: 10.1038/sj.emboj.7601457

152. Frey MR, Golovin A, Polk DB (2004) Epidermal growth factor-stimulated intestinal epithelial cell migration requires Src family kinase-dependent p38 MAPK signaling. J Biol Chem 279:44513-44521. doi:10.1074/jbc.M406253200

153. Froslie KF, Jahnsen J, Moum BA, Vatn MH (2007) Mucosal healing in inflammatory bowel disease: results from a Norwegian population-based cohort. Gastroenterology 133:412-422. doi: 10.1053/j.gastro.2007.05.051

154. Fujino S, Andoh A, Bamba S, Ogawa A, Hata K, Araki Y, Bamba T, Fujiyama Y (2003) Increased expression of interleukin 17 in inflammatory bowel disease. Gut 52:65-70

155. Fukata M, Chen A, Klepper A, Krishnareddy S, Vamadevan AS, Thomas LS, Xu R, Inoue H, Arditi M, Dannenberg AJ, Abreu MT (2006) Cox-2 is regulated by Toll-like receptor-4 (TLR4) signaling: Role in proliferation and apoptosis in the intestine. Gastroenterology 131:862-877. doi:10.1053/j.gastro.2006.06.017

156. Fukata M, Michelsen KS, Eri R, Thomas LS, Hu B, Lukasek K, Nast CC, Lechago J, Xu R, Naiki Y, Soliman A, Arditi M, Abreu MT (2005) Toll-like receptor-4 is required for intestinal response to epithelial injury and limiting bacterial translocation in a murine model of acute colitis. Am J Physiol Gastrointest Liver Physiol 288:G1055-1065. doi:10.1152/ajpgi.00328.2004

157. Furth EE, Li J, Purev E, Solomon AC, Rogler G, Mick R, Putt M, Zhang T, Somasundaram R, Swoboda R, Herlyn D (2006) Serum antibodies to EpCAM in healthy donors but not ulcerative colitis patients. Cancer Immunol Immunother 55:528-537. doi:10.1007/s00262-005-0026-5

158. Furusawa Y, Obata Y, Fukuda S, Endo TA, Nakato G, Takahashi D, Nakanishi Y, Uetake C, Kato K, Kato T, Takahashi M, Fukuda NN, Murakami S, Miyauchi E, Hino S, Atarashi K, Onawa S, Fujimura Y, Lockett T, Clarke JM, Topping DL, Tomita M, Hori S, Ohara O, Morita T, Koseki H, Kikuchi J, Honda K, Hase K, Ohno H (2013) Commensal microbe-derived butyrate induces the differentiation of colonic regulatory T cells. Nature 504:446-450. doi:10.1038/nature12721

159. Fuss IJ, Heller F, Boirivant M, Leon F, Yoshida M, Fichtner-Feigl S, Yang Z, Exley M, Kitani A, Blumberg RS, Mannon P, Strober W (2004) Nonclassical CD1d-restricted NK T cells that produce IL-13 characterize an atypical Th2 response in ulcerative colitis. J Clin Invest 113:1490-1497. doi:10.1172/JCI19836

160. Fuss IJ, Neurath M, Boirivant M, Klein JS, de la Motte C, Strong SA, Fiocchi C, Strober W (1996) Disparate CD4+ lamina propria (LP) lymphokine secretion profiles in inflammatory bowel disease. Crohn's disease LP cells manifest increased secretion of IFN-gamma, whereas ulcerative colitis LP cells manifest increased secretion of IL-5. J Immunol 157:1261-1270

161. Garcia-Espana A, Chung PJ, Sarkar IN, Stiner E, Sun TT, Desalle R (2008) Appearance of new tetraspanin genes during vertebrate evolution. Genomics 91:326-334. doi:10.1016/j.ygeno.2007.12.005

162. Garcia-Lopez MA, Barreiro O, Garcia-Diez A, Sanchez-Madrid F, Penas PF (2005) Role of tetraspanins CD9 and CD151 in primary melanocyte motility. J Invest Dermatol 125:1001-1009. doi:10.1111/j.0022-202X.2005.23882.x

163. Gaugitsch HW, Hofer E, Huber NE, Schnabl E, Baumruker T (1991) A new superfamily of lymphoid and melanoma cell proteins with extensive homology to Schistosoma mansoni antigen Sm23. Eur J Immunol 21:377-383. doi:10.1002/eji.1830210219

164. Gerova VA, Stoynov SG, Katsarov DS, Svinarov DA (2011) Increased intestinal permeability in inflammatory bowel diseases assessed by iohexol test. World J Gastroenterol 17:2211-2215. doi:10.3748/wjg.v17.i17.

165. Ghosh S, Mitchell R (2007) Impact of inflammatory bowel disease on quality of life: Results of the European Federation of Crohn's and Ulcerative Colitis Associations (EFCCA) patient survey. J Crohns Colitis 1:10-20. doi:10.1016/j.crohns.2007.06.005

166. Gilsanz A, Sanchez-Martin L, Gutierrez-Lopez MD, Ovalle S, Machado-Pineda Y, Reyes R, Swart GW, Figdor CG, Lafuente EM, Cabanas C (2013) ALCAM/CD166 adhesive function is regulated by the tetraspanin CD9. Cell Mol Life Sci 70:475-493. doi:10.1007/s00018-012-1132-0

167. Ginzel M, Feng X, Kuebler JF, Klemann C, Yu Y, von Wasielewski R, Park JK, Hornef MW, Vieten G, Ure BM, Kaussen T, Gosemann JH, Mayer S, Suttkus A, Lacher M (2017) Dextran sodium sulfate (DSS) induces necrotizing enterocolitis-like lesions in neonatal mice. PLoS One 12:e0182732. doi:10.1371/journal.pone.0182732

168. Gironella M, Molla M, Salas A, Soriano A, Sans M, Closa D, Engel P, Pique JM, Panes J (2002) The role of P-selectin in experimental colitis as determined by antibody immunoblockade and genetically deficient mice. J Leukoc Biol 72:56-64

169. Goke M, Kanai M, Podolsky DK (1998) Intestinal fibroblasts regulate intestinal epithelial cell proliferation via hepatocyte growth factor. Am J Physiol 274:G809-818

170. Gornacz GE, Al-Mukhtar MY, Ghatei MA, Sagor GR, Wright NA, Bloom SR (1984) Pattern of cell proliferation and enteroglucagon response following small bowel resection in the rat. Digestion 29:65-72. doi:10.1159/000199012

171. Graham DB, Xavier RJ (2013) From genetics of inflammatory bowel disease towards mechanistic insights. Trends Immunol 34:371-378. doi:10.1016/j.it.2013.04.001

172. Gratkowski H, Lear JD, DeGrado WF (2001) Polar side chains drive the association of model transmembrane peptides. Proc Natl Acad Sci U S A 98:880-885. doi:10.1073/pnas.98.3.880

173. Grimm MC, Doe WF (1996) Chemokines in Inflammatory Bowel Disease Mucosa: Expression of RANTES, Macrophage Inflammatory Protein (MIP)-1alpha, MIP-1beta, and gamma-Interferon-Inducible Protein-10 by Macrophages, Lymphocytes, Endothelial Cells, and Granulomas. Inflamm Bowel Dis 2:88-96.

174. Guarner F (2008) What is the role of the enteric commensal flora in IBD? Inflamm Bowel Dis 14 Suppl 2:S83-84. doi:10.1002/ibd.20548

175. Gumbiner B (1988) Cadherins: a family of Ca2+-dependent adhesion molecules. Trends Biochem Sci 13:75-76.

176. Gutierrez-Lopez MD, Gilsanz A, Yanez-Mo M, Ovalle S, Lafuente EM, Dominguez C, Monk PN, Gonzalez-Alvaro I, Sanchez-Madrid F, Cabanas C (2011) The sheddase activity of ADAM17/TACE is regulated by the tetraspanin CD9. Cell Mol Life Sci 68:3275-3292. doi:10.1007/s00018-011-0639-0

177. Guy-Grand D, DiSanto JP, Henchoz P, Malassis-Seris M, Vassalli P (1998) Small bowel enteropathy: role of intraepithelial lymphocytes and of cytokines (IL-12, IFN-gamma, TNF) in the induction of epithelial cell death and renewal. Eur J Immunol 28:730-744. doi:10.1002/(SICI)1521-4141(199802)28:02<730::AID-IMMU730>3.0.CO;2-U.

178. Ha SA, Tsuji M, Suzuki K, Meek B, Yasuda N, Kaisho T, Fagarasan S (2006) Regulation of B1 cell migration by signals through Toll-like receptors. J Exp Med 203:2541-2550. doi:10.1084/jem.20061041

179. Hagiwara C, Tanaka M, Kudo H (2002) Increase in colorectal epithelial apoptotic cells in patients with ulcerative colitis ultimately requiring surgery. J Gastroenterol Hepatol 17:758-764. doi:2791 [pii]

180. Hakansson A, Tormo-Badia N, Baridi A, Xu J, Molin G, Hagslatt ML, Karlsson C, Jeppsson B, Cilio CM, Ahrne S (2015) Immunological alteration and changes of gut microbiota after dextran sulfate sodium (DSS) administration in mice. Clin Exp Med 15:107-120. doi:10.1007/s10238-013-0270-5

181. Halova I, Draber P (2016) Tetraspanins and Transmembrane Adaptor Proteins As Plasma Membrane Organizers-Mast Cell Case. Front Cell Dev Biol 4:43. doi:10.3389/fcell.2016.00043

182. Hamamoto N, Maemura K, Hirata I, Murano M, Sasaki S, Katsu K (1999) Inhibition of dextran sulphate sodium (DSS)-induced colitis in mice by intracolonically administered antibodies against adhesion molecules (endothelial leucocyte adhesion molecule-1 (ELAM-1) or intercellular adhesion molecule-1 (ICAM-1)). Clin Exp Immunol 117:462-468.

183. Han DS, Li F, Holt L, Connolly K, Hubert M, Miceli R, Okoye Z, Santiago G, Windle K, Wong E, Sartor RB (2000) Keratinocyte growth factor-2 (FGF-10) promotes healing of experimental small intestinal ulceration in rats. Am J Physiol Gastrointest Liver Physiol 279:G1011-1022. doi:10.1152/ajpgi.2000.279.5.G1011

184. Harbord MW, Marks DJ, Forbes A, Bloom SL, Day RM, Segal AW (2006) Impaired neutrophil chemotaxis in Crohn's disease relates to reduced production of chemokines and can be augmented by granulocyte-colony stimulating factor. Aliment Pharmacol Ther 24:651-660. doi:10.1111/j.1365-2036.2006.03016.x

185. Hart AL, Lammers K, Brigidi P, Vitali B, Rizzello F, Gionchetti P, Campieri M, Kamm MA, Knight SC, Stagg AJ (2004) Modulation of human dendritic cell phenotype and function by probiotic bacteria. Gut 53:1602-1609. doi:10.1136/gut.2003.037325

186. He XC, Zhang J, Tong WG, Tawfik O, Ross J, Scoville DH, Tian Q, Zeng X, He X, Wiedemann LM, Mishina Y, Li L (2004) BMP signaling inhibits intestinal stem cell self-renewal through suppression of Wnt-beta-catenin signaling. Nat Genet 36:1117-1121. doi:10.1038/ng1430

187. Heller F, Florian P, Bojarski C, Richter J, Christ M, Hillenbrand B, Mankertz J, Gitter AH, Burgel N, Fromm M, Zeitz M, Fuss I, Strober W, Schulzke JD (2005) Interleukin-13 is the key effector Th2 cytokine in ulcerative colitis that affects epithelial tight junctions, apoptosis, and cell restitution. Gastroenterology 129:550-564. doi:10.1016/j.gastro.2005.05.002

188. Hemler ME (2001) Specific tetraspanin functions. J Cell Biol 155:1103-1107. doi:10.1083/jcb.200108061

189. Hemler ME (2003) Tetraspanin proteins mediate cellular penetration, invasion, and fusion events and define a novel type of membrane microdomain. Annu Rev Cell Dev Biol 19:397-422. doi:10.1146/annurev.cellbio.19.111301.153609

190. Hemler ME (2005) Tetraspanin functions and associated microdomains. Nat Rev Mol Cell Biol 6:801-811. doi:10.1038/nrm1736

191. Henkle KJ, Cook GA, Foster LA, Engman DM, Bobek LA, Cain GD, Donelson JE (1990) The gene family encoding eggshell proteins of Schistosoma japonicum. Mol Biochem Parasitol 42:69-82.

192. Hermiston ML, Gordon JI (1995) Inflammatory bowel disease and adenomas in mice expressing a dominant negative N-cadherin. Science 270:1203-1207

193. Hesterberg PE, Winsor-Hines D, Briskin MJ, Soler-Ferran D, Merrill C, Mackay CR, Newman W, Ringler DJ (1996) Rapid resolution of chronic colitis in the cotton-top tamarin with an antibody to a gut-homing integrin alpha 4 beta 7. Gastroenterology 111:1373-1380.

194. Heyman MB, Garnett EA, Wojcicki J, Gupta N, Davis C, Cohen SA, Gold BD, Kirschner BS, Baldassano RN, Ferry GD, Winter HS, Kaplan S (2008) Growth hormone treatment for growth failure in pediatric patients with Crohn's disease. J Pediatr 153:651-658, 658 e651-653. doi:10.1016/j.jpeds.2008.04.064

195. Higashiyama M, Taki T, Ieki Y, Adachi M, Huang CL, Koh T, Kodama K, Doi O, Miyake M (1995) Reduced motility related protein-1 (MRP-1/CD9) gene expression as a factor of poor prognosis in non-small cell lung cancer. Cancer Res 55:6040-6044

196. Higashiyama S, Iwamoto R, Goishi K, Raab G, Taniguchi N, Klagsbrun M, Mekada E (1995) The membrane protein CD9/DRAP 27 potentiates the juxtacrine growth factor activity of the membrane-anchored heparin-binding EGF-like growth factor. J Cell Biol 128:929-938

197. Hines OJ, Ryder N, Chu J, McFadden D (2000) Lysophosphatidic acid stimulates intestinal restitution via cytoskeletal activation and remodeling. J Surg Res 92:23-28. doi:10.1006/jsre.2000.5941

198. Hirotani T, Lee PY, Kuwata H, Yamamoto M, Matsumoto M, Kawase I, Akira S, Takeda K (2005) The nuclear IkappaB protein IkappaBNS selectively inhibits lipopolysaccharide-induced IL-6 production in macrophages of the colonic lamina propria. J Immunol 174:3650-3657.

199. Hoffmann W (2005) Trefoil factors TFF (trefoil factor family) peptide-triggered signals promoting mucosal restitution. Cell Mol Life Sci 62:2932-2938. doi:10.1007/s00018-005-5481-9

200. Hollander D (1988) Crohn's disease--a permeability disorder of the tight junction? Gut 29:1621-1624

201. Hollander D (1993) Permeability in Crohn's disease: altered barrier functions in healthy relatives? Gastroenterology 104:1848-1851. doi:0016-5085(93)90668-3 [pii]

202. Hollander D, Vadheim CM, Brettholz E, Petersen GM, Delahunty T, Rotter JI (1986) Increased intestinal permeability in patients with Crohn's disease and their relatives. A possible etiologic factor. Ann Intern Med 105:883-885

203. Hoorn T, Paul P, Janssen L, Janssen H, Neefjes J (2012) Dynamics within tetraspanin pairs affect MHC class II expression. J Cell Sci 125:328-339. doi:10.1242/jcs.088047

204. Hopkins AM, Pineda AA, Winfree LM, Brown GT, Laukoetter MG, Nusrat A (2007) Organized migration of epithelial cells requires control of adhesion and protrusion through Rho kinase effectors. Am J Physiol Gastrointest Liver Physiol 292:G806-817. doi:10.1152/ajpgi.00333.2006

205. Hori H, Yano S, Koufuji K, Takeda J, Shirouzu K (2004) CD9 expression in gastric cancer and its significance. J Surg Res 117:208-215. doi:10.1016/j.jss.2004.01.014

206. Hormi K, Cadiot G, Kermorgant S, Dessirier V, Le Romancer M, Lewin MJ, Mignon M, Lehy T (2000) Transforming growth factor-alpha and epidermal growth factor receptor in colonic mucosa in active and inactive inflammatory bowel disease. Growth Factors 18:79-91

207. Horvath G, Serru V, Clay D, Billard M, Boucheix C, Rubinstein E (1998) CD19 is linked to the integrin-associated tetraspans CD9, CD81, and CD82. J Biol Chem 273:30537-30543

208. Hosoe N, Miura S, Watanabe C, Tsuzuki Y, Hokari R, Oyama T, Fujiyama Y, Nagata H, Ishii H (2004) Demonstration of functional role of TECK/CCL25 in T lymphocyte-endothelium interaction in inflamed and uninflamed intestinal mucosa. Am J Physiol Gastrointest Liver Physiol 286:G458-466. doi:10.1152/ajpgi.00167.2003

209. Hotta H, Ross AH, Huebner K, Isobe M, Wendeborn S, Chao MV, Ricciardi RP, Tsujimoto Y, Croce CM, Koprowski H (1988) Molecular cloning and characterization of an antigen associated with early stages of melanoma tumor progression. Cancer Res 48:2955-2962

210. Houle CD, Ding XY, Foley JF, Afshari CA, Barrett JC, Davis BJ (2002) Loss of expression and altered localization of KAI1 and CD9 protein are associated with epithelial ovarian cancer progression. Gynecol Oncol 86:69-78.

211. Hsu D, Fukata M, Hernandez YG, Sotolongo JP, Goo T, Maki J, Hayes LA, Ungaro RC, Chen A, Breglio KJ, Xu R, Abreu MT (2010) Toll-like receptor 4 differentially regulates epidermal growth factor-related growth factors in response to intestinal mucosal injury. Lab Invest 90:1295-1305. doi:10.1038/labinvest.2010.100

212. Hu S, Chen M, Wang Y, Wang Z, Pei Y, Fan R, Liu X, Wang L, Zhou J, Zheng S, Zhang T, Lin Y, Zhang M, Tao R, Zhong J (2016) mTOR Inhibition Attenuates Dextran Sulfate Sodium-Induced Colitis by Suppressing T Cell Proliferation and Balancing TH1/TH17/Treg Profile. PLoS One 11:e0154564. doi:10.1371/journal.pone.0154564

213. Huang CI, Kohno N, Ogawa E, Adachi M, Taki T, Miyake M (1998) Correlation of reduction in MRP-1/CD9 and KAI1/CD82 expression with recurrences in breast cancer patients. Am J Pathol 153:973-983.

214. Huang CL, Liu D, Masuya D, Kameyama K, Nakashima T, Yokomise H, Ueno M, Miyake M (2004) MRP-1/CD9 gene transduction downregulates Wnt signal pathways. Oncogene 23:7475-7483. doi:10.1038/sj.onc.1208063

215. Huang CL, Ueno M, Liu D, Masuya D, Nakano J, Yokomise H, Nakagawa T, Miyake M (2006) MRP-1/CD9 gene transduction regulates the actin cytoskeleton through the downregulation of WAVE2. Oncogene 25:6480-6488. doi:10.1038/sj.onc.1209654

216. Huang S, Yuan S, Dong M, Su J, Yu C, Shen Y, Xie X, Yu Y, Yu X, Chen S, Zhang S, Pontarotti P, Xu A (2005) The phylogenetic analysis of tetraspanins projects the evolution of cell-cell interactions from unicellular to multicellular organisms. Genomics 86:674-684. doi:10.1016/j.ygeno.2005.08.004

217. Hueber W, Sands BE, Lewitzky S, Vandemeulebroecke M, Reinisch W, Higgins PD, Wehkamp J, Feagan BG, Yao MD, Karczewski M, Karczewski J, Pezous N, Bek S, Bruin G, Mellgard B, Berger C, Londei M, Bertolino AP, Tougas G, Travis SP (2012) Secukinumab, a human anti-IL-17A monoclonal antibody, for moderate to severe Crohn's disease: unexpected results of a randomised, double-blind placebo-controlled trial. Gut 61:1693-1700. doi:10.1136/gutjnl-2011-301668

218. Hugot JP, Chamaillard M, Zouali H, Lesage S, Cezard JP, Belaiche J, Almer S, Tysk C, O'Morain CA, Gassull M, Binder V, Finkel Y, Cortot A, Modigliani R, Laurent-Puig P, Gower-Rousseau C, Macry J, Colombel JF, Sahbatou M, Thomas G (2001) Association of NOD2 leucine-rich repeat variants with susceptibility to Crohn's disease. Nature 411:599-603. doi:10.1038/35079107

219. Hwang JM, Varma MG (2008) Surgery for inflammatory bowel disease. World J Gastroenterol 14:2678-2690

220. Iizuka M, Konno S (2011) Wound healing of intestinal epithelial cells. World J Gastroenterol 17:2161-2171. doi:10.3748/wjg.v17.i17.2161

221. Ijiri K, Potten CS (1987) Further studies on the response of intestinal crypt cells of different hierarchical status to eighteen different cytotoxic agents. Br J Cancer 55:113-123

222. Indig FE, Diaz-Gonzalez F, Ginsberg MH (1997) Analysis of the tetraspanin CD9-integrin alphaIIbbeta3 (GPIIb-IIIa) complex in platelet membranes and transfected cells. Biochem J 327 (Pt 1):291-298

223. Inui S, Higashiyama S, Hashimoto K, Higashiyama M, Yoshikawa K, Taniguchi N (1997) Possible role of coexpression of CD9 with membrane-anchored heparin-binding EGF-like growth factor and amphiregulin in cultured human keratinocyte growth. J Cell Physiol 171:291-298. doi:10.1002/(SICI)1097-4652(199706)171:3<291::AID-JCP7>3.0.CO;2-J 1

224. Irvine EJ, Marshall JK (2000) Increased intestinal permeability precedes the onset of Crohn's disease in a subject with familial risk. Gastroenterology 119:1740-1744.

225. Ito H (2004) Novel therapy for Crohn's disease targeting IL-6 signalling. Expert Opin Ther Targets 8:287-294. doi:10.1517/14728222.8.4.287

226. Iwamoto M, Koji T, Makiyama K, Kobayashi N, Nakane PK (1996) Apoptosis of crypt epithelial cells in ulcerative colitis. J Pathol 180:152-159. doi:10.1002/(SICI)1096-9896(199610)180:2<152::AID-PATH649>3.0.CO;2-Y

227. Iwamoto R, Higashiyama S, Mitamura T, Taniguchi N, Klagsbrun M, Mekada E (1994) Heparin-binding EGF-like growth factor, which acts as the diphtheria toxin receptor, forms a complex with membrane protein DRAP27/CD9, which up-regulates functional receptors and diphtheria toxin sensitivity. EMBO J 13:2322-2330

228. Jager S, Stange EF, Wehkamp J (2013) Inflammatory bowel disease: an impaired barrier disease. Langenbecks Arch Surg 398:1-12. doi:10.1007/s00423-012-1030-9

229. Jandhyala SM, Talukdar R, Subramanyam C, Vuyyuru H, Sasikala M, Nageshwar Reddy D (2015) Role of the normal gut microbiota. World J Gastroenterol 21:8787-8803. doi:10.3748/wjg.v21.i29.8787

230. Janowitz HD, Croen EC, Sachar DB (1998) The role of the fecal stream in Crohn's disease: an historical and analytic review. Inflamm Bowel Dis 4:29-39

231. Jass JR, Walsh MD (2001) Altered mucin expression in the gastrointestinal tract: a review. J Cell Mol Med 5:327-351.

232. Jess T, Gamborg M, Matzen P, Munkholm P, Sorensen TI (2005) Increased risk of intestinal cancer in Crohn's disease: a meta-analysis of population-based cohort studies. Am J Gastroenterol 100:2724-2729. doi:10.1111/j.1572-0241.2005.00287.x

233. Johansson ME (2014) Mucus layers in inflammatory bowel disease. Inflamm Bowel Dis 20:2124-2131. doi:10.1097/MIB.0000000000000117

234. Johansson ME, Phillipson M, Petersson J, Velcich A, Holm L, Hansson GC (2008) The inner of the two Muc2 mucin-dependent mucus layers in colon is devoid of bacteria. Proc Natl Acad Sci U S A 105:15064-15069. doi:10.1073/pnas.0803124105

235. Johnston RD, Logan RF (2008) What is the peak age for onset of IBD? Inflamm Bowel Dis 14 Suppl 2:S4-5. doi:10.1002/ibd.20545

236. Jones PH, Bishop LA, Watt FM (1996) Functional significance of CD9 association with beta 1 integrins in human epidermal keratinocytes. Cell Adhes Commun 4:297-305

237. Jones SC, Banks RE, Haidar A, Gearing AJ, Hemingway IK, Ibbotson SH, Dixon MF, Axon AT (1995) Adhesion molecules in inflammatory bowel disease. Gut 36:724-730

238. Julian MW, Bao S, Knoell DL, Fahy RJ, Shao G, Crouser ED (2011) Intestinal epithelium is more susceptible to cytopathic injury and altered permeability than the lung epithelium in the context of acute sepsis. Int J Exp Pathol 92:366-376. doi:10.1111/j.1365-2613.2011.00783.x

239. Jung KK, Liu XW, Chirco R, Fridman R, Kim HR (2006) Identification of CD63 as a tissue inhibitor of metalloproteinase-1 interacting cell surface protein. EMBO J 25:3934-3942. doi:10.1038/sj.emboj.7601281

240. Kahrstrom CT, Pariente N, Weiss U (2016) Intestinal microbiota in health and disease. Nature 535:47. doi:10.1038/535047a

241. Kaji K, Takeshita S, Miyake K, Takai T, Kudo A (2001) Functional association of CD9 with the Fc gamma receptors in macrophages. J Immunol 166:3256-3265

242. Kansas GS, Pavalko FM (1996) The cytoplasmic domains of E- and P-selectin do not constitutively interact with alpha-actinin and are not essential for leukocyte adhesion. J Immunol 157:321-325

243. Kaplan GG (2015) The global burden of IBD: from 2015 to 2025. Nat Rev Gastroenterol Hepatol 12:720-727. doi:10.1038/nrgastro.2015.150

244. Kaplan GG, Jess T (2016) The Changing Landscape of Inflammatory Bowel Disease: East Meets West. Gastroenterology 150:24-26. doi:10.1053/j.gastro.2015.11.029

245. Kaplan GG, Ng SC (2017) Understanding and Preventing the Global Increase of Inflammatory Bowel Disease. Gastroenterology 152:313-321 e312. doi:10.1053/j.gastro.2016.10.020

246. Kappelman MD, Rifas-Shiman SL, Porter CQ, Ollendorf DA, Sandler RS, Galanko JA, Finkelstein JA (2008) Direct health care costs of Crohn's disease and ulcerative colitis in US children and adults. Gastroenterology 135:1907-1913. doi:10.1053/j.gastro.2008.09.012

247. Karayiannakis AJ, Syrigos KN, Efstathiou J, Valizadeh A, Noda M, Playford RJ, Kmiot W, Pignatelli M (1998) Expression of catenins and E-cadherin during epithelial restitution in inflammatory bowel disease. J Pathol 185:413-418. doi:10.1002/(SICI)1096-9896(199808)185:4<413::AID-PATH125>3.0.CO;2-K

248. Katz KD, Hollander D, Vadheim CM, McElree C, Delahunty T, Dadufalza VD, Krugliak P, Rotter JI (1989) Intestinal permeability in patients with Crohn's disease and their healthy relatives. Gastroenterology 97:927-931.

249. Kawachi S, Jennings S, Panes J, Cockrell A, Laroux FS, Gray L, Perry M, van der Heyde H, Balish E, Granger DN, Specian RA, Grisham MB (2000) Cytokine and endothelial cell adhesion molecule expression in interleukin-10-deficient mice. Am J Physiol Gastrointest Liver Physiol 278:G734-743. doi:10.1152/ajpgi.2000.278.5.G734

250. Kawachi S, Morise Z, Jennings SR, Conner E, Cockrell A, Laroux FS, Chervenak RP, Wolcott M, van der Heyde H, Gray L, Feng L, Granger DN, Specian RA, Grisham MB (2000) Cytokine and adhesion molecule expression in SCID mice reconstituted with CD4+ T cells. Inflamm Bowel Dis 6:171-180

251. Kedinger M, Lefebvre O, Duluc I, Freund JN, Simon-Assmann P (1998) Cellular and molecular partners involved in gut morphogenesis and differentiation. Philos Trans R Soc Lond B Biol Sci 353:847-856. doi:10.1098/rstb.1998.0249

252. Kenny EE, Pe'er I, Karban A, Ozelius L, Mitchell AA, Ng SM, Erazo M, Ostrer H, Abraham C, Abreu MT, Atzmon G, Barzilai N, Brant SR, Bressman S, Burns ER, Chowers Y, Clark LN, Darvasi A, Doheny D, Duerr RH, Eliakim R, Giladi N, Gregersen PK, Hakonarson H, Jones MR, Marder K, McGovern DP, Mulle J, Orr-Urtreger A, Proctor DD, Pulver A, Rotter JI, Silverberg MS, Ullman T, Warren ST, Waterman M, Zhang W, Bergman A, Mayer L, Katz S, Desnick RJ, Cho JH, Peter I (2012) A genome-wide scan of Ashkenazi Jewish Crohn's disease suggests novel susceptibility loci. PLoS Genet 8:e1002559. doi:10.1371/journal.pgen.1002559

253. Kersey JH, LeBien TW, Abramson CS, Newman R, Sutherland R, Greaves M (1981) P-24: a human leukemia-associated and lymphohemopoietic progenitor cell surface structure identified with monoclonal antibody. J Exp Med 153:726-731

254. Khan KJ, Ullman TA, Ford AC, Abreu MT, Abadir A, Marshall JK, Talley NJ, Moayyedi P (2011) Antibiotic therapy in inflammatory bowel disease: a systematic review and meta-analysis. Am J Gastroenterol 106:661-673. doi:10.1038/ajg.2011.72

255. Khandelwal S, Roche PA (2010) Distinct MHC class II molecules are associated on the dendritic cell surface in cholesterol-dependent membrane microdomains. J Biol Chem 285:35303-35310. doi:10.1074/jbc.M110.147793

256. Khor B, Gardet A, Xavier RJ (2011) Genetics and pathogenesis of inflammatory bowel disease. Nature 474:307-317. doi:10.1038/nature10209

257. Khounlotham M, Kim W, Peatman E, Nava P, Medina-Contreras O, Addis C, Koch S, Fournier B, Nusrat A, Denning TL, Parkos CA (2012) Compromised intestinal epithelial barrier induces adaptive immune compensation that protects from colitis. Immunity 37:563-573. doi:10.1016/j.immuni.2012.06.017

258. Kiesler P, Fuss IJ, Strober W (2015) Experimental Models of Inflammatory Bowel Diseases. Cell Mol Gastroenterol Hepatol 1:154-170. doi:10.1016/j.jcmgh.2015.01.006

259. Kim TW, Seo JN, Suh YH, Park HJ, Kim JH, Kim JY, Oh KI (2006) Involvement of lymphocytes in dextran sulfate sodium-induced experimental colitis. World J Gastroenterol 12:302-305

260. King CL, Xianli J, June CH, Abe R, Lee KP (1996) CD28-deficient mice generate an impaired Th2 response to Schistosoma mansoni infection. Eur J Immunol 26:2448-2455. doi:10.1002/eji.1830261027

261. Kishida K, Kohyama M, Kurashima Y, Kogure Y, Wang J, Hirayasu K, Suenaga T, Kiyono H, Kunisawa J, Arase H (2015) Negative regulation of DSS-induced experimental colitis by PILRalpha. Int Immunol 27:307-314. doi:10.1093/intimm/dxv004

262. Kitadokoro K, Bordo D, Galli G, Petracca R, Falugi F, Abrignani S, Grandi G, Bolognesi M (2001) CD81 extracellular domain 3D structure: insight into the tetraspanin superfamily structural motifs. EMBO J 20:12-18. doi:10.1093/emboj/20.1.12

263. Kitadokoro K, Galli G, Petracca R, Falugi F, Grandi G, Bolognesi M (2001) Crystallization and preliminary crystallographic studies on the large extracellular domain of human CD81, a tetraspanin receptor for hepatitis C virus. Acta Crystallogr D Biol Crystallogr 57:156-158.

264. Ko TC, Yu W, Sakai T, Sheng H, Shao J, Beauchamp RD, Thompson EA (1998) TGF-beta1 effects on proliferation of rat intestinal epithelial cells are due to inhibition of cyclin D1 expression. Oncogene 16:3445-3454. doi:10.1038/sj.onc.1201902

265. Kobayashi H, Hosono O, Iwata S, Kawasaki H, Kuwana M, Tanaka H, Dang NH, Morimoto C (2004) The tetraspanin CD9 is preferentially expressed on the human CD4(+)CD45RA+ naive T cell population and is involved in T cell activation. Clin Exp Immunol 137:101-108. doi:10.1111/j.1365-2249.2004.02494.x

266. Kohmo S, Kijima T, Otani Y, Mori M, Minami T, Takahashi R, Nagatomo I, Takeda Y, Kida H, Goya S, Yoshida M, Kumagai T, Tachibana I, Yokota S, Kawase I (2010) Cell surface tetraspanin CD9 mediates chemoresistance in small cell lung cancer. Cancer Res 70:8025-8035. doi:10.1158/0008-5472.CAN-10-0996

267. Kolaczkowska E, Kubes P (2013) Neutrophil recruitment and function in health and inflammation. Nat Rev Immunol 13:159-175. doi:10.1038/nri3399

268. Kolesnikova TV, Kazarov AR, Lemieux ME, Lafleur MA, Kesari S, Kung AL, Hemler ME (2009) Glioblastoma inhibition by cell surface immunoglobulin protein EWI-2, in vitro and in vivo. Neoplasia 11:77-86, 74p following 86

269. Kolesnikova TV, Stipp CS, Rao RM, Lane WS, Luscinskas FW, Hemler ME (2004) EWI-2 modulates lymphocyte integrin alpha4beta1 functions. Blood 103:3013-3019. doi:10.1182/blood-2003-07-2201

270. Komatsu S, Nimura Y, Granger DN (1999) Intestinal stasis associated bowel inflammation. World J Gastroenterol 5:518-521

271. Kondamudi PK, Kovelamudi H, Mathew G, Nayak PG, Rao CM, Shenoy RR (2013) Modulatory effects of sesamol in dinitrochlorobenzene-induced inflammatory bowel disorder in albino rats. Pharmacol Rep 65:658-665.

272. Korinek V, Barker N, Moerer P, van Donselaar E, Huls G, Peters PJ, Clevers H (1998) Depletion of epithelial stem-cell compartments in the small intestine of mice lacking Tcf-4. Nat Genet 19:379-383. doi:10.1038/1270

273. Korzenik JR, Dieckgraefe BK, Valentine JF, Hausman DF, Gilbert MJ (2005) Sargramostim for active Crohn's disease. N Engl J Med 352:2193-2201. doi:10.1056/NEJMoa041109

274. Kotha J, Longhurst C, Appling W, Jennings LK (2008) Tetraspanin CD9 regulates beta 1 integrin activation and enhances cell motility to fibronectin via a PI-3 kinase-dependent pathway. Exp Cell Res 314:1811-1822. doi:10.1016/j.yexcr.2008.01.024

275. Kovalenko OV, Metcalf DG, DeGrado WF, Hemler ME (2005) Structural organization and interactions of transmembrane domains in tetraspanin proteins. BMC Struct Biol 5:11. doi:10.1186/1472-6807-5-11

276. Kovalenko OV, Yang XH, Hemler ME (2007) A novel cysteine cross-linking method reveals a direct association between claudin-1 and tetraspanin CD9. Mol Cell Proteomics 6:1855-1867. doi:10.1074/mcp.M700183-MCP200

277. Krieglstein CF, Cerwinka WH, Sprague AG, Laroux FS, Grisham MB, Koteliansky VE, Senninger N, Granger DN, de Fougerolles AR (2002) Collagen-binding integrin alpha1beta1 regulates intestinal inflammation in experimental colitis. J Clin Invest 110:1773-1782. doi:10.1172/JCI15256

278. Krishnan K, Arnone B, Buchman A (2011) Intestinal growth factors: potential use in the treatment of inflammatory bowel disease and their role in mucosal healing. Inflamm Bowel Dis 17:410-422. doi:10.1002/ibd.21316

279. Kropshofer H, Spindeldreher S, Rohn TA, Platania N, Grygar C, Daniel N, Wolpl A, Langen H, Horejsi V, Vogt AB (2002) Tetraspan microdomains distinct from lipid rafts enrich select peptide-MHC class II complexes. Nat Immunol 3:61-68. doi:10.1038/ni750

280. Kruger P, Saffarzadeh M, Weber AN, Rieber N, Radsak M, von Bernuth H, Benarafa C, Roos D, Skokowa J, Hartl D (2015) Neutrophils: Between host defence, immune modulation, and tissue injury. PLoS Pathog 11:e1004651. doi:10.1371/journal.ppat.1004651

281. Kucharzik T, Walsh SV, Chen J, Parkos CA, Nusrat A (2001) Neutrophil transmigration in inflammatory bowel disease is associated with differential expression of epithelial intercellular junction proteins. Am J Pathol 159:2001-2009. doi:10.1016/S0002-9440(10)63051-9

282. Kuhl AA, Kakirman H, Janotta M, Dreher S, Cremer P, Pawlowski NN, Loddenkemper C, Heimesaat MM, Grollich K, Zeitz M, Farkas S, Hoffmann JC (2007) Aggravation of different types of experimental colitis by depletion or adhesion blockade of neutrophils. Gastroenterology 133:1882-1892. doi:10.1053/j.gastro.2007.08.073

283. Kuhn KA, Manieri NA, Liu TC, Stappenbeck TS (2014) IL-6 stimulates intestinal epithelial proliferation and repair after injury. PLoS One 9:e114195. doi:10.1371/journal.pone.0114195

284. Kuhn R, Lohler J, Rennick D, Rajewsky K, Muller W (1993) Interleukin-10-deficient mice develop chronic enterocolitis. Cell 75:263-274.

285. Kuhn S, Koch M, Nubel T, Ladwein M, Antolovic D, Klingbeil P, Hildebrand D, Moldenhauer G, Langbein L, Franke WW, Weitz J, Zoller M (2007) A complex of EpCAM, claudin-7, CD44 variant isoforms, and tetraspanins promotes colorectal cancer progression. Mol Cancer Res 5:553-567. doi:10.1158/1541-7786.MCR-06-0384

286. Kullmann F, Messmann H, Alt M, Gross V, Bocker T, Scholmerich J, Ruschoff J (2001) Clinical and histopathological features of dextran sulfate sodium induced acute and chronic colitis associated with dysplasia in rats. Int J Colorectal Dis 16:238-246

287. Lacy ER (1988) Epithelial restitution in the gastrointestinal tract. J Clin Gastroenterol 10 Suppl 1:S72-77

288. Ladwein M, Pape UF, Schmidt DS, Schnolzer M, Fiedler S, Langbein L, Franke WW, Moldenhauer G, Zoller M (2005) The cell-cell adhesion molecule EpCAM interacts directly with the tight junction protein claudin-7. Exp Cell Res 309:345-357. doi:10.1016/j.yexcr.2005.06.013

289. Lagaudriere-Gesbert C, Le Naour F, Lebel-Binay S, Billard M, Lemichez E, Boquet P, Boucheix C, Conjeaud H, Rubinstein E (1997) Functional analysis of four tetraspans, CD9, CD53, CD81, and CD82, suggests a common role in costimulation, cell adhesion, and migration: only CD9 upregulates HB-EGF activity. Cell Immunol 182:105-112.

290. Lajczak NK, Saint-Criq V, O'Dwyer AM, Perino A, Adorini L, Schoonjans K, Keely SJ (2017) Bile acids deoxycholic acid and ursodeoxycholic acid differentially regulate human beta-defensin-1 and -2 secretion by colonic epithelial cells. FASEB J 31:3848-3857. doi:10.1096/fj.201601365R

291. Lakatos PL (2009) Environmental factors affecting inflammatory bowel disease: have we made progress? Dig Dis 27:215-225. doi:10.1159/000228553

292. Laroui H, Ingersoll SA, Liu HC, Baker MT, Ayyadurai S, Charania MA, Laroui F, Yan Y, Sitaraman SV, Merlin D (2012) Dextran sodium sulfate (DSS) induces colitis in mice by forming nano-lipocomplexes with medium-chain-length fatty acids in the colon. PLoS One 7:e32084. doi:10.1371/journal.pone.0032084

293. Larsson JM, Karlsson H, Crespo JG, Johansson ME, Eklund L, Sjovall H, Hansson GC (2011) Altered O-glycosylation profile of MUC2 mucin occurs in active ulcerative colitis and is associated with increased inflammation. Inflamm Bowel Dis 17:2299-2307. doi:10.1002/ibd.21625

294. Laukoetter MG, Nava P, Lee WY, Severson EA, Capaldo CT, Babbin BA, Williams IR, Koval M, Peatman E, Campbell JA, Dermody TS, Nusrat A, Parkos CA (2007) JAM-A regulates permeability and inflammation in the intestine in vivo. J Exp Med 204:3067-3076. doi:10.1084/jem.20071416

295. Laurence A, Tato CM, Davidson TS, Kanno Y, Chen Z, Yao Z, Blank RB, Meylan F, Siegel R, Hennighausen L, Shevach EM, O'Shea J J (2007) Interleukin-2 signaling via STAT5 constrains T helper 17 cell generation. Immunity 26:371-381. doi:10.1016/j.immuni.2007.02.009

296. Le Naour F, Andre M, Boucheix C, Rubinstein E (2006) Membrane microdomains and proteomics: lessons from tetraspanin microdomains and comparison with lipid rafts. Proteomics 6:6447-6454. doi:10.1002/pmic.200600282

297. Le Naour F, Andre M, Greco C, Billard M, Sordat B, Emile JF, Lanza F, Boucheix C, Rubinstein E (2006) Profiling of the tetraspanin web of human colon cancer cells. Mol Cell Proteomics 5:845-857. doi:10.1074/mcp.M500330-MCP200

298. Lee JM, Lee KM (2016) Endoscopic Diagnosis and Differentiation of Inflammatory Bowel Disease. Clin Endosc 49:370-375. doi:10.5946/ce.2016.090

299. Lees CW, Barrett JC, Parkes M, Satsangi J (2011) New IBD genetics: common pathways with other diseases. Gut 60:1739-1753. doi:10.1136/gut.2009.199679

300. Lei-Leston AC, Murphy AG, Maloy KJ (2017) Epithelial Cell Inflammasomes in Intestinal Immunity and Inflammation. Front Immunol 8:1168. doi:10.3389/fimmu.2017.01168

301. Lei Z, Maeda T, Tamura A, Nakamura T, Yamazaki Y, Shiratori H, Yashiro K, Tsukita S, Hamada H (2012) EpCAM contributes to formation of functional tight junction in the intestinal epithelium by recruiting claudin proteins. Dev Biol 371:136-145. doi:10.1016/j.ydbio.2012.07.005

302. Leppkes M, Roulis M, Neurath MF, Kollias G, Becker C (2014) Pleiotropic functions of TNF-alpha in the regulation of the intestinal epithelial response to inflammation. Int Immunol 26:509-515. doi:10.1093/intimm/dxu051

303. Levy S, Shoham T (2005) The tetraspanin web modulates immune-signalling complexes. Nat Rev Immunol 5:136-148. doi:10.1038/nri1548

304. Ley K (2003) The role of selectins in inflammation and disease. Trends Mol Med 9:263-268.

305. Li M, Wu Y, Hu Y, Zhao L, Zhang C (2017) Initial gut microbiota structure affects sensitivity to DSS-induced colitis in a mouse model. Sci China Life Sci. doi:10.1007/s11427-017-9097-0

306. Li X, Sundquist J, Hemminki K, Sundquist K (2011) Risk of inflammatory bowel disease in first- and second-generation immigrants in Sweden: a nationwide follow-up study. Inflamm Bowel Dis 17:1784-1791. doi:10.1002/ibd.21535

307. Liao W, Lin JX, Leonard WJ (2011) IL-2 family cytokines: new insights into the complex roles of IL-2 as a broad regulator of T helper cell differentiation. Curr Opin Immunol 23:598-604. doi:10.1016/j.coi.2011.08.003

308. Liao W, Schones DE, Oh J, Cui Y, Cui K, Roh TY, Zhao K, Leonard WJ (2008) Priming for T helper type 2 differentiation by interleukin 2-mediated induction of interleukin 4 receptor alpha-chain expression. Nat Immunol 9:1288-1296. doi:10.1038/ni.1656

309. Lineberry N, Su L, Soares L, Fathman CG (2008) The single subunit transmembrane E3 ligase gene related to anergy in lymphocytes (GRAIL) captures and then ubiquitinates transmembrane proteins across the cell membrane. J Biol Chem 283:28497-28505. doi:10.1074/jbc.M805092200

310. Lipkin M, Bell B, Sherlock P (1963) Cell Proliferation Kinetics in the Gastrointestinal Tract of Man. I. Cell Renewal in Colon and Rectum. J Clin Invest 42:767-776. doi:10.1172/JCI104769

311. Little KD, Hemler ME, Stipp CS (2004) Dynamic regulation of a GPCR-tetraspanin-G protein complex on intact cells: central role of CD81 in facilitating GPR56-Galpha q/11 association. Mol Biol Cell 15:2375-2387. doi:10.1091/mbc.E03-12-0886

312. Litvinov SV, Velders MP, Bakker HA, Fleuren GJ, Warnaar SO (1994) Ep-CAM: a human epithelial antigen is a homophilic cell-cell adhesion molecule. J Cell Biol 125:437-446

313. Liu JZ, Anderson CA (2014) Genetic studies of Crohn's disease: past, present and future. Best Pract Res Clin Gastroenterol 28:373-386. doi:10.1016/j.bpg.2014.04.009

314. Liu TC, Gurram B, Baldridge MT, Head R, Lam V, Luo C, Cao Y, Simpson P, Hayward M, Holtz ML, Bousounis P, Noe J, Lerner D, Cabrera J, Biank V, Stephens M, Huttenhower C, McGovern DP, Xavier RJ, Stappenbeck TS, Salzman NH (2016) Paneth cell defects in Crohn's disease patients promote dysbiosis. JCI Insight 1:e86907. doi:10.1172/jci.insight.86907

315. Loddo I, Romano C (2015) Inflammatory Bowel Disease: Genetics, Epigenetics, and Pathogenesis. Front Immunol 6:551. doi:10.3389/fimmu.2015.00551

316. Longhurst CM, Jacobs JD, White MM, Crossno JT, Jr., Fitzgerald DA, Bao J, Fitzgerald TJ, Raghow R, Jennings LK (2002) Chinese hamster ovary cell motility to fibronectin is modulated by the second extracellular loop of CD9. Identification of a putative fibronectin binding site. J Biol Chem 277:32445-32452. doi:10.1074/jbc.M204420200

317. Longhurst CM, White MM, Wilkinson DA, Jennings LK (1999) A CD9, alphaIIbbeta3, integrin-associated protein, and GPIb/V/IX complex on the surface of human platelets is influenced by alphaIIbbeta3 conformational states. Eur J Biochem 263:104-111.

318. Longo N, Yanez-Mo M, Mittelbrunn M, de la Rosa G, Munoz ML, Sanchez-Madrid F, Sanchez-Mateos P (2001) Regulatory role of tetraspanin CD9 in tumor-endothelial cell interaction during transendothelial invasion of melanoma cells. Blood 98:3717-3726

319. Lotz MM, Nusrat A, Madara JL, Ezzell R, Wewer UM, Mercurio AM (1997) Intestinal epithelial restitution. Involvement of specific laminin isoforms and integrin laminin receptors in wound closure of a transformed model epithelium. Am J Pathol 150:747-760

320. Lotz MM, Rabinovitz I, Mercurio AM (2000) Intestinal restitution: progression of actin cytoskeleton rearrangements and integrin function in a model of epithelial wound healing. Am J Pathol 156:985-996. doi:10.1016/S0002-9440(10)64966-8

321. Lozahic S, Christiansen D, Manie S, Gerlier D, Billard M, Boucheix C, Rubinstein E (2000) CD46 (membrane cofactor protein) associates with multiple beta1 integrins and tetraspans. Eur J Immunol 30:900-907. doi:10.1002/1521-4141(200003)30:3<900::AID-IMMU900>3.0.CO;2-X

322. Luckheeram RV, Zhou R, Verma AD, Xia B (2012) CD4(+)T cells: differentiation and functions. Clin Dev Immunol 2012:925135. doi:10.1155/2012/925135

323. Lund PK, Moats-Staats BM, Hynes MA, Simmons JG, Jansen M, D'Ercole AJ, Van Wyk JJ (1986) Somatomedin-C/insulin-like growth factor-I and insulin-like growth factor-II mRNAs in rat fetal and adult tissues. J Biol Chem 261:14539-14544

324. Lynch SV, Pedersen O (2016) The Human Intestinal Microbiome in Health and Disease. N Engl J Med 375:2369-2379. doi:10.1056/NEJMra1600266

325. Llopis M, Antolin M, Carol M, Borruel N, Casellas F, Martinez C, Espin-Basany E, Guarner F, Malagelada JR (2009) Lactobacillus casei downregulates commensals' inflammatory signals in Crohn's disease mucosa. Inflamm Bowel Dis 15:275-283. doi:10.1002/ibd.20736

326. Macpherson AJ (2006) IgA adaptation to the presence of commensal bacteria in the intestine. Curr Top Microbiol Immunol 308:117-136

327. Maecker HT, Todd SC, Levy S (1997) The tetraspanin superfamily: molecular facilitators. FASEB J 11:428-442

328. Maetzel D, Denzel S, Mack B, Canis M, Went P, Benk M, Kieu C, Papior P, Baeuerle PA, Munz M, Gires O (2009) Nuclear signalling by tumour-associated antigen EpCAM. Nat Cell Biol 11:162-171. doi:10.1038/ncb1824

329. Mankertz J, Schulzke JD (2007) Altered permeability in inflammatory bowel disease: pathophysiology and clinical implications. Curr Opin Gastroenterol 23:379-383. doi:10.1097/MOG.0b013e32816aa392

330. Manninen A (2015) Epithelial polarity--generating and integrating signals from the ECM with integrins. Exp Cell Res 334:337-349. doi:10.1016/j.yexcr.2015.01.003

331. Mannon PJ, Fuss IJ, Mayer L, Elson CO, Sandborn WJ, Present D, Dolin B, Goodman N, Groden C, Hornung RL, Quezado M, Yang Z, Neurath MF, Salfeld J, Veldman GM, Schwertschlag U, Strober W (2004) Anti-interleukin-12 antibody for active Crohn's disease. N Engl J Med 351:2069-2079. doi:10.1056/NEJMoa033402

332. Mantegazza AR, Barrio MM, Moutel S, Bover L, Weck M, Brossart P, Teillaud JL, Mordoh J (2004) CD63 tetraspanin slows down cell migration and translocates to the endosomal-lysosomal-MIICs route after extracellular stimuli in human immature dendritic cells. Blood 104:1183-1190. doi:10.1182/blood-2004-01-0104

333. Marchiando AM, Graham WV, Turner JR (2010) Epithelial barriers in homeostasis and disease. Annu Rev Pathol 5:119-144. doi:10.1146/annurev.pathol.4.110807.092135

334. Mariadason JM, Bordonaro M, Aslam F, Shi L, Kuraguchi M, Velcich A, Augenlicht LH (2001) Down-regulation of beta-catenin TCF signaling is linked to colonic epithelial cell differentiation. Cancer Res 61:3465-3471

335. Marjon KD, Termini CM, Karlen KL, Saito-Reis C, Soria CE, Lidke KA, Gillette JM (2016) Tetraspanin CD82 regulates bone marrow homing of acute myeloid leukemia by modulating the molecular organization of N-cadherin. Oncogene 35:4132-4140. doi:10.1038/onc.2015.449

336. Marlin SD, Springer TA (1987) Purified intercellular adhesion molecule-1 (ICAM-1) is a ligand for lymphocyte function-associated antigen 1 (LFA-1). Cell 51:813-819. doi:0092-8674(87)90104-8 [pii]

337. Martinez C, Lobo B, Pigrau M, Ramos L, Gonzalez-Castro AM, Alonso C, Guilarte M, Guila M, de Torres I, Azpiroz F, Santos J, Vicario M (2013) Diarrhoea-predominant irritable bowel syndrome: an organic disorder with structural abnormalities in the jejunal epithelial barrier. Gut 62:1160-1168. doi:10.1136/gutjnl-2012-302093

338. Matsuura M, Okazaki K, Nishio A, Nakase H, Tamaki H, Uchida K, Nishi T, Asada M, Kawasaki K, Fukui T, Yoshizawa H, Ohashi S, Inoue S, Kawanami C, Hiai H, Tabata Y, Chiba T (2005) Therapeutic effects of rectal administration of basic fibroblast growth factor on experimental murine colitis. Gastroenterology 128:975-986.

339. Maunder RG (2005) Evidence that stress contributes to inflammatory bowel disease: evaluation, synthesis, and future directions. Inflamm Bowel Dis 11:600-608.

340. Mawdsley JE, Rampton DS (2005) Psychological stress in IBD: new insights into pathogenic and therapeutic implications. Gut 54:1481-1491. doi:10.1136/gut.2005.064261

341. May GR, Sutherland LR, Meddings JB (1993) Is small intestinal permeability really increased in relatives of patients with Crohn's disease? Gastroenterology 104:1627-1632.

342. McCafferty DM, Smith CW, Granger DN, Kubes P (1999) Intestinal inflammation in adhesion molecule-deficient mice: an assessment of P-selectin alone and in combination with ICAM-1 or E-selectin. J Leukoc Biol 66:67-74

343. McConnell BB, Kim SS, Bialkowska AB, Yu K, Sitaraman SV, Yang VW (2011) Kruppel-like factor 5 protects against dextran sulfate sodium-induced colonic injury in mice by promoting epithelial repair. Gastroenterology 140:540-549 e542. doi:10.1053/j.gastro.2010.10.061

344. McGee DW, Vitkus SJ (1996) IL-4 enhances IEC-6 intestinal epithelial cell proliferation yet has no effect on IL-6 secretion. Clin Exp Immunol 105:274-277

345. McGovern DP, Kugathasan S, Cho JH (2015) Genetics of Inflammatory Bowel Diseases. Gastroenterology 149:1163-1176 e1162. doi:10.1053/j.gastro.2015.08.001

346. Meenan J, Hommes DW, Mevissen M, Dijkhuizen S, Soule H, Moyle M, Buller HR, ten Kate FW, Tytgat GN, van Deventer SJ (1996) Attenuation of the inflammatory response in an animal colitis model by neutrophil inhibitory factor, a novel beta 2-integrin antagonist. Scand J Gastroenterol 31:786-791

347. Melgar S, Karlsson L, Rehnstrom E, Karlsson A, Utkovic H, Jansson L, Michaelsson E (2008) Validation of murine dextran sulfate sodium-induced colitis using four therapeutic agents for human inflammatory bowel disease. Int Immunopharmacol 8:836-844. doi:10.1016/j.intimp.2008.01.036

348. Merger M, Viney JL, Borojevic R, Steele-Norwood D, Zhou P, Clark DA, Riddell R, Maric R, Podack ER, Croitoru K (2002) Defining the roles of perforin, Fas/FasL, and tumour necrosis factor alpha in T cell induced mucosal damage in the mouse intestine. Gut 51:155-163

349. Merritt AJ, Potten CS, Watson AJ, Loh DY, Nakayama K, Hickman JA (1995) Differential expression of bcl-2 in intestinal epithelia. Correlation with attenuation of apoptosis in colonic crypts and the incidence of colonic neoplasia. J Cell Sci 108 (Pt 6):2261-2271

350. Miao WM, Vasile E, Lane WS, Lawler J (2001) CD36 associates with CD9 and integrins on human blood platelets. Blood 97:1689-1696

351. Miceli R, Hubert M, Santiago G, Yao DL, Coleman TA, Huddleston KA, Connolly K (1999) Efficacy of keratinocyte growth factor-2 in dextran sulfate sodium-induced murine colitis. J Pharmacol Exp Ther 290:464-471

352. Michielan A, D'Inca R (2015) Intestinal Permeability in Inflammatory Bowel Disease: Pathogenesis, Clinical Evaluation, and Therapy of Leaky Gut. Mediators Inflamm 2015:628157. doi:10.1155/2015/628157

353. Min G, Wang H, Sun TT, Kong XP (2006) Structural basis for tetraspanin functions as revealed by the cryo-EM structure of uroplakin complexes at 6-A resolution. J Cell Biol 173:975-983. doi:10.1083/jcb.200602086

354. Mittelbrunn M, Martinez del Hoyo G, Lopez-Bravo M, Martin-Cofreces NB, Scholer A, Hugues S, Fetler L, Amigorena S, Ardavin C, Sanchez-Madrid F (2009) Imaging of plasmacytoid dendritic cell interactions with T cells. Blood 113:75-84. doi:10.1182/blood-2008-02-139865

355. Miyake M, Inufusa H, Adachi M, Ishida H, Hashida H, Tokuhara T, Kakehi Y (2000) Suppression of pulmonary metastasis using adenovirally motility related protein-1 (MRP-1/CD9) gene delivery. Oncogene 19:5221-5226. doi:10.1038/sj.onc.1203919

356. Miyake M, Koyama M, Seno M, Ikeyama S (1991) Identification of the motility-related protein (MRP-1), recognized by monoclonal antibody M31-15, which inhibits cell motility. J Exp Med 174:1347-1354

357. Miyake M, Nakano K, Ieki Y, Adachi M, Huang CL, Itoi S, Koh T, Taki T (1995) Motility related protein 1 (MRP-1/CD9) expression: inverse correlation with metastases in breast cancer. Cancer Res 55:4127-4131

358. Miyake M, Nakano K, Itoi SI, Koh T, Taki T (1996) Motility-related protein-1 (MRP-1/CD9) reduction as a factor of poor prognosis in breast cancer. Cancer Res 56:1244-1249

359. Monteleone G, Biancone L, Marasco R, Morrone G, Marasco O, Luzza F, Pallone F (1997) Interleukin 12 is expressed and actively released by Crohn's disease intestinal lamina propria mononuclear cells. Gastroenterology 112:1169-1178.

360. Monteleone G, MacDonald TT, Wathen NC, Pallone F, Pender SL (1999) Enhancing Lamina propria Th1 cell responses with interleukin 12 produces severe tissue injury. Gastroenterology 117:1069-1077.

361. Monteleone G, Pallone F (2015) Mongersen, an Oral SMAD7 Antisense Oligonucleotide, and Crohn's Disease. N Engl J Med 372:2461. doi:10.1056/NEJMc1504845

362. Moore RJ, Stanley D (2016) Experimental design considerations in microbiota/inflammation studies. Clin Transl Immunology 5:e92. doi:10.1038/cti.2016.41

363. Mori M, Mimori K, Shiraishi T, Haraguchi M, Ueo H, Barnard GF, Akiyoshi T (1998) Motility related protein 1 (MRP1/CD9) expression in colon cancer. Clin Cancer Res 4:1507-1510

364. Morrissey PJ, Charrier K, Braddy S, Liggitt D, Watson JD (1993) CD4+ T cells that express high levels of CD45RB induce wasting disease when transferred into congenic severe combined immunodeficient mice. Disease development is prevented by cotransfer of purified CD4+ T cells. J Exp Med 178:237-244

365. Moss SF, Attia L, Scholes JV, Walters JR, Holt PR (1996) Increased small intestinal apoptosis in coeliac disease. Gut 39:811-817

366. Mottet C, Uhlig HH, Powrie F (2003) Cutting edge: cure of colitis by CD4+CD25+ regulatory T cells. J Immunol 170:3939-3943

367. Mucida D, Park Y, Kim G, Turovskaya O, Scott I, Kronenberg M, Cheroutre H (2007) Reciprocal TH17 and regulatory T cell differentiation mediated by retinoic acid. Science 317:256-260. doi:10.1126/science.1145697

368. Mueller JL, McGeough MD, Pena CA, Sivagnanam M (2014) Functional consequences of EpCam mutation in mice and men. Am J Physiol Gastrointest Liver Physiol 306:G278-288. doi:10.1152/ajpgi.00286.2013

369. Munz M, Baeuerle PA, Gires O (2009) The emerging role of EpCAM in cancer and stem cell signaling. Cancer Res 69:5627-5629. doi:10.1158/0008-5472.CAN-09-0654

370. Munz M, Kieu C, Mack B, Schmitt B, Zeidler R, Gires O (2004) The carcinoma-associated antigen EpCAM upregulates c-myc and induces cell proliferation. Oncogene 23:5748-5758. doi:10.1038/sj.onc.1207610

371. Murayama Y, Miyagawa J, Oritani K, Yoshida H, Yamamoto K, Kishida O, Miyazaki T, Tsutsui S, Kiyohara T, Miyazaki Y, Higashiyama S, Matsuzawa Y, Shinomura Y (2004) CD9-mediated activation of the p46 Shc isoform leads to apoptosis in cancer cells. J Cell Sci 117:3379-3388. doi:10.1242/jcs.01201

372. Murayama Y, Miyagawa J, Shinomura Y, Kanayama S, Isozaki K, Yamamori K, Mizuno H, Ishiguro S, Kiyohara T, Miyazaki Y, Taniguchi N, Higashiyama S, Matsuzawa Y (2002) Significance of the association between heparin-binding epidermal growth factor-like growth factor and CD9 in human gastric cancer. Int J Cancer 98:505-513. doi:10.1002/ijc.10198

373. Murayama Y, Oritani K, Tsutsui S (2015) Novel CD9-targeted therapies in gastric cancer. World J Gastroenterol 21:3206-3213. doi:10.3748/wjg.v21.i11.3206

374. Murayama Y, Shinomura Y, Oritani K, Miyagawa J, Yoshida H, Nishida M, Katsube F, Shiraga M, Miyazaki T, Nakamoto T, Tsutsui S, Tamura S, Higashiyama S, Shimomura I, Hayashi N (2008) The tetraspanin CD9 modulates epidermal growth factor receptor signaling in cancer cells. J Cell Physiol 216:135-143. doi:10.1002/jcp.21384

375. Myhre GM, Toruner M, Abraham S, Egan LJ (2004) Metalloprotease disintegrin-mediated ectodomain shedding of EGFR ligands promotes intestinal epithelial restitution. Am J Physiol Gastrointest Liver Physiol 287:G1213-1219. doi:10.1152/ajpgi.00149.2004

376. Nakamura K, Iwamoto R, Mekada E (1995) Membrane-anchored heparin-binding EGF-like growth factor (HB-EGF) and diphtheria toxin receptor-associated protein (DRAP27)/CD9 form a complex with integrin alpha 3 beta 1 at cell-cell contact sites. J Cell Biol 129:1691-1705

377. Nakamura K, Mitamura T, Takahashi T, Kobayashi T, Mekada E (2000) Importance of the major extracellular domain of CD9 and the epidermal growth factor (EGF)-like domain of heparin-binding EGF-like growth factor for up-regulation of binding and activity. J Biol Chem 275:18284-18290. doi:10.1074/jbc.M907971199

378. Natsui M, Kawasaki K, Takizawa H, Hayashi SI, Matsuda Y, Sugimura K, Seki K, Narisawa R, Sendo F, Asakura H (1997) Selective depletion of neutrophils by a monoclonal antibody, RP-3, suppresses dextran sulphate sodium-induced colitis in rats. J Gastroenterol Hepatol 12:801-808

379. Nava P, Koch S, Laukoetter MG, Lee WY, Kolegraff K, Capaldo CT, Beeman N, Addis C, Gerner-Smidt K, Neumaier I, Skerra A, Li L, Parkos CA, Nusrat A (2010) Interferon-gamma regulates intestinal epithelial homeostasis through converging beta-catenin signaling pathways. Immunity 32:392-402. doi:10.1016/j.immuni.2010.03.001

380. Negroni A, Cucchiara S, Stronati L (2015) Apoptosis, Necrosis, and Necroptosis in the Gut and Intestinal Homeostasis. Mediators Inflamm 2015:250762. doi:10.1155/2015/250762

381. Neufert C, Becker C, Neurath MF (2007) An inducible mouse model of colon carcinogenesis for the analysis of sporadic and inflammation-driven tumor progression. Nat Protoc 2:1998-2004. doi:10.1038/nprot.2007.279

382. Neurath MF (2014) Cytokines in inflammatory bowel disease. Nat Rev Immunol 14:329-342. doi:10.1038/nri3661

383. Neurath MF (2014) New targets for mucosal healing and therapy in inflammatory bowel diseases. Mucosal Immunol 7:6-19. doi:10.1038/mi.2013.73

384. Neurath MF (2017) Current and emerging therapeutic targets for IBD. Nat Rev Gastroenterol Hepatol 14:269-278. doi:10.1038/nrgastro.2016.208

385. Neurath MF, Travis SP (2012) Mucosal healing in inflammatory bowel diseases: a systematic review. Gut 61:1619-1635. doi:10.1136/gutjnl-2012-302830

386. Ng SC, Shi HY, Hamidi N, Underwood FE, Tang W, Benchimol EI, Panaccione R, Ghosh S, Wu JCY, Chan FKL, Sung JJY, Kaplan GG (2018) Worldwide incidence and prevalence of inflammatory bowel disease in the 21st century: a systematic review of population-based studies. Lancet 390:2769-2778. doi:10.1016/S0140-6736(17)32448-0

387. Ng SC, Tang W, Ching JY, Wong M, Chow CM, Hui AJ, Wong TC, Leung VK, Tsang SW, Yu HH, Li MF, Ng KK, Kamm MA, Studd C, Bell S, Leong R, de Silva HJ, Kasturiratne A, Mufeena MN, Ling KL, Ooi CJ, Tan PS, Ong D, Goh KL, Hilmi I, Pisespongsa P, Manatsathit S, Rerknimitr R, Aniwan S, Wang YF, Ouyang Q, Zeng Z, Zhu Z, Chen MH, Hu PJ, Wu K, Wang X, Simadibrata M, Abdullah M, Wu JC, Sung JJ, Chan FK (2013) Incidence and phenotype of inflammatory bowel disease based on results from the Asia-pacific Crohn's and colitis epidemiology study. Gastroenterology 145:158-165 e152. doi:10.1053/j.gastro.2013.04.007

388. Ng WK, Wong SH, Ng SC (2016) Changing epidemiological trends of inflammatory bowel disease in Asia. Intest Res 14:111-119. doi:10.5217/ir.2016.14.2.111

389. Nguyen TL, Vieira-Silva S, Liston A, Raes J (2015) How informative is the mouse for human gut microbiota research? Dis Model Mech 8:1-16. doi:10.1242/dmm.017400

390. Ni J, Li X, He Z, Xu M (2017) A novel method to determine the minimum number of sequences required for reliable microbial community analysis. J Microbiol Methods 139:196-201. doi:10.1016/j.mimet.2017.06.006

391. Nishimura S, Takahashi M, Ota S, Hirano M, Hiraishi H (1998) Hepatocyte growth factor accelerates restitution of intestinal epithelial cells. J Gastroenterol 33:172-178

392. Noah TK, Donahue B, Shroyer NF (2011) Intestinal development and differentiation. Exp Cell Res 317:2702-2710. doi:10.1016/j.yexcr.2011.09.006

393. Noguchi M, Hiwatashi N, Liu Z, Toyota T (1995) Enhanced interferon-gamma production and B7-2 expression in isolated intestinal mononuclear cells from patients with Crohn's disease. J Gastroenterol 30 Suppl 8:52-55

394. Nourshargh S, Alon R (2014) Leukocyte migration into inflamed tissues. Immunity 41:694-707. doi:10.1016/j.immuni.2014.10.008

395. Nubel T, Preobraschenski J, Tuncay H, Weiss T, Kuhn S, Ladwein M, Langbein L, Zoller M (2009) Claudin-7 regulates EpCAM-mediated functions in tumor progression. Mol Cancer Res 7:285-299. doi:10.1158/1541-7786.MCR-08-0200

396. O'Carroll C, Moloney G, Hurley G, Melgar S, Brint E, Nally K, Nibbs RJ, Shanahan F, Carmody RJ (2013) Bcl-3 deficiency protects against dextran-sodium sulphate-induced colitis in the mouse. Clin Exp Immunol 173:332-342. doi:10.1111/cei.12119

397. Odenwald MA, Choi W, Buckley A, Shashikanth N, Joseph NE, Wang Y, Warren MH, Buschmann MM, Pavlyuk R, Hildebrand J, Margolis B, Fanning AS, Turner JR (2017) ZO-1 interactions with F-actin and occludin direct epithelial polarization and single lumen specification in 3D culture. J Cell Sci 130:243-259. doi:10.1242/jcs.188185

398. Odenwald MA, Turner JR (2017) The intestinal epithelial barrier: a therapeutic target? Nat Rev Gastroenterol Hepatol 14:9-21. doi:10.1038/nrgastro.2016.169

399. Oficjalska K, Raverdeau M, Aviello G, Wade SC, Hickey A, Sheehan KM, Corr SC, Kay EW, O'Neill LA, Mills KH, Creagh EM (2015) Protective role for caspase-11 during acute experimental murine colitis. J Immunol 194:1252-1260. doi:10.4049/jimmunol.1400501

400. Oikonomou KA, Kapsoritakis AN, Kapsoritaki AI, Manolakis AC, Tsiopoulos FD, Germenis AE, Potamianos SP (2010) Downregulation of serum epidermal growth factor in patients with inflammatory bowel disease. Is there a link with mucosal damage? Growth Factors 28:461-466. doi:10.3109/08977194.2010.527967

401. Okayasu I, Hatakeyama S, Yamada M, Ohkusa T, Inagaki Y, Nakaya R (1990) A novel method in the induction of reliable experimental acute and chronic ulcerative colitis in mice. Gastroenterology 98:694-702. doi:0016-5085(90)90290-H

402. Okayasu I, Yamada M, Mikami T, Yoshida T, Kanno J, Ohkusa T (2002) Dysplasia and carcinoma development in a repeated dextran sulfate sodium-induced colitis model. J Gastroenterol Hepatol 17:1078-1083.

403. Ono M, Handa K, Withers DA, Hakomori S (1999) Motility inhibition and apoptosis are induced by metastasis-suppressing gene product CD82 and its analogue CD9, with concurrent glycosylation. Cancer Res 59:2335-2339

404. Opstelten JL, Leenders M, Dik VK, Chan SS, van Schaik FD, Khaw KT, Luben R, Hallmans G, Karling P, Lindgren S, Grip O, Key TJ, Crowe FL, Boeing H, Bergmann MM, Overvad K, Palli D, Masala G, Racine A, Carbonnel F, Boutron-Ruault MC, Tjonneland A, Olsen A, Andersen V, Kaaks R, Katzke VA, Tumino R, Trichopoulou A, Siersema PD, Bueno-de-Mesquita HB, Hart AR, Oldenburg B (2016) Dairy Products, Dietary Calcium, and Risk of Inflammatory Bowel Disease: Results From a European Prospective Cohort Investigation. Inflamm Bowel Dis 22:1403-1411. doi:10.1097/MIB.0000000000000798

405. Oren R, Takahashi S, Doss C, Levy R, Levy S (1990) TAPA-1, the target of an antiproliferative antibody, defines a new family of transmembrane proteins. Mol Cell Biol 10:4007-4015

406. Orholm M, Fonager K, Sorensen HT (1999) Risk of ulcerative colitis and Crohn's disease among offspring of patients with chronic inflammatory bowel disease. Am J Gastroenterol 94:3236-3238. doi:10.1111/j.1572-0241.1999.01526.x

407. Ortega-Gomez A, Perretti M, Soehnlein O (2013) Resolution of inflammation: an integrated view. EMBO Mol Med 5:661-674. doi:10.1002/emmm.201202382

408. Oshima T, Miwa H, Joh T (2008) Changes in the expression of claudins in active ulcerative colitis. J Gastroenterol Hepatol 23 Suppl 2:S146-150. doi:10.1111/j.1440-1746.2008.05405.x

409. Ostanin DV, Bao J, Koboziev I, Gray L, Robinson-Jackson SA, Kosloski-Davidson M, Price VH, Grisham MB (2009) T cell transfer model of chronic colitis: concepts, considerations, and tricks of the trade. Am J Physiol Gastrointest Liver Physiol 296:G135-146. doi:10.1152/ajpgi.90462.2008

410. Ovalle S, Gutierrez-Lopez MD, Olmo N, Turnay J, Lizarbe MA, Majano P, Molina-Jimenez F, Lopez-Cabrera M, Yanez-Mo M, Sanchez-Madrid F, Cabanas C (2007) The tetraspanin CD9 inhibits the proliferation and tumorigenicity of human colon carcinoma cells. Int J Cancer 121:2140-2152. doi:10.1002/ijc.22902

411. Owczarek D, Rodacki T, Domagala-Rodacka R, Cibor D, Mach T (2016) Diet and nutritional factors in inflammatory bowel diseases. World J Gastroenterol 22:895-905. doi:10.3748/wjg.v22.i3.895

412. Owen KA, Abshire MY, Tilghman RW, Casanova JE, Bouton AH (2011) FAK regulates intestinal epithelial cell survival and proliferation during mucosal wound healing. PLoS One 6:e23123. doi:10.1371/journal.pone.0023123

413. Palejwala AA, Watson AJ (2000) Apoptosis and gastrointestinal disease. J Pediatr Gastroenterol Nutr 31:356-361

414. Park CS, Yashiro Y, Tai XG, Toyo-oka K, Hamaoka T, Yagita H, Okumura K, Neben S, Fujiwara H (1998) Differential involvement of a Fas-CPP32-like protease pathway in apoptosis of TCR/CD9-costimulated, naive T cells and TCR-restimulated, activated T cells. J Immunol 160:5790-5796

415. Pearson AD, Eastham EJ, Laker MF, Craft AW, Nelson R (1982) Intestinal permeability in children with Crohn's disease and coeliac disease. Br Med J (Clin Res Ed) 285:20-21

416. Peeters M, Geypens B, Claus D, Nevens H, Ghoos Y, Verbeke G, Baert F, Vermeire S, Vlietinck R, Rutgeerts P (1997) Clustering of increased small intestinal permeability in families with Crohn's disease. Gastroenterology 113:802-807.

417. Peeters M, Nevens H, Baert F, Hiele M, de Meyer AM, Vlietinck R, Rutgeerts P (1996) Familial aggregation in Crohn's disease: increased age-adjusted risk and concordance in clinical characteristics. Gastroenterology 111:597-603.

418. Peng WM, Yu CF, Kolanus W, Mazzocca A, Bieber T, Kraft S, Novak N (2011) Tetraspanins CD9 and CD81 are molecular partners of trimeric FcvarepsilonRI on human antigen-presenting cells. Allergy 66:605-611. doi:10.1111/j.1398-9995.2010.02524.x

419. Perse M, Cerar A (2012) Dextran sodium sulphate colitis mouse model: traps and tricks. J Biomed Biotechnol 2012:718617. doi:10.1155/2012/718617

420. Peterson LW, Artis D (2014) Intestinal epithelial cells: regulators of barrier function and immune homeostasis. Nat Rev Immunol 14:141-153. doi:10.1038/nri3608

421. Petersson J, Schreiber O, Hansson GC, Gendler SJ, Velcich A, Lundberg JO, Roos S, Holm L, Phillipson M (2011) Importance and regulation of the colonic mucus barrier in a mouse model of colitis. Am J Physiol Gastrointest Liver Physiol 300:G327-333. doi:10.1152/ajpgi.00422.2010

422. Picarella D, Hurlbut P, Rottman J, Shi X, Butcher E, Ringler DJ (1997) Monoclonal antibodies specific for beta 7 integrin and mucosal addressin cell adhesion molecule-1 (MAdCAM-1) reduce inflammation in the colon of scid mice reconstituted with CD45RBhigh CD4+ T cells. J Immunol 158:2099-2106

423. Pickert G, Neufert C, Leppkes M, Zheng Y, Wittkopf N, Warntjen M, Lehr HA, Hirth S, Weigmann B, Wirtz S, Ouyang W, Neurath MF, Becker C (2009) STAT3 links IL-22 signaling in intestinal epithelial cells to mucosal wound healing. J Exp Med 206:1465-1472. doi:10.1084/jem.20082683

424. Piguet PF, Vesin C, Guo J, Donati Y, Barazzone C (1998) TNF-induced enterocyte apoptosis in mice is mediated by the TNF receptor 1 and does not require p53. Eur J Immunol 28:3499-3505. doi: 10.1002/(SICI)1521-4141(199811)28:11<3499::AID-IMMU3499>3.0.CO;2-Q

425. Pils MC, Bleich A, Prinz I, Fasnacht N, Bollati-Fogolin M, Schippers A, Rozell B, Muller W (2011) Commensal gut flora reduces susceptibility to experimentally induced colitis via T-cell-derived interleukin-10. Inflamm Bowel Dis 17:2038-2046. doi:10.1002/ibd.21587

426. Pineton de Chambrun G, Peyrin-Biroulet L, Lemann M, Colombel JF (2010) Clinical implications of mucosal healing for the management of IBD. Nat Rev Gastroenterol Hepatol 7:15-29. doi:10.1038/nrgastro.2009.203

427. Platt AM, Bain CC, Bordon Y, Sester DP, Mowat AM (2010) An independent subset of TLR expressing CCR2-dependent macrophages promotes colonic inflammation. J Immunol 184:6843-6854. doi:10.4049/jimmunol.0903987

428. Playford RJ, Shaw-Smith C (1996) Growth factors and ulcerative gastrointestinal disease. Baillieres Clin Gastroenterol 10:135-149

429. Podolsky DK (2002) Inflammatory bowel disease. N Engl J Med 347:417-429. doi:10.1056/NEJMra020831

430. Polk DB (1998) Epidermal growth factor receptor-stimulated intestinal epithelial cell migration requires phospholipase C activity. Gastroenterology 114:493-502.

431. Popp V, Gerlach K, Mott S, Turowska A, Garn H, Atreya R, Lehr HA, Ho IC, Renz H, Weigmann B, Neurath MF (2017) Rectal Delivery of a DNAzyme That Specifically Blocks the Transcription Factor GATA3 and Reduces Colitis in Mice. Gastroenterology 152:176-192 e175. doi:10.1053/j.gastro.2016.09.005

432. Poritz LS, Garver KI, Green C, Fitzpatrick L, Ruggiero F, Koltun WA (2007) Loss of the tight junction protein ZO-1 in dextran sulfate sodium induced colitis. J Surg Res 140:12-19. doi:10.1016/j.jss.2006.07.050

433. Potten CS, Owen G, Roberts SA (1990) The temporal and spatial changes in cell proliferation within the irradiated crypts of the murine small intestine. Int J Radiat Biol 57:185-199.

434. Powner D, Kopp PM, Monkley SJ, Critchley DR, Berditchevski F (2011) Tetraspanin CD9 in cell migration. Biochem Soc Trans 39:563-567. doi:10.1042/BST0390563

435. Powrie F, Correa-Oliveira R, Mauze S, Coffman RL (1994) Regulatory interactions between CD45RBhigh and CD45RBlow CD4+ T cells are important for the balance between protective and pathogenic cell-mediated immunity. J Exp Med 179:589-600

436. Powrie F, Leach MW, Mauze S, Caddle LB, Coffman RL (1993) Phenotypically distinct subsets of CD4+ T cells induce or protect from chronic intestinal inflammation in C. B-17 scid mice. Int Immunol 5:1461-1471

437. Prasad S, Mingrino R, Kaukinen K, Hayes KL, Powell RM, MacDonald TT, Collins JE (2005) Inflammatory processes have differential effects on claudins 2, 3 and 4 in colonic epithelial cells. Lab Invest 85:1139-1162. doi:10.1038/labinvest.3700316

438. Prideaux L, Kamm MA, De Cruz PP, Chan FK, Ng SC (2012) Inflammatory bowel disease in Asia: a systematic review. J Gastroenterol Hepatol 27:1266-1280. doi:10.1111/j.1440-1746.2012.07150.x

439. Probert CS, Jayanthi V, Hughes AO, Thompson JR, Wicks AC, Mayberry JF (1993) Prevalence and family risk of ulcerative colitis and Crohn's disease: an epidemiological study among Europeans and south Asians in Leicestershire. Gut 34:1547-1551

440. Procaccino F, Reinshagen M, Hoffmann P, Zeeh JM, Lakshmanan J, McRoberts JA, Patel A, French S, Eysselein VE (1994) Protective effect of epidermal growth factor in an experimental model of colitis in rats. Gastroenterology 107:12-17.

441. Pulendran B, Artis D (2012) New paradigms in type 2 immunity. Science 337:431-435. doi:10.1126/science.1221064

442. Pullan RD, Thomas GA, Rhodes M, Newcombe RG, Williams GT, Allen A, Rhodes J (1994) Thickness of adherent mucus gel on colonic mucosa in humans and its relevance to colitis. Gut 35:353-359

443. Qi JC, Wang J, Mandadi S, Tanaka K, Roufogalis BD, Madigan MC, Lai K, Yan F, Chong BH, Stevens RL, Krilis SA (2006) Human and mouse mast cells use the tetraspanin CD9 as an alternate interleukin-16 receptor. Blood 107:135-142. doi:10.1182/blood-2005-03-1312

444. Qin J, Li R, Raes J, Arumugam M, Burgdorf KS, Manichanh C, Nielsen T, Pons N, Levenez F, Yamada T, Mende DR, Li J, Xu J, Li S, Li D, Cao J, Wang B, Liang H, Zheng H, Xie Y, Tap J, Lepage P, Bertalan M, Batto JM, Hansen T, Le Paslier D, Linneberg A, Nielsen HB, Pelletier E, Renault P, Sicheritz-Ponten T, Turner K, Zhu H, Yu C, Jian M, Zhou Y, Li Y, Zhang X, Qin N, Yang H, Wang J, Brunak S, Dore J, Guarner F, Kristiansen K, Pedersen O, Parkhill J, Weissenbach J, Bork P, Ehrlich SD (2010) A human gut microbial gene catalogue established by metagenomic sequencing. Nature 464:59-65. doi:10.1038/nature08821

445. Qiu W, Wu B, Wang X, Buchanan ME, Regueiro MD, Hartman DJ, Schoen RE, Yu J, Zhang L (2011) PUMA-mediated intestinal epithelial apoptosis contributes to ulcerative colitis in humans and mice. J Clin Invest 121:1722-1732. doi:10.1172/JCI42917

446. Qiu X, Zhang M, Yang X, Hong N, Yu C (2013) Faecalibacterium prausnitzii upregulates regulatory T cells and anti-inflammatory cytokines in treating TNBS-induced colitis. J Crohns Colitis 7:e558-568. doi:10.1016/j.crohns.2013.04.002

447. Quiros M, Nishio H, Neumann PA, Siuda D, Brazil JC, Azcutia V, Hilgarth R, O'Leary MN, Garcia-Hernandez V, Leoni G, Feng M, Bernal G, Williams H, Dedhia PH, Gerner-Smidt C, Spence J, Parkos CA, Denning TL, Nusrat A (2017) Macrophage-derived IL-10 mediates mucosal repair by epithelial WISP-1 signaling. J Clin Invest 127:3510-3520. doi:10.1172/JCI90229

448. Qureshi FG, Leaphart C, Cetin S, Li J, Grishin A, Watkins S, Ford HR, Hackam DJ (2005) Increased expression and function of integrins in enterocytes by endotoxin impairs epithelial restitution. Gastroenterology 128:1012-1022.

449. Raab Y, Gerdin B, Ahlstedt S, Hallgren R (1993) Neutrophil mucosal involvement is accompanied by enhanced local production of interleukin-8 in ulcerative colitis. Gut 34:1203-1206

450. Rakoff-Nahoum S, Paglino J, Eslami-Varzaneh F, Edberg S, Medzhitov R (2004) Recognition of commensal microflora by toll-like receptors is required for intestinal homeostasis. Cell 118:229-241. doi:10.1016/j.cell.2004.07.002

451. Ramachandran A, Madesh M, Balasubramanian KA (2000) Apoptosis in the intestinal epithelium: its relevance in normal and pathophysiological conditions. J Gastroenterol Hepatol 15:109-120

452. Ranganathan P, Jayakumar C, Li DY, Ramesh G (2014) UNC5B receptor deletion exacerbates DSS-induced colitis in mice by increasing epithelial cell apoptosis. J Cell Mol Med 18:1290-1299. doi:10.1111/jcmm.12280

453. Rao JN, Rathor N, Zhuang R, Zou T, Liu L, Xiao L, Turner DJ, Wang JY (2012) Polyamines regulate intestinal epithelial restitution through TRPC1-mediated Ca(2)+ signaling by differentially modulating STIM1 and STIM2. Am J Physiol Cell Physiol 303:C308-317. doi:10.1152/ajpcell.00120.2012

454. Ray G (2016) Inflammatory bowel disease in India - Past, present and future. World J Gastroenterol 22:8123-8136. doi:10.3748/wjg.v22.i36.8123

455. Regueiro M, Kip KE, Cheung O, Hegazi RA, Plevy S (2005) Cigarette smoking and age at diagnosis of inflammatory bowel disease. Inflamm Bowel Dis 11:42-47.

456. Renes IB, Verburg M, Van Nispen DJ, Taminiau JA, Buller HA, Dekker J, Einerhand AW (2002) Epithelial proliferation, cell death, and gene expression in experimental colitis: alterations in carbonic anhydrase I, mucin MUC2, and trefoil factor 3 expression. Int J Colorectal Dis 17:317-326. doi:10.1007/s00384-002-0409-4

457. Reyes R, Monjas A, Yanez-Mo M, Cardenes B, Morlino G, Gilsanz A, Machado-Pineda Y, Lafuente E, Monk P, Sanchez-Madrid F, Cabanas C (2015) Different states of integrin LFA-1 aggregation are controlled through its association with tetraspanin CD9. Biochim Biophys Acta 1853:2464-2480. doi:10.1016/j.bbamcr.2015.05.018

458. Rhodes D, Revis D, Lacy ER (1994) Extracellular matrix constituents affect superficial gastric epithelial cell adhesion. J Gastroenterol Hepatol 9 Suppl 1:S72-77

459. Riviere A, Selak M, Lantin D, Leroy F, De Vuyst L (2016) Bifidobacteria and Butyrate-Producing Colon Bacteria: Importance and Strategies for Their Stimulation in the Human Gut. Front Microbiol 7:979. doi:10.3389/fmicb.2016.00979

460. Rivollier A, He J, Kole A, Valatas V, Kelsall BL (2012) Inflammation switches the differentiation program of Ly6Chi monocytes from antiinflammatory macrophages to inflammatory dendritic cells in the colon. J Exp Med 209:139-155. doi:10.1084/jem.20101387

461. Rocha-Perugini V, Gonzalez-Granado JM, Tejera E, Lopez-Martin S, Yanez-Mo M, Sanchez-Madrid F (2014) Tetraspanins CD9 and CD151 at the immune synapse support T-cell integrin signaling. Eur J Immunol 44:1967-1975. doi:10.1002/eji.201344235

462. Rocha-Perugini V, Martinez Del Hoyo G, Gonzalez-Granado JM, Ramirez-Huesca M, Zorita V, Rubinstein E, Boucheix C, Sanchez-Madrid F (2017) CD9 Regulates Major Histocompatibility Complex Class II Trafficking in Monocyte-Derived Dendritic Cells. Mol Cell Biol 37. doi:10.1128/MCB.00202-17

463. Rocha-Perugini V, Zamai M, Gonzalez-Granado JM, Barreiro O, Tejera E, Yanez-Mo M, Caiolfa VR, Sanchez-Madrid F (2013) CD81 controls sustained T cell activation signaling and defines the maturation stages of cognate immunological synapses. Mol Cell Biol 33:3644-3658. doi:10.1128/MCB.00302-13

464. Rogler G (2017) Resolution of inflammation in inflammatory bowel disease. Lancet Gastroenterol Hepatol 2:521-530. doi:10.1016/S2468-1253(17)30031-6

465. Rose DM, Han J, Ginsberg MH (2002) Alpha4 integrins and the immune response. Immunol Rev 186:118-124.

466. Rosen MJ, Dhawan A, Saeed SA (2015) Inflammatory Bowel Disease in Children and Adolescents. JAMA Pediatr 169:1053-1060. doi:10.1001/jamapediatrics.2015.1982

467. Roth MP, Petersen GM, McElree C, Feldman E, Rotter JI (1989) Geographic origins of Jewish patients with inflammatory bowel disease. Gastroenterology 97:900-904.

468. Round JL, Mazmanian SK (2010) Inducible Foxp3+ regulatory T-cell development by a commensal bacterium of the intestinal microbiota. Proc Natl Acad Sci U S A 107:12204-12209. doi:10.1073/pnas.0909122107

469. Rubinstein E, Le Naour F, Billard M, Prenant M, Boucheix C (1994) CD9 antigen is an accessory subunit of the VLA integrin complexes. Eur J Immunol 24:3005-3013. doi:10.1002/eji.1830241213

470. Rubinstein E, Le Naour F, Lagaudriere-Gesbert C, Billard M, Conjeaud H, Boucheix C (1996) CD9, CD63, CD81, and CD82 are components of a surface tetraspan network connected to HLA-DR and VLA integrins. Eur J Immunol 26:2657-2665. doi:10.1002/eji.1830261117

471. Ruemmele FM, Gurbindo C, Mansour AM, Marchand R, Levy E, Seidman EG (1998) Effects of interferon gamma on growth, apoptosis, and MHC class II expression of immature rat intestinal crypt (IEC-6) cells. J Cell Physiol 176:120-126. doi:10.1002/(SICI)1097-4652(199807)176:1<120::AID-JCP14>3.0.CO;2-B

472. Rutgeerts P, Sandborn WJ, Feagan BG, Reinisch W, Olson A, Johanns J, Travers S, Rachmilewitz D, Hanauer SB, Lichtenstein GR, de Villiers WJ, Present D, Sands BE, Colombel JF (2005) Infliximab for induction and maintenance therapy for ulcerative colitis. N Engl J Med 353:2462-2476. doi:10.1056/NEJMoa050516

473. Rutgeerts P, Vermeire S, Van Assche G (2007) Mucosal healing in inflammatory bowel disease: impossible ideal or therapeutic target? Gut 56:453-455. doi:10.1136/gut.2005.088732

474. Safarpour AR, Hosseini SV, Mehrabani D (2013) Epidemiology of inflammatory bowel diseases in iran and Asia; a mini review. Iran J Med Sci 38:140-149

475. Sahin U, Weskamp G, Kelly K, Zhou HM, Higashiyama S, Peschon J, Hartmann D, Saftig P, Blobel CP (2004) Distinct roles for ADAM10 and ADAM17 in ectodomain shedding of six EGFR ligands. J Cell Biol 164:769-779. doi:10.1083/jcb.200307137

476. Saito Y, Tachibana I, Takeda Y, Yamane H, He P, Suzuki M, Minami S, Kijima T, Yoshida M, Kumagai T, Osaki T, Kawase I (2006) Absence of CD9 enhances adhesion-dependent morphologic differentiation, survival, and matrix metalloproteinase-2 production in small cell lung cancer cells. Cancer Res 66:9557-9565. doi:10.1158/0008-5472.CAN-06-1131

477. Sala-Valdes M, Ursa A, Charrin S, Rubinstein E, Hemler ME, Sanchez-Madrid F, Yanez-Mo M (2006) EWI-2 and EWI-F link the tetraspanin web to the actin cytoskeleton through their direct association with ezrin-radixin-moesin proteins. J Biol Chem 281:19665-19675. doi:10.1074/jbc.M602116200

478. Salim SY, Soderholm JD (2011) Importance of disrupted intestinal barrier in inflammatory bowel diseases. Inflamm Bowel Dis 17:362-381. doi:10.1002/ibd.21403

479. Sandborn WJ, Ghosh S, Panes J, Vranic I, Wang W, Niezychowski W (2014) A phase 2 study of tofacitinib, an oral Janus kinase inhibitor, in patients with Crohn's disease. Clin Gastroenterol Hepatol 12:1485-1493 e1482. doi:10.1016/j.cgh.2014.01.029

480. Sandborn WJ, Sands BE, Wolf DC, Valentine JF, Safdi M, Katz S, Isaacs KL, Wruble LD, Katz J, Present DH, Loftus EV, Jr., Graeme-Cook F, Odenheimer DJ, Hanauer SB (2003) Repifermin (keratinocyte growth factor-2) for the treatment of active ulcerative colitis: a randomized, double-blind, placebo-controlled, dose-escalation trial. Aliment Pharmacol Ther 17:1355-1364.

481. Sander LE, Obermeier F, Dierssen U, Kroy DC, Singh AK, Seidler U, Streetz KL, Lutz HH, Muller W, Tacke F, Trautwein C (2008) Gp130 signaling promotes development of acute experimental colitis by facilitating early neutrophil/macrophage recruitment and activation. J Immunol 181:3586-3594.

482. Sands BE (2015) Biomarkers of Inflammation in Inflammatory Bowel Disease. Gastroenterology 149:1275-1285 e1272. doi:10.1053/j.gastro.2015.07.003

483. Sans M, Danese S, de la Motte C, de Souza HS, Rivera-Reyes BM, West GA, Phillips M, Katz JA, Fiocchi C (2007) Enhanced recruitment of CX3CR1+ T cells by mucosal endothelial cell-derived fractalkine in inflammatory bowel disease. Gastroenterology 132:139-153. doi:10.1053/j.gastro.2006.10.010

484. Sans M, Salas A, Soriano A, Prats N, Gironella M, Pizcueta P, Elena M, Anderson DC, Pique JM, Panes J (2001) Differential role of selectins in experimental colitis. Gastroenterology 120:1162-1172. doi:10.1053/gast.2001.23252

485. Santos MF, McCormack SA, Guo Z, Okolicany J, Zheng Y, Johnson LR, Tigyi G (1997) Rho proteins play a critical role in cell migration during the early phase of mucosal restitution. J Clin Invest 100:216-225. doi:10.1172/JCI119515

486. Santos MPC, Gomes C, Torres J (2018) Familial and ethnic risk in inflammatory bowel disease. Ann Gastroenterol 31:14-23. doi:10.20524/aog.2017.0208

487. Sartor RB (2006) Mechanisms of disease: pathogenesis of Crohn's disease and ulcerative colitis. Nat Clin Pract Gastroenterol Hepatol 3:390-407. doi:10.1038/ncpgasthep0528

488. Sartor RB (2008) Microbial influences in inflammatory bowel diseases. Gastroenterology 134:577-594. doi:10.1053/j.gastro.2007.11.059

489. Sasaki H, Hirai K, Yamamoto H, Tanooka H, Sakamoto H, Iwamoto T, Takahashi T, Terada M, Ochiya T (2004) HST-1/FGF-4 plays a critical role in crypt cell survival and facilitates epithelial cell restitution and proliferation. Oncogene 23:3681-3688. doi:10.1038/sj.onc.1207348

490. Sauer G, Windisch J, Kurzeder C, Heilmann V, Kreienberg R, Deissler H (2003) Progression of cervical carcinomas is associated with down-regulation of CD9 but strong local re-expression at sites of transendothelial invasion. Clin Cancer Res 9:6426-6431

491. Scarpellini E, Lupo M, Iegri C, Gasbarrini A, De Santis A, Tack J (2014) Intestinal permeability in non-alcoholic fatty liver disease: the gut-liver axis. Rev Recent Clin Trials 9:141-147.

492. Scheffold A, Huhn J, Hofer T (2005) Regulation of CD4+CD25+ regulatory T cell activity: it takes (IL-)two to tango. Eur J Immunol 35:1336-1341. doi:10.1002/eji.200425887

493. Schenk GJ, Dijkstra S, van het Hof AJ, van der Pol SM, Drexhage JA, van der Valk P, Reijerkerk A, van Horssen J, de Vries HE (2013) Roles for HB-EGF and CD9 in multiple sclerosis. Glia 61:1890-1905. doi:10.1002/glia.22565

494. Scherberich A, Giannone G, Perennou E, Takeda K, Boucheix C, Rubinstein E, Lanza F, Beretz A (2002) FAK-mediated inhibition of vascular smooth muscle cell migration by the tetraspanin CD9. Thromb Haemost 87:1043-1050

495. Scherberich A, Moog S, Haan-Archipoff G, Azorsa DO, Lanza F, Beretz A (1998) Tetraspanin CD9 is associated with very late-acting integrins in human vascular smooth muscle cells and modulates collagen matrix reorganization. Arterioscler Thromb Vasc Biol 18:1691-1697

496. Schippers A, Muschaweck M, Clahsen T, Tautorat S, Grieb L, Tenbrock K, Gassler N, Wagner N (2016) beta7-Integrin exacerbates experimental DSS-induced colitis in mice by directing inflammatory monocytes into the colon. Mucosal Immunol 9:527-538. doi:10.1038/mi.2015.82

497. Schmidt C, Giese T, Ludwig B, Mueller-Molaian I, Marth T, Zeuzem S, Meuer SC, Stallmach A (2005) Expression of interleukin-12-related cytokine transcripts in inflammatory bowel disease: elevated interleukin-23p19 and interleukin-27p28 in Crohn's disease but not in ulcerative colitis. Inflamm Bowel Dis 11:16-23.

498. Schmidt DS, Klingbeil P, Schnolzer M, Zoller M (2004) CD44 variant isoforms associate with tetraspanins and EpCAM. Exp Cell Res 297:329-347. doi:10.1016/j.yexcr.2004.02.023

499. Schmitz H, Barmeyer C, Fromm M, Runkel N, Foss HD, Bentzel CJ, Riecken EO, Schulzke JD (1999) Altered tight junction structure contributes to the impaired epithelial barrier function in ulcerative colitis. Gastroenterology 116:301-309.

500. Schneider MR, Dahlhoff M, Horst D, Hirschi B, Trulzsch K, Muller-Hocker J, Vogelmann R, Allgauer M, Gerhard M, Steininger S, Wolf E, Kolligs FT (2010) A key role for E-cadherin in intestinal homeostasis and Paneth cell maturation. PLoS One 5:e14325. doi:10.1371/journal.pone.0014325

501. Secondulfo M, de Magistris L, Fiandra R, Caserta L, Belletta M, Tartaglione MT, Riegler G, Biagi F, Corazza GR, Carratu R (2001) Intestinal permeability in Crohn's disease patients and their first degree relatives. Dig Liver Dis 33:680-685.

502. Sedghi S, Fields JZ, Klamut M, Urban G, Durkin M, Winship D, Fretland D, Olyaee M, Keshavarzian A (1993) Increased production of luminol enhanced chemiluminescence by the inflamed colonic mucosa in patients with ulcerative colitis. Gut 34:1191-1197

503. Segal AW, Loewi G (1976) Neutrophil dysfunction in Crohn's disease. Lancet 2:219-221.

504. Seigneuret M (2006) Complete predicted three-dimensional structure of the facilitator transmembrane protein and hepatitis C virus receptor CD81: conserved and variable structural domains in the tetraspanin superfamily. Biophys J 90:212-227. doi:10.1529/biophysj.105.069666

505. Seigneuret M, Delaguillaumie A, Lagaudriere-Gesbert C, Conjeaud H (2001) Structure of the tetraspanin main extracellular domain. A partially conserved fold with a structurally variable domain insertion. J Biol Chem 276:40055-40064. doi:10.1074/jbc.M105557200

506. Seno H, Miyoshi H, Brown SL, Geske MJ, Colonna M, Stappenbeck TS (2009) Efficient colonic mucosal wound repair requires Trem2 signaling. Proc Natl Acad Sci U S A 106:256-261. doi:10.1073/pnas.0803343106

507. Serbina NV, Pamer EG (2006) Monocyte emigration from bone marrow during bacterial infection requires signals mediated by chemokine receptor CCR2. Nat Immunol 7:311-317. doi:10.1038/ni1309

508. Shaw AR, Domanska A, Mak A, Gilchrist A, Dobler K, Visser L, Poppema S, Fliegel L, Letarte M, Willett BJ (1995) Ectopic expression of human and feline CD9 in a human B cell line confers beta 1 integrin-dependent motility on fibronectin and laminin substrates and enhanced tyrosine phosphorylation. J Biol Chem 270:24092-24099

509. Shaw SY, Blanchard JF, Bernstein CN (2011) Association between the use of antibiotics and new diagnoses of Crohn's disease and ulcerative colitis. Am J Gastroenterol 106:2133-2142. doi:10.1038/ajg.2011.304

510. Shi M, Lin TH, Appell KC, Berg LJ (2008) Janus-kinase-3-dependent signals induce chromatin remodeling at the Ifng locus during T helper 1 cell differentiation. Immunity 28:763-773. doi:10.1016/j.immuni.2008.04.016

511. Shi W, Fan H, Shum L, Derynck R (2000) The tetraspanin CD9 associates with transmembrane TGF-alpha and regulates TGF-alpha-induced EGF receptor activation and cell proliferation. J Cell Biol 148:591-602

512. Shimoda M, Horiuchi K, Sasaki A, Tsukamoto T, Okabayashi K, Hasegawa H, Kitagawa Y, Okada Y (2016) Epithelial Cell-Derived a Disintegrin and Metalloproteinase-17 Confers Resistance to Colonic Inflammation Through EGFR Activation. EBioMedicine 5:114-124. doi:10.1016/j.ebiom.2016.02.007

513. Sho M, Adachi M, Taki T, Hashida H, Konishi T, Huang CL, Ikeda N, Nakajima Y, Kanehiro H, Hisanaga M, Nakano H, Miyake M (1998) Transmembrane 4 superfamily as a prognostic factor in pancreatic cancer. Int J Cancer 79:509-516. doi:10.1002/(SICI)1097-0215(19981023)79:5<509::AID-IJC11>3.0.CO;2-X

514. Si Z, Hersey P (1993) Expression of the neuroglandular antigen and analogues in melanoma. CD9 expression appears inversely related to metastatic potential of melanoma. Int J Cancer 54:37-43

515. Singh B, Read S, Asseman C, Malmstrom V, Mottet C, Stephens LA, Stepankova R, Tlaskalova H, Powrie F (2001) Control of intestinal inflammation by regulatory T cells. Immunol Rev 182:190-200.

516. Singh H, Grewal N, Arora E, Kumar H, Kakkar AK (2016) Vedolizumab: A novel anti-integrin drug for treatment of inflammatory bowel disease. J Nat Sci Biol Med 7:4-9. doi:10.4103/0976-9668.175016

517. Sinha A, Nightingale J, West KP, Berlanga-Acosta J, Playford RJ (2003) Epidermal growth factor enemas with oral mesalamine for mild-to-moderate left-sided ulcerative colitis or proctitis. N Engl J Med 349:350-357. doi:10.1056/NEJMoa013136

518. Slonim AE, Bulone L, Damore MB, Goldberg T, Wingertzahn MA, McKinley MJ (2000) A preliminary study of growth hormone therapy for Crohn's disease. N Engl J Med 342:1633-1637. doi:10.1056/NEJM200006013422203

519. Slupsky JR, Kamiguti AS, Rhodes NP, Cawley JC, Shaw AR, Zuzel M (1997) The platelet antigens CD9, CD42 and integrin alpha IIb beta IIIa can be topographically associated and transduce functionally similar signals. Eur J Biochem 244:168-175

520. Smith AM, Rahman FZ, Hayee B, Graham SJ, Marks DJ, Sewell GW, Palmer CD, Wilde J, Foxwell BM, Gloger IS, Sweeting T, Marsh M, Walker AP, Bloom SL, Segal AW (2009) Disordered macrophage cytokine secretion underlies impaired acute inflammation and bacterial clearance in Crohn's disease. J Exp Med 206:1883-1897. doi:10.1084/jem.20091233

521. Smith JM, Johanesen PA, Wendt MK, Binion DG, Dwinell MB (2005) CXCL12 activation of CXCR4 regulates mucosal host defense through stimulation of epithelial cell migration and promotion of intestinal barrier integrity. Am J Physiol Gastrointest Liver Physiol 288:G316-326. doi:10.1152/ajpgi.00208.2004

522. Smith PD, Smythies LE, Mosteller-Barnum M, Sibley DA, Russell MW, Merger M, Sellers MT, Orenstein JM, Shimada T, Graham MF, Kubagawa H (2001) Intestinal macrophages lack CD14 and CD89 and consequently are down-regulated for LPS- and IgA-mediated activities. J Immunol 167:2651-2656

523. Smythies LE, Sellers M, Clements RH, Mosteller-Barnum M, Meng G, Benjamin WH, Orenstein JM, Smith PD (2005) Human intestinal macrophages display profound inflammatory anergy despite avid phagocytic and bacteriocidal activity. J Clin Invest 115:66-75. doi:10.1172/JCI19229

524. Smythies LE, Shen R, Bimczok D, Novak L, Clements RH, Eckhoff DE, Bouchard P, George MD, Hu WK, Dandekar S, Smith PD (2010) Inflammation anergy in human intestinal macrophages is due to Smad-induced IkappaBalpha expression and NF-kappaB inactivation. J Biol Chem 285:19593-19604. doi:10.1074/jbc.M109.069955

525. Soderholm JD, Olaison G, Lindberg E, Hannestad U, Vindels A, Tysk C, Jarnerot G, Sjodahl R (1999) Different intestinal permeability patterns in relatives and spouses of patients with Crohn's disease: an inherited defect in mucosal defence? Gut 44:96-100

526. Soderholm JD, Olaison G, Peterson KH, Franzen LE, Lindmark T, Wiren M, Tagesson C, Sjodahl R (2002) Augmented increase in tight junction permeability by luminal stimuli in the non-inflamed ileum of Crohn's disease. Gut 50:307-313

527. Soderholm JD, Peterson KH, Olaison G, Franzen LE, Westrom B, Magnusson KE, Sjodahl R (1999) Epithelial permeability to proteins in the noninflamed ileum of Crohn's disease? Gastroenterology 117:65-72.

528. Sood A, Midha V, Sood N, Bhatia AS, Avasthi G (2003) Incidence and prevalence of ulcerative colitis in Punjab, North India. Gut 52:1587-1590

529. Souza HS, Tortori CJ, Castelo-Branco MT, Carvalho AT, Margallo VS, Delgado CF, Dines I, Elia CC (2005) Apoptosis in the intestinal mucosa of patients with inflammatory bowel disease: evidence of altered expression of FasL and perforin cytotoxic pathways. Int J Colorectal Dis 20:277-286. doi:10.1007/s00384-004-0639-8

530. Soyuer S, Soyuer I, Unal D, Ucar K, Yildiz OG, Orhan O (2010) Prognostic significance of CD9 expression in locally advanced gastric cancer treated with surgery and adjuvant chemoradiotherapy. Pathol Res Pract 206:607-610. doi:10.1016/j.prp.2010.04.004

531. Spadaccini M, D'Alessio S, Peyrin-Biroulet L, Danese S (2017) PDE4 Inhibition and Inflammatory Bowel Disease: A Novel Therapeutic Avenue. Int J Mol Sci 18. doi:10.3390/ijms18061276

532. Stipp CS, Kolesnikova TV, Hemler ME (2001) EWI-2 is a major CD9 and CD81 partner and member of a novel Ig protein subfamily. J Biol Chem 276:40545-40554. doi:10.1074/jbc.M107338200

533. Stipp CS, Kolesnikova TV, Hemler ME (2003) EWI-2 regulates alpha3beta1 integrin-dependent cell functions on laminin-5. J Cell Biol 163:1167-1177. doi:10.1083/jcb.200309113

534. Stipp CS, Kolesnikova TV, Hemler ME (2003) Functional domains in tetraspanin proteins. Trends Biochem Sci 28:106-112. doi:10.1016/S0968-0004(02)00014-2

535. Stipp CS, Orlicky D, Hemler ME (2001) FPRP, a major, highly stoichiometric, highly specific CD81- and CD9-associated protein. J Biol Chem 276:4853-4862. doi:10.1074/jbc.M009859200

536. Strober W, Fuss IJ, Blumberg RS (2002) The immunology of mucosal models of inflammation. Annu Rev Immunol 20:495-549. doi:10.1146/annurev.immunol.20.100301.064816

537. Sturm A, Sudermann T, Schulte KM, Goebell H, Dignass AU (1999) Modulation of intestinal epithelial wound healing in vitro and in vivo by lysophosphatidic acid. Gastroenterology 117:368-377. doi:S0016508599001559 [pii]

538. Su L, Shen L, Clayburgh DR, Nalle SC, Sullivan EA, Meddings JB, Abraham C, Turner JR (2009) Targeted epithelial tight junction dysfunction causes immune activation and contributes to development of experimental colitis. Gastroenterology 136:551-563. doi:10.1053/j.gastro.2008.10.081

539. Su Y, Yang J, Besner GE (2013) HB-EGF promotes intestinal restitution by affecting integrin-extracellular matrix interactions and intercellular adhesions. Growth Factors 31:39-55. doi:10.3109/08977194.2012.755966

540. Sun CM, Hall JA, Blank RB, Bouladoux N, Oukka M, Mora JR, Belkaid Y (2007) Small intestine lamina propria dendritic cells promote de novo generation of Foxp3 T reg cells via retinoic acid. J Exp Med 204:1775-1785. doi:10.1084/jem.20070602

541. Sun FF, Lai PS, Yue G, Yin K, Nagele RG, Tong DM, Krzesicki RF, Chin JE, Wong PY (2001) Pattern of cytokine and adhesion molecule mRNA in hapten-induced relapsing colon inflammation in the rat. Inflammation 25:33-45

542. Sunnarborg SW, Hinkle CL, Stevenson M, Russell WE, Raska CS, Peschon JJ, Castner BJ, Gerhart MJ, Paxton RJ, Black RA, Lee DC (2002) Tumor necrosis factor-alpha converting enzyme (TACE) regulates epidermal growth factor receptor ligand availability. J Biol Chem 277:12838-12845. doi:10.1074/jbc.M112050200

543. Suzuki M, Tachibana I, Takeda Y, He P, Minami S, Iwasaki T, Kida H, Goya S, Kijima T, Yoshida M, Kumagai T, Osaki T, Kawase I (2009) Tetraspanin CD9 negatively regulates lipopolysaccharide-induced macrophage activation and lung inflammation. J Immunol 182:6485-6493. doi:10.4049/jimmunol.0802797

544. Swanson PA, 2nd, Kumar A, Samarin S, Vijay-Kumar M, Kundu K, Murthy N, Hansen J, Nusrat A, Neish AS (2011) Enteric commensal bacteria potentiate epithelial restitution via reactive oxygen species-mediated inactivation of focal adhesion kinase phosphatases. Proc Natl Acad Sci U S A 108:8803-8808. doi:10.1073/pnas.1010042108

545. Tabbekh M, Mokrani-Hammani M, Bismuth G, Mami-Chouaib F (2013) T-cell modulatory properties of CD5 and its role in antitumor immune responses. Oncoimmunology 2:e22841. doi:10.4161/onci.22841

546. Tai XG, Toyooka K, Yashiro Y, Abe R, Park CS, Hamaoka T, Kobayashi M, Neben S, Fujiwara H (1997) CD9-mediated costimulation of TCR-triggered naive T cells leads to activation followed by apoptosis. J Immunol 159:3799-3807

547. Tai XG, Yashiro Y, Abe R, Toyooka K, Wood CR, Morris J, Long A, Ono S, Kobayashi M, Hamaoka T, Neben S, Fujiwara H (1996) A role for CD9 molecules in T cell activation. J Exp Med 184:753-758

548. Takeda T, Hattori N, Tokuhara T, Nishimura Y, Yokoyama M, Miyake M (2007) Adenoviral transduction of MRP-1/CD9 and KAI1/CD82 inhibits lymph node metastasis in orthotopic lung cancer model. Cancer Res 67:1744-1749. doi:10.1158/0008-5472.CAN-06-3090

549. Takeda Y, He P, Tachibana I, Zhou B, Miyado K, Kaneko H, Suzuki M, Minami S, Iwasaki T, Goya S, Kijima T, Kumagai T, Yoshida M, Osaki T, Komori T, Mekada E, Kawase I (2008) Double deficiency of tetraspanins CD9 and CD81 alters cell motility and protease production of macrophages and causes chronic obstructive pulmonary disease-like phenotype in mice. J Biol Chem 283:26089-26097. doi:10.1074/jbc.M801902200

550. Takeuchi K, Yokota A, Tanaka A, Takahira Y (2006) Factors involved in upregulation of inducible nitric oxide synthase in rat small intestine following administration of nonsteroidal anti-inflammatory drugs. Dig Dis Sci 51:1250-1259. doi:10.1007/s10620-006-8045-4

551. Tambuwala MM, Cummins EP, Lenihan CR, Kiss J, Stauch M, Scholz CC, Fraisl P, Lasitschka F, Mollenhauer M, Saunders SP, Maxwell PH, Carmeliet P, Fallon PG, Schneider M, Taylor CT (2010) Loss of prolyl hydroxylase-1 protects against colitis through reduced epithelial cell apoptosis and increased barrier function. Gastroenterology 139:2093-2101. doi:10.1053/j.gastro.2010.06.068

552. Tang M, Yin G, Wang F, Liu H, Zhou S, Ni J, Chen C, Zhou Y, Zhao Y (2015) Downregulation of CD9 promotes pancreatic cancer growth and metastasis through upregulation of epidermal growth factor on the cell surface. Oncol Rep 34:350-358. doi:10.3892/or.2015.3960

553. Taniguchi T, Tsukada H, Nakamura H, Kodama M, Fukuda K, Saito T, Miyasaka M, Seino Y (1998) Effects of the anti-ICAM-1 monoclonal antibody on dextran sodium sulphate-induced colitis in rats. J Gastroenterol Hepatol 13:945-949

554. Targan SR (2006) Current limitations of IBD treatment: where do we go from here? Ann N Y Acad Sci 1072:1-8. doi:10.1196/annals.1326.032

555. Taupin D, Podolsky DK (2003) Trefoil factors: initiators of mucosal healing. Nat Rev Mol Cell Biol 4:721-732. doi:10.1038/nrm1203

556. Taylor RG, Fuller PJ (1994) Humoral regulation of intestinal adaptation. Baillieres Clin Endocrinol Metab 8:165-183

557. Tessner TG, Cohn SM, Schloemann S, Stenson WF (1998) Prostaglandins prevent decreased epithelial cell proliferation associated with dextran sodium sulfate injury in mice. Gastroenterology 115:874-882.

558. Todres E, Nardi JB, Robertson HM (2000) The tetraspanin superfamily in insects. Insect Mol Biol 9:581-590.

559. Tomlinson MG, Wright MD (1996) A new transmembrane 4 superfamily molecule in the nematode, Caenorhabditis elegans. J Mol Evol 43:312-314

560. Tontini GE, Pastorelli L, Ishaq S, Neumann H (2015) Advances in endoscopic imaging in ulcerative colitis. Expert Rev Gastroenterol Hepatol 9:1393-1405. doi:10.1586/17474124.2015.1087848

561. Toyo-oka K, Tai XG, Yashiro Y, Ahn HJ, Abe R, Hamaoka T, Kobayashi M, Neben S, Fujiwara H (1997) Synergy between CD28 and CD9 costimulation for naive T-cell activation. Immunol Lett 58:19-23.

562. Toyo-oka K, Yashiro-Ohtani Y, Park CS, Tai XG, Miyake K, Hamaoka T, Fujiwara H (1999) Association of a tetraspanin CD9 with CD5 on the T cell surface: role of particular transmembrane domains in the association. Int Immunol 11:2043-2052

563. Tozun N, Atug O, Imeryuz N, Hamzaoglu HO, Tiftikci A, Parlak E, Dagli U, Ulker A, Hulagu S, Akpinar H, Tuncer C, Suleymanlar I, Ovunc O, Hilmioglu F, Aslan S, Turkdogan K, Bahcecioglu HI,

Yurdaydin C (2009) Clinical characteristics of inflammatory bowel disease in Turkey: a multicenter epidemiologic survey. J Clin Gastroenterol 43:51-57. doi:10.1097/MCG.0b013e3181574636

564. Trzpis M, McLaughlin PM, de Leij LM, Harmsen MC (2007) Epithelial cell adhesion molecule: more than a carcinoma marker and adhesion molecule. Am J Pathol 171:386-395. doi:10.2353/ajpath.2007.070152

565. Tsai YC, Mendoza A, Mariano JM, Zhou M, Kostova Z, Chen B, Veenstra T, Hewitt SM, Helman LJ, Khanna C, Weissman AM (2007) The ubiquitin ligase gp78 promotes sarcoma metastasis by targeting KAI1 for degradation. Nat Med 13:1504-1509. doi:10.1038/nm1686

566. Tsukita S, Furuse M, Itoh M (2001) Multifunctional strands in tight junctions. Nat Rev Mol Cell Biol 2:285-293. doi:10.1038/35067088

567. Turnbaugh PJ, Quince C, Faith JJ, McHardy AC, Yatsunenko T, Niazi F, Affourtit J, Egholm M, Henrissat B, Knight R, Gordon JI (2010) Organismal, genetic, and transcriptional variation in the deeply sequenced gut microbiomes of identical twins. Proc Natl Acad Sci U S A 107:7503-7508. doi:10.1073/pnas.1002355107

568. Turner JR (2009) Intestinal mucosal barrier function in health and disease. Nat Rev Immunol 9:799-809. doi:10.1038/nri2653

569. Tysk C, Lindberg E, Jarnerot G, Floderus-Myrhed B (1988) Ulcerative colitis and Crohn's disease in an unselected population of monozygotic and dizygotic twins. A study of heritability and the influence of smoking. Gut 29:990-996

570. Uchida S, Shimada Y, Watanabe G, Li ZG, Hong T, Miyake M, Imamura M (1999) Motility-related protein (MRP-1/CD9) and KAI1/CD82 expression inversely correlate with lymph node metastasis in oesophageal squamous cell carcinoma. Br J Cancer 79:1168-1173. doi:10.1038/sj.bjc.6690186

571. Uchiyama K, Naito Y, Takagi T, Mizushima K, Hayashi N, Harusato A, Hirata I, Omatsu T, Handa O, Ishikawa T, Yagi N, Kokura S, Yoshikawa T (2010) Carbon monoxide enhance colonic epithelial restitution via FGF15 derived from colonic myofibroblasts. Biochem Biophys Res Commun 391:1122-1126. doi:10.1016/j.bbrc.2009.12.035

572. Uguccioni M, Gionchetti P, Robbiani DF, Rizzello F, Peruzzo S, Campieri M, Baggiolini M (1999) Increased expression of IP-10, IL-8, MCP-1, and MCP-3 in ulcerative colitis. Am J Pathol 155:331-336. doi:10.1016/S0002-9440(10)65128-0

573. Uhlig HH (2013) Monogenic diseases associated with intestinal inflammation: implications for the understanding of inflammatory bowel disease. Gut 62:1795-1805. doi:10.1136/gutjnl-2012-303956

574. Ukabam SO, Clamp JR, Cooper BT (1983) Abnormal small intestinal permeability to sugars in patients with Crohn's disease of the terminal ileum and colon. Digestion 27:70-74. doi:10.1159/000198932

575. Unternaehrer JJ, Chow A, Pypaert M, Inaba K, Mellman I (2007) The tetraspanin CD9 mediates lateral association of MHC class II molecules on the dendritic cell surface. Proc Natl Acad Sci U S A 104:234-239. doi:10.1073/pnas.0609665104

576. van den Brink GR, Bleuming SA, Hardwick JC, Schepman BL, Offerhaus GJ, Keller JJ, Nielsen C, Gaffield W, van Deventer SJ, Roberts DJ, Peppelenbosch MP (2004) Indian Hedgehog is an antagonist of Wnt signaling in colonic epithelial cell differentiation. Nat Genet 36:277-282. doi:10.1038/ng1304

577. van der Gun BT, Melchers LJ, Ruiters MH, de Leij LF, McLaughlin PM, Rots MG (2010) EpCAM in carcinogenesis: the good, the bad or the ugly. Carcinogenesis 31:1913-1921. doi:10.1093/carcin/bgq187

578. Van der Sluis M, De Koning BA, De Bruijn AC, Velcich A, Meijerink JP, Van Goudoever JB, Buller HA, Dekker J, Van Seuningen I, Renes IB, Einerhand AW (2006) Muc2-deficient mice spontaneously

develop colitis, indicating that MUC2 is critical for colonic protection. Gastroenterology 131:117-129. doi:10.1053/j.gastro.2006.04.020

579. van der Valk ME, Mangen MJ, Leenders M, Dijkstra G, van Bodegraven AA, Fidder HH, de Jong DJ, Pierik M, van der Woude CJ, Romberg-Camps MJ, Clemens CH, Jansen JM, Mahmmod N, van de Meeberg PC, van der Meulen-de Jong AE, Ponsioen CY, Bolwerk CJ, Vermeijden JR, Siersema PD, van Oijen MG, Oldenburg B (2014) Healthcare costs of inflammatory bowel disease have shifted from hospitalisation and surgery towards anti-TNFalpha therapy: results from the COIN study. Gut 63:72-79. doi:10.1136/gutjnl-2012-303376

580. van Deventer SJ, Wedel MK, Baker BF, Xia S, Chuang E, Miner PB, Jr. (2006) A phase II dose ranging, double-blind, placebo-controlled study of alicaforsen enema in subjects with acute exacerbation of mild to moderate left-sided ulcerative colitis. Aliment Pharmacol Ther 23:1415-1425. doi:10.1111/j.1365-2036.2006.02910.x

581. Vaughn BP, Shah S, Cheifetz AS (2014) The role of mucosal healing in the treatment of patients with inflammatory bowel disease. Curr Treat Options Gastroenterol 12:103-117. doi:10.1007/s11938-013-0008-1

582. Vazeille E, Buisson A, Bringer MA, Goutte M, Ouchchane L, Hugot JP, de Vallee A, Barnich N, Bommelaer G, Darfeuille-Michaud A (2015) Monocyte-derived macrophages from Crohn's disease patients are impaired in the ability to control intracellular adherent-invasive Escherichia coli and exhibit disordered cytokine secretion profile. J Crohns Colitis 9:410-420. doi:10.1093/ecco-jcc/jjv053

583. Vermeire S, O'Byrne S, Keir M, Williams M, Lu TT, Mansfield JC, Lamb CA, Feagan BG, Panes J, Salas A, Baumgart DC, Schreiber S, Dotan I, Sandborn WJ, Tew GW, Luca D, Tang MT, Diehl L, Eastham-Anderson J, De Hertogh G, Perrier C, Egen JG, Kirby JA, van Assche G, Rutgeerts P (2014) Etrolizumab as induction therapy for ulcerative colitis: a randomised, controlled, phase 2 trial. Lancet 384:309-318. doi:10.1016/S0140-6736(14)60661-9

584. Vermeire S, Schreiber S, Petryka R, Kuehbacher T, Hebuterne X, Roblin X, Klopocka M, Goldis A, Wisniewska-Jarosinska M, Baranovsky A, Sike R, Stoyanova K, Tasset C, Van der Aa A, Harrison P (2017) Clinical remission in patients with moderate-to-severe Crohn's disease treated with filgotinib (the FITZROY study): results from a phase 2, double-blind, randomised, placebo-controlled trial. Lancet 389:266-275. doi:10.1016/S0140-6736(16)32537-5

585. Vetuschi A, Latella G, Sferra R, Caprilli R, Gaudio E (2002) Increased proliferation and apoptosis of colonic epithelial cells in dextran sulfate sodium-induced colitis in rats. Dig Dis Sci 47:1447-1457

586. Victoria CR, Sassak LY, Nunes HR (2009) Incidence and prevalence rates of inflammatory bowel diseases, in midwestern of Sao Paulo State, Brazil. Arq Gastroenterol 46:20-25.

587. Vongsa RA, Zimmerman NP, Dwinell MB (2009) CCR6 regulation of the actin cytoskeleton orchestrates human beta defensin-2- and CCL20-mediated restitution of colonic epithelial cells. J Biol Chem 284:10034-10045. doi:10.1074/jbc.M805289200

588. Wan MX, Riaz AA, Schramm R, Wang Y, Vestweber D, Menger MD, Thorlacius H (2002) Leukocyte rolling is exclusively mediated by P-selectinin colonic venules. Br J Pharmacol 135:1749-1756. doi:10.1038/sj.bjp.0704638

589. Wang GP, Han XF (2015) CD9 modulates proliferation of human glioblastoma cells via epidermal growth factor receptor signaling. Mol Med Rep 12:1381-1386. doi:10.3892/mmr.2015.3466

590. Wang JC, Begin LR, Berube NG, Chevalier S, Aprikian AG, Gourdeau H, Chevrette M (2007) Down-regulation of CD9 expression during prostate carcinoma progression is associated with CD9 mRNA modifications. Clin Cancer Res 13:2354-2361. doi:10.1158/1078-0432.CCR-06-1692

591. Wang JY, Johnson LR (1990) Luminal polyamines stimulate repair of gastric mucosal stress ulcers. Am J Physiol 259:G584-592. doi:10.1152/ajpgi.1990.259.4.G584

592. Wang L, Ray A, Jiang X, Wang JY, Basu S, Liu X, Qian T, He R, Dittel BN, Chu Y (2015) T regulatory cells and B cells cooperate to form a regulatory loop that maintains gut homeostasis and suppresses dextran sulfate sodium-induced colitis. Mucosal Immunol 8:1297-1312. doi:10.1038/mi.2015.20

593. Wang SL, Wang ZR, Yang CQ (2012) Meta-analysis of broad-spectrum antibiotic therapy in patients with active inflammatory bowel disease. Exp Ther Med 4:1051-1056. doi:10.3892/etm.2012.718

594. Wang Y, Tong X, Omoregie ES, Liu W, Meng S, Ye X (2012) Tetraspanin 6 (TSPAN6) negatively regulates retinoic acid-inducible gene I-like receptor-mediated immune signaling in a ubiquitination-dependent manner. J Biol Chem 287:34626-34634. doi:10.1074/jbc.M112.390401

595. Waterhouse R, Ha C, Dveksler GS (2002) Murine CD9 is the receptor for pregnancy-specific glycoprotein 17. J Exp Med 195:277-282

596. Wehkamp J, Schmid M, Fellermann K, Stange EF (2005) Defensin deficiency, intestinal microbes, and the clinical phenotypes of Crohn's disease. J Leukoc Biol 77:460-465. doi:10.1189/jlb.0904543

597. Weimers P, Munkholm P (2018) The Natural History of IBD: Lessons Learned. Curr Treat Options Gastroenterol. doi:10.1007/s11938-018-0173-3

598. Welcker K, Martin A, Kolle P, Siebeck M, Gross M (2004) Increased intestinal permeability in patients with inflammatory bowel disease. Eur J Med Res 9:456-460

599. Wen YA, Li X, Goretsky T, Weiss HL, Barrett TA, Gao T (2015) Loss of PHLPP protects against colitis by inhibiting intestinal epithelial cell apoptosis. Biochim Biophys Acta 1852:2013-2023. doi:10.1016/j.bbadis.2015.07.012

600. Wilson AJ, Gibson PR (1997) Short-chain fatty acids promote the migration of colonic epithelial cells in vitro. Gastroenterology 113:487-496.

601. Wilson AJ, Gibson PR (1999) Role of epidermal growth factor receptor in basal and stimulated colonic epithelial cell migration in vitro. Exp Cell Res 250:187-196. doi:10.1006/excr.1999.4496

602. Williams CS, Bradley AM, Chaturvedi R, Singh K, Piazuelo MB, Chen X, McDonough EM, Schwartz DA, Brown CT, Allaman MM, Coburn LA, Horst SN, Beaulieu DB, Choksi YA, Washington MK, Williams AD, Fisher MA, Zinkel SS, Peek RM, Jr., Wilson KT, Hiebert SW (2013) MTG16 contributes to colonic epithelial integrity in experimental colitis. Gut 62:1446-1455. doi:10.1136/gutjnl-2011-301439

603. Williams IR, Parkos CA (2007) Colonic neutrophils in inflammatory bowel disease: double-edged swords of the innate immune system with protective and destructive capacity. Gastroenterology 133:2049-2052. doi:10.1053/j.gastro.2007.10.031

604. Williams KL, Fuller CR, Dieleman LA, DaCosta CM, Haldeman KM, Sartor RB, Lund PK (2001) Enhanced survival and mucosal repair after dextran sodium sulfate-induced colitis in transgenic mice that overexpress growth hormone. Gastroenterology 120:925-937.

605. Withers DR, Hepworth MR, Wang X, Mackley EC, Halford EE, Dutton EE, Marriott CL, Brucklacher-Waldert V, Veldhoen M, Kelsen J, Baldassano RN, Sonnenberg GF (2016) Transient inhibition of ROR-gammat therapeutically limits intestinal inflammation by reducing TH17 cells and preserving group 3 innate lymphoid cells. Nat Med 22:319-323. doi:10.1038/nm.4046

606. Wolfe MM, Lichtenstein DR, Singh G (1999) Gastrointestinal toxicity of nonsteroidal antiinflammatory drugs. N Engl J Med 340:1888-1899. doi:10.1056/NEJM199906173402407

607. Won WJ, Kearney JF (2002) CD9 is a unique marker for marginal zone B cells, B1 cells, and plasma cells in mice. J Immunol 168:5605-5611

608. Wong PY, Yue G, Yin K, Miyasaka M, Lane CL, Manning AM, Anderson DC, Sun FF (1995) Antibodies to ICAM-1 ameliorate inflammation in acetic acid induced inflammatory bowel disease. Adv Prostaglandin Thromboxane Leukot Res 23:337-339

609. Wright MD, Henkle KJ, Mitchell GF (1990) An immunogenic Mr 23,000 integral membrane protein of Schistosoma mansoni worms that closely resembles a human tumor-associated antigen. J Immunol 144:3195-3200

610. Wyatt J, Vogelsang H, Hubl W, Waldhoer T, Lochs H (1993) Intestinal permeability and the prediction of relapse in Crohn's disease. Lancet 341:1437-1439.

611. Xia XM, Wang FY, Zhou J, Hu KF, Li SW, Zou BB (2011) CXCR4 antagonist AMD3100 modulates claudin expression and intestinal barrier function in experimental colitis. PLoS One 6:e27282. doi:10.1371/journal.pone.0027282

612. Xiao W, Yin M, Wu K, Lu G, Deng B, Zhang Y, Qian L, Jia X, Ding Y, Gong W (2017) High-dose wogonin exacerbates DSS-induced colitis by up-regulating effector T cell function and inhibiting Treg cell. J Cell Mol Med 21:286-298. doi:10.1111/jcmm.12964

613. Yamada S, Koyama T, Noguchi H, Ueda Y, Kitsuyama R, Shimizu H, Tanimoto A, Wang KY, Nawata A, Nakayama T, Sasaguri Y, Satoh T (2014) Marine hydroquinone zonarol prevents inflammation and apoptosis in dextran sulfate sodium-induced mice ulcerative colitis. PLoS One 9:e113509. doi:10.1371/journal.pone.0113509

614. Yamazaki K, McGovern D, Ragoussis J, Paolucci M, Butler H, Jewell D, Cardon L, Takazoe M, Tanaka T, Ichimori T, Saito S, Sekine A, Iida A, Takahashi A, Tsunoda T, Lathrop M, Nakamura Y (2005) Single nucleotide polymorphisms in TNFSF15 confer susceptibility to Crohn's disease. Hum Mol Genet 14:3499-3506. doi:10.1093/hmg/ddi379

615. Yan F, Cao H, Cover TL, Washington MK, Shi Y, Liu L, Chaturvedi R, Peek RM, Jr., Wilson KT, Polk DB (2011) Colon-specific delivery of a probiotic-derived soluble protein ameliorates intestinal inflammation in mice through an EGFR-dependent mechanism. J Clin Invest 121:2242-2253. doi:10.1172/JCI44031

616. Yan F, Polk DB (2010) Probiotics: progress toward novel therapies for intestinal diseases. Curr Opin Gastroenterol 26:95-101. doi:10.1097/MOG.0b013e328335239a

617. Yan Y, Kolachala V, Dalmasso G, Nguyen H, Laroui H, Sitaraman SV, Merlin D (2009) Temporal and spatial analysis of clinical and molecular parameters in dextran sodium sulfate induced colitis. PLoS One 4:e6073. doi:10.1371/journal.pone.0006073

618. Yanez-Mo M, Barreiro O, Gordon-Alonso M, Sala-Valdes M, Sanchez-Madrid F (2009) Tetraspanin-enriched microdomains: a functional unit in cell plasma membranes. Trends Cell Biol 19:434-446. doi:10.1016/j.tcb.2009.06.004

619. Yanez-Mo M, Tejedor R, Rousselle P, Sanchez -Madrid F (2001) Tetraspanins in intercellular adhesion of polarized epithelial cells: spatial and functional relationship to integrins and cadherins. J Cell Sci 114:577-587

620. Yang Q, Bermingham NA, Finegold MJ, Zoghbi HY (2001) Requirement of Math1 for secretory cell lineage commitment in the mouse intestine. Science 294:2155-2158. doi:10.1126/science.1065718

621. Yashiro-Ohtani Y, Zhou XY, Toyo-Oka K, Tai XG, Park CS, Hamaoka T, Abe R, Miyake K, Fujiwara H (2000) Non-CD28 costimulatory molecules present in T cell rafts induce T cell costimulation by enhancing the association of TCR with rafts. J Immunol 164:1251-1259.

622. Yashiro Y, Tai XG, Toyo-oka K, Park CS, Abe R, Hamaoka T, Kobayashi M, Neben S, Fujiwara H (1998) A fundamental difference in the capacity to induce proliferation of naive T cells between CD28 and other co-stimulatory molecules. Eur J Immunol 28:926-935. doi:10.1002/(SICI)1521-4141(199803)28:03<926::AID-IMMU926>3.0.CO;2-0

623. Yauch RL, Hemler ME (2000) Specific interactions among transmembrane 4 superfamily (TM4SF) proteins and phosphoinositide 4-kinase. Biochem J 351 Pt 3:629-637

624. Yazbeck R, Howarth GS, Butler RN, Geier MS, Abbott CA (2011) Biochemical and histological changes in the small intestine of mice with dextran sulfate sodium colitis. J Cell Physiol 226:3219-3224. doi:10.1002/jcp.22682

625. Ye D, Ma I, Ma TY (2006) Molecular mechanism of tumor necrosis factor-alpha modulation of intestinal epithelial tight junction barrier. Am J Physiol Gastrointest Liver Physiol 290:G496-504. doi:10.1152/ajpgi.00318.2005

626. Yen D, Cheung J, Scheerens H, Poulet F, McClanahan T, McKenzie B, Kleinschek MA, Owyang A, Mattson J, Blumenschein W, Murphy E, Sathe M, Cua DJ, Kastelein RA, Rennick D (2006) IL-23 is essential for T cell-mediated colitis and promotes inflammation via IL-17 and IL-6. J Clin Invest 116:1310-1316. doi:10.1172/JCI21404

627. Yoshida N, Yamaguchi T, Nakagawa S, Nakamura Y, Naito Y, Yoshikawa T (2001) Role of P-selectin and intercellular adhesion molecule-1 in TNB-induced colitis in rats. Digestion 63 Suppl 1:81-86. doi:10.1159/000051916

628. Yu CF, Basson MD (2000) Matrix-specific FAK and MAPK reorganization during Caco-2 cell motility. Microsc Res Tech 51:191-203. doi:10.1002/1097-0029(20001015)51:2<191::AID-JEMT10>3.0.CO;2-1

629. Yu S, Gao N (2015) Compartmentalizing intestinal epithelial cell toll-like receptors for immune surveillance. Cell Mol Life Sci 72:3343-3353. doi:10.1007/s00018-015-1931-1

630. Yu SJ, Liu Y, Deng Y, Zhu XY, Zhan N, Dong WG (2015) CARD3 deficiency protects against colitis through reduced epithelial cell apoptosis. Inflamm Bowel Dis 21:862-869. doi:10.1097/MIB.0000000000000322

631. Yuan B, Zhou S, Lu Y, Liu J, Jin X, Wan H, Wang F (2015) Changes in the Expression and Distribution of Claudins, Increased Epithelial Apoptosis, and a Mannan-Binding Lectin-Associated Immune Response Lead to Barrier Dysfunction in Dextran Sodium Sulfate-Induced Rat Colitis. Gut Liver 9:734-740. doi:10.5009/gnl14155

632. Zaki MH, Boyd KL, Vogel P, Kastan MB, Lamkanfi M, Kanneganti TD (2010) The NLRP3 inflammasome protects against loss of epithelial integrity and mortality during experimental colitis. Immunity 32:379-391. doi:10.1016/j.immuni.2010.03.003

633. Zeissig S, Burgel N, Gunzel D, Richter J, Mankertz J, Wahnschaffe U, Kroesen AJ, Zeitz M, Fromm M, Schulzke JD (2007) Changes in expression and distribution of claudin 2, 5 and 8 lead to discontinuous tight junctions and barrier dysfunction in active Crohn's disease. Gut 56:61-72. doi:10.1136/gut.2006.094375

634. Zhang HL, Zheng YJ, Pan YD, Xie C, Sun H, Zhang YH, Yuan MY, Song BL, Chen JF (2016) Regulatory T-cell depletion in the gut caused by integrin beta7 deficiency exacerbates DSS colitis by evoking aberrant innate immunity. Mucosal Immunol 9:391-400. doi:10.1038/mi.2015.68

635. Zhang R, Borges CM, Fan MY, Harris JE, Turka LA (2015) Requirement for CD28 in Effector Regulatory T Cell Differentiation, CCR6 Induction, and Skin Homing. J Immunol 195:4154-4161. doi:10.4049/jimmunol.1500945

636. Zhang XA, Bontrager AL, Hemler ME (2001) Transmembrane-4 superfamily proteins associate with activated protein kinase C (PKC) and link PKC to specific beta(1) integrins. J Biol Chem 276:25005-25013. doi:10.1074/jbc.M102156200

637. Zhang XA, Lane WS, Charrin S, Rubinstein E, Liu L (2003) EWI2/PGRL associates with the metastasis suppressor KAI1/CD82 and inhibits the migration of prostate cancer cells. Cancer Res 63:2665-2674

638. Zhao J, Ng SC, Lei Y, Yi F, Li J, Yu L, Zou K, Dan Z, Dai M, Ding Y, Song M, Mei Q, Fang X, Liu H, Shi Z, Zhou R, Xia M, Wu Q, Xiong Z, Zhu W, Deng L, Kamm MA, Xia B (2013) First prospective, population-based inflammatory bowel disease incidence study in mainland of China: the emergence of "western" disease. Inflamm Bowel Dis 19:1839-1845. doi:10.1097/MIB.0b013e31828a6551

639. Zheng R, Yano S, Zhang H, Nakataki E, Tachibana I, Kawase I, Hayashi S, Sone S (2005) CD9 overexpression suppressed the liver metastasis and malignant ascites via inhibition of proliferation and motility of small-cell lung cancer cells in NK cell-depleted SCID mice. Oncol Res 15:365-372

640. Zhou B, Liu L, Reddivari M, Zhang XA (2004) The palmitoylation of metastasis suppressor KAI1/CD82 is important for its motility- and invasiveness-inhibitory activity. Cancer Res 64:7455-7463. doi:10.1158/0008-5472.CAN-04-1574

641. Zhou FX, Merianos HJ, Brunger AT, Engelman DM (2001) Polar residues drive association of polyleucine transmembrane helices. Proc Natl Acad Sci U S A 98:2250-2255. doi:10.1073/pnas.041593698

642. Zhou XY, Yashiro-Ohtani Y, Nakahira M, Park WR, Abe R, Hamaoka T, Naramura M, Gu H, Fujiwara H (2002) Molecular mechanisms underlying differential contribution of CD28 versus non-CD28 costimulatory molecules to IL-2 promoter activation. J Immunol 168:3847-3854

643. Zigmond E, Varol C, Farache J, Elmaliah E, Satpathy AT, Friedlander G, Mack M, Shpigel N, Boneca IG, Murphy KM, Shakhar G, Halpern Z, Jung S (2012) Ly6C hi monocytes in the inflamed colon give rise to proinflammatory effector cells and migratory antigen-presenting cells. Immunity 37:1076-1090. doi:10.1016/j.immuni.2012.08.026

644. Zilber MT, Setterblad N, Vasselon T, Doliger C, Charron D, Mooney N, Gelin C (2005) MHC class II/CD38/CD9: a lipid-raft-dependent signaling complex in human monocytes. Blood 106:3074-3081. doi:10.1182/blood-2004-10-4094

645. Zoller M (2009) Tetraspanins: push and pull in suppressing and promoting metastasis. Nat Rev Cancer 9:40-55. doi:10.1038/nrc2543

646. Zuidscherwoude M, Gottfert F, Dunlock VM, Figdor CG, van den Bogaart G, van Spriel AB (2015) The tetraspanin web revisited by super-resolution microscopy. Sci Rep 5:12201. doi:10.1038/srep12201

647. Zuidscherwoude M, Worah K, van der Schaaf A, Buschow SI, van Spriel AB (2017) Differential expression of tetraspanin superfamily members in dendritic cell subsets. PLoS One 12:e0184317. doi:10.1371/journal.pone.0184317

648. Zushi S, Shinomura Y, Kiyohara T, Minami T, Sugimachi M, Higashimoto Y, Kanayama S, Matsuzawa Y (1996) Role of prostaglandins in intestinal epithelial restitution stimulated by growth factors. Am J Physiol 270:G757-762. doi:10.1152/ajpgi.1996.270.5.G757

Annexes

9. Annexes

9.1 Publications related with this thesis work

I. **Saiz ML**, Cibrian D, Ramírez-Huesca M, Torralba D, Moreno-Gonzalo O, Sánchez-Madrid F.Tetraspanin CD9 Limits Mucosal Healing in Experimental Colitis. Front Immunol. 2017 Dec 19;8:1854. doi: 10.3389/fimmu.2017.01854. eCollection 2017.

II. **Saiz ML**, Rocha-Perugini V and Sánchez-Madrid F. Tetraspanins as Organizers of Antigen-Presenting Cell Function. Front. Immunol. 2018 May 9:1074. doi: 10.3389/fimmu.2018.01074

9.2 Other publications

I. Roig J, **Saiz ML**, Galiano A, Trelis M, Cantalapiedra F, Monteagudo C, Giner E, Giner RM, Recio MC, Bernal D, Sánchez-Madrid F and Marcilla A. Extracellular Vesicles From the Helminth Fasciola hepatica Prevent DSS-Induced Acute Ulcerative Colitis in a T-Lymphocyte Independent Mode. Front. Microbiol. 2018 May 9:1036. doi: 10.3389/fmicb.2018.01036.

II. Cibrian D, **Saiz ML**, de la Fuente H, Sánchez-Díaz R, Moreno-Gonzalo O, Jorge I, Ferrarini A, Vázquez J, Punzón C, Fresno M, Vicente-Manzanares M, Daudén E, Fernández-Salguero PM, Martín P, Sánchez-Madrid F. CD69 controls the uptake of L-tryptophan through LAT1-CD98 and AhR-dependent secretion of IL-22 in psoriasis. Nat Immunol. 2016 Aug;17(8):985-96. doi: 10.1038/ni.3504. Epub 2016 Jul 4. Erratum in: Nat Immunol. 2016 Sep 20;17 (10):1235.

III. Moreno-Gonzalo O, Ramírez-Huesca M, Blas-Rus N, Cibrián D, **Saiz ML**, Jorge I, Camafeita E, Vázquez J, Sánchez-Madrid F. HDAC6 controls innate immune and autophagy responses to TLR-mediated signalling by the intracellular bacteria Listeria monocytogenes. PLoS Pathog. 2017 Dec 27;13(12):e1006799. doi: 10.1371/journal.ppat.1006799. eCollection 2017 Dec.

IV. González-Terán B, Matesanz N, Nikolic I, Verdugo MA, Sreeramkumar V, Hernández-Cosido L, Mora A, Crainiciuc G, **Saiz ML**, Bernardo E, Leiva-Vega L, Rodríguez E, Bondía V, Torres JL, Perez-Sieira S, Ortega L, Cuenda A, Sanchez-Madrid F, Nogueiras R, Hidalgo A, Marcos M, Sabio G. p38γ and p38δ reprogram liver metabolism by modulating neutrophil infiltration. EMBO J. 2016 Mar 1;35(5):536-52. doi: 10.15252/embj.201591857. Epub 2016 Feb 3.

frontiers in Immunology

ORIGINAL RESEARCH
published: 19 December 2017
doi: 10.3389/fimmu.2017.01854

Tetraspanin CD9 Limits Mucosal Healing in Experimental Colitis

*María Laura Saiz[1,2], Danay Cibrian[1,2,3], Marta Ramírez-Huesca[2], Daniel Torralba[1,2], Olga Moreno-Gonzalo[1,2] and Francisco Sánchez-Madrid[1,2,3]**

[1] Immunology Service, Hospital de la Princesa, Universidad Autónoma de Madrid, Instituto de Investigación Sanitaria del Hospital Universitario de La Princesa, Madrid, Spain, [2] Department of Vascular Biology and Inflammation, Centro Nacional de Investigaciones Cardiovasculares (CNIC), Madrid, Spain, [3] CIBER Cardiovascular, Madrid, Spain

Tetraspanins are a family of proteins with four transmembrane domains that associate between themselves and cluster with other partner proteins, conforming a distinct class of membrane domains, the tetraspanin-enriched microdomains (TEMs). These TEMs constitute macromolecular signaling platforms that regulate key processes in several cellular settings controlling signaling thresholds and avidity of receptors. In this study, we investigated the role of CD9, a tetraspanin that regulates major biological processes such as cell migration and immunological responses, in two mouse models of colitis that have been used to study the pathogenesis of inflammatory bowel disease (IBD). Previous *in vitro* studies revealed an important role in the interaction of leukocytes with inflamed endothelium, but *in vivo* evidence of the involvement of CD9 in inflammatory diseases is scarce. Here, we studied the role of CD9 in the pathogenesis of colitis *in vivo*. Colitis was induced by administration of dextran sodium sulfate (DSS), a chemical colitogen that causes epithelial disruption and intestinal inflammation. $CD9^{-/-}$ mice showed less severe colitis than wild-type counterparts upon exposure to DSS (2% solution) and enhanced survival in response to a lethal DSS dose (4%). Decreased neutrophil and macrophage cell infiltration was observed in colonic tissue from $CD9^{-/-}$ animals, in accordance with their lower serum levels of TNF-α, IL-6, and other proinflammatory cytokines in the colon. The specific role of CD9 in IBD was further dissected by transfer of $CD4^{+}$ $CD45RB^{hi}$ naive T cells into the $Rag1^{-/-}$ mouse colitis model. However, no significant differences were observed in these settings between both groups, ruling out a role for CD9 in IBD in the lymphoid compartment. Experiments with bone marrow chimeras revealed that CD9 in the non-hematopoietic compartment is involved in colon injury and limits the proliferation of epithelial cells. Our data indicate that CD9 in non-hematopoietic cells plays an important role in colitis by limiting epithelial cell proliferation. Future strategies to repress CD9 expression may be of therapeutic benefit in the treatment of IBD.

Keywords: tetraspanins, CD9, mucosal healing, dextran sodium sulfate, colitis

OPEN ACCESS

Edited by:
Annemiek van Spriel, Radboud University Nijmegen Medical Center, Netherlands

Reviewed by:
Peter Monk, University of Sheffield, United Kingdom
Gernot Sellge, Uniklinik RWTH Aachen, Germany

***Correspondence:**
Francisco Sánchez-Madrid
fsmadrid@salud.madrid.org

Specialty section:
This article was submitted to Molecular Innate Immunity, a section of the journal Frontiers in Immunology

Received: *03 October 2017*
Accepted: *07 December 2017*
Published: *19 December 2017*

Citation:
Saiz ML, Cibrian D, Ramírez-Huesca M, Torralba D, Moreno-Gonzalo O and Sánchez-Madrid F (2017) Tetraspanin CD9 Limits Mucosal Healing in Experimental Colitis. Front. Immunol. 8:1854. doi: 10.3389/fimmu.2017.01854

INTRODUCTION

Inflammatory bowel disease (IBD) defines a group of intestinal disorders, principally, ulcerative colitis (UC) and Crohn's disease (CD). Both diseases are characterized by chronic inflammation of the gastrointestinal tract interspersed with relapsing phases (1). Much progress has been made in understanding UC and CD disease mechanisms, for example, through genome-wide association

studies in patients; however, these diseases remain incompletely understood. Identified genetic risk loci have revealed defects in IBD patients affecting genes crucial for intestinal homeostasis, including epithelial barrier function, restitution, and wounding (2). Moreover, recent clinical studies have revealed mucosal healing (MH) as the major prognostic predictor of long-term remission in IBD patients (3, 4), suggesting that epithelial regeneration is critical to improving IBD therapy (5).

Tetraspanins are proteins that span the cell membrane four times and play an important role in plasma membrane organization through the formation of tetraspanin-enriched microdomains, which enable them to associate with multiple proteins, including other tetraspanins (6). The tetraspanin CD9 is broadly expressed on the surface of several cell types, including many malignant tumor cells, as well as normal hematopoietic, endothelial, and epithelial cells (7, 8). Soon after its identification, CD9 was found to associate with several integrins (9), enabling CD9 to exert pro- or anti-migratory effects (10). CD9 can also interact with the immunoglobulin superfamily members EWI-2 and EWI-F (11), DDR1 (12), other tetraspanins (e.g., CD81 and CD151) (13), claudin-1 (14), ADAM10 (15), and ADAM17 (16) metalloproteases, epidermal growth factor receptor (EGFR) (17), and membrane-bound EGFR ligands (18, 19). Moreover, CD9 has been reported to regulate endothelial nanoscopic organization and expression levels of ICAM-1 and VCAM-1 upon TNF-α activation, enabling formation of the docking structure required for leukocyte extravasation (20, 21). Anti-CD9 agonistic antibodies or ectopic expression of CD9 both exert an antiproliferative effect on human colon carcinoma cell lines (22). However, the role of CD9 in IBD has not been previously addressed *in vivo*. Here, we show that CD9 acts as a limiting factor for epithelial regeneration and colonic MH in dextran sodium sulfate (DSS)-induced colitis.

MATERIALS AND METHODS

Mice

Experiments were performed with sex and age matched (8- to 12-week old) $CD9^{-/-}$ and WT mice on the C57BL/6 background. $CD9^{-/-}$ mice have been described previously (23). $Rag1^{-/-}$ mice (24) used in the adoptive transfer colitis model were kindly provided by Dr. J. M. Fernández-Granado (CNIC). For chimeric reconstitution experiments, B6SJL CD45.1 mice (Jackson Laboratories) were used. All animals were housed in pathogen-free conditions at the CNIC animal facility. Experimental procedures were approved by the local research ethics committee and conformed to EU Directive 2010/63EU and Recommendation 2007/526/EC, enforced in Spanish law under Real Decreto 53/2013.

Induction and Assessment of DSS-Induced Colitis

Dextran sulfate sodium salt (DSS, MP Biomedicals; $M_W = 36{,}000$–$50{,}000$) was dissolved at 2 or 4% (w/v) in sterile drinking water provided to mice *ad libitum*. Mice were checked daily for development of colitis by monitoring body weight, fecal occult blood (Hemoccult II Sensa; Beckman Coulter) or gross rectal bleeding, and stool consistency. Overall disease severity was assessed by a clinical scoring system defined as follows: weight loss: 0 (no loss), 1 (1–5%), 2 (5–10%), 3 (10–20%), and 4 (>20%); stool consistency: 0 (normal), 2 (loose stool), and 4 (diarrhea); and bleeding: 0 (no blood), 1 (Hemoccult positive), 2 (Hemoccult positive and visual pellet bleeding), and 4 (gross bleeding, blood around anus). At the end of the experiment, tissues were fixed in 10% neutral buffered formalin (Bio Optica) for 24 h and transferred to 70% ethanol. After embedding in paraffin, transverse sections (4–5 μm) of proximal and distal colon were stained with H&E for histological studies. Images were digitized using Hamamatsu Nanozoomer 2.0 RS scan and NDP.scan 2.5 digitization software. Three images of two serial sections cut at a separation of 100 μm (six sections in total) were evaluated for each mouse for each part of the colon (proximal and distal). Histological scoring evaluated inflammation severity, crypt damage, and ulceration. Inflammation severity was scored as follows: 0, rare inflammatory cells in the lamina propria; 1, increased numbers of granulocytes in the lamina propria; 2, confluence of inflammatory cells extending into the submucosa; 3, transmural extension of the inflammatory infiltrate. Crypt damage was scored as follows: 0, intact crypts; 1, loss of the basal one-third; 2, loss of the basal two-thirds; 3, entire crypt loss; 4, change of epithelial surface with erosion; 5, confluent erosion. Ulceration was scored as follows: 0, absence of ulcers; 1, 1–2 ulceration foci; 2, 3–4 ulceration foci; 3, confluent or extensive ulceration. Scores for each parameter were summed to give a maximum histological score of 11.

T Cell-Mediated Colitis

Naive $CD4^+$ T cells were sorted (FACSaria sorter, BD) from single-cell spleen suspensions of $CD9^{-/-}$ or WT mice. Live cells were isolated after labeling with antibodies to CD4, CD62, CD25, and CD45RB (eBiosciences) and hoescht 33258. Cells were transferred to recipient mice ($4–5 \times 10^5$ cells per mouse) by intraperitoneal injection.

Bone Marrow Chimeras

Bone marrow transfer was used to create chimeric mice in which genetic deficiency for CD9 was confined to either circulating cells ($CD9^{-/-}$ > WT) or nonhematopoietic tissue (WT > $CD9^{-/-}$). Briefly, bone marrows were collected from femur and tibia of congenic WT donor mice (expressing CD45.1 leukocyte antigen) or $CD9^{-/-}$ and WT donor mice (expressing CD45.2 leukocyte antigen) by flushing with PBS. Erythrocytes were lysed (ACK lysis buffer, Lonza) for 1 min on ice. After a washing step, cells were resuspended in PBS at 1×10^8/ml. This cell suspension (100 μl) was injected intravenously into 13 Gy-irradiated recipient mice 48 h postirradiation. Four chimera groups were generated: WT > WT (WT cells expressing CD45.1 into WT mice expressing CD45.2); WT > $CD9^{-/-}$ (WT cells expressing CD45.1 into $CD9^{-/-}$ mice expressing CD45.2); WT > WT (WT cells expressing CD45.2 into WT mice expressing CD45.1); $CD9^{-/-}$ > WT ($CD9^{-/-}$ cells expressing CD45.2 into WT mice expressing CD45.1). Bone marrow reconstitution was verified after 8 weeks by staining for CD45.1 or CD45.2 in blood cells with anti-CD45.1 or anti-CD45.2 specific antibodies (BD Biosciences).

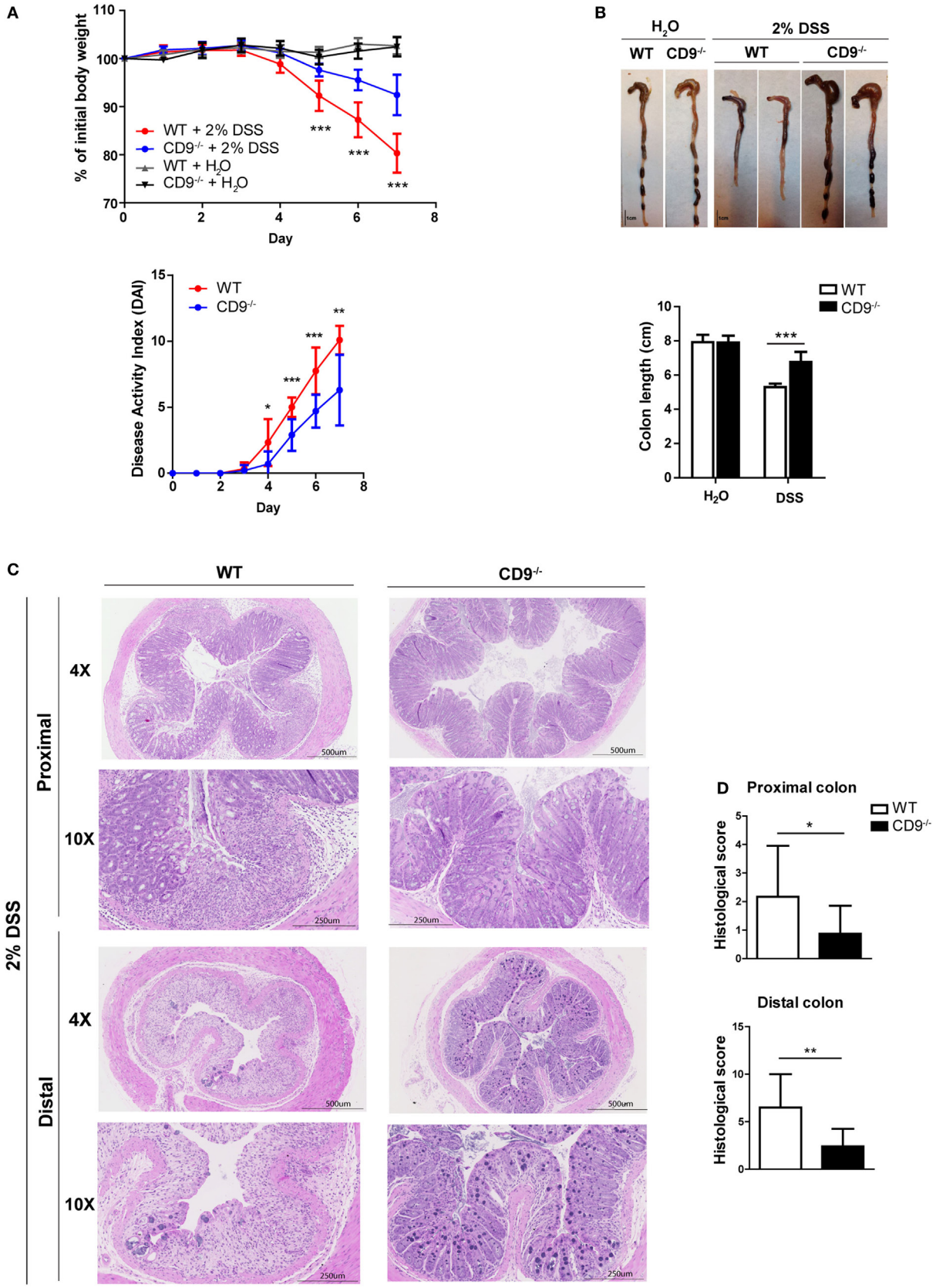

FIGURE 1 | Continued

FIGURE 1 | CD9-deficiency reduces sensitivity to dextran sodium sulfate (DSS)-induced colitis. **(A)** *Top,* body-weight loss in WT and CD9$^{-/-}$ mice after administration of 2% DSS in drinking water for 7 days. Controls for each genotype were administered with unadulterated drinking water. *Bottom*, disease activity index (DAI) score in WT and CD9$^{-/-}$ mice after administration of 2% DSS for 7 days. n = 10–12 per group; $^{*}P < 0.05$; $^{**}P < 0.005$; $^{***}P < 0.001$, unpaired t-test. **(B)** Macroscopic colon damage in DSS-treated WT and CD9$^{-/-}$ mice. *Top*, Colon shrinkage. *Bottom*, changes in colon length. Representative colons are shown of n = 10–12 mice per group. **(C)** Representative photomicrographs of proximal colon (near the cecum) and distal colon (near the anus) from WT and CD9$^{-/-}$ mice at day 7 of DSS administration (H&E; magnifications: 4× and 10×). **(D)** Histological scores obtained from H&E-stained proximal and distal colon tissue sections from DSS-treated WT and CD9$^{-/-}$ mice. Data are pooled from two independent experiments (n = 4). Values represent mean ± SD of the mean: $^{*}P < 0.05$; $^{**}P < 0.005$; $^{***}P < 0.001$, unpaired t-test.

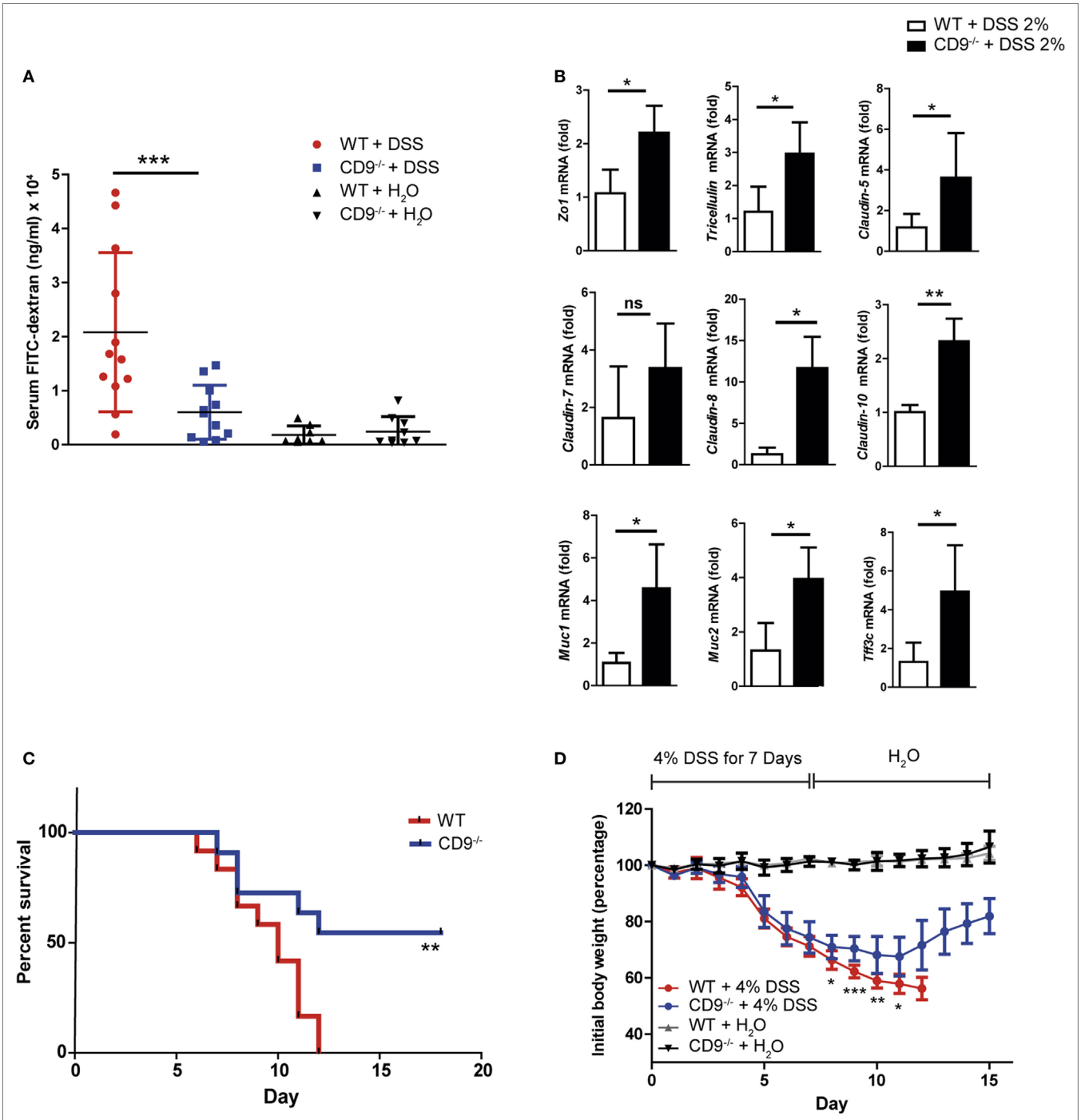

FIGURE 2 | Continued

FIGURE 2 | Enhanced epithelial barrier integrity and survival in CD9$^{-/-}$ mice after dextran sodium sulfate (DSS) challenge **(A)** *In vivo* colon permeability, indexed from the serum level of 4 kDa FITC-dextran 4 h after feeding by gavage. Data are pooled from two independent experiments, $n = 5$–6 animals per group. Data were analyzed by one-way ANOVA and the Newman–Keuls multiple comparison test; $^{***}P < 0.001$. **(B)** qPCR analysis of tight junction and mucin gene expression in colon samples after 7 days of DSS exposure. Data are from one experiment repeated two times with similar results. **(C)** Kaplan–Meier survival for WT and CD9$^{-/-}$ mice given 4% DSS in drinking water. $^{**}P < 0.01$, Log-rank (Mantel–Cox) test. **(D)** Percentage of initial body weight of WT and CD9$^{-/-}$ mice after 7-day intake of 4% DSS chased by unadulterated water. $n = 11$–12 per group: $^{*}P < 0.05$; $^{**}P < 0.005$; $^{***}P < 0.001$; unpaired *t*-test for WT and CD9$^{-/-}$ groups in **(B,C)**.

In Vivo Permeability Assay

Food was withdrawn overnight and mice were gavaged with the permeability tracer FITC-dextran (MW 4,000; Sigma-Aldrich) at 60 mg/100 g body weight. After 4 h, blood was collected by heart puncture and serum FITC-dextran was measured with a fluorescence spectrophotometer (Fluoroskan Ascent; Thermo Labsystems) using emission and excitation wavelengths of 490 and 520 nm, respectively. FITC-dextran concentration was determined from a standard curve generated by serialdilution.

Isolation and Flow Cytometry Analysis of Colonic Leukocytes

Colons were dissected longitudinally, washed several times with PBS to remove feces, and cut into small pieces. Samples were digested with 0.25 mg/ml Liberase TM (Roche), 50 µg/ml DNAseI (Roche), and 1 mM DTT diluted in Hank's Balanced Solution for 30 min at 37°C. At the end of the incubation period, enzyme activity was blocked by adding 50 ml PBS supplemented with 0.5% BSA and 0.05 mM EDTA (PBS–BSA–EDTA), and the sample was mechanically disrupted by passing through a 70-µm cell strainer to obtain a cell suspension. When only epithelial cells were required, samples were incubated in 5 mM EDTA, 1 mM DTT for 20 min before enzyme digestion. Before all staining procedures, colon cell suspensions were incubated with anti-mouse FcRII/III (clone 2.4G2, TONBO Biosciences) for 10 min at 4°C in PBS-BSA-EDTA. Flow cytometry analysis of DSS-induced inflammation was performed with anti-mouse antibodies to the following antigens: CD45 (BD Horizon) and CD11b, CD64, and Ly6G (BD Pharmingen). For epithelial cell proliferation analysis, antibodies were used targeting EpCAM (Biolegend) and Ki67 (BD Pharmingen). Absolute cell numbers were obtained using TruCount Tubes (BD Biosciences). Cell samples were acquired in a FACSCanto Flow Cytometer (BD Biosciences), and the data were analyzed with FlowJo (Tree Star) or FACSDiva (BD Biosciences) software.

Flow Cytometric Bead Array (CBA)

Serum TNF-α, IL-6, and IFNγ were determined using the mouse Th1/Th2/Th17 BD CBA.

RNA Extraction and Real-time Quantitative PCR

RNA was isolated by disrupting colon tissue samples with TRIzol Reagent (1 ml per 50–100 mg tissue, Qiagen) and homogenizing in a tissue disruptor (Ika ultra-turrax T10 homogenizer). DSS traces were removed by the LiCl method (Ambion). Residual DNA contamination was eliminated with the Turbo DNA-free Kit (Ambion). Total RNA (1 µg) was reverse transcribed to cDNA with a Reverse Trancription Kit (Applied Biosystems). Quantitative PCR was then performed in an AB7900_384 (Applied Biosystems) using SYBR Green (Applied Biosystems) as the reporter. Gene-specific primers used are listed in Table S1 in Supplementary Material. Expression of each gene of interest was normalized to housekeeping gene GAPDH. Data are presented as relative fold differences calculated by the $2^{-\Delta\Delta Ct}$ method.

In Vitro T Cell Differentiation

Naive CD4$^+$ T cells were obtained by incubating single-cell suspensions of spleen and lymph nodes with biotinylated antibodies to CD8, CD16, CD19, F4/80, Gr-1, MHC class II (I-Ab), CD11b, CD11c, and DX5 followed by incubation with Streptavidin Microbeads (MACS, Miltenyi Biotec). CD4$^+$ T cells were isolated by negative selection in an auto-MACSTM Pro Separator (Miltenyi Biotec). Next, cells were activated with plate-bound anti-CD3 (5 µg/ml) and anti-CD28 (2 µg/ml) in RPMI 1640 medium (Sigma-Aldrich) supplemented with 10% FCS, 2×10^{-3} M L-glutamine, 100 U/ml penicillin, 100 µg/ml streptomycin, 50 µM 2-mercaptoethanol, and the corresponding cytokine cocktail: for Th0, anti-IFNγ (4 µg/ml), anti-IL-4 (4 µg/ml), and IL-2 (10 ng/ml); for Th1 anti-IL-4 (4 µg/ml), IL-12 (10 ng/ml), and IL-2 (10 ng/ml); for Th17 anti-IFNγ (4 µg/ml), anti-IL-4 (4 µg/ml), IL-6 (20 ng/ml), IL-23 (10 ng/ml), and TGF-β1 (5 ng/ml); and for Treg anti-IFNγ (4 µg/ml), anti-IL-4 (4 µg/ml), and TGF-β1 (10 ng/ml). After 72 h of culture, IFNγ, IL-17, or IL-10 in the supernatant were measured by ELISA (Ready-SET-Go, eBiosciences). For FACS analysis, intracellular cytokine staining was preceded by restimulation for 4 h with 50 ng/ml phorbol dibutyrate (PMA) and 500 ng/ml ionomycin in the presence of brefeldin A (1 µg/ml) (BD Biosciences).

Immunofluorescence and Immunohistochemical Analysis

For IF and IHC staining, colon sections were deparaffinized, boiled in antigen retrieval solution (10 mM Tris Base, 1 mM EDTA Solution, 0.05% Tween 20, pH 9.0 for Ki67 and 10 mM sodium citrate, 0.05% Tween 20, pH = 6 for caspase-3), and incubated with the rabbit monoclonal anti-mouse Ki67 primary antibody (Master Diagnostica, clon SP6) for IF or anti active caspase-3 rabbit polyclonal antibody for IHC (R&D system, catalog AF835). Bound antibodies were detected with a goat anti-rabbit 647 (ThermoFischer Scientific) for IF or the anti-rabbit EnVision FLEX-HRP detection system (Agilent) for IHC. Staining was developed with DAB substrate (Dako K3468), and slides were counterstained with Mayers Hematoxylin. Ki67 and

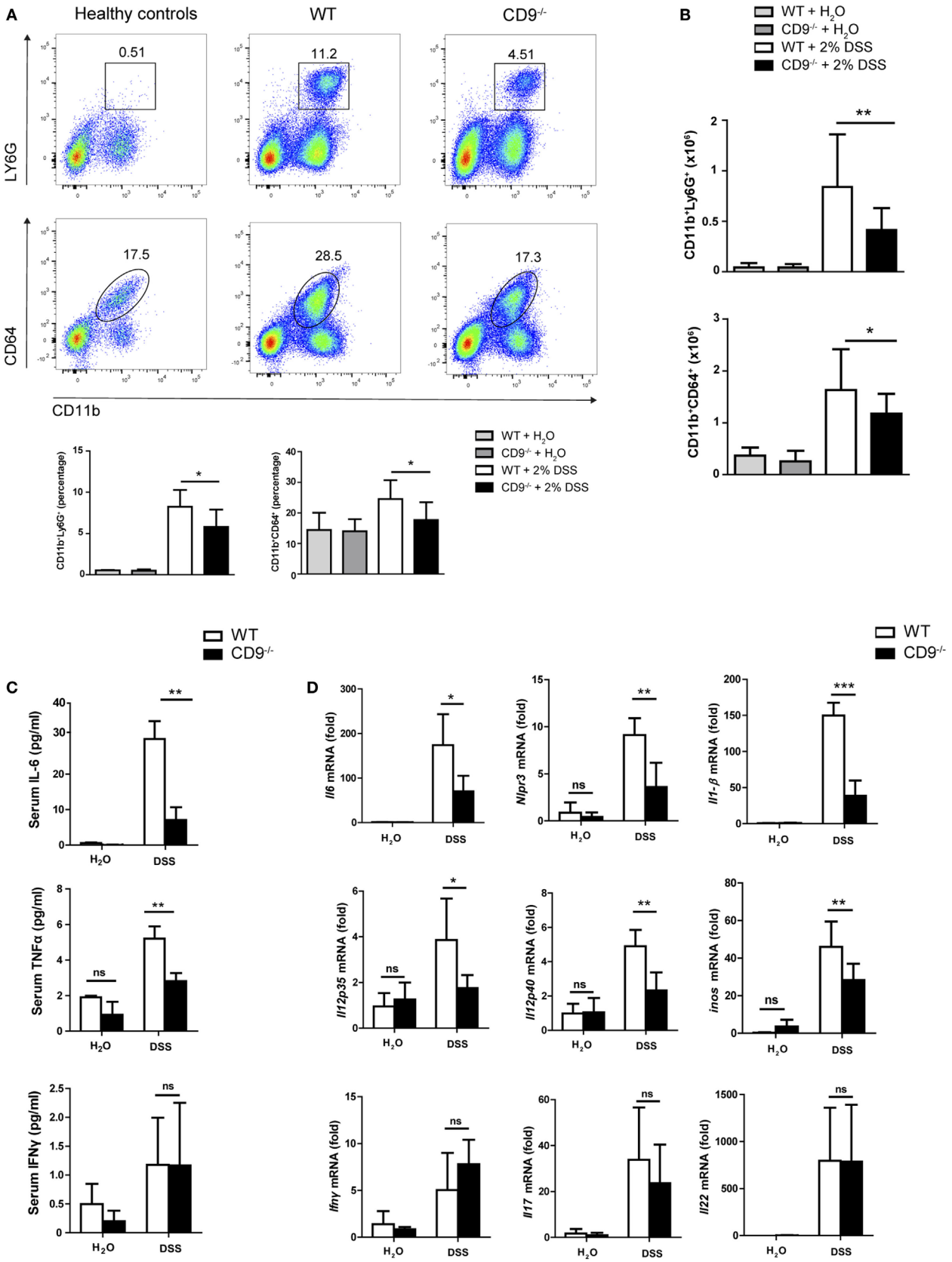

FIGURE 3 | Continued

FIGURE 3 | CD9$^{-/-}$ mice exhibit lower leukocyte infiltration and proinflammatory cytokines in serum and colon after 2% dextran sodium sulfate (DSS) administration. **(A)** Flow cytometry analysis of whole colon from WT and CD9$^{-/-}$ mice after 7-day 2% DSS intake. Representative dot plots and percentage quantification of CD45^{+} populations show similar DSS-induced infiltration by neutrophils (Ly6G^{+}) and macrophages (CD64^{+}) in both genotypes. **(B)** Total neutrophil and macrophage numbers in the CD45^{+}-gated population, determined by TruCount Tubes. Data are pooled from two independent experiments. For **(A,B)**, n = 6–7 mice per group with two repeats and analysis by one-way ANOVA and the Newman–Keuls multiple comparison test. *P < 0.05; **P < 0.005; ***P < 0.001. **(C)** Serum levels of TNF-α, IL-6, and IFNγ measured by cytometric bead array assay. **(D)** qPCR analysis of colonic proinflammatory cytokine mRNA expression. Bars denote the mean ± SD of n = 4–5 mice per genotype. Data from **(C,D)** were analyzed by two-way ANOVA and the Bonferroni multiple comparison test.

active caspase-3 staining in epithelial cells were quantified in the whole colon sections from each DSS-treated mouse (4–5 mice per group). Image J (1.46r) was used to measure Ki67 positive individual nuclei and to measure caspase-3 intensity relative to the total area corresponding to the complete epithelial layer in each image.

Statistical Analysis

Data are presented as mean ± SD. Normal data distribution was assessed with the Kolmogorov Smirnov test, and the statistical significance of between-group differences was assessed by one-tailed unpaired Student's *t*-test or one-way ANOVA with Newman–Keuls multiple comparison *t*-test, as required. All statistical analyses were performed with GraphPad Prism (GraphPad Software Inc.).

RESULTS

CD9$^{-/-}$ Mice Are Protected against DSS-Induced Colonic Injury

To explore the function of CD9 in colitis development, we challenged CD9$^{-/-}$ and WT mice with the toxic compound DSS (2% solution) in drinking water for 7 days. CD9$^{-/-}$ animals lost less than 10% of their initial body weight, whereas WT counterparts lost around 20% (**Figure 1A**, top). To monitor disease activity, we recorded a daily disease activity index (DAI) combining weight loss, stool consistency, and bleeding. From day 4, DAI values were lower in CD9$^{-/-}$ mice than in WT counterparts (**Figure 1A**, bottom). Autopsy revealed that DSS-treated CD9$^{-/-}$ mice had significantly larger colons than WT counterparts (**Figure 1B**). Histology revealed a better preservation of tissue architecture in CD9$^{-/-}$ mice, in both the proximal and the distal colon. DSS-treated WT animals showed more pronounced epithelial denudation, crypt distortion, leukocyte infiltration of the lamina propria, and submucosal swelling (**Figure 1C**). Histological sections were scored for the severity of DSS-induced inflammation as described in Section "Materials and Methods." In both proximal and distal colon, histological scores were lower in CD9$^{-/-}$ mice than in WT mice, with the difference more pronounced in the distal colon (**Figure 1D**).

CD9 Exacerbates Tissue Injury and Decreases Mouse Survival after a Lethal DSS Dose

Intestinal epithelial integrity is necessary for efficient defense against intraluminal toxins, antigens, and enteric bacteria. Cells are tightly joined in a healthy epithelium, and transepithelial permeability can thus be determined as an index of epithelial integrity. To monitor gut barrier function *in vivo*, we treated CD9$^{-/-}$ and WT animals with 2% DSS for 7 days and then orally administered 4KDa FITC-Dextran. Fluorescence spectrophotometry detection of serum FITC after 4 h revealed markedly lower gastrointestinal permeability in CD9$^{-/-}$ mice than in WT mice (**Figure 2A**). Serum FITC levels in non-treated animals showed no significant between-genotype differences and remained below 5 μg/ml, consistent with an intact intestinal barrier function in the steady state (**Figure 2A**). Consistent with the FITC-Dextran data, qPCR of colon samples from DSS-treated CD9$^{-/-}$ mice revealed elevated expression of genes encoding epithelial tight junction proteins, such as ZO-1, tricellulin, and claudin family members (**Figure 2B**). CD9$^{-/-}$ colon also showed elevated expression of genes encoding epithelial globet cell proteins, such as the secretory mucin glycoproteins MUC1, MUC2, and trefoil factor 3, indicating normal intestinal function (**Figure 2B**). In a further approach, we exposed mice to a lethal DSS dose (4%) for 7 days followed by unadulterated drinking water for a further 8 days. At the end of the experiment all WT mice had died, whereas only 45% of the CD9$^{-/-}$ group were dead (**Figure 2C**). Moreover, the surviving CD9$^{-/-}$ mice showed a recovery in body weight (**Figure 2D**). These results show that CD9 impedes epithelial repair and contributes to colon injury at both sublethal and lethal DSS doses.

Reduced Myeloid Cell Infiltration and Proinflammatory Cytokine Expression in the Colon of CD9$^{-/-}$ Mice

To characterize the immune mechanisms of colonic mucosa damage, we analyzed CD9$^{-/-}$ and WT colon cells by flow cytometry. After 7-day exposure to 2% DSS, CD9$^{-/-}$ colon showed markedly lower neutrophil and macrophage infiltration than WT colon (**Figures 3A,B**). In contrast, in non-treated mice, gut populations of these immune cell subsets were comparable between genotypes (**Figures 3A,B**), as were mesenteric lymph nodes, intraepithelial lymphocyte and lamina propria populations (Figure S1 in Supplementary Material). DSS-treated CD9$^{-/-}$ mice also had lower serum levels of IL-6 and TNFα than WT mice, whereas IFNγ was similarly increased in response to DSS in both genotypes (**Figure 3C**). Analysis of colon samples by qPCR revealed lower DSS-induced levels of IL-6, IL-1β, NLPR3, iNOS, IL-12p35, and IL-12p40 mRNA in CD9$^{-/-}$animals, whereas IL-17, IL-22, and IFNγ showed no significant between-genotype differences (**Figure 3D**).

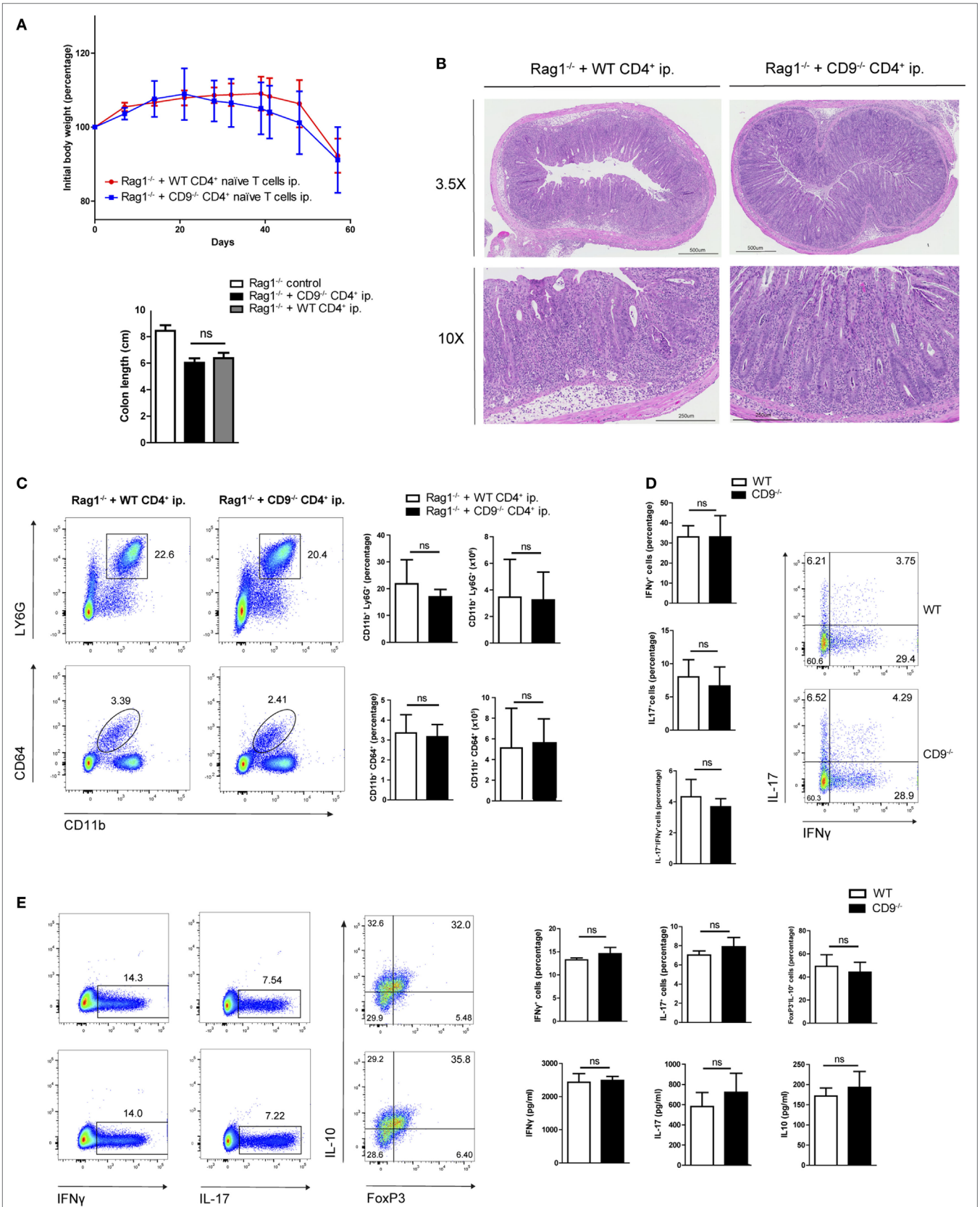

FIGURE 4 | Continued

FIGURE 4 | $CD4^+$ T cell-expressed CD9 does not contribute to adoptive transfer-mediated colitis or T cell differential subset skewing. **(A)** *Top,* body weight after intraperitoneal adoptive transfer of $CD4^+CD45RB^{hi}$ $CD62L^+CD25^-$ T cells from WT and $CD9^{-/-}$ donors into $Rag1^{-/-}$ recipients. *Bottom*, colon length at sacrifice on day 57. Data are from a representative experiment repeated three times with similar results. $n = 5$–6 mice per group; unpaired *t*-test. ns, non significant. **(B)** Representative 3.5× and 10× magnification H&E-stained colonic sections from $Rag1^{-/-}$ mice injected with WT and $CD9^{-/-}$ $CD4^+$ cells, showing transmural infiltration affecting all colon layers in both settings. **(C)** FACS analysis of myeloid cell infiltration. Representative dot plots are shown on the left; quantification of $CD45^+$-gated cell percentages and total numbers is shown on the right. **(D)** Flow cytometry analysis of intracellular staining for IFNγ and IL-17 in T cells from the mesenteric lymph nodes (MLNs) of $RAG1^{-/-}$ mice 2 months after $CD4^+$ T cell transfer. Cells were cultured for 72 h on an anti-CD3/CD28-coated plate and brefeldin A was added for the last 4 h. Representative dot plots and bar quantifications are shown of $CD4^+CD25^+$-gated cells. $n = 5$–6 mice per group; unpaired *t*-test. **(E)** *In vitro* T cell differentiation toward Th1, Th17, and Treg $CD4^+$ T cell subsets. Representative dots plots are shown of intracellular IFNγ, IL-17, and IL-10 in sorted populations, with quantification on the right (top row). Cytokine release was quantified by ELISA (bottom). Data are from a representative independent experiment of three performed and are presented as mean ± SD. $n = 5$ per genotype; unpaired *t*-test.

CD9 Expressed on $CD4^+$ T Cells Does Not Contribute to Immune-Cell Adoptive Transfer-Mediated Colitis

To further explore possible CD9-mediated immune mechanisms in IBD, we used an alternative model of colitis induced by intraperitoneal transfer into $Rag1^{-/-}$ mice of $CD4^+CD62L^+$ $CD25^-CD45RB^{hi}$ naive T cells sorted from WT or $CD9^{-/-}$ mice. Body weight was recorded over 2 months, showing no between-group differences (**Figure 4A**, top). Colon shortening was also similar in both genotypes (**Figure 4A**, bottom). Consistent with these findings, histological analysis revealed a similar extent of transmural inflammation in injected animals (**Figure 4B**), and flow cytometry showed similar increases in neutrophil and macrophage infiltration (**Figure 4C**). Restimulation of mesenteric lymph node $CD4^+$ cells with CD3/CD28 revealed no significant differences in Th1 and Th17 effector cell populations or cytokine production (**Figure 4D**). Likewise, no between-genotype differences were observed in the percentages of Th1, Th17, and Treg cells upon *in vitro* polyclonal differentiation of $CD4^+$ naive T cells from $CD9^{-/-}$ and WT mice (**Figure 4E**).

$CD9^{-/-}$ Bone Marrow Cells Transplanted into WT Mice Do Not Provide Protection against Colonic Injury

We next investigated the possible role of CD9 in myeloid cell populations or the resident non-hematopoietic cell compartment (mainly endothelial and epithelial cells). Two groups of chimeric mice were generated using the CD45.1 and CD45.2 haplotypes. Flow cytometry showed reconstitution levels of 95–99% (data not shown). Reconstitution experiments were carried out with WT CD45.1 mice and $CD9^{-/-}$ or WT CD45.2 mice, with irradiation and transplantation in either direction. Protection against DSS-induced colitis was observed only when irradiated $CD9^{-/-}$ mice were used as recipients of WT bone marrow (**Figures 5A,B**). Histology revealed typical DSS-induced changes in the distal and proximal colon of WT recipients and less pronounced alterations in $CD9^{-/-}$ recipients reconstituted with CD45.1 WT bone marrow (**Figures 5C,D**). Only $CD9^{-/-}$ recipients had lower DSS-induced levels of serum IL-6 measured by ELISA (**Figure 5E**), and colon samples from $CD9^{-/-}$ recipients also had lower induced transcript expression of proinflammatory cytokines measured by qPCR (**Figure 5F**). These results underscore the conclusion that susceptibility to DSS-induced colitis is increased by CD9 expression in the non-hematopoietic compartment.

Enhanced Colonocyte Proliferation after DSS-Induced Injury in $CD9^{-/-}$ Mice

After DSS-induced epithelial cell damage, the colonic epithelium actively proliferates to restore intestinal barrier integrity. Flow cytometry analysis of the proliferation marker Ki67 in colonic $EpCAM^+$ intestinal epithelial cells (IECs) from mice revealed that CD9 deficiency supports elevated colonic epithelial cell proliferation after DSS exposure (**Figure 6A**, top). However, no differences were detected in the proliferation of epithelial cells extracted from non-treated animals (Figure S2 in Supplementary Material). Remarkably, although the percentage of $Ki67^+$ cells was slightly higher in $CD9^{-/-}$ colon after 2 and 4 days of DSS exposure, the significant difference was observed at day 6. This is coincident with significant lower body weight loss and higher colon length in $CD9^{-/-}$ mice (**Figure 6A**, bottom). Moreover, $CD9^{-/-}$ colon showed higher mRNA expression of c-myc, c-fos, and cyclin D1 (**Figure 6B**). Analysis of the apoptosis marker caspase-3 was carried out by IHC in DSS-treated chimeric mice, with no differences between genotypes (Figure S3 in Supplementary Material). Proliferation in DSS-exposed colon of these animals was determined by counting immunostained $Ki67^+$ cells in colon crypts on histological sections. The percentage of $Ki67^+$ colonic cells was higher after DSS exposure in $CD9^{-/-}$ recipients than in WT recipients (**Figures 6C,D**). Taken together, these results demonstrate that CD9 limits epithelial cell proliferation in response to injury.

DISCUSSION

Inflammatory bowel disease arises through close interaction between genetics, immunology, environment, and microbiome. The development and progression of this multifactorial disorder is affected by several factors, including diet, lifestyle, and behavior. Moreover, perturbations of the gut microbiota due to antibiotic medication may also play an important role in IBD. DSS-induced colitis has become a widely used model for studying IBD in the mouse (25, 26). DSS is a chemical colitogen toxic to gut epithelial cells, interfering with intestinal barrier function and stimulating local inflammation. This

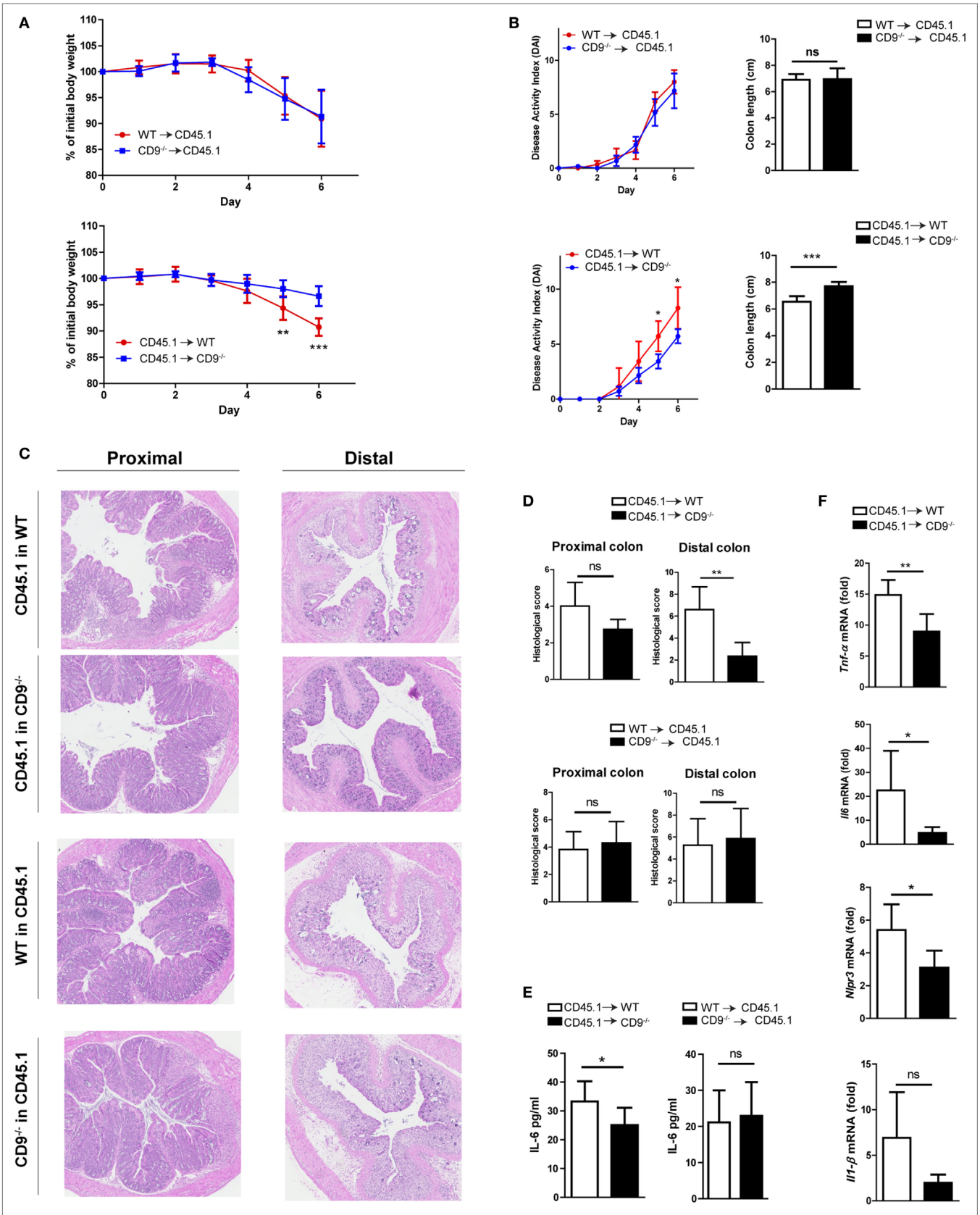

FIGURE 5 | Continued

FIGURE 5 | Lack of CD9 in the resident non-hematopoietic compartment confers the reduced susceptibility to dextran sodium sulfate (DSS)-mediated colitis. Lethally irradiated WT CD45.1 mice were rescued with WT or CD9$^{-/-}$ CD45.2 bone marrow, whereas lethally irradiated WT and CD9$^{-/-}$ CD45.2 mice were rescued with WT CD45.1 bone marrow. Three months post-transplantation mice were treated with 2% DSS. **(A)** Body weight evolution. **(B)** Disease activity index and colon shortening. **(C)** H&E stained proximal and distal colon sections. **(D)** Histological injury scores. **(E)** Serum IL-6 measured by ELISA. **(F)** qPCR analysis of proinflammatory cytokine expression in the colon of WT or CD9$^{-/-}$ CD45.2 recipients. Experiments were perfomed twice, giving similar results. $n = 6–7$ per group. All between-group comparisons were analyzed by unpaired *t*-test; $^{*}P < 0.05$; $^{**}P < 0.005$; $^{***}P < 0.001$.

model is suitable for studying events triggered by temporary failure of mucosal homeostasis after epithelial cell shedding and loss of barrier integrity, and can also provide insight into the mechanisms that lead to MH after initial injury (27). Here, we report protection against DSS-induced colonic mucosal damage in CD9-deficient mice. These mice show lower DAI scores throughout treatment, larger colons, and have a less severe histological injury. The protection conferred by CD9 absence was confirmed by the increased survival of CD9$^{-/-}$ mice upon administration of a lethal 4% DSS dose. Epithelial preservation *in vivo* was demonstrated by lower colonic transepithelial FITC-dextran leakage in CD9$^{-/-}$ mice, and the importance of CD9 in the control of intestinal epithelial barrier function and integrity was further demonstrated by preserved expression of tight junction and other barrier-related genes in CD9$^{-/-}$ mice.

CD9 is ubiquitously expressed, and we therefore performed chimeric reconstitution experiments to determine which cell compartment is responsible for mediating DSS-induced toxicity. Our data clearly demonstrated that protection in CD9$^{-/-}$ animals was not dependent on the hematopoietic cell compartment. In CD9$^{-/-}$ colon, crypt and villous distortion is minimal and surface epithelium is more preserved; this keeps luminal pathogens outside the lamina propria, and therefore proinflammatory cytokine and chemokine release is lower and there is less inflammatory cell recruitment. Specifically, the myeloid-derived cytokines involved in the inflammatory response in DSS acute colitis iNOs, TNF-α, IL-6, IL-12, and the inflammasome drivers NLRP3 and IL-1β were enhanced in WT mice versus CD9$^{-/-}$ mice, but no differences were observed in either IFNγ, IL-17, or IL-22 cytokines. DSS colitis can be exacerbated by granulocyte recruitment (28–30). However, the reconstitution experiments ruled out a contribution to colon protection from CD9 deficiency in innate immune cells. The role of endothelial CD9 could not be completely discarded, and additional research with endothelium-specific deletion of CD9 would be required to resolve this issue. In addition, CD9 plays an important role in T cell activation (31–34). However, our data in the adoptive T cell transfer-mediated colitis model and *in vitro* T cell polyclonal experiments showed no significant differences in the differentiation and activation of CD9-deficient and WT Th1 and Th17 T cell subsets.

Flow cytometry and immunohistochemistry analysis revealed a higher percentage of Ki67 IECs in DSS-exposed CD9$^{-/-}$ colon. In the distal colon, the percentage Ki67^{+} cells is lower than in the proximal colon. This likely reflects the more severe colitis in the middle and distal third of the colon in DSS-exposed mice, causing a predominantly distal injury characterized by epithelial ulceration and impaired regeneration (35). Notably, the difference in proliferation was observed after 6 days of DSS exposure, suggesting that it is related to mechanisms of post-injury epithelial recovery. CD9 absence thus does not increase IEC proliferation *per se* and only supports MH after injury. Indeed, hyperplasia and dysplasia were not observed in any CD9$^{-/-}$ animals after cessation of DSS exposure.

Dextran sodium sulfate treatment leads to the exposure of the Toll-like receptors on the IEC basolateral surface. This triggers a proliferation that contributes to mucosal repair after injury, and DSS-induced colitis is exacerbated in mice with gene deletions affecting TLR signaling such as Tlr2$^{-/-}$, Tlr4$^{-/-}$, and Myd88$^{-/-}$ (36–38). TLR signaling is linked to EGFR activation (39), which is required for intestinal homeostasis in the setting of acute mucosal damage (40, 41). CD9 could be playing several roles in these settings. EGFR signaling is increased in CD9-deficient cell lines (17, 42), and CD9 also negatively regulates ADAM17 (16) metalloproteinase activity, which is known to shed some EGFR ligands. CD9 deficiency will thus translate into increased EGFR phosphorylation and activation. Aside from a direct control of proliferation, CD9 might regulate epithelial restitution, its deficiency ultimately resulting in increased epithelial proliferation (43). In this context, CD9 absence might facilitate rapid resealing of the intestinal epithelial barrier and could promote IEC migration through impaired localization of talin-1 to focal adhesions (10) or increase CXCR4/CXCL12-mediated migration (44), a route that directly regulates epithelial cell migration, barrier maturation, and restitution (45). Compared with CD9-positive cells, CD9-negative or depleted epithelial and tumor cells have a much higher migratory capacity, thereby supporting epithelial restitution (42, 46).

Inflammatory bowel disease is effectively treated with anti-TNF-α monoclonal antibody (Infliximab), either as monotherapy or in combination with other immunomodulators, and current efforts are directed toward the crucial goal of achieving MH in order to accomplish long-term remission (4, 47). However, pharmacological anti-inflammatory agents such as glucocorticosteroids or 5-aminosalicylic acid do not heal the bowel mucosa (4), and the efficacy of growth factors such as GH and EGF has yet to be established (48). There is thus a clear need to identify new therapeutic targets for MH. Our results indicate that CD9 depletion enhances IEC proliferation, resulting in a high regenerative response and reduced susceptibility to DSS-induced colitis. Our findings thus reveal a critical role for the tetraspanin CD9 in colon inflammation and suggest a novel therapeutic opportunity. Growing recent evidence suggests that targeting tetraspanins by an array of

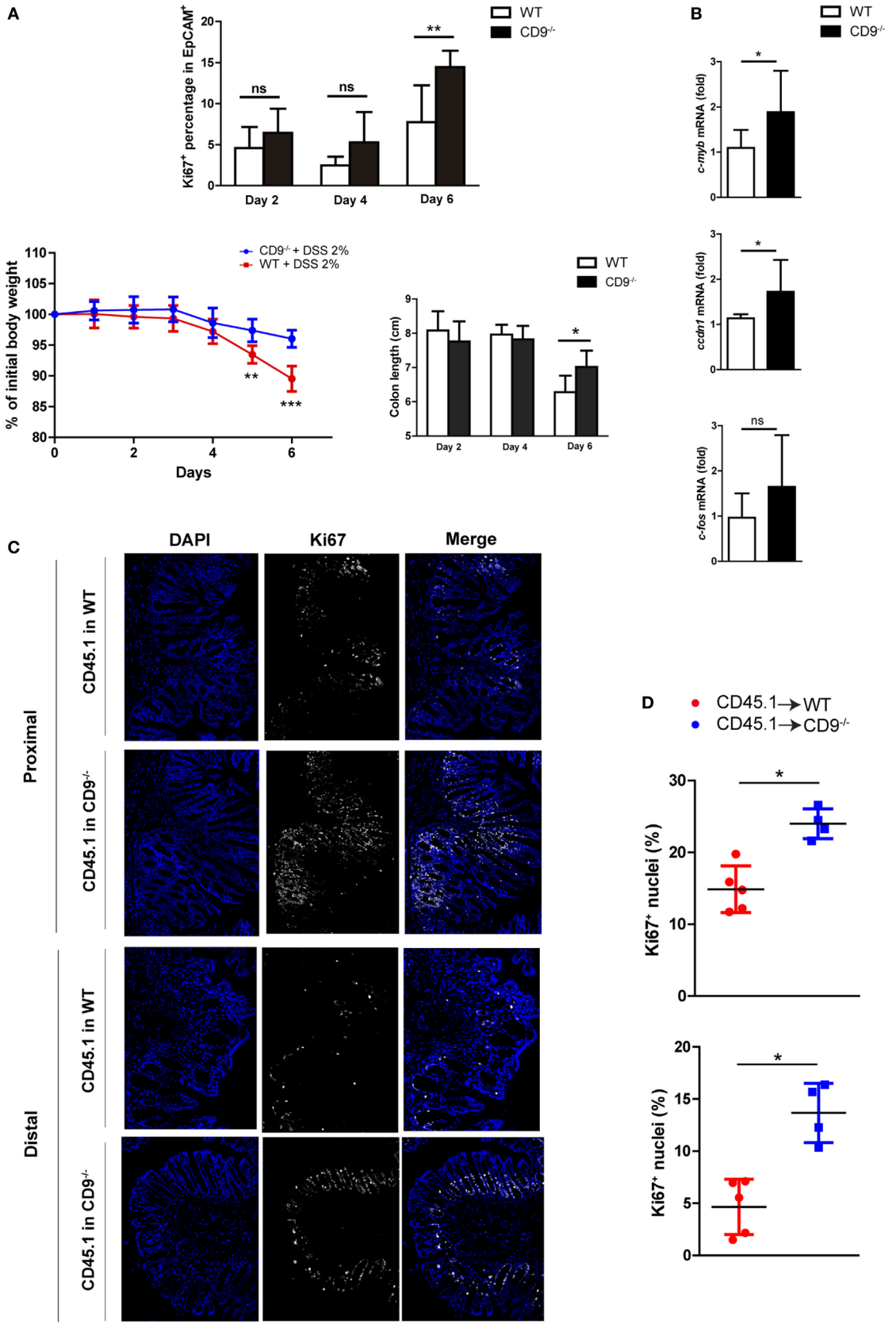

FIGURE 6 | Continued

FIGURE 6 | CD9 limits epithelial cell proliferation upon dextran sodium sulfate (DSS) challenge. **(A)** *Top*, FACS analysis of Ki67$^+$ cells in the EpCAM$^+$CD45$^-$ gated population after days 2, 4, and 6 days 2% DSS exposure (upper panel). *Bottom,* body weight loss and colon shortening, $n = 5$–6 mice per group. **(B)** qPCR analysis of colonic mRNA expression of the cell-cycle genes *c-myb*, *ccdn1*, and *c-fos*. Data are pooled from two independent experiments, $n = 4$–6 mice per group. **(C)** Ki67 immunofluorescence staining on proximal and distal colon sections from untreated or 6-day DSS-treated chimeric mice. Representative magnification images are shown. **(D)** Quantification of Ki67$^+$ cells in the epithelial layer of proximal (upper), and distal (lower) colons from 6-day DSS-fed chimeric mice. Each dot corresponds to the percentage of Ki67$^+$ nuclei from all the epithelial nuclei of whole colon sections $n = 4$–5 mice per genotype. Between-group comparisons were analyzed by unpaired *t*-test for **(A,B)** and Mann–Whitney *U*-test for **(D)**; $^*P < 0.05$; $^{**}P < 0.005$; $^{***}P < 0.001$.

tools including monoclonal antibodies, soluble large-loop proteins, and RNAi technology may be used to improve the course of IBDs.

ETHICS STATEMENT

All animals were housed in pathogen-free conditions at the CNIC animal facility. Experimental procedures were approved by the local research ethics committee and conformed to EU Directive 2010/63EU and Recommendation 2007/526/EC, enforced in Spanish law under Real Decreto 53/2013.

AUTHOR CONTRIBUTIONS

MS designed research plan and performed all mice studies, analyzed and interpreted all data, and wrote the manuscript. DC helped to designed research plan and in mice experimentation, data interpretation, and writing of the manuscript. MR-H, DT, and OM-G performed experimental work. FS-M planned research, discussed results, and collaborated to write the manuscript.

ACKNOWLEDGMENTS

We thank Dr. S. Bartlett for assistance with English editing and M. Vicente-Manzanares for critical reading of the manuscript. We also thank Cellomics and Histopathology CNIC units for technical advice.

FUNDING

This work was supported by grants to FS-M (SAF2014-55579-R; INDISNET-S2011/BMD-2332; ERC-2011-AdG 294340-GENTRIS; PIE13/00041; and CIBER CARDIOVASCULAR) and was cofunded by Fondo Europeo de Desarrollo Regional (FEDER). The CNIC is supported by the Spanish Ministry of Economy, Industry and Competitiveness (MINECO) and by the Pro CNIC Foundation.

SUPPLEMENTARY MATERIAL

The Supplementary Material for this article can be found online at http://www.frontiersin.org/articles/10.3389/fimmu.2017.01854/full#supplementary-material.

REFERENCES

1. Podolsky DK. Inflammatory bowel disease. *N Engl J Med* (2002) 347:417–29. doi:10.1056/NEJMra020831
2. Khor B, Gardet A, Xavier RJ. Genetics and pathogenesis of inflammatory bowel disease. *Nature* (2011) 474:307–17. doi:10.1038/nature10209
3. Froslie KF, Jahnsen J, Moum BA, Vatn MH, IBSEN Group. Mucosal healing in inflammatory bowel disease: results from a Norwegian population-based cohort. *Gastroenterology* (2007) 133:412–22. doi:10.1053/j.gastro.2007.05.051
4. Rutgeerts P, Vermeire S, Van Assche G. Mucosal healing in inflammatory bowel disease: impossible ideal or therapeutic target? *Gut* (2007) 56:453–5. doi:10.1136/gut.2005.088732
5. Pineton de Chambrun G, Peyrin-Biroulet L, Lemann M, Colombel JF. Clinical implications of mucosal healing for the management of IBD. *Nat Rev Gastroenterol Hepatol* (2010) 7:15–29. doi:10.1038/nrgastro.2009.203
6. Hemler ME. Tetraspanin functions and associated microdomains. *Nat Rev Mol Cell Biol* (2005) 6:801–11. doi:10.1038/nrm1736
7. Boucheix C, Duc GH, Jasmin C, Rubinstein E. Tetraspanins and malignancy. *Expert Rev Mol Med* (2001) 2001:1–17. doi:10.1017/1462399401002381
8. Yáñez-Mó M, Barreiro O, Gordon-Alonso M, Sala-Valdés M, Sánchez-Madrid F. Tetraspanin-enriched microdomains: a functional unit in cell plasma membranes. *Trends Cell Biol* (2009) 19:434–46. doi:10.1016/j.tcb.2009.06.004
9. Berditchevski F. Complexes of tetraspanins with integrins: more than meets the eye. *J Cell Sci* (2001) 114:4143–51.
10. Powner D, Kopp PM, Monkley SJ, Critchley DR, Berditchevski F. Tetraspanin CD9 in cell migration. *Biochem Soc Trans* (2011) 39:563–7. doi:10.1042/BST0390563
11. Charrin S, le Naour F, Silvie O, Milhiet PE, Boucheix C, Rubinstein E. Lateral organization of membrane proteins: tetraspanins spin their web. *Biochem J* (2009) 420:133–54. doi:10.1042/BJ20082422
12. Castro-Sanchez L, Soto-Guzman A, Navarro-Tito N, Martinez-Orozco R, Salazar EP. Native type IV collagen induces cell migration through a CD9 and DDR1-dependent pathway in MDA-MB-231 breast cancer cells. *Eur J Cell Biol* (2010) 89:843–52. doi:10.1016/j.ejcb.2010.07.004
13. Kovalenko OV, Yang X, Kolesnikova TV, Hemler ME. Evidence for specific tetraspanin homodimers: inhibition of palmitoylation makes cysteine residues available for cross-linking. *Biochem J* (2004) 377:407–17. doi:10.1042/bj20031037
14. Kovalenko OV, Yang XH, Hemler ME. A novel cysteine cross-linking method reveals a direct association between claudin-1 and tetraspanin CD9. *Mol Cell Proteomics* (2007) 6:1855–67. doi:10.1074/mcp.M700183-MCP200
15. Arduise C, Abache T, Li L, Billard M, Chabanon A, Ludwig A, et al. Tetraspanins regulate ADAM10-mediated cleavage of TNF-alpha and epidermal growth factor. *J Immunol* (2008) 181:7002–13. doi:10.4049/jimmunol.181.10.7002
16. Gutiérrez-López MD, Gilsanz A, Yáñez-Mó M, Ovalle S, Lafuente EM, Domínguez C, et al. The sheddase activity of ADAM17/TACE is regulated by the tetraspanin CD9. *Cell Mol Life Sci* (2011) 68:3275–92. doi:10.1007/s00018-011-0639-0
17. Murayama Y, Shinomura Y, Oritani K, Miyagawa J, Yoshida H, Nishida M, et al. The tetraspanin CD9 modulates epidermal growth factor receptor signaling in cancer cells. *J Cell Physiol* (2008) 216:135–43. doi:10.1002/jcp.21384

18. Inui S, Higashiyama S, Hashimoto K, Higashiyama M, Yoshikawa K, Taniguchi N. Possible role of coexpression of CD9 with membrane-anchored heparin-binding EGF-like growth factor and amphiregulin in cultured human keratinocyte growth. *J Cell Physiol* (1997) 171:291–8. doi:10.1002/(SICI)1097-4652(199706)171:3<291::AID-JCP7>3.0.CO;2-J
19. Shi W, Fan H, Shum L, Derynck R. The tetraspanin CD9 associates with transmembrane TGF-alpha and regulates TGF-alpha-induced EGF receptor activation and cell proliferation. *J Cell Biol* (2000) 148:591–602. doi:10.1083/jcb.148.3.591
20. Barreiro O, Yáñez-Mó M, Sala-Valdés M, Gutiérrez-López MD, Ovalle S, Higginbottom A, et al. Endothelial tetraspanin microdomains regulate leukocyte firm adhesion during extravasation. *Blood* (2005) 105:2852–61. doi:10.1182/blood-2004-09-3606
21. Barreiro O, Zamai M, Yáñez-Mó M, Tejera E, López-Romero P, Monk PN, et al. Endothelial adhesion receptors are recruited to adherent leukocytes by inclusion in preformed tetraspanin nanoplatforms. *J Cell Biol* (2008) 183:527–42. doi:10.1083/jcb.200805076
22. Ovalle S, Gutiérrez-López MD, Olmo N, Turnay J, Lizarbe MA, Majano P, et al. The tetraspanin CD9 inhibits the proliferation and tumorigenicity of human colon carcinoma cells. *Int J Cancer* (2007) 121:2140–52. doi:10.1002/ijc.22902
23. Le Naour F, Rubinstein E, Jasmin C, Prenant M, Boucheix C. Severely reduced female fertility in CD9-deficient mice. *Science* (2000) 287:319–21. doi:10.1126/science.287.5451.319
24. Mombaerts P, Iacomini J, Johnson RS, Herrup K, Tonegawa S, Papaioannou VE. RAG-1-deficient mice have no mature B and T lymphocytes. *Cell* (1992) 68:869–77. doi:10.1016/0092-8674(92)90030-G
25. Okayasu I, Hatakeyama S, Yamada M, Ohkusa T, Inagaki Y, Nakaya R. A novel method in the induction of reliable experimental acute and chronic ulcerative colitis in mice. *Gastroenterology* (1990) 98:694–702. doi:10.1016/0016-5085(90)90290-H
26. Cooper HS, Murthy SN, Shah RS, Sedergran DJ. Clinicopathologic study of dextran sulfate sodium experimental murine colitis. *Lab Invest* (1993) 69:238–49.
27. Kiesler P, Fuss IJ, Strober W. Experimental models of inflammatory bowel diseases. *Cell Mol Gastroenterol Hepatol* (2015) 1:154–70. doi:10.1016/j.jcmgh.2015.01.006
28. Natsui M, Kawasaki K, Takizawa H, Hayashi SI, Matsuda Y, Sugimura K, et al. Selective depletion of neutrophils by a monoclonal antibody, RP-3, suppresses dextran sulphate sodium-induced colitis in rats. *J Gastroenterol Hepatol* (1997) 12:801–8. doi:10.1111/j.1440-1746.1997.tb00375.x
29. Williams IR, Parkos CA. Colonic neutrophils in inflammatory bowel disease: double-edged swords of the innate immune system with protective and destructive capacity. *Gastroenterology* (2007) 133:2049–52. doi:10.1053/j.gastro.2007.10.031
30. Chami B, Yeung AW, van Vreden C, King NJ, Bao S. The role of CXCR3 in DSS-induced colitis. *PLoS One* (2014) 9:e101622. doi:10.1371/journal.pone.0101622
31. Tai XG, Yashiro Y, Abe R, Toyooka K, Wood CR, Morris J, et al. A role for CD9 molecules in T cell activation. *J Exp Med* (1996) 184:753–8. doi:10.1084/jem.184.2.753
32. Tai XG, Toyooka K, Yashiro Y, Abe R, Park CS, Hamaoka T, et al. CD9-mediated costimulation of TCR-triggered naive T cells leads to activation followed by apoptosis. *J Immunol* (1997) 159:3799–807.
33. Toyo-oka K, Tai XG, Yashiro Y, Ahn HJ, Abe R, Hamaoka T, et al. Synergy between CD28 and CD9 costimulation for naive T-cell activation. *Immunol Lett* (1997) 58:19–23. doi:10.1016/S0165-2478(97)02706-5
34. Rocha-Perugini V, González-Granado JM, Tejera E, López-Martín S, Yañez-Mó M, Sánchez-Madrid F. Tetraspanins CD9 and CD151 at the immune synapse support T-cell integrin signaling. *Eur J Immunol* (2014) 44:1967–75. doi:10.1002/eji.201344235
35. Perse M, Cerar A. Dextran sodium sulphate colitis mouse model: traps and tricks. *J Biomed Biotechnol* (2012) 2012:718617. doi:10.1155/2012/718617
36. Fukata M, Michelsen KS, Eri R, Thomas LS, Hu B, Lukasek K, et al. Toll-like receptor-4 is required for intestinal response to epithelial injury and limiting bacterial translocation in a murine model of acute colitis. *Am J Physiol Gastrointest Liver Physiol* (2005) 288:G1055–65. doi:10.1152/ajpgi.00328.2004
37. Rakoff-Nahoum S, Paglino J, Eslami-Varzaneh F, Edberg S, Medzhitov R. Recognition of commensal microflora by toll-like receptors is required for intestinal homeostasis. *Cell* (2004) 118:229–41. doi:10.1016/j.cell.2004.07.002
38. Cario E, Gerken G, Podolsky DK. Toll-like receptor 2 controls mucosal inflammation by regulating epithelial barrier function. *Gastroenterology* (2007) 132:1359–74. doi:10.1053/j.gastro.2007.02.056
39. Fukata M, Chen A, Klepper A, Krishnareddy S, Vamadevan AS, Thomas LS, et al. Cox-2 is regulated by Toll-like receptor-4 (TLR4) signaling: role in proliferation and apoptosis in the intestine. *Gastroenterology* (2006) 131:862–77. doi:10.1053/j.gastro.2006.06.017
40. Playford RJ, Hanby AM, Gschmeissner S, Peiffer LP, Wright NA, McGarrity T. The epidermal growth factor receptor (EGF-R) is present on the basolateral, but not the apical, surface of enterocytes in the human gastrointestinal tract. *Gut* (1996) 39:262–6. doi:10.1136/gut.39.2.262
41. Sinha A, Nightingale J, West KP, Berlanga-Acosta J, Playford RJ. Epidermal growth factor enemas with oral mesalamine for mild-to-moderate left-sided ulcerative colitis or proctitis. *N Engl J Med* (2003) 349:350–7. doi:10.1056/NEJMoa013136
42. Tang M, Yin G, Wang F, Liu H, Zhou S, Ni J, et al. Downregulation of CD9 promotes pancreatic cancer growth and metastasis through upregulation of epidermal growth factor on the cell surface. *Oncol Rep* (2015) 34:350–8. doi:10.3892/or.2015.3960
43. Iizuka M, Konno S. Wound healing of intestinal epithelial cells. *World J Gastroenterol* (2011) 17:2161–71. doi:10.3748/wjg.v17.i17.2161
44. Leung KT, Chan KY, Ng PC, Lau TK, Chiu WM, Tsang KS, et al. The tetraspanin CD9 regulates migration, adhesion, and homing of human cord blood CD34+ hematopoietic stem and progenitor cells. *Blood* (2011) 117:1840–50. doi:10.1182/blood-2010-04-281329
45. Smith JM, Johanesen PA, Wendt MK, Binion DG, Dwinell MB. CXCL12 activation of CXCR4 regulates mucosal host defense through stimulation of epithelial cell migration and promotion of intestinal barrier integrity. *Am J Physiol Gastrointest Liver Physiol* (2005) 288:G316–26. doi:10.1152/ajpgi.00208.2004
46. Takeda Y, He P, Tachibana I, Zhou B, Miyado K, Kaneko H, et al. Double deficiency of tetraspanins CD9 and CD81 alters cell motility and protease production of macrophages and causes chronic obstructive pulmonary disease-like phenotype in mice. *J Biol Chem* (2008) 283:26089–97. doi:10.1074/jbc.M801902200
47. Shah SC, Colombel JF, Sands BE, Narula N. Mucosal healing is associated with improved long-term outcomes of patients with ulcerative colitis: a systematic review and meta-analysis. *Clin Gastroenterol Hepatol* (2016) 14:1245–1255.e1248. doi:10.1016/j.cgh.2016.01.015
48. Neurath MF. New targets for mucosal healing and therapy in inflammatory bowel diseases. *Mucosal Immunol* (2014) 7:6–19. doi:10.1038/mi.2013.73

Conflict of Interest Statement: The authors declare that the research was conducted in the absence of any commercial or financial relationships that could be construed as a potential conflict of interest.

frontiers in Immunology

REVIEW
published: 23 May 2018
doi: 10.3389/fimmu.2018.01074

Tetraspanins as Organizers of Antigen-Presenting Cell Function

Maria Laura Saiz[1,2], *Vera Rocha-Perugini*[1,2]* *and Francisco Sánchez-Madrid*[1,2,3]*

[1] Servicio de Inmunología, Hospital de la Princesa, Instituto de Investigación Sanitaria La Princesa, Madrid, Spain,
[2] Vascular Pathophysiology Research Area, Centro Nacional de Investigaciones Cardiovasculares, Madrid, Spain,
[3] CIBER Cardiovascular, Madrid, Spain

Professional antigen-presenting cells (APCs) include dendritic cells, monocytes, and B cells. APCs internalize and process antigens, producing immunogenic peptides that enable antigen presentation to T lymphocytes, which provide the signals that trigger T-cell activation, proliferation, and differentiation, and lead to adaptive immune responses. After detection of microbial antigens through pattern recognition receptors (PRRs), APCs migrate to secondary lymphoid organs where antigen presentation to T lymphocytes takes place. Tetraspanins are membrane proteins that organize specialized membrane platforms, called tetraspanin-enriched microdomains, which integrate membrane receptors, like PRR and major histocompatibility complex class II (MHC-II), adhesion proteins, and signaling molecules. Importantly, through the modulation of the function of their associated membrane partners, tetraspanins regulate different steps of the immune response. Several tetraspanins can positively or negatively regulate the activation threshold of immune receptors. They also play a role during migration of APCs by controlling the surface levels and spatial arrangement of adhesion molecules and their subsequent intracellular signaling. Finally, tetraspanins participate in antigen processing and are important for priming of naïve T cells through the control of T-cell co-stimulation and MHC-II-dependent antigen presentation. In this review, we discuss the role of tetraspanins in APC biology and their involvement in effective immune responses.

Keywords: tetraspanins, tetraspanin-enriched microdomains, antigen-presenting cells, immune receptors, cell migration, antigen presentation

OPEN ACCESS

Edited by:
Annemiek van Spriel, Radboud University Nijmegen Medical Center, Netherlands

Reviewed by:
Laura Santambrogio, Albert Einstein College of Medicine, United States
Bénédicte Manoury, Institut National de la Santé et de la Recherche Médicale (INSERM), France
Mark Dexter Wright, Monash University, Australia

***Correspondence:**
Vera Rocha-Perugini
verapfrp@gmail.com;
Francisco Sánchez-Madrid
fsmadrid@salud.madrid.org

Specialty section:
This article was submitted to Antigen Presenting Cell Biology, a section of the journal Frontiers in Immunology

Received: *18 January 2018*
Accepted: *30 April 2018*
Published: *23 May 2018*

Citation:
Saiz ML, Rocha-Perugini V and Sánchez-Madrid F (2018) Tetraspanins as Organizers of Antigen-Presenting Cell Function. Front. Immunol. 9:1074. doi: 10.3389/fimmu.2018.01074

INTRODUCTION

Professional antigen-presenting cells (APCs), which include dendritic cells (DCs), monocytes/macrophages, and B cells, are essential players of the immune system. Once an infection occurs, the innate immune system is stimulated, beginning the inflammation process to prevent the infection from spreading. Then, adaptive immune responses are required for the effective and specific clearance of the pathogen. This vital task lies on APCs, which operate at the interface between the innate and adaptive immunities. First, APCs detect foreign pathogens thanks to specialized receptors, known as pattern recognition receptors (PRRs). PRRs recognize conserved repeated motifs in microbial species, called pathogen associated molecular patterns (PAMPs), and enable APCs to discriminate between self and non-self (1). After engulfment of exogenous pathogens, APCs use their unique machinery to break down molecular antigens into small peptides and present a representative repertoire of these through a specialized immune receptor, namely, the major histocompatibility complex class II (MHC-II) molecule. This process triggers APC activation and maturation, with

upregulation of surface expression of MHCII and co-stimulatory molecules. APC migration from peripheral tissues to secondary lymphoid organs is a key step for the generation of proper adaptive immunity, since antigen presentation to naïve T lymphocytes by APCs takes place primarily in secondary lymphoid organs (2). DCs have been extensively characterized and different subsets have been described (3, 4). Moreover, these cells precisely alternate their sentinel capacities with their antigenic presentation properties to favor antigen detection and migration, and antigen processing and presentation.

Tetraspanins belong to a family of small proteins (20–30 kDa) that contain four transmembrane regions spanning the plasma membrane. They also share other structural features: a small and a large extracellular loop with conserved residues, and short N- and C- terminal tails (5). In humans and mice, 33 tetraspanin members have been identified. These proteins are widely distributed in cells and tissues. Some of them are ubiquitous (CD81, CD82, CD9, or CD63), whereas others have a tissue-restricted expression (CD37 or CD53 in immune cells) (6). Tetraspanins do not have the characteristics of prototype membrane receptors. They have small cytoplasmic tails that lack known motifs involved in signal transduction (5), and there are only few reports claiming tetraspanin ligands (7). Instead, tetraspanins function as molecular organizers of multimolecular membrane complexes, which facilitate signal transduction processes (8). Through the association with proteins and lipids, they organize specific membrane microdomains with a particular composition and detergent-solubilization properties, conforming the so-called tetraspanin-enriched microdomains (TEMs) (9, 10). TEMs are distinct from other well-known membrane domains, like lipid rafts, caveolae, and GPI-linked protein nanodomains (10).

Early studies using biochemical approaches have shown that TEMs follow a hierarchical network of associations based on the strength of the interactions (5, 9). The first level comprises the direct and specific interaction of a tetraspanin with its protein partner and is resistant to strong detergent conditions. The second level is characterized by interactions between tetraspanins. These interactions are more labile, resistant to mild detergents, and regulated by palmitoylation. Cutting edge fluorescence microscopy techniques, as single-molecule tracking, phasorFLIM-FRET and super-resolution microscopy, have more recently demonstrated that TEM organization and composition is highly dynamic (10–14). Accordingly, several studies have suggested that TEM composition can differ between cells. Through the organization of TEMs, tetraspanins regulate the function of their associated partners, finely tuning a breadth of biological processes. They may have overlapping functions in some cases or can have unique roles or even opposing functions. Their importance for several pathological and physiological processes has been discussed in detail elsewhere (15–22).

Tetraspanins have been widely studied in the mammalian immune system, and thanks to the generation of tetraspanin knockout mice a deeper comprehension is being achieved. Interestingly, the existence of tetraspanins in the innate immune system of invertebrates and non-mammalian vertebrates has also been described. Marine gastropod mollusks show ubiquitous expression of CD63 and Tspn33, which are upregulated upon different immune stimulation challenges, like toll-like receptor (TLR) ligands, bacteria or viral infection (23). Similarly, CD9 expression is induced in lamprey fish after LPS stimulation (24), or in turtles after bacterial infection (25). CD37 expression is highly increased in Atlantic salmons after a secondary viral infection (26). Conversely, treatment with several immune stimulators downregulate CD9, CD53, and CD63 expression in leukocytes from teleost fishes (27, 28). The study of the innate defense mechanisms in non-mammalian vertebrates can give additional hints for the comprehension of vertebrate innate immunity. In mammals, tetraspanins are master regulators of APC function, mediating the crosstalk between the immunogenic environment and APCs, and the interplay between innate and adaptive immune cells.

Herein, we will review the function of tetraspanins in regulating each step of APC function: at the cellular level, by modulating clustering and trafficking of immune receptors; during the process of APC migration, and finally during MHC-II-dependent antigen presentation. We will also discuss the growing evidence on tetraspanins as markers of specific DC subsets.

Tetraspanins, Negative Regulators of PRRs

Recognition and uptake of microbial antigens by APCs is mediated by PRRs, which bind conserved pathogen structures known as PAMPs (1). Membrane-bound PRRs include TLRs, C-type lectin receptors (CLRs), scavenger receptors (SRs) and NOD-like receptors. The efficiency of antigen recognition greatly depends on the supramolecular organization of PRRs at the APC surface, and tetraspanins play an important role in this process (**Figure 1**).

Toll-like receptors multimerization at the APC surface promotes the recruitment of signaling molecules (29), a process influenced by the inclusion of TLRs and associated co-receptors into TEMs. LPS stimulation triggers TLR-4 and CD81 co-clustering in peripheral blood monocytes (30). How CD81 regulates TLR-4 signaling has not been assessed; however, it has been shown that CD9 restricts LPS-induced macrophage activation and TNF-α production by preventing the TLR-4 co-receptor CD14 localization into lipid rafts (**Figure 1**). Through this mechanism, CD9 deficiency in mice enhances macrophage infiltration and lung inflammation after *in vivo* intranasal LPS administration (31). In DCs, bacterial antigens can be recognized by TLR-dependent pathways, sensing cell surface or endosomal antigens, and by cytosolic pathways, like the cytosolic sensor stimulator of IFN genes (STING) (32). Interestingly, CD81 negatively regulates STING/IFNAR signaling through its interaction with Rac1 and the inhibition of STAT-1 activation, thus leading to reduced TNF-α and NO production by inflammatory monocytes and DCs (**Figure 1**). As a consequence, CD81 deficient mice are protected against systemic *Listeria monocytogenes* infection (33).

Among the CLRs, Dectin-1 specifically recognizes β-glucans in fungal cell walls and is important for efficient immune response against fungi (34). Dectin-1 associates with tetraspanins CD37 and CD63 at the membrane of APCs when using CHAPS 1% (35, 36), a mild detergent extraction condition that only keeps third level molecular interactions within TEMs (7, 10). Dectin-1 direct association with CD37 was however observed in transfected HEK293 cells when using Triton X-100 1%, which preserves

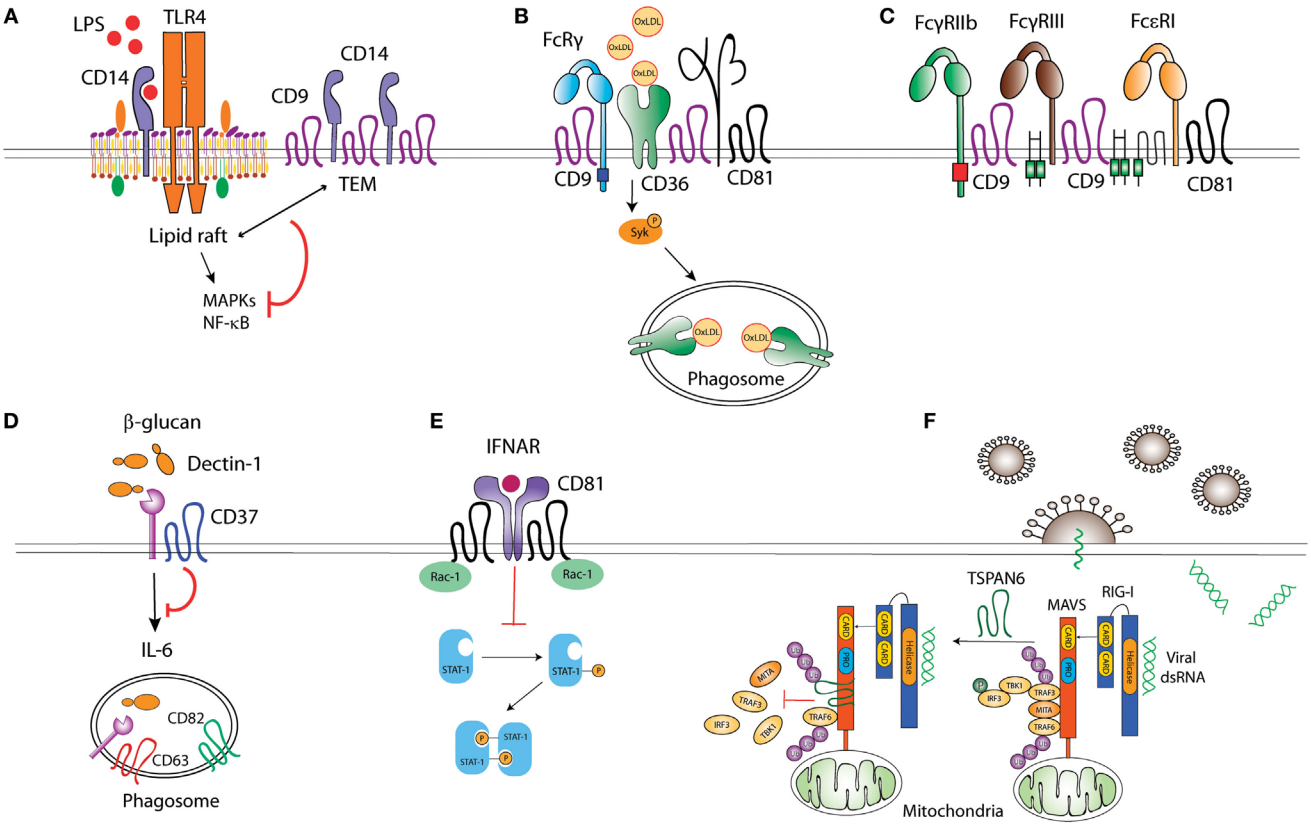

FIGURE 1 | Tetraspanins act as molecular organizers of pattern recognition receptors (PRRs). **(A)** CD9 sequesters TLR4 co-receptor CD14 into tetraspanin-enriched microdomains (TEMs), impairing its localization into lipid rafts, and thus preventing TLR4 downstream signaling. **(B)** CD36 coupling to the adaptor FcRγ is mediated by the complex formed between CD36, β1, and/or β2 integrins, and CD9 and/or CD81 tetraspanins. CD36 association with tetraspanins regulates its engagement with Src and Syk kinases, and its internalization when bound to ligands like oxidized low-density lipoproteins. **(C)** CD9 collaborates with FcγRIIb and FcγRIII upon macrophage activation, and, together with CD81, associates with FcεRI. **(D)** CD37 stabilizes membrane C-type lectin receptor Dectin-1 and inhibits IL-6 production. **(E)** CD81 interaction with Rac-1 prevents STAT-1 activation downstream of interferon-α/β receptor (IFNAR) stimulation. **(F)** The interaction between ubiquitinated Tspan6 and MAVS (mitochondrial antiviral signaling) interferes with RIG-I (retinoic acid-inducible gene I)-induced recruitment of downstream molecules TRAF3, MITA, and IRF3 to MAVS after viral RNA detection.

tetraspanin-partner primary complexes, but not in B cells (36), indicating that this interaction could be affected by other proteins expressed on APCs or that it is dynamically dependent on the cell activation status. CD37 stabilizes Dectin-1 surface expression and impairs its internalization, and Dectin-1-mediated TNF-α and IL-6 production in response to yeast cell walls (36) (**Figure 1**). Accordingly, CD37$^{-/-}$ mice are protected against systemic *Candida albicans* infection, producing high levels of IL-6 and specific IgA antibodies (37). On the other hand, CD37 mRNA expression positively correlates with Dectin-1 and IL-6 mRNA in brains of mice infected with *Toxoplasma gondii* (38); however, further studies are necessary to evaluate this effect at the protein level and if there is any causal relationship. CD63 also seems to cooperate with Dectin-1 during yeast phagocytosis by human monocyte-derived DCs (MoDCs) (35), being specifically recruited to phagosomes containing *Cryptococcus neoformans* (39) in a process dependent on acidification and thought to be required for tethering the antigen-loading machinery together.

CD36 is a SR that recognizes proteinaceous or lipidic antigens from microbes, or self-ligands. In mouse macrophages, CD81 and CD9 are required for CD36 internalization after binding to oxidized low-density lipoprotein (oxLDL) ligands (40, 41). CD9 would be important for signaling in response to oxLDL, since oxLDL uptake and subsequent JNK phosphorylation are impaired in CD9$^{-/-}$ macrophages (40). Moreover, CD9 and CD81-dependent scaffolding of CD36, and β1 and β2 integrins in membrane multimolecular complexes is essential for CD36 association with FcγR (Fc receptor for IgG) and with Src and Syk kinases; and for its subsequent antigen uptake (41) (**Figure 1**). CD9 is also associated with the scavenger-like receptor CD5, which recognizes β-glucans expressed on fungi (42), although there is no experimental evidence about the functional implications of this interaction.

Pathogens can be opsonized with IgGs produced in response to microbial invasion, and recognized by FcγRs associated with PRRs. This combined stimulation triggers cytokine production and pathogen-specific innate immune responses. FcγRs seem to be included in TEMs in phagocytic cells. CD9 antibody cross-linking, but not Fc fragment alone, stimulates intracellular signaling dependent on FcγRIIB and FcγRIII, thus promoting mouse macrophage

activation (43). Antibody cross-linking of tetraspanin CD82 enhances FcR-dependent activation of intracellular signaling in human monocytic cell lines (44). Importantly, IgG-opsonized HIV-1 particles are targeted to TEMs in endosomes of immature DCs (45). Other Fc receptors are also associated with TEMs, as the FcεRI (Fc receptor for IgE), which is a molecular partner of CD9 and CD81 in human monocytes and skin-derived DCs (46) (**Figure 1**). The importance of TEMs as organizers of FcεRI signalosome in mast cells has been recently reviewed elsewhere (47).

Tetraspanins can also regulate signaling of cytoplasmic PRRs, like the RIG-I-like receptors (RLRs). RLRs recognize viral RNA and trigger signaling pathways that induce type I IFN responses (48). In the presence of viral RNA, ubiquitination of human tetraspanin 6 (Tspn6) promotes its interaction with RIG-I, MDA5, and mitochondrial antiviral signaling (MAVS) signalosome, impairing the activation of IFN-stimulated response element (ISRE), NF-κB, and IFN-β promoters (49) (**Figure 1**).

In summary, increasing evidence shows that tetraspanins usually act as negative regulators of PRR clustering and/or signaling. Thus, tetraspanins constitute key players to avoid uncontrolled immune responses, which are harmful to the host.

Tetraspanins Tightly Control APC Migration

Leukocyte migration is of fundamental importance for the efficient development of immune responses against pathogens. Innate immune cells capture antigens in peripheral tissues and then migrate to secondary lymphoid organs where antigen presentation to T lymphocytes takes place. Immune cells can also migrate out of the bloodstream toward the inflammation site, where adaptive immune responses occur (**Figure 2**). Thus, leukocytes modify their adhesive properties depending on the immune scenario (50). Innate immune cells usually need inflammation signals to initiate migration, whereas naïve lymphocytes efficiently migrate to secondary lymphoid organs, and after activation signals acquire specific migratory patterns. Tetraspanins have emerged as key regulators of cell migration, since they modulate the function of proteins involved in cell-cell adhesion, cell-ECM (extracellular matrix) adhesion, cytoskeletal protrusion/contraction, and proteolytic ECM remodeling. Indeed, tetraspanins associate with integrins, cadherins, members of the Ig superfamily, signaling molecules like Rac and Rho GTPases, and matrix metalloproteinases (MMP); regulating their membrane compartmentalization, intracellular trafficking, and proteolytic activity. Most of the information on tetraspanin regulation of cell migration comes from studies with adherent and tumor cells and has been reviewed in detail (20, 51). In this section, we will delineate the importance of tetraspanins for migration and extravasation of APCs.

Early studies employed cross-linking with monoclonal antibodies (mAbs) to investigate the role of tetraspanins in immune cell migration. Human MoDC *in vitro* migration toward MIP-5 and MIP-1α chemokines was increased by the treatment with mAbs against CD9, CD63, CD81, or CD82 (35). These chemokines are

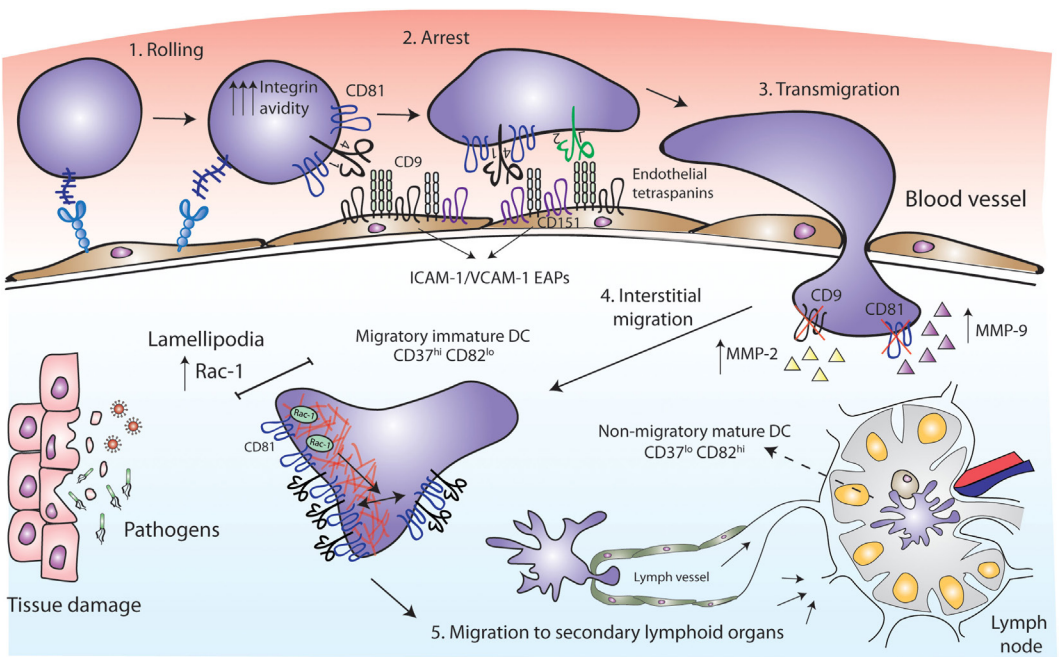

FIGURE 2 | Tetraspanins act as key players in antigen-presenting cell (APC) migration. CD81 facilitates rolling and arrest under shear flow, increasing the avidity of VLA-4 integrin. Tetraspanins CD9 and CD151 congregate the endothelial adhesion receptors (ICAM-1 and VCAM-1) in clusters called endothelial adhesive platforms, thus controlling their adhesive properties and leukocyte extravasation. CD9 and CD81 deficiency results in an increase of MMP-2 and MMP-9 metalloproteinases production and activity, required for interstitial migration. Once in the tissue, CD81 tetraspanin controls cell migration *via* Rac-1-dependent mobilization of preformed integrin clusters at the leading edge and contributes to the formation of lamellipodia. While migratory immature dendritic cells (DCs) are $CD37^{hi}$ and $CD82^{lo}$, mature DCs at the lymph nodes are $CD37^{lo}$ $CD82^{hi}$, and display reduced migratory capacity and efficient antigen presentation machinery.

strong chemoattractants required for the recruitment of inmature DCs to the surrounding tissue at the sites of injury (52, 53). After antigen capture, DCs mature, lose their responsiveness to inflammatory chemokines and express CCR7 (54, 55). CCR7 is the receptor for CCL19 and CCL21, which are chemokines highly present in lymphoid T-cell zones of secondary lymphoid organs (56), where DCs home to present their processed antigen to T lymphocytes. Opposite to that observed with MoDC migration toward MIP-5 and MIP-1α, the same mAb against CD81 (clone JS-81) or a CD81 ligand [the Hepatitis C Virus E2 envelope glycoprotein (57)] inhibited MoDC migration in response to CCL21 *in vitro* (58). These contradictory results could be due to different chemokine stimuli or to technical issues. Subsequent studies were all in line with a positive role for tetraspanins in cell migration. Monocyte transmigration across brain endothelial cell monolayers was significantly inhibited by an anti-CD9 mAb and several anti-CD81 mAbs, in both rodent and human *in vitro* models, by acting on the leukocyte side and on endothelial tetraspanins (59, 60). Accordingly, CD81 mAb (clone Eat2) administration reduced spinal cord inflammation *in vivo*, alleviating autoimmune encephalomyelitis (EAE) (59). Ly6C$^+$ monocytes, which can derive in MoDCs (61), are key determinants for Th17 differentiation in the EAE mouse model (62, 63). Moreover, since ICAM-1 and VCAM-1 adhesion molecules are the ligands of leukocyte integrins Mac-1 (αMβ2) and LFA-1 (αLβ2) (for ICAM-1) and VLA-4 (α4β1) (for VCAM-1), we must emphasize the importance of endothelial tetraspanins as organizers of ICAM-1 and VCAM-1 containing docking structures during leukocyte extravasation (11, 64). Importantly, loss-of-function studies have demonstrated that CD81 is essential for cell rolling, arrest, and migration. In both monocytic cell lines and mouse primary splenocytes, CD81 facilitates rolling and arrest under shear flow, increasing the avidity of integrin VLA-4 (65) (**Figure 2**). The link between tetraspanins and MMP during immune cell migration has also been investigated. Bone marrow-derived macrophages (BMDMs) from CD9 and CD81 double deficient mice show reduced motility, through a mechanism dependent on the regulation of MMP-2 and MMP-9 expression and activity (**Figure 2**). Interestingly, CD81 and CD9 double deficient mice spontaneously develop pulmonary emphysema, with elevated numbers of alveolar macrophages and increased MMP activity (66). A similar increase in MMP-2 and MMP-9 production and activity was observed in BMDMs from CD9-deficient mice, which showed decreased macrophage motility with an increase in macrophage infiltration after intranasal administration of LPS (31).

It is important to mention that DC motility behavior depends on the environmental context. DC migration on two-dimensional (2D) surfaces, like endothelial cell surfaces of the circulatory system, require adhesive forces and integrin functionality; whereas migration in three-dimensional (3D) environments, as interstitial ECM, is ameboid and less adhesive, and largely driven by cytoskeletal deformability (67–69). Importantly, tetraspanins fine-tune DC migratory capabilities by tightly controlling Rac1 and RhoA spatiotemporal activation. CD81 controls the migration of MoDCs, by regulating the formation of lamellipodia, and the mobilization of preformed integrin clusters at the leading edge of migratory cells (70). This tetraspanin is essential for the formation of actin protrusions through a mechanism dependent on its interaction with the small GTPase Rac-1 (70, 71) (**Figure 2**). Integrin adhesiveness and lamellipodia formation are required for DCs migration on 2D surfaces, thus this kind of migration is impaired in the absence of CD81. However, CD81 is not required for DCs migration within 3D collagen scaffolds, corresponding with unaffected Rho-A activity (70) and pointing out the differential molecular requirements of DCs migration. CD37 also promotes Rac-1 activation, while CD82 inhibits RhoA (72). Consequently, CD37 deficient DCs have impaired migration from the skin to the draining lymph nodes *in vivo*, and reduced *ex vivo* DC migration in response to CCL19 (73). CD82 deficient DCs display the opposite phenotype (72). Absence of CD37 in BMDCs also reduces adhesion to fibronectin under low shear flow, and cell spreading (73), while CD82 deficiency increases DC spreading (72). Thus, CD37^{hi}CD82^{lo} DCs would correspond to immature cells, showing increased migration and reduced capacity to activate naïve T cells, while CD37^{lo}CD82^{hi} DCs would have an activated phenotype, being less motile and endowed with the proper presentation machinery to efficiently activate naïve T cells (72) (**Figure 2**). It is becoming increasingly clear that through the regulation of cytoskeletal rearrangement, integrins, and signaling molecules, tetraspanins constitute key players in APCs migration.

MHC-II Trafficking and Antigen Presentation Take Place Within TEMs

Upon their arrival to the lymph nodes, DCs transfer the information collected at peripheral tissues to T lymphocytes triggering adaptive immune responses. This process of antigen presentation is mediated by MHC-II molecules, which are able to stably bind to antigenic peptides, and then present these fragments of exogenous proteins to effector T lymphocytes. MHC-II is expressed on professional APCs and associates with several tetraspanins, including CD9, CD37, CD53, CD81, and CD82, at the surface of APCs (74–76). It has been suggested that different tetraspanins may play a role in MHC-II clustering (**Figure 3**). CD37 negatively regulates MHC-II clustering, thus limiting antigen presentation by mouse splenic CD11c$^+$ DCs. CD37 knock-out splenic DCs show increased T-cell stimulatory capacity, by a mechanism strictly dependent on peptide-bound MHC-II signals (77). CD81 and CD9 co-immunoprecipitate with I-A MHC-II molecules in mouse BM-derived DCs and B blasts, and I-A/I-E heterologous multimerization is reduced in CD9-deficient BM-derived DCs (78). However, functional analyses were not performed in the study of Unternaehrer and collaborators. Another study has also suggested that MHC-II, together with HLA-DM and CD86, was included in TEMs containing tetraspanins CD9, CD63, CD81, and CD82 (79). This study was performed using the CDw78 antibody, which recognizes a specific determinant on an MHC-II subpopulation. However, this biochemical analysis of MHC-II multimerization was performed using mild detergent conditions (CHAPS 1%). It was later demonstrated that CD9 and CD81 co-immunoprecipitation with MHC-II I-A/I-E multimers only occurs under these mild detergent conditions (80), not being observed when using more stringent conditions (Triton X-100). Thus, deficiency in CD9 or CD81 does not affect MHC-II clustering at the surface of mouse BM-derived DCs, while surface

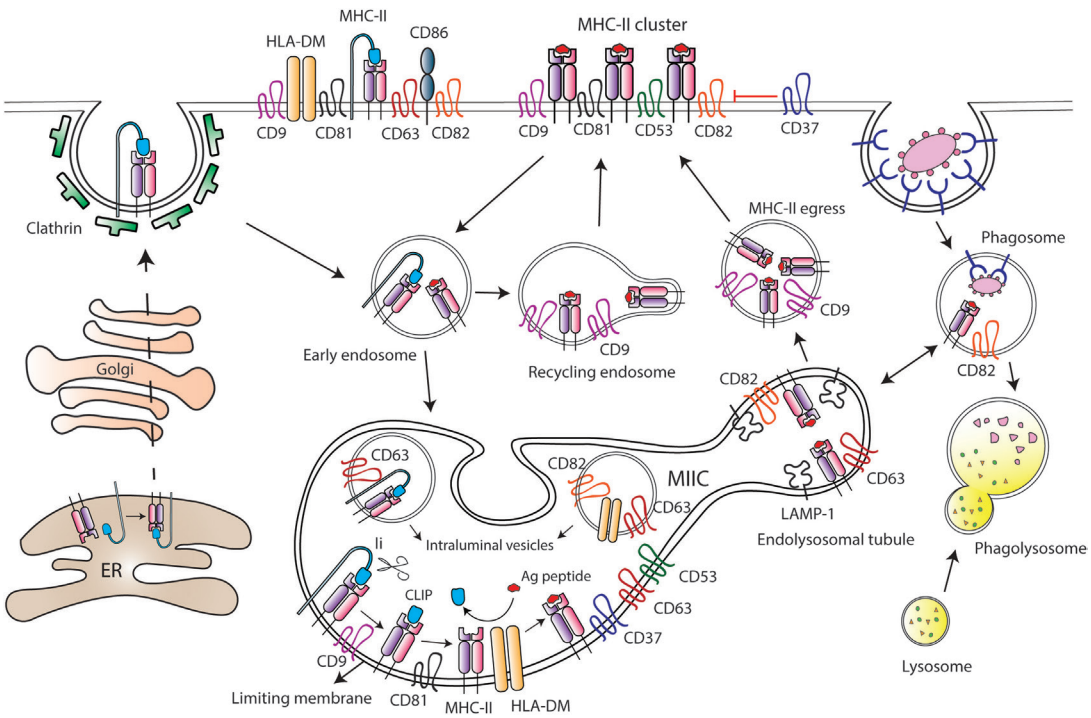

FIGURE 3 | Tetraspanins regulate major histocompatibility complex class II (MHC-II) trafficking and surface expression at antigen-presenting cells (APCs). After synthesis, MHC-II molecules are transported to the plasma membrane of APCs in association with the chaperone Ii, which drives MHC-II internalization through clathrin-coated pits. Then, Ii is sequentially degraded by different proteases at the MHC-II-enriched endosomal compartment (MIIC), until MHC-II molecules remain bound only to the CLIP (class II-associated invariant chain peptide) fragment. Peptides derived from internalized antigens are subsequently loaded to MHC-II molecules with the help of the class-II-like chaperone HLA-DM. Several tetraspanins are greatly enriched at the MIIC compartment, and peptide-bound MHC-II molecules coupled to Ii are included into tetraspanin-enriched microdomains (TEMs). Tetraspanin CD9 is required for the efficient egress of MHC-II from MIIC to the cell surface, and it is essential for MHC-II endocytosis and recycling. CD82 together with CD63 accumulate in LAMP-1-enriched endolysosomal tubules that emanate from the MIIC. In MIIC intraluminal vesicles, CD63 is associated with MHC-II and HLA-DM; while CD82 only interacts with HLA-DM. In addition, CD82 is preferentially associated with peptide-bound MHC-II, and it is found in phagosomes prior to their fusion with lysosomes. At the APC surface, tetraspanins CD9, CD53, CD81, and CD82 are associated with MHC-II, and tetraspanin CD37 negatively regulates MHC-II clustering. Moreover, TEMs containing CD9, CD63, CD81, and CD82 include MHC-II, HLA-DM, and CD86 molecules.

cholesterol content is essential for multimerization (80, 81). In addition, it was later demonstrated that the CDw78 determinant also recognizes peptide-bound MHC-II molecules coupled to the chaperone class-II associated invariant chain (Ii) (82). Intracellular trafficking of MHC-II molecules in APCs is a tightly regulated process, essential for proper antigen internalization, processing and subsequent presentation to T lymphocytes. Newly synthesized MHC II molecules associate with the chaperon Ii in the endoplasmic reticulum, which prevents premature peptide loading of MHC-II until MHCII-Ii complex enters the endocytic pathway (83) (**Figure 3**). The observation that peptide-bound MHC-II molecules coupled to the chaperone Ii (recognized by the CDw78 determinant) are included in TEMs (79, 82) suggests that tetraspanins could regulate MHC-II trafficking at the MHC Class II compartment (MIIC). Accordingly, there is considerable evidence supporting this hypothesis.

The MIIC is a multilamellar compartment that has similarities with late endosomes, being enriched in classical late endocytic markers, like LAMP-1, and in resident proteases, like cathepsins (84–86). Several tetraspanins, including CD37, CD53, CD63, CD81, and CD82, are highly enriched at the MIIC of human MoDCs and B cell lines (76, 87–89) (**Figure 3**). MHC-II diffusion rates are comparable to the diffusion values of CD63 and CD82, indicating inclusion into TEMs (89). Indeed, CD63 associates with MHC-II at both intraluminal vesicles and limiting membranes of the MIIC, and with the chaperone HLA-DM at the intraluminal vesicles. On the contrary, CD82 associates with HLA-DM at MIIC intraluminal vesicles and limiting membranes, but it only associates with MHC-II molecules at the limiting membrane (88, 89). CD82 would be mostly associated with peptide-bound MHC-II molecules, since it does not interact with MHC-II-coupled to Ii (88). Accordingly, CD82 and MHC-II are recruited together to phagosomes containing fungi or bacteria, before the fusion with lysosomes (90). Moreover, CD82 deficiency in DCs slightly reduces the maturation of MHC-II/peptide complexes (72). However, despite abundant evidence that tetraspanins dynamically interact with MHC-II and HLA-DM at the MIIC, they do not seem to be essential for peptide loading to MHC-II molecules. Downregulation of CD9, CD63, CD81, and CD82 in human cell lines does not affect surface expression of peptide-bound MHC-II (89), and CD9 deficiency in BMDCs does not affect antigen proteolysis (91). The dynamic interactions between these molecules

at the MIIC compartment would rather indicate that TEMs are important organizers of MHC-II trafficking in APCs.

After being loaded with antigenic peptides, MHC-II molecules egress from the MIIC to the APC surface, a process that remains largely undefined. Recently, it has been reported that tetraspanin CD9 is important for MHC-II egress to the surface of mouse immature MoDCs (91). CD9-deficient MoDCs display increased accumulation of MHC-II molecules in acidic compartments, in which MHC-II colocalizes with LAMP-1. As a consequence, surface expression of MHC-II is decreased in the absence of CD9 (91). Upon DC maturation, tubular extensions emanate from the MIIC in a process dependent on microtubules and microtubule-adaptor proteins (92–94), thus transporting peptide-bound MHC-II molecules to the plasma membrane (95, 96). In mouse BMDCs stimulated with LPS, these dynamic tubular extensions are enriched in LAMP-1 and tetraspanins CD63 and CD82 and show accumulation of fluorescent OVA protein (93) (**Figure 3**). In mature MoDCs, CD9 is not involved in MHC-II egress from the MIIC to the plasma membrane, which would take place only in a CD9-independent manner (91). Therefore, transport of peptide-bound MHC-II to the cell surface might be dependent on different TEMs, whose composition would be tightly controlled before and after cell maturation.

After arriving at the APC plasma membrane, peptide-bound MHCII molecules are actively endocytosed and then recycled back to the surface *via* early endocytic compartments. MHC-II endocytosis occurs through clathrin- and dynamin-independent pathway(s) (83). Early studies suggested that in immature DCs, MHC-II internalization is facilitated through ubiquitination by the ubiquitin E3 ligase MARCH-I (97, 98). MHC-II ubiquitination would be less efficient in mature DCs due to reduced MARCH-I expression, which would result in an increase in MHC-II surface expression (98, 99). However, subsequent studies have challenged this view (100–102). MHC-II ubiquitination enhances the kinetics of degradation of peptide-bound MHC-II molecules in immature DCs (101) and prevents recycling of internalized molecules back to the membrane (102), without affecting endocytosis. MHC-II recycling back to the surface is highly increased upon DC maturation, greatly contributing to boost MHC-II surface expression (102). Other members of the MARCH family have been shown to be involved in tetraspanin turnover. CD81 is targeted to lysosomes in the presence of MARCH-IV and -VIII, but not MARCH-I. Accordingly, MARCH-IV downregulation by siRNA increases CD81 surface expression (103). The effect of MARCH proteins on CD81 turnover could also affect the expression levels of CD81-interacting partners included in TEMs. Importantly, a recent study showed that CD9 is essential for MHC-II endocytosis in both immature and mature MoDCs, by a mechanism independent on MHC-II ubiquitination. Moreover, CD9 deficiency prevents MHC-II recycling in mature MoDCs (91). Tetraspanins are therefore important players in MHC-II trafficking and surface expression at APCs.

Tetraspanins are relevant for antigen presentation to T lymphocytes. Early studies have suggested that disruption of TEMs by cholesterol depletion, which is an essential component of these microdomains (104), affects the capacity of APCs to stimulate T cell activation (79, 81). However, cholesterol depletion can also disrupt lipid rafts, which are also required for proper antigen presentation (105). More recently, the specific functions of individual tetraspanins during antigen presentation have been established. CD37 negatively regulates MHC-dependent antigen presentation to $CD4^+$ and $CD8^+$ T cells, while CD151 inhibits T-cell co-stimulation by mouse $CD11c^+$ splenic DCs. As a consequence, mouse deficiency in those tetraspanins triggers $CD4^+$ and $CD8^+$ T-cell hyperstimulation (77). Sheng and collaborators have suggested that CD37 and CD151 could negatively regulate MHC clustering; however, despite the functional evidence demonstrated in their study, the molecular mechanisms behind CD37 and CD151 function remain to be determined. A similar phenotype was also observed with $Tssc6^{-/-}$ and $CD37^{-/-}Tssc6^{-/-}$ mice, through a mechanism independent on DC costimulatory signals (106). CD63 knock-down in human B cell lines also enhances MHC-II-dependent $CD4^+$ T cell stimulation, but in this case, the mechanism seems to be related with increased production of extracellular vesicles (107). In this sense, T cell activation can be induced by extracellular vesicles derived from mature DCs (18, 108), which are enriched in MHC-I and MHC-II, and several tetraspanins, like CD9, CD63, CD81, and CD82 (87, 109). MHC-II sorting into extracellular vesicles has been suggested to depend on its recruitment to TEMs (110–112). Together, these data suggest negative roles for some tetraspanins during antigen presentation. However, other tetraspanins can have the opposite effect. Indeed, mouse $CD9^{-/-}$ MoDCs induce less $CD4^+$ T-cell activation and proliferation than wild-type MoDCs, due to reduced surface expression of MHC-II (91). Strikingly, CD9-deficient Flt3L conventional DC (cDC) showed similar T-cell stimulatory capacity as wild-type cDCs, triggering comparable $CD4^+$ T proliferation *in vivo* (91). The role of CD9 in antigen presentation seems therefore to be DC subset-specific, and it would be interesting to investigate the molecular mechanisms behind this difference. CD9 interacts with MHC-II, and engagement of this tetraspanin with antibodies promotes the formation of antigen-dependent conjugates between human $CD14^+$ monocytes and T cells (113). CD9 could also play a role in antigen presentation through extracellular vesicles, since both are found at the MIIC and exosomes from mature splenic mouse DC lines (114). Together, these studies indicate that the strength of antigen presentation by professional APCs can be tightly regulated by TEM composition, with some tetraspanins playing positive roles while others limit T-cell activation signals.

Tetraspanins Define Distinct DC Subsets

Dendritic cells can be classified in several subsets that differentially control the strength and duration of T-cell responses. The main populations that have been described are plasmacytoid DCs (pDCs) and cDCs, which can be divided into several subpopulations. Monocytes can also be precursors of different subsets of DCs found in different tissues in the steady state and can generate MoDCs during inflammatory reactions (61). Both human and mice individual DC subsets display different TEM composition (115). In addition, expression of specific tetraspanins can be modulated by DC differentiation and maturation. For instance, CD9 is differentially expressed on conventional and pDCs (115, 116).

Regarding cDCs, it has been suggested that they have a higher capacity to sense, process and present phagocytosed antigens to T cells than pDCs. cDCs are classified in two main subsets: $CD141^+$ ($BDCA3^+$) in humans and $CD8\alpha^+$ ($CD11b^-CD11c^+$) in mice; or

$CD1c^+$ ($BDCA1^+$) in humans and $CD4^+$ ($CD11b^+CD11c^+$) in mice (3, 4). Murine and human DC subsets have some similarities in their functional properties. In mice, $CD8\alpha^+$ cDC are found in lymphoid tissues and show similar phenotype and functional specialization to $CD103^+$ cDCs, which are found in non-lymphoid organs. Both subsets express comparable levels of TLRs, CLRs, and chemokine receptors and have a higher capability to cross-present antigens to $CD8^+$ T lymphocytes compared to $CD11b^+$ DCs (3). Interestingly, $CD141^+$ human and $CD8\alpha^+$ mouse cDCs show high expression of tetraspanins CD9, CD53, and CD81 (115), which associate with MHC-I (75, 117). $CD141^+$ cDCs also display high levels of CD37, CD82, CD151, and Tspan31 (115). The other main subset of cDC is $CD11b^+$ cDCs, which seem to be more efficient in MHC-II-dependent antigen presentation to $CD4^+$ T lymphocytes, thus triggering polarization to Th2 and Th17 responses (3). The tetraspanin expression profile was somewhat variable when comparing $CD1c^+$ human and $CD11b^+CD11c^+$ mouse cDCs (115). Indeed, $CD1c^+$ human cDCs express very high levels of CD37, CD53, and CD81 and display intermediate to high levels of CD9, CD82, and CD151. In mice, $CD4^+CD11b^+$ cDCs show intermediate to low levels of CD9, CD53, CD81, and CD151 (115). As previously discussed, several of these tetraspanins are described to regulate different steps of MHC-II trafficking and antigen presentation by APCs. However, further studies are necessary to ascertain whether specific tetraspanin expression profiles can be used as markers of cDC subsets and/or define APC functions.

Plasmacytoid DCs, both in humans and mice, have the capacity to produce large amounts of type I interferons (IFN-α/β) in response to invading pathogens (118, 119). pDCs ($BDCA2^+$ in humans, and $B220^+$ in mice) are a small subset, and in mice express low levels of MHC-II, co-stimulatory molecules, integrin CD11c, and PRRs (119). Importantly, tetraspanins can be used as markers for the identification of different mouse and human pDC subpopulations. CD9 expression allows the recognition of immature and mature mouse pDCs subsets. $CD9^+$Siglec-H^{low} pDCs have an immature phenotype, producing high levels of type I IFN and other pro-inflammatory cytokines. These cells are mainly present in mouse bone marrow and spleen, and when stimulated can induce strong $CD4^+$ and $CD8^+$ T cell responses *in vitro* and *in vivo* (120). In contrast, tissue resident pDCs are negative for CD9, do not produce IFN-α, and have a tolerogenic phenotype, increasing the numbers of $Foxp3^+CD4^+$ Treg cells in tumor-draining lymph nodes (120). Therefore, these two pDC subsets ($CD9^+$ and $CD9^-$) define cells at different maturation stages at steady state. Upon infection, cell activation would induce migration of $CD9^+$ pDCs to the periphery, allowing the secretion of inflammatory cytokines at the infection site. Interestingly, upon maturation, $CD9^+$ pDC upregulate markers of pDC differentiation but gradually lose CD9 expression (120). Distinct pDC mouse subsets can also be distinguished when looking at tetraspanin CD81. A small subpopulation of $B220^+CD5^+CD81^+$ cells could be observed in blood, spleen, and bone marrow. This small subset does not produce IFN-α, while splenic $CD5^-CD81^-$ pDCs secrete high amounts of the cytokine (121). Similar $CD81^-$ and $CD81^+$ pDC subpopulations were observed in humans. Human pDCs are divided in two subsets depending on CD2 expression (122), and it has been recently demonstrated that $CD2^{high}$ pDCs include $CD2^{hi}CD5^-CD81^-$ and $CD2^{hi}CD5^+CD81^+$ cells (121). Similarly to mice, human $CD2^{hi}CD5^+CD81^+$ pDCs represent a relatively rare subpopulation that produce little or no IFN-α (121). This subset can, however, secrete other pro-inflammatory cytokines, like IL-12p40 and IL-6, and is capable of inducing B-cell proliferation and differentiation to plasma cells. In addition, $CD2^{hi}CD5^+CD81^+$ pDCs are efficient inducers of $CD4^+$ T cell proliferation and Treg differentiation (121). Interestingly, antibodies against CD81 and CD9, but not CD63, specifically inhibited IFN-α production by pDCs when co-cultured with HCV-infected hepatoma cells. This effect was specifically related to CD81 expression in pDCs and required Rac GTPase activity (123). Hence, the absence of tetraspanins CD9 and CD81 seems to identify small pDC subpopulations that do not produce type I IFN. However, whether these tetraspanin expression profiles define overlapping pDC subsets and/or if differential expression of tetraspanins is associated with specific APC phenotypes remain to be determined.

CONCLUSION

In APCs, surface immune receptors and adhesion molecules, such as MHC molecules, co-receptors, PRRs, and integrins, associate with tetraspanins. Through the inclusion of these receptors in TEMs, tetraspanins can regulate their clustering, internalization, and intracellular trafficking, then affecting their downstream signaling. TEMs are thus important regulators of proper antigen uptake, processing and presentation. In addition, by modulating cytoskeleton-dependent processes, like outside-in integrin signaling, actin polymerization and cell spreading, tetraspanins are also key players in APC migration. Increasing evidence shows that different subsets of DCs having distinct requirements for antigen presentation and/or motility capabilities express specific repertoires of tetraspanins. This fine-tuned regulation warrants appropriate adaptive immune responses. Therefore, tetraspanins are potential targets for therapeutical interventions aiming to balance exaggerated immune responses in pathological inflammations and in immune-mediated chronic diseases.

AUTHOR CONTRIBUTIONS

MS and VR-P designed and wrote the review. VRP and FSM coordinated and edited the manuscript.

ACKNOWLEDGMENTS

We thank Dr Manuel Gomez-Gutierrez for critical reading and editing of the manuscript.

FUNDING

This work was supported by grants to FS-M (SAF2014-54705-R; SAF2017-82886-R; B2017/BMD-3671-INFLAMUNE; ERC-2011-AdG 294340-GENTRIS; PIE13/00041; and CIBER CARDIOVASCULAR) and was co-funded by Fondo Europeo de Desarrollo Regional (FEDER). The CNIC is supported by the Spanish Ministry of Economy, Industry and Competitiveness (MINECO) and by the Pro CNIC Foundation.

REFERENCES

1. Mogensen TH. Pathogen recognition and inflammatory signaling in innate immune defenses. *Clin Microbiol Rev* (2009) 22(2):240–273, Table of Contents. doi:10.1128/CMR.00046-08
2. Alvarez D, Vollmann EH, von Andrian UH. Mechanisms and consequences of dendritic cell migration. *Immunity* (2008) 29(3):325–42. doi:10.1016/j.immuni.2008.08.006
3. Merad M, Sathe P, Helft J, Miller J, Mortha A. The dendritic cell lineage: ontogeny and function of dendritic cells and their subsets in the steady state and the inflamed setting. *Annu Rev Immunol* (2013) 31:563–604. doi:10.1146/annurev-immunol-020711-074950
4. Guilliams M, Ginhoux F, Jakubzick C, Naik SH, Onai N, Schraml BU, et al. Dendritic cells, monocytes and macrophages: a unified nomenclature based on ontogeny. *Nat Rev Immunol* (2014) 14(8):571–8. doi:10.1038/nri3712
5. Boucheix C, Rubinstein E. Tetraspanins. *Cell Mol Life Sci* (2001) 58(9):1189–205. doi:10.1007/PL00000933
6. Hemler ME. Specific tetraspanin functions. *J Cell Biol* (2001) 155(7):1103–7. doi:10.1083/jcb.200108061
7. Charrin S, le Naour F, Silvie O, Milhiet PE, Boucheix C, Rubinstein E. Lateral organization of membrane proteins: tetraspanins spin their web. *Biochem J* (2009) 420(2):133–54. doi:10.1042/BJ20082422
8. Hemler ME. Tetraspanin functions and associated microdomains. *Nat Rev Mol Cell Biol* (2005) 6(10):801–11. doi:10.1038/nrm1736
9. Hemler ME. Tetraspanin proteins mediate cellular penetration, invasion, and fusion events and define a novel type of membrane microdomain. *Annu Rev Cell Dev Biol* (2003) 19:397–422. doi:10.1146/annurev.cellbio.19.111301.153609
10. Yanez-Mo M, Barreiro O, Gordon-Alonso M, Sala-Valdes M, Sanchez-Madrid F. Tetraspanin-enriched microdomains: a functional unit in cell plasma membranes. *Trends Cell Biol* (2009) 19(9):434–46. doi:10.1016/j.tcb.2009.06.004
11. Barreiro O, Zamai M, Yanez-Mo M, Tejera E, Lopez-Romero P, Monk PN, et al. Endothelial adhesion receptors are recruited to adherent leukocytes by inclusion in preformed tetraspanin nanoplatforms. *J Cell Biol* (2008) 183(3):527–42. doi:10.1083/jcb.200805076
12. Espenel C, Margeat E, Dosset P, Arduise C, Le Grimellec C, Royer CA, et al. Single-molecule analysis of CD9 dynamics and partitioning reveals multiple modes of interaction in the tetraspanin web. *J Cell Biol* (2008) 182(4):765–76. doi:10.1083/jcb.200803010
13. Rocha-Perugini V, Zamai M, Gonzalez-Granado JM, Barreiro O, Tejera E, Yanez-Mo M, et al. CD81 controls sustained T cell activation signaling and defines the maturation stages of cognate immunological synapses. *Mol Cell Biol* (2013) 33(18):3644–58. doi:10.1128/MCB.00302-13
14. Zuidscherwoude M, Gottfert F, Dunlock VM, Figdor CG, van den Bogaart G, Spriel AB. The tetraspanin web revisited by super-resolution microscopy. *Sci Rep* (2015) 5:12201. doi:10.1038/srep12201
15. Levy S, Shoham T. The tetraspanin web modulates immune-signalling complexes. *Nat Rev Immunol* (2005) 5(2):136–48. doi:10.1038/nri1548
16. Zoller M. Tetraspanins: push and pull in suppressing and promoting metastasis. *Nat Rev Cancer* (2009) 9(1):40–55. doi:10.1038/nrc2543
17. Jones EL, Demaria MC, Wright MD. Tetraspanins in cellular immunity. *Biochem Soc Trans* (2011) 39(2):506–11. doi:10.1042/BST0390506
18. Andreu Z, Yanez-Mo M. Tetraspanins in extracellular vesicle formation and function. *Front Immunol* (2014) 5:442. doi:10.3389/fimmu.2014.00442
19. Charrin S, Jouannet S, Boucheix C, Rubinstein E. Tetraspanins at a glance. *J Cell Sci* (2014) 127(Pt 17):3641–8. doi:10.1242/jcs.154906
20. Jiang X, Zhang J, Huang Y. Tetraspanins in cell migration. *Cell Adh Migr* (2015) 9(5):406–15. doi:10.1080/19336918.2015.1005465
21. Rocha-Perugini V, Sanchez-Madrid F, Martinez Del Hoyo G. Function and dynamics of tetraspanins during antigen recognition and immunological synapse formation. *Front Immunol* (2015) 6:653. doi:10.3389/fimmu.2015.00653
22. Termini CM, Gillette JM. Tetraspanins function as regulators of cellular signaling. *Front Cell Dev Biol* (2017) 5:34. doi:10.3389/fcell.2017.00034
23. Priyathilaka TT, Bathige S, Herath H, Lee S, Lee J. Molecular identification of disk abalone (*Haliotis discus*) tetraspanin 33 and CD63: insights into potent players in the disk abalone host defense system. *Fish Shellfish Immunol* (2017) 69:173–84. doi:10.1016/j.fsi.2017.08.020
24. Wu F, Su P, Chen L, Li M, Liu X, Li Q. Cloning of arctic lamprey *Lethenteron camtschaticum* cd9 with roles in the immune response. *J Fish Biol* (2012) 81(4):1147–57. doi:10.1111/j.1095-8649.2012.03299.x
25. Zhou X, Feng H, Guo Q, Dai H. Identification and characterization of the first reptilian CD9, and its expression analysis in response to bacterial infection. *Dev Comp Immunol* (2010) 34(2):150–7. doi:10.1016/j.dci.2009.09.001
26. LeBlanc F, Arseneau JR, Leadbeater S, Glebe B, Laflamme M, Gagne N. Transcriptional response of *Atlantic salmon* (*Salmo salar*) after primary versus secondary exposure to infectious salmon anemia virus (ISAV). *Mol Immunol* (2012) 51(2):197–209. doi:10.1016/j.molimm.2012.03.021
27. Castro R, Abos B, Gonzalez L, Aquilino C, Pignatelli J, Tafalla C. Molecular characterization of CD9 and CD63, two tetraspanin family members expressed in trout B lymphocytes. *Dev Comp Immunol* (2015) 51(1):116–25. doi:10.1016/j.dci.2015.03.002
28. Hou CY, Lin JH, Lin SJ, Kuo WC, Lin HT. Down-regulation of CD53 expression in *Epinephelus coioides* under LPS, poly (I:C), and cytokine stimulation. *Fish Shellfish Immunol* (2016) 51:143–52. doi:10.1016/j.fsi.2015.11.032
29. Song DH, Lee JO. Sensing of microbial molecular patterns by toll-like receptors. *Immunol Rev* (2012) 250(1):216–29. doi:10.1111/j.1600-065X.2012.01167.x
30. Pfeiffer A, Bottcher A, Orso E, Kapinsky M, Nagy P, Bodnar A, et al. Lipopolysaccharide and ceramide docking to CD14 provokes ligand-specific receptor clustering in rafts. *Eur J Immunol* (2001) 31(11):3153–64. doi:10.1002/1521-4141(200111)31:11<3153::AID-IMMU3153>3.0.CO;2-0
31. Suzuki M, Tachibana I, Takeda Y, He P, Minami S, Iwasaki T, et al. Tetraspanin CD9 negatively regulates lipopolysaccharide-induced macrophage activation and lung inflammation. *J Immunol* (2009) 182(10):6485–93. doi:10.4049/jimmunol.0802797
32. Witte CE, Archer KA, Rae CS, Sauer JD, Woodward JJ, Portnoy DA. Innate immune pathways triggered by *Listeria monocytogenes* and their role in the induction of cell-mediated immunity. *Adv Immunol* (2012) 113:135–56. doi:10.1016/B978-0-12-394590-7.00002-6
33. Martinez del Hoyo G, Ramirez-Huesca M, Levy S, Boucheix C, Rubinstein E, Minguito de la Escalera M, et al. CD81 controls immunity to *Listeria* infection through rac-dependent inhibition of proinflammatory mediator release and activation of cytotoxic T cells. *J Immunol* (2015) 194(12):6090–101. doi:10.4049/jimmunol.1402957
34. Taylor PR, Tsoni SV, Willment JA, Dennehy KM, Rosas M, Findon H, et al. Dectin-1 is required for beta-glucan recognition and control of fungal infection. *Nat Immunol* (2007) 8(1):31–8. doi:10.1038/ni1408
35. Mantegazza AR, Barrio MM, Moutel S, Bover L, Weck M, Brossart P, et al. CD63 tetraspanin slows down cell migration and translocates to the endosomal-lysosomal-MIICs route after extracellular stimuli in human immature dendritic cells. *Blood* (2004) 104(4):1183–90. doi:10.1182/blood-2004-01-0104
36. Meyer-Wentrup F, Figdor CG, Ansems M, Brossart P, Wright MD, Adema GJ, et al. Dectin-1 interaction with tetraspanin CD37 inhibits IL-6 production. *J Immunol* (2007) 178(1):154–62. doi:10.4049/jimmunol.178.1.154
37. van Spriel AB, Sofi M, Gartlan KH, van der Schaaf A, Verschueren I, Torensma R, et al. The tetraspanin protein CD37 regulates IgA responses and anti-fungal immunity. *PLoS Pathog* (2009) 5(3):e1000338. doi:10.1371/journal.ppat.1000338
38. Yan J, Wu B, Huang B, Huang S, Jiang S, Lu F. Dectin-1-CD37 association regulates IL-6 expression during Toxoplasma gondii infection. *Parasitol Res* (2014) 113(8):2851–60. doi:10.1007/s00436-014-3946-1
39. Artavanis-Tsakonas K, Love JC, Ploegh HL, Vyas JM. Recruitment of CD63 to *Cryptococcus neoformans* phagosomes requires acidification. *Proc Natl Acad Sci U S A* (2006) 103(43):15945–50. doi:10.1073/pnas.0607528103
40. Huang W, Febbraio M, Silverstein RL. CD9 tetraspanin interacts with CD36 on the surface of macrophages: a possible regulatory influence on uptake of oxidized low density lipoprotein. *PLoS One* (2011) 6(12):e29092. doi:10.1371/journal.pone.0029092
41. Heit B, Kim H, Cosio G, Castano D, Collins R, Lowell CA, et al. Multimolecular signaling complexes enable Syk-mediated signaling of CD36 internalization. *Dev Cell* (2013) 24(4):372–83. doi:10.1016/j.devcel.2013.01.007
42. Toyo-oka K, Yashiro-Ohtani Y, Park CS, Tai XG, Miyake K, Hamaoka T, et al. Association of a tetraspanin CD9 with CD5 on the T cell surface: role of

particular transmembrane domains in the association. *Int Immunol* (1999) 11(12):2043–52. doi:10.1093/intimm/11.12.2043
43. Kaji K, Takeshita S, Miyake K, Takai T, Kudo A. Functional association of CD9 with the Fc gamma receptors in macrophages. *J Immunol* (2001) 166(5):3256–65. doi:10.4049/jimmunol.166.5.3256
44. Lebel-Binay S, Lagaudriere C, Fradelizi D, Conjeaud H. CD82, tetraspan-transmembrane protein, is a regulated transducing molecule on U937 monocytic cell line. *J Leukoc Biol* (1995) 57(6):956–63. doi:10.1002/jlb.57.6.956
45. Wilflingseder D, Banki Z, Garcia E, Pruenster M, Pfister G, Muellauer B, et al. IgG opsonization of HIV impedes provirus formation in and infection of dendritic cells and subsequent long-term transfer to T cells. *J Immunol* (2007) 178(12):7840–8. doi:10.4049/jimmunol.178.12.7840
46. Peng WM, Yu CF, Kolanus W, Mazzocca A, Bieber T, Kraft S, et al. Tetraspanins CD9 and CD81 are molecular partners of trimeric FcvarepsilonRI on human antigen-presenting cells. *Allergy* (2011) 66(5):605–11. doi:10.1111/j.1398-9995.2010.02524.x
47. Halova I, Draber P. Tetraspanins and transmembrane adaptor proteins as plasma membrane organizers-mast cell case. *Front Cell Dev Biol* (2016) 4:43. doi:10.3389/fcell.2016.00043
48. Ding SW. RNA-based antiviral immunity. *Nat Rev Immunol* (2010) 10(9):632–44. doi:10.1038/nri2824
49. Wang Y, Tong X, Omoregie ES, Liu W, Meng S, Ye X. Tetraspanin 6 (TSPAN6) negatively regulates retinoic acid-inducible gene I-like receptor-mediated immune signaling in a ubiquitination-dependent manner. *J Biol Chem* (2012) 287(41):34626–34. doi:10.1074/jbc.M112.390401
50. Ley K, Laudanna C, Cybulsky MI, Nourshargh S. Getting to the site of inflammation: the leukocyte adhesion cascade updated. *Nat Rev Immunol* (2007) 7(9):678–89. doi:10.1038/nri2156
51. Yanez-Mo M, Gutierrez-Lopez MD, Cabanas C. Functional interplay between tetraspanins and proteases. *Cell Mol Life Sci* (2011) 68(20):3323–35. doi:10.1007/s00018-011-0746-y
52. Dieu MC, Vanbervliet B, Vicari A, Bridon JM, Oldham E, Ait-Yahia S, et al. Selective recruitment of immature and mature dendritic cells by distinct chemokines expressed in different anatomic sites. *J Exp Med* (1998) 188(2):373–86. doi:10.1084/jem.188.2.373
53. Sozzani S, Allavena P, Vecchi A, Mantovani A. The role of chemokines in the regulation of dendritic cell trafficking. *J Leukoc Biol* (1999) 66(1):1–9. doi:10.1002/jlb.66.1.1
54. Sallusto F, Schaerli P, Loetscher P, Schaniel C, Lenig D, Mackay CR, et al. Rapid and coordinated switch in chemokine receptor expression during dendritic cell maturation. *Eur J Immunol* (1998) 28(9):2760–9. doi:10.1002/(SICI)1521-4141(199809)28:09<2760::AID-IMMU2760>3.0.CO;2-N
55. Sozzani S, Allavena P, D'Amico G, Luini W, Bianchi G, Kataura M, et al. Differential regulation of chemokine receptors during dendritic cell maturation: a model for their trafficking properties. *J Immunol* (1998) 161(3):1083–6.
56. Martin-Fontecha A, Sebastiani S, Hopken UE, Uguccioni M, Lipp M, Lanzavecchia A, et al. Regulation of dendritic cell migration to the draining lymph node: impact on T lymphocyte traffic and priming. *J Exp Med* (2003) 198(4):615–21. doi:10.1084/jem.20030448
57. Pileri P, Uematsu Y, Campagnoli S, Galli G, Falugi F, Petracca R, et al. Binding of hepatitis C virus to CD81. *Science* (1998) 282(5390):938–41. doi:10.1126/science.282.5390.938
58. Nattermann J, Zimmermann H, Iwan A, von Lilienfeld-Toal M, Leifeld L, Nischalke HD, et al. Hepatitis C virus E2 and CD81 interaction may be associated with altered trafficking of dendritic cells in chronic hepatitis C. *Hepatology* (2006) 44(4):945–54. doi:10.1002/hep.21350
59. Dijkstra S, Kooij G, Verbeek R, van der Pol SM, Amor S, Geisert EE Jr, et al. Targeting the tetraspanin CD81 blocks monocyte transmigration and ameliorates EAE. *Neurobiol Dis* (2008) 31(3):413–21. doi:10.1016/j.nbd.2008.05.018
60. Schenk GJ, Dijkstra S, van het Hof AJ, van der Pol SM, Drexhage JA, van der Valk P, et al. Roles for HB-EGF and CD9 in multiple sclerosis. *Glia* (2013) 61(11):1890–905. doi:10.1002/glia.22565
61. Dominguez PM, Ardavin C. Differentiation and function of mouse monocyte-derived dendritic cells in steady state and inflammation. *Immunol Rev* (2010) 234(1):90–104. doi:10.1111/j.0105-2896.2009.00876.x
62. King IL, Dickendesher TL, Segal BM. Circulating Ly-6C+ myeloid precursors migrate to the CNS and play a pathogenic role during autoimmune demyelinatingdisease.*Blood*(2009)113(14):3190–7.doi:10.1182/blood-2008-07-168575
63. Ko HJ, Brady JL, Ryg-Cornejo V, Hansen DS, Vremec D, Shortman K, et al. GM-CSF-responsive monocyte-derived dendritic cells are pivotal in Th17 pathogenesis. *J Immunol* (2014) 192(5):2202–9. doi:10.4049/jimmunol.1302040
64. Barreiro O, Yanez-Mo M, Sala-Valdes M, Gutierrez-Lopez MD, Ovalle S, Higginbottom A, et al. Endothelial tetraspanin microdomains regulate leukocyte firm adhesion during extravasation. *Blood* (2005) 105(7):2852–61. doi:10.1182/blood-2004-09-3606
65. Feigelson SW, Grabovsky V, Shamri R, Levy S, Alon R. The CD81 tetraspanin facilitates instantaneous leukocyte VLA-4 adhesion strengthening to vascular cell adhesion molecule 1 (VCAM-1) under shear flow. *J Biol Chem* (2003) 278(51):51203–12. doi:10.1074/jbc.M303601200
66. Takeda Y, He P, Tachibana I, Zhou B, Miyado K, Kaneko H, et al. Double deficiency of tetraspanins CD9 and CD81 alters cell motility and protease production of macrophages and causes chronic obstructive pulmonary disease-like phenotype in mice. *J Biol Chem* (2008) 283(38):26089–97. doi:10.1074/jbc.M801902200
67. Lammermann T, Bader BL, Monkley SJ, Worbs T, Wedlich-Soldner R, Hirsch K, et al. Rapid leukocyte migration by integrin-independent flowing and squeezing. *Nature* (2008) 453(7191):51–5. doi:10.1038/nature06887
68. Petrie RJ, Yamada KM. At the leading edge of three-dimensional cell migration. *J Cell Sci* (2012) 125(Pt 24):5917–26. doi:10.1242/jcs.093732
69. Wilson K, Lewalle A, Fritzsche M, Thorogate R, Duke T, Charras G. Mechanisms of leading edge protrusion in interstitial migration. *Nat Commun* (2013) 4:2896. doi:10.1038/ncomms3896
70. Quast T, Eppler F, Semmling V, Schild C, Homsi Y, Levy S, et al. CD81 is essential for the formation of membrane protrusions and regulates Rac1-activation in adhesion-dependent immune cell migration. *Blood* (2011) 118(7):1818–27. doi:10.1182/blood-2010-12-326595
71. Tejera E, Rocha-Perugini V, Lopez-Martin S, Perez-Hernandez D, Bachir AI, Horwitz AR, et al. CD81 regulates cell migration through its association with Rac GTPase. *Mol Biol Cell* (2013) 24(3):261–73. doi:10.1091/mbc.E12-09-0642
72. Jones EL, Wee JL, Demaria MC, Blakeley J, Ho PK, Vega-Ramos J, et al. Dendritic cell migration and antigen presentation are coordinated by the opposing functions of the tetraspanins CD82 and CD37. *J Immunol* (2016) 196(3):978–87. doi:10.4049/jimmunol.1500357
73. Gartlan KH, Wee JL, Demaria MC, Nastovska R, Chang TM, Jones EL, et al. Tetraspanin CD37 contributes to the initiation of cellular immunity by promoting dendritic cell migration. *Eur J Immunol* (2013) 43(5):1208–19. doi:10.1002/eji.201242730
74. Angelisova P, Hilgert I, Horejsi V. Association of four antigens of the tetraspans family (CD37, CD53, TAPA-1, and R2/C33) with MHC class II glycoproteins. *Immunogenetics* (1994) 39(4):249–56. doi:10.1007/BF00188787
75. Szollosi J, Horejsi V, Bene L, Angelisova P, Damjanovich S. Supramolecular complexes of MHC class I, MHC class II, CD20, and tetraspan molecules (CD53, CD81, and CD82) at the surface of a B cell line JY. *J Immunol* (1996) 157(7):2939–46.
76. Engering A, Pieters J. Association of distinct tetraspanins with MHC class II molecules at different subcellular locations in human immature dendritic cells. *Int Immunol* (2001) 13(2):127–34. doi:10.1093/intimm/13.2.127
77. Sheng KC, van Spriel AB, Gartlan KH, Sofi M, Apostolopoulos V, Ashman L, et al. Tetraspanins CD37 and CD151 differentially regulate Ag presentation and T-cell co-stimulation by DC. *Eur J Immunol* (2009) 39(1):50–5. doi:10.1002/eji.200838798
78. Unternaehrer JJ, Chow A, Pypaert M, Inaba K, Mellman I. The tetraspanin CD9 mediates lateral association of MHC class II molecules on the dendritic cell surface. *Proc Natl Acad Sci U S A* (2007) 104(1):234–9. doi:10.1073/pnas.0609665104
79. Kropshofer H, Spindeldreher S, Rohn TA, Platania N, Grygar C, Daniel N, et al. Tetraspan microdomains distinct from lipid rafts enrich select peptide-MHC class II complexes. *Nat Immunol* (2002) 3(1):61–8. doi:10.1038/ni750

80. Khandelwal S, Roche PA. Distinct MHC class II molecules are associated on the dendritic cell surface in cholesterol-dependent membrane microdomains. *J Biol Chem* (2010) 285(46):35303–10. doi:10.1074/jbc.M110.147793
81. Bosch B, Heipertz EL, Drake JR, Roche PA. Major histocompatibility complex (MHC) class II-peptide complexes arrive at the plasma membrane in cholesterol-rich microclusters. *J Biol Chem* (2013) 288(19):13236–42. doi:10.1074/jbc.M112.442640
82. Poloso NJ, Denzin LK, Roche PA. CDw78 defines MHC class II-peptide complexes that require Ii chain-dependent lysosomal trafficking, not localization to a specific tetraspanin membrane microdomain. *J Immunol* (2006) 177(8):5451–8. doi:10.4049/jimmunol.177.8.5451
83. ten Broeke T, Wubbolts R, Stoorvogel W. MHC class II antigen presentation by dendritic cells regulated through endosomal sorting. *Cold Spring Harb Perspect Biol* (2013) 5(12):a016873. doi:10.1101/cshperspect.a016873
84. Calafat J, Nijenhuis M, Janssen H, Tulp A, Dusseljee S, Wubbolts R, et al. Major histocompatibility complex class II molecules induce the formation of endocytic MIIC-like structures. *J Cell Biol* (1994) 126(4):967–77. doi:10.1083/jcb.126.4.967
85. Honey K, Rudensky AY. Lysosomal cysteine proteases regulate antigen presentation. *Nat Rev Immunol* (2003) 3(6):472–82. doi:10.1038/nri1110
86. Roche PA, Furuta K. The ins and outs of MHC class II-mediated antigen processing and presentation. *Nat Rev Immunol* (2015) 15(4):203–16. doi:10.1038/nri3818
87. Escola JM, Kleijmeer MJ, Stoorvogel W, Griffith JM, Yoshie O, Geuze HJ. Selective enrichment of tetraspan proteins on the internal vesicles of multivesicular endosomes and on exosomes secreted by human B-lymphocytes. *J Biol Chem* (1998) 273(32):20121–7. doi:10.1074/jbc.273.32.20121
88. Hammond C, Denzin LK, Pan M, Griffith JM, Geuze HJ, Cresswell P. The tetraspan protein CD82 is a resident of MHC class II compartments where it associates with HLA-DR, -DM, and -DO molecules. *J Immunol* (1998) 161(7):3282–91.
89. Hoorn T, Paul P, Janssen L, Janssen H, Neefjes J. Dynamics within tetraspanin pairs affect MHC class II expression. *J Cell Sci* (2012) 125(Pt 2):328–39. doi:10.1242/jcs.088047
90. Artavanis-Tsakonas K, Kasperkovitz PV, Papa E, Cardenas ML, Khan NS, Van der Veen AG, et al. The tetraspanin CD82 is specifically recruited to fungal and bacterial phagosomes prior to acidification. *Infect Immun* (2011) 79(3):1098–106. doi:10.1128/IAI.01135-10
91. Rocha-Perugini V, Martinez Del Hoyo G, Gonzalez-Granado JM, Ramirez-Huesca M, Zorita V, Rubinstein E, et al. CD9 regulates major histocompatibility complex class II trafficking in monocyte-derived dendritic cells. *Mol Cell Biol* (2017) 37(15):e202–17. doi:10.1128/MCB.00202-17
92. Wubbolts R, Fernandez-Borja M, Jordens I, Reits E, Dusseljee S, Echeverri C, et al. Opposing motor activities of dynein and kinesin determine retention and transport of MHC class II-containing compartments. *J Cell Sci* (1999) 112(Pt 6):785–95.
93. Vyas JM, Kim YM, Artavanis-Tsakonas K, Love JC, Van der Veen AG, Ploegh HL. Tubulation of class II MHC compartments is microtubule dependent and involves multiple endolysosomal membrane proteins in primary dendritic cells. *J Immunol* (2007) 178(11):7199–210. doi:10.4049/jimmunol.178.11.7199
94. van Nispen tot Pannerden HE, Geerts WJ, Kleijmeer MJ, Heijnen HF. Spatial organization of the transforming MHC class II compartment. *Biol Cell* (2010) 102(11):581–91. doi:10.1042/BC20100046
95. Barois N, de Saint-Vis B, Lebecque S, Geuze HJ, Kleijmeer MJ. MHC class II compartments in human dendritic cells undergo profound structural changes upon activation. *Traffic* (2002) 3(12):894–905. doi:10.1034/j.1600-0854.2002.31205.x
96. Chow A, Toomre D, Garrett W, Mellman I. Dendritic cell maturation triggers retrograde MHC class II transport from lysosomes to the plasma membrane. *Nature* (2002) 418(6901):988–94. doi:10.1038/nature01006
97. Shin JS, Ebersold M, Pypaert M, Delamarre L, Hartley A, Mellman I. Surface expression of MHC class II in dendritic cells is controlled by regulated ubiquitination. *Nature* (2006) 444(7115):115–8. doi:10.1038/nature05261
98. van Niel G, Wubbolts R, Ten Broeke T, Buschow SI, Ossendorp FA, Melief CJ, et al. Dendritic cells regulate exposure of MHC class II at their plasma membrane by oligoubiquitination. *Immunity* (2006) 25(6):885–94. doi:10.1016/j.immuni.2006.11.001
99. De Gassart A, Camosseto V, Thibodeau J, Ceppi M, Catalan N, Pierre P, et al. MHC class II stabilization at the surface of human dendritic cells is the result of maturation-dependent MARCH I down-regulation. *Proc Natl Acad Sci U S A* (2008) 105(9):3491–6. doi:10.1073/pnas.0708874105
100. Matsuki Y, Ohmura-Hoshino M, Goto E, Aoki M, Mito-Yoshida M, Uematsu M, et al. Novel regulation of MHC class II function in B cells. *EMBO J* (2007) 26(3):846–54. doi:10.1038/sj.emboj.7601556
101. Walseng E, Furuta K, Bosch B, Weih KA, Matsuki Y, Bakke O, et al. Ubiquitination regulates MHC class II-peptide complex retention and degradation in dendritic cells. *Proc Natl Acad Sci U S A* (2010) 107(47):20465–70. doi:10.1073/pnas.1010990107
102. Cho KJ, Walseng E, Ishido S, Roche PA. Ubiquitination by march-I prevents MHC class II recycling and promotes MHC class II turnover in antigen-presenting cells. *Proc Natl Acad Sci U S A* (2015) 112(33):10449–54. doi:10.1073/pnas.1507981112
103. Bartee E, Eyster CA, Viswanathan K, Mansouri M, Donaldson JG, Fruh K. Membrane-associated RING-CH proteins associate with Bap31 and target CD81 and CD44 to lysosomes. *PLoS One* (2010) 5(12):e15132. doi:10.1371/journal.pone.0015132
104. Charrin S, Manie S, Thiele C, Billard M, Gerlier D, Boucheix C, et al. A physical and functional link between cholesterol and tetraspanins. *Eur J Immunol* (2003) 33(9):2479–89. doi:10.1002/eji.200323884
105. Anderson HA, Hiltbold EM, Roche PA. Concentration of MHC class II molecules in lipid rafts facilitates antigen presentation. *Nat Immunol* (2000) 1(2):156–62. doi:10.1038/7784277842
106. Gartlan KH, Belz GT, Tarrant JM, Minigo G, Katsara M, Sheng KC, et al. A complementary role for the tetraspanins CD37 and Tssc6 in cellular immunity. *J Immunol* (2010) 185(6):3158–66. doi:10.4049/jimmunol.0902867
107. Petersen SH, Odintsova E, Haigh TA, Rickinson AB, Taylor GS, Berditchevski F. The role of tetraspanin CD63 in antigen presentation via MHC class II. *Eur J Immunol* (2011) 41(9):2556–61. doi:10.1002/eji.201141438
108. Tkach M, Kowal J, Zucchetti AE, Enserink L, Jouve M, Lankar D, et al. Qualitative differences in T-cell activation by dendritic cell-derived extracellular vesicle subtypes. *EMBO J* (2017) 36(20):3012–28. doi:10.15252/embj.201696003
109. Thery C, Regnault A, Garin J, Wolfers J, Zitvogel L, Ricciardi-Castagnoli P, et al. Molecular characterization of dendritic cell-derived exosomes. Selective accumulation of the heat shock protein hsc73. *J Cell Biol* (1999) 147(3):599–610. doi:10.1083/jcb.147.3.599
110. Wubbolts R, Leckie RS, Veenhuizen PT, Schwarzmann G, Mobius W, Hoernschemeyer J, et al. Proteomic and biochemical analyses of human B cell-derived exosomes. Potential implications for their function and multivesicular body formation. *J Biol Chem* (2003) 278(13):10963–72. doi:10.1074/jbc.M207550200
111. Saunderson SC, Schuberth PC, Dunn AC, Miller L, Hock BD, MacKay PA, et al. Induction of exosome release in primary B cells stimulated via CD40 and the IL-4 receptor. *J Immunol* (2008) 180(12):8146–52. doi:10.4049/jimmunol.180.12.8146
112. Perez-Hernandez D, Gutierrez-Vazquez C, Jorge I, Lopez-Martin S, Ursa A, Sanchez-Madrid F, et al. The intracellular interactome of tetraspanin-enriched microdomains reveals their function as sorting machineries toward exosomes. *J Biol Chem* (2013) 288(17):11649–61. doi:10.1074/jbc.M112.445304
113. Zilber MT, Setterblad N, Vasselon T, Doliger C, Charron D, Mooney N, et al. MHC class II/CD38/CD9: a lipid-raft-dependent signaling complex in human monocytes. *Blood* (2005) 106(9):3074–81. doi:10.1182/blood-2004-10-4094
114. Buschow SI, Nolte-'t Hoen EN, van Niel G, Pols MS, ten Broeke T, Lauwen M, et al. MHC II in dendritic cells is targeted to lysosomes or T cell-induced exosomes via distinct multivesicular body pathways. *Traffic* (2009) 10(10):1528–42. doi:10.1111/j.1600-0854.2009.00963.x
115. Zuidscherwoude M, Worah K, van der Schaaf A, Buschow SI, van Spriel AB. Differential expression of tetraspanin superfamily members in dendritic cell subsets. *PLoS One* (2017) 12(9):e0184317. doi:10.1371/journal.pone.0184317
116. Mittelbrunn M, Martinez del Hoyo G, Lopez-Bravo M, Martin-Cofreces NB, Scholer A, Hugues S, et al. Imaging of plasmacytoid dendritic cell interactions with T cells. *Blood* (2009) 113(1):75–84. doi:10.1182/blood-2008-02-139865
117. Lagaudriere-Gesbert C, Lebel-Binay S, Wiertz E, Ploegh HL, Fradelizi D, Conjeaud H. The tetraspanin protein CD82 associates with both free HLA

class I heavy chain and heterodimeric beta 2-microglobulin complexes. *J Immunol* (1997) 158(6):2790–7.
118. Liu YJ. IPC: professional type 1 interferon-producing cells and plasmacytoid dendritic cell precursors. *Annu Rev Immunol* (2005) 23:275–306. doi:10.1146/annurev.immunol.23.021704.115633
119. Swiecki M, Colonna M. The multifaceted biology of plasmacytoid dendritic cells. *Nat Rev Immunol* (2015) 15(8):471–85. doi:10.1038/nri3865
120. Bjorck P, Leong HX, Engleman EG. Plasmacytoid dendritic cell dichotomy: identification of IFN-alpha producing cells as a phenotypically and functionally distinct subset. *J Immunol* (2011) 186(3):1477–85. doi:10.4049/jimmunol.1000454
121. Zhang H, Gregorio JD, Iwahori T, Zhang X, Choi O, Tolentino LL, et al. A distinct subset of plasmacytoid dendritic cells induces activation and differentiation of B and T lymphocytes. *Proc Natl Acad Sci U S A* (2017) 114(8):1988–93. doi:10.1073/pnas.1610630114
122. Matsui T, Connolly JE, Michnevitz M, Chaussabel D, Yu CI, Glaser C, et al. CD2 distinguishes two subsets of human plasmacytoid dendritic cells with distinct phenotype and functions. *J Immunol* (2009) 182(11):6815–23. doi:10.4049/jimmunol.0802008
123. Zhang S, Kodys K, Babcock GJ, Szabo G. CD81/CD9 tetraspanins aid plasmacytoid dendritic cells in recognition of hepatitis C virus-infected cells and induction of interferon-alpha. *Hepatology* (2013) 58(3):940–9. doi:10.1002/hep.25827

Conflict of Interest Statement: The authors declare that the research was conducted in the absence of any commercial or financial relationships that could be construed as a potential conflict of interest.

frontiers in Microbiology

ORIGINAL RESEARCH
published: 23 May 2018
doi: 10.3389/fmicb.2018.01036

Extracellular Vesicles From the Helminth *Fasciola hepatica* Prevent DSS-Induced Acute Ulcerative Colitis in a T-Lymphocyte Independent Mode

*Javier Roig[1,2†], Maria L. Saiz[3†], Alicia Galiano[1†], Maria Trelis[1,4], Fernando Cantalapiedra[1,5], Carlos Monteagudo[6], Elisa Giner[7], Rosa M. Giner[7], M. C. Recio[7], Dolores Bernal[8], Francisco Sánchez-Madrid[2,9,10] and Antonio Marcilla[1,4]**

[1] Àrea de Parasitologia, Departament de Farmàcia i Tecnologia Farmacèutica i Parasitologia, Universitat de València, Burjassot, Spain, [2] Facultad de Ciencias de la Salud, Universidad Europea de Valencia, Burjassot, Spain, [3] Vascular Pathophysiology Area, Centro Nacional de Investigaciones Cardiovasculares, Madrid, Spain, [4] Joint Research Unit on Endocrinology, Nutrition and Clinical Dietetics, Health Research Institute La Fe, Universitat de València, Burjassot, Spain, [5] Veterinari de Salut Pública, Centre de Salut Pública de Manises, Burjassot, Spain, [6] Departament de Patologia, Universitat de València, Burjassot, Spain, [7] Departament de Farmacologia, Universitat de València, Burjassot, Spain, [8] Departament de Bioquímica i Biologia Molecular, Universitat de València, Burjassot, Spain, [9] Immunology Service, Hospital de La Princesa, Instituto de Investigación Sanitaria Hospital Universitario de La Princesa, Universidad Autónoma de Madrid, Madrid, Spain, [10] Centro de Investigación Biomédica en Red Enfermedades Cardiovasculares, Madrid, Spain

OPEN ACCESS

Edited by:
Ana Claudia Torrecilhas,
Federal University of São Paulo, Brazil

Reviewed by:
Werner Solbach,
Universität zu Lübeck, Germany
Patricia Xander,
Federal University of São Paulo, Brazil

***Correspondence:**
Antonio Marcilla
antonio.marcilla@uv.es

[†] These authors have contributed equally to this work.

Specialty section:
This article was submitted to Microbial Physiology and Metabolism, a section of the journal Frontiers in Microbiology

Received: 02 March 2018
Accepted: 01 May 2018
Published: 23 May 2018

Citation:
Roig J, Saiz ML, Galiano A, Trelis M, Cantalapiedra F, Monteagudo C, Giner E, Giner RM, Recio MC, Bernal D, Sánchez-Madrid F and Marcilla A (2018) Extracellular Vesicles From the Helminth Fasciola hepatica Prevent DSS-Induced Acute Ulcerative Colitis in a T-Lymphocyte Independent Mode. Front. Microbiol. 9:1036. doi: 10.3389/fmicb.2018.01036

The complexity of the pathogenesis of inflammatory bowel disease (ulcerative colitis and Crohn's disease) has led to the quest of empirically drug therapies, combining immunosuppressant agents, biological therapy and modulators of the microbiota. Helminth parasites have been proposed as an alternative treatment of these diseases based on the hygiene hypothesis, but ethical and medical problems arise. Recent reports have proved the utility of parasite materials, mainly excretory/secretory products as therapeutic agents. The identification of extracellular vesicles on those secreted products opens a new field of investigation, since they exert potent immunomodulating effects. To assess the effect of extracellular vesicles produced by helminth parasites to treat ulcerative colitis, we have analyzed whether extracellular vesicles produced by the parasitic helminth *Fasciola hepatica* can prevent colitis induced by chemical agents in a mouse model. Adult parasites were cultured *in vitro* and secreted extracellular vesicles were purified and used for immunizing both wild type C57BL/6 and RAG1$^{-/-}$ mice. Control and immunized mice groups were treated with dextran sulfate sodium 7 days after last immunization to promote experimental colitis. The severity of colitis was assessed by disease activity index and histopathological scores. Mucosal cytokine expression was evaluated by ELISA. The activation of NF-kB, COX-2, and MAPK were evaluated by immunoblotting. Administration of extracellular vesicles from *F. hepatica* ameliorates the pathological symptoms reducing the amount of pro-inflammatory cytokines and interfering with both MAPK and NF-kB pathways. Interestingly, the

observed effects do not seem to be mediated by T-cells. Our results indicate that extracellular vesicles from parasitic helminths can modulate immune responses in dextran sulfate sodium (DSS)-induced colitis, exerting a protective effect that should be mediated by other cells distinct from B- and T-lymphocytes.

Keywords: inflammatory bowel disease, DSS-ulcerative colitis, *Fasciola hepatica*, extracellular vesicles

INTRODUCTION

Ulcerative colitis and Crohn's disease are two major clinical entities included in IBD, which may affect 0.5% of Western world population (1 million people in the United States, and 2.5–3 million people in Europe), with 37 new cases per 10^5 inhabitants in Europe (Molodecky et al., 2012; Kaplan and Ng, 2017). IBD is also spreading in developing countries, where the prevalence is lower than in developed ones (Molodecky et al., 2012; Ng et al., 2013). Most of IBD patients are affected in their productive age, originating not only important social problems, but also economic losses (Kaplan, 2015).

The etiology of the disease is not well understood and because of the complexity of this pathology, the development of effective treatments will require studies using multidisciplinary approaches, where animal models have proved to be highly informative (Lin and Hackam, 2011).

Due to the absence of a curative treatment for IBD, there have been numerous attempts to incorporate new therapies. Some of these include new drugs or nutritional supplements to correct or enhance the effectiveness of the currently authorized treatments. In fact, the complexity of the pathogenesis of these diseases has led to empirically evolved current drug therapies, which primarily treat inflammation. The latest therapies attempt to restore the intestinal immune balance by efficiently combining immunosuppressant agents, biological therapy and modulators of the microbiota (Vanhove et al., 2016).

Interestingly, previous epidemiologic studies and clinic trials suggested that helminths, either by natural or artificial infections, might protect people from IBD (Smallwood et al., 2017). This has been confirmed by Ramanan et al. (2016), which have demonstrated that alteration of commensal and pathogenic bacteria produced by gastrointestinal helminths infection in turn protects the host against IBD (Ramanan et al., 2016). Still, major concerns of the helminthic therapy are related to ethical issues and the ability of controlling the course of the infection. In this sense, the identification of helminth-derived molecules that ultimately mediate host immune modulation is attracting much attention.

Extracellular vesicles, including exosomes and microvesicles, have been described as participating in intercellular communications with important roles in physiological and pathological processes, where they can be used as diagnostic and therapeutic weapons (Yáñez-Mó et al., 2015; Barile and Vassalli, 2017). EVs have been described to participate in inflammation, like EVs from granulocytes, which have been used for IBD treatment in a mice model (Wang et al., 2016; Song et al., 2017).

Fasciola hepatica is a flatworm that excretes/secretes a large number of molecules to the host-parasite interplay, including immune modulators (Dalton et al., 2013). Our group has identified some of these molecules in EVs released by parasite adults in culture (Marcilla et al., 2012; Cwiklinski et al., 2015; Fromm et al., 2015). To assess the functional role of these EVs in the host and exploring their usefulness as therapeutic agents against IBD, we have studied their potential in preventing ulcerative colitis in a DSS induced colitis model in C57BL/6 mice. Our data support that *F. hepatica* EVs (FhEVs) can protect from IBD in this model, since their inoculation prevents intestinal damage in acute colitis by altering the local immune response. Thus, FhEVs might be employed for preventing relapses in IBD patients and could be explored as a potential new therapy for treating IBD.

MATERIALS AND METHODS

Materials

Unless otherwise specified, all reagents were purchased from Sigma-Aldrich (Madrid, Spain) and Bio-Rad Laboratories (Madrid, Spain). DSS, colitis grade (36–50 kDa) was purchased from MP Biomedical (United States). Specific antibodies for COX-2, p38 and p65 subunit nuclear factor-κβ (NF-κB) were purchased from Millipore (Billerica, MA, United States); antibodies against p38 MAPK and P-p38 MAPK were obtained from were obtained from Cell Signaling Technology (Danvers, MA, United States) and Santa Cruz Biotechnology (Santa Cruz, CA, United States), respectively. Anti-GAPDH polyclonal sera was kindly provided by Dr. Daniel Gozalbo, Universitat de València. ELISA kits for cytokines were purchased from Affymetrix eBioscience (San Diego, CA, United States).

Isolation and Characterization of *Fasciola hepatica* Extracellular Vesicles

Extracellular vesicles from *F. hepatica* adults (FhEVs) were purified and monitored by TEM as previously described (Marcilla et al., 2012). Briefly, adult parasites, collected from cow livers from local abattoirs, were thoroughly washed with PBS and cultured in 0.2 μm filtered RPMI -1640 culture medium containing 100 U penicillin and 100 μg/mL streptomycin (all from Sigma), at concentrations of 2 worms/mL at 37°C for 5 h. After the incubation period, the parasite culture media was collected and centrifuged at low speed (first at 300 g/10 min,

Abbreviations: COX-2, cyclooxygenase 2; DAI, disease activity index; DSS, dextran sulfate sodium; EVs, extracellular vesicles; FABPs, fatty acid-binding proteins; Fh, *Fasciola hepatica*; IBD, inflammatory bowel disease; IL, interleukin; MAPK, mitogen activated protein kinase; MPO, myeloperoxidase; NF-kB, nuclear factor kappa B; TEM, transmission electron microscopy; TNF-α, tumor necrosis factor alpha.

and then at 700 g/30 min) to remove larger debris, and the resulting supernatant was centrifuged at 15,000 *g* for 45 min at 4°C. Supernatants were then filtered using an ultrafiltration membrane (0.2 μm; Schleicher and Schuell) and centrifuged at 120000 *g*/1 h at 4°C in an Optima TL100 tabletop ultracentrifuge (Beckman) using a TLA-55 rotor.

Extracellular vesicles were aliquoted, frozen-drying in PBS containing 20% sucrose, and kept at 4°C until use. Before inoculating animals, protein content was determined following Bradford's method (Bio-Rad).

Animals

Female C57BL/6 mice (Harlan Interfauna Iberica, Barcelona, Spain), 6–8 weeks of age, weighing 18–20 g were previously acclimatized in 12 h light/dark cycles at 22°C and 60% humidity, for 7 days before performing the experiments, and fed with a standard laboratory rodent diet and water *ad libitum*. All animal care and experimental protocols were approved by the Institutional Ethics Committee of the Universitat de València and Generalitat Valènciana, Spain (No. 2015/VSC/PEA/00045 type 2, 12-03-2015).

Rag1$^{-/-}$ mice were housed in pathogen-free conditions at the CNIC animal facility. Experimental procedures were approved by the local research ethics committee and conformed to EU Directive 2010/63EU and Recommendation 2007/526/EC, enforced in Spanish law under Real Decreto 53/2013.

Induction of Dextran Sulfate Sodium (DSS) Colitis and Inoculation With FhEVs

Acute colitis was induced in mice by administering drinking water with 3% (w/v) DSS for 7 days, as previously described (Giner et al., 2016). Animals were randomly assigned to four groups: Control group (mice received only regular drinking water); DSS group (mice received 3% DSS in drinking water); FhEV + DSS group (mice were subcutaneously inoculated three times with *F. hepatica* EVs resuspended in PBS, and received 3% DSS in drinking water); and FhEV group (mice subcutaneously inoculated three times with *F. hepatica* EVs, and received regular drinking water) (see **Figure 1B**). At day 49 mice were sacrificed, their colons were removed and samples analyzed. Every effort was made to minimize animal suffering and reduce the number of animals used.

Disease Activity Index

Disease Activity Index was used to assess the severity of colitis as indicated by Giner et al. (2013). Mice were checked daily for development of colitis by monitoring body weight, fecal occult blood (Hemoccult® II Sensa; Beckman Coulter), or gross rectal bleeding, and stool consistency. Overall disease severity was assessed by a clinical scoring system defined as follows: weight loss: 0 (no loss), 1 (1–5%), 2 (5–10%), 3 (10–15%), and 4 (>15%); stool consistency: 0 (normal), 2 (loose stool), and 4 (diarrhea); and bleeding: 0 (no blood), 1 (Hemoccult® positive), 2 (Hemoccult® positive and visual pellet bleeding), and 4 (gross bleeding, blood around anus).

Histological Analysis

Distal colon parts were cut and fixed as previously reported (Giner et al., 2016). Five-micrometer tissue sections were stained with hematoxylin and eosin and evaluated using an Optiphot Nikkon, microscope by an expert pathologist (CM). A well-accepted histology score in an scale of 0 to 6 was used (Melgar et al., 2008) (0 = no signs of damage; 1 = few inflammatory cells, no signs of epithelial degeneration; 2 = mild inflammation, few signs of epithelial degeneration; 3 = moderate inflammation, few epithelial ulcerations; 4 = moderate to severe inflammation, ulcerations in more than 25% of the tissue section; 5 = moderate to severe inflammation, large ulcerations of more than 50% of the tissue section; and 6 = severe inflammation and ulcerations of more than 75% of the tissue section). In addition, the precise percentage of ulcerated mucosa in every transversal section of the colon was recorded. Median histopathology score and median percentage of ulcerated mucosa were used for comparison between groups.

Cytokine Production in Tissue

TNF-α, IL-6, IL-17A, and IL-10 concentrations were measured as previously described (Giner et al., 2016), by using specific enzyme immunoassay kits, following manufacturer's instructions. Reads were done in an iMark^{TM} microplate absorbance reader (Bio-Rad, CA, United States). Values of cytokines were expressed as pg per mg of total protein.

Determination of Neutrophil Infiltration in Colon Tissue

Neutrophil infiltration was determined by assaying MPO activity, as previously described (Giner et al., 2011, 2013). Absorbance was measured spectrophotometrically at 630 nm, and MPO activity was expressed as the amount of enzyme necessary to produce a change in absorbance of 1.0 Unit g^{-1} of tissue (Recio et al., 2000).

Cytosolic and Nuclear Protein Extraction

The differential extraction of proteins from intestines and their concentration were determined as previously reported (Giner et al., 2011).

Western Blot Analysis

Equal amounts of protein (25 μg) were separated by SDS-PAGE in 10% polyacrylamide gels, transferred onto nitrocellulose membranes, blocked, and incubated overnight at 4°C with anti-COX-2 (1:8000), anti-p65 NF-κB (1:500) subunit, or anti-GAPDH, anti-p38 MAPK, anti-Pp38 MAPK (all at 1:1000). Blots were washed with TBS (10 mM Tris-HCl pH 7.4, NaCl 150 mM), incubated with secondary antibodies (1:10000), and immune reactive bands were visualized with the aid of Amersham^{TM} ECL Select western blotting system (GE Healthcare, Madrid, Spain) (Marcilla et al., 1995; Giner et al., 2013).

To unify Western blot densitometry to result in the processed images, data from the DSS group were taken as reference and assigned the value of 100. Relative percentages of the other groups were then calculated.

Statistical Analysis

The results are expressed as the mean ± SE values. Statistical significance was determined with a one-way analysis of variance (ANOVA), and Dunnett's *t*-test for multiple comparisons using GraphPad Prism, version 6 (GraphPad Software Inc., La Jolla, CA, United States). Values of $p < 0.05$ were considered to be statistically significant, and the symbols *, $^{\#}$ and $^{+}$ were used to indicate the statistical significance.

Software

Images for all Western blot experiments were acquired with a ChemiDoc MP imager (Bio Rad, CA, United States). Digital images were processed and band density measurements were made with the aid of NIH Image J software (Schneider et al., 2012).

RESULTS

Preventive Treatment With *F. hepatica* EVs Ameliorates Clinical Symptoms and Attenuates Histological Alterations in DSS-Induced Acute Colitis

Previous evidence suggests that EVs from parasitic helminths could be potential new therapeutic alternatives against autoimmune diseases (Buck et al., 2014; Montaner et al., 2014). We therefore assessed their putative preventive effect in IBD. EVs were purified from *F. hepatica* parasites cultured as described previously (Marcilla et al., 2012), showing to be a clean and homogeneous preparation, with most vesicles ranging in the size of 50–100 nm (**Figure 1A**).

To test whether FhEVs could prevent colitis, C57BL/6 mice were injected subcutaneously with 10 μg of FhEVs/mouse/injection on days 0, 15, and 30 before colitis induction by DSS at day 42 (**Figure 1B**). We used these amounts of EVs based on previous studies (Trelis et al., 2016). FhEVs-treated mice were considerably less susceptible to DSS-induced colitis and lost around 10% of their initial body weight, whereas non-treated mice lost around 20% after 7 days of DSS treatment (data not shown). Accordingly, DAI of FhEVs-treated colitic mice was lower than in colitic mice on day 5 after the initiation of DSS treatment. Moreover, this difference gradually increased over time (**Figure 1C**). On autopsy, a significant colonic shortening was detected in the DSS-administered groups as compared to the water-administered ones injected or not with FhEVs. However, between DSS-treated mice, FhEVs injected mice had significant larger colons than their non-injected counterparts (**Figures 1D,E**).

FhEVs Attenuate Histological Alterations and Suppress Neutrophil Infiltration Upon DSS Challenge

Histologic analyses of colonic sections revealed complete disruption of the colonic architecture in colitic mice, whereas FhEVs-treated colitic mice display a better preservation of tissue architecture and reduced epithelial denudation, crypts distortion, and leukocyte infiltration of the lamina propria (**Figure 2A**), thus resulting in a lower histopathological mean score in this group (**Figure 2B**). Consistent with the histological findings, the ulceration score of FhEVs-treated colitic mice was significantly lower than in DSS-induced colitic mice (**Figure 2C**).

Furthermore, the reduction in neutrophil infiltration observed by histological inspection in FhEVs-treated colitic mice was confirmed by the reduced MPO activity detection in colon tissues from these mice (**Figure 2D**). Altogether, these results strongly support the view that injection of FhEVs could ameliorate DSS-induced murine experimental colitis.

FhEVs Decrease Pro-inflammatory Cytokines in Colon Tissues

To address the effect of FhEVs in colitis we next analyzed the immune response involved by determining the tissue levels of cytokines known to participate in IBD (Giner et al., 2016). Amounts of TNF-α, IL-6, IL-17A, and IL-10 were determined in intestine by ELISA. As shown in **Figures 3A,B**, treatment with FhEVs markedly prevented the increase in the levels of the pro-inflammatory cytokines TNF-α and IL-6 observed in the intestine of DSS-treated mice.

Recent studies have identified that the expression of genes involved in Th17 immune response can distinguish patients with ulcerative colitis from patients with Crohn disease (Rosen et al., 2017). To address whether Th17 response was also modified in the mice model of ulcerative colitis, IL-17A levels in intestine were determined by ELISA. As shown in **Figure 3C**, IL-17A levels were lower in FhEVs-treated colitic mice in comparison to DSS-induced colitic mice, indicating the anti-inflammatory effect of FhEVs. As a parameter of the anti-inflammatory activity of regulatory T lymphocytes (Treg), IL10 was also monitored. Interestingly, the amount of this cytokine did not change significantly in the groups of mice analyzed (**Figure 3D**). Taken together these results indicated that *F. hepatica* EVs exerted their preventive effect by altering the pro-inflammatory effect of DSS, not depending of a role of Treg cells.

FhEVs Decrease the Activation of the Pro-inflammatory Effector Molecules COX-2, NFkB, and Phosphorylated p38 MAPK in DSS-Induced Acute Colitis

It is well known that several key factors participate in the inflammatory cascade leading to colitis (Talero et al., 2008; Giner et al., 2011). In this context, different studies have documented the role of COX-2 in mediating the prolonged epithelial secretion, and the barrier dysfunction observed in colonic inflammation in mice (Zamuner et al., 2003; Sanchez-Fidalgo et al., 2013). To address whether *F. hepatica* EVs administration could also affect the expression of COX-2, as pro-inflammatory mediator in DSS-induced colitis, we next analyzed its levels in colon tissue by western blot. As shown in **Figure 4**, the DSS-induced colitic mice showed higher levels of COX-2 in colon tissues than their FhEVs-pretreated counterparts (only 33% of COX-2 was detected

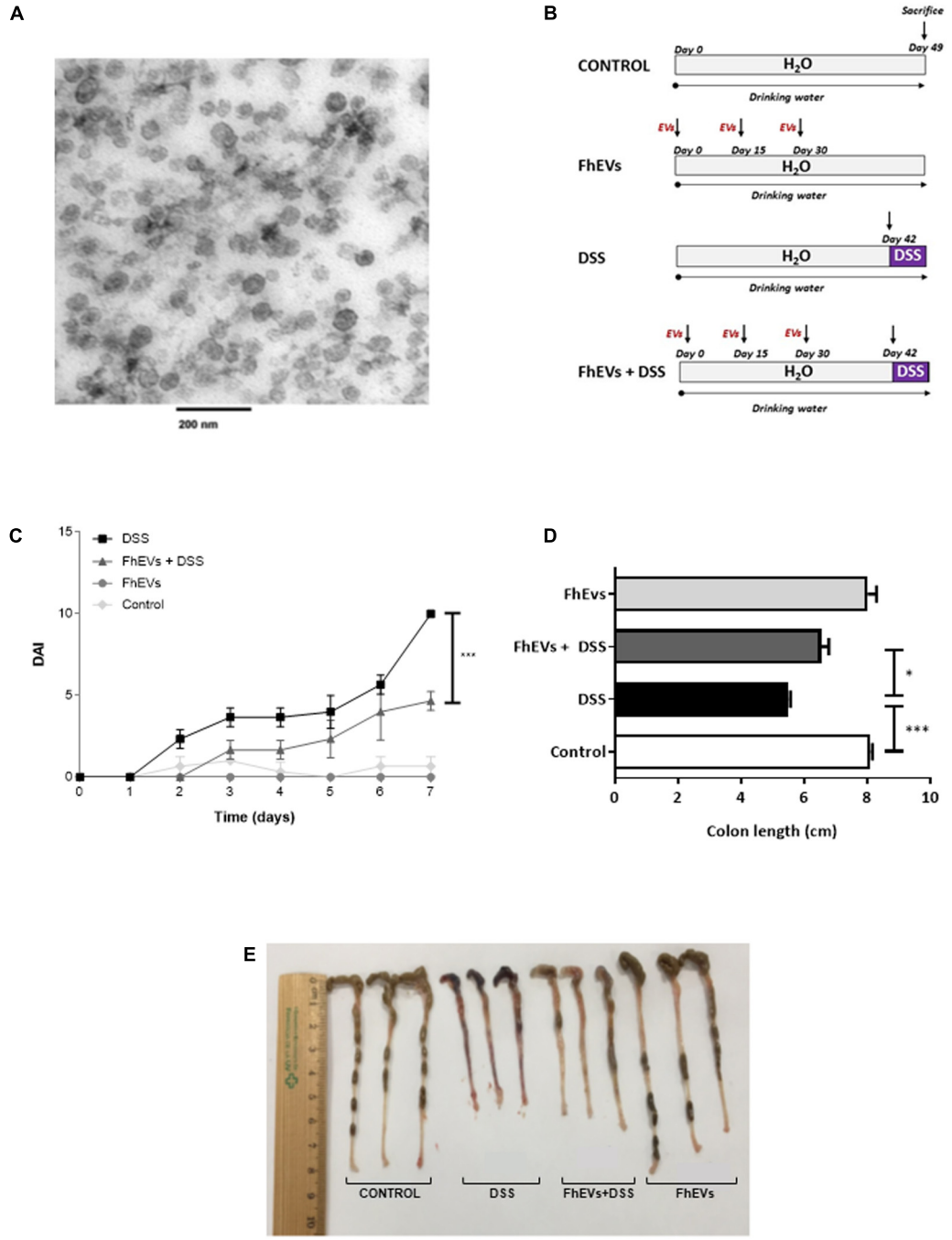

FIGURE 1 | Treatment with *Fasciola hepatica* EVs ameliorates clinical symptoms and partially avoids colon shortening in DSS-induced acute colitis. **(A)** Extracellular vesicles were obtained by differential ultracentrifugation and ultrastructure was confirmed by TEM. **(B)** Schematic time schedule of immunization with *F. hepatica* EVs (FhEVs) and DSS-induction of colitis in C57B/L6 mice. **(C)** Disease activity index (DAI) was evaluated daily using the parameters of weight loss, diarrhea, and bleeding as described in methods. Statistical significance between two experimental groups was assessed using the Independent-Sample *t*-test (***$p < 0.001$, significantly different between the control and DSS group; *$p < 0.05$ significantly different between the immunized group and the DSS group; using one-way ANOVA followed by Dunnett's *t*-test). **(D,E)** Colon length was measured as an indirect marker of inflammation.

as compared to the levels observed in DSS-induced colitic mice, **Figure 4B**).

Furthermore, colonic cells showed variations in different signaling pathways as in the mitogen-activated protein kinase (p38 MAPK), and NF-kB pathways. As shown in **Figure 4**, DSS increased the phosphorylation of p38 MAPK, but pre-treatment of colitic mice with FhEVs produced lower levels of phosphorylation of p38 MAPK (around 39%),

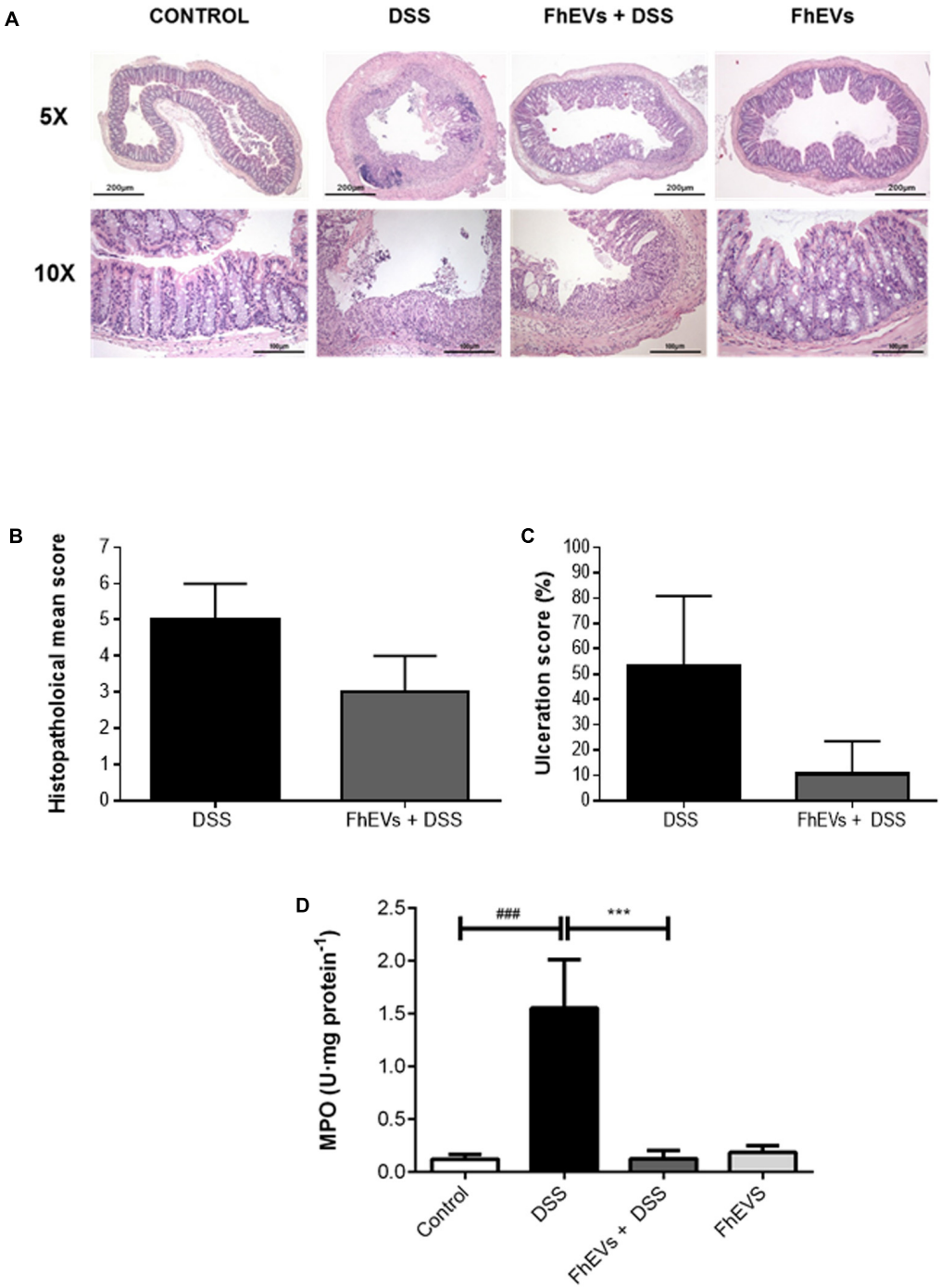

FIGURE 2 | Histopathological changes in the colons of acute colitis mice. **(A)** Distal colon tissue samples were examined using haematoxylin-eosin staining (5× and 10×). **(B)** Histopathological score of colon tissue samples as a mean histopathology score in DSS and FhEVs+DSS mice. **(C)** Percentage of ulcerated colonic mucosa in DSS and FhEVs+DSS mice. **(D)** Myeloperoxidase (MPO) activity was determined by a spectrophotometric method and expressed as the amount of enzyme necessary to produce a change in absorbance of 1.0 unit/mg of tissue. Each bar chart represents the mean ± SEM for at least three independent experiments (n = 3 animals) ($^{###}p < 0.001$, significantly different from the DSS group vs. control group; $^{***}p < 0.001$ significantly different between the DSS group and the group immunized with FhEVs; using one-way ANOVA followed by Dunnett's t-test).

although still higher than in colon from control and FhEVs-injected mice groups (both without DSS administration) (**Figure 4B**).

The levels of NF-kB in the nuclear fraction of colon cells were also quantified, and colon tissues from both DSS-induced colitis mice contained higher levels of this nuclear factor than controls.

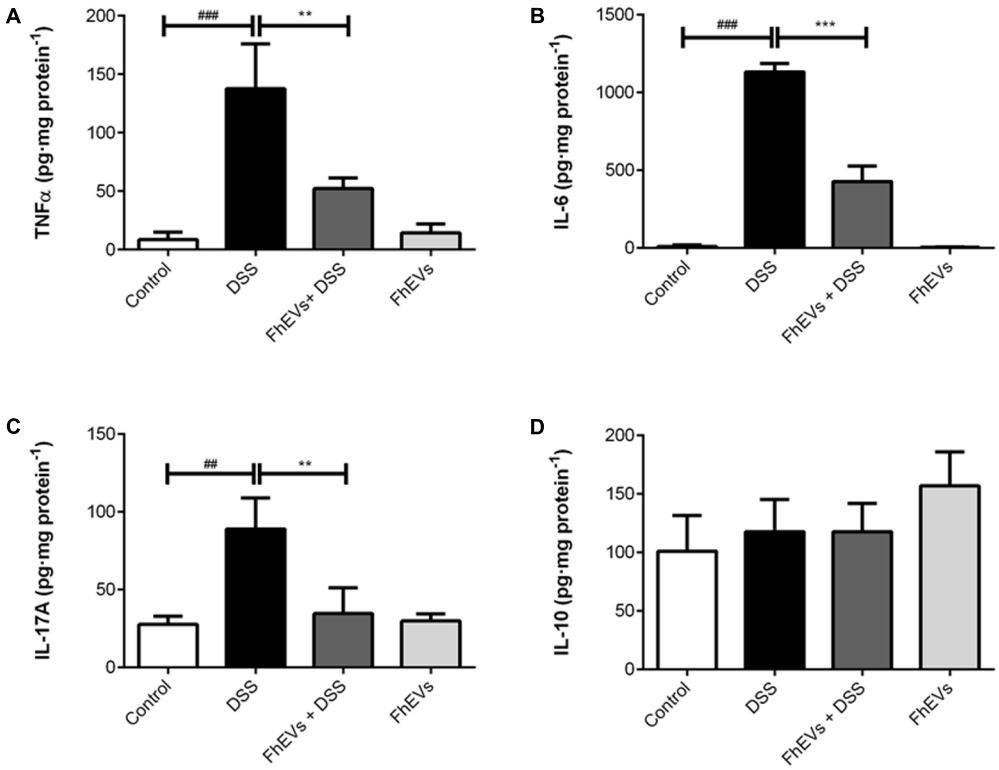

FIGURE 3 | Effect of FhEVs on the profile of cytokine levels in colon tissue samples. At day 49 cytokine levels in colon homogenates were determined by ELISA. The amount of cytokines was expressed as pg per mg of protein. **(A)** TNFα levels, **(B)** IL-6 levels, **(C)** IL-17A levels, **(D)** IL-10 levels. Each bar chart represents the mean ± SEM for at least three independent experiments (n = 3 animals). $^{###}p < 0.001$ significantly different from the DSS and control for TNFα and IL6; $^{##}p < 0.01$ significantly different from the DSS and control for IL17A; $^{***}p < 0.001$ significantly different from the DSS and immunized group for IL6; $^{**}p < 0.01$ significantly different from the DSS and immunized group for TNFα and IL6, using one-way ANOVA followed by Dunnett's t-test.

Nevertheless, FhEVs treated colitic mice contained around 25% less amount of NF-kB when comparing to DSS-induced colitic mice (**Figures 4A,B**).

Altogether, our results indicate that *F. hepatica* EVs interfere with signaling pathways involved in acute ulcerative colitis promoted by DSS, and suggest their role in preventing pro-inflammatory cascades in which these key molecules participate.

The Preventive Effect of FhEVs in Colitis Is Not Mediated by Lymphocytes

To assess whether lymphocytes were the cells accounting for the protection, similar *in vivo* experiments of immunization with FhEVs before DSS administration were carried out in Rag1$^{-/-}$ mice. These mice lack lymphoid B and T cells (Mombaerts et al., 1992), and are susceptible to DSS-induced colitis (Kim et al., 2006; Kiesler et al., 2015). Rag1$^{-/-}$ mice were injected with FhEVs subcutaneously. Interestingly, FhEVs exhibited protection against the chemical treatment (**Figure 5**), similarly to what happened in C57BL/6 mice (see **Figures 1**, **2**).

Fasciola hepatica EVs-treated mice lost around 9% of their initial body weight, whereas non-treated mice lost around 18%, after 7 days of DSS treatment (data not shown). Accordingly, the DAI of FhEVs-treated colitic mice was lower than in colitic mice on day 4 after the initiation of DSS treatment, increasing this difference over time (**Figure 5A**). DSS-administered mice treated with FhEVs had significant larger colons than their non-injected counterparts, although not reaching the length observed in control animals (**Figure 5B**).

When histological analyses of colonic sections were performed, they revealed large disruption areas of the colonic architecture in colitic mice, whereas FhEVs-treated colitic mice displayed preservation of tissue architecture and reduced epithelial denudation and crypts distortion (**Figure 5C**). Altogether, these results supported the notion that neither T nor B cells are involved in the preventive effect observed with the parasite EVs.

DISCUSSION

Intestinal bowel disease is one of the most important diseases affecting developing countries, and it is currently spreading in undeveloped ones (Molodecky et al., 2012; Ng et al., 2013). The etiology of the disease is not well understood, with a complex pathology which has no effective treatment available. In fact, the development of effective treatments require studies using multidisciplinary approaches, where animal models have proven

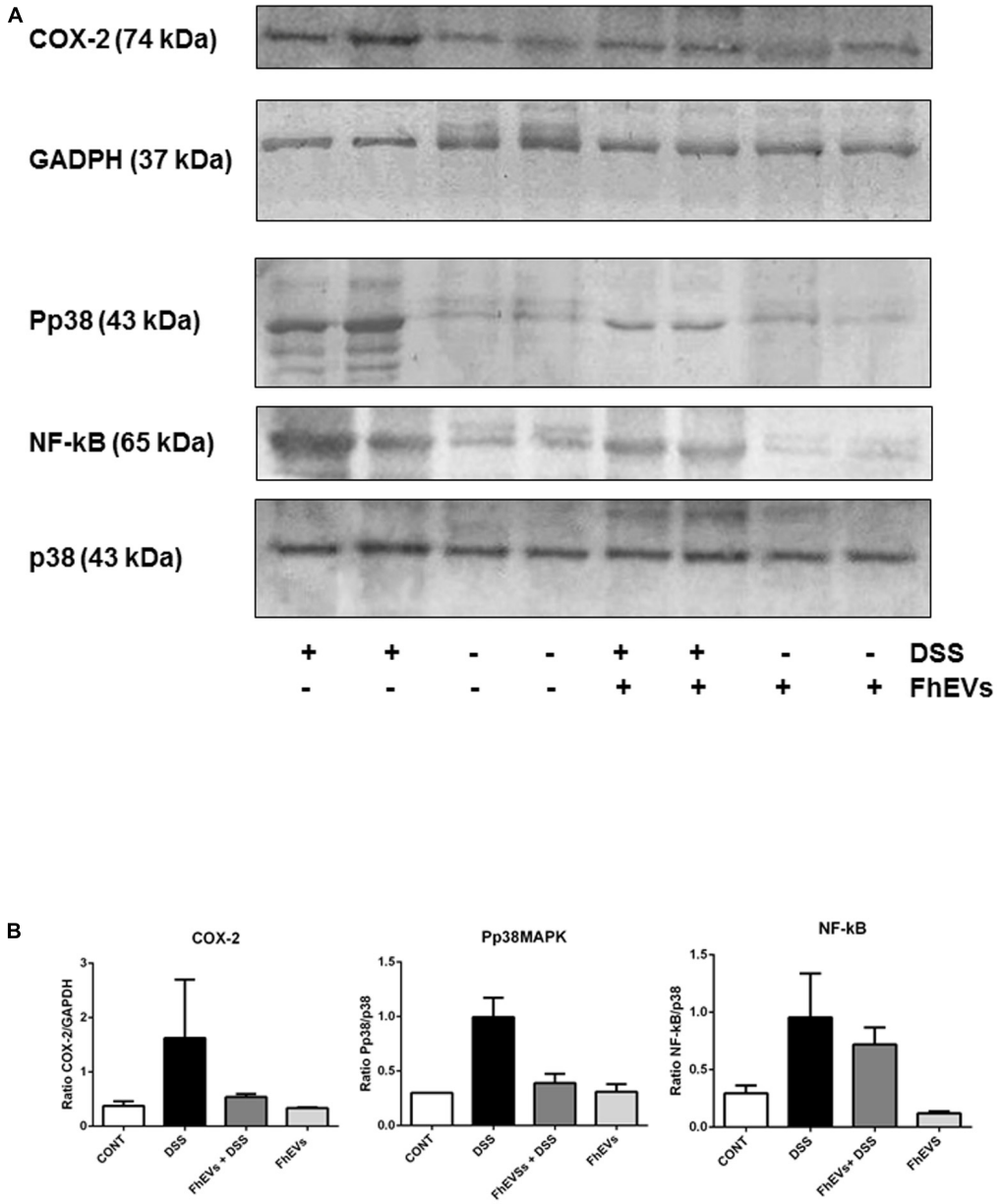

FIGURE 4 | Effects of FhEVs on COX-2 and NF-kB expression, and phosphorylation of p38MAPK (pp38) in DSS-induced acute colitis in mice. At day 49 colon tissues were powdered in a mortar with liquid nitrogen, and tissue proteins were extracted. **(A)** Representative western blot analyses are shown (from three different experiments, $n = 3$). The amount of COX-2 was determined by densitometry analysis, and normalized to GAPDH content for each sample. The amount of phosphorylated p38MAPK (pp38MAPK) and p65 NF-kappaB were determined by densitometry analysis, and normalized to p38MAPK content. Quantification measures were done using NIH ImageJ software (Schneider et al., 2012), considering the amount of protein in DSS group as 100%. **(B)** The histograms representing the data derived from representative western blots following densitometry analysis of each group are also shown.

highly useful (Lin and Hackam, 2011). DSS-induced colitis model has been widely used to explore new therapeutic options (Wirtz and Neurath, 2007; Kiesler et al., 2015).

Among the new treatments, the use of biologicals is gaining attention (Rogler, 2015; Maizels, 2016). In this context, and following the Hygiene hypothesis (Strachan, 1989), clinical trials with parasitic helminths have been initiated, and some are underway (Smallwood et al., 2017). Some concerns about using helminths to treat IBD have arisen, with the possibility of producing malignancy (Bonovas et al., 2016). In fact, a recent report has shown that the treatment with the parasitic nematode *Heligmosomoides polygyrus* can induce tumor progression in a DSS-induced colitis in Balb/c mice (Pastille et al., 2017).

Along with those potential clinical problems, the use of parasites to treat IBD also face ethical problems (McSorley and Maizels, 2012), so the alternative of using parasite defined

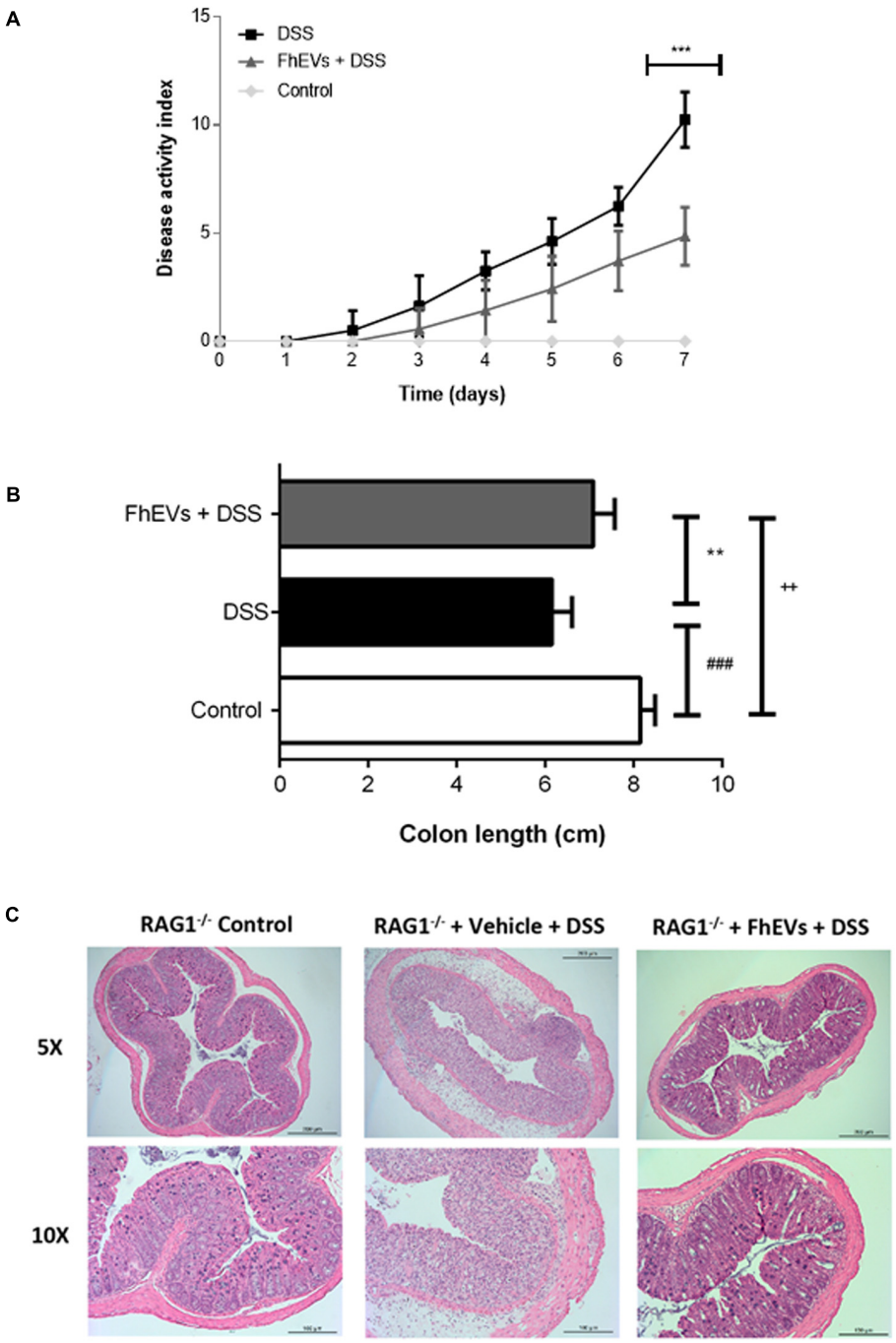

FIGURE 5 | Lymphocytes do not mediate the preventive effect of FhEVs in DSS-induced colitis. **(A)** Disease activity index (DAI) evaluated daily combining the parameters of weight loss, diarrhea, and bleeding in Rag1$^{-/-}$ mice (n = 7 animals) as described in methods. Statistical analyses were performed using a one-way ANOVA followed by Dunnett's multiple comparison *post hoc* test (***$p < 0.001$, FhEVs+DSS versus DSS). **(B)** Colon length was measured as an indirect marker of inflammation. Statistical significance between two experimental groups was assessed using the Independent-Sample t-test ($^{###}p < 0.001$, significantly different between the control and DSS group; **$p < 0.01$ significantly different between the immunized group and the control; $^{++}p < 0.01$ significantly different between the immunized group and the DSS group; using one-way ANOVA followed by Dunnett's t-test). **(C)** The histopathological changes of colons in mice were examined using H&E staining (5× and 10×).

products, like excretory/secretory products (ESP), or isolated molecules seem to be a good option. In this context, studies with a crude extract from the laminated layer of *Echinococcus granulosus* (a tapeworm parasite) showed not only its preventive effect but also played a beneficial role in maintaining the integrity of the intestinal mucosal barrier against DSS-induced injury

(Soufli et al., 2015). Those results supported the role of EVs as promoters of the epithelial barrier function (Xu et al., 2016).

Previous studies had shown that EVs administered either orally or injected could reach the colon of mice and exert their therapeutic effect on induced colitis (Ju et al., 2013; Yang et al., 2015). Very recently, Wang et al. (2017) have reported a protective effect in a similar mice model when using EVs produced by dendritic cells previously exposed to eggs from the parasitic trematode *Schistosoma japonicum* (Wang et al., 2017). In this regard, our data highlight that the parasite *F. hepatica* EVs have a potent modulatory effect on the immune response in DSS-induced colitis in mice. We provide evidence that *F. hepatica* EVs can prevent DSS-induced colitis by down regulating pro-inflammatory cytokines like TNFα, IL-6, and IL17A, as well as suppressing MAPK/NF-κB signaling pathways. Accordingly, FhEVs treatment decreased MPO activity, indicating a reduction in neutrophil infiltration in damaged colon and which has also been corroborated in the histological sections. In accordance, reduce levels of cytokines TNF-α and IL-17A have been detected in the colon of FhEVs-treated mice, which are inducers of neutrophil transmigration (Kolls and Lindén, 2004; Griffin et al., 2012). DSS colitis can be exacerbated by granulocyte recruitment (Natsui et al., 1997; Williams and Parkos, 2007; Sander et al., 2008; Chami et al., 2014; Kishida et al., 2015). The activity of many enzymes and chemicals produced by neutrophils is not specific to pathogens, so they can damage host tissues when released extracellularly, contributing to the aggravation of mucosal inflammation. Likewise, in UC, unrestricted neutrophil activation may cause significant tissue damage that further leads to chronic pathology and the extent of neutrophil infiltration correlates with the severity of the disease (Bressenot et al., 2015). Therefore, the reduced neutrophil infiltration in FhEVs-treated mice, would provide for the protection effect detected in this model of acute colitis induced by DSS, and may be crucial for the treatment of UC patients. In $Rag1^{-/-}$ mice, a decreased neutrophil infiltration is also observed in the histology sections after FhEVs treatment, in accordance with the results obtained in C57B/L6 mice. It is important to remark that though $Rag1^{-/-}$ mice have no mature T and B lymphocytes (Mombaerts et al., 1992), develop totally normal granulocytes, like WT mice, as has been demonstrated in reports which use these mice in infection models (Smith et al., 2009; Seymour et al., 2015; Carey et al., 2016; Papp et al., 2016).

Furthermore, our results suggest that neither lymphocytes nor IL-10 are involved in the protective effect by FhEVs in DSS-induced colitis mice model. This seems to be at odds with previous reports showing that either splenic B cells or EVs from granulocytic myeloid-derived suppressor cells, attenuate DSS-induced colitis by promoting Tregs expansion, and inhibit Th1 cells proliferation (Reyes et al., 2015; Wang et al., 2016).

The accurate identification of the molecules responsible for the anti-inflammatory effect is underway, but suitable candidates are molecules previously identified in FhEVs, like FABPs (Cwiklinski et al., 2015), which have been shown to induce anti-inflammatory response in animal models by diminishing the levels of TNFα (Ramos-Benitez et al., 2017). Other exosome-contained molecules like miRNAs represent potential candidates as they may act as immunomodulators of the intestinal innate immune response (Buck et al., 2014). Interestingly, a repertoire of miRNAs with immune-regulatory function have been found in *F. hepatica* EVs previously by our group (Fromm et al., 2015).

Resident intestinal macrophages and colonic dendritic cells have been reported to have a high anti-inflammatory phenotype and are hypo-responsive to microbial stimuli in rodents and humans (Bilsborough and Viney, 2004; Kelsall and Leon, 2005; Smith et al., 2005). In line with this, it has been described that depletion of both dendritic cells and macrophages from the intestinal lamina propria in C57BL/6, BALB/c, and SCID mice (without T and B cells) increased DSS colitis severity. These mice had increased neutrophilic inflammation, epithelial injury, and enhanced mucin depletion from globet cells (Qualls et al., 2006). On the other hand, helminth infections are associated with the induction of immunosuppressive M2/Alternatively Activated Macrophages (AAMs) (Loke et al., 2000; Herbert et al., 2004). It is therefore conceivable that FhEVs are enhancing the anti-inflammatory functions of these innate cell populations as they are protective in $Rag1^{-/-}$ mice that lack T and B cells populations. Other helminth infections have been shown to prevent colitis development independently of Tregs stimulation, through the inhibition of prostaglandins by AAMs (Ledesma-Soto et al., 2015) or recruitment of a novel macrophage population distinct to AAMs or $Gr1^{+}$ macrophages (Smith et al., 2007). Moreover, in addition to their immunosuppressive role, lamina propria macrophages play an important role in the regeneration of damaged epithelium by controlling the epithelial progenitor niche after DSS-induced colitis (Pull et al., 2005). On the other hand, the reduced neutrophil infiltration detected in FhEVs-treated mice might be a consequence of the decreased epithelial barrier damage and diminished production of pro-inflammatory cytokines from the resident myeloid cell populations in the gut as observed in the foregoing reports, because of the preventive role of these exosomes. Moreover, some reports described that subcutaneously injected exosomes can be detected in several organs including the gastrointestinal tract even after 24 h of administration, and cleared from the bloodstream in a few minutes (Wiklander et al., 2015). However, in our experimental settings the exosomes are administered 12 days before DSS administration, which makes us to think that they are exerting their role in the gut resident populations. A plausible mechanism may be epigenetic reprogramming of these innate cell populations, a process that has been recently termed as trained immunity (Netea et al., 2016), or even of the intestinal epithelial cells. Whether, in addition, FhEVs could be exerting their function by altering granulopoiesis at the bone marrow level, or influencing in endothelial cells the level of expression of adhesion molecules, requires further experimentation and biodistribution analyses.

Apart from the induction of strong Th2 responses and IgE production, which can be discarded in our experimental setting due to the maintenance of the protective effect in $Rag1^{-/-}$ mice that lack mature T and B lymphocytes, helminths also promote the expansion of eosinophils, mast cells and basophils which could not be discarded. Levels of these cell populations can be measured by flow cytometry to evaluate if

there were differences among FhEVs-treated versus non-treated mice. Interestingly, among these cell populations, the only one which have been described to promote a protective role in acute DSS colitis are the eosinophils, due to the production of anti-inflammatory lipid mediators (Masterson et al., 2015). To further elucidate which innate cell population is mediating the protection, adoptive transfer experiments could be performed by injecting specific sorted cell populations derived from FhEVs-immunized Rag1$^{-/-}$ mice into non-immunize ones. Our most likely candidates are macrophages, as stated in the foregoing works. Besides, macrophages are highly phagocytic cells that could be acquiring a highest number of exosomes. Moreover, the role of dendritic cells is typically focused on T cell polarization, which are not involved. Specific deletion of macrophages can be performed by the use of liposomal clodronate agent. If they turn to be involved in the conferred protection to DSS-colitis, it would be very informative to evaluate the role of FhEVs in M1 and M2 polarization, which could be performed by flow cytometry or RNA-seq.

Our findings suggest that other immune cells aside lymphocytes are involved in the protective response (Masterson et al., 2015; Coakley et al., 2017; Wang et al., 2017; Campbell et al., 2018). Future studies will address the identification of the immune cells involved in the FhEVs protective effect and the mechanisms behind it. The fact that the conferred protection against intestinal inflammation is mediated by EVs is of great importance to move this research forward into translational applications.

AUTHOR CONTRIBUTIONS

AM, MT, DB, MR, RG, and FS-M: participated in the study concept and design. JR, AG, MS, FC, CM, DB, and MT: acquisition of data. JR, AG, MS, EG, CM, MR, RG, DB, FS-M, and AM analyzed and interpreted data. MR, RG, DB, FS-M, and AM drafted and critically revised the manuscript.

FUNDING

This work was supported by the Conselleria d' Educació, Investigació, Cultura i Esport, Generalitat Valenciana, Valencia, Spain (PROMETEO/2016/156 to AM), Fundación Ramón Areces and REDIEX to AM and FS-M. The Spanish Ministry of Economy and Competitiveness (SAF2014-55579-R to FS-M), Comunidad de Madrid, Spain (INDISNET-S2011/BMD-2332 to FS-M), and the European Research Council (ERC-2011-AdG 294340-GENTRIS to FS-M). JR was supported by a Generalitat Valenciana (Valencia, Spain) predoctoral fellowship. MS was supported by FPI Programme (Spanish Ministry of Economy).

ACKNOWLEDGMENTS

The Serveis of Microscopia and Producción Animal, Servei Central de Suport a l'Investigació Experimental (SCSIE), Universitat de València are acknowledged.

REFERENCES

Barile, L., and Vassalli, G. (2017). Exosomes: therapy delivery tools and biomarkers of diseases. *Pharmacol. Ther.* 174, 63–78. doi: 10.1016/j.pharmthera.2017.02.020

Bilsborough, J., and Viney, J. L. (2004). Gastrointestinal dendritic cells play a role in immunity, tolerance, and disease. *Gastroenterology* 127, 300–309. doi: 10.1053/j.gastro.2004.01.028

Bonovas, S., Fiorino, G., Allocca, M., Lytras, T., Nikolopoulos, G. K., Peyrin-Biroulet, L., et al. (2016). Biologic therapies and risk of infection and malignancy in patients with inflammatory bowel disease: a systematic review and network meta-analysis. *Clin. Gastroenterol. Hepatol.* 14, 1385.e10–1397.e10. doi: 10.1016/j.cgh.2016.04.039

Bressenot, A., Salleron, J., Bastien, C., Danese, S., Boulagnon-Rombi, C., and Peyrin-Biroulet, L. (2015). Comparing histological activity indexes in UC. *Gut* 64, 1412–1418. doi: 10.1136/gutjnl-2014-307477

Buck, A. H., Coakley, G., Simbari, F., McSorley, H. J., Quintana, J. F., Le Bihan, T., et al. (2014). Exosomes secreted by nematode parasites transfer small RNAs to mammalian cells and modulate innate immunity. *Nat. Commun.* 5:5488. doi: 10.1038/ncomms6488

Campbell, S. M., Knipper, J. A., Ruckerl, D., Finlay, C. M., Logan, N., Minutti, C. M., et al. (2018). Myeloid cell recruitment versus local proliferation differentiates susceptibility from resistance to filarial infection. *eLife* 7:e30947. doi: 10.7554/eLife.30947

Carey, A. J., Weinberg, J. B., Dawid, S. R., Venturini, C., Lam, A. K., Nizet, V., et al. (2016). Interleukin-17A contributes to the control of *Streptococcus pyogenes* colonization and inflammation of the female genital tract. *Sci. Rep.* 6:26836. doi: 10.1038/srep26836

Chami, B., Yeung, A. W., van Vreden, C., King, N. J., and Bao, S. (2014). The role of CXCR3 in DSS-induced colitis. *PLOS One* 9:e101622. doi: 10.1371/journal.pone.0101622

Coakley, G., McCaskill, J. L., Borger, J. G., Simbari, F., Robertson, E., Millar, M., et al. (2017). Extracellular vesicles from a helminth parasite suppress macrophage activation and constitute an effective vaccine for protective immunity. *Cell Rep.* 19, 1545–1557. doi: 10.1016/j.celrep.2017.05.001

Cwiklinski, K., de la Torre-Escudero, E., Trelis, M., Bernal, D., Dufresne, P. J., Brennan, G. P., et al. (2015). The extracellular vesicles of the helminth pathogen, *Fasciola hepatica*: biogenesis pathways and cargo molecules involved in parasite pathogenesis. *Mol. Cell. Proteomics* 14, 3258–3273. doi: 10.1074/mcp.M115.053934

Dalton, J. P., Robinson, M. W., Mulcahy, G., O'Neill, S. M., and Donnelly, S. (2013). Immunomodulatory molecules of Fasciola hepatica: candidates for both vaccine and immunotherapeutic development. *Vet. Parasitol.* 195, 272–285. doi: 10.1016/j.vetpar.2013.04.008

Fromm, B., Trelis, M., Hackenberg, M., Cantalapiedra, F., Bernal, D., and Marcilla, A. (2015). The revised microRNA complement of Fasciola hepatica reveals a plethora of overlooked microRNAs and evidence for enrichment of immuno-regulatory microRNAs in extracellular vesicles. *Int. J. Parasitol.* 45, 697–702. doi: 10.1016/j.ijpara.2015.06.002

Giner, E., Andujar, I., Recio, M. C., Rios, J. L., Cerda-Nicolas, J. M., and Giner, R. M. (2011). Oleuropein ameliorates acute colitis in mice. *J. Agric. Food Chem.* 59, 12882–12892. doi: 10.1021/jf203715m

Giner, E., Recio, M. C., Rios, J. L., Cerda-Nicolas, J. M., and Giner, R. M. (2016). Chemopreventive effect of oleuropein in colitis-associated colorectal cancer in C57BL/6 mice. *Mol. Nutr. Food Res.* 60, 242–255. doi: 10.1002/mnfr.201500605

Giner, E., Recio, M. C., Rios, J. L., and Giner, R. M. (2013). Oleuropein protects against dextran sodium sulfate-induced chronic colitis in mice. *J. Nat. Prod.* 76, 1113–1120. doi: 10.1021/np400175b

Griffin, G. K., Newton, G., Tarrio, M. L., Bu, D. X., Maganto-Garcia, E., Azcutia, V., et al. (2012). IL-17 and TNF-α sustain neutrophil recruitment during inflammation through synergistic effects on endothelial activation. *J. Immunol.* 188, 6287–6299. doi: 10.4049/jimmunol.1200385

Herbert, D. R., Hölscher, C., Mohrs, M., Arendse, B., Schwegmann, A., Radwanska, M., et al. (2004). Alternative macrophage activation is essential for survival during schistosomiasis and down modulates T helper 1 responses and immunopathology. *Immunity* 20, 623–635. doi: 10.1016/S1074-7613(04)00107-4

Ju, S., Mu, J., Dokland, T., Zhuang, X., Wang, Q., Jiang, H., et al. (2013). Grape exosome-like nanoparticles induce intestinal stem cells and protect mice from DSS-induced colitis. *Mol. Ther.* 21, 1345–1357. doi: 10.1038/mt.2013.64

Kaplan, G. G. (2015). The global burden of IBD: from 2015 to 2025. *Nat. Rev. Gastroenterol. Hepatol.* 12, 720–727. doi: 10.1038/nrgastro.2015.150

Kaplan, G. G., and Ng, S. C. (2017). Understanding and preventing the global increase of inflammatory bowel disease. *Gastroenterology* 152, 313.e2–321.e2. doi: 10.1053/j.gastro.2016.10.020

Kelsall, B. L., and Leon, F. (2005). Involvement of intestinal dendritic cells in oral tolerance, immunity to pathogens, and inflammatory bowel disease. *Immunol. Rev.* 206, 132–148. doi: 10.1111/j.0105-2896.2005.00292.x

Kiesler, P., Fuss, I. J., and Strober, W. (2015). Experimental models of inflammatory bowel diseases. *Cell. Mol. Gastroenterol. Hepatol.* 1, 154–170. doi: 10.1016/j.jcmgh.2015.01.006

Kim, T. W., Seo, J. N., Suh, Y. H., Park, H. J., Kim, J. H., Kim, J. Y., et al. (2006). Involvement of lymphocytes in dextran sulfate sodium-induced experimental colitis. *World J. Gastroenterol.* 12, 302–305. doi: 10.3748/wjg.v12.i2.302

Kishida, K., Kohyama, M., Kurashima, Y., Kogure, Y., Wang, J., Hirayasu, K., et al. (2015). Negative regulation of DSS-induced experimental colitis by PILRα. *Int. Immunol.* 27, 307–314. doi: 10.1093/intimm/dxv004

Kolls, J. K., and Lindén, A. (2004). Interleukin-17 family members and inflammation. *Immunity* 21, 467–476. doi: 10.1016/j.immuni.2004.08.018

Ledesma-Soto, Y., Callejas, B. E., Terrazas, C. A., Reyes, J. L., Espinoza-Jiménez, A., González, M. I., et al. (2015). Extraintestinal helminth infection limits pathology and proinflammatory cytokine expression during DSS-induced ulcerative colitis: a role for alternatively activated macrophages and prostaglandins. *Biomed. Res. Int.* 2015:563425. doi: 10.1155/2015/563425

Lin, J., and Hackam, D. J. (2011). Worms, flies and four-legged friends: the applicability of biological models to the understanding of intestinal inflammatory diseases. *Dis. Mod. Mech.* 4, 447–456. doi: 10.1242/dmm.007252

Loke, P., MacDonald, A. S., Robb, A., Maizels, R. M., and Allen, J. E. (2000). Alternatively activated macrophages induced by nematode infection inhibit proliferation via cell-to-cell contact. *Eur. J. Immunol.* 30, 2669–2678.

Maizels, R. M. (2016). Parasitic helminth infections and the control of human allergic and autoimmune disorders. *Clin. Microbiol. Infect.* 22, 481–486. doi: 10.1016/j.cmi.2016.04.024

Marcilla, A., Rivero-Lezcano, O. M., Agarwal, A., and Robbins, K. C. (1995). Identification of the major tyrosine kinase substrate in signaling complexes formed after engagement of Fc gamma receptors. *J. Biol. Chem.* 270, 9115–9120. doi: 10.1074/jbc.270.16.9115

Marcilla, A., Trelis, M., Cortes, A., Sotillo, J., Cantalapiedra, F., Minguez, M. T., et al. (2012). Extracellular vesicles from parasitic helminths contain specific excretory/secretory proteins and are internalized in intestinal host cells. *PLoS One* 7:e45974. doi: 10.1371/journal.pone.0045974

Masterson, J. C., McNamee, E. N., Fillon, S. A., Hosford, L., Harris, R., Fernando, S. D., et al. (2015). Eosinophil-mediated signalling attenuates inflammatory responses in experimental colitis. *Gut* 64, 1236–1247. doi: 10.1136/gutjnl-2014-306998

McSorley, H. J., and Maizels, R. M. (2012). Helminth infections and host immune regulation. *Clin. Microbiol. Rev.* 25, 585–608. doi: 10.1128/CMR.05040-11

Melgar, S., Karlsson, L., Rehnström, E., Karlsson, A., Utkovic, H., Jansson, L., et al. (2008). Validation of murine dextran sulfate sodium-induced colitis using four therapeutic agents for human inflammatory bowel disease. *Int. Immunopharmacol.* 8, 836–844. doi: 10.1016/j.intimp.2008.01.036

Molodecky, N. A., Soon, I. S., Rabi, D. M., Ghali, W. A., Ferris, M., Chernoff, G., et al. (2012). Increasing incidence and prevalence of the inflammatory bowel diseases with time, based on systematic review. *Gastroenterology* 142, 46.e42–54.e42. doi: 10.1053/j.gastro.2011.10.001

Mombaerts, P., Iacomini, J., Johnson, R. S., Herrup, K., Tonegawa, S., and Papaioannou, V. E. (1992). RAG-1-deficient mice have no mature B and T lymphocytes. *Cell* 68, 869–877. doi: 10.1016/0092-8674(92)90030-G

Montaner, S., Galiano, A., Trelis, M., Martin-Jaular, L., Del Portillo, H. A., Bernal, D., et al. (2014). The role of extracellular vesicles in modulating the host immune response during parasitic infections. *Front. Immunol.* 5:433. doi: 10.3389/fimmu.2014.00433

Natsui, M., Kawasaki, K., Takizawa, H., Hayashi, S. I., Matsuda, Y., Sugimura, K., et al. (1997). Selective depletion of neutrophils by a monoclonal antibody, RP-3, suppresses dextran sulfate sodium-induced colitis in rats. *J. Gastroenterol. Hepatol.* 12, 801–808.

Netea, M. G., Joosten, L. A., Latz, E., Mills, K. H., Natoli, G., Stunnenberg, H. G., et al. (2016). Trained immunity: a program of innate immune memory in health and disease. *Science* 352:aaf1098. doi: 10.1126/science.aaf1098

Ng, S. C., Bernstein, C. N., Vatn, M. H., Lakatos, P. L., Loftus, E. V. Jr., Tysk, C., et al. (2013). Geographical variability and environmental risk factors in inflammatory bowel disease. *Gut* 62, 630–649. doi: 10.1136/gutjnl-2012-303661

Papp, S., Moderzynski, K., Rauch, J., Heine, L., Kuehl, S., Richardt, U., et al. (2016). Liver necrosis and lethal systemic inflammation in a murine model of *Rickettsia typhi* infection: role of neutrophils, macrophages and NK cells. *PLoS Neglect. Trop. Dis.* 10:e0004935. doi: 10.1371/journal.pntd.0004935

Pastille, E., Frede, A., McSorley, H. J., Grab, J., Adamczyk, A., Kollenda, S., et al. (2017). Intestinal helminth infection drives carcinogenesis in colitis-associated colon cancer. *PLoS Pathog.* 13:e1006649. doi: 10.1371/journal.ppat.1006649

Pull, S. L., Doherty, J. M., Mills, J. C., Gordon, J. I., and Stappenbeck, T. S. (2005). Activated macrophages are an adaptive element of the colonic epithelial progenitor niche necessary for regenerative responses to injury. *Proc. Natl. Acad. Sci. U.S.A.* 102, 99–104. doi: 10.1073/pnas.0405979102

Qualls, J. E., Kaplan, A. M., van Rooijen, N., and Cohen, D. A. (2006). Suppression of experimental colitis by intestinal mononuclear phagocytes. *J. Leukoc. Biol.* 80, 802–815. doi: 10.1189/jlb.1205734

Ramanan, D., Bowcutt, R., Lee, S. C., Tang, M. S., Kurtz, Z. D., Ding, Y., et al. (2016). Helminth infection promotes colonization resistance via type 2 immunity. *Science* 352, 608–612. doi: 10.1126/science.aaf3229

Ramos-Benitez, M. J., Ruiz-Jimenez, C., Aguayo, V., and Espino, A. M. (2017). Recombinant Fasciola hepatica fatty acid binding protein suppresses toll-like receptor stimulation in response to multiple bacterial ligands. *Sci. Rep.* 7:5455. doi: 10.1038/s41598-017-05735-w

Recio, M. C., Giner, R. M., Uriburu, L., Manez, S., Cerda, M., De la Fuente, J. R., et al. (2000). In vivo activity of pseudoguaianolide sesquiterpene lactones in acute and chronic inflammation. *Life Sci.* 66, 2509–2518. doi: 10.1016/S0024-3205(00)00585-3

Reyes, J. L., Wang, A., Fernando, M. R., Graepel, R., Leung, G., van Rooijen, N., et al. (2015). Splenic B cells from *Hymenolepis diminuta*-infected mice ameliorate colitis independent of T cells and via cooperation with macrophages. *J. Immunol.* 194, 364–378. doi: 10.4049/jimmunol.1400738

Rogler, G. (2015). Where are we heading to in pharmacological IBD therapy? *Pharmacol. Res.* 100, 220–227. doi: 10.1016/j.phrs.2015.07.005

Rosen, M. J., Karns, R., Vallance, J. E., Bezold, R., Waddell, A., Collins, M. H., et al. (2017). Mucosal expression of type 2 and type 17 immune response genes distinguishes ulcerative colitis from colon-only Crohn's disease in treatment-naive pediatric patients. *Gastroenterology* 152, 1335.e7–1357.e7. doi: 10.1053/j.gastro.2017.01.016

Sanchez-Fidalgo, S., Cardeno, A., Sanchez-Hidalgo, M., Aparicio-Soto, M., and de la Lastra, C. A. (2013). Dietary extra virgin olive oil polyphenols supplementation modulates DSS-induced chronic colitis in mice. *J. Nutr. Biochem.* 24, 1401–1413. doi: 10.1016/j.jnutbio.2012.11.008

Sander, L. E., Obermeier, F., Dierssen, U., Kroy, D. C., Singh, A. K., Seidler, U., et al. (2008). Gp130 signaling promotes development of acute experimental colitis by facilitating early neutrophil/macrophage recruitment and activation. *J. Immunol.* 181, 3586–3594. doi: 10.4049/jimmunol.181.5.3586

Schneider, C. A., Rasband, W. S., and Eliceiri, K. W. (2012). NIH image to ImageJ: 25 years of image analysis. *Nat. Methods* 9, 671–675. doi: 10.1038/nmeth.2089

Seymour, R. L., Adams, A. P., Leal, G., Alcorn, M. D., and Weaver, S. C. (2015). A rodent model of chikungunya virus infection in RAG1 -/- mice, with features of persistence, for vaccine safety evaluation. *PLoS Neglect. Trop. Dis.* 9:e0003800. doi: 10.1371/journal.pntd.0003800

Smallwood, T. B., Giacomin, P. R., Loukas, A., Mulvenna, J. P., Clark, R. J., and Miles, J. J. (2017). Helminth immunomodulation in autoimmune disease. *Front. Immunol.* 8:453. doi: 10.3389/fimmu.2017.00453

Smith, E., von Vietinghoff, S., Stark, M. A., Zarbock, A., Sanders, J. M., Duley, A., et al. (2009). T-lineage cells require the thymus but not VDJ recombination

to produce IL-17A and regulate granulopoiesis in vivo. *J. Immunol.* 183, 5685–5693. doi: 10.4049/jimmunol.0900887

Smith, P., Mangan, N. E., Walsh, C. M., Fallon, R. E., McKenzie, A. N. J., van Rooijen, N., et al. (2007). Infection with a helminth parasite prevents experimental colitis via a macrophage-mediated mechanism. *J. Immunol.* 178, 4557–4566. doi: 10.4049/jimmunol.178.7.4557

Smith, P. D., Ochsenbauer-Jambor, C., and Smythies, L. E. (2005). Intestinal macrophages: unique effector cells of the innate immune system. *Immunol. Rev.* 206, 149–159. doi: 10.1111/j.0105-2896.2005.00288.x

Song, W. J., Li, Q., Ryu, M. O., Ahn, J. O., Ha Bhang, D., Chan Jung, Y., et al. (2017). TSG-6 secreted by human adipose tissue-derived mesenchymal stem cells ameliorates DSS-induced colitis by inducing M2 macrophage polarization in mice. *Sci. Rep.* 7:7. doi: 10.1038/s41598-017-04766-7

Soufli, I., Toumi, R., Rafa, H., Amri, M., Labsi, M., Khelifi, L., et al. (2015). Crude extract of hydatid laminated layer from *Echinococcus granulosus* cyst attenuates mucosal intestinal damage and inflammatory responses in dextran sulfate sodium induced colitis in mice. *J. Inflamm.* 12:19. doi: 10.1186/s12950-015-0063-6

Strachan, D. P. (1989). Hay fever, hygiene, and household size. *BMJ* 299, 1259–1260. doi: 10.1136/bmj.299.6710.1259

Talero, E., Sanchez-Fidalgo, S., de la Lastra, C. A., Illanes, M., Calvo, J. R., and Motilva, V. (2008). Acute and chronic responses associated with adrenomedullin administration in experimental colitis. *Peptides* 29, 2001–2012. doi: 10.1016/j.peptides.2008.07.013

Trelis, M., Galiano, A., Bolado, A., Toledo, R., Marcilla, A., and Bernal, D. (2016). Subcutaneous injection of exosomes reduces symptom severity and mortality induced by *Echinostoma caproni* infection in BALB/c mice. *Int. J. Parasitol.* 46, 799–808. doi: 10.1016/j.ijpara.2016.07.003

Vanhove, W., Nys, K., and Vermeire, S. (2016). Therapeutic innovations in inflammatory bowel diseases. *Clin. Pharmacol. Ther.* 99, 49–58. doi: 10.1002/cpt.286

Wang, L., Yu, Z., Wan, S., Wu, F., Chen, W., Zhang, B., et al. (2017). Exosomes derived from dendritic cells treated with *Schistosoma japonicum* soluble egg antigen attenuate DSS-induced colitis. *Front. Pharmacol.* 8:651. doi: 10.3389/fphar.2017.00651

Wang, Y., Tian, J., Tang, X., Rui, K., Tian, X., Ma, J., et al. (2016). Exosomes released by granulocytic myeloid-derived suppressor cells attenuate DSS-induced colitis in mice. *Oncotarget* 7, 15356–15368. doi: 10.18632/oncotarget.7324

Wiklander, O. P., Nordin, J. Z., O'Loughlin, A., Gustafsson, Y., Corso, G., Mäger, I., et al. (2015). Extracellular vesicle in vivo biodistribution is determined by cell source, route of administration and targeting. *J. Extracell. Vesicles* 4:26316. doi: 10.3402/jev.v4.26316

Williams, I. R., and Parkos, C. A. (2007). Colonic neutrophils in inflammatory bowel disease: double-edged swords of the innate immune system with protective and destructive capacity. *Gastroenterology* 133, 2049–2052. doi: 10.1053/j.gastro.2007.10.031

Wirtz, S., and Neurath, M. F. (2007). Mouse models of inflammatory bowel disease. *Adv. Drug Deliv. Rev.* 59, 1073–1083. doi: 10.1016/j.addr.2007.07.003

Xu, A. T., Lu, J. T., Ran, Z. H., and Zheng, Q. (2016). Exosome in intestinal mucosal immunity. *J. Gastroenterol. Hepatol.* 31, 1694–1699. doi: 10.1111/jgh.13413

Yáñez-Mó, M., Siljander, P. R., Andreu, Z., Zavec, A. B., Borràs, F. E., Buzas, E. I., et al. (2015). Biological properties of extracellular vesicles and their physiological functions. *J. Extracell. Vesicles* 4:27066. doi: 10.3402/jev.v4.27066

Yang, J., Liu, X., Fan, H., Tang, Q., Shou, Z., Zuo, D., et al. (2015). Extracellular vesicles derived from bone marrow mesenchymal stem cells protect against experimental colitis via attenuating colon inflammation, oxidative stress and apoptosis. *PLoS One* 10:e0140551. doi: 10.1371/journal.pone.0140551

Zamuner, S. R., Warrier, N., Buret, A. G., MacNaughton, W. K., and Wallace, J. L. (2003). Cyclooxygenase 2 mediates post-inflammatory colonic secretory and barrier dysfunction. *Gut* 52, 1714–1720. doi: 10.1136/gut.52.12.1714

Conflict of Interest Statement: The authors declare that the research was conducted in the absence of any commercial or financial relationships that could be construed as a potential conflict of interest.

The reviewer PX and handling Editor declared their shared affiliation.

nature immunology

CD69 controls the uptake of L-tryptophan through LAT1-CD98 and AhR-dependent secretion of IL-22 in psoriasis

Danay Cibrian[1], María Laura Saiz[1], Hortensia de la Fuente[1], Raquel Sánchez-Díaz[2], Olga Moreno-Gonzalo[1], Inmaculada Jorge[2], Alessia Ferrarini[2], Jesús Vázquez[2], Carmen Punzón[3], Manuel Fresno[3], Miguel Vicente-Manzanares[1], Esteban Daudén[4], Pedro M Fernández-Salguero[5], Pilar Martín[2] & Francisco Sánchez-Madrid[1,2]

The activation marker CD69 is expressed by skin γδ T cells. Here we found that CD69 controlled the aryl hydrocarbon receptor (AhR)-dependent secretion of interleukin 22 (IL-22) by γδ T cells, which contributed to the development of psoriasis induced by IL-23. CD69 associated with the aromatic-amino-acid-transporter complex LAT1-CD98 and regulated its surface expression and uptake of L-tryptophan (L-Trp) and the intracellular quantity of L-Trp-derived activators of AhR. *In vivo* administration of L-Trp, an inhibitor of AhR or IL-22 abrogated the differences between CD69-deficient mice and wild-type mice in skin inflammation. We also observed LAT1-mediated regulation of AhR activation and IL-22 secretion in circulating $V_\gamma9^+$ γδ T cells of psoriatic patients. Thus, CD69 serves as a key mediator of the pathogenesis of psoriasis by controlling LAT1-CD98-mediated metabolic cues.

Psoriasis is one of the most common chronic inflammatory skin diseases, affecting about 2% of the population worldwide[1]. It is defined by a thickened epidermis (acanthosis) caused by keratinocyte proliferation and massive infiltration of leukocytes into the skin. Psoriatic lesions contain larger amounts of the pro-inflammatory cytokines interleukin 17 (IL-17), IL-21, IL-22 and IL-23, which has led to the classification of psoriasis as a disease mediated by IL-17-producing helper T cells (T_H17 cells)[2]. The importance of IL-23 and IL-17 in psoriatic patients is demonstrated by the efficacy of treatment with monoclonal antibodies to IL-17 and to the cytokine receptor IL-23R[3]. Furthermore, intradermal administration of recombinant IL-23 to mice induces a psoriasiform dermatitis that mimics the human disease in histological and immunological aspects[4].

In addition to IL-17, IL-22 also acts as a master regulator of psoriasis[5–7]. Polymorphisms in *IL22* result in enhanced susceptibility to psoriasis[8], and serum concentrations of IL-22 positively correlate with disease severity and negatively correlate with responsiveness to therapy[9]. IL-22 signaling in keratinocytes induces expression and phosphorylation of the transcription factor STAT3, which increases epidermal proliferation and de-differentiation[10]. IL-22 expression is regulated by the ligand-dependent transcription factor AhR in T_H17 cells and some populations of γδ T cells[11] and innate lymphocytes[12]. Currently described endogenous ligands for AhR also include naturally occurring dietary substances, such as L-tryptophan (L-Trp)-derived metabolites[13]. After being exposed to light, L-Trp can be metabolized to several products, including the high-affinity AhR agonist FICZ (6-formylindolo [3, 2-b] carbazole). A light-independent, H_2O_2-dependent pathway for the systemic generation of FICZ from L-Trp has also been described[14]. Uptake of aromatic amino acids by activated lymphoid cells is conducted mainly via the system L1 transporter, an heterodimer comprising the heavy chain CD98 (also known as SLC3A2 or 4F2) and the light chain LAT1 ('L-type amino acid transporter 1'; also known as SLC7A5). Regulation of amino acid transport through the LAT1-CD98 heterodimer is linked to T cell–activation and T cell–differentiation processes[15].

Although T_H17 cells were once considered an important source of IL-17 and IL-22 in psoriatic skin, evidence now indicates that these cytokines are produced mainly by a population of dermal γδ T cells already identified in both humans and mice[16–19]. Skin γδ T cells bear several markers of memory and effector T cells, including CD69 (ref. 20). Lymphocytes from CD69-deficient mice show enhanced differentiation toward the T_H17 lineage[21], and CD69-deficient mice exhibit increased severity of T_H17 cell–mediated inflammatory diseases, including collagen II–induced arthritis[22], allergic asthma and skin contact hypersensitivity[23], autoimmune myocarditis[24] and colitis[25]. Whether CD69 exerts an immunomodulatory effect on psoriasis by controlling IL-17 and IL-22 responses in skin γδ T cells has remained unexplored until now.

In this study we found that CD69-deficient mice developed an attenuated skin inflammatory response to the administration of

[1]Immunology Service, Hospital de la Princesa, Universidad Autónoma de Madrid, Instituto Investigación Sanitaria Princesa, Madrid, Spain. [2]Department of Vascular Biology and Inflammation, Centro Nacional de Investigaciones Cardiovasculares, Madrid, Spain. [3]Department of Molecular Biology, Centro de Biología Molecular Severo Ochoa, Universidad Autónoma de Madrid, Madrid, Spain. [4]Dermatology Service, Hospital de la Princesa, Madrid, Spain. [5]Department of Biochemistry, Molecular Biology and Genetic, Faculty of Sciences, University of Extremadura, Badajoz, Spain. Correspondence should be addressed to F.S.-M. (fsmadrid@salud.madrid.org).

Received 4 March; accepted 1 June; published online 4 July 2016; corrected online 11 July 2016 (details online); doi:10.1038/ni.3504

IL-23, with decreased expression of IL-22 and STAT3 in the epidermis. We also found that CD69 associated with the heterodimeric amino-acid transporter LAT1-CD98 and regulated the uptake of L-Trp. This promoted the AhR-induced secretion of IL-22 by skin γδ T cells.

RESULTS

IL-23-induced psoriasiform inflammation requires CD69

To assess the role of CD69 in psoriasis, we administered consecutive intradermal injections of mouse IL-23 protein into the ears of wild-type and CD69-deficient mice. IL-23 induced more swelling, epidermal acanthosis, dermal inflammation and keratinocyte proliferation (Ki67$^+$ nuclei) in the ears of wild-type mice than in those of CD69-deficient mice (**Fig. 1a–c**). IL-23 also significantly increased the total number of CD45$^+$ cells in wild-type mice relative to that in CD69-deficient mice (**Fig. 1d**). These were mostly CD45$^+$CD11c$^-$CD11b$^+$ myeloid (non-dendritic) cells, particularly Gr-1$^+$F4/80$^-$neutrophils, F4/80^{lo} monocytes and F4/80^{hi} macrophages (**Fig. 1d**). Immunohistochemistry also revealed more Ly6G$^+$ neutrophils and F4/80$^+$ monocytes and macrophages in wild-type mice than in CD69-deficient mice after treatment with IL-23 (**Fig. 1c**) These results indicated that the absence of CD69 prevented the development of psoriasis after intradermal injection of IL-23.

Reduced expression of IL-22 and STAT3 in CD69 deficiency

We next determined whether CD69 controls the expression of inflammatory mediators in the skin. IL-23 induced higher expression of *Cxcl1*, *S100a8* and *S100a9* mRNA in wild-type mice than in CD69-deficient mice, while both genotypes showed a similar increase in *Ccl20* mRNA (**Fig. 2a**). IL-23 treatment increased the expression of *Il6*, *Tnf*, *Il1b* and IL-17 mRNA to a similar extent in wild-type mice and CD69-deficient mice, while the expression of *Tgfb* mRNA in the skin was not altered (**Fig. 2b**,**c**). In contrast, IL-23 induced a very modest increase in IL-22 expression in the skin of CD69-deficient relative to that in the skin of wild-type mice (**Fig. 2d**). Neither genotype showed detectable expression of IL-22 or IL-17 in CD4$^+$ T cells obtained from the ear-draining lymph nodes of mice given injection of IL-23, followed by re-stimulation of the cells *in vitro* (data not shown). These results indicated that the weak

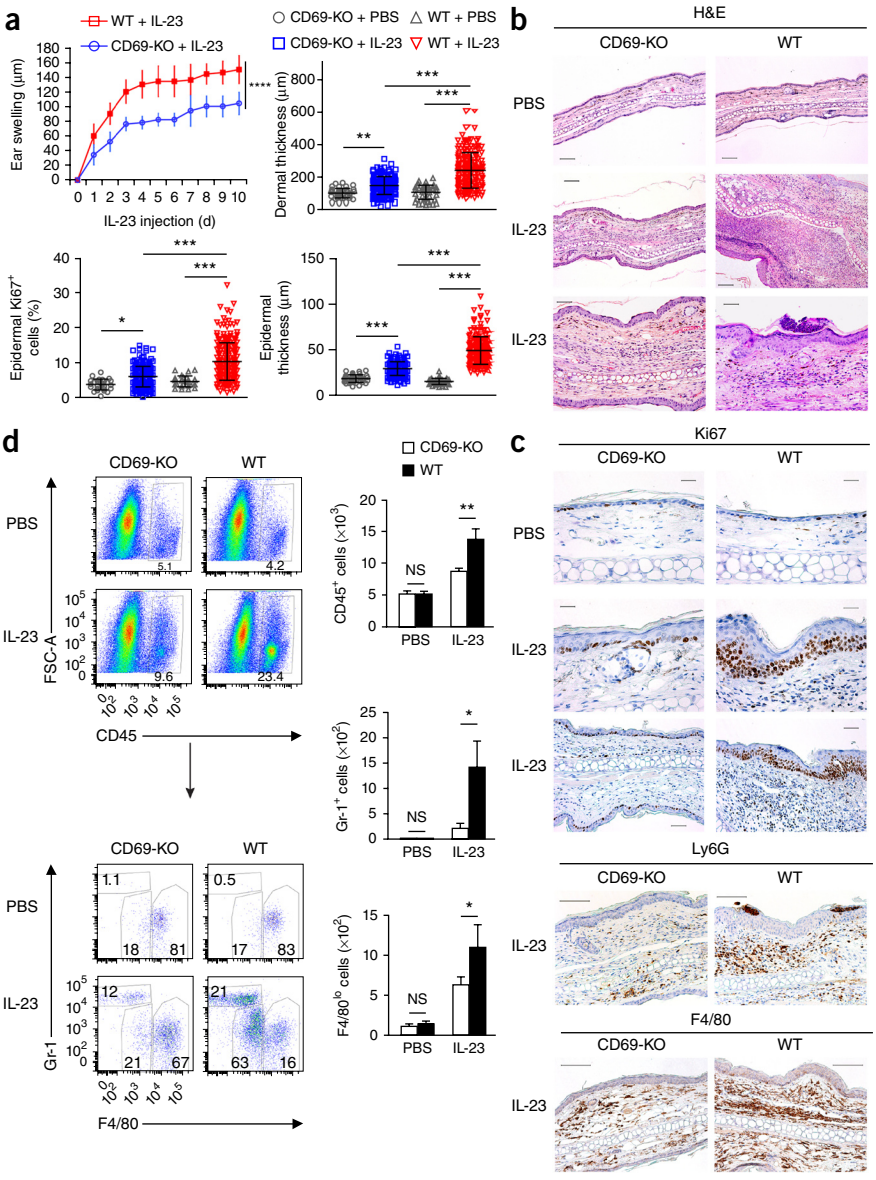

Figure 1 CD69-deficient mice develop a mild form of IL-23-induced psoriasis. (**a**) Ear thickness of CD69-deficient (CD69-KO) and wild-type (WT) mice after each intradermal injection of IL-23 (horizontal axis) (top left), and dermal and epidermal thickness and quantification of Ki67$^+$ nuclei in histological sections of ears from CD69-deficient and wild-type mice after ten doses of IL-23 (top right and bottom row). Each symbol (top right and bottom row) represents an individual image; small horizontal lines indicate the mean (± s.d.). (**b**) Hematoxylin-and-eosin (H&E)-stained sections of ear skin from CD69-deficient and wild-type mice treated with PBS or IL-23 (left margin). Scale bars, 100 μm (top and middle) or 50 μm (bottom); original magnification, ×10 (top and middle) or ×20 (bottom). (**c**) Immunohistochemistry of Ki67, Ly6G and F4/80 (above images) in the skin of CD69-deficient and wild-type mice treated with PBS or IL-23 (left margin). Scale bars, 25 μm (top and second row), 50 μm (third row) or 100 μm (bottom two rows); original magnification, ×40 (top and second row) or ×20 (bottom three rows). (**d**) Flow cytometry (left) of cells that infiltrated the ears of CD69-deficient and wild-type mice (above plots) given ten doses of PBS or IL-23 (left margin). Numbers adjacent to outlined areas indicate percent of CD45$^+$ cells among live gated cells (top group), or Gr-1$^+$ granulocytes (top left), F4/80^{lo} cells (bottom left) or F4/80^{hi} monocytes and macrophages (bottom right) among CD45$^+$CD11b$^+$CD11c$^-$ live gated cells. Right, quantification of the populations gated at left (per 1×10^4 live gated cells). FSC, forward scatter. NS, not significant ($P > 0.05$); $^*P < 0.05$, $^{**}P < 0.01$, $^{***}P < 0.001$ and $^{****}P < 0.0001$ (unpaired *t*-test (**a**, top left), one-way analysis of variance (ANOVA) with Newman-Keuls multiple-comparisons post-test (**a**, top right and bottom row) or two-way ANOVA with Bonferroni's multiple-comparisons test (**d**, right)). Data are representative of three experiments (mean ± s.d. (**a**, top left) or mean + s.e.m. (**d**); $n = 5$ mice per group).

cutaneous inflammatory response to IL-23 injection observed in the CD69-deficient mice might have been related to attenuated skin production of IL-22.

Expression of the cytokine receptor IL-22R in skin is restricted to non-hematopoietic cells, such as keratinocytes and fibroblasts. In these cells, the binding of IL-22 to IL-22R activates STAT3 (ref. 26). Injections of IL-23 into the ear caused a uniform increase in epidermal STAT3 expression and phosphorylation (at Ser727 and Tyr705) in wild-type mice, compared with only patchy induction of these parameters in CD69-deficient mice (**Fig. 2e**,**f**). This indicated that CD69 controlled the expression of IL-22 and STAT3.

Enhancement of the expression of AhR and IL-22 by CD69

CD69 is a negative regulator of the secretion of IL-17 by T_H17 cells[27], but its effect on IL-22 secretion is not known. This is a crucial question, since IL-22 is produced by T_H17 lymphocytes[13]. Naive $CD4^+$ T cells from CD69-deficient mice polarized for 48 h *in vitro* into T_H17 cells secreted less IL-22 than did their wild-type counterparts (**Supplementary Fig. 1a**). Moreover, flow cytometry after intracellular staining showed that CD69-deficient T_H17 cells had lower expression of AhR than that of wild type T_H17 cells (**Supplementary Fig. 1b**). We found that expression of mRNA from the AhR target genes *Il22*, *Ahr*, *Ahrr*, *Cyp1a* and *Cyp1b* was impaired in CD69-deficient T_H17 cells relative to that in wild-type T_H17 cells (**Supplementary Fig. 1c**).

In IL-23-driven psoriasis, IL-22 and IL-17 are secreted by dermal γδ T cells[16,18]. To characterize the resident T cell populations in the skin of both wild-type mice and CD69-deficient mice, we analyzed total skin-cell suspensions and separated dermal and epidermal layers by flow cytometry. These experiments indicated that $CD3^{hi}$ cells were dendritic epidermal γδ T cells, while 50–80% of dermal $CD3^{lo}$ cells were γδ T cells (**Supplementary Fig. 1d**). Both $CD3^{hi}$ γδ T cell populations and $CD3^{lo}$ γδ T cell populations in untreated skin had high expression of CD69 (**Supplementary Fig. 1e**). Although CD69 expression is linked to the generation and migration of skin-resident memory T cells[28], the frequency of skin-resident epidermal ($CD3^{hi}$) and dermal ($CD3^{lo}$) γδ T cell populations was similar in wild-type mice and CD69-deficient mice (**Supplementary Fig. 1f**).

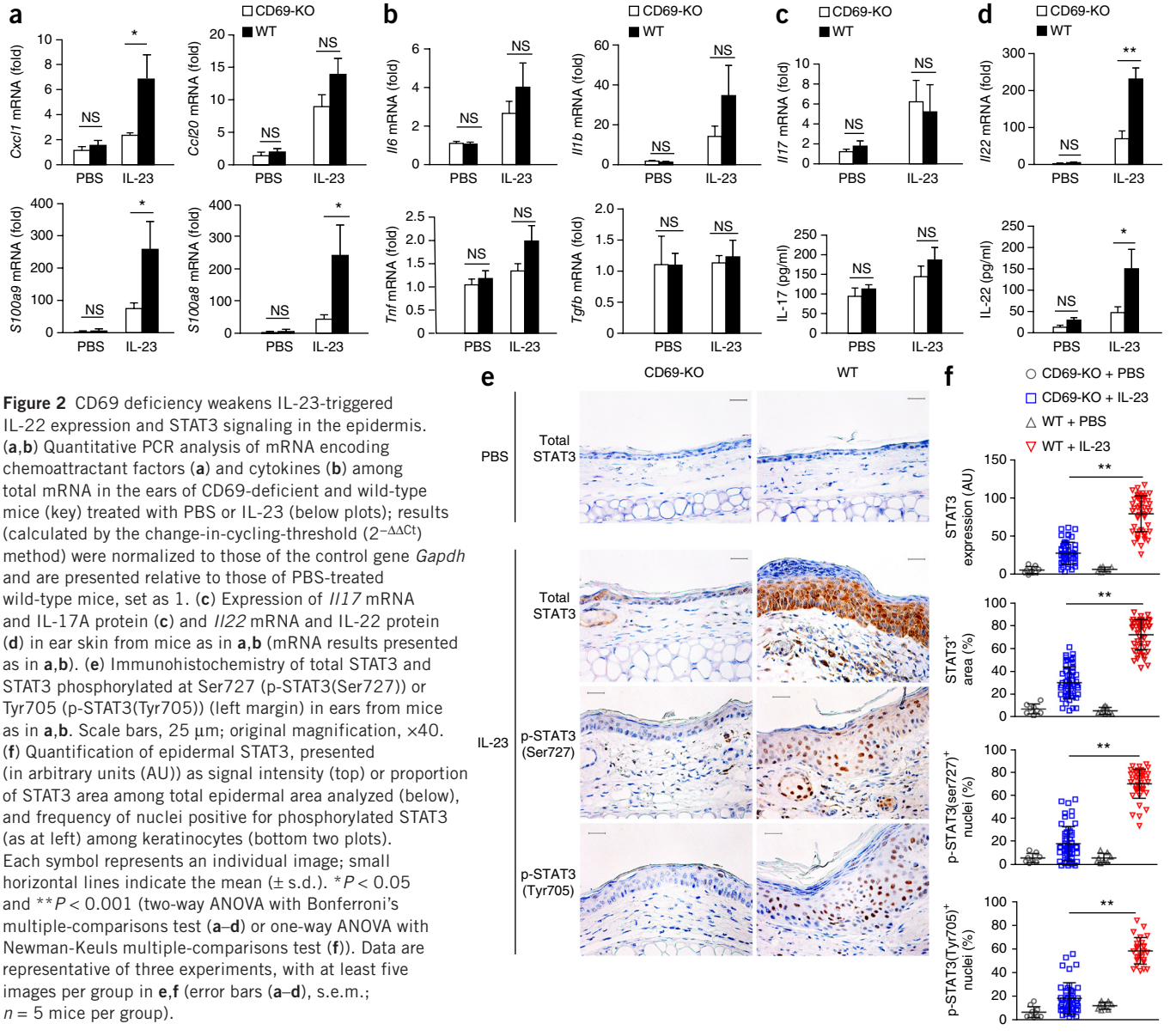

Figure 2 CD69 deficiency weakens IL-23-triggered IL-22 expression and STAT3 signaling in the epidermis. (**a**,**b**) Quantitative PCR analysis of mRNA encoding chemoattractant factors (**a**) and cytokines (**b**) among total mRNA in the ears of CD69-deficient and wild-type mice (key) treated with PBS or IL-23 (below plots); results (calculated by the change-in-cycling-threshold ($2^{-\Delta\Delta Ct}$) method) were normalized to those of the control gene *Gapdh* and are presented relative to those of PBS-treated wild-type mice, set as 1. (**c**) Expression of *Il17* mRNA and IL-17A protein (**c**) and *Il22* mRNA and IL-22 protein (**d**) in ear skin from mice as in **a**,**b** (mRNA results presented as in **a**,**b**). (**e**) Immunohistochemistry of total STAT3 and STAT3 phosphorylated at Ser727 (p-STAT3(Ser727)) or Tyr705 (p-STAT3(Tyr705)) (left margin) in ears from mice as in **a**,**b**. Scale bars, 25 µm; original magnification, ×40. (**f**) Quantification of epidermal STAT3, presented (in arbitrary units (AU)) as signal intensity (top) or proportion of STAT3 area among total epidermal area analyzed (below), and frequency of nuclei positive for phosphorylated STAT3 (as at left) among keratinocytes (bottom two plots). Each symbol represents an individual image; small horizontal lines indicate the mean (± s.d.). $*P < 0.05$ and $**P < 0.001$ (two-way ANOVA with Bonferroni's multiple-comparisons test (**a**–**d**) or one-way ANOVA with Newman-Keuls multiple-comparisons test (**f**)). Data are representative of three experiments, with at least five images per group in **e**,**f** (error bars (**a**–**d**), s.e.m.; $n = 5$ mice per group).

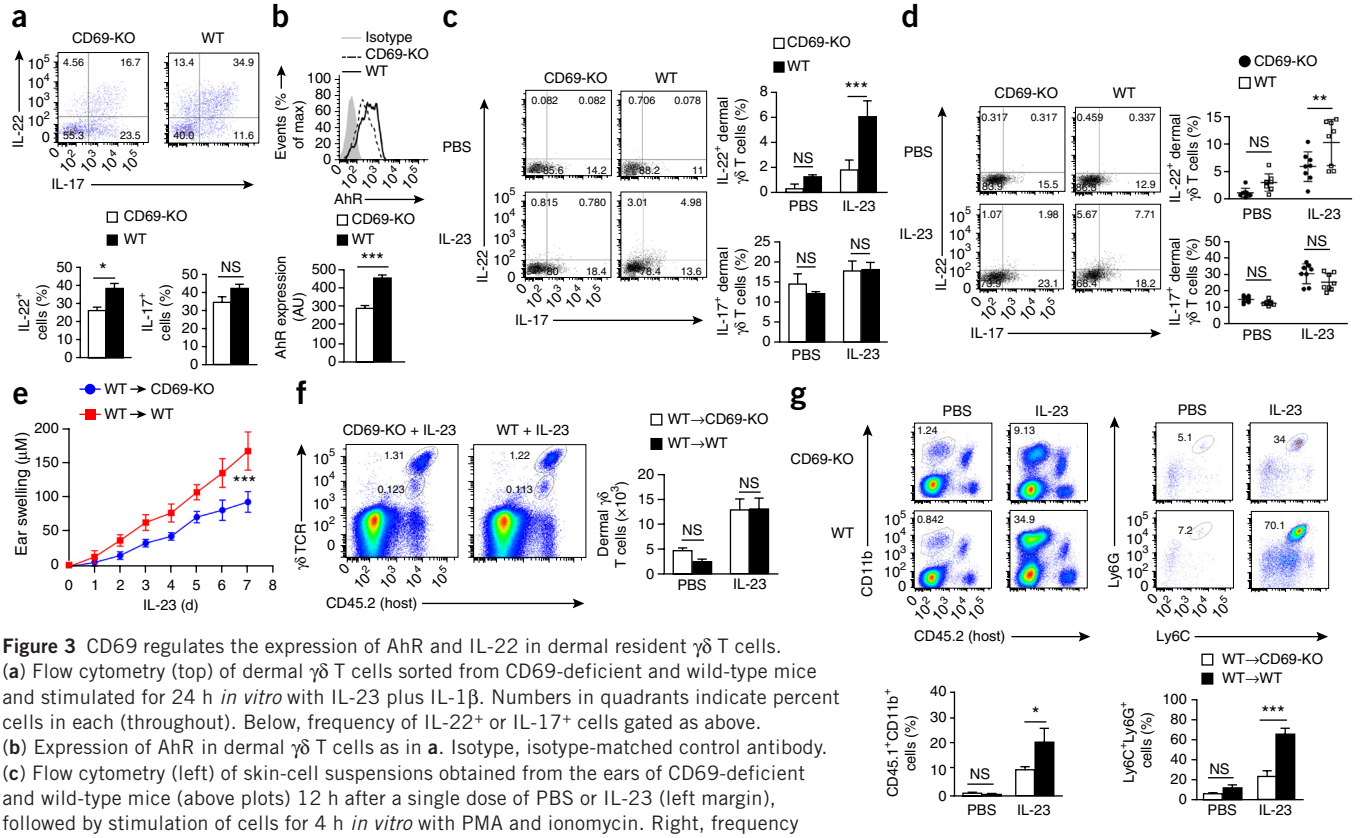

Figure 3 CD69 regulates the expression of AhR and IL-22 in dermal resident γδ T cells. (**a**) Flow cytometry (top) of dermal γδ T cells sorted from CD69-deficient and wild-type mice and stimulated for 24 h *in vitro* with IL-23 plus IL-1β. Numbers in quadrants indicate percent cells in each (throughout). Below, frequency of IL-22$^+$ or IL-17$^+$ cells gated as above. (**b**) Expression of AhR in dermal γδ T cells as in **a**. Isotype, isotype-matched control antibody. (**c**) Flow cytometry (left) of skin-cell suspensions obtained from the ears of CD69-deficient and wild-type mice (above plots) 12 h after a single dose of PBS or IL-23 (left margin), followed by stimulation of cells for 4 h *in vitro* with PMA and ionomycin. Right, frequency of IL-22$^+$ or IL-17$^+$ cells gated as at left ($n = 8$ mice per group). (**d**) Flow cytometry (left) of cells obtained from CD69-deficient and wild-type mice (above plots) 12 h after injection of a single dose of PBS and brefeldin A or IL-23 and brefeldin A (left margin). Right, frequency of IL-22$^+$ or IL-17$^+$ cells gated as at left. Each symbol represents an individual mouse ($n = 8$ per group); small horizontal lines indicated the mean (± s.d.). (**e**) Ear thickness of lethally irradiated CD69-deficient and wild-type host mice (CD45.2$^+$) reconstituted by intravenous injection of wild-type whole bone marrow cells (CD45.1$^+$) for 2 months, then given seven doses of PBS or IL-23 intradermally (assessed after each dose; horizontal axis). (**f**) Flow cytometry (left) analyzing dermal γδ T cells in CD69-deficient or wild-type (CD45.2$^+$) host chimeric mice as in **e**. Numbers adjacent to outlined areas indicate percent CD45.2$^+$ (host-resident) dermal or epidermal γδ T cells identified by high expression (top right; epidermal) or low expression (bottom right; dermal) of the γδ TCR. Right, quantification of total dermal γδ T cells (per ear) in host mice as at left after intradermal treatment with PBS or IL-23 (horizontal axis). (**g**) Flow cytometry (top) of cells from mice as in **e**. Numbers adjacent to outlined areas indicate percent CD45.1$^+$CD11b$^+$ cells among live cells (left group) or Ly6G$^+$Ly6C$^+$ cells among CD45.1$^+$CD11b$^+$F4/80$^-$ gated cells (right group). Bottom, frequency of CD45.1$^+$CD11b$^+$ and CD45.1$^+$CD11b$^+$F480$^-$Ly6G$^+$Ly6C$^+$ cells as above. *$P < 0.05$, **$P < 0.01$ and ***$P < 0.001$ (unpaired *t*-test (**a**,**b**) or two-way ANOVA and Bonferroni's multiple-comparisons test (**c**,**d**,**f**,**g**)). Data are representative of three experiments (**a**,**b**; mean + s.e.m.; $n = 3$ or 4 mice per experiment), one experiment (**c**,**d**; mean + s.d. of $n = 8$ mice per group in **c**) or two experiments (**e**–**g**; mean + s.e.m. of $n = 5$ mice per group).

Simultaneous intradermal injection of IL-23 (into the ears) and systemic (intraperitoneal) administration of the secretion inhibitor brefeldin A to wild-type mice promoted the accumulation of IL-22 in dermal CD3^{lo} γδ T cells (**Supplementary Fig. 2a**). Moreover, flow cytometry of dermal γδ T cells sorted from wild-type mice and stimulated *in vitro* with IL-23 plus IL-1β revealed an acute peak of IL-22 (maximal at 24 h after stimulation) and higher AhR expression than that of unstimulated cells (**Supplementary Fig. 2b**). However, the secretion of IL-17 from sorted dermal γδ T cells was sustained for up to 72 h after stimulation (**Supplementary Fig. 2b**).

Sorted CD69-deficient dermal γδ T cells released less IL-22 than did wild-type dermal γδ T cells when stimulated with IL-23 and IL-1β *in vitro*, whereas their IL-17 production was similar (**Fig. 3a**). Moreover, the expression of AhR induced by IL-23 and IL-1β *in vitro* stimulation was lower in CD69-deficient dermal γδ T cells than in wild-type dermal γδ T cells (**Fig. 3b**).

To parse the function of CD69 in IL-22 secretion by dermal γδ T cells *in vivo*, we prepared skin-cell suspensions 12 h after the administration of a single dose of IL-23 into the ears of wild-type and CD69-deficient mice, followed by stimulation of the cell suspensions with the phorbol ester PMA and ionomycin. Flow cytometry showed lower IL-22 expression in CD69-deficient dermal γδ T cells than in wild-type dermal γδ T cells (**Fig. 3c**). Simultaneous intradermal injection of IL-23 and intraperitoneal administration of brefeldin A resulted in lower expression of IL-22 in dermal γδ T cells from CD69-deficient mice than in those from wild-type mice (**Fig. 3d**).

We observed a similar expression of the transcription factor RORγt in dermal γδ T cells from CD69-deficient and those from wild-type mice (**Supplementary Fig. 2c**). Likewise, phosphorylation of STAT3 and STAT5 following stimulation with IL-23 plus IL-1β was similar in CD69-deficient dermal γδ T cells and wild-type dermal γδ T cells (**Supplementary Fig. 2c**). Flow cytometry of skin suspensions from mice with sequence encoding green fluorescent protein (GFP) reporter knocked into the gene encoding IL-23R[29] showed that dermal γδ T cells (CD3^{lo}) were the main population among IL-23R$^+$ (GFP$^+$) cells in the skin at steady state, while epidermal γδ T cells (CD3^{hi}) were IL-23R$^-$ (GFP$^-$) (**Supplementary Fig. 2d**). Staining of IL-23R showed that the number of IL-23R$^+$ dermal γδ T cells and their molecular density of IL-23R were similar for CD69-deficient mice and wild-type mice (**Supplementary Fig. 2e**).

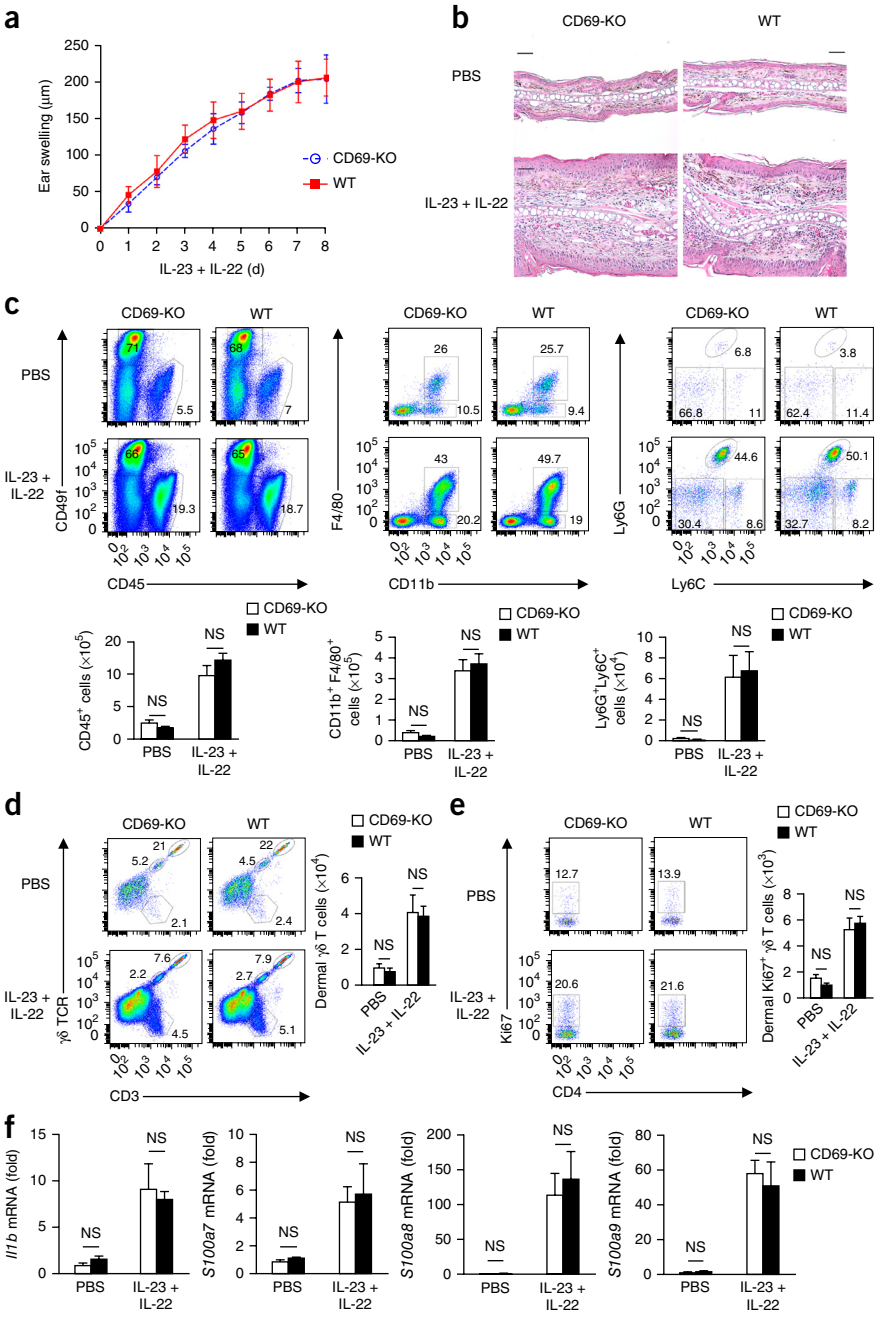

Figure 4 IL-22 mediates skin inflammation downstream of CD69. (**a**) Ear thickness of CD69-deficient and wild-type mice during the administration of eight doses of IL-23 plus IL-22 (500 ng of each; horizontal axis). (**b**) H&E-stained sections of ears from wild-type and CD69-deficient mice (above plots) treated with eight doses of PBS or with IL-23 plus IL-22 (left margin). Scale bars, 50 μm; original magnification, ×20. (**c**) Flow cytometry (top) of cells in skin suspensions from mice as in **a**. Numbers adjacent to outlined areas indicate percent CD49f$^+$CD45$^-$ keratinocytes (top left) or CD49f$^-$CD45$^+$ cells (bottom right) among live gated cells (left group), CD11b$^+$F4/80$^+$ macrophages (top) or CD11b$^+$F4/80$^-$ cells (bottom) among CD45$^+$CD11c$^-$ live gated cells (middle group), or Ly6G$^+$Ly6C$^+$ neutrophils (top), Ly6G$^-$Ly6C$^-$ cells (bottom left) or Ly6G$^-$Ly6C$^+$ cells (bottom right) among live CD45$^+$ CD11b$^+$F4/80$^-$ gated cells (right group). Below, total CD45$^+$ cells, macrophages and neutrophils (per ear) in mice as above. (**d**) Flow cytometry (left) of skin suspensions from mice as in **a**. Numbers adjacent to outlined areas indicate percent γδTCR$^-$CD3$^+$ T cells (bottom), γδTCR$^+$CD3$^+$ dermal T cells (top right) and γδTCR^{++}CD3^{++} epidermal T cells (top left) among live CD45$^+$ gated cells. Right, total dermal γδ T cells (per ear) in mice as at left. (**e**) Flow cytometry (left) of skin suspensions from mice as in **a**. Numbers adjacent to outlined areas indicate percent Ki67$^+$ cells among CD45$^+$CD3^{lo}γδTCR^{lo} gated cells. Right, total dermal Ki67$^+$ γδ T cells as at left. (**f**) Quantitative PCR analysis of *Il1b*, *S100a7*, *S100a8* and *S100a9* mRNA in the skin of mice as in **a** (presented as in **Fig. 2a**,**b**). *P* values (NS), unpaired *t*-test (**a**) or two-way ANOVA followed by Bonferroni's multiple-comparisons test (**c**–**f**). Data are representative of two independent experiments with similar results (mean ± s.d. (**a**) or mean + s.e.m. (**c**–**f**); $n = 5$ mice per group in each experiment).

CD69 is known to modulate the trafficking of effector T cells[30]. To investigate whether CD69-mediated egress of lymphocytes from the lymph node was involved in the IL-23 skin-inflammation model, we transferred wild-type (CD45.1$^+$) whole bone marrow cells intravenously into lethally γ-irradiated CD69-deficient or wild-type (CD45.2$^+$) host mice (**Fig. 3e**). After 2 months of reconstitution, we administered IL-23 intradermally to the mice. CD69-deficient host mice displayed less skin inflammation than that of wild-type host mice (**Fig. 3e**). Flow cytometry of skin-cell suspensions showed a similar increase in host-derived (CD45.2$^+$) dermal γδ T cells in CD69-deficient mice and wild-type host mice after treatment with IL-23 (**Fig. 3f**). We observed significantly more infiltrating CD11b$^+$ myeloid cells and Ly6G$^+$Ly6C$^+$ neutrophils of donor (CD45.1$^+$) origin in the skin of wild-type mice than in that of CD69-deficient mice (**Fig. 3g**). Because skin-resident dermal γδ T cells are radioresistant and proliferate *in situ*[20], they persisted in the bone-marrow-chimeric hosts, which would account for the differences between the wild-type hosts and CD69-deficient hosts. These observations ruled out the possibility of a role for the migration of CD69$^+$ T lymphocytes from the lymph nodes as a triggering mechanism.

IL-22- and AhR-mediated skin inflammation downstream of CD69

To address whether the attenuated skin inflammation observed in CD69-deficient mice was due to reduced secretion of IL-22 from the skin, we simultaneously injected IL-22 and IL-23 intradermally into wild-type mice and CD69-deficient mice. We observed a similar degree of ear swelling in mice of each genotype (**Fig. 4a**), as well as substantial acanthosis (**Fig. 4b**) and similar infiltration of myeloid cells into the skin (**Fig. 4c**), proliferation of dermal γδ T cells (**Fig. 4d**,**e**), and expression of *Il1b* and IL-22-related genes, such *S100a7*, *S100a8* and *S100a9*, in mice of each genotype (**Fig. 4f**). Moreover, intradermal injection of IL-22 alone induced

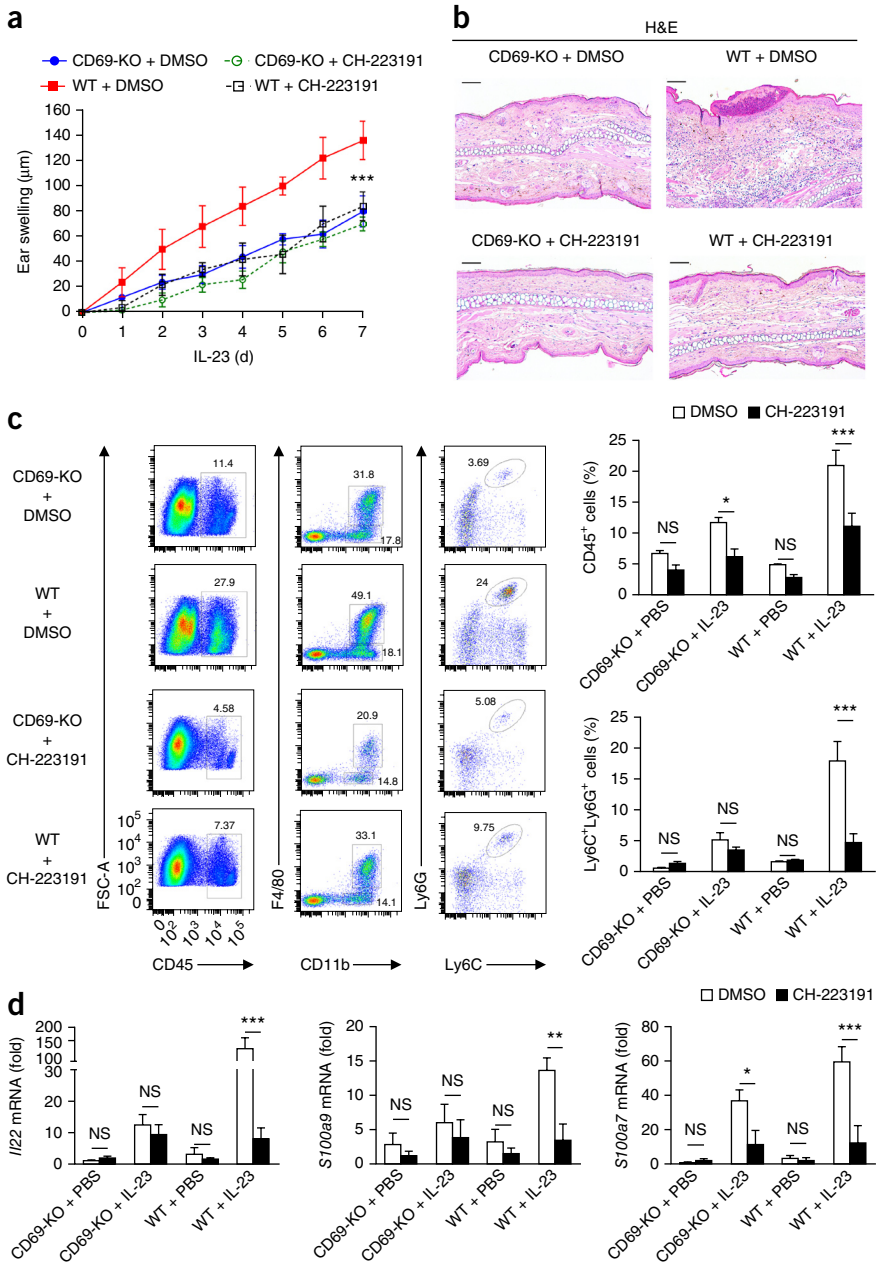

Figure 5 IL-23-induced skin inflammation is prevented by inhibition of AhR. (**a**) Ear thickness of CD69-deficient and wild-type mice during the administration of seven doses of IL-23 (horizontal axis) with concomitant daily intraperitoneal injection of CH-223191 or vehicle (DMSO). (**b**) H&E-stained sections of ears from wild-type and CD69-deficient mice treated intradermally with seven doses of IL-23 along with systemic administration of CH-223191 or DMSO. Scale bars, 100 μm; original magnification, ×10. (**c**) Flow cytometry of cells from wild-type and CD69-deficient mice treated as in **a** (left margin). Numbers adjacent to outlined areas indicate percent $CD45^+$ cells among live gated cells (left), $CD11b^+F4/80^+$ macrophages (top) or $CD11b^+F4/80^-$ cells (bottom) among $CD45^+CD11c^-$ live gated cells (middle), or $Ly6G^+Ly6C^+$ neutrophils among $CD11b^+F4/80^-$ gated cells (right). Right, frequency of $CD45^+$ cells among live-gated skin cells (top) and of $Ly6C^+Ly6G^+$ cells in the $CD45^+CD11c^-CD11b^+F4/80^-$ subset (bottom) in wild-type and CD69-deficient mice treated with PBS or IL-23 (horizontal axis) and with CH-223191 or DMSO (key). (**d**) Quantitative PCR analysis of *Il22*, *S100a9* and *S100a7* mRNA in the skin of mice as in **a** (presented as in **Fig. 2a**,**b**). $*P < 0.05$, $**P < 0.01$ and $***P < 0.001$ (two-way ANOVA with Bonferroni's multiple-comparisons test). Data are representative of two independent experiments with similar results (mean ± s.d. (**a**) or mean + s.e.m. (**c**,**d**); $n = 5$ mice per group).

similar ear swelling and expression of *Il1b*, *S100a8* and *S100a9* in CD69-deficient skin and wild-type skin (**Supplementary Fig. 3a**). These observations suggested that the effect of IL-22 in the context of IL-23-induced skin inflammation was independent of CD69 expression.

Direct involvement of AhR in the secretion of IL-22 by dermal γδ T cells was addressed by simultaneous administration of three intradermal injections of IL-23 into the ears of AhR-deficient and wild-type mice, as well as intraperitoneal administration of brefeldin A. Flow cytometry of skin-cell suspensions showed fewer $IL\text{-}22^+$ dermal γδ T cells in AhR-deficient mice than in wild-type mice, while the number of $IL\text{-}17^+$ γδ T cells was increased similarly in the skin of each genotype (**Supplementary Fig. 3b**). In addition, we stimulated sorted CD69-deficient and wild-type dermal γδ T cells *in vitro* with IL-23 plus IL-1β in the presence of the AhR inhibitor CH-223191, which prevented secretion of IL-22 by cells of each genotype (**Supplementary Fig. 3c**). To assess whether IL-22 secretion depended on CD69 in γδ T subsets in locations other than the skin, we studied splenic $CD27^-$ γδ T cells, which secrete IL-17 and IL-22 after being stimulated with IL-23 (ref. 31). These cells expressed CD69 after being stimulated with IL-23 and/or IL-1β (**Supplementary Fig. 3d**). Splenic $CD27^-$ γδ T cells from CD69-deficient mice had lower expression of IL-22 than that of their wild-type counterparts, and this was abrogated by CH-223191 (**Supplementary Fig. 3e**). These observations indicated that activation of AhR was required for CD69 to regulate the IL-23-induced IL-22 expression.

To address whether inhibition of AhR controlled IL-23-dependent skin inflammation, we injected IL-23 intradermally into wild-type and CD69-deficient mice, together with daily intraperitoneal administration of CH-223191. This treatment decreased inflammation in wild-type mice but had a very modest effect on CD69-deficient mice (**Fig. 5a**,**b**). Systemic administration of CH-223191 also reduced the number of IL-23-driven $Ly6G^+Ly6C^+$ neutrophils in wild-type skin to numbers similar to those in CD69-deficient skin (**Fig. 5c**). Also, the expression of *Il22* mRNA and of the IL-22 target genes *S100a9* and *S100a7* in whole skin was significantly lower in wild-type mice that received CH-223191 plus IL-23 than in wild-type mice that received IL-23 alone and was similar to that in CD69-deficient mice treated with IL-23 (**Fig. 5d**). These results indicated that AhR and IL-22 contributed to skin inflammation controlled by CD69.

CD69 associates with LAT1-CD98 and controls amino acid uptake

To address the mechanism by which CD69 regulated the AhR-mediated expression of IL-22, we used mass spectrometry to explore possible interactions of CD69 with regulators of AhR. We found that CD69 associated with several nutrient transporters, including CD98, LAT1, MOT1 and GTR1 (**Supplementary Table 1** and **Supplementary Fig. 4a**). The LAT1-CD98 complex is a major intake receptor for aromatic amino acids such as L-Trp, which is a source of ligands for AHR[14]. Immunoprecipitation experiments showed that CD69 associated with both chains of the LAT1-CD98 transporter in human Jurkat T cells activated with PMA and ionomycin (**Fig. 6a**). Confocal imaging and a proximity-ligation assay also indicated an

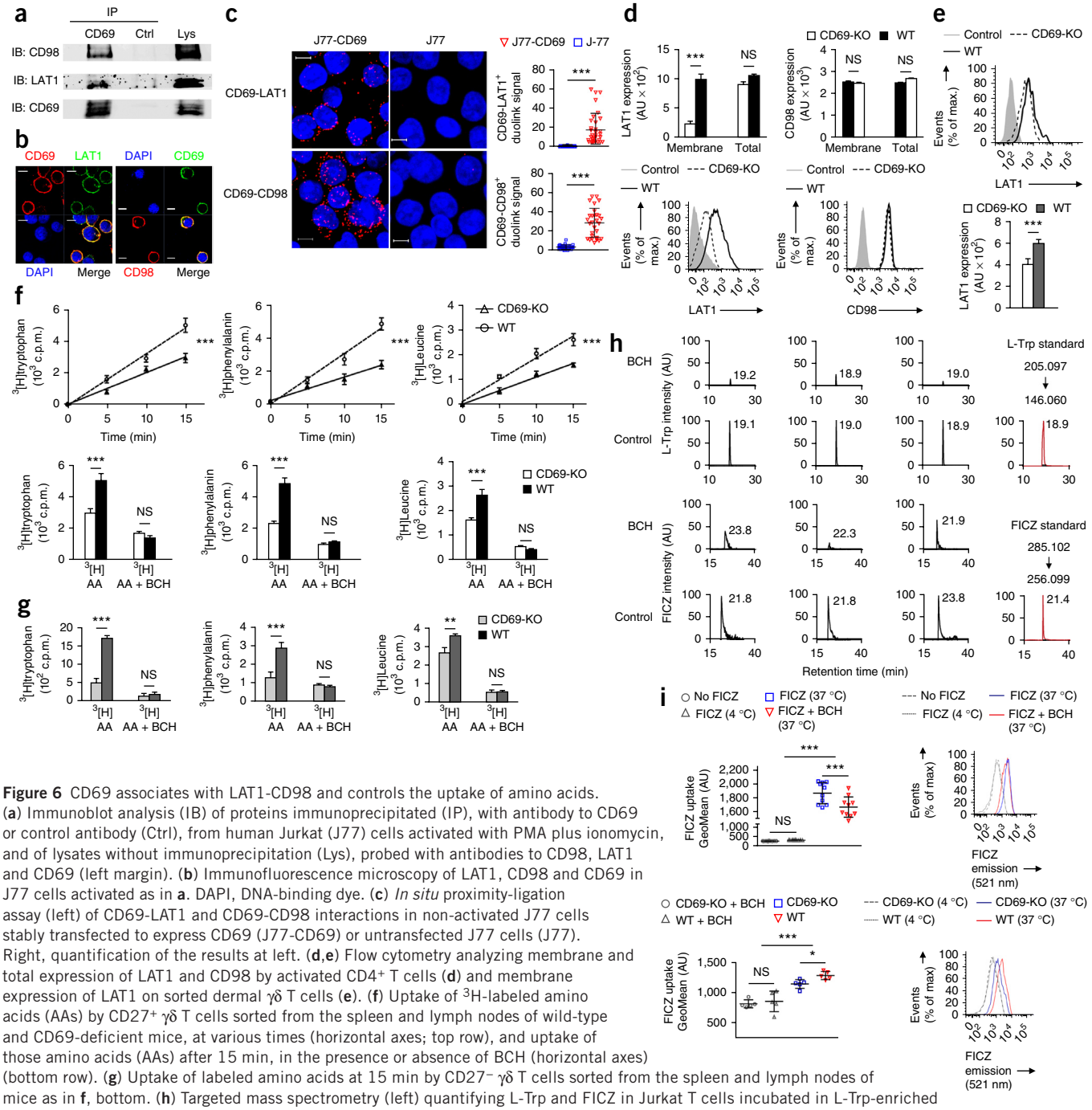

Figure 6 CD69 associates with LAT1-CD98 and controls the uptake of amino acids. (**a**) Immunoblot analysis (IB) of proteins immunoprecipitated (IP), with antibody to CD69 or control antibody (Ctrl), from human Jurkat (J77) cells activated with PMA plus ionomycin, and of lysates without immunoprecipitation (Lys), probed with antibodies to CD98, LAT1 and CD69 (left margin). (**b**) Immunofluorescence microscopy of LAT1, CD98 and CD69 in J77 cells activated as in **a**. DAPI, DNA-binding dye. (**c**) *In situ* proximity-ligation assay (left) of CD69-LAT1 and CD69-CD98 interactions in non-activated J77 cells stably transfected to express CD69 (J77-CD69) or untransfected J77 cells (J77). Right, quantification of the results at left. (**d**,**e**) Flow cytometry analyzing membrane and total expression of LAT1 and CD98 by activated CD4$^+$ T cells (**d**) and membrane expression of LAT1 on sorted dermal γδ T cells (**e**). (**f**) Uptake of ^{3}H-labeled amino acids (AAs) by CD27$^+$ γδ T cells sorted from the spleen and lymph nodes of wild-type and CD69-deficient mice, at various times (horizontal axes; top row), and uptake of those amino acids (AAs) after 15 min, in the presence or absence of BCH (horizontal axes) (bottom row). (**g**) Uptake of labeled amino acids at 15 min by CD27$^-$ γδ T cells sorted from the spleen and lymph nodes of mice as in **f**, bottom. (**h**) Targeted mass spectrometry (left) quantifying L-Trp and FICZ in Jurkat T cells incubated in L-Trp-enriched medium and left untreated (Control) or treated with BCH, presented as mass-spectrometry-2-extracted values reflecting the intensity (AU) of each compound in each sample, with retention times used for identification (three biological replicates: top, middle, left); far right (red), ion chromatograms of reference standards for L-Trp and FICZ (confirmation of retention times; presented as at left). (**i**) Flow cytometry analyzing the uptake of FICZ by wild-type activated CD4$^+$ T cells after 16 h of incubation with no FICZ or 1 μM FICZ (top row) or by CD69-deficient and wild-type activated CD4$^+$ T cells after 1 h of incubation with 100 nM FICZ (bottom row), with or without BCH, at 4 °C or 37 °C (key). Each symbol (**c**,**i**) represents an individual replicate (cell (**c**) or well (**i**)); small horizontal lines indicate the mean (± s.d.). $^*P < 0.05$, $^{**}P < 0.01$ and $^{***}P < 0.001$ (unpaired *t*-test (**c**,**e**) or one- or two-way ANOVA and Newman-Keuls or Bonferroni's test (**d**,**f**,**g**)). Data are representative of two experiments (**a**–**c**,**f**,**g**,**i**; mean + s.e.m. in **f**,**g**), three experiments with at least $n = 5$ replicates (wells) per group (**d**,**e**; mean + s.d.) or three independent experiments with one biological replicate (**h**).

association of CD69 with CD98 and LAT1 on the plasma membrane of activated Jurkat T cells (**Fig. 6b**,**c**).

Activated $CD4^+$ T cells from CD69-deficient mice had lower surface expression of LAT1 but not lower total expression of LAT1 than that of their wild-type counterparts, while plasma-membrane expression and global expression of CD98 were similar in cells of each genotype (**Fig. 6d**). Membrane expression of LAT1 was also significantly higher in sorted wild-type dermal γδ T cells than in their CD69-deficient counterparts (**Fig. 6e**). After stimulation with antibody to the invariant signaling protein CD3 (anti-CD3), wild-type $CD4^+$ T cells and CD69-deficient $CD4^+$ T cells showed a similar increase in *Slc7a5* mRNA (which encodes LAT1) and *Slc3a2* mRNA (which encodes CD98) (**Supplementary Fig. 4b**); this suggested that CD69 might have been regulating LAT1 dynamics and/or its stability at the membrane. Moreover, no significant difference between activated $CD4^+$ T cells from CD69-deficient and those from wild-type mice was observed in the expression of mRNA encoding other amino acid transporters, except for higher expression of *Slc38a2* mRNA (which encodes the transporter SNAT2), regulated by amino-acid starvation[32], in CD69-deficient $CD4^+$ T cells than in their wild-type counterparts (**Supplementary Fig. 4c**).

Assays of the uptake of ^{3}H-labeled L-Trp, L-Phe and L-Leu showed that CD69-deficient γδ T cells isolated from spleen and lymph nodes had slower uptake of L-Trp via LAT1 than that of their wild-type counterparts (**Fig. 6f**,**g**). Likewise, less uptake of amino acids via LAT1 was detected in CD69-deficient $CD4^+$ T cells than in wild-type $CD4^+$ T cells (**Supplementary Fig. 5a**). Incubation with an antibody that promotes CD69 internalization[23] also triggered the internalization of LAT1 in $CD4^+$ T cells but had no effect on surface expression of CD98 (**Supplementary Fig. 5b**). HEK-293 human embryonic kidney cells were co-transfected with plasmids encoding CD69-GFP and LAT1-Cherry fusion proteins and then incubated with labeled anti-CD69; this showed co-internalization of CD69 and LAT1 (**Supplementary Fig. 5c**). Moreover, antibody-induced internalization of CD69 impaired the uptake of L-Trp and L-Phe in $CD4^+$ wild-type T cells relative to their uptake after treatment with control antibody, but it had no effect on amino acid uptake in CD69-deficient cells (**Supplementary Fig. 5d**). These observations indicated that CD69 was associated with LAT1 and regulated its localization at the plasma membrane and amino acid transport.

Mass-spectrometry analysis showed less intracellular accumulation of FICZ (a metabolic and photoxidative product of L-Trp that activates AhR) in Jurkat T cells cultured in L-Trp-enriched medium treated with the LAT1 inhibitor BCH than in cells not treated with BCH (**Fig. 6h**). Moreover, through use of the intrinsic fluorescence of FICZ, we observed enhanced intracellular transport of FICZ into T cells at 37 °C but not at 4 °C (**Fig. 6i**). Uptake of FICZ from the extracellular medium was lower in CD69-deficient T cells than in wild-type T cells, and these differences were abrogated by the LAT1 inhibitor (**Fig. 6i**). These results demonstrated that LAT1-CD98 facilitated the intracellular transport of FICZ in a CD69-regulated manner.

CD69-LAT1-CD98 regulate mTORC and AhR-mediated IL-22 expression

The LAT1-mediated transport of amino acids is required for activation of the metabolic-checkpoint-kinase complex mTORC pathway[33]. CD69-deficient and wild-type naive $CD4^+$ T cells were polarized toward T_H17 cells *in vitro* and mTORC signaling was assessed as phosphorylation of the kinases mTORC1, S6 and 4E-BP1 (at 24–96 h). CD69 expression was dispensable for early activation of mTORC at 24 h after engagement of the T cell antigen receptor (TCR) (**Supplementary Fig. 6a**). However, the maintenance of mTORC signaling is influenced by amino acid uptake[33]. T_H17 cells from CD69-deficient mice showed impaired phosphorylation of S6 and 4E-BP1 after 96 h relative to that of their wild-type counterparts (**Supplementary Fig. 6b**).

We next addressed the role of LAT1-CD98–mediated transport of aromatic amino acids in AhR-dependent responses. Addition of the LAT1 inhibitor BCH abrogated IL-22 production in CD69-deficient and wild-type T_H17 cells (**Supplementary Fig. 6c**). In contrast, addition of the AhR ligand FICZ induced the secretion of IL-22 from cells of each genotype (**Supplementary Fig. 6c**). Culture of T_H17 cells with L-Trp-enriched Iscove's modified Dulbecco's medium (IMDM)[13] restored the secretion of IL-22 from CD69–deficient T_H17 to the secretion of IL-22 by wild-type cells (**Supplementary Fig. 6c**). Moreover, in the presence of LAT1 inhibitor BCH, the IL-22 expression in dermal γδ T cells stimulated *in vitro* with IL-23 plus IL-1β was reduced in wild-type cells to an amount similar to that observed in their CD69-deficient counterparts (**Fig. 7a**). Conversely, culture in IMDM or the addition of FICZ induced similar IL-22 expression in CD69-deficient dermal γδ T cells and wild-type dermal γδ T cells (**Fig. 7a**). Supplementation of RPMI medium with L-Trp also increased the release of IL-22 from CD69-deficient and wild-type $CD4^+$ T_H17 cells (**Fig. 7b**), although differences in IL-17 secretion remained (**Fig. 7b**). Expression of the AhR-regulated genes *Ahrr* and *Il22* was higher in CD69-deficient and wild-type $CD4^+$ naive cells polarized *in vitro* into the T_H17 subset and cultured in RPMI medium supplemented with L-Trp or IMDM than in cells activated with anti-CD3 and antibody to the costimulatory receptor CD28 (anti-CD28) (the 'T_H0-polarizing' condition) (**Fig. 7c**). The addition of BCH decreased the expression of *Ahrr* and *Il22* mRNA in CD69-deficient and wild-type cells (**Fig. 7c**).

Psoriatic skin displays increased expression of the tryptophan-degrading enzymes IDO (indoleamine 2,3-dyoxigenase) and TDO (tryptophan 2,3-dioxygenase), which catalyze the first step in L-Trp catabolism by the kynurenine pathway, and higher expression of the enzyme L-kynureninase, which further degrades kynurenine[34]. Thus, we assessed their expression in whole skin after intradermal injection of IL-23 alone or IL-23 plus IL-22. The expression of mRNA encoding IDO or L-kynureninase was induced similarly in CD69-deficient skin and wild-type skin, while the expression of mRNA encoding TDO was not induced by IL-23 (**Supplementary Fig. 6d**).

To determine whether uptake of L-Trp *in vivo* by dermal γδ T cells modulated psoriasis in CD69-deficient and wild-type mice, we administered L-Trp daily (intraperitoneally) simultaneously with intradermal injection of IL-23. The administration of L-Trp resulted in similar skin swelling in CD69-deficient mice and wild-type mice (**Fig. 7d**) and similar numbers of infiltrating $CD45^+CD11b^+F4/80^+$ macrophages and $CD45^+CD11b^+F4/80^-Ly6G^+Ly6C^+$ neutrophils in the skin of CD69-deficient mice and that of wild-type mice (**Fig. 7e**,**f**). We also observed similar numbers of IL-22^+ dermal γδ T cells in CD69-deficient mice and wild-type mice following the administration of L-Trp (**Fig. 7g**). Hence, these results indicated that CD69 regulated the surface expression of LAT1, the uptake of L-Trp, an intracellular increase in FICZ, and subsequent AhR activation and IL-22 secretion in dermal γδ T cells (**Supplementary Fig. 7**).

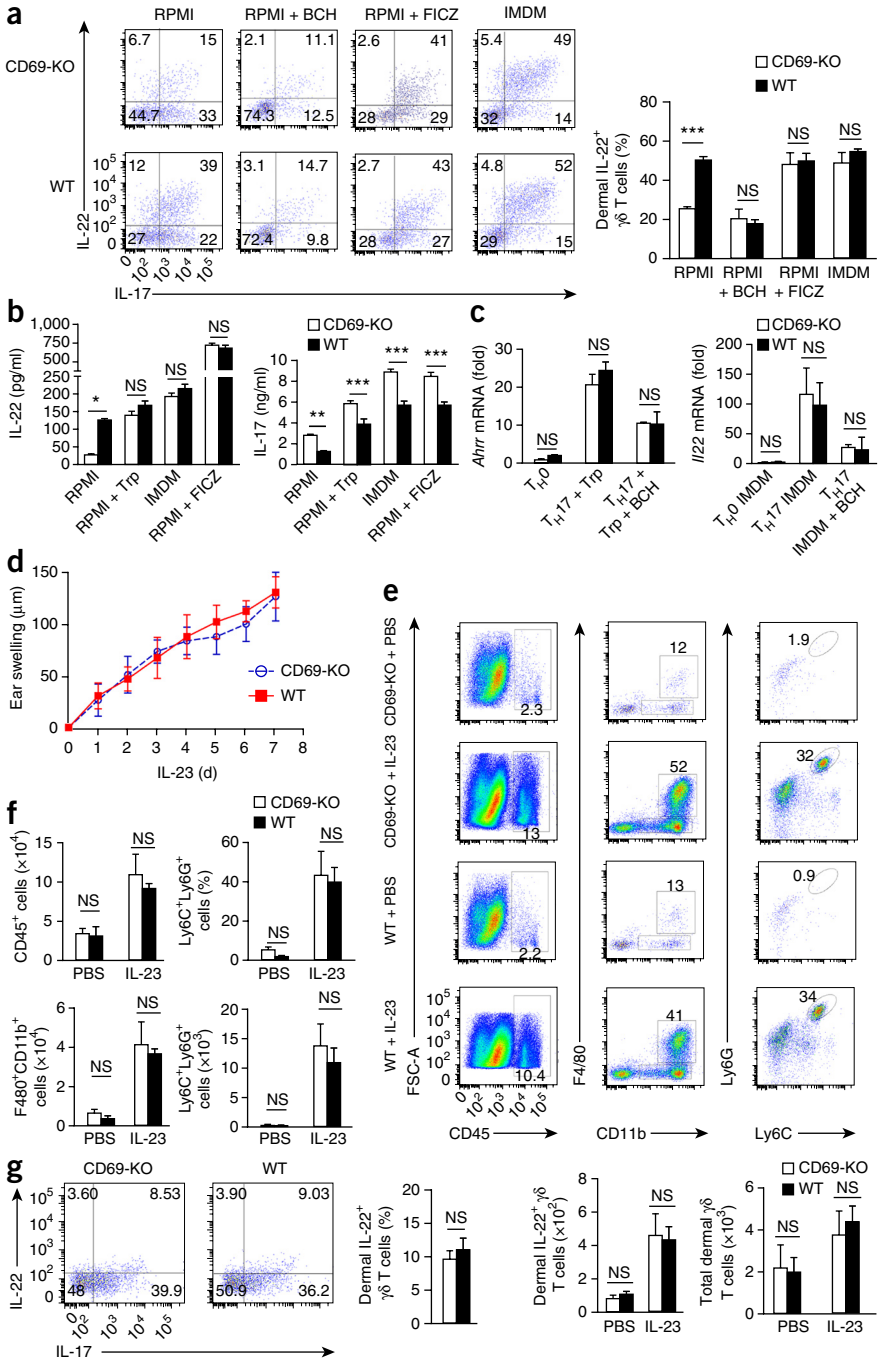

Figure 7 CD69 regulates AhR-induced secretion of IL-22 by dermal γδ T cells *in vitro* and *in vivo* through control of L-Trp uptake. (**a**) Flow cytometry (left) analyzing the expression of IL-22 and IL-17 by wild-type and CD69-deficient sorted dermal γδ T cells stimulated *in vitro* with IL-23 plus IL-1β in RPMI medium alone or supplemented with BCH or FICZ, or in IMDM (above plots). Right, frequency of IL-22$^+$ cells as at left. (**b**) ELISA of IL-22 and IL-17 in supernatants of wild-type and CD69-deficient CD4$^+$ T_H17 cells cultured in RPMI medium alone or supplemented with L-Trp or FICZ, or in IMDM (horizontal axes). (**c**) Quantitative PCR analysis of *Ahrr* and *Il22* mRNA in T_H0 and T_H17 cells cultured for 48 h *in vitro* in various conditions in RPMI medium (for *Ahrr*) or in IMDM (for *Il22*) (horizontal axes) (presented as in **Fig. 2a**,**b**). (**d**) Ear swelling of CD69-deficient and wild-type mice during the administration of IL-23 plus L-Trp. (**e**) Flow cytometry of cells in ears from mice given systemic injection of L-Trp in addition to intradermal administration of PBS or IL-23 (numbers adjacent to outlined areas, as in **Fig. 5c**). (**f**) Frequency (top right) and total number (top left and bottom row) of CD45$^+$ cells from live gated skin cells (top left) and of Ly6C$^+$Ly6G$^+$ cells in the CD45$^+$CD11b$^+$F4/80$^-$ subset (top right). (**g**) Flow cytometry (left) of dermal γδ T cells in CD69-deficient and wild-type mice treated with IL-23 and L-Trp and given injection of brefeldin A. Right, frequency and total number of IL-22$^+$ cells, and total dermal γδ T cells. Each symbol (**c**,**i**) represents an individual replicate (well); small horizontal lines indicate the mean (± s.d.). $*P < 0.05$, $**P < 0.01$ and $***P < 0.001$ (two-way ANOVA and Bonferroni's test). Data are representative of two experiments (mean + s.e.m. (**a**–**c**,**f**,**g**) or mean ± s.d. (**d**); $n = 5$ mice per group in **d**–**g**).

Upregulation of CD69, LAT1 and IL-22 in psoriasis

We next assessed whether CD69$^+$ γδ T cells were present in skin samples from patients with moderate to severe psoriasis. CD69 expression was detected by immunofluorescence in $V_\gamma9^+$ T cells in psoriatic skin lesions (**Fig. 8a**). The frequency of $V_\gamma9^+$CD69$^+$ T cells positively correlated with the psoriasis area severity index (**Fig. 8b**). Immunofluorescence staining showed that IL-22-secreting $V_\gamma9^+$ T cells in the dermal layer expressed CD69 (**Fig. 8c**). In agreement with that, expression of *IL22* and *TNF* mRNA was higher in psoriatic skin than in biopsies of healthy skin (**Fig. 8d**).

The frequency of circulating CD69$^+$CLA$^+$$V_\gamma9^+$ T cells was greater in psoriatic patients than in healthy control subjects (**Fig. 8e**). To assess the ability of these cells to produce IL-22, we stimulated circulating γδ T cells from psoriatic patients *in vitro* with a cytokine 'cocktail' (IL-23 plus IL-1β plus IL-6 plus TGF-β). IL-22 expression in human $V_\gamma9^+$ γδ T cells was decreased by the addition of inhibitors of AhR or LAT1 (**Fig. 8f**,**g**). Quantitative RT-PCR analysis of mRNA from whole-skin biopsies showed significantly higher expression of *SLC7A5* and *CD69* mRNA in psoriatic lesions than in unaffected regions, whereas *SLC3A2* mRNA was not expressed differentially in these regions (**Fig. 8h**). These results demonstrated LAT1-mediated regulation of AhR and IL-22 in γδ T cells from patients with psoriasis.

DISCUSSION

The pathogenesis of psoriasis involves cross-talk between skin-resident innate immune cells and keratinocytes, which is orchestrated by cytokines such as IL-22 and IL-17 (refs. 1,35). Here we found that CD69 associated with the transporter complex LAT1-CD98 and enhanced the uptake of L-Trp, a metabolic precursor of AhR ligands that promoted IL-22 secretion[13,14]. The transcriptional activity of STAT3 induced by IL-22 in keratinocytes upregulates the expression of pro-inflammatory molecules such as keratin 17, S100A7, S100A8 and S100A9, as well as several CXCL chemokines[6,36].

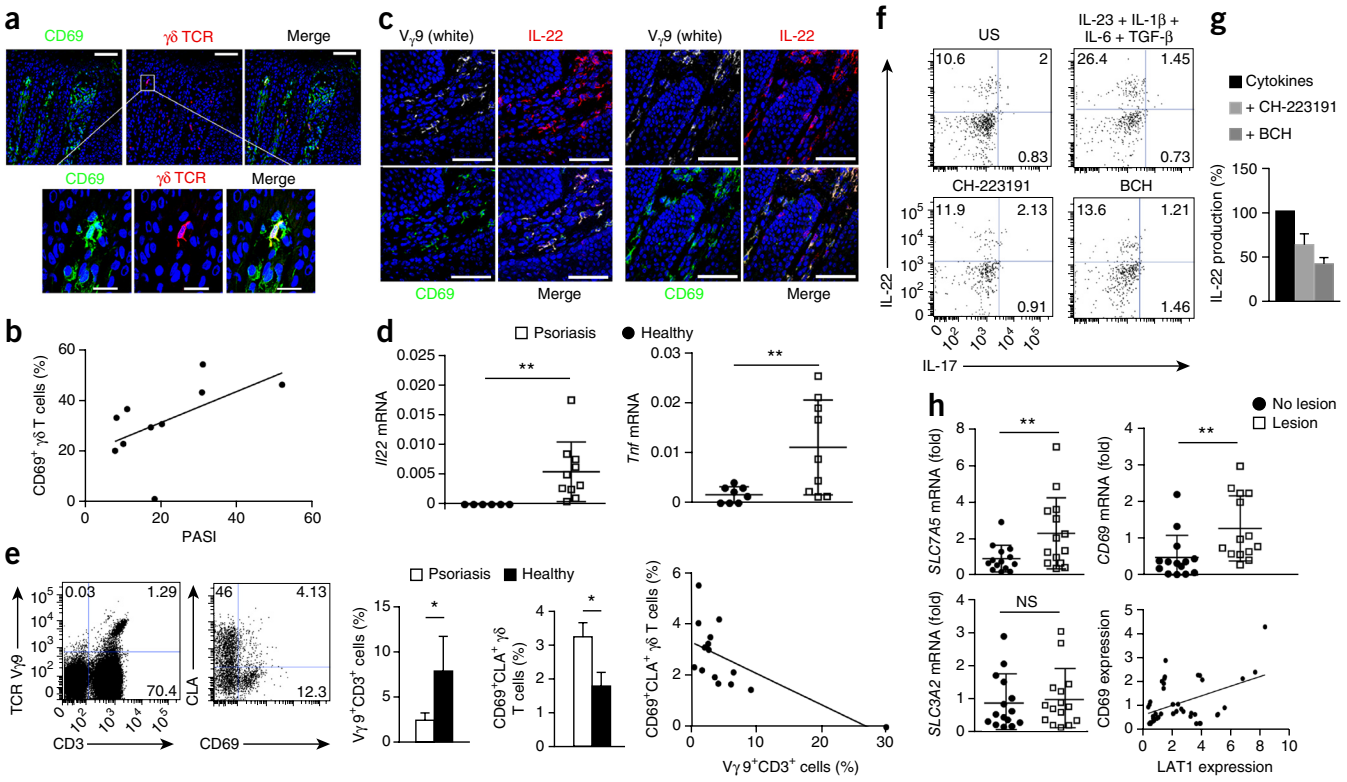

Figure 8 CD69 expression is detected in skin and circulating $V_\gamma9^+$ T cells from psoriatic patients. (**a**) Microscopy of frozen section of human psoriatic lesions immunostained for CD69, the γδ TCR and nuclei (DAPI); outlined area (top middle) is enlarged below. Scale bars, 50 μm (top row) or 25 μm (bottom row). (**b**) Correlation between the frequency of dermal $V_\gamma9^+CD69^+$ T cells and the clinical psoriasis area severity index (PASI) of psoriatic patients ($r = 0.64$ (Spearman test); $P < 0.05$. (**c**) Microscopy of frozen sections from psoriatic lesions immunostained for $V_\gamma9$, IL-22 and CD69. Scale bars, 50 μm. (**d**) Quantitative PCR analysis of *IL22* and *TNF* mRNA in lesional skin from patients and skin from healthy subjects; results (calculated by the standard-curve method) were normalized to those of the control gene *ACTB*. (**e**) Flow cytometry analyzing the expression of $V_\gamma9$ and CD3 (left) and of CLA and CD69 by $CD3^+V_\gamma9^+$ gated cells (right) among peripheral blood mononuclear cells from a psoriatic patient. Middle, frequency of $V_\gamma9^+CD3^+$ cells (left) among live cells and of CLA^+ and $CD69^+$ cells among $V_\gamma9^+$ peripheral γδ T cells from psoriatic patients and healthy subjects. Far right, frequency of $CD69^+CLA^+V_\gamma9^+$ cells plotted against that of $V_\gamma9^+CD3^+$ cells. (**f**) Flow cytometry analyzing the expression of IL-22 and IL-17 by peripheral γδ T cells obtained from psoriatic patients, then subjected to population expansion and left unstimulated (US) or stimulated with various cytokines alone (top left) or in the presence of CH-223191 (bottom left) or BCH (bottom right). (**g**) ELISA of IL-22-producing cells as in **f**. (**h**) Quantitative PCR analysis of *SLC7A5*, *CD69* and *SLC3A2* in lesion and non-lesional areas of psoriatic patients (presented as in **Fig. 2a**,**b**), and correlation analysis of *CD69* and *SLC7A5* (bottom right: $r = 0.34$; $P = 0.02$). Each symbol (**b**,**d**,**e**,**h**) represents an individual donor; small horizontal lines indicate the mean (± s.d.). $^*P < 0.05$ and $^{**}P < 0.001$ (unpaired *t*-test). Data are representative of experiments with ten patients (**a**–**c**) ten patients and nine healthy subjects (**d**), nine patients and six healthy subjects (**e**; mean + s.e.m.), three patients (**f**), three patients and six healthy subjects (pooled) (**g**; mean + s.e.m.) or fifteen patients (**h**).

IL-22 also induces keratinocyte proliferation through the PI3K-Akt-mTORC signaling pathway[37]. The deficient expression of IL-22 and activation of STAT3 in the skin of CD69-deficient mice we found here provides a mechanistic link that explains the attenuated dermal inflammation and keratinocyte proliferation observed after administration of IL-23.

γδ TCR–deficient mice display attenuated psoriatic plaque formation in response to IL-23 (ref. 16) and imiquimod[18]. The role of CD69 as an enhancer of AhR activity and IL-22 release in γδ T cells *in vitro* and *in vivo* correlates well with clinical data showing increased CD69 expression on $V_\gamma9^+$ T cells from the skin and the bloodstream of psoriatic patients.

CD69 associated with the amino-acid transporter complex LAT1-CD98 on the plasma membrane of activated T cells and controlled the activation of mTORC. Further studies are needed to ascertain whether CD69 regulates other targets of mTORC, such as the autophagy route[38] and HIF-1α through AhR[39]. Different regions of CD98 control the uptake of amino acids and β_1-integrin-mediated cell proliferation[40]. However, published studies have shown no difference in the proliferation rate of CD69-deficient T lymphocytes and that of wild-type T lymphocytes[41], which suggests that the association of CD69 with the LAT1-CD98 complex in activated immune cells modulates the uptake of amino acids specifically.

Cytoplasmic L-Trp acts as a chromophore that is converted by exposure to light into active AhR ligands, including FICZ[13]. The characterization of a light-independent metabolic route for the generation of FICZ from the intracellular pool of L-Trp[14] suggests that regulation of entry of the precursor might determine the amount of cellular FICZ and AhR activation. Our results demonstrated that LAT1-CD98 regulated the intracellular accumulation of FICZ.

Inhibition of AhR protects against inflammation induced by IL-23 without substantial alteration of the keratinocyte layers. However, depletion of AhR in keratinocytes disrupts epidermal homeostasis, which enhances psoriasis in response to imiquimod, although lower expression of IL-22 in the skin of fully AhR-deficient mice than in the skin of wild-type mice has been detected[42]. Differences between the IL-23-induced psoriasis model and imiquimod-induced psoriasis model exist[2]. Toll-like-receptor-7-independent epidermal hyperproliferative responses induced by keratinocyte damage are involved in the induction of psoriasis in the imiquimod model[18,43].

AhR controls the terminal differentiation of epidermal cells and the expression of genes encoding proteins linked to skin barrier function, such as filaggrin[44,45]. Hence, AhR in keratinocytes is required for skin homeostasis, but its activation in inflammatory cells mediates inflammation.

CD69 did not affect the secretion of IL-17 by innate γδ T cells, in contrast to its effect on $CD4^+$ T_H17 T cells[27]. The greater secretion of IL-17 by CD69-deficient $CD4^+$ T_H17 cells than by wild-type $CD4^+$ T_H17 cells is due to increased phosphorylation of STAT3 and increased RORγt expression[27]. This was not observed in dermal γδ T cells, owing to the fact that the transcription factors that control the T_H17 differentiation $CD4^+$ T cells, such as STAT3, are not required for the development of IL-17^+ (RORγt$^+$) γδ T cells that originated in fetal thymus[46,47].

Prevention of the uptake of L-Trp via LAT1 abrogated the AhR-dependent secretion of IL-22 from human peripheral γδ T cells from psoriatic patients, which would suggest a possible role for the uptake of dietary L-Trp in psoriasis. Notably, *in vivo* administration of L-Trp increased the severity of inflammatory responses elicited by IL-23 independently of CD69 expression. Overall, these data indicate that L-Trp catabolism has an important role in the pathophysiology of psoriasis, not only due to the regulation of kynurenine but also by its effect on other metabolites that might contribute to skin inflammation. In conclusion, our study has established a biological role for CD69 in the control of amino acid uptake and the regulation of AhR activation and IL-22 expression in γδ and T_H17 cells and indicates that CD69 contributes to the development of psoriasis.

METHODS

Methods and any associated references are available in the online version of the paper.

Note: Any Supplementary Information and Source Data files are available in the online version of the paper.

ACKNOWLEDGMENTS

We thank D. Rotin (University of Toronto) for the plasmid for the expression of LAT1-mCherry; P. Taylor (University of Dundee) for antiserum to human LAT1; M. Navarro (Universidad Autónoma de Madrid, Spain) for IL-23R-GFP reporter mice; S. Bartlett for English editing; and T. Hernandez and R. Brid Doohan for technical assistance with immunohistochemistry. Supported by the Spanish Ministry of Economy and Competitiveness (SAF2011-25834 and SAF2014-55579-R to F.S.-M.; SAF2011-27330 to P.M.; and SAF2013-42850 to M.F.), Comunidad de Madrid (INDISNET-S2011/BMD-2332 to F.S.-M.; and 2010/BMD-2332 from M.F. and F.S.-M.), Instituto Salud Carlos III (Red Cardiovascular RD 12-0042-0056 to F.S.-M.; BIOIMID to M.F. and F.S.-M.), the European Research Council (ERC-2011-AdG 294340-GENTRIS to F.S.-M.) and the Ramón Areces foundation (M.F. and F.S.-M.).

AUTHOR CONTRIBUTIONS

D.C. performed mice experimentation, analyzed and interpreted data and wrote the manuscript; M.L.S. collaborated on mice experimentation, data interpretation and writing of the manuscript; H.d.l.F. performed analysis of psoriatic patients; R.S.-D. and O.M.-G. performed quantitative PCR; I.J., A.F. and J.V. performed proteomic and metabolic-mass spectrometry analyses; C.P. contributed expertise in radioactive assays; M.F., M.V.-M. and P.M.F.-S. provided reagents and helped with the revision of the manuscript; E.D. provided biopsies from psoriatic patients and their clinical diagnostics; P.M. helped to design research, provided reagents, collaborated in data interpretation and manuscript writing; and F.S.-M. planned research, discussed results and collaborated in writing the manuscript.

COMPETING FINANCIAL INTERESTS

The authors declare no competing financial interests.

1. Di Meglio, P., Villanova, F. & Nestle, F.O. Psoriasis. *Cold Spring Harb. Perspect. Med.* **4**, a015354 (2014).
2. Lowes, M.A., Suárez-Fariñas, M. & Krueger, J.G. Immunology of psoriasis. *Annu. Rev. Immunol.* **32**, 227–255 (2014).
3. Leonardi, C. *et al.* Anti-interleukin-17 monoclonal antibody ixekizumab in chronic plaque psoriasis. *N. Engl. J. Med.* **366**, 1190–1199 (2012).
4. Chan, J.R. *et al.* IL-23 stimulates epidermal hyperplasia via TNF and IL-20R2-dependent mechanisms with implications for psoriasis pathogenesis. *J. Exp. Med.* **203**, 2577–2587 (2006).
5. Zheng, Y. *et al.* Interleukin-22, a T_H17 cytokine, mediates IL-23-induced dermal inflammation and acanthosis. *Nature* **445**, 648–651 (2007).
6. Wolk, K. *et al.* IL-22 and IL-20 are key mediators of the epidermal alterations in psoriasis while IL-17 and IFN-γ are not. *J. Mol. Med.* **87**, 523–536 (2009).
7. Van Belle, A.B. *et al.* IL-22 is required for imiquimod-induced psoriasiform skin inflammation in mice. *J. Immunol.* **188**, 462–469 (2012).
8. Prans, E. *et al.* Copy number variations in *IL22* gene are associated with psoriasis vulgaris. *Hum. Immunol.* **74**, 792–795 (2013).
9. Shimauchi, T. *et al.* Serum interleukin-22 and vascular endothelial growth factor serve as sensitive biomarkers but not as predictors of therapeutic response to biologics in patients with psoriasis. *J. Dermatol.* **40**, 805–812 (2013).
10. Wolk, K. *et al.* IL-22 regulates the expression of genes responsible for antimicrobial defense, cellular differentiation, and mobility in keratinocytes: a potential role in psoriasis. *Eur. J. Immunol.* **36**, 1309–1323 (2006).
11. Martin, B., Hirota, K., Cua, D.J., Stockinger, B. & Veldhoen, M. Interleukin-17-producing γδ T cells selectively expand in response to pathogen products and environmental signals. *Immunity* **31**, 321–330 (2009).
12. Qiu, J. *et al.* The aryl hydrocarbon receptor regulates gut immunity through modulation of innate lymphoid cells. *Immunity* **36**, 92–104 (2012).
13. Veldhoen, M., Hirota, K., Christensen, J., O'Garra, A. & Stockinger, B. Natural agonists for aryl hydrocarbon receptor in culture medium are essential for optimal differentiation of Th17 T cells. *J. Exp. Med.* **206**, 43–49 (2009).
14. Smirnova, A. *et al.* Evidence for new light-independent pathways for generation of the endogenous aryl hydrocarbon receptor agonist FICZ. *Chem. Res. Toxicol.* **29**, 75–86 (2016).
15. Sinclair, L.V. *et al.* Control of amino-acid transport by antigen receptors coordinates the metabolic reprogramming essential for T cell differentiation. *Nat. Immunol.* **14**, 500–508 (2013).
16. Cai, Y. *et al.* Pivotal role of dermal IL-17-producing γδ T cells in skin inflammation. *Immunity* **35**, 596–610 (2011).
17. Laggner, U. *et al.* Identification of a novel proinflammatory human skin-homing Vγ9Vδ2 T cell subset with a potential role in psoriasis. *J. Immunol.* **187**, 2783–2793 (2011).
18. Pantelyushin, S. *et al.* Rorγt$^+$ innate lymphocytes and γδ T cells initiate psoriasiform plaque formation in mice. *J. Clin. Invest.* **122**, 2252–2256 (2012).
19. Ahlfors, H. *et al.* IL-22 fate reporter reveals origin and control of IL-22 production in homeostasis and infection. *J. Immunol.* **193**, 4602–4613 (2014).
20. Sumaria, N. *et al.* Cutaneous immunosurveillance by self-renewing dermal γδ T cells. *J. Exp. Med.* **208**, 505–518 (2011).
21. González-Amaro, R., Cortés, J.R., Sánchez-Madrid, F. & Martín, P. Is CD69 an effective brake to control inflammatory diseases? *Trends Mol. Med.* **19**, 625–632 (2013).
22. Sancho, D. *et al.* CD69 downregulates autoimmune reactivity through active transforming growth factor-β production in collagen-induced arthritis. *J. Clin. Invest.* **112**, 872–882 (2003).
23. Martín, P. *et al.* The leukocyte activation antigen CD69 limits allergic asthma and skin contact hypersensitivity. *J. Allergy Clin. Immunol.* **126**, 355–365, 365.e1–365.e3 (2010).
24. Cruz-Adalia, A. *et al.* CD69 limits the severity of cardiomyopathy after autoimmune myocarditis. *Circulation* **122**, 1396–1404 (2010).
25. Radulovic, K. *et al.* CD69 regulates type I IFN-induced tolerogenic signals to mucosal CD4 T cells that attenuate their colitogenic potential. *J. Immunol.* **188**, 2001–2013 (2012).
26. Rutz, S., Eidenschenk, C. & Ouyang, W. IL-22, not simply a Th17 cytokine. *Immunol. Rev.* **252**, 116–132 (2013).
27. Martín, P. *et al.* CD69 association with Jak3/Stat5 proteins regulates Th17 cell differentiation. *Mol. Cell. Biol.* **30**, 4877–4889 (2010).
28. Mackay, L.K. *et al.* The developmental pathway for $CD103^+CD8^+$ tissue-resident memory T cells of skin. *Nat. Immunol.* **14**, 1294–1301 (2013).
29. Awasthi, A. *et al.* Cutting edge: IL-23 receptor gfp reporter mice reveal distinct populations of IL-17-producing cells. *J. Immunol.* **182**, 5904–5908 (2009).
30. Shiow, L.R. *et al.* CD69 acts downstream of interferon-α/β to inhibit S1P1 and lymphocyte egress from lymphoid organs. *Nature* **440**, 540–544 (2006).
31. Ribot, J.C. *et al.* CD27 is a thymic determinant of the balance between interferon-γ- and interleukin 17-producing gammadelta T cell subsets. *Nat. Immunol.* **10**, 427–436 (2009).
32. Kashiwagi, H., Yamazaki, K., Takekuma, Y., Ganapathy, V. & Sugawara, M. Regulatory mechanisms of SNAT2, an amino acid transporter, in L6 rat skeletal muscle cells by insulin, osmotic shock and amino acid deprivation. *Amino Acids* **36**, 219–230 (2009).
33. Taylor, P.M. Role of amino acid transporters in amino acid sensing. *Am. J. Clin. Nutr.* **99**, S223–S230 (2014).
34. Harden, J.L. *et al.* The tryptophan metabolism enzyme L-kynureninase is a novel inflammatory factor in psoriasis and other inflammatory diseases. *J. Allergy Clin. Immunol.* **137**, 1830–1840 (2016).

35. Rizzo, H.L. *et al.* IL-23-mediated psoriasis-like epidermal hyperplasia is dependent on IL-17A. *J. Immunol.* **186**, 1495–1502 (2011).
36. Boniface, K. *et al.* IL-22 inhibits epidermal differentiation and induces proinflammatory gene expression and migration of human keratinocytes. *J. Immunol.* **174**, 3695–3702 (2005).
37. Mitra, A., Raychaudhuri, S.K. & Raychaudhuri, S.P. IL-22 induced cell proliferation is regulated by PI3K/Akt/mTOR signaling cascade. *Cytokine* **60**, 38–42 (2012).
38. Finlay, D.K. *et al.* PDK1 regulation of mTOR and hypoxia-inducible factor 1 integrate metabolism and migration of $CD8^+$ T cells. *J. Exp. Med.* **209**, 2441–2453 (2012).
39. Mascanfroni, I.D. *et al.* Metabolic control of type 1 regulatory T cell differentiation by AHR and HIF1-α. *Nat. Med.* **21**, 638–646 (2015).
40. Fenczik, C.A. *et al.* Distinct domains of CD98hc regulate integrins and amino acid transport. *J. Biol. Chem.* **276**, 8746–8752 (2001).
41. Lauzurica, P. *et al.* Phenotypic and functional characteristics of hematopoietic cell lineages in CD69-deficient mice. *Blood* **95**, 2312–2320 (2000).
42. Di Meglio, P. *et al.* Activation of the aryl hydrocarbon receptor dampens the severity of inflammatory skin conditions. *Immunity* **40**, 989–1001 (2014).
43. Walter, A. *et al.* Aldara activates TLR7-independent immune defence. *Nat. Commun.* **4**, 1560 (2013).
44. van den Bogaard, E.H. *et al.* Genetic and pharmacological analysis identifies a physiological role for the AHR in epidermal differentiation. *J. Invest. Dermatol.* **135**, 1320–1328 (2015).
45. Furue, M. *et al.* Gene regulation of filaggrin and other skin barrier proteins via aryl hydrocarbon receptor. *J. Dermatol. Sci.* **80**, 83–88 (2015).
46. Serre, K. & Silva-Santos, B. Molecular mechanisms of differentiation of murine pro-inflammatory γδ T cell subsets. *Front. Immunol.* **4**, 431 (2013).
47. Shibata, K. *et al.* Notch-Hes1 pathway is required for the development of IL-17-producing γδ T cells. *Blood* **118**, 586–593 (2011).

ONLINE METHODS

Mice. Wild-type, CD69-deficient, OT-II and OT-II CD69-deficient mice (C57BL/6 background) were previously described[27]. Homozygous AhR-deficient and wild-type littermate mice (C57BL/6 background) were obtained from P. M. Fernández-Salguero's group (University of Extremadura, Badajoz, Spain). IL-23R-GFP.KI reporter mice (C57BL/6 background) were previously described[29]. For experiments with chimeric mice, wild-type B6SJL CD45.1 mice (Jackson) were used as donor of bone marrow progenitor cells. Sex- and age-matched mice (8–12 weeks) were used for *in vitro* and *in vivo* experiments. All animals were kept in pathogen-free conditions at the animal facility of Centro Nacional de Investigaciones Cardiovasculares. Experimental procedures were approved by the local Committee for Research Ethics and are in accordance to Spanish and European guidelines.

Human subjects. Patients with moderate to severe psoriasis that were recruited in the study had a psoriasis area and severity index of ≥8.0 and washout periods of 14 d for topical corticosteroids; 28 d for conventional systemic therapy, including corticosteroids, methotrexate, cyclosporine, acitretin and phototherapy; and 84 d for biological agents. Skin punch biopsies (5 mm) were obtained from lesional-plaque-type psoriasis and non-lesional area. Healthy skin biopsies were also collected from nine surgical patients without cutaneous disease. Half of each skin biopsy was immediately frozen and processed for RNA extraction, while remaining sample was embedded in OCT for immunofluorescence staining. Blood samples were also collected from ten psoriatic patients and five healthy volunteers, for flow cytometry analysis. The study was approved by the Hospital La Princesa ethics committee. All the participants gave their written informed consent.

Establishment of psoriasis-like model. CD69-deficient and wild-type mice were intradermally injected in the ears with 20 µl of vehicle (PBS) or 500 ng of recombinant mouse IL-23 (eBioscience) using a 33-gauge needle. Injections were repeated on alternate days for a total of seven to ten doses. Ear thickness was measured on days without injections with an AccuteRemote 0.5-mm-thickness gauge dial micrometer (TECLOCK). All measurements were performed blinded. Mice were sacrificed and skin samples were collected for staining with H&E and immunohistochemistry. If required, half of ears were rapidly frozen in liquid nitrogen for subsequent isolation of total RNA or detection of tissue cytokines. Recombinant mouse IL-22 (eBioscience) (500 ng in 20 µl of PBS) was intradermally injected alone or in combination with IL-23, where indicated. In addition, in some experiments mice received an intraperitoneal injection of CH-223191 (10 mg per kg body weight) or vehicle (DMSO) together with the IL-23 intradermal administration. When indicated, 250 µg/mice of secretion inhibitor brefeldin A dissolved in ethanol (SIGMA) was intraperitoneally administrated 5 h before sacrifice. For experiments with chimeric mice, wild-type and CD69-deficient mice (CD45.2 haplotype) were lethally irradiated (13 Gy divided in two sessions) and transplanted with 5×10^6 per mice of whole bone marrow cells obtained from B6 SJL (CD45.1 haplotype) wild-type mice. Reconstitution was allowed for 2 months before starting the protocol of IL-23 injections. In some experiments, mice received a daily intraperitoneal administration of L-Trp (50 mg per kg body weight) or its vehicle (DMSO) along the IL-23 protocol. L-Trp dose was chosen by published assays that proved it to be safe for mice and that it induced *Cyp1a1* transcriptional expression in the liver[48]. As described, FICZ can be found in light-oxidized preparation of L-Trp[13]; for this reason, fresh solutions were daily prepared and kept protected from light.

Skin histology and immunohistochemistry staining. Skin samples were fixed in formaldehyde and embedded in paraffin using routine methods. Slices (4–5 µm) were stained with H&E and analyzed by two evaluators 'blinded' to sample identity. Consecutive images were acquired at several magnifications with an optical microscope (DM2500; Leica) equipped with a CCD camera (DFC420; Leica), with Leica Application Suite software (version 4.3.0). Dermal and epidermal thickness were measured every 100 µm, from the ear surface to a depth of about 5 mm, using ImageJ software. For immunohistochemical staining, skin sections were deparaffinized, boiled in antigen retrieval solution (10 mM sodium citrate, 0,05% Tween 20, pH6), and incubated with the following primary monoclonal antibodies (**Supplementary Table 2**): rabbit anti-mouse Ki67 (Master Diagnostica),rat anti-mouse F4/80 and Ly6G (Abcam), rabbit anti-mouse STAT3, phospho-STAT3 (Tyr 705) and phospho-STAT3 (Ser727) (Cell Signaling); followed by specific secondary antibodies from Dako (**Supplementary Table 2**): envision flex system for Ki67, Rabbit anti rat HRP for F480 and Ly6G; and Goat anti Rabbit HRP for STAT3-related antibodies. Slides were developed with DAB substrate (Dako K3468) and then counterstained with Mayers hematoxylin. Epidermal $Ki67^+$ frequency was determined as the number of $Ki67^+$ nuclei observed each 100 µm, also from the ear surface to a depth of about 5 mm, $n = 5$ mice per group. STAT3 staining in keratinocytes was quantified in at least five fields (×40 magnification) from each IL-23-treated mouse (five mice per group). Fields were quantified for mean gray value in the epidermal layer with ImageJ software. Percentage of epidermal area stained for STAT3 was also assessed. Nuclear staining of each phosphorylation site for STAT3 in keratinocytes was also counted as indicative of its transcriptional activity.

RNA extraction and real-time quantitative PCR. RNA from mouse and human samples was isolated using a QIAGEN RNeasy Kit (Qiagen). Residual DNA contamination was removed with the Turbo DNA-free Kit (Ambion). Total RNA (200ng) was reverse transcribed to cDNA with a Reverse Trancription Kit (Applied Biosystem). Quantitative PCR was then performed in an AB7900_384 (Applied Biosystem) using SYBR Green (Applied Biosystems) as reporter. Gene-specific primers used are listed in **Supplementary Table 3**. Expression of each gene of interest was normalized to at least two housekeeping genes (*Actb* or *Gapdh*). Data (calculated by the $2^{-\Delta\Delta Ct}$ method or the standard-curve method (for human samples)) are presented as results for CD69-deficient mice relative to those of wild-type mice samples, or treated samples relative to control samples, or psoriatic patients relative to the mean value obtained for healthy donors.

Flow cytometry and sorting of skin γδ T cells. Animals were euthanized and ears were collected and digested with Liberase TM (Roche) (0.25 mg/ml in free-serum medium RPMI), for 60 min at 37 °C. Enzyme was inhibited by adding 50 ml of PBS supplemented with 0.5% of BSA and 0.05mM of EDTA (PBS-BSA-EDTA) and tissue was mechanically disrupted and filtered to obtain a skin cell suspension. Epidermis and dermis separation was conducted after incubation of ears with trypsin-EDTA solution 1X (Sigma), 45 min at 37 °C. The two layers were separated with forceps, and the epidermis was directly homogenized while the dermis was incubated with Liberase TM by 30 min. Incubation of skin cell suspensions with anti-FcRII/III (clone 2.4G2; **Supplementary Table 2**) was always conducted before staining. For flow cytometry analysis of IL-23 -induced inflammation the following anti-mouse antibodies were used (**Supplementary Table 2**): CD45, F480 and γδTCR obtained from eBioscience, CD11c, CD11b, GR1, Ly6G, Ly6C and CD3 from BD Bioscience. Absolute count of cells in the skin was conducted using BD Trucount Tubes (BD). For sorting skin γδ T cells, cell suspensions obtained from ears were stained with DAPI, anti-CD3 (BD Biosciences) and anti-γδTCR (eBioscience). Directed labeled antibodies against mouse IL-23R (R&D) and RORγt (EBioscience) (**Supplementary Table 2**) were also used in skin suspensions. To analyze the expression of CD69 in human circulating γδ T cells, freshly obtained peripheral blood mononuclear cells (PBMCs) (1×10^6) from psoriatic patients and healthy subjects were stained with the following mouse anti-human mAbs: anti-CLA (BD Bioscience), anti-TCR $V_\gamma 9$ (BioLegend) and anti-CD8, anti-CD69, anti-CD4 and anti-CD3 (BD Bioscience) (**Supplementary Table 2**). Cell samples were acquired in a FACSCanto Flow Cytometer (BD), and analyzed with FlowJo software (Tree Star).

Cell cultures for T_H17 and γδ T cells. Cells were routinely cultured in RPMI 1640 medium (Sigma-Aldrich) supplemented with 5% FCS, 2 mM L-glutamine, 100 U/ml penicillin 100 µg/ml streptomycin, and 50 nM of β-mercaptoethanol. In some cases, IMDM (Sigma-Aldrich) was used, supplemented as for RPMI. Also, in some cases, RPMI medium was supplemented with 11 mg/liter L-Trp (Invitrogen) to adjust it to the concentrations found in IMDM. Naive $CD4^+$ T cells were obtained by negative selection using an auto-MACSTM Pro Separator (Miltenyi Biotec) and subjected to *in vitro* T_H17 differentiation (1×10^6 cells/ml) with the following cytokine cocktail: blocking anti-IFN-γ (5 µg/ml) and anti-IL-4 (5 µg/ml) mAbs, IL-6 (50 ng/ml), IL-23 (10 ng/ml),

IL-1β (10 ng/ml) and TGF-β1 (5 ng/ml) for 2-4 d (**Supplementary Table 2**). Naive CD4$^+$ T cells obtained from OT-II and OT-II CD69-deficient were cultured in the presence of irradiated antigen-presenting cells (T cell–depleted splenocytes) and OVA peptide 323-339 (OVA; 10 μg/ml). Those experiments with OT-II mice were specifically used for flow cytometry analysis and ELISA. When T_H17 cells were required for mRNA analysis expression and western blot, naive CD4 T cells were isolated from wild-type and CD69-deficient mice and were activated with plate-bound anti-CD3 (5 μg/ml) plus anti-CD28 (2 μg/ml) (**Supplementary Table 2**), using the same cytokine cocktail described above for OT-II mice. The AhR ligand 6-formylindolo (3,2-b) carbazole (FICZ) (Enzo Life Science) (350 nM), the AhR specific inhibitor CH-223191 (Sigma) (3 μM) and the LAT1/CD98 inhibitor 2-amino-2-norbornanecarboxylic acid (BCH) (Sigma) (50 mM) were added at the start of some cultures. Before intracellular cytokine staining, cells were restimulated for 4 h with 50 ng/ml phorbol dibutyrate (PMA) and 500 ng/ml ionomycin in the presence of brefeldin A (1 μg/ml) (BD Biosciences).

Sorted dermal and epidermal γδ T cells (1×10^4 cells/ml) from CD69-deficient and wild-type mice were incubated for 24 h on plate-bound anti-CD3 (5 μg/ml), soluble anti-CD28 (2 μg/ml) (**Supplementary Table 2**) and IL-23 plus IL-1β (10 ng/ml each one). For γδ T cells, no re-stimulation was required, and only brefeldin A (1 μg/ml) was added for last 4 h of culture.

Both γδ and *in vitro*–skewed T_H17 cells were fixed and permeabilized with Fix & Perm solution (BD Biosciences) and stained with anti-IL-22 (eBioscience) and anti-CD69, anti-CD25 and anti-IL-17 (BD Pharmingen) (**Supplementary Table 2**). IL-22 and IL-17 production in the cultures supernatants was quantified with the IL-22/IL-17 Ready-Set-Go ELISA kits (eBioscience). In some experiments, AhR nuclear expression was analyzed by flow cytometry using the Foxp3/Transcription Factor Staining Buffer Set (eBioscience) and rabbit anti-mouse AhR (Enzo Life Science) followed by Alexa-647 conjugated Goat anti rabbit. CD98 expression was detected with an Alexa 647-conjugated rat anti-mouse antibody (BioLegend) while for LAT1 expression a rabbit anti mouse antibody (Santa Cruz Biotech) followed by an Alexa-647 conjugated goat anti rabbit was used (all antibodies, **Supplementary Table 2**). Directed labeled 647-mouse anti STAT5 (pY694) and PE-mouse anti-STAT3 (pY705) (BD Bioscience) was used with Fix&Perm kit (life technologies) modified for methanol permeabilization (antibodies, **Supplementary Table 2**). Mouse isotype-matched control antibodies obtained from BD were used as required (**Supplementary Table 2**).

IL-22 production in human γδ T cells. PBMCs from psoriatic patients ($n = 3$) were adjusted at 1×10^6 cells/ml in culture medium EX-VIVO 15 (Lonza, Belgium) supplemented with L-Trp (15 mg/L) and expanded with zoledronic acid (5 μM) as previously reported[49]. At day 0 (d0), PBMCs (1×10^6) were stimulated in a 24-well plate in the presence or absence of IL-23 (50 ng/ml), IL-1b (50 ng/ml), IL-6 (100 ng/ml) and TGF-β (1 ng/ml). Where indicated, LAT-1 inhibitor BCH (50 mM) or CH-223191 (3 μM) were also added to the cultures. At d2, IL-2 (100 U/ml) was added and cells were analyzed for IL-22 production at d4 of culture. First, PBMCs were incubated with human PercP-anti-Vδ2 (Biolegend) during 30 min at 4 °C, then cells were fixed (PFA 2% 10 min TA) and incubated in saponin (0.3% 10 min TA) before incubation with APC anti-human IL-22 (eBioscience). Cells were analyzed in a FACSCanto flow cytometer. Dead cell were excluded using fixable viability staining 510 (BD Biosciences). IL-22 secretion was quantified in the supernatant using Human IL-22 Ready-Set-Go ELISA kit (eBioscience).

Immunofluorescence staining and *in situ* proximity ligation assay (PLA). Frozen sections of human skin biopsies were fixed in cold acetone and blocked in PBS containing 5% of donkey serum and 100 mM/ml human γ-globulin (Sigma-Aldrich, St Louis, MO, USA). Sections were incubated with the following anti-human primary Abs (**Supplementary Table 2**): mouse monoclonal anti-CD69 (TP1.55), rabbit polyclonal anti-IL-22 (Bios, Mass USA) and goat anti-TCR-γ9 (Santa Cruz Biotechnology) for 1 h. The secondary Abs used were: AlexaFluor 488-conjugated donkey anti-rabbit, AlexaFluor 568-conjugated donkey anti-goat and AlexaFluor 647-conjugated donkey anti-mouse. Nuclei were counterstained with DAPI. Immunofluorescence pictures were taken using a Zeiss LSM Confocal microscope and analyzed with LSM image browser software.

J77 Jurkat cells or CD69-stable overexpressing J77 Jurkat cells were fixed in ice-cold methanol at -20 °C for 10 min and blocked with 1% BSA and 10% donkey serum in PBS for 2 h at room temperature. Then cells were incubated with mouse anti human CD69 mAb (TP1/55), Rabbit anti human LAT1 (Cell Signaling) or rabbit anti human CD98 (Santa Cruz) for 1 h at 37 °C (antibodies, **Supplementary Table 2**). Secondary antibodies from donkey species (**Supplementary Table 2**) or PLA detection kit reagents (SIGMA) were added for visualization of co-localization or proximity assay of these molecules in the membrane. For each duolink pair confocal microphotographs quantification of red dots per cells was conducted using Imaris Software.

Amino acid uptake assay. Naive CD4$^+$ T cells obtained from CD69-deficient and wild-type mice were cultured (1×10^6 cells/ml) in RPMI medium for 24 h, in the presence of anti-CD3 (5 μg/ml) and anti-CD28 (2 μg/ml) (**Supplementary Table 2**). Similarly, spleen/lymph-nodes γδ T cells were sorted as CD27$^+$ and CD27$^-$ and stimulated for 24 h with IL-23 (10 ng/ml) and IL-1β (10 ng/ml) in RPMI medium (1×10^5 cells/ml). ^{3}H-radiolabeled L-Trp, L-Phe and L-Leu (PerkinElmer) were added (0.5 μCi/ml) in HBSS (GIBCO) with a final extracellular L-Leu concentration of 5 μM. Amino acid uptake was measured at 5, 10, 15 and 20 min at 37 °C. Uptake was stopped by the addition of 20 mM cold L-Leu to quench System L. For the purpose of kinetic analysis, uptake at 5-min was defined as the initial uptake rate and data were analyzed only at the time interval where incorporation was linear. At the end of the assay period, cells were harvested onto glass-fiber filters using a Tomtec 96-well parallel harvester and washed vigorously for 30 s with PBS solution. β-radioactivity was counted in a Beckman LS 6500 Multi-Purpose Scintillation Counter (Beckman Coulter). Nonspecific binding of radioactivity to the filters (based on wells containing radiolabeled substrate without cells) was typically <10% of the total signal and was subtracted from each data point. Five replicates were assessed for each data point.

CD69 internalization assay. Plasmid for LAT1-mCherry expression was provided by D. Rotin(University of Toronto, USA). CD69-eGFP plasmid has been generated in our lab. HEK 293 cells maintained in Dulbecco's Modified Eagle Medium (DMEM) supplemented with 4 mM L-glutamine and 10% FBS were transfected with plasmids expressing LAT1-mCherry and CD69-eGFP using Lipofectamine Reagent (ThermoFisher). Mouse anti human CD69 monoclonal antibody (TP1/55; **Supplementary Table 2**) was directly labeled with Zenon Alexa-647 labeling Kit (Life Technologies) and incubated for 30 min with transfected cells at 37 °C. Cells were washed with PBS and fixed with 1% paraformaldehyde. Immunofluorescence pictures were taken using a Zeiss LSM Confocal microscope and analyzed with LSM image browser software.

Proteomic study design and in-gel protein digestion. For the proteomics assay, naive CD4$^+$ T cells obtained from CD69-deficient and wild-type mice were activated with PMA (50 ng/ml) plus ionomycin (750 ng/ml) for 18 h. After assessing CD69 expression by flow cytometry in wild-type cells, about 5×10^6 whole cells were incubated with hamster anti-mouse CD69 mAb (clone: H1. 2F3, Abcam) and isotype-matched control mAb (hamster anti-mouse CD31, clone 2H8, AbD Serotec) (**Supplementary Table 2**), already immobilized in Dynabeads Protein G (Life Technologies), in serum-free RPMI medium, for 1 h at 4 °C. Thereafter, cells were lysed in ice-cold 1% CHAPS lysis buffer containing 1 mM $CaCl_2$ and protease inhibitor cocktail (Complete, Roche) for 1 h at 4 °C. Magnetic separation of beads allows collecting proteins associated to CD69 and consecutive washes with ice-cold lysis buffer for 4 h for reduction of nonspecific interactions.

Proteins were digested in the gel using the following protocol. 15 μl of beads were resuspended in 30 μl of sample buffer and loaded into SDS-PAGE gel. The run was stopped as soon as the front entered 2 mm into the resolving gel. The protein band was excised and digested with 20 ng/μl trypsin at 10:1 protein: trypsin (w/w) ratio. The resulting peptides were desalted onto C18 OMIX tips (Agilent Technologies) before LC-MS/MS analysis.

Mass spectrometry. Analyses were performed using a nano-HPLC Easy nLC 1000 coupled to a linear ion trap-Orbitrap Elite hybrid mass spectrometer (Thermo Scientific). Peptides samples were loaded onto a home-made C18 reversed-phase (RP) nano-column (100 μm I.D., 45 cm) and separated in

doi:10.1038/ni.3504

a continuous gradient consisting of 8–35% B for 20 min and 35–90% B for 2 min (B = 90% acetonitrile, 0.1% formic acid) at 300 nL/min. A Picotip emitter nanospray needle (New Objective) was used for peptide ionization. An enhanced FT-resolution spectrum in the mass range of m/z 390–1,600 followed by data-dependent MS/MS spectra of the 20 most intense parent ions were acquired along the chromatographic run. Normalized CID collision energy was set to 35% and a 2-Da of parent ion mass isolation width.

Peptide identification and statistics. Peptide identification from MS/MS spectra was done using Sequest running under Proteome Discoverer 1.4 (Thermo Scientific), allowing two missed cleavages, and using 800 ppm and 0.02 ppm precursor and fragment mass tolerances, respectively. Met oxidation and Cys carbamydomethylation were selected as dynamic modifications. The MS/MS raw files were searched against the Human Uniprot database (March 2013) and results were analyzed using the probability ratio method. Post-search result filtering by mass error was done as described. For each scan, if the mass deviation fell outside the ± 5 ppm window, the corresponding XCorr was rescored to 0, whereas the pRatio was reassigned a value of 2. The false-discovery rate (1% FDR) was estimated from the search results against a decoy database.

Co-immunoprecipitation and immunoblot analysis. A human-Jurkat-cell-derived T cell line (J77) activated with PMA (50 ng/ml) and Ionomycin (500 ng/ml) for 18 h was used for co-immunoprecipitation experiments. The following mouse anti human mAbs generated in the laboratory were used (**Supplementary Table 2**): anti-CD69 (TP1/8), anti-CD98 (FG1/8), and anti-CD13 (Tea1/8) as negative control, using the same protocol and lysis buffer described for the proteomic assay. Co-immunoprecipitated proteins were separated by SDS-PAGE and immunoblotted with the following rabbit polyclonal anti human Abs (**Supplementary Table 2**): anti-CD69 (Abcam) and anti-CD98 (Santa Cruz Biotechnology). Anti-human LAT1 antiserum was provided by P. Taylor (Dundee, UK).

Immunoblot analysis of mTORC signaling was conducted with *in vitro* cultured T_H17 cells from CD69-deficient and wild-type mice. After the lysis with RIPA buffer supplemented with protease and phosphatase inhibitor cocktails (Roche), the lysates were separated by SDS-PAGE and immunoblotted with the following rabbit Abs (**Supplementary Table 2**): antibody to mTORC1 phosphorylated at Ser2448, antibody to total mTORC1, antibody to S6 phosphorylated at Ser235 and Ser236, antibody to total S6, antibody to 4E-BP1 phosphorylated at Thr37 and Thr46, and antibody to total 4E-BP1 (Cell Signaling). Control of protein quantity was assessed with rabbit anti mouse β actin antibody (Santa Cruz; **Supplementary Table 2**). All primary antibodies were detected with HRP conjugated goat anti-rabbit (Pierce; **Supplementary Table 2**). Protein bands were analyzed using the LAS-3000 CCD system and Image Gauge 3.4 (Fuji Photo Film Co., Tokyo, Japan).

Treatment of samples for L-Trp and FICZ quantification. Three biological replicates of 50×10^6 Jurkat T cells were incubated in RPMI 1640 medium w/o amino acids (US Biological Life Sciences) supplemented with 5% FCS, 2 mM L-glutamine, 100 U/ml penicillin 100 µg/ml streptomycin, non-essential amino acids (Hyclone) and L-Trp (50 mg/ml), and were treated or not with BCH (50 mM) for 24 h. The cell pellets were thawed on ice and subjected to three freeze–thaw cycles for complete cell disruption, protein precipitation and metabolite extraction. Samples were suspended in 100 µL mixture composed by MeOH:MTBE (1:1 v/v), vortex-mixed, placed in liquid nitrogen for 10 s and thaw in an ice bath (for 10 s) three times. Samples were then sonicated for 6 min and vortex-mixed for 1 min. The entire protocol was repeated three times. Subsequently samples were centrifuge at 18,000*g* for 20 min at 10 °C and the supernatants were collected (extract A) and stored at –20 °C. The residual cell pellets were extracted again with 100 µL of MeOH:MTBE (1:1 v/v), following the same procedure. Supernatants were collected after centrifugation (extract B) and the two extracts were combined.

Cell culture medium samples were thaw on ice and vortex-mixed few seconds. Then, 300 µL of MeOH:MTBE (1:1 v/v), were added to 100 µL of sample, vortex-mixed and incubated on ice for 20 min. Supernatants were collected by centrifugation at 18000*g* for 20 min at 4 °C. Finally, cells and media extracts were diluted 1:5 (for analysis of FICZ) and 1:1,000 (for the analysis of Trp) with acetonitrile:water (10:90 v/v) containing 0.1% of formic acid. Samples were vortex-mixed, centrifuged at 18,000*g* for 10 min at 10 °C to allow particle precipitation and transfer in a HPLC glass vial with 300 µL insert.

Liquid chromatography–mass spectrometry determination of FICZ and L-Trp. LC-MS grade water, formic acid, acetonitrile, and HPLC grade methyl tert-butyl ether (MTBE) and Tryptophan (Trp) were purchased from Sigma-Aldrich. Methanol (MeOH), was purchased form Fischer Chemical and formylindolo (3,2-b)carbazole (FICZ) from Enzo Life Science.

High-resolution parallel reaction monitoring (PRM) of FICZ and Trp were carried out on an Easy-nLC 1000 nano HPLC (Thermo Scientific, Waltham, Massachusetts, USA) coupled to a trihybrid quadrupole-linear ion trap-orbitrap mass spectrometer (Orbitrap Fusion Tribrid, Thermo Scientific) operating in positive polarity mode. A volume of 10 µL of diluted extracts were loaded onto an Easy-Spray (Thermo Scientific) C-18 reversed-phase nano-column (75 µm I.D., 50 cm) and metabolites were separated with mobile phase composed by A) water with 0.1% of formic acid and B) acetonitrile:water (90:10 v/v) with 0.1% of formic acid, at 200 nL/min and 50 °C. For analysis of FICZ, the gradient started at 35% B to 100% B in 10 min, holding 100% B for 12 min and returned to starting condition in 2 min, keeping the re-equilibration time for 30 min. For analysis of Trp, the gradient started at 35% B to 100% B in 15 min, holding 100% B for 9 min and returned to starting condition in 2 min, keeping the re-equilibration time for 30 min.

Metabolites were monitored by targeting the corresponding [M+H]+ ions to acquire complete MS2 spectra. Precursor ion of the FICZ and Trp (corresponding to m/z 285.10224 and 205.09715, respectively) were isolated by the quadrupole analyzer and targeted for higher-energy collisional dissociation (HCD). HCD collision energy was optimized for each compound and fragments were detected with 15000 resolution in orbitrap. Targeted parameters included a 3 Thompson isolation window around the m/z values of interest, 2.7 kV spray voltage and 310 °C as capillary temperature. Data analysis was performed with Xcalibur 2.2 (Thermo Scientific).

Statistical analysis. After analysis of data distribution with Kolmogorov Smirnov test, the statistical significance was assessed by one-tailed unpaired Student's *t*-test, one-way ANOVA with Newman-Keuls multiple-comparisons *t*-test or two-way ANOVA with Bonferroni's multiple-comparisons post-test, as required. For kinetic assay of amino acid uptake, a linear regression with slopes comparison was conducted. All analysis was performed with GrapPhad software. Differences were considered significant at $P < 0.05$.

48. Mukai, M. & Tischkau, S.A. Effects of tryptophan photoproducts in the circadian timing system: searching for a physiological role for aryl hydrocarbon receptor. *Toxicol. Sci.* **95**, 172–181 (2007).
49. Kondo, M. *et al.* Expansion of human peripheral blood gammadelta T cells using zoledronate. *JoVE* **55**, 3152 (2011).

PLOS | PATHOGENS

RESEARCH ARTICLE

HDAC6 controls innate immune and autophagy responses to TLR-mediated signalling by the intracellular bacteria *Listeria monocytogenes*

Olga Moreno-Gonzalo[1,2], Marta Ramírez-Huesca[1,2], Noelia Blas-Rus[1,2], Danay Cibrián[1,2,3], María Laura Saiz[1,2], Inmaculada Jorge[4], Emilio Camafeita[4], Jesús Vázquez[3,4], Francisco Sánchez-Madrid[1,2,3]*

1 Cell-cell Communication Laboratory, Vascular Pathophysiology Area, Centro Nacional Investigaciones Cardiovasculares (CNIC), Madrid, Spain, **2** Servicio de Inmunología, Hospital Universitario de la Princesa, Instituto Investigación Sanitaria Princesa (IIS-IP)-Universidad Autónoma de Madrid (UAM), Madrid, Spain, **3** CIBER CARDIOVASCULAR, Madrid, Spain, **4** Proteomics Unit, Vascular Pathophysiology Area, Centro Nacional Investigaciones Cardiovasculares (CNIC), Madrid, Spain

* fsmadrid@salud.madrid.org

Citation: Moreno-Gonzalo O, Ramírez-Huesca M, Blas-Rus N, Cibrián D, Saiz ML, Jorge I, et al. (2017) HDAC6 controls innate immune and autophagy responses to TLR-mediated signalling by the intracellular bacteria *Listeria monocytogenes*. PLoS Pathog 13(12): e1006799. https://doi.org/10.1371/journal.ppat.1006799

Editor: Igor Eric Brodsky, University of Pennsylvania, UNITED STATES

Received: May 29, 2017

Accepted: December 8, 2017

Published: December 27, 2017

Data Availability Statement: All relevant data are within the paper and its Supporting Information files.

Funding: The funders had no role in study design, data collection and analysis, decision to publish, or preparation of the manuscript. This study was supported by the following grants to FSM: SAF2014-55579-R from the Spanish Ministry of Economy and Competitiveness, INDISNET-S2011/BMD-2332 from the Comunidad de Madrid, CIBER

Abstract

Recent evidence on HDAC6 function underlines its role as a key protein in the innate immune response to viral infection. However, whether HDAC6 regulates innate immunity during bacterial infection remains unexplored. To assess the role of HDAC6 in the regulation of defence mechanisms against intracellular bacteria, we used the *Listeria monocytogenes* (*Lm*) infection model. Our data show that *Hdac6*$^{-/-}$ bone marrow-derived dendritic cells (BMDCs) have a higher bacterial load than *Hdac6*$^{+/+}$ cells, correlating with weaker induction of IFN-related genes, pro-inflammatory cytokines and nitrite production after bacterial infection. *Hdac6*$^{-/-}$ BMDCs have a weakened phosphorylation of MAPK signalling in response to *Lm* infection, suggesting altered Toll-like receptor signalling (TLR). Compared with *Hdac6*$^{+/+}$ counterparts, *Hdac6*$^{-/-}$ GM-CSF-derived and FLT3L-derived dendritic cells show weaker pro-inflammatory cytokine secretion in response to various TLR agonists. Moreover, HDAC6 associates with the TLR-adaptor molecule Myeloid differentiation primary response gene 88 (*MyD88*), and the absence of HDAC6 seems to diminish the NF-κB induction after TLR stimuli. *Hdac6*$^{-/-}$ mice display low serum levels of inflammatory cytokine IL-6 and correspondingly an increased survival to a systemic infection with *Lm*. The impaired bacterial clearance in the absence of HDAC6 appears to be caused by a defect in autophagy. Hence, *Hdac6*$^{-/-}$ BMDCs accumulate higher levels of the autophagy marker p62 and show defective phagosome-lysosome fusion. These data underline the important function of HDAC6 in dendritic cells not only in bacterial autophagy, but also in the proper activation of TLR signalling. These results thus demonstrate an important regulatory role for HDAC6 in the innate immune response to intracellular bacterial infection.

CARDIOVASCULAR and grant PIE13/00041 from the Instituto de Salud Carlos III (Fondo de Investigación Sanitaria del Instituto de Salud Carlos III with co-funding from the Fondo Europeo de Desarrollo Regional; FEDER), and ERC-2011-AdG 294340- GENTRIS and COST-Action BM1202 from the European Comission. The Centro Nacional de Investigaciones Cardiovasculares (CNIC) is supported by the Spanish Ministry of Economy and Competitiveness (MINECO) and the Pro-CNIC Foundation and is a Severo Ochoa Center of Excellence (MINECO award SEV-2015-0505). OMG was supported by the fellowship FPU programme (Spanish Ministry of Education). MLS was supported by the fellowship FPI programme (Spanish Ministry of Economy).

Competing interests: The authors have declared that no competing interests exist.

Author summary

Listeria monocytogenes (Lm) is a food-borne intracellular bacterium that causes listeriosis to 1.600 people each year, being responsible of approximately 260 deaths. This pathogen mostly affects immunocompromised individuals and pregnant women. It is particularly dangerous for the later due to its ability to pass across the placenta and the blood-brain barrier. *Lm* is extensively used as a *Gram* positive infection model in the laboratory to study innate and adaptive immune responses. HDAC6 is an important regulatory enzyme of the tubulin and actin cytoskeletons. Its inhibition or deficiency quells the immune response against different virus infections. Previous work has shown its involvement in the regulation of viral RNA-sensing activity and in interferon signalling. In this study, we report that HDAC6 is an essential component of the innate immune response to fight against intracellular bacterial infections. Genetic ablation of HDAC6 impairs activation of the pertinent Toll-like receptor pathway to induce the pro-inflammatory transcriptional program of the cell. Moreover, this enzyme controls cytoskeletal proteins that mediate the fusion of phagosome-contained bacteria with the lysosome during pathogen degradation.

Introduction

Histone deacetylase 6 (HDAC6) is a cytoplasmic deacetylase involved in the regulation of several biological processes, including migration, transport, angiogenesis, and tumour progression [1–5]. This enzyme is able to deacetylate α-tubulin and cortactin, regulating not only the microtubule cytoskeleton, but also actin [6, 7]. Both cytoskeletal interactions underline a crucial role of HDAC6 in many cellular functions such as phagosome-lysosome fusion, cargo transport through microtubules, and cell motility [8–10]. The role of HDAC6 has also been described in two of the main cellular degradation mechanisms: autophagy, through interaction with the autophagy marker p62; and the proteasome, mediated by deacetylation of HSP90 and its intersection with the ubiquitin-proteasome system (UPS) [11–15]. In addition, HDAC6 is involved in the transport of damaged mitochondria (mitophagy) and misfolded proteins (aggrephagy) to lysosomes and the proteasome for degradation [16–18]. The absence of HDAC6 impairs the deacetylation of mitofusin 1, preventing the mitochondrial fusion induced by glucose deprivation and causing excessive ROS production that provokes oxidative damage [19].

HDAC6 regulates the replication of human immunodeficiency virus (HIV) by deacetylating Tat and thus inhibiting viral transactivation [20, 21]. HDAC6 also participates in Sendai virus infection through the deacetylation of β-catenin, which acts as a co-activator of IRF3-mediated transcription [22]. During infection with Influenza Virus A (IVA), HDAC6 appears to play a dual role. IVA capsids mimic misfolded-protein aggregates to take advantage of the host cell aggresome pathway, thereby achieving disassembly and successful viral uncoating [23]. On the other hand, HDAC6-mediated microtubule deacetylation impairs the IVA cycle, preventing trafficking of viral components to the viral assembly site in the host plasma membrane and the spread of infection to surrounding cells [24]. The role of HDAC6 in the adaptive CD4 + T-cell response has been studied in several autoimmune and inflammatory situations such as colitis and cardiac allograft rejection; however, little is known about its role in innate immunity and bacterial diseases [25, 26].

Listeria monocytogenes (*Lm*) is a *Gram*-positive bacteria that causes severe infection in immunocompromised individuals and is able to cross the blood-brain barrier and the placenta [27]. *Lm* is widely used as a model of innate and adaptive immune responses to intracellular

bacterial infection [27–29]. From the first hours of infection, professional phagocytic cells trap bacteria in the blood and target organs, exerting a degree of control on bacterial growth [28]. After internalization by phagocytic cells, *Lm* is eliminated by fusion of the phagosome with lysosomes; however, some bacteria escape the phagosome into the cytoplasm through the action of listeriolysin O (LLO). In the cytoplasm, *Lm* replicates and is able to infect neighbouring cells [30–32]. Interestingly, phagosome-contained bacteria are also eliminated by the action of reactive oxygen species (ROS) and nitric oxide (NO), produced by NADPH oxidase 2 (NOX2) and inducible NO synthase (iNOS), respectively [33]. Moreover, *Lm* bacteria contain an ARP2/3-mimicking protein that enables their propulsion to neighbouring cells through the directional assembly of actin filaments (actin rockets) [34]. *Lm* can spread from cell to cell without exiting the intracellular compartment by a process called paracytophagy, which evades immune detection. However, the host cell is able to develop a specific $CD8^+$T cell response to cytosolic *Lm*, which is crucial for the control of infection [35–38].

Early control of *Listeria* burden largely depends on the innate immune response occurring in the spleen, which relies on two main cell populations of dendritic cells (DCs). On one hand, a subset of monocyte-derived DCs namely TNF/iNOS–producing DCs (Tip-DCs) has the ability to produce TNFα and NO [39]. The other splenic DC subset is $CD8\alpha^+$ conventional DCs (cDCs), and it is responsible for the final resolution of infection against *Listeria* through the antigen presentation of bacterial-derived antigens to specific CD8+T cells to induce cytotoxicity [40, 41]. The response of dendritic cells (DC) to live *Lm* is mediated by toll-like receptors (TLRs), nucleotide-binding oligomerization domain (NODs)-like receptors (NLRs), and other cytosolic receptors and involves two signalling pathways: TLR-dependent and independent signalling. TLR-dependent signalling, triggered by sensing of cell-surface and endo-phagosomal bacteria, mediating the activation of a MyD88-dependent response; and the cytosolic pathway, triggered by bacterial DNA after the escape of *Lm* into the cytosol, is responsible for the activation of sensor stimulator of interferon (IFN) genes (STING). STING activation leads to IFN regulatory factor (IRF)3–dependent production of IFN-β and activation of downstream signals that control the transcription of IFN target genes essential for antiviral and antibacterial responses [42, 43].

To determine the role of HDAC6 in the innate response to bacterial infection, we explored the impact of HDAC6 deficiency on the response of myeloid cells to *Lm*. Our results reveal that *Hdac6*$^{-/-}$ BMDCs are less efficient than *Hdac6*$^{+/+}$ at clearing *Lm*. This is due to defective maturation of phagosome-contained bacteria. Moreover, *Hdac6*$^{-/-}$ DCs display lower activation after *Lm* infection and TLR stimuli. These data support the view that HDAC6 positively regulates innate defence mechanisms against *Lm* and that its absence weakens the pro-inflammatory response.

Results

Deficient intracellular bacteria clearance in *Hdac6*$^{-/-}$ BMDCs

To assess the possible role of HDAC6 in innate immune responses during bacterial pathogenesis, we performed a time-course infection with *Lm* in granulocyte and monocyte colony-stimulating factor (GM-CSF)-derived BMDCs from *Hdac6*$^{+/+}$ and *Hdac6*$^{-/-}$ mice. Increasing levels of HDAC6 expression were detected in the *Hdac6*$^{+/+}$ DCs as the infection progressed (Fig 1A). However, BMDC differentiation was not noticeably affected in the absence of HDAC6 (S1 Fig part A). Next, *Hdac6*$^{+/+}$ and *Hdac6*$^{-/-}$ BMDCs were infected for different times with *Gram*-negative bacteria (*Salmonella* Typhimurium and *Escherichia coli DH5α*) and *Gram*-positive bacteria (*Listeria monocytogenes* and *Staphylococcus aureus*) at a multiplicity of infection (MOI) of 10, with colony-formed units (CFUs) corresponding to intracellular live bacteria. Bacterial

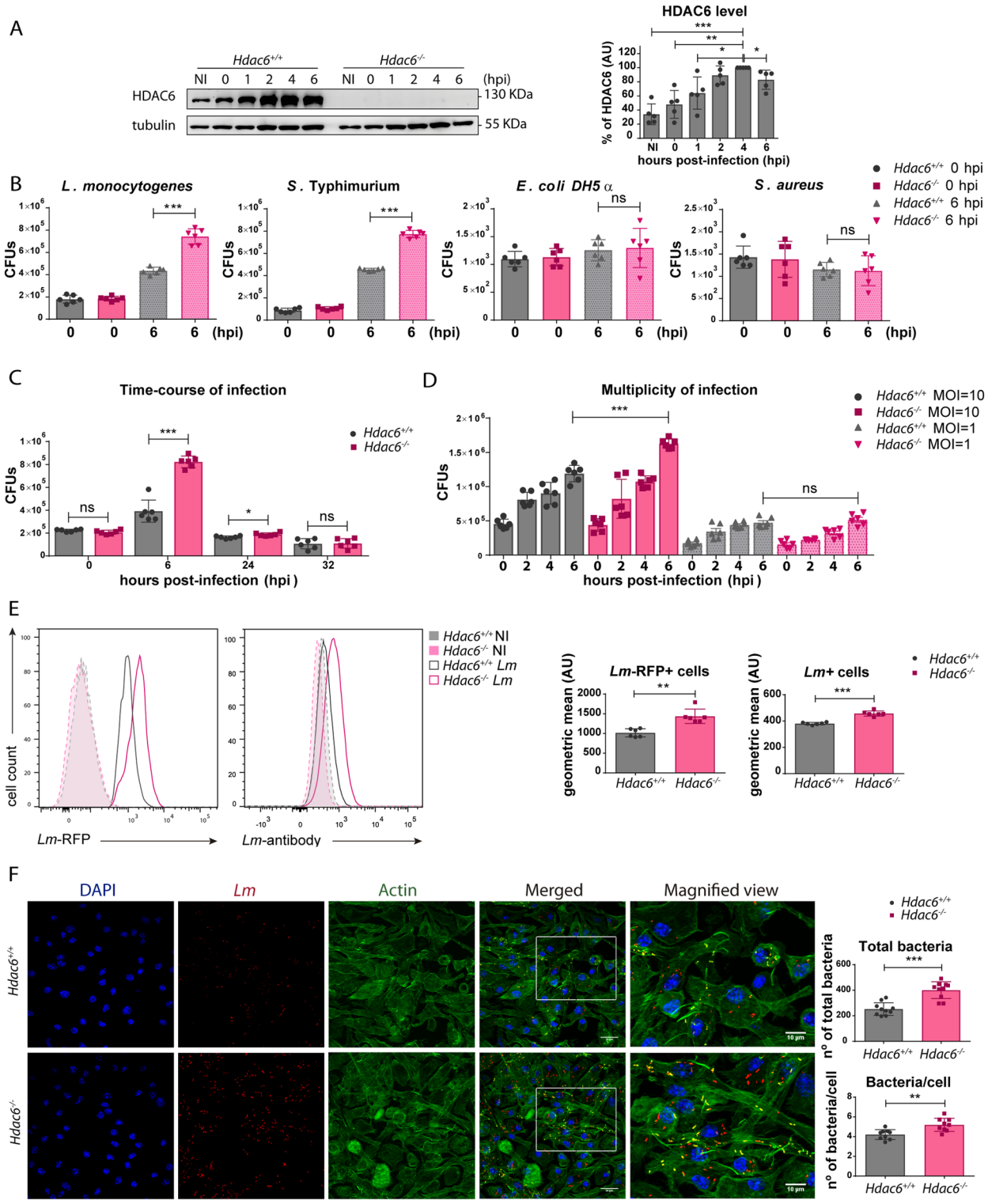

Fig 1. Deficient intracellular bacteria clearance in *Hdac6*$^{-/-}$ BMDCs. A) Western blot analysis of HDAC6 in a time-course of infection of BMDCs with *Lm*. Tubulin was used as a loading control. HDAC6 levels were quantified in five independent experiments. $^{***}p\leq0.001$, $^{**}p\leq0.01$ $^{*}p\leq0.05$. B) CFUs obtained at 0 and 6 hpi from BMDCs infected with *L. monocytogenes*, *S.* Typhimurium, *E. coli DHDα*, and *S. aureus* at a MOI of 10. Data from 0 hpi are shown as a bacteria entry control. $^{***}p\leq0.001$, ns>0.05 non-significant; n = 6. C) CFUs of *Lm*-infected BMDCs obtained at 0, 6, 24 and 32 hpi with a MOI = 10. $^{***}p\leq0.001$, $^{*}p\leq0.05$, ns>0.05 non-significant; n = 6. D) CFUs of *Lm*-infected BMDCs obtained at 0, 2, 4 and 6 hpi with a MOI = 10 and 1. $^{***}p\leq0.001$, $^{*}p\leq0.05$, ns>0.05 non-significant; n = 6. E) BMDCs were infected with *Lm* or *Lm*-RFP for 6 h and the bacterial signal

was determined by flow cytometry. The panel shows representative histograms and the geometric mean of the *Lm* signal. $^{***}p\leq0.001$, ** $p\leq0.01$; n = 6. F) Confocal microscopy determination of bacterial load at 6 hpi. *Left panel*: Maximum intensity z-projections of confocal microscopy images of *Lm*-infected *Hdac6*$^{+/+}$ and *Hdac6*$^{-/-}$ BMDCs at 6 hpi. The panel shows DAPI (blue), *Lm* (red), β-actin (green), merged views of three channels, and magnified views of the boxed areas from the merged view. Yellow indicates *Lm* and β-actin co-localization. Scale bars 20 μm (main panels) and 10 μm magnified views). *Right panel*: ImarisCell Module analysis of the number of cells and the number of bacteria per cell in all pictures (10 pictures per genotype). Statistical analysis of Imaris quantification of total bacteria and bacteria per cell in *Hdac6*$^{+/+}$ and *Hdac6*$^{-/-}$ BMDCs. $^{***}p\leq0.001$, ** $p\leq0.01$; n = 10.

https://doi.org/10.1371/journal.ppat.1006799.g001

entry was similar in *Hdac6*$^{+/+}$ and *Hdac6*$^{-/-}$ DCs at 0 h post-infection (hpi), while bacterial proliferation, measured at 6 hpi, was significantly higher in *Hdac6*$^{-/-}$ BMDCs for both types of intracellular pathogens, *Lm* and *S*. Typhimurium (Fig 1B). This was not due to differences in cell viability at 6 hpi (S1 Fig part B). In contrast, no significant difference was observed in the proliferation of the non-intracellular pathogens *S. aureus* and *E. coli*, indicating that HDAC6 is an important component of cellular mechanisms for the clearance of intracellular pathogens (Fig 1B).

Time-course analysis showed that differences between *Lm* infection in *Hdac6*$^{+/+}$ and *Hdac6*$^{-/-}$ BMDCs CFUs peaked at 6 hpi and were sustained until 24 hpi (Fig 1C). This effect was clearly observed at a MOI of 10, which did not affect cell viability (Fig 1D and S1 Fig part B). A similar pattern was observed with macrophage colony-stimulating factor (M-CSF)-derived macrophages, demonstrating the lineage independence of the role of HDAC6 in bacterial clearance (S1 Fig part C). Although the difference between *Hdac6*$^{+/+}$ and *Hdac6*$^{-/-}$ cells was observed in both macrophages and DCs, the clearance capacity of macrophages was ten-fold higher than that of DCs at 6 hpi (S1 Fig part C).

Bacterial load was also determined by flow cytometry using two strategies: a specific antibody against *Lm*, and RFP-expressing bacteria. Both approaches showed that *Hdac6*-deficient DCs contained more bacteria at 6 hpi (Fig 1E). Higher numbers of bacteria in *Hdac6*$^{-/-}$ BMDCs were also detected by confocal fluorescence microscopy at 6 hpi (Fig 1F). Some bacteria co-localized with filamentous actin, showing clear actin rockets (Fig 1F). Image quantification confirmed that *Hdac6*$^{-/-}$ BMDCs contained more bacteria per cell and more total bacteria, remarking a higher percentage of cells hosting a large number of bacteria in *Hdac6*$^{-/-}$ cells (see distribution of bacteria per cell, 6–7) (S1 Fig part D). ImarisCell Module view of Fig 1F images showed the number of bacteria per cell using actin transparency to easily visualize individual bacteria (S1 Fig part E).

To ascertain whether *Hdac6*$^{-/-}$ cells display higher bacterial burden than *Hdac6*$^{+/+}$ cells *in vivo*, *Hdac6*$^{+/+}$ and *Hdac6*$^{-/-}$ mice were intravenously injected with *Lm* and total CFUs per gram of liver and spleen were determined at 6 hpi. In agreement with the higher numbers of *Lm* observed in GM-CSF-DCs and M-CSF-Macrophages, we observed increased bacterial titres in spleen and liver cell suspensions (Fig 2A). Next, to determine the specific cell populations underlying this phenotype, a multicolour gating strategy was used to identify the myeloid cell compartment, including monocytes, neutrophils, Tips DCs, total cDCs, cCDs CD8^{-} and cDCs CD8^{+} (S2 Fig part A). Higher numbers of *Lm* were observed in different myeloid cells at 6 hpi (Fig 2B and S2 Fig part B). These data highlight the impairment of *Hdac6*$^{-/-}$ myeloid cells to clear intracellular *Lm*.

Impaired bacterial clearance in *Hdac6*$^{-/-}$ BMDCs is caused by a defect in autophagy

To test the involvement of autophagy in the mechanism by which HDAC6 regulates *Lm* infection, we treated DCs with 3-methyladenine (3-MA), an inhibitor of autophagosome formation. Treatment with 3-MA increased bacterial load in *Hdac6*$^{+/+}$ BMDCs at 6 hpi, while having no

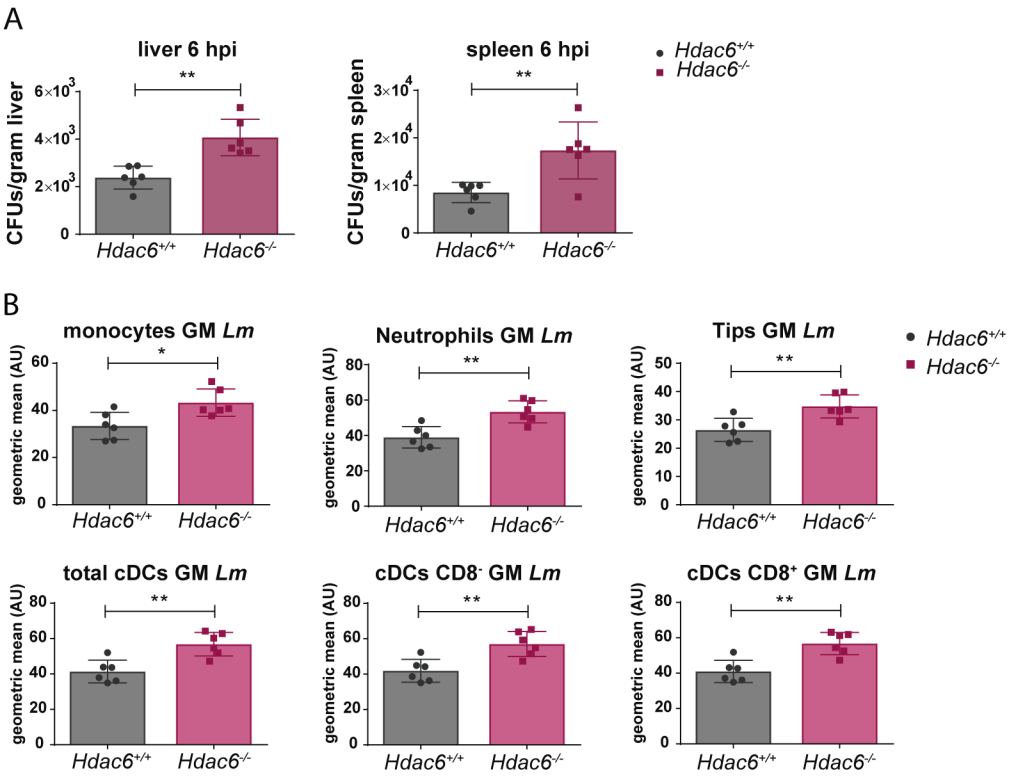

Fig 2. Deficient intracellular bacteria clearance in *Hdac6*$^{-/-}$ splenic myeloid populations. A) Quantification of bacterial load in target organs (spleen and liver) at 6 hpi in *Hdac6*$^{+/+}$ and *Hdac6*$^{-/-}$ mice injected with a lethal dose of *Lm*. Bacterial load is expressed by CFUs per gram of liver (left graph) and per gram of spleen (right graph). $^{**}p \leq 0.01$, n = 6. B) The charts show geometric means of *Lm* of different splenic populations (monocytes, neutrophils, Tips DCs, total cDCs, cDCs CD8$^-$ and cDCs CD8$^+$) gated in the live CD3$^-$CD19$^-$DX5$^-$ population of *Hdac6*$^{+/+}$ and *Hdac6*$^{-/-}$ mice injected with a lethal dose of *Lm* at 6 hpi. $^{**}p \leq 0.01$; n = 6.

https://doi.org/10.1371/journal.ppat.1006799.g002

effect on *Hdac6*$^{-/-}$ BMDCs (Fig 3A), suggesting autophagy as the bacterial clearance mechanism impaired in *Hdac6*-deficient DCs. A similar result was observed upon treatment of BMDCs with bafilomycin A1, an inhibitor of vascular proton pump that indirectly inhibits phagosome-lysosome fusion, and with the lysosome acidification inhibitors chloroquine and NH_4Cl (Fig 3A). In contrast, increasing autophagy flux with rapamycin did not restore the impaired autophagy in *Hdac6*$^{-/-}$ BMDCs (Fig 3B). No significant effects were observed with control vehicles (S3 Fig part A). To explore other possible mechanisms, we treated BMDCs with inhibitors of NADPH oxidase (DPI) and iNOS (1400W). These treatments did not alter the difference in CFU number at 6 hpi between treated and non-treated *Hdac6*$^{+/+}$ and *Hdac6*$^{-/-}$ BMDCs, indicating that the activity of either enzyme is not accounting for the existing phenotype (Fig 3B).

The defective autophagy phenotype of *Hdac6*$^{-/-}$ BMDCs was not due to transcriptional alterations to autophagy or lysosome components, since *Lm*-infected *Hdac6*$^{+/+}$ and *Hdac6*$^{-/-}$ BMDCs showed no mRNA expression differences at 6 hpi in the autophagy components LC3A and B, p62, ATG2, 5, 7 and 12, and Beclin-1 or in the lysosome components LAMP-1 and 2 (S3 Fig part B).

To determine whether these findings can be extended to other phagocytic cells, we carried out CFU assays with macrophages obtained from *Hdac6*$^{+/+}$ and *Hdac6*$^{-/-}$ mice four days after intraperitoneal thioglycollate injection. Higher bacterial load was observed only in *Hdac6*$^{-/-}$

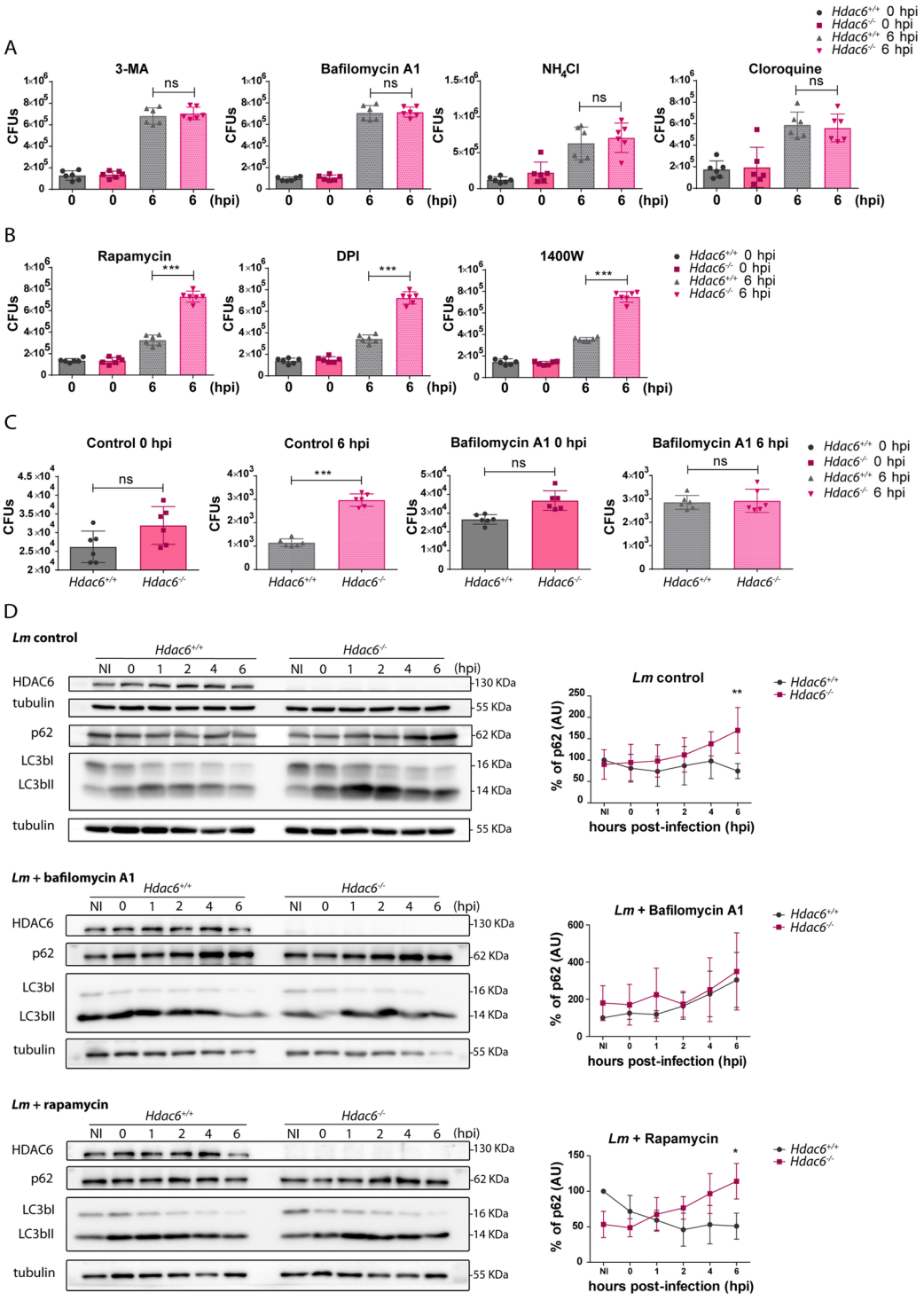

Fig 3. Impaired bacterial clearance in *Hdac6*$^{-/-}$ BMDCs is caused by a defect in autophagy. A) Total CFUs in *Lm*-infected BMDCs treated with inhibitors. CFUs were detected at entry (0 hpi) and 6 hpi (bacterial proliferation) using the autophagy inhibitors (3-MA and bafilomycin A1 and the lysosome acidification inhibitors (NH4Cl and cloroquine), ns>0.05 non-significant; n = 6. B) Total CFUs at 0 and 6 hpi in *Lm*-infected BMDCs treated with the autophagy activator (rapamycin), the NADPH oxidase inhibitor (DPI) and the iNOS inhibitor (1400W). $^{***}p\leq0.001$; n = 6. C) Total CFUs at 0 and 6 hpi in *Lm*-infected thioglycollate-elicited macrophages treated with or without bafilomycin A1. $^{***}p\leq0.001$, ns>0.05 non-significant; n = 6. D) Western-blot analysis of autophagy markers over the time-course of *Lm* infection in *Hdac6*$^{+/+}$ and *Hdac6*$^{-/-}$ BMDCs. *Left panels*: Levels were detected of p62, LC3bI and II and HDAC6 in control cells and cells treated

with bafilomycin A1 and rapamycin. Tubulin was used as a loading control. HDAC6 was as a genotype check of *Hdac6*$^{+/+}$ and *Hdac6*$^{-/-}$ BMDCs and to monitor HDAC6 induction during infection. *Right panels*: Accompanying charts show quantification of the p62 percentage of control, bafilomycin A1 and rapamycin western blots. ** $p \leq 0.01$, * $p \leq 0.05$, ns>0.05 non-significant; n = 5.

https://doi.org/10.1371/journal.ppat.1006799.g003

macrophages at 6 hpi, and this difference was abrogated by treatment with bafilomycin A1 (Fig 3C). These data indicate that the phenotype observed in BMDCs is also extendable in other *Hdac6*-deficient phagocytic cells such as peritoneal macrophages, indicating a widespread defect in intracellular killing ability due to lack of HDAC6. Moreover, the killing ability shown by peritoneal macrophages is similar to that of M-CSF-derived macrophages and higher than GM-CSF-derived DCs (Fig 3C compared with S1 Fig part C).

To gain further insight into the autophagy mechanism affected by HDAC6, we monitored the autophagosome markers p62 and LC3bI and II in *Lm*-infected BMDCs. *Hdac6*$^{-/-}$ BMDCs showed a 2-fold higher accumulation of p62 than *Hdac6*$^{+/+}$ cells at 6 hpi and increased LC3bII level in *Hdac6*$^{+/+}$ cells from 1 to 6 hpi (Fig 3D). However, differences in p62 and LC3b levels were not noticed at early times of *Lm* infection of *Hdac6*$^{+/+}$ and *Hdac6*$^{-/-}$ BMDCs, indicating that the induction of autophagy is not affected in the absence of HDAC6 (Fig 3D). The treatment with bafilomycin A1 enhances the accumulation of p62 during the infection at the same level in both genotypes, abrogating the deficiency in autophagy observed in *Hdac6*$^{+/+}$ BMDCs (Fig 3D). Although rapamycin also increased p62 accumulation at early times in *Hdac6*$^{+/+}$ and *Hdac6*$^{-/-}$ BMDCs, only *Hdac6*$^{+/+}$ cells are able to diminished p62 at 6 hpi (Fig 3D). This treatment confirmed the results obtained in the CFUs functional assays with this inhibitor (Fig 3D compared with Fig 3B). The similarity of the autophagy defect detected in *Hdac6*$^{-/-}$ BMDCs in control condition to that in rapamycin-treated *Hdac6*$^{-/-}$ cells, suggests an impairment in phagocytic vesicle fusion with the lysosome.

Hdac6$^{-/-}$ BMDCs accumulate p62

In order to further understand the defective autophagy of *Hdac6*$^{-/-}$ BMDCs, the accumulation of p62 was studied in more detail. Flow cytometry at 6 hpi revealed significantly higher p62 content in *Hdac6*$^{-/-}$ BMDCs, indicating accumulation of this phagosome marker due to defective fusion of this organelle with the lysosome (Fig 4A). Bafilomycin A1 treatment completely abrogated this difference, suggesting that *Hdac6*$^{-/-}$ BMDCs displayed an impairment in the final step of autophagy (Fig 4A). More signal of *Lm* is displayed in *Hdac6*$^{-/-}$ DCs (Fig 4A). In this regard, bafilomycin A1 treatment increased the low *Lm* signal in *Hdac6*$^{+/+}$ DCs to the level observed in *Hdac6*$^{-/-}$ cells (Fig 4A).

Confocal fluorescent analysis of *Lm*-infected DCs revealed increased levels of p62 in *Hdac6*$^{-/-}$ BMDCs (Fig 4B). *Hdac6*$^{-/-}$ BMDCs also showed a higher percentage of p62-*Lm* co-localization than *Hdac6*$^{+/+}$ cells, indicating that *Hdac6*$^{-/-}$ cells have more number of phagosome-contained bacteria (Fig 4B in accordance with p62 accumulation observed in Figs 3D and 4A). Confocal fluorescent microscopy study of actin and *Lm* revealed more frequent co-localization in *Hdac6*$^{-/-}$ than in *Hdac6*$^{+/+}$ BMDCs, indicating that more bacteria are at the cytoplasm to form actin rockets in *Hdac6*-deficient cells (Fig 4C). Moreover, more signal of acetylated-cortactin is detected in *Hdac6*$^{-/-}$ BMDCs and also higher percentage of acetylated-cortactin-*Lm* co-localization (Fig 4D). These data could explain the accumulation of p62 and the delay in phagocytic vesicle fusion observed in *Hdac6*$^{-/-}$ BMDCs, necessary to degrade phagocytosed *Lm*.

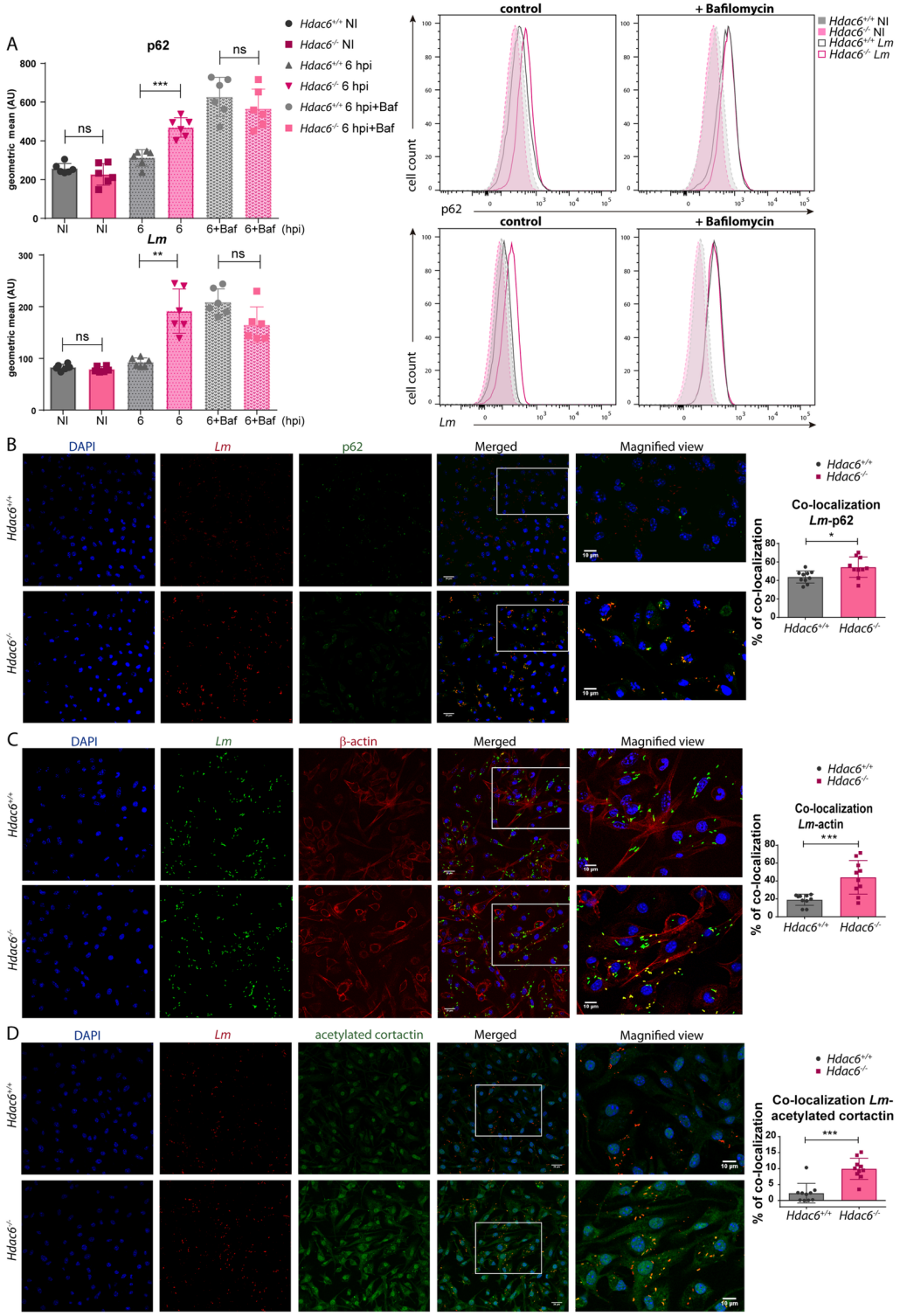

Fig 4. *Hdac6*$^{-/-}$ BMDCs accumulate higher levels of p62. A) *Left panels*: The charts show geometric means of p62 *and* *Lm* gated in the MHCII^{+}CD11c^{+} population of *Hdac6*$^{+/+}$ and *Hdac6*$^{-/-}$ BMDCs without infection (NI) and at 6 hpi, with and without bafilomycin A1 treatment. The representative histograms on the right show p62 and *Lm* with and without bafilomycin A1. $^{***}p \leq 0.001$, $^{**}p \leq 0.01$, ns>0.05 non-significant; n = 6. B) Confocal microscopy analysis of p62-*Lm* co-localization in *Lm*-infected *Hdac6*$^{+/+}$ and *Hdac6*$^{-/-}$ BMDCs at 6 hpi. Panels show DAPI (blue), *Lm* (red), p62 (green), and merged views of the three channels, with magnified views of the boxed areas. Yellow indicates p62-*Lm* co-localization.

Scale bars 20 μm (main panels) and 10 μm (magnified views). *Right panel*: The chart shows ImarisCell Module analysis of the number of cells and the number of bacteria per cell in all pictures (10 pictures per genotype). Co-localization percentages were obtained by measuring the p62 channel on the bacterial surface using a threshold of 100. The statistical analysis of Imaris quantifications corresponds to the percentage of p62-*Lm* co-localization at 6 hpi. $^{*}p \leq 0.05$; n = 10. C) Confocal microscopy analysis of actin-*Lm* co-localization in *Lm*-infected *Hdac6*$^{+/+}$ and *Hdac6*$^{-/-}$ BMDCs at 6 hpi. Panels show DAPI (blue), *Lm* (green), β-actin (red), and merged views of the three channels, with magnified views of the boxed areas. Yellow indicates β-actin-*Lm* co-localization. Scale bars 20 μm (main panels) and 10 μm (magnified views). *Right panel*: The chart shows ImarisCell Module analysis of the number of cells and the number of bacteria per cell in all pictures (10 pictures per genotype). Co-localization percentages were obtained by measuring the actin channel on the bacterial surface using a threshold of 40.6. The statistical analysis of Imaris quantifications corresponds to the percentage of actin-*Lm* co-localization at 6 hpi. *** $p \leq 0.001$; n = 10. D) Confocal microscopy analysis of acetylated cortactin-*Lm* co-localization in *Lm*-infected *Hdac6*$^{+/+}$ and *Hdac6*$^{-/-}$ BMDCs at 6 hpi. Panels show DAPI (blue), *Lm* (red), acetylated cortactin (green), and merged views of the three channels, with magnified views of the boxed areas. Yellow indicates acetylated cortactin-*Lm* co-localization. Scale bars 20 μm (main panels) and 10 μm (magnified views). *Right panel*: The chart shows ImarisCell Module analysis of the number of cells and the number of bacteria per cell in all pictures (10 pictures per genotype). Co-localization percentages were obtained by measuring the acetylated cortactin channel on the bacterial surface using a threshold of 184. The statistical analysis of Imaris quantifications corresponds to the percentage of acetylated cortactin-*Lm* co-localization at 6 hpi. *** $p \leq 0.001$; n = 10.

https://doi.org/10.1371/journal.ppat.1006799.g004

Defective pro-inflammatory cytokine response to *Lm* in *Hdac6*$^{-/-}$ BMDCs

The effect of HDAC6 on the response of BMDCs to *Lm* was evaluated by measuring pro-inflammatory cytokine gene induction. The relative mRNA levels of type I interferons (interferons α and β) were lower in *Hdac6*$^{-/-}$ BMDCs at 6 hpi (Fig 5A). Accordingly, expression of downstream interferon-response genes such as Mx1, IFIT3, and ISG15 was also lower in *Hdac6*$^{-/-}$ BMDCs (Fig 5A). Lack of HDAC6 also decreased the relative mRNA levels of the pro-inflammatory cytokines TNFα, IL-1β and IL12p40, indicating impaired cytokine activation after infection (Fig 5A). Similarly, *Hdac6*$^{-/-}$ DCs expressed lower levels than their *Hdac6*$^{+/+}$ counterparts of the chemokine receptor CXCR1 and chemokines CXCL5 and CXCL10 (Fig 5A). These data demonstrate that *Hdac6*-deficient DCs have a weakened activation response to *Lm* infection at 6 hpi, which suggests a defect in bacterial clearance, consistent with the increased bacterial load in these cells. To confirm these data, we monitored pro-inflammatory cytokines and IFN-β in the supernatants of *Lm*-infected DCs. Early after infection, TNFα, IL-1β, IL-6, IL12p70 and IFN-β levels were lower in supernatants from *Hdac6*$^{-/-}$ cells than in those from *Hdac6*$^{+/+}$ cells, and this difference held at 12 and 24 hpi (Fig 5B). To exclude a defect in cytokine secretion, we compared cytokine levels in supernatants (S) with the levels in supernatants plus their corresponding cell pellets (S+P). Both analyses showed decreased cytokine levels in *Hdac6*$^{-/-}$ cells, indicating an impaired antibacterial response in *Hdac6*-deficient DCs (S4 Fig).

Measurement of nitrite in supernatants of infected-BMDCs revealed higher nitric oxide production by *Hdac6*$^{+/+}$ DCs than in *Hdac6*$^{-/-}$ DCs at 24 hpi (Fig 6A). In agreement, western blot revealed lower levels of inducible nitric oxide synthase (iNOS) in *Hdac6*$^{-/-}$ BMDCs at 4 and 6 hpi (Fig 6B), indicating a delay of the enzyme induction in *Hdac6*$^{-/-}$ BMDCs. Likewise, flow cytometry after exposure of DCs to live or heat-killed *L. monocytogenes* (HKLM) revealed higher expression of iNOS in *Hdac6*$^{+/+}$ BMDCs in both cases (Fig 6C). These data support the involvement of HDAC6 in the activation of DC-mediated iNOS microbicidal responses to *Lm* infection and in the clearance of this intracellular pathogen.

Hdac6$^{-/-}$ BMDCs show defective activation of Toll-like receptor signalling pathway

The diminished activation response against *Lm* in *Hdac6*$^{-/-}$ BMDCs is consistent with impaired TLR-related signalling. To investigate this question, we determined the phosphorylation levels

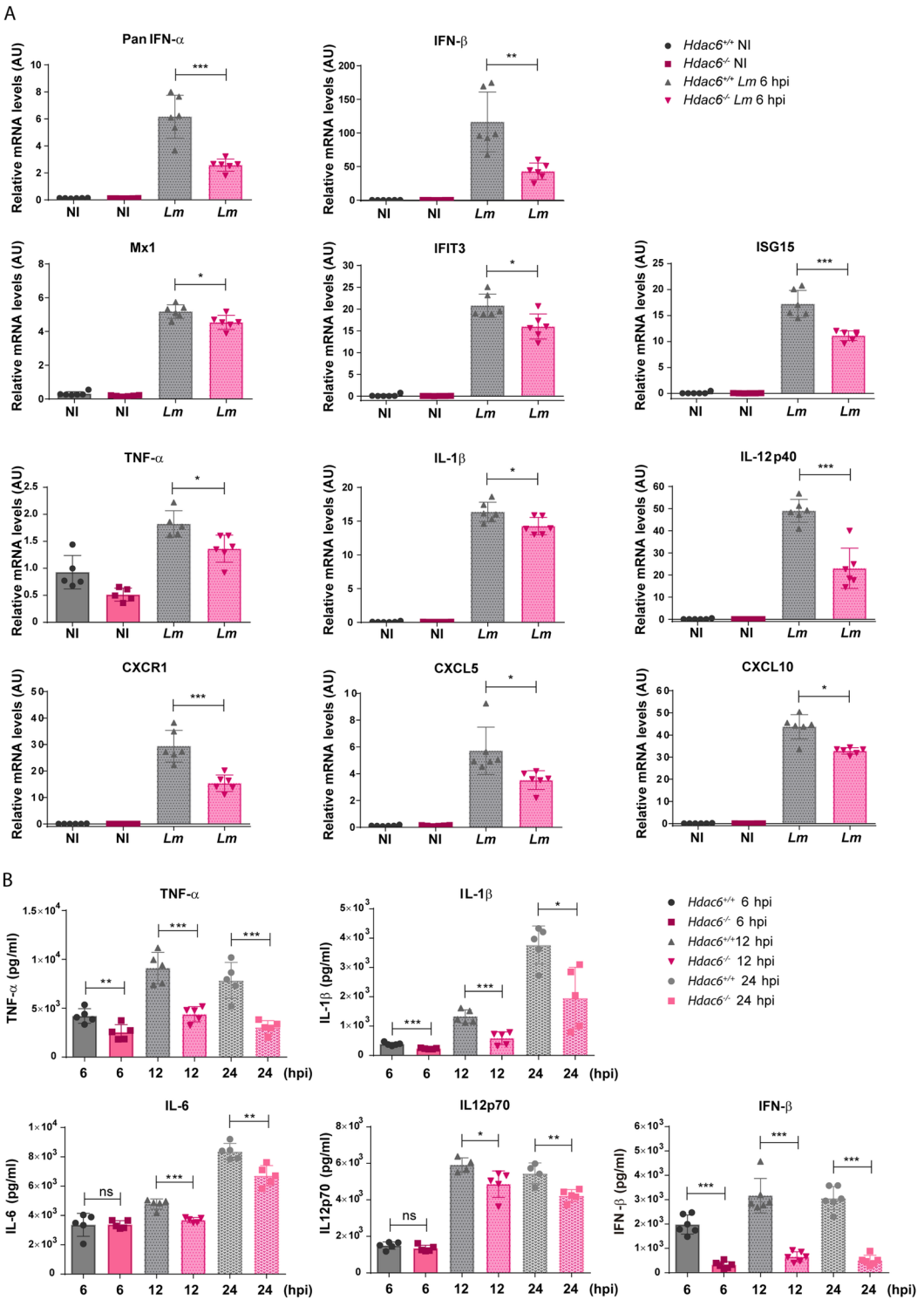

Fig 5. Defective pro-inflammatory cytokine response to *Lm* in *Hdac6*$^{-/-}$ BMDCs. A) PCR analysis of type-I interferons (PanIFN-α and IFN-β), interferon downstream proteins (Mx1, IFIT3 and ISG15), pro-inflammatory cytokines (TNF-α, IL-1β and IL-12p40) chemokine receptor (CXCR1) and chemokines (CXCL5 and CXCL10) of *Hdac6*$^{+/+}$ and *Hdac6*$^{-/-}$ BMDCs non-infected (NI) and infected with *Lm* at 6 hpi (arbitrary units). $^{***}p\leq0.001$, ** $p\leq0.01$, * $p\leq0.05$; n = 5–6. B) ELISA analysis of the pro-inflammatory cytokines TNFα, IL1β, IL6 and IL12p70 (pg/ml) and IFN-β in supernatants of *Hdac6*$^{+/+}$ and *Hdac6*$^{-/-}$ BMDCs at 6, 12 and 24 hpi with *Lm*. $^{***}p\leq0.001$, ** $p\leq0.01$, * $p\leq0.05$ ns>0.05 non-significant; n = 5–6.

https://doi.org/10.1371/journal.ppat.1006799.g005

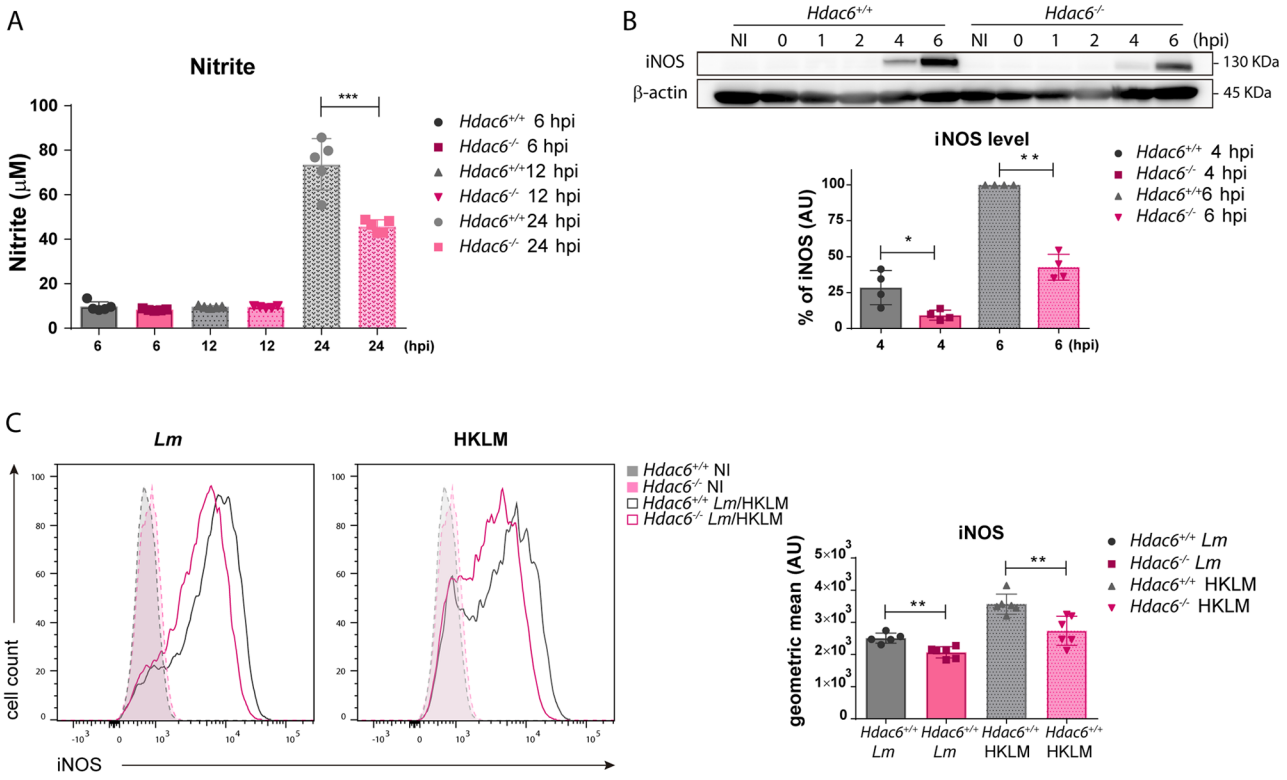

Fig 6. Defective iNOS response to *Lm* in *Hdac6*$^{-/-}$ BMDCs. A) *Lm*-activated iNOS activity. Nitrite levels in supernatants of *Lm*-infected BMDCs at 6, 12 and 24 hpi. ***p≤0.001; n = 5. B) Western-blot analysis of iNOS induction over the time-course of *Lm* infection. β-actin was used as a loading control (top panel). The chart shows quantification of iNOS at 4 and 6 hpi. ** p≤0.01, * p≤0.05; n = 4 (lower panel). C) The panel shows representative histograms of iNOS expressed by *Hdac6*$^{+/+}$ and *Hdac6*$^{-/-}$ BMDCs after exposure to live *Lm* or HKLM for 24 h (left). The right chart shows the geometric mean of iNOS expression. Non-infected (NI) BMDCs were used as a control of iNOS induction. **p≤0.01; n = 6.

https://doi.org/10.1371/journal.ppat.1006799.g006

of TLR downstream mediators by western blot. Compared with *Hdac6*$^{+/+}$ BMDCs, *Hdac6*$^{-/-}$ BMDCs showed weaker phosphorylation signals for ERK and AKT after *Lm* infection (Fig 7A). We next examined the effect of HDAC6 deficiency on TLR-signalling pathways using other TLR stimuli, including HKLM and LPS. AKT phosphorylation in *Hdac6*$^{-/-}$ BMDCs was decreased after LPS or HKLM treatment compared to *Hdac6*$^{+/+}$, confirming defective TLR activation (S5 Fig part A). These effects are not related to a defect in *Lm*-induced transcriptional induction since mRNA levels of different *Lm*-related TLRs (TLR1, 2, and 6) were similar in *Hdac6*$^{+/+}$ and *Hdac6*$^{-/-}$ BMDCs (S5 Fig part B). Moreover, *Hdac6*$^{-/-}$ BMDCs showed weaker phosphorylation of mTORC1 pathway proteins (mTORC1 downstream substrates p70S6K and S6), consistent with a less pronounced pro-inflammatory response after TLR-activation by pathogen-associated molecular patterns (PAMPs) (Fig 7B).

To determine if *Hdac6*$^{-/-}$ BMDCs showed a similarly defective response to other TLR agonists, we first examined secretion of pro-inflammatory cytokines in response to agonists of TLR1-2 (Pam3GSK4), TLR-4 (LPS), TLR-7-9 (Imiquimod), and multiple TLRs (heat-killed *Salmonella* Typhimurium; HKST). *Hdac6*$^{-/-}$ BMDCs showed a defective cytokine response to these stimuli, determined from the release of TNFα, IL-6, IL-1β and IL12p70 (Fig 8A–8D).

To assess the pro-inflammatory cytokine response to TLR3 and TLR5 ligands, we generated Fms-related tyrosine kinase 3 ligand dendritic cells (FLT3L-DCs). Differentiation with the cytokine FLT3L yielded similar percentages of CD24^{+} and CD24^{-} subpopulations (CD11c^{+}CD11b^{+}B220^{-}CD24^{+} and CD11c^{+}CD11b^{+}B220^{-}CD24^{-}, respectively) from *Hdac6*$^{+/+}$

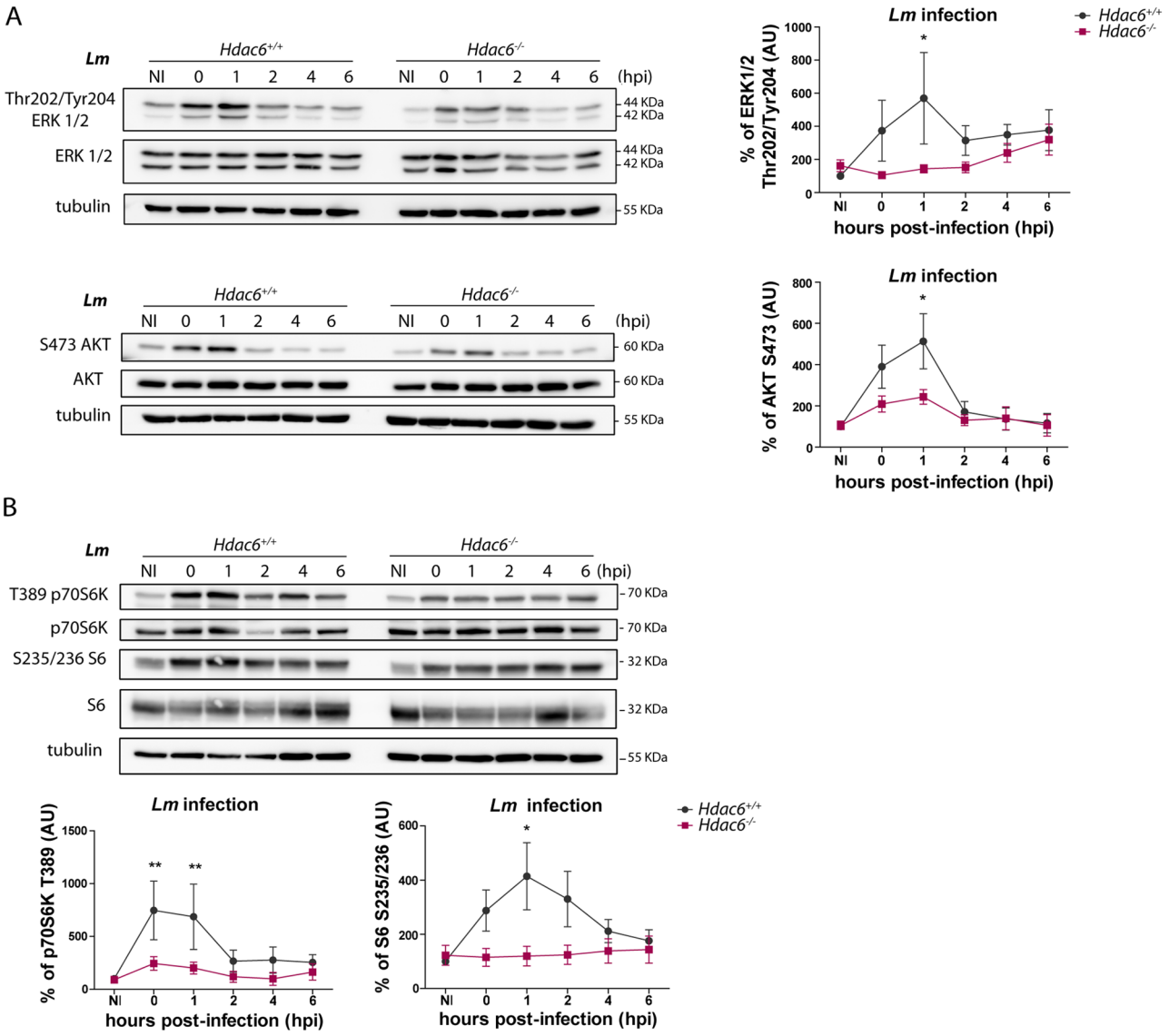

Fig 7. *Hdac6*$^{-/-}$ BMDCs show defective activation of the Toll-like receptor signalling pathway. A) Western-blot analysis of MAPK activation over the time-course of *Lm* infection in *Hdac6*$^{+/+}$ and *Hdac6*$^{-/-}$ BMDCs. Total and phosphorylated ERK and AKT were detected. Tubulin was used as a loading control (left). Accompanying charts show quantification of phERK/totalERK and phAKT/totalAKT ratios relative to the loading control, ns non-significant; n = 7 (right). B) Western-blot analysis of mTORC1 pathway activation over the time-course of *Lm* infection in *Hdac6*$^{+/+}$ and *Hdac6*$^{-/-}$ BMDCs. Levels of phosphorylated and total p70S6K and S6 were detected. Tubulin was used as a loading control (top panel). Accompanying charts show quantification of php70S6K/total70S6K (n = 5) and phS6/totalS6 (n = 7) ratios relative to the loading control. ** $p \leq 0.01$, ns non-significant; (lower panel).

https://doi.org/10.1371/journal.ppat.1006799.g007

and *Hdac6*$^{-/-}$ DCs, indicating that differentiation is unaffected by HDAC6 absence (S6 Fig part A). The TLR agonists Pam3GSK4 (TLR1-2), Poly(I:C) (TLR3), LPS (TLR4), flagellin (TLR5), Imiquimod (TLR-7-9), *Lm*, HKLM, and HKST (which activates several TLRs simultaneously) elicited similar cytokine secretion profiles in GM-CSF DCs and FLT3L-DCs (Fig 9A and S6 Fig part B compared to Fig 8A–8D). *Hdac6*$^{-/-}$ DCs of both derivations showed an impaired cytokine response to each TLR agonist, indicating that HDAC6 likely regulates a common TLR signalling adaptor.

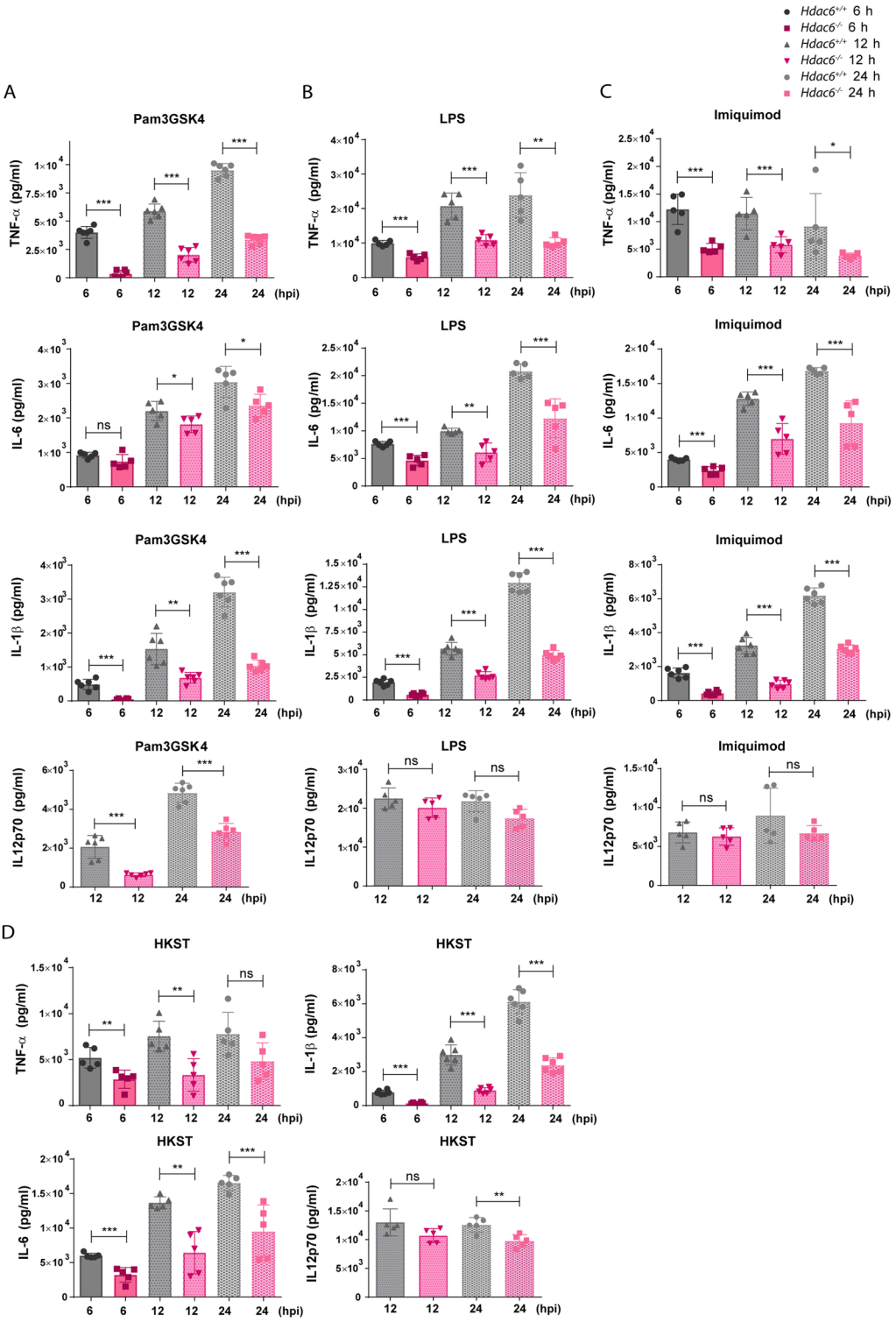

Fig 8. *Hdac6*$^{-/-}$ BMDCs show defective inflammatory cytokine response to Toll-like receptor stimuli. A) ELISA analysis of the pro-inflammatory cytokines TNFα, IL-1β, IL-6 and IL12p70 (pg/ml) in supernatants of *Hdac6*$^{+/+}$ and *Hdac6*$^{-/-}$ BMDCs after treatment for 6, 12 and 24 h with Pam3GSK4. $^{***}p \leq 0.001$, ** $p \leq 0.01$, * $p \leq 0.05$, ns>0.05 non-significant; n = 5–6. B) ELISA analysis of the pro-inflammatory cytokines TNFα, IL-1β, IL-6 and IL12p70 (pg/ml) in supernatants of *Hdac6*$^{+/+}$ and *Hdac6*$^{-/-}$ BMDCs after treatment for 6, 12 and 24 h with LPS. $^{***}p \leq 0.001$, ** $p \leq 0.01$, ns>0.05 non-significant; n = 5–6. C) ELISA analysis of the pro-inflammatory cytokines TNFα, IL-1β, IL-6 and IL12p70

(pg/ml) in supernatants of *Hdac6*$^{+/+}$ and *Hdac6*$^{-/-}$ BMDCs after treatment for 6, 12 and 24 h with Imiquimod. $^{***}p \leq 0.001$, * $p \leq 0.05$, ns>0.05 non-significant; n = 5–6. D) ELISA analysis of the pro-inflammatory cytokines TNFα, IL-1β, IL-6 and IL12p70 (pg/ml) in supernatants of *Hdac6*$^{+/+}$ and *Hdac6*$^{-/-}$ BMDCs after treatment for 6, 12 and 24 h with HKST. $^{***}p \leq 0.001$, ** $p \leq 0.01$, ns>0.05 non-significant; n = 5–6.

https://doi.org/10.1371/journal.ppat.1006799.g008

In this view, the TLR adaptor MyD88 participates in the transmission of signals by all TLRs except for TLR3. We decided to study MyD88 levels in a time-course infection with *Lm* by western blot, demonstrating that the quantity of this molecule was the same between *Hdac6*$^{+/+}$ and *Hdac6*$^{-/-}$ DCs and remaining stable during infection (S6 Fig part C). Remarkably, MyD88-HDAC6 molecular association was observed by co-immunoprecipitations of endogenous proteins using human dendritic cells after Pam2GSK4, Pam3GSK4 and HKLM stimulation (Fig 9B). Likewise, the MyD88 immunoprecipitation in *MyD88*- and *HDAC6*-overexpressed HEK cell line was also able to co-precipitate HDAC6 (S6 Fig part D). These results were corroborated by mass spectrometry analysis of MyD88 immunoprecipitates; which in addition detected two acetylated peptides corresponding to MyD88 (S6 Fig parts E and F). The same approach was used to determine MyD88-HDAC6 molecular association after TLR-2 activation with HKLM using a constitutively expressed human TLR-2 HEK cell line, rendering the same result (Fig 9C). This association is also maintained using a double-deacetylase domain mutant of HDAC6 (H216A:H611A), called HDAC6-DD, indicating that HDAC6-MyD88 interaction is independent of its catalytic activity (Fig 9C and S6 Fig part D). The knock-down of HDAC6 expression using a small harping plasmid (sh-HDAC6) blocked this interaction (Fig 9C and S6 Fig part D). However, no acetylated peptides could be detected in the mass spectrometry analysis of the MyD88 immunoprecipitation from HKLM-stimulated TLR-2 HEK cell line (Fig 9D). Moreover, assessment of NF-κB induction in TLR-2-expressing HEK cell line after HKLM, Pam2GSK4 and Pam3GSK4 stimulation shows lower activation only in shHDAC6 transfected cells, without affecting the activity of HDAC6-DD-transfected ones (Fig 9E).

Taking into account all these data, HDAC6 associates with the TLR-adaptor molecule MyD88, and the absence of HDAC6 in DCs seems to diminish the TLR-response after a variety of stimuli, underlining the scaffold role of HDAC6 in determining the ability of MyD88 to mediate TLR signalling.

To ascertain the defective TLR-dependent inflammatory response *in vivo* due to the molecular association of MyD88-HDAC6, *Hdac6*$^{+/+}$ and *Hdac6*$^{-/-}$ mice were intravenously injected with a lethal dose of *Lm* (Fig 9F) [44]. A protective effect against *Lm*-induced septic shock was observed from 3 to 10 days post-infection (dpi) (Fig 9F). Accordingly, lower levels of the pro-inflammatory cytokine IL-6 were detected in the serum of *Hdac6*$^{-/-}$ mice at 72 hpi, highlighting a reduced systemic cytokine-driven inflammatory response after *Lm* infection in these mice (Fig 9G).

Discussion

Recent studies have revealed the involvement of HDAC6 in the innate immune response against Influenza Virus A (IVA), Sendai virus (SeV), and vesicular stomatitis virus (VSV) [21–24]. Given the similarities between the innate responses to viruses and intracellular bacteria, this prompted us to investigate the role of HDAC6 in a model of *Lm* infection. In this work, we demonstrated a dual role of HDAC6 in the innate response against *Lm*, not only due to its enzymatic activity but also dependent of its function as a scaffold (Fig 10). Our data clearly demonstrate that *Hdac6*$^{-/-}$ BMDCs have an impaired immune response against *Lm* and *S.* Typhimurium infection *in vitro*. Moreover, higher *Lm* titres observed in *Hdac6*$^{-/-}$ dendritic cells, M-CSF-derived macrophages and peritoneal macrophages were corroborated during *in*

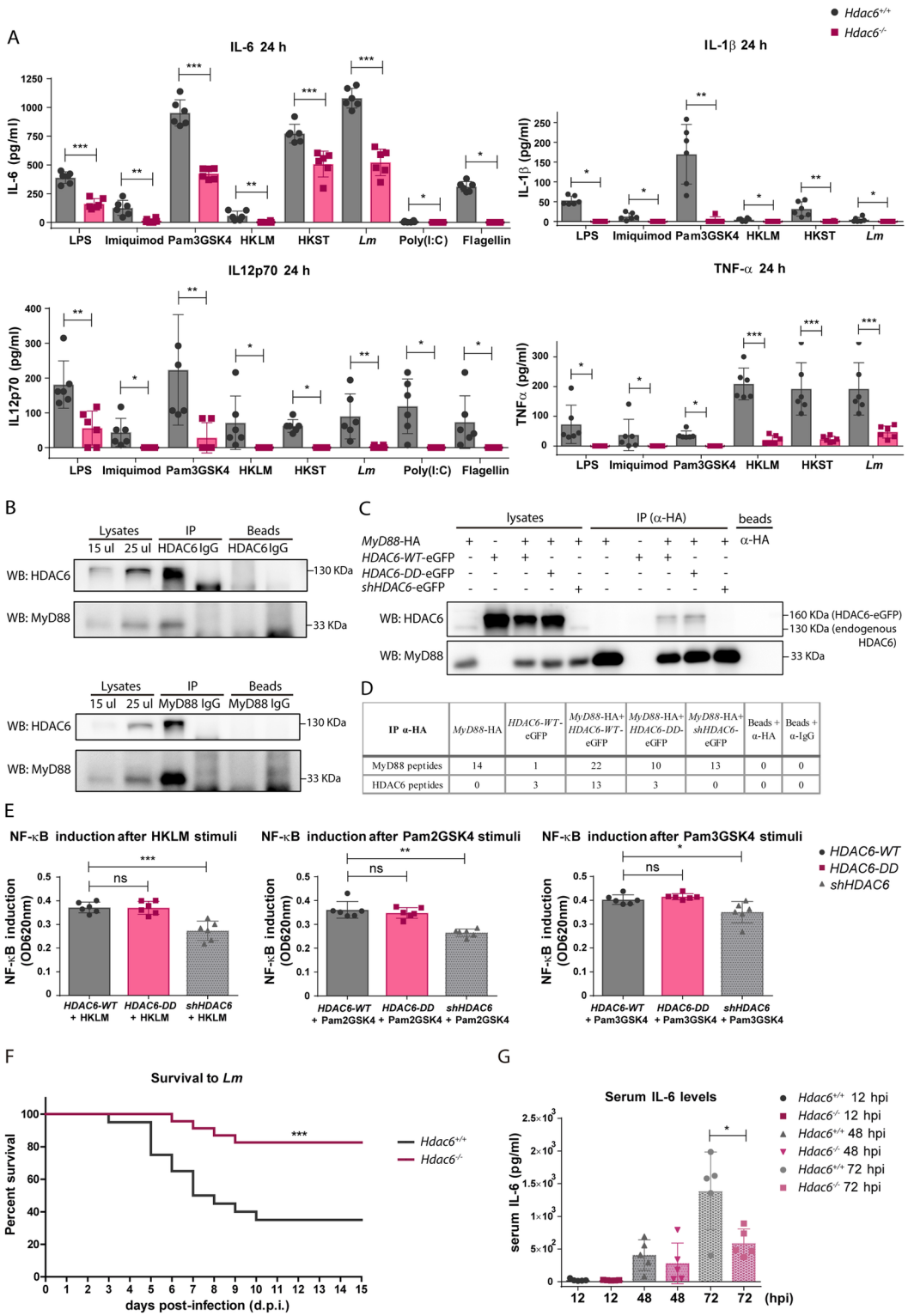

Fig 9. Association of HDAC6 with TLR-adaptor MyD88 and its contribution to the inflammatory response to *Lm*. A) ELISA analysis of the pro-inflammatory cytokines TNFα, IL-1β, IL-6 and IL12p70 (pg/ml) in supernatants of *Hdac6*$^{+/+}$ and *Hdac6*$^{-/-}$ FLT3L-DCs activated with LPS, Imiquimod, Pam3GSK4, HKLM, HKST, *Lm*, Poly(I:C) and flagellin for 24 h. $^{***}p \leq 0.001$, ** $p \leq 0.01$, * $p \leq 0.05$; n = 6. B) Immunoprecipitation of endogenous HDAC6 and MyD88 followed by western-blot for both proteins. Immunoprecipitations were carried out using human moDCs after 30 min of stimulation with

Pam2GSK4, Pam3GSK4 and HKLM. Endogenous HDAC6 (130 KDa) and MyD88 (33 KDa) are indicated at right of western-blot. Similar results were obtained in two independent experiments. C) Immunoprecipitation of HA (MyD88) followed by western-blot for HDAC6 and MyD88. Immunoprecipitations were carried out using different HDAC6-eGFP plasmids co-transfected with MyD88-HA in HEK-Blue hTLR2 cell line after 30 min of stimulation with HKLM. Over-expressed (HDAC6-eGFP, 160 KDa) and endogenous HDAC6 (130 KDa) are indicated at right of western-blot. Similar results were obtained in four independent experiments. D) Immunoprecipitation of HA (MyD88) followed by mass spectrometry analysis. Immunoprecipitations were carried out using different HDAC6-eGFP plasmids co-transfected with MyD88-HA in HEK-Blue hTLR2 cell line after 30 min of stimulation with HKLM. The number of unique MyD88 and HDAC6 peptides is indicated. No acetylated peptides from MyD88 were detected in any sample. Similar results were obtained in four independent experiments. E) Graph of NF-κB induction in transfected *HDAC6-WT*, *HDAC6-DD* and *shHDAC6* HEK-Blue hTLR2 cell line after activation with HKLM, Pam2GSK4 and Pam3GSK4 during 8 h. NF-κB induction was calculated by the ratio of the signal of stimulated cells with its corresponding transfected cells in basal condition (without stimuli), $^{***}p\leq0.001$, ** $p\leq0.01$, * $p\leq0.05$, ns>0.05 non-significant; n = 6. F) Survival curve to intravenous injection with a lethal dose of *Lm* in $Hdac6^{+/+}$ and $Hdac6^{-/-}$ is showed. This curve corresponds to two different experiment of survival to *Lm* with a n = 24–21. $^{***}p\leq0.001$. G) Pro-inflammatory cytokine IL-6 was measured in sera of $Hdac6^{+/+}$ and $Hdac6^{-/-}$ mice intravenously injected with a lethal dose of *Lm* at 12, 48 and 72 hpi. $^{*}p\leq0.05$, n = 5.

https://doi.org/10.1371/journal.ppat.1006799.g009

vivo Lm infection at 6 hpi in various myeloid subsets of the spleen. The absence of this effect during BMDC *in vitro* infection by the non-intracellular bacteria *S. aureus* and *E. coli* DH5α indicates that $Hdac6^{-/-}$ BMDCs are specifically unable to efficiently clear intracellular pathogens. HDAC6 is involved in two of the most important cellular clearance systems, autophagy and ubiquitin-proteasome system (UPS) [9, 13]. In the case of *Lm* and *S.* Typhimurium, the main molecular mechanism for degradation of vesicle-contained bacteria is fusion with lysosomes in a process called autophagy [45–47]. In agreement with this, our data show that impaired phagosome-lysosome fusion underlies the phenotype observed in $Hdac6^{-/-}$ BMDCs. Unsuccessful fusion depends on acetylated-cortactin in *Hdac6*-deficient cells [9]. A similar mechanism has been described in *Hdac6*-deficient MEFs during quality-control autophagy [9]. We demonstrated that in $Hdac6^{-/-}$ BMDCs co-localized higher levels of acetylated-cortactin with intracellular *Lm*. The delay in vesicle fusion caused by the acetylation of cortactin, impairs the phagosome-lysosome fusion and provides more opportunities for phagosome-containing bacteria to escape to the cytosol, resulting in the higher bacterial load detected in $Hdac6^{-/-}$ BMDCs. Based on this experimental evidence, it is conceivable to postulate that the enzymatic activity of HDAC6 on its substrate cortactin controls autophagy of intracellular bacteria for their efficient clearance (Fig 10).

Pharmacological autophagy inhibitors erased the observed differences between $Hdac6^{+/+}$ and $Hdac6^{-/-}$ BMDCs. Conversely, rapamycin did not overcome the $Hdac6^{-/-}$ autophagy defect, indicating a defect in phagosome-lysosome fusion. However, other authors have reported opposite observations using pan-HDAC inhibitors or specific inhibitors of HDAC6 during infection of human macrophages with the *Gram*-negative intracellular pathogens *S.* Typhimurium and *E. coli* [48]. These inhibitors, when added at the time of infection, increase mitochondrial ROS production [48]. However, overnight pre-treatment before infection hampered bacterial clearance and reduced phagocytosis [48]. These data indicate that specific HDAC6 chemical inhibitors can have side-effects, including effects on other HDAC members, potentially interfering with the acetylation of other substrates upstream of cortactin that also have a role during bacterial infection. Our genetic approach unequivocally assigns a specific role to HDAC6 in innate cells during bacterial infection.

Although we observed an impairment in phagosome-lysosome fusion, we cannot rule out an involvement of HDAC6 in the anti-microbial response through its BUZ domain, with a contribution from ubiquitin. The characterized interaction between p62 and HDAC6 through their ubiquitin-binding domains provides a clue about the possible role of ubiquitin in the activation of innate immunity through the recognition of ubiquitinated-molecules [15]. For example, the ubiquitin-binding regions of HDAC6 and p62 are both essential for MyD88

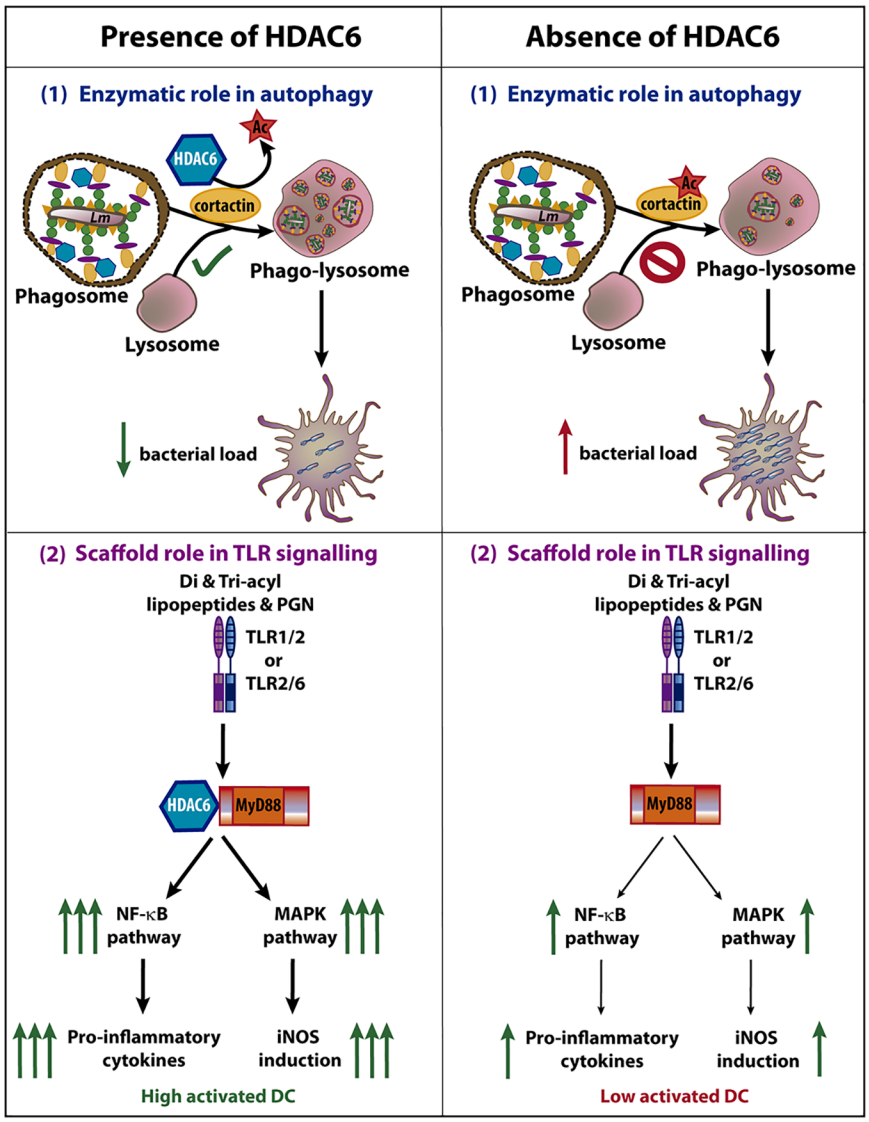

Fig 10. Dual role of HDAC6 during *Lm* infection in dendritic cells. The scheme shows the involvement of HDAC6 in two different functions of dendritic cell during *Lm* infection, the autophagy and the TLR signalling. **(1)** The fusion of phagosome with lysosome is dependent on cortactin and F-actin. The deacetylation of cortactin by HDAC6 allows the correct fusion, followed by an autophagic clearance of *Lm*. The absence of this enzyme delays the fusion of phagosome and lysosome, facilitating *Lm* to escape from phagosome leading to an increased bacterial load. **(2)** Di- and tri-acyl lipopeptides and peptidoglycan (PGN) of *Lm* are recognized by TLR1/2 or TLR2/6, activating the TLR pathway. HDAC6 is able to interact with the TLR-adaptor protein MyD88 which caused an enhanced down-stream signalling of TLR pathway, increasing NF-κB and MAPK activation. This stronger activation (independent on HDAC6 enzymatic activity) results in higher pro-inflammatory cytokine production and iNOS induction, reinforcing the ability of the DC to combat against this intracellular pathogen. Although the absence of HDAC6 does not fully abolish the activation of the DC, a lower induction of NF-κB and MAPK pathways promotes a lower activation of the anti-bacterial transcriptional program of the DCs. Note that both processes occur during *Lm* infection and the pro-inflammatory cytokines and iNOS induction can impact on the autophagic process. The images in the figure are not scaled.

https://doi.org/10.1371/journal.ppat.1006799.g010

aggregation and the downstream activation of MyD88-dependent signal transduction [49]. Furthermore, ubiquitin-binding platforms formed by HDAC6 and p62 are able to interact with interferon stimulated gene 15 (ISG15) to eliminate ISGylated proteins tagged after interferon stimulation by autophagy [50]. HDAC6 is able to bind to either mono- and poly-

ubiquitinated proteins, but shows a preference for proteins modified with k63-linked ubiquitin chains, which share structural similarities with ISG15 [51]. *S*. Typhimurium is decorated with this kind of ubiquitin chain for recognition by host cells, and can be recovered with phagosome proteins to initiate autophagy [52, 53]. Nevertheless, our data demonstrate that autophagy induction does not differ between *Hdac6*$^{+/+}$ and *Hdac6*$^{-/-}$ BMDCs, indicating that this phenotype is due to p62 accumulation in *Hdac6*$^{-/-}$ BMDCs as a consequence of impaired phagosome-lysosome fusion. Intact autophagy activation in *Hdac6*$^{-/-}$ BMDCs could be explained by compensatory p62 binding to ubiquitinated bacteria in the absence of HDAC6.

Our data also underscore other different function of HDAC6, independent of its enzymatic activity, in innate immune response to intracellular bacteria and various TLR stimuli (Fig 10). Hence, we provide evidence for a dampened inflammatory response in the absence of HDAC6, as shown by lower RNA levels of pro-inflammatory cytokines, chemokines, type-I interferons, and interferon-related proteins in *Hdac6*$^{-/-}$ BMDCs than in *Hdac6*$^{+/+}$ cells at 6 hpi, as well as the lower pro-inflammatory cytokine production and IFN-β secretion by infected *Hdac6*$^{-/-}$ BMDCs from 6 to 24 hpi. Moreover, *Hdac6*$^{-/-}$ BMDCs showed diminished iNOS induction at 6 hpi associated with low nitrite production and iNOS expression at longer times of *Lm* infection (24 hpi). These results agree with a lower phosphorylation of the MAPK pathway after *Lm* infection in *Hdac6*$^{-/-}$ dendritic cells, controlling the activation of AP-1 family transcription factors, which is necessary to switch inflammatory responses on [54]. In addition, the lower phosphorylation of mTORC1 pathway components in *Hdac6*$^{-/-}$ DCs is consistent with a lower pro-inflammatory response, as reported in trained macrophages and dendritic cells, in which a metabolic switch to glycolysis has been described [55]. These data may indicate that HDAC6 also appears to play a role in the activation of mTOR pathway after *Lm* infection to initiate the antibacterial transcriptional response to combat this pathogen. In summary, our results reveal a defect in DC activation after *Lm* entry.

Remarkably, this impaired anti-inflammatory response in *Hdac6*$^{-/-}$ BMDCs was also observed with other TLR-agonists such as LPS, Imiquimod, poly(I:C) and Pam3GSK4, highlighting HDAC6 as an important player in TLR signalling activation. Broad-spectrum HDAC inhibitors such as TSA exert immunosuppressive effects [56]. Genome-wide expression profiling arrays have revealed that 60% of genes transcriptionally increased by TLR2 or TLR4 stimulation are inhibited in TSA-treated cells, whereas 16% of genes are potentiated [56]. However, these observations do not provide any demonstrative evidence for a specific role of HDAC6, since other HDACs may also be involved.

Because GM-CSF-derived DCs express low levels of TLR3 and 5 in the membrane, we stimulated FLT3-L-derived DCs with poly(I:C) and flagellin to measure pro-inflammatory cytokines [57, 58], noting maintained failure in the inflammatory response in *Hdac6*$^{-/-}$ cells. Moreover, we detected impaired responses to PAMPs activation in GM-CSF-derived and FLT3L-derived *Hdac6*$^{-/-}$ DCs. In addition, all TLRs except for TLR3 signal through the adaptor MyD88, and the result obtained with the TLR3 ligand poly(I:C) was similar to that showed for the rest of TLR stimuli, thereby indicating that the TLR3-response is also affected by absence of HDAC6. In this regard, these data are in agreement with a recent study showing that acetylated retinoic-acid-inducible gene-1 (RIG-1) makes *Hdac6*$^{-/-}$ cells less sensitive to the presence of RNA viruses, resulting in a higher viral titre [59]. While this mechanism could explain the difference between the response of *Hdac6*$^{+/+}$ and *Hdac6*$^{-/-}$ FLT3L-DCs to TLR3 stimulation, the deficient activation by other TLRs in *Hdac6*$^{-/-}$ DCs also requires an explanation. In this respect, we demonstrate the molecular association of HDAC6 with MyD88 with endogenous proteins and in an overexpression system. Conceivably, the depletion of HDAC6 and therefore prevention of HDAC6-MyD88 binding, could inhibit TLR-2-signalling pathway activation, which is in accordance with a lower NF-κB induction measured in *Hdac6*$^{-/-}$ cells after various

TLR-2 agonist stimulation. A diminished NF-κB induction in *Hdac6*$^{-/-}$ cells could explain a reduced initiation of the pro-inflammatory response observed in *Hdac6*$^{-/-}$ dendritic cells, needed to alert the innate and adaptive immune response to *Lm*. However, NF-κB activity of HDAC6-DD-transfected HEK cell line after TLR-2 stimuli did not display any significant change compared to HDAC6-WT-transfected ones, supporting that enzymatic activity of HDAC6 is not involved in this signalling pathway. Two acetylated peptides corresponding to MyD88 have been found in basal condition in HEK transfected with HDAC6-DD and shHDAC6 constructions, which are different from the residue previously described in MyD88 [60]. However, no changes in the acetylation marks on MyD88 were detected after HKLM incubation, highlighting the scaffold role of HDAC6 in the proper activation of TLR-signalling pathway (Fig 10). Unexpectedly, a protective effect against systemic infection to a lethal dose of *Lm* were observed in *Hdac6*$^{-/-}$ mice. The reduced level of the inflammatory cytokine IL-6 detected in *Hdac6*$^{-/-}$ mice are in accordance with its higher resistance to *Lm* infection. The defective systemic inflammatory response after *Lm* infection of *Hdac6*$^{-/-}$ mice may indicate an impaired TLR-response in the absence of HDAC6 and might therefore be attributed to the absence of the molecular association of MyD88 and HDAC6. In this regard, mice resistance to *Lm* infection can be mediated by sequential MyD88-independent and -dependent responses [61–64]. However, the role of TLR-2 during *Lm* infection does not appear to be clear enough [62, 63]. On one hand, *Tlr-2*$^{-/-}$ mice display a deficit in circulating TNF-α and IL-12p40 production during intravenously injected *Lm* infection combined with a lower mice survival and increased bacterial burden in the liver [61, 63]. Other authors have obtained similar resistance to intraperitoneal-injected *Lm* infection between *Tlr-2*$^{-/-}$ and *Tlr-2*$^{+/+}$ mice, indicating that different inoculation routes of bacteria may render different immune outcomes [62]. Although handling and direct killing of *Lm* by activated macrophages can be mediated by TLR-2- and MyD88-independent mechanisms, the role of TLR-signalling has been observed necessary for nitric oxide and cytokine production [61, 63]. In fact, MyD88 not only works as TLR-adaptor protein, but also as adaptor of IL-1 and IL-18 receptors, both cytokine responses affected in *Lm*-MyD88$^{-/-}$ mice [62, 63, 65].

Overall, our data support a dual role for HDAC6 in the regulation of innate immunity against intracellular bacteria. An increased bacterial load in different *Hdac6*$^{-/-}$ myeloid cells can be explained by the autophagy mechanism, where a permanently acetylated cortactin may impair the phagosome-lysosome fusion, necessary for the clearance of this pathogen. Our experiments also show the importance of HDAC6 in DC activation, uncovering a novel mechanism of HDAC6 action mediated by the appropriate signalling via the TLR pathway, due to the association of HDAC6 with the TLR-adaptor protein MyD88. This molecular association seems to be required for a response to TLR stimuli to initiate the inflammatory response of an activated dendritic cell. Taken together, both HDAC6 functions described in this manuscript, reinforce the importance of this molecule to combat intracellular bacteria as *Lm* by autophagy and to completely activate the inflammatory response after TLR activation.

Materials and methods

Ethical statement

Mice were housed under specific pathogen-free conditions at the Centro Nacional de Investigaciones Cardiovasculares Carlos III (CNIC), and experiments were approved by the CNIC Ethical Committee for Animal Welfare and by the Spanish Ministry of Agriculture, Food, and the Environment. Animal care and animal procedures license were reviewed and approved by the local Ethics Committee for Basic research at the CNIC Ethical Committee for Animal Welfare and the Órgano Encargado del Bienestar Animal (OEBA) del Gabinete Veterinario de la

Universidad Autónoma de Madrid (UAM). This committee approved the document with an associated identification number PROEX 158/15 (CNIC 04/15).

Buffy coats of healthy donors were received from the Blood Transfusion Center of Comunidad de Madrid, and all donors signed their consent for the use of samples for research purposes. All the procedures using primary human cells were approved by the Ethics Committee of the Hospital Universitario de la Princesa.

Mice

HDAC6$^{-/-}$ mice were generated through targeting of exons from 10 to 13 by inserting a neomycin (Neo) and zeocin (Zeo) cassette, resulting in the disruption of the first catalytic domain of HDAC6 [66]. These mice were intercrossed on a C57BL/6 background to generate sex and age matched wild-type (*wt*) and knockout.

Bacteria strains

We used the *Listeria monocytogenes EGD* (BUG 600) strain, provided by Dr. Esteban Veiga (Centro Nacional de Biotecnología, CNB, Madrid). *Staphylococcus aureus* 132 and *Escherichia coli* K12, strain DH5α, were purchased from Invitrogen. BUG600 and *S. aureus* bacteria were grown in BHI broth. RFP-expressing *Listeria monocytogenes* (RFP-*Lm*) was provided by Dr Carlos Ardavín´s laboratory (Centro Nacional de Biotecnología, CNB, Madrid). *Salmonella enterica* serovar Thyphimurium strain SL1344 was provided by Dr. J. Garaude (Centro Nacional de Investigaciones Cardiovasculares, CNIC, Madrid). SL1344 and DH5α bacteria were grown in LB broth supplemented with 50 μg/ml streptomycin (Sigma). For phagocytosis experiments, *Lm* and *S. aureus* were grown overnight in Brain Herat Infusion (BHI) broth and *E. coli* and *S.* Thyphimurium in Luria-Bertani (LB) broth with shaking, diluted 1/50, and grown until log-phase (optical density 0.8–1.2 at 600 nm) without shaking. Bacteria were washed with phosphate-buffered saline (PBS) to remove LB salts before addition to cells.

Cell culture

The HEK293T cell line (ATCC) was cultured in DMEM medium (Sigma) containing 10% FBS (Invitrogen), 2 mM L-glutamine, 100 mg/ml penicillin and 100 mg/ml streptomycin. HEK Blue hTLR2 cell line (Invivogen), the HEK293 cell line expressing human TLR2, CD14 and NF-κB-SEAP (secreted embryonic alkaline phosphatase) reporter gene was cultured in DMEM medium (Sigma) containing 10% FBS (Invitrogen), 2 mM L-glutamine, 100 μg/ml Normocin (Invivogen) and 1X HEK-Blue Selection (Invitrogen).

Generation of bone marrow-derived dendritic cells (GM-CSF) and macrophages (M-CSF)

Mouse primary dendritic cells (BMDCs) and macrophages (BMDMs) were obtained from bone marrow cell suspensions after culture on non-treated 150-mm Petri dishes in complete RPMI 1640 supplemented with 10% FBS, 2 mM L-glutamine, 100 mg/ml penicillin, 100 mg/ml streptomycin, 50 mM 2-ME, and 20 ng/ml granulocyte-macrophage colony-stimulating factor (GM-CSF, PeproTech, London, U.K.) for BMDCs and macrophage colony-stimulating factor (30% mycoplasma-free L929 cell supernatant, NCBI Biosample accession number SAMN00155972) for BMDMs. BMDCs were collected at day 9 and BMDCs were characterized as $CD11c^{+}MHC\text{-}II^{+}Gr\text{-}1^{-}$ cells by flow cytometry. BMDMs were collected at day 6 and BMDMs were characterized as $CD11b^{+}F4/80^{+}$ or $CD11b^{+}CD64^{+}$ cells.

Generation of bone marrow-derived dendritic cells (FLT3L)

Bone marrow cell suspensions were culture on treated 6 well plates in complete RPMI 1640 supplemented with 10% FBS, 2 mM L-glutamine, 100 mg/ml penicillin, 100 mg/ml streptomycin, 50 mM 2-ME, and 150 ng/ml (FLT3L, PeproTech, London, U.K.). After 9–11 days of differentiation cells were collected to be characterized by flow cytometry as $CD11c^{+}B220^{-}CD11b^{+}CD24^{-}$ (60% of the culture) and $CD11c^{+}B220^{-}CD11b^{+}CD24^{+}$(40%).

Obtainment of thioglycollate-elicited macrophages (TEMs)

Mice received peritoneal injections with 1ml 4% TG. The peritoneal exudate was collected after 4 days and cultured in complete RPMI 1640 supplemented with 10% FBS, 2 mM L-glutamine, 100 mg/ml penicillin, 100 mg/ml streptomycin, and 50 mM 2-ME. To enrich the culture for macrophages, non-adherent cells were eliminated after a few hours by washing five times with warm PBS and gentle swirling.

Obtainment of human monocyte-derived dendritic cells (moDCs)

Peripheral blood mononuclear cells (PBMCs) from Buffy coats of healthy donors were isolated using Biocoll separating solution (Millipore) by centrifugation at 700 g 30 min at RT. Monocytes were purified from peripheral blood mononuclear cells (PBMCs) by an adherence step at 37˚C in incomplete RPMI 1640 medium during 1 h. Non-adherent cells were removed and adherent monocytes were washed three times with warm 1xPBS to remove residual PBMCs. Monocytes were cultured in complete RPMI 1640 supplemented with 10% FBS, 2 mM L-glutamine, 100 mg/ml penicillin, 100 mg/ml streptomycin, 500 U/ml IL-4 (R&D) and 500 U/ml GM-CSF (Immunotools) for 6 days. Fresh medium and cytokines were added every 48 hours to differentiate monocytes to immature human dendritic cells. Cells were characterized by flow cytometry as $HLA\text{-}DR^{+}CD3^{-}DC\text{-}SIGN^{+}CD14^{-}CD11c^{+}$. Activation of dendritic cells was induced with Pam2GSK4, Pam3GSK4 and HKLM for 30 min (Invivogen).

In vitro Lm-infection of BMDCs, BMDMs and TEMs

Cells were incubated with *Lm* and assessed for survival to gentamicin exposure [67]. Cells were infected with *Lm* at a multiplicity of infection (MOI) of 10 for 30 min at 37˚C. To determine the number of bacteria entering the cells, extracellular bacteria were killed by treatment with 100 μg/ml gentamicin (Sigma-Aldrich, St. Louis, MO) for an additional 30 min at 37˚C. Then, infected cells were washed with PBS three times and lysed with 0.05% Triton X-100 (Sigma-Aldrich, St. Louis, MO) in distilled water. Serial dilutions were seeded on brain-heart infusion (BHI) agar plates and CFUs were counted after 36 hours.

In vivo Lm systemic infections

$Hdac6^{+/+}$ and $Hdac6^{-/-}$ were intravenously injected with *Listeria monocytogenes* EGD (125.000 CFUs/mouse) using a 29-gauge needle. For survival experiments mice were monitored twice a day in order to detect casualties during 15 days of infection.

Determination of CFUs in target organs

After 12, 24, 48 and 72 hpi, mice were perfused with 1X PBS to clean blood form organs and spleens and livers were weight. To determine bacterial load, spleens and livers were digested with 0.1 mg/ml type IV collagenase and 0.5 mg/ml DNAse I (Roche, Mannheim, Germany) for 30 min at 37˚C. After digestion, organs were homogenized in 70 μm filters and red blood cells were lysed with ammonium chloride potassium lysis buffer (ACK, Sigma). Splenic cell

suspensions were resuspended in PBS and cells were counted. Serial dilutions were grown on BHI agar plates. CFUs were counted after 36 hours of incubation at 37˚C. CFUs were calculated by cell number and by gram per organ.

Antibodies and reagents

Antibodies were used in western blotting, flow cytometry and immunofluorescence; detailed information is available in S1 Table. Poly-L-lysine (PLL) was purchased from Sigma. Phalloidin-Alexa488 and 647 were from BD Biosciences. Zenon Alexa Fluor 488 rabbit IgG labelling kit, DAPI and Prolong Gold anti-fade mounting medium were from Thermofisher Scientific. Anti-human CD3 antibody (T3b hybridoma) was generated in Dr. F. Sánchez-Madrid laboratory (Hospital Universitario de la Princesa, HUP, Madrid) [68]. Rapamycin, bafilomycin A1, 3-MA, cloroquine, NH_4Cl, 1400W and DPI were from Sigma-Aldrich.

Gene overexpression and silencing

HEK293 cells were co-transfected with plasmids encoding human MyD88 fused to the HA-tag (Addgene plasmid #12287) together with plasmids encoding *HDAC6-WT* or double deacetylase domain mutant DD (mutated human HDAC6-H216A/H611A) fused to the eGFP tag (*HDAC6-WT* and *HDAC6-DD* have been previously described [26]. When indicated, cells were co-transfected with the appropriate small harping RNA plasmid pLVX-IRES-ZsGreen1, where *shHDAC6*-2049 (TRCN0000004842) was cloned between BamH1 and EcoR1 sites. Cells were transfected using Lipofectamine 2000 (Invitrogen). Experiments were performed after 24 h after transfection.

RNA extraction and real-time quantitative PCR

RNA from mouse BMDCs was isolated with the QIAGEN RNeasy Kit (Qiagen). Residual DNA contamination was removed with the Turbo DNA-free Kit (Ambion). Total RNA (1–2 μg) was reverse transcribed to cDNA with a Reverse Trancription Kit (Applied Biosystems). Quantitative PCR was then performed in an AB7900-384 thermocycler (Applied Biosystem) using SYBR Green master mix (Applied Biosystems, Warrington, UK) as the reporter. Expression levels of target genes were normalized to the expression of housekeeping genes β-actin, GAPDH, β2-microglobulin and Yhwaz (tyrosine 3-monooxygenase/tryptophan 5-monooxygenase activation protein, ζ) for presentation of relative mRNA levels. Data were analysed with Biogazelle qBasePlus version 2.3 (Biogazelle) and graphs are represented as a normalized expression scaled to average of all samples. Gene-specific primers used are listed in S2 Table.

Soluble embryonic alkaline phosphatase (SEAP)-NF-κB detection

50.000 transfected HEK-Blue hTLR2 cells with different HDAC6 constructions were place in bottom p96 well plates resuspended in HEK-Blue Detection medium (Invivogen) without stimulus (negative control) and with TLR-2 agonists (HKLM stimulus, MOI = 10). After 8–12 h of incubation, SEAP activity was measured by optical density at 620 nm with a microplate reader. To calculate the NF-κB induction, the signal obtained from each mutant condition without stimuli (background) was depleted of the signal of each condition of activation with Pam2GSK4, Pam3GSK4 or HKLM.

ELISAs and nitrite measurement

Cytokine and NO production was analysed in the supernatants of BMDC cultures at 6, 12 and 24 h after stimulation with *Lm*, heat-killed *Listeria monocytogenes* (HKLM), heat-killed

Salmonella Typhimurium (HKST), Pam3CSK4, Flagellin, Imiquimod, polyinosinic-polycytidylic acid (Poly(I:C)) (InvivoGen, San Diego, CA), or LPS from *Escherichia coli* (Sigma-Aldrich). TNF-α and IL12p70 were analysed with OptEIA ELISA kits (BD Biosciences, San Diego, CA), IL-1β and IL-6 with the mouse ELISA Ready-SET-Go! kit from eBioscience (Affymetrix, San Diego, CA) and Interferon-β was measured with Legend max mouse IFN-β ELISA kit (Biolegend). The detection was based on colorimetric quantification of absorbance at 450 nm, corrected with subtraction at 570 nm measured in a microplate reader (Bio-Rad Model 550). NO was estimated from the nitrite concentration measured with a Griess reagent kit at 548 nm (Molecular Probes/Life Technologies, Thermo Fisher Scientific). Results were expressed as the means of duplicate wells.

Immunoblotting

Total cell extracts from BMDCs stimulated with *Lm*, HKLM or the indicated TLR ligands for the indicated times were prepared in lysis buffer (0.5% Triton X100, 25 mM Tris-HCl pH 7.5, 0.5 mM EGTA, 0.5 mM EDTA, 25 mM NaF, 0.5 sodium glycerol-phosphate, 2.5 mM pyrophosphate, 0.135 M sacarose) with a cocktail of protease and phosphatase inhibitors (Roche). Cell lysates were cleared of nuclei by centrifugation at 15,000 g for 15 min. Protein extracts were separated by 8–15% SDS-PAGE and transferred to a PVDF membrane (Biorad). Proteins were visualized with LAS-3000 after membrane incubation with specific antibodies (see S1 Table) and peroxidase-conjugated secondary antibodies (5 μg ml^{-1}). Band intensities were quantified using Image Gauge software (Fuji Photo Film, Co., Ltd) and results are expressed relative to loading controls. For quantification of western-blots, phosphorylated/total ratios were divided by loading control signal. Non-infection (NI) time was considered as 100%, and following times were relativized to it.

Immunoprecipitation of MyD88 and HDAC6 proteins

Human moDCs (1×10^7 per condition) were lysed (10 mM Tris pH 7.4, 150 mM NaCl, 5% glycerol, 1mM EDTA, 1mM $MgCl_2$, 1mM $CaCl_2$, 1% CHAPS (Sigma) and protease and phosphatase inhibitors (Roche)) for 1 h at 4˚C. Lysates were incubated for pre-clearing with pre-washed Protein G Dynabeads (Invitrogen; 50 μl per condition; 2 h, 4˚C). Pre-cleared lysates were incubated with 6 μg rabbit anti-MyD88 antibody (Cell Signaling) or 6 μg rabbit anti-HDAC6 antibody (Assay bioTech) per condition O/N at 4˚C. Similar μg of control isotype antibody for rabbit were used. Fifty microlitres of Dynabeads per condition were washed three times in wash buffer (10 mM Tris pH 7.4, 150 mM NaCl, 5% glycerol, 1mM EDTA, 1mM $MgCl_2$, 1mM $CaCl_2$, 0.1% CHAPS) and added to antibody-conjugated lysates for 2 h 4C. Antibody-conjugated Dynabeads were washed six times with wash buffer and transferred to clean tubes.

HEK293T cells or HEK-Blue hTLR2 (1×10^7 per condition) were lysed (25 mM Tris pH 8, 150 mM NaCl, 0.5% NP-40 and protease and phosphatase inhibitors) and incubated for pre-clearing with pre-washed Protein G Dynabeads (Invitrogen; 50 μl per condition; 3 h, 4˚C). Fifty microlitres of Dynabeads per condition were washed three times in wash buffer (25 mM Tris pH 8, 150 mM NaCl, 0.05% NP-40) and re-suspended in 600 μl of wash buffer containing 1–2 μg mouse anti-HA antibody (Roche) per condition and incubated 3 h at 4˚C. Similar μg of control isotype antibody for mouse were used. Pre-cleared lysates were incubated with antibody-conjugated Dynabeads (O/N, 4˚C). Antibody-conjugated Dynabeads were washed six times with lysis buffer and transferred to clean tubes. Then, were washed twice with wash buffer. Protein loading buffer was added, samples were boiled at 95˚C for 5 min and processed for immunoblotting.

Flow cytometry

Cells were stained in ice-cold PBS containing FBS (0.5%) and EDTA (5 mM) using appropriate antibody-fluorophore conjugates. Multiparameter analysis was performed on a FACSCANTO II flow cytometer (BD Biosciences) and analysed with FlowJo software (Tree Star). Prior to fixing, cells were resuspended in PBS/0.5% BSA/5 mM EDTA solution containing yellow fluorescent reactive dye to exclude dead cells (Life Technologies). For intracellular staining, cells were fixed and permeabilized using the CytoFix/Cytoperm kit (BD).

Fluorescence confocal microscopy

For immunofluorescence assays, cells were plated onto slides coated with poly-L-lysine (50 μg ml^{-1}) and incubated for 1 h at 37˚C. Infection experiment were carried out at the indicated times. Cells were then fixed, blocked and stained with the indicated primary antibodies (5 μg ml^{-1}) followed by alexa488- or Rhodamine Red X-labelled secondary antibodies (5 μg ml^{-1}). Samples were examined under a Leica SP5 confocal microscope (Leica) fitted with a 63X objective. Images were acquired with sequential xyz acquisition mode scans with laser ranges of 418–473 nm for DAPI, 502–548 nm for Alexa-488, 584–644 nm for Rhodamine X and 737–779 nm for Alexa-647. Z-stacks of 2–5 μm were obtained using a maximum z-step size of 0.3 μm.

Imaris quantification

Images were processed and assembled using Image J 1.51p (Fiji). Confocal 3D images assembled with Imaris 7.7.2 (Bitplane) using the ImarisCell module. Every cell and its corresponding intracellular bacteria were calculated in each image. Surfaces corresponding to bacteria were used to calculate the maximal fluorescence intensity of the channels to co-localize with bacteria. Two-channel co-localization was quantified in at least 10 images per genotype, corresponding to 10 biological samples.

In-gel protein digestion

Proteins were in-gel digested using a previously described protocol [69]. Briefly, the coimmunoprecipitate was heated at 95˚C for 5 min, after which the magnetic beads were removed using a magnet. The resulting solution was added sample buffer and loaded in 0.5-cm-wide wells of an SDS-PAGE gel. The run was stopped as soon as the front entered into the resolving gel. The protein band was visualized by Coomassie Blue staining, excised, and digested overnight at 37˚C with 60 ng/μl sequencing-grade modified trypsin (Promega) at 10:1 protein: enzyme (w/w) ratio in 50 mM ammonium bicarbonate, pH 8.8, containing 10% acetonitrile. The resulting tryptic peptides were desalted onto C18 OMIX tips (Agilent), dried down and kept at -80˚C until further use.

Mass spectrometry

The resulting peptides were analyzed by liquid chromatography coupled to tandem mass spectrometry (LC-MS/MS) on an Easy nLC-1000 nano-HPLC apparatus (Thermo Scientific, San Jose, CA, USA) coupled to a hybrid quadrupole-orbitrap mass spectrometer (Q Exactive HF, Thermo Scientific). The dried peptides were taken up in 0.1% (v/v) formic acid and then loaded onto a PepMap100 C18 LC pre-column (75 μm I.D., 2 cm, Thermo Scientific) and eluted on line onto an analytical NanoViper PepMap 100 C18 LC column (75 μm I.D., 50 cm, Thermo Scientific) with a continuous gradient consisting of 8–31% B in 240 min (B = 80% ACN, 0.1% formic acid) at 200 nL/min. Peptides were ionized using a Picotip emitter

nanospray needle (New Objective). Each MS run consisted of enhanced FT-resolution spectra (120,000 resolution) in the 400–1,200 m/z range followed by data-dependent MS/MS spectra of the 20 most intense parent ions acquired along the chromatographic run. The AGC target value in the Orbitrap for the survey scan was set to 1,000,000. Fragmentation in the linear ion trap was performed at 30% normalized collision energy with a target value of 10,000 ions. The full target was set to 30,000, with 1 microscan and 50 ms injection time, and the dynamic exclusion was set to 0.5 min.

Peptide identification

For peptide identification the MS/MS spectra were searched with the Sequest algorithm implemented in Proteome Discoverer 1.4 (Thermo Scientific). Database searching against human protein sequences from the UniProt database (March 2017, 158,382 entries) was performed with the following parameters: trypsin digestion with 4 maximum missed cleavage sites; precursor and fragment mass tolerances of 800 ppm and 0.02 Da, respectively; Cys carbamidomethylation as static modifications; and Met oxidation and Lys acetylation as dynamic modifications. The results were analyzed using the probability ratio method [70] and a false discovery rate (FDR) for peptide identification was calculated based on the search results against a decoy database using the refined method [71].

Statistical analysis

Data were analysed with GraphPad prism software (La Jolla, CA) for normality (Kolmogorov-Smirnov test for small samples). Normal data were analysed by Student t-test, non-normal data by Mann-Whitney test, and grouped data by 2-tailed One-way ANOVA with a Bonferroni post-test. For western blot quantification, the sample with the maximum signal was assigned a value of 100%, and signals in other samples were expressed as a percentage of this; significance was determined by a one-sample test. Long-rank (Mantel-Cox) test and Cehan-Breslow-Wilcoxon test were used for the analysis of the Kaplan-Meier curve (survival curve).

Supporting information

S1 Fig. Differentiation of GM-CSF-derived DCs, their viability at 6 hpi, comparison of CFUs of GM-CSF- and M-CSF-derived cells and fluorescent confocal microscopy of *Lm*. A) Left: Dot-plots showing CD11c and MHC-II markers, with gating for $CD11c^{+}MHC\text{-}II^{+}$ and $CD11c^{+}MHC\text{-}II^{-}$ populations (percentages indicated). Right: Dot-plots on differentiation day 11 showing FSC-H versus Gr-1, gating the $Gr\text{-}1^{+}$ population corresponding to neutrophil contamination in GM-CSF-derived DC cultures. Charts show the percentages of $CD11c^{+}MHC\text{-}II^{+}$, $CD11c^{+}MHC\text{-}II^{-}$ and $Gr\text{-}1^{+}$ populations. ns>0.05 non-significant; n = 6. B) Percentage viability of BMDCs before infections and at 6 hpi with *Lm*, ns>0.05 non-significant; n = 6. C) Comparison of CFUs in GM-CSF-derived DCs and M-CSF-derived macrophages over the time-course of *Lm* infection. $^{***}p\leq0.001$, $^{**}p\leq0.01$, ns>0.05 non-significant; n = 6. D) ImarisCell Module analysis of the number of cells and the number of bacteria per cell in all pictures (10 pictures per genotype). The graph shows the distribution of cells with a specific number of bacteria per cell. The number of cells with 6 and 7 bacteria differed significantly between the $Hdac6^{+/+}$ and $Hdac6^{-/-}$ genotypes. $^{*}p\leq0.05$, n = 10. E) Confocal microscopy determination of bacterial load of the Fig 1F. Maximum intensity z-projections of confocal microscopy images of *Lm*-infected $Hdac6^{+/+}$ and $Hdac6^{-/-}$ BMDCs at 6 hpi. ImarisCell Module view of the number of nucleus and bacteria per cell. Actin transparency is used to visualize bacteria (number indicated on the right). Images show DAPI (blue),

Lm (red), β-actin (green). Scale bars 20 μm.
(TIF)

S2 Fig. Gating strategy of myeloid populations of the spleen. A) Dot-plots showing the gating of myeloid populations of spleen. Dot-plots showing SSC-A versus FSC-A indicates p1, FSC-H versus FSC-W and SSC-H versus SSC-W were used to avoid doublets and FSC-H versus viability shows live and dead cells. Singlets and live cells were used to choose $CD3^-CD19^-DX5^-Ly6G^+$ cell population. From this population, neutrophils were gated as Ly6G +Ly6C+ cells, monocytes as $CD11b^+CD11c^{lo}$, Tips DCs as intermedium levels of CD11b and CD11c, conventional dendritic cells (cDCs) as $CD11c^{hi}$; inside this population cDCs $CD8^-$ were distinguish as $CD11c^{hi}CD11b^+$ and cDCs $CD8^-$ as $CD11c^{hi}CD11b^{lo}$. B) Representative histograms of different splenic populations (monocytes, neutrophils, Tips DCs, total cDCs, cDCs $CD8^-$ and cDCs $CD8^+$) show *Lm* signal of $Hdac6^{+/+}$ and $Hdac6^{-/-}$ mice injected with a lethal dose of *Lm* at 6 hpi. A pool of $Hdac6^{+/+}$ and $Hdac6^{-/-}$ spleens non-infected was used as a control sample without infection (NI). $^{**}p\leq0.01$, $^{*}p\leq0.05$; n = 6.
(TIF)

S3 Fig. Control vehicles and autophagy markers. A) Total CFUs at 0 and 6 hpi in *Lm*-infected BMDCs (MOI of 10) treated with different control vehicles (H_2O, DMSO and ethanol). H_2O were the control vehicle used for NH_4Cl and cloroquine, DMSO for 3-MA, bafilomycin A1, DPI and 1400W and ethanol for rapamycin. Time 0 is included as a bacterial entry control. $^{***}p\leq0.001$, ns>0.05 non-significant; n = 6. B) PCR analysis of autophagy markers (ATG-2, 5, 7 and 12, LC3A and B, p62 and Beclin-1) and lysosome markers (LAMP-1 and 2) (arbitrary units) after 6 hpi with *Lm*, ns>0.05 non-significant; n = 5.
(TIF)

S4 Fig. Pro-inflammatory cytokine secretion. ELISA detection of the pro-inflammatory cytokines IL-1β and IL12p70 (pg/ml) in supernatants (S) and in supernatants plus the corresponding cell pellets (S+P) of *Lm*-infected $Hdac6^{+/+}$ and $Hdac6^{-/-}$ BMDCs at 6, 12 and 24 hpi. $^{***}p\leq0.001$, $^{**}p\leq0.01$, $^{*}p\leq0.05$, ns>0.05 non-significant; n = 5.
(TIF)

S5 Fig. TLR expression and TLR-signalling pathway activation by LPS and HKLM. A) Western-blot analysis in $Hdac6^{+/+}$ and $Hdac6^{-/-}$ BMDCs over the time-course of LPS or HKLM treatment. Total and phosphorylated AKT were detected for both treatments. Accompanying charts on the right show quantification, indicating the percentage of phAKT/total AKT ratio. $^{**}p\leq0.01$, $^{*}p\leq0.05$; n = 4. B) PCR analysis of TLR-1, 2 and 6 (arbitrary units) in $Hdac6^{+/+}$ and $Hdac6^{-/-}$ BMDCs non-infected (NI) and after *Lm*-infection at 6 hpi. ns>0.05 non-significant; n = 6.
(TIF)

S6 Fig. Differentiation of FLT3-L DCs, their pro-inflammatory cytokine secretion at 6 hpi and association of HDAC6 with TLR-adaptor MyD88. A) Left: Dot-plots of FLT3-L DC cultures at day 11 of differentiation, showing gating for the CD11c+ population (percentages indicated). Centre: Dot-plots showing CD11b versus B220 to select two populations: $CD11c^+CD11b^+B220^+$ (plasmacytoid DCs, pDCs) and $CD11c^+CD11b^+B220^-$ (conventional DCs, cDCs) (percentages indicated). Right: Dot-plots showing CD11b versus CD24 to select the $CD11b^+CD24^+$ and $CD11b^+CD24^-$ populations (gated from cDCs) (percentages indicated). The charts on the right show the percentages of $CD11c^+$, $CD11c^+CD11b^+B220^-CD24^-$ and $CD11c^+CD11b^+B220^-CD24^+$ populations, ns>0.05 non-significant; n = 6. B) ELISA detection of the pro-inflammatory cytokines IL-1β and IL-6 (pg/ml) in supernatants of

Hdac6$^{+/+}$ and *Hdac6*$^{-/-}$ FLT3L-DCs activated with LPS, Imiquimod, Pam3GSK4, HKLM, HKST, *Lm*, Poly(I:C) or flagellin for 6 h. $^{***}p \leq 0.001$, ** $p \leq 0.01$, * $p \leq 0.05$; n = 6. C) MyD88 adaptor protein in *Hdac6*$^{+/+}$ and *Hdac6*$^{-/-}$ BMDCs. Western-blot analysis of MyD88 over the time-course of *Lm* infection in *Hdac6*$^{+/+}$ and *Hdac6*$^{-/-}$ BMDCs (left). Accompanying charts on the right show quantification of the percentage of MyD88; ns non-significant; n = 5. D) Immunoprecipitation of HA (MyD88) followed by western-blot for HDAC6 and MyD88. Immunoprecipitations were carried out using different HDAC6-eGFP plasmids co-transfected with MyD88-HA in HEK cell line. Over-expressed (HDAC6-eGFP, 160 kDa) is indicated at right of western-blot. E) Immunoprecipitation of HA (MyD88) followed by mass spectrometry analysis. Immunoprecipitations were carried out using different HDAC6-eGFP plasmids co-transfected with MyD88-HA in HEK cell line. The number of unique MyD88 and HDAC6 peptides identified is indicated. (*) indicates the presence of acetylated MyD88 peptides. Similar results were obtained in three independent experiments. F) MS^2 fragmentation spectra from the peptides showing at 1217.0699 (Top), and 599.3803 (Bottom). Ion adscription to carboxy- (*y* ions, blue) and amino-terminal (*b* ions, red) fragmentation series is indicated. K_{ac} denotes acetylated lysine and C_{cm} indicates carbamidomethylated cysteine. Fragment ion sequence coverage is schematically indicated. Similar results were obtained in three independent experiments.
(TIF)

S1 Table. Antibody table. Table of antibodies used in experimental procedures disclosed by reference, brand, host, application and dilution.
(PDF)

S2 Table. qPCR primers. Table of qPCR primers used in experimental procedures disclosed by gene name and sequence 5′-3′.
(PDF)

Acknowledgments

We thank Dr S. Bartlett for assistance with English editing and M.V. Manzanares for critical reading of the manuscript. Some experiments were performed in the CNIC Proteomics Units.

Author Contributions

Conceptualization: Olga Moreno-Gonzalo, Danay Cibrián, María Laura Saiz, Francisco Sánchez-Madrid.

Data curation: Inmaculada Jorge, Emilio Camafeita, Jesús Vázquez.

Formal analysis: Olga Moreno-Gonzalo, María Laura Saiz, Inmaculada Jorge, Emilio Camafeita.

Funding acquisition: Francisco Sánchez-Madrid.

Investigation: Olga Moreno-Gonzalo, Marta Ramírez-Huesca, Noelia Blas-Rus, Danay Cibrián, María Laura Saiz, Francisco Sánchez-Madrid.

Methodology: Olga Moreno-Gonzalo, Marta Ramírez-Huesca, Noelia Blas-Rus, Danay Cibrián, María Laura Saiz, Inmaculada Jorge, Emilio Camafeita, Jesús Vázquez.

Project administration: Francisco Sánchez-Madrid.

Supervision: Francisco Sánchez-Madrid.

Validation: Olga Moreno-Gonzalo, Marta Ramírez-Huesca, Noelia Blas-Rus.

Writing – original draft: Olga Moreno-Gonzalo, Emilio Camafeita, Francisco Sánchez-Madrid.

Writing – review & editing: Olga Moreno-Gonzalo, Francisco Sánchez-Madrid.

References

1. Valenzuela-Fernandez A, Cabrero JR, Serrador JM, Sanchez-Madrid F. HDAC6: a key regulator of cytoskeleton, cell migration and cell-cell interactions. Trends Cell Biol. 2008; 18(6):291–7. https://doi.org/10.1016/j.tcb.2008.04.003 PMID: 18472263.
2. Kaluza D, Kroll J, Gesierich S, Yao TP, Boon RA, Hergenreider E, et al. Class IIb HDAC6 regulates endothelial cell migration and angiogenesis by deacetylation of cortactin. EMBO J. 2011; 30(20):4142–56. https://doi.org/10.1038/emboj.2011.298 PMID: 21847094.
3. Birdsey GM, Dryden NH, Shah AV, Hannah R, Hall MD, Haskard DO, et al. The transcription factor Erg regulates expression of histone deacetylase 6 and multiple pathways involved in endothelial cell migration and angiogenesis. Blood. 2012; 119(3):894–903. https://doi.org/10.1182/blood-2011-04-350025 PMID: 22117042.
4. Schulz R, Marchenko ND, Holembowski L, Fingerle-Rowson G, Pesic M, Zender L, et al. Inhibiting the HSP90 chaperone destabilizes macrophage migration inhibitory factor and thereby inhibits breast tumor progression. J Exp Med. 2012; 209(2):275–89. https://doi.org/10.1084/jem.20111117 PMID: 22271573.
5. Cabrero JR, Serrador JM, Barreiro O, Mittelbrunn M, Naranjo-Suarez S, Martin-Cofreces N, et al. Lymphocyte chemotaxis is regulated by histone deacetylase 6, independently of its deacetylase activity. Molecular biology of the cell. 2006; 17(8):3435–45. https://doi.org/10.1091/mbc.E06-01-0008 PMID: 16738306.
6. Zhang X, Yuan Z, Zhang Y, Yong S, Salas-Burgos A, Koomen J, et al. HDAC6 modulates cell motility by altering the acetylation level of cortactin. Molecular cell. 2007; 27(2):197–213. https://doi.org/10.1016/j.molcel.2007.05.033 PMID: 17643370.
7. Hubbert C, Guardiola A, Shao R, Kawaguchi Y, Ito A, Nixon A, et al. HDAC6 is a microtubule-associated deacetylase. Nature. 2002; 417(6887):455–8. https://doi.org/10.1038/417455a PMID: 12024216.
8. Matsuyama A, Shimazu T, Sumida Y, Saito A, Yoshimatsu Y, Seigneurin-Berny D, et al. In vivo destabilization of dynamic microtubules by HDAC6-mediated deacetylation. EMBO J. 2002; 21(24):6820–31. https://doi.org/10.1093/emboj/cdf682 PMID: 12486003.
9. Lee JY, Koga H, Kawaguchi Y, Tang W, Wong E, Gao YS, et al. HDAC6 controls autophagosome maturation essential for ubiquitin-selective quality-control autophagy. EMBO J. 2010; 29(5):969–80. https://doi.org/10.1038/emboj.2009.405 PMID: 20075865.
10. Lafarga V, Aymerich I, Tapia O, Mayor F Jr., Penela P. A novel GRK2/HDAC6 interaction modulates cell spreading and motility. EMBO J. 2012; 31(4):856–69. https://doi.org/10.1038/emboj.2011.466 PMID: 22193721.
11. Iwata A, Riley BE, Johnston JA, Kopito RR. HDAC6 and microtubules are required for autophagic degradation of aggregated huntingtin. The Journal of biological chemistry. 2005; 280(48):40282–92. https://doi.org/10.1074/jbc.M508786200 PMID: 16192271.
12. Pandey UB, Batlevi Y, Baehrecke EH, Taylor JP. HDAC6 at the intersection of autophagy, the ubiquitin-proteasome system and neurodegeneration. Autophagy. 2007; 3(6):643–5. PMID: 17912024.
13. Pandey UB, Nie Z, Batlevi Y, McCray BA, Ritson GP, Nedelsky NB, et al. HDAC6 rescues neurodegeneration and provides an essential link between autophagy and the UPS. Nature. 2007; 447(7146):859–63. https://doi.org/10.1038/nature05853 PMID: 17568747.
14. Boyault C, Gilquin B, Zhang Y, Rybin V, Garman E, Meyer-Klaucke W, et al. HDAC6-p97/VCP controlled polyubiquitin chain turnover. EMBO J. 2006; 25(14):3357–66. https://doi.org/10.1038/sj.emboj.7601210 PMID: 16810319.
15. Yan J, Seibenhener ML, Calderilla-Barbosa L, Diaz-Meco MT, Moscat J, Jiang J, et al. SQSTM1/p62 interacts with HDAC6 and regulates deacetylase activity. PloS one. 2013; 8(9):e76016. https://doi.org/10.1371/journal.pone.0076016 PMID: 24086678.
16. Ding WX, Yin XM. Sorting, recognition and activation of the misfolded protein degradation pathways through macroautophagy and the proteasome. Autophagy. 2008; 4(2):141–50. PMID: 17986870.
17. Lee JY, Nagano Y, Taylor JP, Lim KL, Yao TP. Disease-causing mutations in parkin impair mitochondrial ubiquitination, aggregation, and HDAC6-dependent mitophagy. J Cell Biol. 2010; 189(4):671–9. https://doi.org/10.1083/jcb.201001039 PMID: 20457763.

18. Kawaguchi Y, Kovacs JJ, McLaurin A, Vance JM, Ito A, Yao TP. The deacetylase HDAC6 regulates aggresome formation and cell viability in response to misfolded protein stress. Cell. 2003; 115(6):727–38. PMID: 14675537.

19. Lee JY, Kapur M, Li M, Choi MC, Choi S, Kim HJ, et al. MFN1 deacetylation activates adaptive mitochondrial fusion and protects metabolically challenged mitochondria. Journal of cell science. 2014; 127 (Pt 22):4954–63. https://doi.org/10.1242/jcs.157321 PMID: 25271058.

20. Huo L, Li D, Sun X, Shi X, Karna P, Yang W, et al. Regulation of Tat acetylation and transactivation activity by the microtubule-associated deacetylase HDAC6. The Journal of biological chemistry. 2011; 286(11):9280–6. https://doi.org/10.1074/jbc.M110.208884 PMID: 21220424.

21. Valenzuela-Fernandez A, Alvarez S, Gordon-Alonso M, Barrero M, Ursa A, Cabrero JR, et al. Histone deacetylase 6 regulates human immunodeficiency virus type 1 infection. Molecular biology of the cell. 2005; 16(11):5445–54. https://doi.org/10.1091/mbc.E05-04-0354 PMID: 16148047.

22. Zhu J, Coyne CB, Sarkar SN. PKC alpha regulates Sendai virus-mediated interferon induction through HDAC6 and beta-catenin. EMBO J. 2011; 30(23):4838–49. https://doi.org/10.1038/emboj.2011.351 PMID: 21952047.

23. Banerjee I, Miyake Y, Nobs SP, Schneider C, Horvath P, Kopf M, et al. Influenza A virus uses the aggresome processing machinery for host cell entry. Science. 2014; 346(6208):473–7. https://doi.org/10.1126/science.1257037 PMID: 25342804.

24. Husain M, Cheung CY. Histone deacetylase 6 inhibits influenza A virus release by downregulating the trafficking of viral components to the plasma membrane via its substrate, acetylated microtubules. Journal of virology. 2014; 88(19):11229–39. https://doi.org/10.1128/JVI.00727-14 PMID: 25031336.

25. de Zoeten EF, Wang L, Butler K, Beier UH, Akimova T, Sai H, et al. Histone deacetylase 6 and heat shock protein 90 control the functions of Foxp3(+) T-regulatory cells. Mol Cell Biol. 2011; 31(10):2066–78. https://doi.org/10.1128/MCB.05155-11 PMID: 21444725.

26. Serrador JM, Cabrero JR, Sancho D, Mittelbrunn M, Urzainqui A, Sanchez-Madrid F. HDAC6 deacetylase activity links the tubulin cytoskeleton with immune synapse organization. Immunity. 2004; 20 (4):417–28. PMID: 15084271.

27. Pamer EG. Immune responses to Listeria monocytogenes. Nature reviews Immunology. 2004; 4 (10):812–23. https://doi.org/10.1038/nri1461 PMID: 15459672.

28. Tam MA, Wick MJ. Dendritic cells and immunity to Listeria: TipDCs are a new recruit. Trends Immunol. 2004; 25(7):335–9. https://doi.org/10.1016/j.it.2004.05.004 PMID: 15207498.

29. Hamon M, Bierne H, Cossart P. Listeria monocytogenes: a multifaceted model. Nat Rev Microbiol. 2006; 4(6):423–34. https://doi.org/10.1038/nrmicro1413 PMID: 16710323.

30. Pizarro-Cerda J, Cossart P. Listeria monocytogenes membrane trafficking and lifestyle: the exception or the rule? Annu Rev Cell Dev Biol. 2009; 25:649–70. https://doi.org/10.1146/annurev.cellbio.042308.113331 PMID: 19575658.

31. Burrack LS, Harper JW, Higgins DE. Perturbation of vacuolar maturation promotes listeriolysin O-independent vacuolar escape during Listeria monocytogenes infection of human cells. Cell Microbiol. 2009; 11(9):1382–98. https://doi.org/10.1111/j.1462-5822.2009.01338.x PMID: 19500109.

32. Birmingham CL, Canadien V, Kaniuk NA, Steinberg BE, Higgins DE, Brumell JH. Listeriolysin O allows Listeria monocytogenes replication in macrophage vacuoles. Nature. 2008; 451(7176):350–4. https://doi.org/10.1038/nature06479 PMID: 18202661.

33. MacMicking JD, Nathan C, Hom G, Chartrain N, Fletcher DS, Trumbauer M, et al. Altered responses to bacterial infection and endotoxic shock in mice lacking inducible nitric oxide synthase. Cell. 1995; 81 (4):641–50. PMID: 7538909.

34. Kocks C, Hellio R, Gounon P, Ohayon H, Cossart P. Polarized distribution of Listeria monocytogenes surface protein ActA at the site of directional actin assembly. Journal of cell science. 1993; 105 (Pt 3):699–710. PMID: 8408297.

35. Michel E, Reich KA, Favier R, Berche P, Cossart P. Attenuated mutants of the intracellular bacterium Listeria monocytogenes obtained by single amino acid substitutions in listeriolysin O. Mol Microbiol. 1990; 4(12):2167–78. PMID: 1965218.

36. Hamilton SE, Badovinac VP, Khanolkar A, Harty JT. Listeriolysin O-deficient Listeria monocytogenes as a vaccine delivery vehicle: antigen-specific CD8 T cell priming and protective immunity. Journal of immunology. 2006; 177(6):4012–20. PMID: 16951364.

37. Bahjat KS, Meyer-Morse N, Lemmens EE, Shugart JA, Dubensky TW, Brockstedt DG, et al. Suppression of cell-mediated immunity following recognition of phagosome-confined bacteria. PLoS Pathog. 2009; 5(9):e1000568. https://doi.org/10.1371/journal.ppat.1000568 PMID: 19730694.

38. Condotta SA, Richer MJ, Badovinac VP, Harty JT. Probing CD8 T cell responses with Listeria monocytogenes infection. Adv Immunol. 2012; 113:51–80. https://doi.org/10.1016/B978-0-12-394590-7.00005-1 PMID: 22244579.

39. Serbina NV, Salazar-Mather TP, Biron CA, Kuziel WA, Pamer EG. TNF/iNOS-producing dendritic cells mediate innate immune defense against bacterial infection. Immunity. 2003; 19(1):59–70. PMID: 12871639.

40. Edelson BT, Bradstreet TR, Hildner K, Carrero JA, Frederick KE, Kc W, et al. CD8alpha(+) dendritic cells are an obligate cellular entry point for productive infection by Listeria monocytogenes. Immunity. 2011; 35(2):236–48. https://doi.org/10.1016/j.immuni.2011.06.012 PMID: 21867927.

41. Jung S, Unutmaz D, Wong P, Sano G, De los Santos K, Sparwasser T, et al. In vivo depletion of CD11c + dendritic cells abrogates priming of CD8+ T cells by exogenous cell-associated antigens. Immunity. 2002; 17(2):211–20. PMID: 12196292.

42. Witte CE, Archer KA, Rae CS, Sauer JD, Woodward JJ, Portnoy DA. Innate immune pathways triggered by Listeria monocytogenes and their role in the induction of cell-mediated immunity. Adv Immunol. 2012; 113:135–56. https://doi.org/10.1016/B978-0-12-394590-7.00002-6 PMID: 22244582.

43. Honda K, Takaoka A, Taniguchi T. Type I interferon [corrected] gene induction by the interferon regulatory factor family of transcription factors. Immunity. 2006; 25(3):349–60. https://doi.org/10.1016/j.immuni.2006.08.009 PMID: 16979567.

44. Martinez del Hoyo G, Ramirez-Huesca M, Levy S, Boucheix C, Rubinstein E, Minguito de la Escalera M, et al. CD81 controls immunity to Listeria infection through rac-dependent inhibition of proinflammatory mediator release and activation of cytotoxic T cells. Journal of immunology. 2015; 194(12):6090–101. https://doi.org/10.4049/jimmunol.1402957 PMID: 25972472.

45. Rich KA, Burkett C, Webster P. Cytoplasmic bacteria can be targets for autophagy. Cell Microbiol. 2003; 5(7):455–68. PMID: 12814436.

46. Py BF, Lipinski MM, Yuan J. Autophagy limits Listeria monocytogenes intracellular growth in the early phase of primary infection. Autophagy. 2007; 3(2):117–25. PMID: 17204850.

47. Birmingham CL, Smith AC, Bakowski MA, Yoshimori T, Brumell JH. Autophagy controls Salmonella infection in response to damage to the Salmonella-containing vacuole. The Journal of biological chemistry. 2006; 281(16):11374–83. https://doi.org/10.1074/jbc.M509157200 PMID: 16495224.

48. Ariffin JK, das Gupta K, Kapetanovic R, Iyer A, Reid RC, Fairlie DP, et al. Histone deacetylase inhibitors promote mitochondrial reactive oxygen species production and bacterial clearance by human macrophages. Antimicrob Agents Chemother. 2015. https://doi.org/10.1128/AAC.01876-15 PMID: 26711769.

49. Into T, Inomata M, Niida S, Murakami Y, Shibata K. Regulation of MyD88 aggregation and the MyD88-dependent signaling pathway by sequestosome 1 and histone deacetylase 6. The Journal of biological chemistry. 2010; 285(46):35759–69. https://doi.org/10.1074/jbc.M110.126904 PMID: 20837465.

50. Nakashima H, Nguyen T, Goins WF, Chiocca EA. Interferon-stimulated gene 15 (ISG15) and ISG15-linked proteins can associate with members of the selective autophagic process, histone deacetylase 6 (HDAC6) and SQSTM1/p62. The Journal of biological chemistry. 2015; 290(3):1485–95. https://doi.org/10.1074/jbc.M114.593871 PMID: 25429107.

51. Olzmann JA, Li L, Chudaev MV, Chen J, Perez FA, Palmiter RD, et al. Parkin-mediated K63-linked polyubiquitination targets misfolded DJ-1 to aggresomes via binding to HDAC6. J Cell Biol. 2007; 178 (6):1025–38. https://doi.org/10.1083/jcb.200611128 PMID: 17846173.

52. Rytkonen A, Poh J, Garmendia J, Boyle C, Thompson A, Liu M, et al. SseL, a Salmonella deubiquitinase required for macrophage killing and virulence. Proc Natl Acad Sci U S A. 2007; 104(9):3502–7. https://doi.org/10.1073/pnas.0610095104 PMID: 17360673.

53. Olzmann JA, Chin LS. Parkin-mediated K63-linked polyubiquitination: a signal for targeting misfolded proteins to the aggresome-autophagy pathway. Autophagy. 2008; 4(1):85–7. PMID: 17957134.

54. Kawasaki T, Kawai T. Toll-like receptor signaling pathways. Front Immunol. 2014; 5:461. https://doi.org/10.3389/fimmu.2014.00461 PMID: 25309543.

55. Netea MG, Joosten LA, Latz E, Mills KH, Natoli G, Stunnenberg HG, et al. Trained immunity: A program of innate immune memory in health and disease. Science. 2016; 352(6284):aaf1098. https://doi.org/10.1126/science.aaf1098 PMID: 27102489.

56. Roger T, Lugrin J, Le Roy D, Goy G, Mombelli M, Koessler T, et al. Histone deacetylase inhibitors impair innate immune responses to Toll-like receptor agonists and to infection. Blood. 2011; 117(4):1205–17. https://doi.org/10.1182/blood-2010-05-284711 PMID: 20956800.

57. Dearman RJ, Cumberbatch M, Maxwell G, Basketter DA, Kimber I. Toll-like receptor ligand activation of murine bone marrow-derived dendritic cells. Immunology. 2009; 126(4):475–84. https://doi.org/10.1111/j.1365-2567.2008.02922.x PMID: 18778283.

58. Xu Y, Zhan Y, Lew AM, Naik SH, Kershaw MH. Differential development of murine dendritic cells by GM-CSF versus Flt3 ligand has implications for inflammation and trafficking. Journal of immunology. 2007; 179(11):7577–84. PMID: 18025203.

59. Choi SJ, Lee HC, Kim JH, Park SY, Kim TH, Lee WK, et al. HDAC6 regulates cellular viral RNA sensing by deacetylation of RIG-I. EMBO J. 2016. 15; 35(4):429–42. https://doi.org/10.15252/embj.201592586 PMID: 26746851.

60. New M, Sheikh S, Bekheet M, Olzscha H, Thezenas ML, Care MA, et al. TLR Adaptor Protein MYD88 Mediates Sensitivity to HDAC Inhibitors via a Cytokine-Dependent Mechanism. Cancer research. 2016; 76(23):6975–87. https://doi.org/10.1158/0008-5472.CAN-16-0504 PMID: 27733371.

61. Seki E, Tsutsui H, Tsuji NM, Hayashi N, Adachi K, Nakano H, et al. Critical roles of myeloid differentiation factor 88-dependent proinflammatory cytokine release in early phase clearance of Listeria monocytogenes in mice. Journal of immunology. 2002; 169(7):3863–8. PMID: 12244183.

62. Edelson BT, Unanue ER. MyD88-dependent but Toll-like receptor 2-independent innate immunity to Listeria: no role for either in macrophage listericidal activity. Journal of immunology. 2002; 169 (7):3869–75. PMID: 12244184.

63. Torres D, Barrier M, Bihl F, Quesniaux VJ, Maillet I, Akira S, et al. Toll-like receptor 2 is required for optimal control of Listeria monocytogenes infection. Infect Immun. 2004; 72(4):2131–9. https://doi.org/10.1128/IAI.72.4.2131-2139.2004 PMID: 15039335.

64. Serbina NV, Kuziel W, Flavell R, Akira S, Rollins B, Pamer EG. Sequential MyD88-independent and -dependent activation of innate immune responses to intracellular bacterial infection. Immunity. 2003; 19(6):891–901. PMID: 14670305.

65. Arnold-Schrauf C, Dudek M, Dielmann A, Pace L, Swallow M, Kruse F, et al. Dendritic cells coordinate innate immunity via MyD88 signaling to control Listeria monocytogenes infection. Cell Rep. 2014; 6 (4):698–708. https://doi.org/10.1016/j.celrep.2014.01.023 PMID: 24529704.

66. Gao YS, Hubbert CC, Lu J, Lee YS, Lee JY, Yao TP. Histone deacetylase 6 regulates growth factor-induced actin remodeling and endocytosis. Mol Cell Biol. 2007; 27(24):8637–47. https://doi.org/10.1128/MCB.00393-07 PMID: 17938201.

67. Vaudaux P, Waldvogel FA. Gentamicin antibacterial activity in the presence of human polymorphonuclear leukocytes. Antimicrob Agents Chemother. 1979; 16(6):743–9. PMID: 533256.

68. Montoya MC, Sancho D, Bonello G, Collette Y, Langlet C, He HT, et al. Role of ICAM-3 in the initial interaction of T lymphocytes and APCs. Nat Immunol. 2002; 3(2):159–68. https://doi.org/10.1038/ni753 PMID: 11812993.

69. Bonzon-Kulichenko E, Perez-Hernandez D, Nunez E, Martinez-Acedo P, Navarro P, Trevisan-Herraz M, et al. A robust method for quantitative high-throughput analysis of proteomes by 18O labeling. Mol Cell Proteomics. 2011; 10(1):M110 003335. https://doi.org/10.1074/mcp.M110.003335 PMID: 20807836.

70. Martinez-Bartolome S, Navarro P, Martin-Maroto F, Lopez-Ferrer D, Ramos-Fernandez A, Villar M, et al. Properties of average score distributions of SEQUEST: the probability ratio method. Mol Cell Proteomics. 2008; 7(6):1135–45. https://doi.org/10.1074/mcp.M700239-MCP200 PMID: 18303013.

71. Navarro P, Vazquez J. A refined method to calculate false discovery rates for peptide identification using decoy databases. J Proteome Res. 2009; 8(4):1792–6. https://doi.org/10.1021/pr800362h PMID: 19714873.

Published online: February 3, 2016

Article

TRANSPARENT PROCESS

THE EMBO JOURNAL

p38γ and p38δ reprogram liver metabolism by modulating neutrophil infiltration

Bárbara González-Terán[1,†], Nuria Matesanz[1,†], Ivana Nikolic[1,†], María Angeles Verdugo[1,2], Vinatha Sreeramkumar[1], Lourdes Hernández-Cosido[3,4], Alfonso Mora[1], Georgiana Crainiciuc[1], María Laura Sáiz[1], Edgar Bernardo[1], Luis Leiva-Vega[1], Elena Rodríguez[1], Victor Bondía[1], Jorge L Torres[5,6], Sonia Perez-Sieira[7,8], Luis Ortega[3,4], Ana Cuenda[2], Francisco Sanchez-Madrid[1], Rubén Nogueiras[7,8], Andrés Hidalgo[1], Miguel Marcos[5,6] & Guadalupe Sabio[1,*]

Abstract

Non-alcoholic fatty liver disease (NAFLD) is a major health problem and the main cause of liver disease in Western countries. Although NAFLD is strongly associated with obesity and insulin resistance, its pathogenesis remains poorly understood. The disease begins with an excessive accumulation of triglycerides in the liver, which stimulates an inflammatory response. Alternative p38 mitogen-activated kinases (p38γ and p38δ) have been shown to contribute to inflammation in different diseases. Here we demonstrate that p38δ is elevated in livers of obese patients with NAFLD and that mice lacking p38γ/δ in myeloid cells are resistant to diet-induced fatty liver, hepatic triglyceride accumulation and glucose intolerance. This protective effect is due to defective migration of p38γ/δ-deficient neutrophils to the damaged liver. We further show that neutrophil infiltration in wild-type mice contributes to steatosis development by means of inflammation and liver metabolic changes. Therefore, p38γ and p38δ in myeloid cells provide a potential target for NAFLD therapy.

Keywords diabetes; inflammation; obesity; steatosis; stress kinases
Subject Categories Immunology; Metabolism; Molecular Biology of Disease
DOI 10.15252/embj.201591857 | Received 20 April 2015 | Revised 18 December 2015 | Accepted 22 December 2015 | Published online 3 February 2016
The EMBO Journal (2016) 35: 536–552

Introduction

Non-alcoholic fatty liver disease (NAFLD) is the leading cause of chronic liver disease in Western countries and estimates of its worldwide prevalence range from 6 to 35% (Vernon *et al*, 2011). NAFLD refers to a wide spectrum of liver damage, ranging from simple steatosis caused by intracellular triglyceride accumulation to inflammation (non-alcoholic steatohepatitis [NASH]), fibrosis, and cirrhosis (Marchesini *et al*, 2003). NAFLD is a main cause of cryptogenic cirrhosis and may also predispose to hepatocarcinoma (Farrell & Larter, 2006).

The pathogenesis of NAFLD is strongly associated with insulin resistance, obesity and type 2 diabetes (Fabbrini *et al*, 2010). However, the mechanisms involved in the accumulation of triglycerides in the liver and subsequent hepatocellular damage are multifactorial and not completely understood. Metabolic deregulation and hepatic steatosis have been linked to stress signaling (Sabio & Davis, 2010; Sabio *et al*, 2010), and the activation of stress kinases in steatosis and obesity suggests a role for these proteins in this disease (Sabio & Davis, 2010). The stress-activated protein kinase group consists of two subfamilies: p38 mitogen-activated kinases (p38 MAPKs) and c-Jun N-terminal kinases (JNKs). While the role of JNKs in the development of steatosis has been widely studied (Sabio *et al*, 2008, 2009), less is known about the role of the p38 MAPK signaling pathway. In mammals, four p38 MAPK isoforms have been identified: p38α, -β, -γ, and -δ. Despite biochemical evidence of specific roles for the individual isoforms, redundancy and embryonic lethality have impeded attempts to establish their distinct functions *in vivo* (Sabio & Davis, 2014). Embryos lacking p38α die due to defects in placental development (Adams *et al*, 2000; Allen *et al*, 2000; Tamura *et al*, 2000), but mice lacking p38β, -γ, and -δ are viable without any obvious defects under basal conditions (Beardmore *et al*, 2005; Sabio *et al*, 2005). Kinases p38γ and -δ were recently shown to control inflammation by regulating

1 Fundación Centro Nacional de Investigaciones Cardiovasculares Carlos III, Madrid, Spain
2 Department of Immunology and Oncology, Centro Nacional de Biotecnología/CSIC, Madrid, Spain
3 Bariatric Surgery Unit, Department of General Surgery, University Hospital of Salamanca, Salamanca, Spain
4 Department of Surgery, University of Salamanca, Salamanca, Spain
5 Department of Internal Medicine, University Hospital of Salamanca-IBSAL, Salamanca, Spain
6 Department of Medicine, University of Salamanca, Salamanca, Spain
7 Department of Physiology, CIMUS, University of Santiago de Compostela-Instituto de Investigación Sanitaria, Santiago de Compostela, Spain
8 CIBER Fisiopatología de la Obesidad y Nutrición (CIBERobn), Santiago de Compostela, Spain
*Corresponding author. Tel: +34 91453 12 00; E-mail: guadalupe.sabio@cnic.es
†These authors contributed equally to this work

macrophage production of tumor necrosis factor (TNF)-α (Risco *et al*, 2012; Gonzalez-Teran *et al*, 2013) and T-cell activation (Criado *et al*, 2014); moreover, p38δ also influences neutrophil inflammatory responses in the lung (Ittner *et al*, 2012).

Since chronic inflammation is central to the progression of NAFLD, we aimed to define the role of p38γ and p38δ in the development of this disorder. We detected elevated liver expression of p38δ in a cohort of obese patients with NAFLD and found that p38γ and p38δ are responsible for the development of steatosis and NASH in three animal models of NAFLD: mice fed a high-fat diet (HFD), mice fed a high-fat fructose diet (HFF), and mice fed a methionine–choline-deficient (MCD) diet. Lack of p38γ and p38δ in myeloid cells impaired neutrophil migration to the liver and thus protected against steatosis and further hepatic damage. These results highlight the importance of p38 kinases and neutrophils in NAFLD and open a new avenue for the treatment of this disease.

Results

p38γ and p38δ are overexpressed in NAFLD

Analysis of liver biopsies from obese NAFLD patients (body mass index [BMI] > 35 kg/m^2) revealed elevated mRNA expression of *MAPK13* (p38delta) compared with non-obese individuals without NAFLD, and a similar tendency was detected for *MAPK12* (p38gamma) (Fig 1A). Further, among individuals with a BMI < 35 kg/m^2, hepatic *MAPK12* and *MAPK13* mRNA was elevated in individuals with liver steatosis compared with control individuals without liver disease (Fig 1B). Western blot analysis confirmed higher liver expression of p38δ protein in obese individuals with steatosis (Fig 1C). To corroborate these results in a mouse model of steatosis, we studied the expression and activation of p38γ and p38δ in livers from mice fed a methionine–choline-deficient (MCD) diet, which induces macrovesicular steatosis and is widely used in NASH research (Anstee & Goldin, 2006). MCD diet increased the mRNA expression of p38δ (Fig 1D) and induced the activation of p38γ and p38δ after 1 week (Fig 1E). This activation remained high during the 3 weeks of the diet (Fig 1E and F). These results indicate a possible role of p38γ and p38δ in the development of steatosis.

Mice lacking p38γ and p38δ are protected against MCD-induced steatosis

To study how these kinases affect the development of fatty liver, we fed a MCD diet to WT mice and mice lacking p38γ (p38γ$^{-/-}$), p38δ (p38δ$^{-/-}$), and both p38γ and p38δ (p38γ/δ$^{-/-}$). Compared with MCD-diet WT mice, MCD-diet p38γ$^{-/-}$ and p38δ$^{-/-}$ mice showed only a slightly milder liver steatosis as evaluated by H&E and Oil Red staining (Appendix Fig S1A); in contrast, the development of steatosis and inflammation was strongly attenuated in p38γ/δ$^{-/-}$ mice (Fig 2A and Appendix Fig S2A). These findings were confirmed by biochemical analysis of hepatic triglyceride content (Fig 2B and Appendix Fig S1B). Moreover, whereas MCD diet increased serum levels of alanine transaminase (ALT) in WT, p38γ$^{-/-}$, and p38δ$^{-/-}$ mice, the level in p38γ/δ$^{-/-}$ mice was significantly lower, indicating milder liver necrosis (Fig 2C and Appendix Fig S1C). The appearance of steatosis protection only in mice doubly deficient for p38γ and p38δ probably reflects the previously described partial functional redundancy between the two isoforms (Risco *et al*, 2012; Gonzalez-Teran *et al*, 2013).

An early event in MCD-induced choline deficiency is the appearance in liver of oxidized lipids, DNA, and proteins. Assay of thiobarbituric acid reactive substances in the livers of MCD-fed animals detected lower oxidized lipid content in p38γ/δ$^{-/-}$ mice than in WT animals, correlating with lower levels of hydrogen peroxide in the double-knockout mice (Fig 2D). Liver fibrosis is a hallmark of NASH. Livers of MCD-diet WT mice expressed higher levels of *Col1a1* and *Acta2* than MCD-diet p38γ/δ$^{-/-}$ mice (Fig 2E), correlating with higher Masson's trichrome staining (Fig 2F). These results demonstrate that p38γ/δ$^{-/-}$ mice are protected against MCD-diet-induced steatosis and NASH.

Inflammation plays a key role in the pathogenesis of NAFLD, and the development of hepatic steatosis is associated with increased liver infiltration by myeloid cells (Tiniakos *et al*, 2010). p38γ/δ kinases regulate inflammation through the control of TNF-α production in macrophages and Kupffer cells (Risco *et al*, 2012; Gonzalez-Teran *et al*, 2013), and p38δ modulates neutrophil motility in lung disease (Ittner *et al*, 2012), prompting us to examine the mRNA expression levels of myeloid cell markers and pro-inflammatory cytokines in mice fed the MCD diet. Liver expression

Figure 1. p38γ and p38δ are up-regulated in NAFDL.

A Left: qRT–PCR analysis of mRNA expression of *MAPK12* (p38gamma) and *MAPK13* (p38delta) in liver extracts prepared from obese patients with alcoholic fatty liver disease (NAFLD) and control individuals without NAFLD. mRNA expression was normalized to the amount of *Gapdh* mRNA (n = 11–74). Right: representative H&E-stained liver sections. Scale bar: 50 μm.

B Left: qRT–PCR analysis of mRNA expression of *MAPK12* (p38gamma) and *MAPK13 (*p38delta) in liver extracts prepared from control patients with NAFLD/non-alcoholic steatohepatitis (NASH) and control individuals without NAFLD/NASH. mRNA expression was normalized to the amount of *Gapdh* mRNA (n = 9–11). Right: representative H&E-stained liver sections. Scale bar: 50 μm.

C Quantification of immunoblot analysis of p38δ expression in liver extracts prepared from obese patients with NAFLD and individuals without NAFLD. Representative blots are shown (n = 7–40).

D qRT–PCR analysis of *Mapk12* (p38gamma) and *Mapk13 (*p38delta) mRNA expression in liver extracts prepared from wild-type mice (WT) fed a diet deficient in methionine and choline (MCD) or control diet (ND) for 3 weeks; mRNA expression was normalized to the amount of *Gapdh* mRNA (n = 5–10).

E Immunoprecipitation analysis of activation and protein levels of p38γ and p38δ isoforms in liver extracts prepared from WT fed a MCD or ND diet for the times indicated.

F Immunoprecipitation analysis of activation and protein levels of p38γ and p38δ isoforms in liver extracts prepared from WT fed a MCD or ND for 3 weeks (n = 5). Western blot against vinculin was used to assay the protein amount in the total lysate (TL) used for each IP. Protein expression was normalized to vinculin.

Data information: Data are means ± SEM. *P < 0.05; **P < 0.01. Statistical significance by two-tailed Student's t-test. Characteristics of patients and controls were compared by means of χ^2 or Mann–Whitney U-tests.

Published online: February 3, 2016
The EMBO Journal

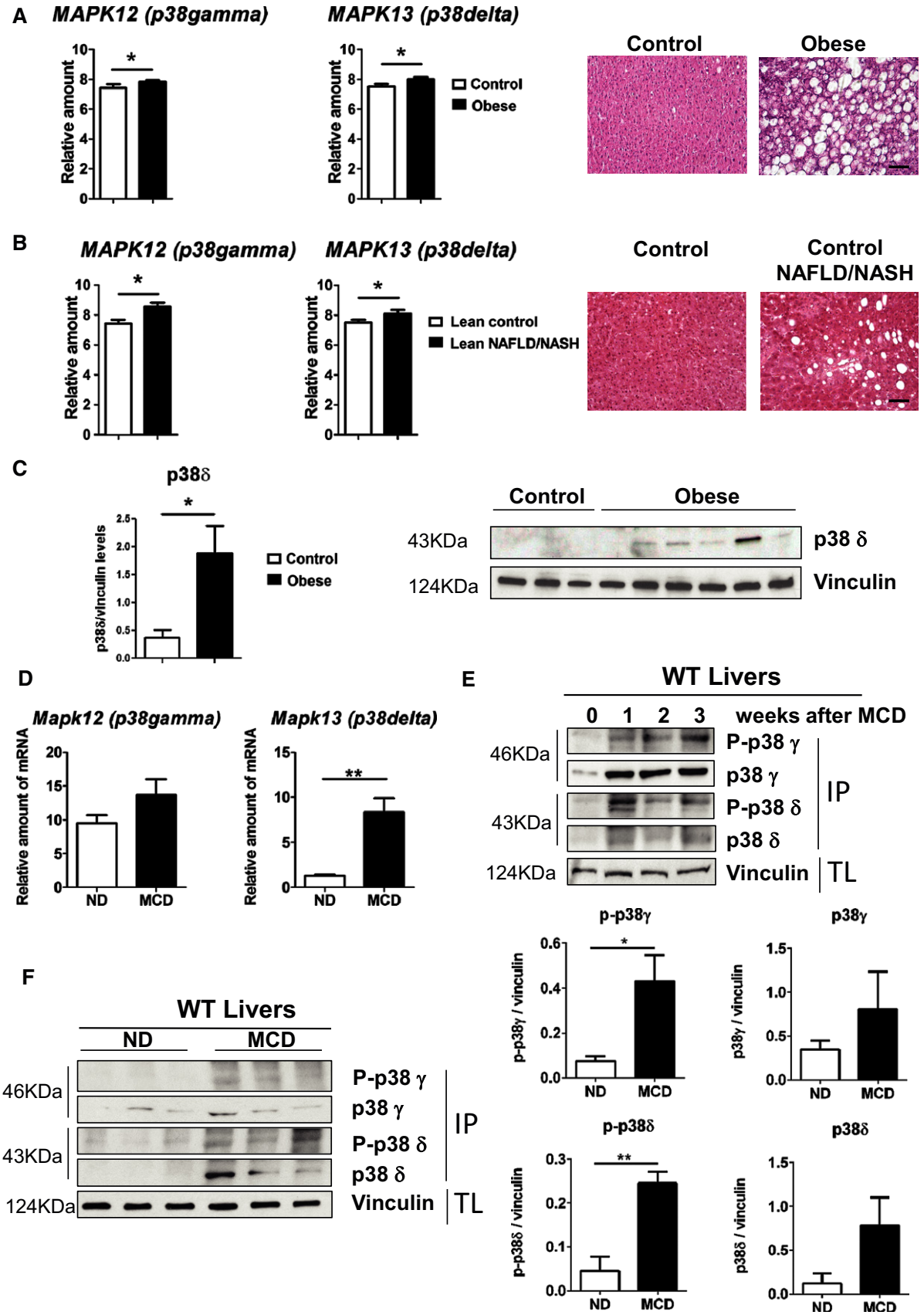

Figure 1.

Published online: February 3, 2016

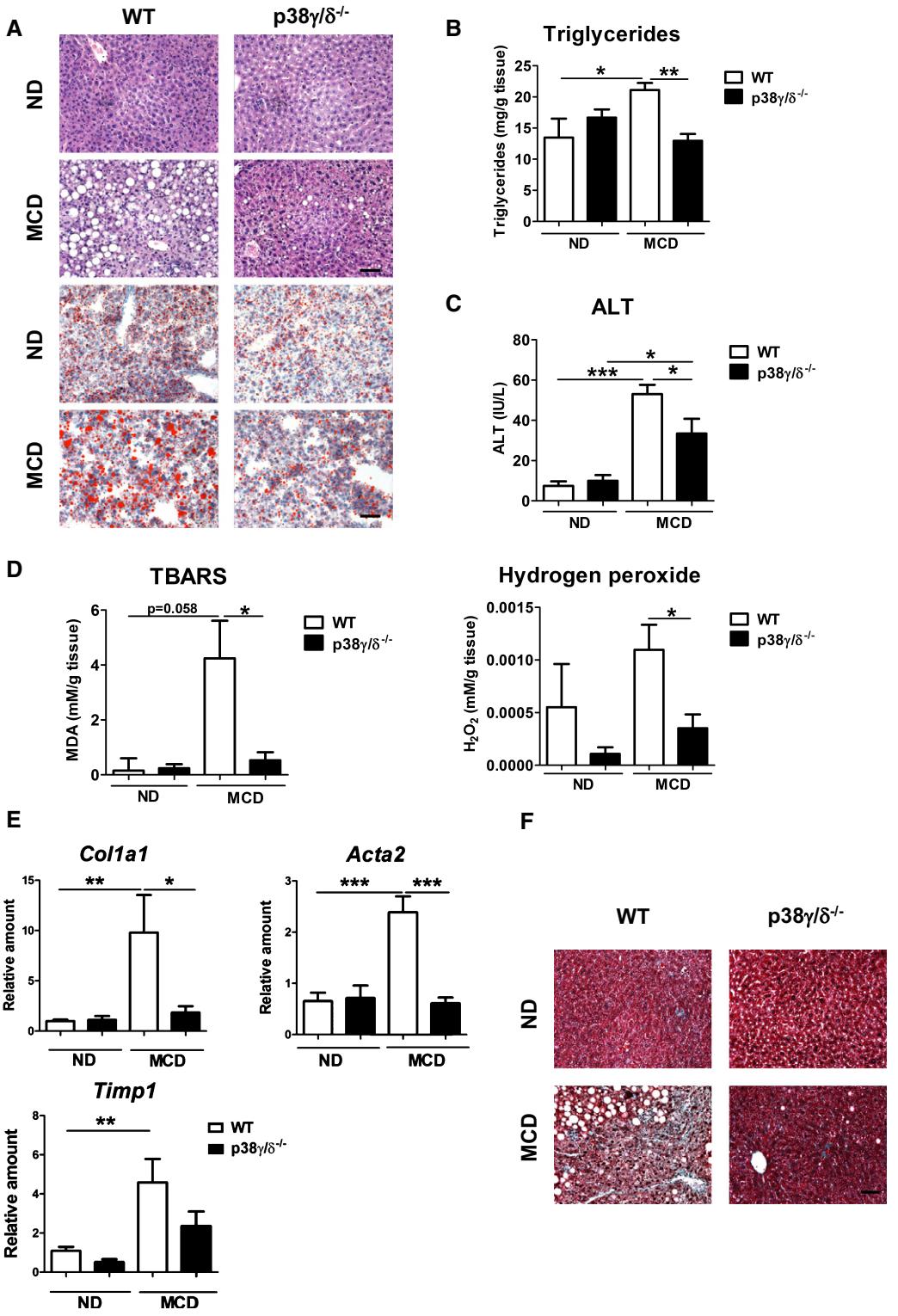

Figure 2. p38γ/δ$^{-/-}$ mice are protected against steatohepatitis and fibrosis.

A Representative H&E- and Oil Red-stained liver sections prepared from WT and p38γ/δ$^{-/-}$ mice fed a ND or the MCD diet for 3 weeks. Scale bar: 50 μm.

B, C Liver triglycerides (B) and plasma transaminase activity (ALT) (C) measured in WT and p38γ/δ$^{-/-}$ mice after 3 weeks of MCD diet.

D TBARS and hydrogen peroxide detected in liver samples from mice fasted overnight after the 3-week MCD diet.

E qRT–PCR analysis of *Col1a1*, *Acta2*, and *Timp1* mRNA expression. mRNA expression was normalized to the amount of *Gapdh* mRNA.

F Representative Masson's trichrome-stained liver sections prepared from WT and p38γ/δ$^{-/-}$ mice fed a ND or the MCD diet for 3 weeks. Scale bar: 50 μm.

Data information: Data are means ± SEM (n = 5–10). *P < 0.05; **P < 0.01; ***P < 0.001 (one-way ANOVA coupled to Bonferroni's post-tests).

levels of the myeloid cell marker *F4/80* and the cytokines *Tnfa* and *Il6* were significantly lower in p38γ/δ$^{-/-}$ mice than in WT mice (Appendix Fig S2B). However, analysis of M1 and M2 macrophage-differentiation markers revealed no differences in M1 (*Ifng*, *Il23)* and M2 markers (*Il10, Il13* or *Arg)* between WT and p38γ/δ$^{-/-}$ mice (Appendix Fig S2C).

Effect of myeloid cell expression of p38γ and p38δ on MCD-induced steatosis

To elucidate the role of myeloid-expressed p38γ/δ in the development of steatosis, we analyzed mice lacking p38γ/δ in myeloid cells. These mice have complete deletion of p38γ and p38δ in macrophages, and neutrophils infiltrated in liver and spleen while only partial deletion of p38δ was observed in dendritic cells (Appendix Fig S3A). Control mice expressing Cre recombinase (Lyzs-Cre mice) developed the typical hepatic steatosis in response to the MCD diet, with associated liver accumulation of triglycerides and hepatocyte necrosis indexed by serum ALT (Fig 3A–C). In contrast, the response of p38γ/δ$^{Lyzs\text{-}KO}$ mice to the MCD diet was milder for all three parameters (Fig 3A–C), demonstrating a protection similar to that seen in global p38γ/δ$^{-/-}$ mice. The p38γ/δ$^{Lyzs\text{-}KO}$ mice also had lower circulating levels of TNF-α and IL-6 than Lyzs-Cre mice after the MCD diet (Fig 3D), and gene expression analysis revealed significantly lower levels of the pro-inflammatory and myeloid cell markers *Il6, Gr1, Lyzs*, and *F4/80* (Fig 3E). In contrast, there were no between-genotype differences in the M1/M2 polarization of liver-infiltrated macrophages (Fig 3F).

Myeloid-specific p38γ and p38δ deficiencies do not affect diet-induced obesity, but protect against steatosis and diabetes

To confirm that the protection against liver steatosis in MCD-diet p38γ/δ$^{Lyzs\text{-}KO}$ mice was independent of the model used to induce the disease, we fed Lyzs-Cre and p38γ/δ$^{Lyzs\text{-}KO}$ mice with a high-fat diet (HFD). Weight gain was the same in p38γ/δ$^{Lyzs\text{-}KO}$ and Lyzs-Cre mice (Fig 4A), consistent with their similar lean and fat mass (Fig 4B). Liver mass was slightly lower in p38γ/δ$^{Lyzs\text{-}KO}$ mice (Fig 4C), while white adipose tissue mass was similar in both genotypes (Fig 4D). Histological analysis revealed less severe liver HFD-induced steatosis in the p38γ/δ$^{Lyzs\text{-}KO}$ mice (Fig 5A and B), correlating with lower circulating ALT levels (Fig 5C). We found higher energy expenditure in p38γ/δ$^{Lyzs\text{-}KO}$ animals with no differences in the respiratory exchange quotient [VCO_2]/[VO_2] between p38γ/δ$^{Lyzs\text{-}KO}$ and Lyzs-Cre mice (Fig 4E).

To study whether the protection against steatosis ameliorates HFD-induced diabetes, we performed a glucose tolerance test (GTT). HFD-fed p38γ/δ$^{Lyzs\text{-}KO}$ mice showed significantly higher glucose tolerance (Fig 5D) and lower fasting glucose (Fig 5E) than age-matched Lyzs-Cre controls on the same diet. These results indicate that the protection against steatosis in mice lacking p38γ/δ in myeloid cells also protects against HFD-induced diabetes.

A diet high in cholesterol, saturated fat, and fructose (HFF) has been found to recapitulate features of metabolic syndrome and NASH better than the traditional HFD (Charlton *et al*, 2011). Histological analysis of p38γ/δ$^{Lyzs\text{-}KO}$ and Lyzs-Cre mice fed a HFF diet revealed less severe liver steatosis in the p38γ/δ$^{Lyzs\text{-}KO}$ mice (Appendix Fig S3B and F), inflammation and fibrosis (Appendix Fig S3F), correlating with lower triglyceride accumulation and circulating ALT levels (Appendix Fig S3C and D). This protection against liver steatosis was associated with an improvement in fasting glucose (Appendix Fig S3E).

p38γ-floxed mice have below-normal expression of p38γ in muscle and fat (data not shown), raising the possibility that this defective expression might contribute to the protection against steatosis. To exclude this, we generated radiation chimeras by transplanting p38γ/δ$^{Lyzs\text{-}KO}$ or Lyzs-Cre bone marrow cells into lethally irradiated WT mice and fed a HFD or MCD diet. Efficient reconstitution of B6.SJL (CD45.1) mice with p38γ/δ$^{Lyzs\text{-}KO}$ or Lyzs-Cre bone marrow from C57BL/6J (CD45.2) mice was confirmed by staining peripheral blood leukocytes and liver-infiltrated leukocytes with antibodies to CD45.1/CD45.2 and analysis by flow cytometry (Fig 6A). Histological analysis showed milder steatosis (Fig 6B and C and Appendix Fig S4A), correlating with lower circulating ALT levels (Fig 6D and Appendix Fig S4B) after MCD or HFD in CX BM p38γ/δ$^{Lyzs\text{-}KO}$ than in the control CX BM Lyzs-Cre mice. Protection against HFD-induced steatosis associated with lower fasting glucose in CX BM p38γ/δ$^{Lyzs\text{-}KO}$ (Fig 6E). These results confirmed that this protection is a specific consequence of the loss of p38γ/δ in bone marrow-derived cells.

p38γ and p38δ control neutrophil infiltration during steatosis by regulating neutrophil adhesion

The protection of p38γ/δ myeloid KO mice against steatosis and liver inflammation, together with the low levels of myeloid cell markers in the livers of these animals suggested a possible effect on liver infiltration in animals fed a MCD diet or HFD. Characterization of liver-infiltrating leukocyte subsets in mice fed either diet revealed that the diet-induced increase in liver-infiltrating neutrophil counts (CD11b^{+}Gr-1^{high}) was significantly bigger in Lyzs-Cre mice than in p38γ/δ$^{Lyzs\text{-}KO}$ mice (Fig 7A), and similar results were observed in radiation chimeras restored by bone marrow from Lyzs-Cre mice versus p38γ/δ$^{Lyzs\text{-}KO}$ mice (Appendix Figs S4C and S5). This result correlated with lower levels of circulating neutrophils in p38γ/δ$^{Lyzs\text{-}KO}$ mice after both diets (Fig 7B and C).

Figure 3. p38γ/δ$^{Lyzs\text{-}KO}$ mice are protected against steatohepatitis induced by MCD diet.
Lyzs-Cre and p38γ/δ$^{Lyzs\text{-}KO}$ mice were fed a ND or a MCD diet for 3 weeks.

A Representative H&E- and Oil Red-stained liver sections. Scale bar: 50 μm.
B, C Liver triglycerides (B) and plasma ALT (C) at the end of the diet period.
D Measurement of plasma TNF-α and IL-6.
E qRT–PCR analysis of myeloid cell markers and cytokine mRNA expression from liver tissue; mRNA expression was normalized to the amount of *Gapdh* mRNA.
F qRT–PCR analysis of M1 and M2 polarization cell markers from liver-infiltrated macrophages. mRNA expression was normalized to the amount of *Gapdh* mRNA.

Data information: Data are means ± SEM (n = 5–10). *P < 0.05; **P < 0.01; ***P < 0.001 (one-way ANOVA coupled to Bonferroni's post-tests).

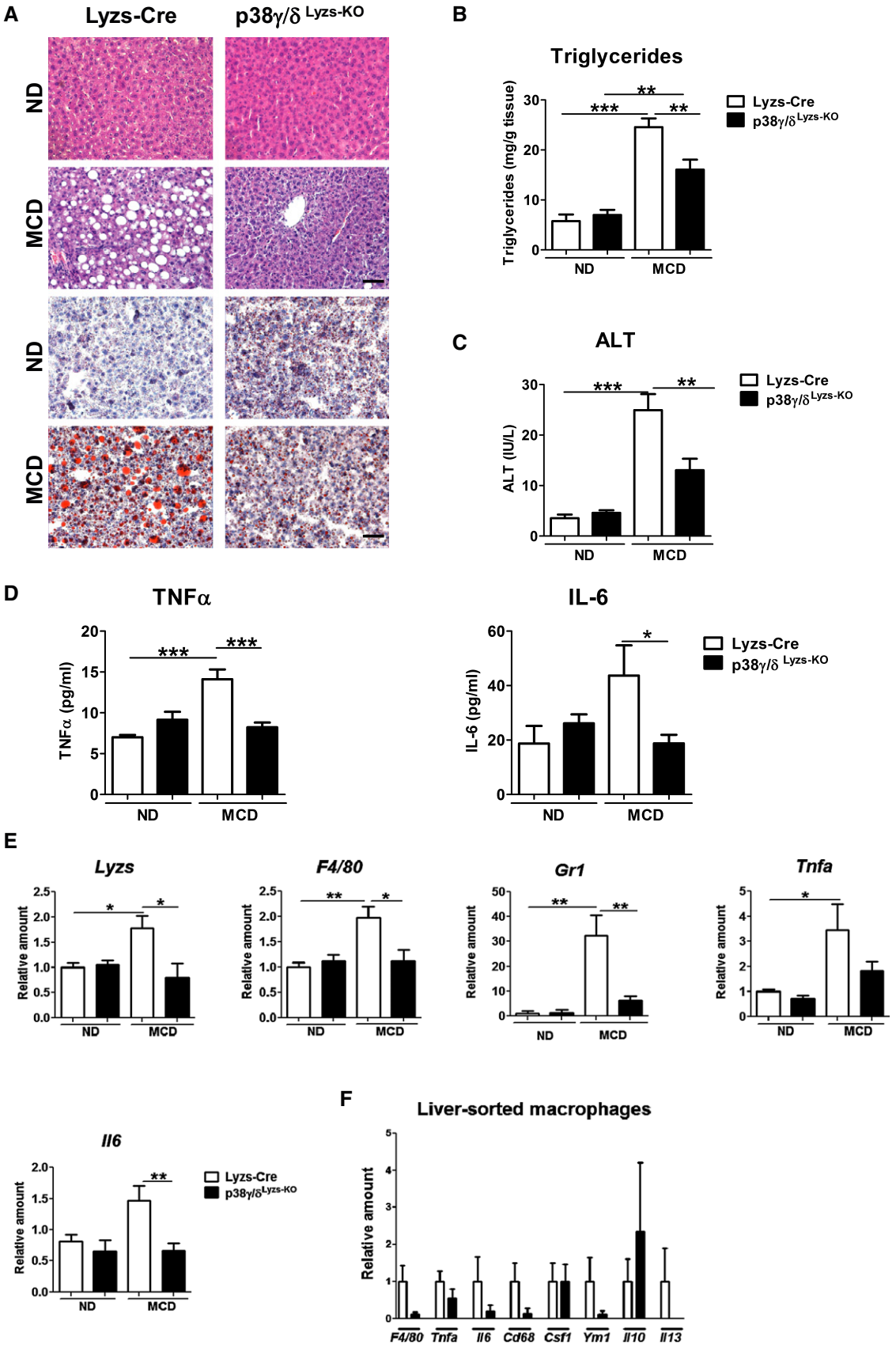
A
Lyzs-Cre
p38γ/δ Lyzs-KO
ND
MCD
ND
MCD
B
Triglycerides
Triglycerides (mg/g tissue)
Lyzs-Cre
p38γ/δ Lyzs-KO
ND
MCD
C
ALT
ALT (IU/L)
Lyzs-Cre
p38γ/δ Lyzs-KO
ND
MCD
D
TNFα
TNFα (pg/ml)
ND
MCD
IL-6
IL-6 (pg/ml)
Lyzs-Cre
p38γ/δ Lyzs-KO
ND
MCD
E
Lyzs
F4/80
Gr1
Tnfa
Relative amount
ND
MCD
Il6
Lyzs-Cre
p38γ/δ Lyzs-KO
F
Liver-sorted macrophages
Relative amount
F4/80
Tnfa
Il6
Cd68
Csf1
Ym1
Il10
Il13

Figure 3.

Published online: February 3, 2016
The EMBO Journal

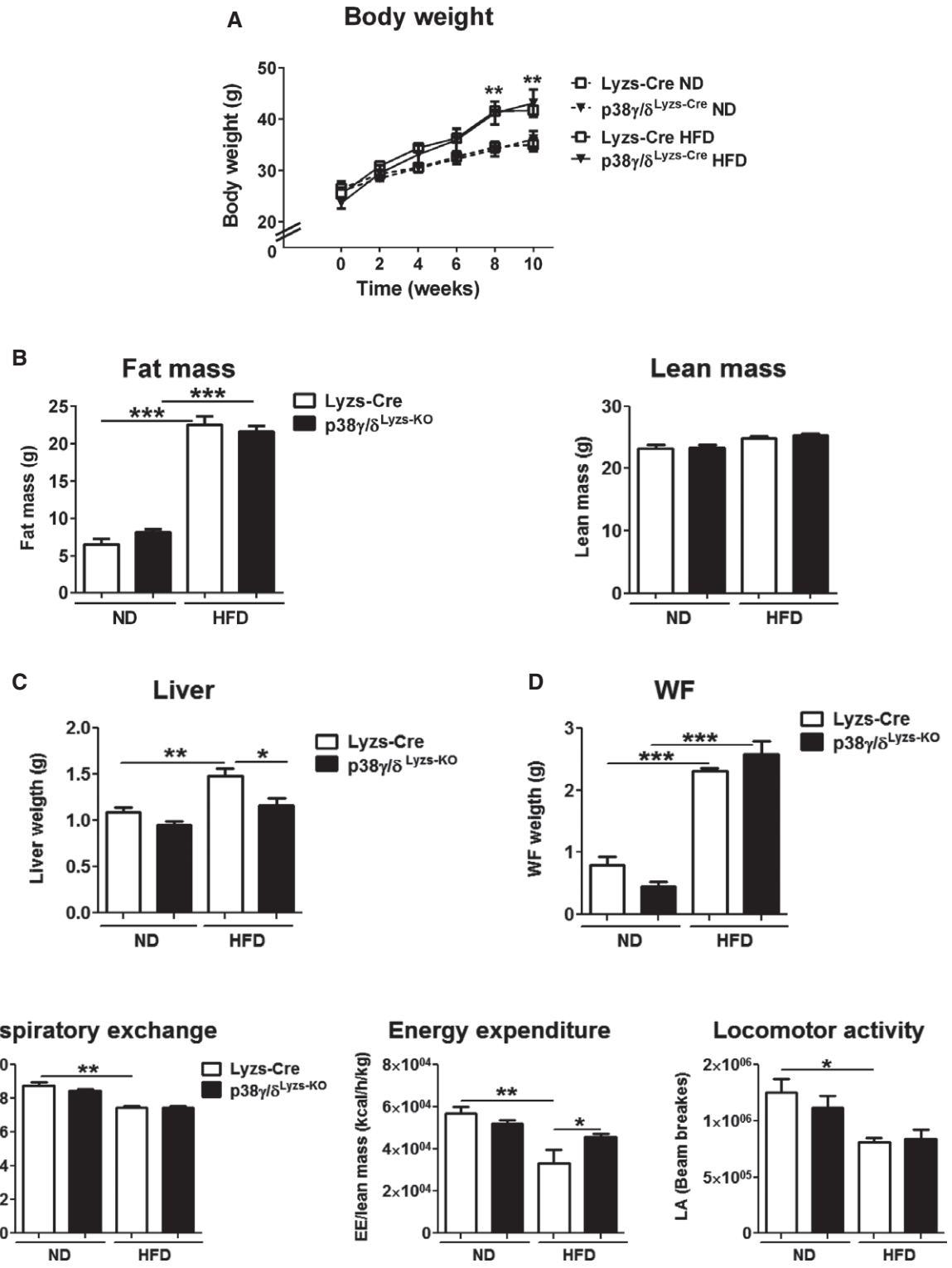

Figure 4. p38γ and p38δ deficiency in myeloid cells improves glucose metabolism in an obesity model.
Lyzs-Cre and p38γ/δ$^{Lyzs-KO}$ mice were fed a ND or a high-fat diet (HFD) for 10 weeks.

A Body weight measured at the indicated times during HFD treatment.

B Fat mass and lean mass determined by MRI at the end of the diet period.

C, D Liver mass and white fat (WF) mass.

E Respiratory exchange quotient, energy expenditure, and locomotor activity, detected in metabolic cages.

Data information: Data are means ± SEM (n = 5–10). *P < 0.05; **P < 0.01; ***P < 0.001 (one-way ANOVA coupled to Bonferroni's post-tests).

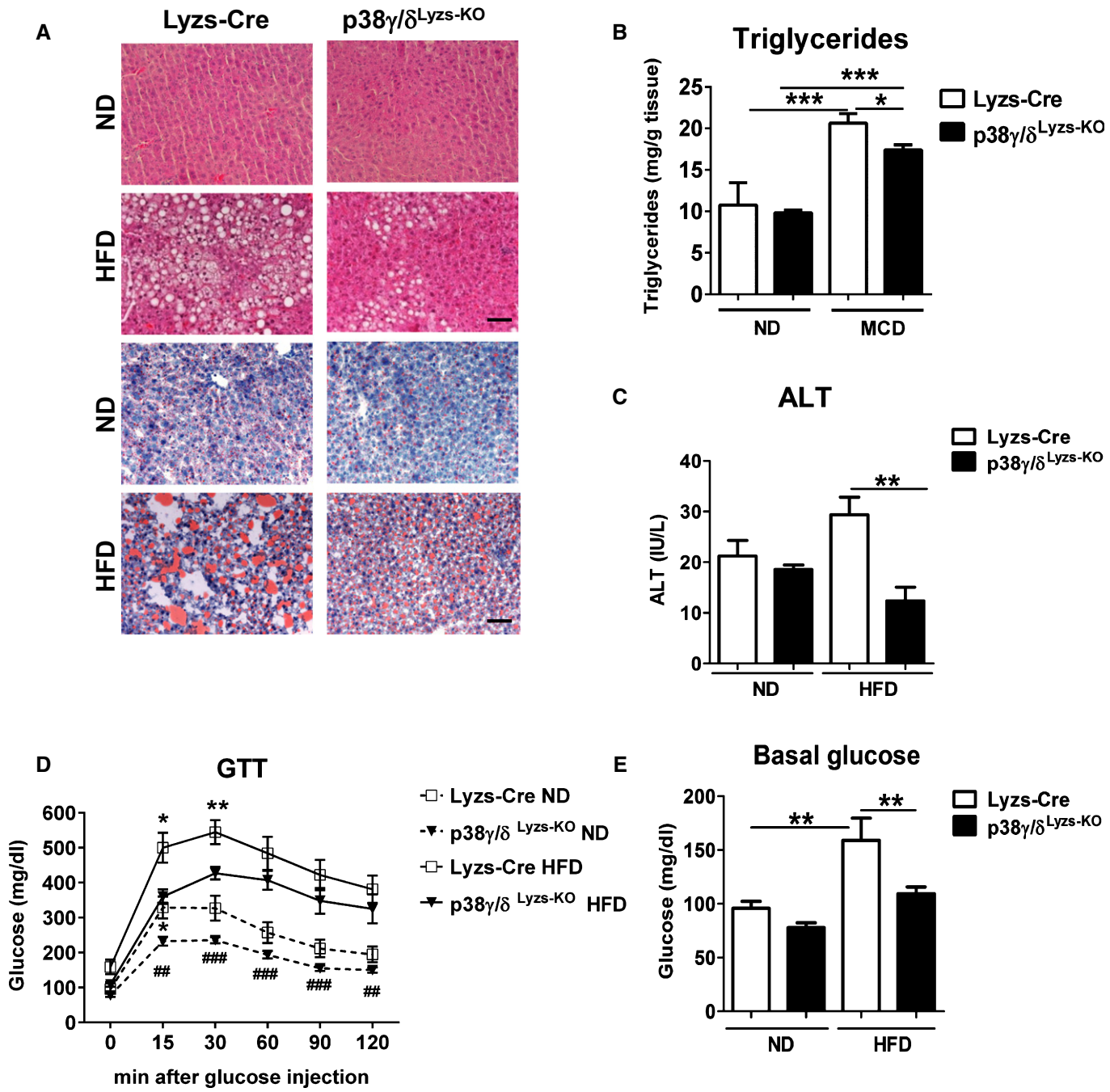

Figure 5. p38γ/δ$^{Lyzs-KO}$ mice are protected against steatohepatitis induced by HFD.
Lyzs-Cre and p38γ/δ$^{Lyzs-KO}$ mice were fed a ND or a HFD for 10 weeks.

A, B Representative H&E- and Oil Red-stained liver sections (scale bar: 50 μm) (A) and liver triglycerides (B).

C Plasma ALT at the end of the diet period.

D Glucose tolerance measured at the end of the diet period. Blood glucose concentration was measured in mice given an intraperitoneal glucose injection (1 g/kg) after overnight fasting.

E Basal blood glucose in overnight-fasted ND and HFD-fed Lyzs-Cre and p38γ/δ$^{Lyzs-KO}$ mice.

Data information: Data are means ± SEM (n = 5–10). *P < 0.05; **P < 0.01; ***P < 0.001 refers to p38γ/δ$^{Lyzs-KO}$ versus Lyzs-Cre; $^{\#\#}P$ < 0.01; $^{\#\#\#}P$ < 0.001 refers to ND versus HFD (one-way ANOVA coupled to Bonferroni's post-tests or Newman–Keuls post-test for liver triglycerides).

Neutrophils are the first immune cell type to respond to inflammation and can induce a chronic inflammatory state by promoting macrophage recruitment and interacting with antigen-presenting cells (Mantovani *et al*, 2011; Talukdar *et al*, 2012). Neutrophil levels by defensin 1–3 and neutrophils activation by nitrotyrosine staining, a measure of NO production, were elevated in the livers of obese

Published online: February 3, 2016
The EMBO Journal

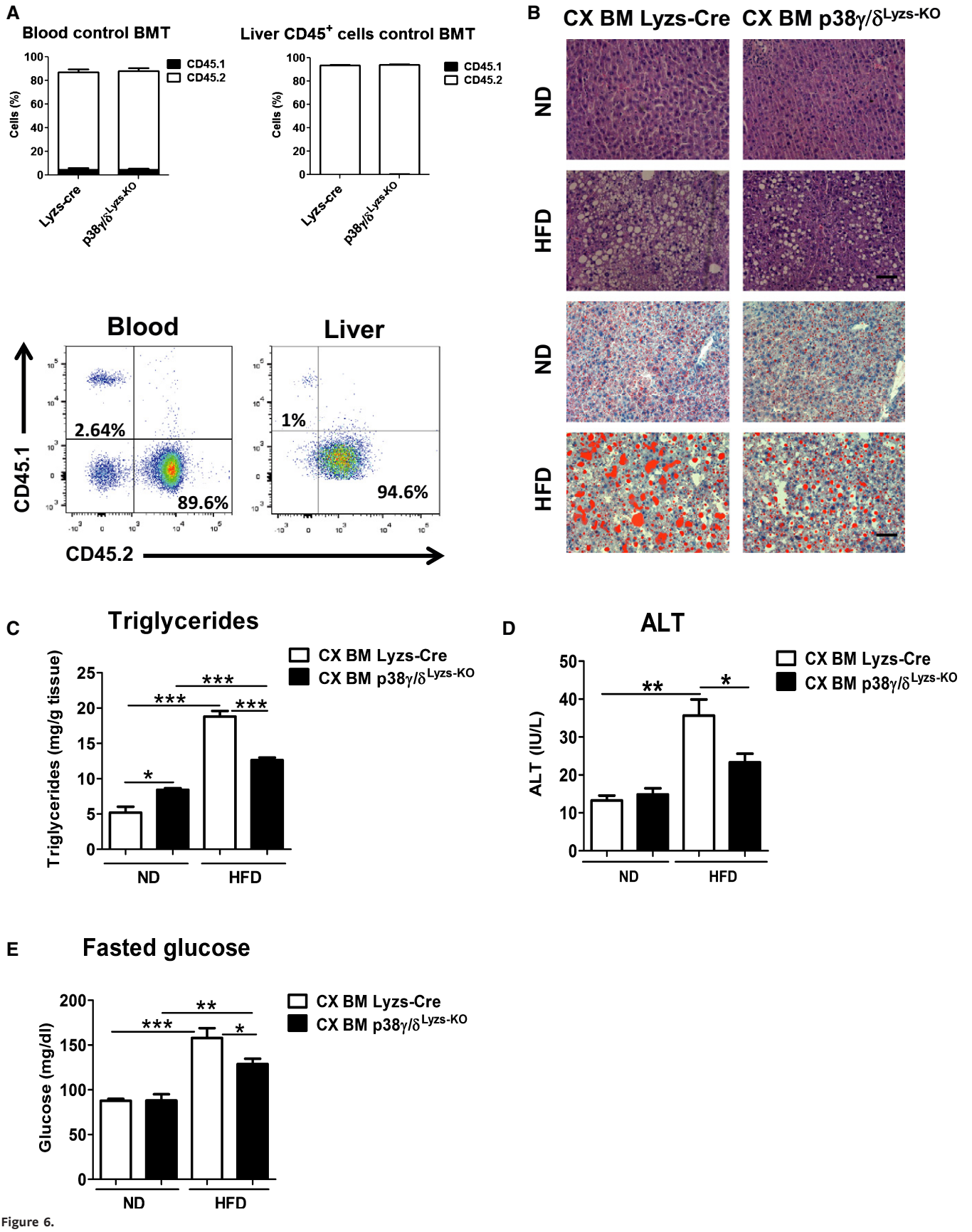

Figure 6.

Figure 6. p38γ/δ$^{Lyzs\text{-}KO}$ hematopoietic cells protect mice against HFD-induced steatosis.
Lethally irradiated WT mice were reconstituted with BM from Lyzs-Cre (Cx BM Lyzs-Cre) or p38γ/δ$^{Lyzs\text{-}KO}$ mice (Cx BM p38γ/δ$^{Lyzs\text{-}KO}$). Two months after the transplant, mice were fed the HFD for 10 weeks.

A Freshly prepared CD45.2 whole BM mononuclear cells (2×10^7) were transplanted into lethally irradiated B6.SJL (CD45.1) mice, and engraftment by CD45.2 cells (%) was analyzed by antibody staining and FACS of peripheral blood and liver CD45$^+$ cells. Charts show CD45.1 and CD45.2 expression in blood cells (left) and liver cells (right) isolated from transplanted mice (n = 3). Representative FACS dot plots of CD45.1 and CD45.2 expression are shown beneath the charts.

B Representative H&E- and Oil Red-stained liver sections. Scale bar: 50 μm.

C Liver triglyceride content.

D Plasma transaminase ALT activity.

E Fasted glucose, detected at the end of the diet period in overnight-fasted mice.

Data information: Data are means ± SEM (n = 5–10). *P < 0.05; **P < 0.01; ***P < 0.001 (one-way ANOVA coupled to Bonferroni's post-tests).

patients with NAFLD (Appendix Fig S6A and B). To test the possible role of neutrophil p38γ/δ expression in the etiology of inflammation-induced liver steatosis, we first compared the capacity of WT and p38γ/δ-neutrophils to migrate to steatotic liver. For this, we performed a competitive cell migration assay that allows direct and simultaneous comparison of the migration of multiple cell subsets in the same mouse. MCD-diet WT mice were i.v. injected with a 1:1 mix of DiO-labeled WT and DiD-labeled p38γ/δ$^{-/-}$ neutrophils (6×10^6 cells in total). WT neutrophils arrived at the steatotic liver 1 h after injection, but recruitment of p38γ/δ$^{-/-}$ neutrophils was markedly curtailed (Fig 7D and E). The more extensive recruitment of WT neutrophils appear to be not due to better survival since neutrophils from both genotypes showed the same survival ratio; however, we cannot rule out some role of p38γ/δ in neutrophil survival (Appendix Fig S7A).

Using intravital microscopy (IVM), we further quantified TNF-α-stimulated neutrophil migration in the microcirculation of the cremaster muscle of mice reconstituted with bone marrow (BM) from Lyzs-Cre or p38γ/δ$^{Lyzs\text{-}KO}$ mice (Movies EV1 and EV2). Numbers of rolling neutrophils were slightly higher in mice receiving p38γ/δ$^{Lyzs\text{-}KO}$ BM, accompanied by higher rolling velocity and contrasting with lower numbers of adherent neutrophils (Fig 7F). This higher rolling velocity is consistent with increased expression of L-selectin observed in neutrophils lacking p38γ/δ. Moreover, the defective adhesion might be explained by the lower expression in p38γ/δ$^{Lyzs\text{-}KO}$ neutrophils of CD11b, an integrin that regulates neutrophil adhesion and migration (Appendix Fig S7B). These results show that neutrophil adhesion and recruitment are compromised in the absence of p38γ/δ. Neutrophil rolling under flow conditions is mediated by L-selectin (Abbassi *et al*, 1993). To test the involvement L-selectin in the impaired rolling of p38γ/δ$^{Lyzs\text{-}KO}$ neutrophils, we assayed neutrophil migration under flow conditions on plates coated with the CD11b ligand ICAM-1 and the L-selectin ligand E-selectin. Our results indicated that p38γ/δ$^{Lyzs\text{-}KO}$ neutrophils presented a higher rolling velocity than Lyzs-Cre neutrophils (Appendix Fig S7C).

To investigate whether the altered migration capacity of p38γ/δ$^{Lyzs\text{-}KO}$ neutrophils is due to an autonomous effect or a defective production of chemokines, we performed a parabiosis experiment. Efficiency of parabiosis was evaluated by using congenic markers to distinguish blood cells in parabiotic pairs, in which one partner was CD45.1$^+$. Parabiotic exposure of p38γ/δ$^{Lyzs\text{-}KO}$ mice to the circulation of WT (CD45.1) mice, both fed the MCD diet, was enough to worsen the steatosis phenotype of p38γ/δ$^{Lyzs\text{-}KO}$ (Appendix Fig S8A). The exacerbated steatosis correlated with a higher proportion of CD45.1 (WT) neutrophils in p38γ/δ$^{Lyzs\text{-}KO}$ livers compared to the proportion observed in livers from Lyzs-Cre mice (Appendix Fig S8B). There were no differences in macrophage infiltration (Appendix Fig S8B), indicating that the wild-type circulation specifically increases liver neutrophil infiltration in p38γ/δ$^{Lyzs\text{-}KO}$ mice. Neutrophils thus appear to be crucial to the steatosis protection in p38γ/δ$^{Lyzs\text{-}KO}$ mice.

Neutrophil-specific p38δ deficiency protects against steatosis

The most abundant p38 isoform in neutrophils is p38δ (Ittner *et al*, 2012). To test the implication of neutrophil p38δ in liver steatosis, we crossed p38δ-floxed mice with Mrp8-Cre mice (Passegue *et al*, 2004) to generate mice lacking p38δ specifically in neutrophils (p38δ$^{Mrp8\text{-}KO}$ mice; Appendix Fig S9A). H&E and Oil Red staining of liver sections revealed that these mice were partially protected against MCD-induced steatosis (Appendix Fig S9B). Moreover, p38δ$^{Mrp8\text{-}KO}$ mice had below-normal levels of MCD-induced ALT (Appendix Fig S9C). This protection was associated with low

Figure 7. p38γ/δ$^{Lyzs\text{-}KO}$ neutrophils have deficient migration to the liver.

A Flow cytometry analysis of liver myeloid subsets (CD11b$^+$ Gr-1^{high}, CD11b$^+$ Gr-1^{intermediate}, CD11b$^+$ Gr-1$^-$) isolated from Lyzs-Cre and p38γ/δ$^{Lyzs\text{-}KO}$ mice fed a MCD for 3 weeks or HFD for 10 weeks. Representative dot plots are shown, and bar charts show the diet-induced increase in each population as a percentage of the total intrahepatic CD11b$^+$ leukocyte population. Myeloid infiltrating cells isolated from livers were sorted by FACS and stained with H&E. Representative cells are shown next to the appropriate myeloid subsets.

B, C Neutrophils and monocytes as a percentage of total circulating leukocytes, measured in total blood in animals fed the MCD diet for 3 weeks (B) or the HFD for 10 weeks (C).

D, E WT mice fed the MCD diet were i.v. injected with a 1:1 mix of DiO-labeled Lyzs-Cre neutrophils and DiD-labeled p38γ/δ$^{Lyzs\text{-}KO}$ neutrophils (6×10^6 cells in total; n = 10). One hour after injection, liver-infiltrating neutrophils were assessed by flow cytometry (D) and fluorescence micrography on liver sections (E).

F Intravital microscopy quantification of the rolling and adhesion frequencies and rolling velocities of neutrophils recruited to venules irrigating inflamed (TNF-α-injected) cremaster muscle.

Data information: Data are means ± SEM (n = 5–10). *P < 0.05; **P < 0.01; ***P < 0.001 (one-way ANOVA coupled to Bonferroni's post-tests).

Published online: February 3, 2016
The EMBO Journal

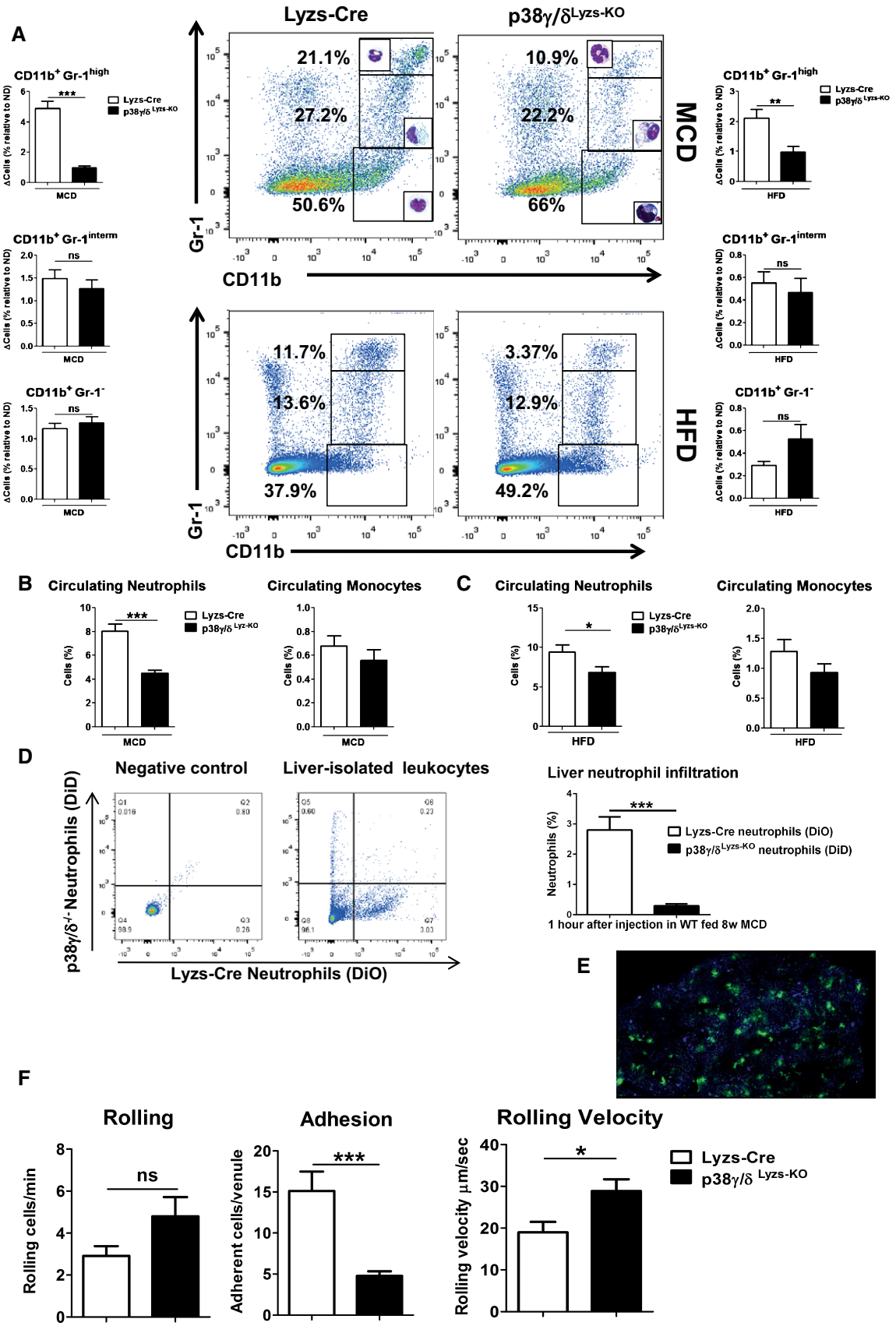

Figure 7.

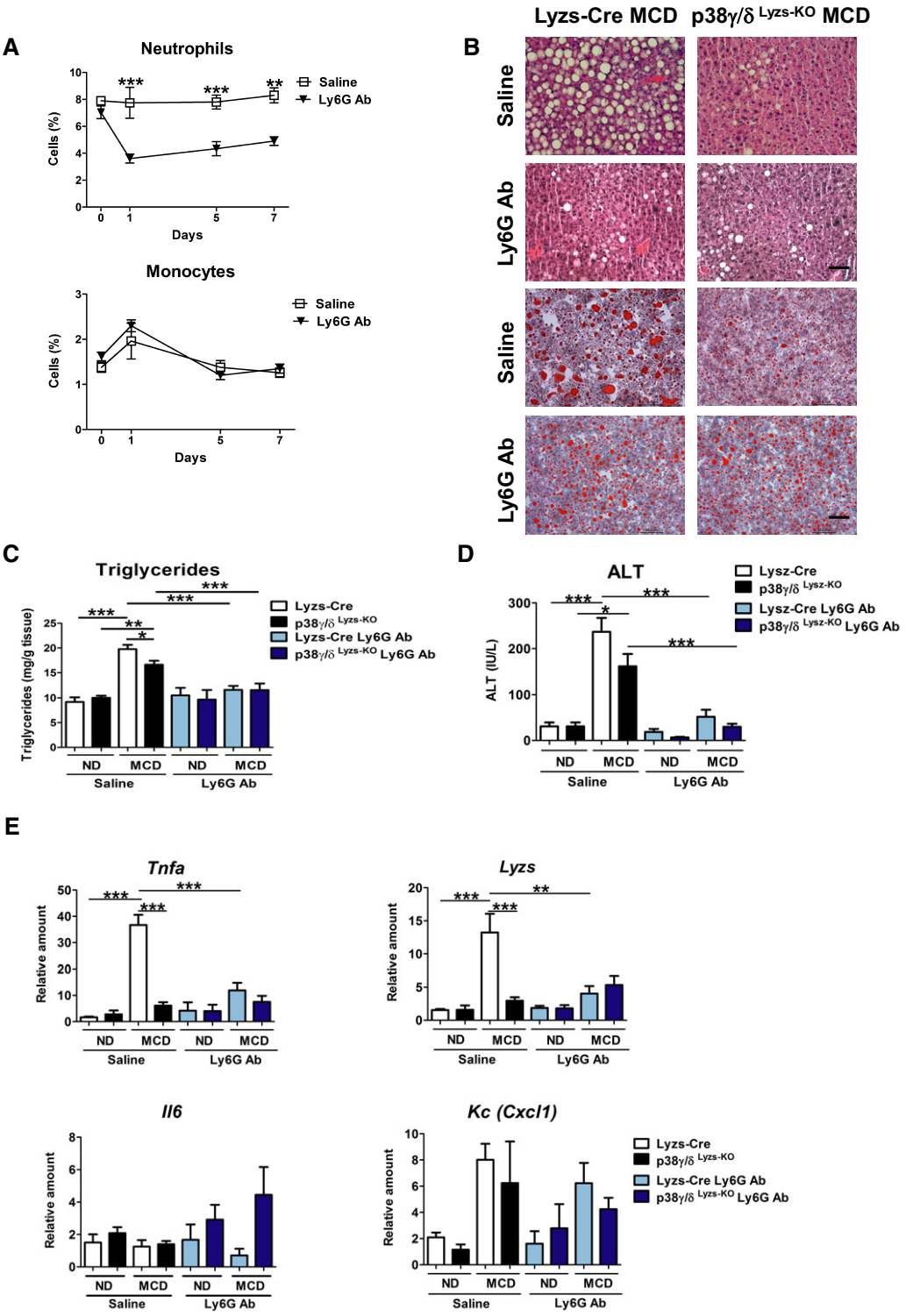

Figure 8. Neutrophil depletion protects against steatosis.

Osmotic minipumps containing saline or Ly6G antibody were implanted subcutaneously in Lyzs-Cre and p38γ/δ$^{Lyzs\text{-}KO}$ mice. These animals were fed a ND or MCD for 3 weeks.

A Neutrophils and monocytes as a percentage of circulating leukocytes, measured in total blood.

B Representative H&E- and Oil Red-stained liver sections after 3 weeks of treatment. Scale bar: 50 μm.

C, D Liver triglyceride (C) and plasma transaminase activity (ALT) (D) at the end of the diet period.

E Total RNA was extracted from livers, and chemokine and cytokine mRNA levels were determined by qRT–PCR. mRNA expression was normalized to the amount of *Gapdh* mRNA.

Data information: Data are means ± SEM (n = 5–10). *P < 0.05; **P < 0.01; ***P < 0.001 (one-way ANOVA coupled to Bonferroni's post-tests).

Published online: February 3, 2016
The EMBO Journal

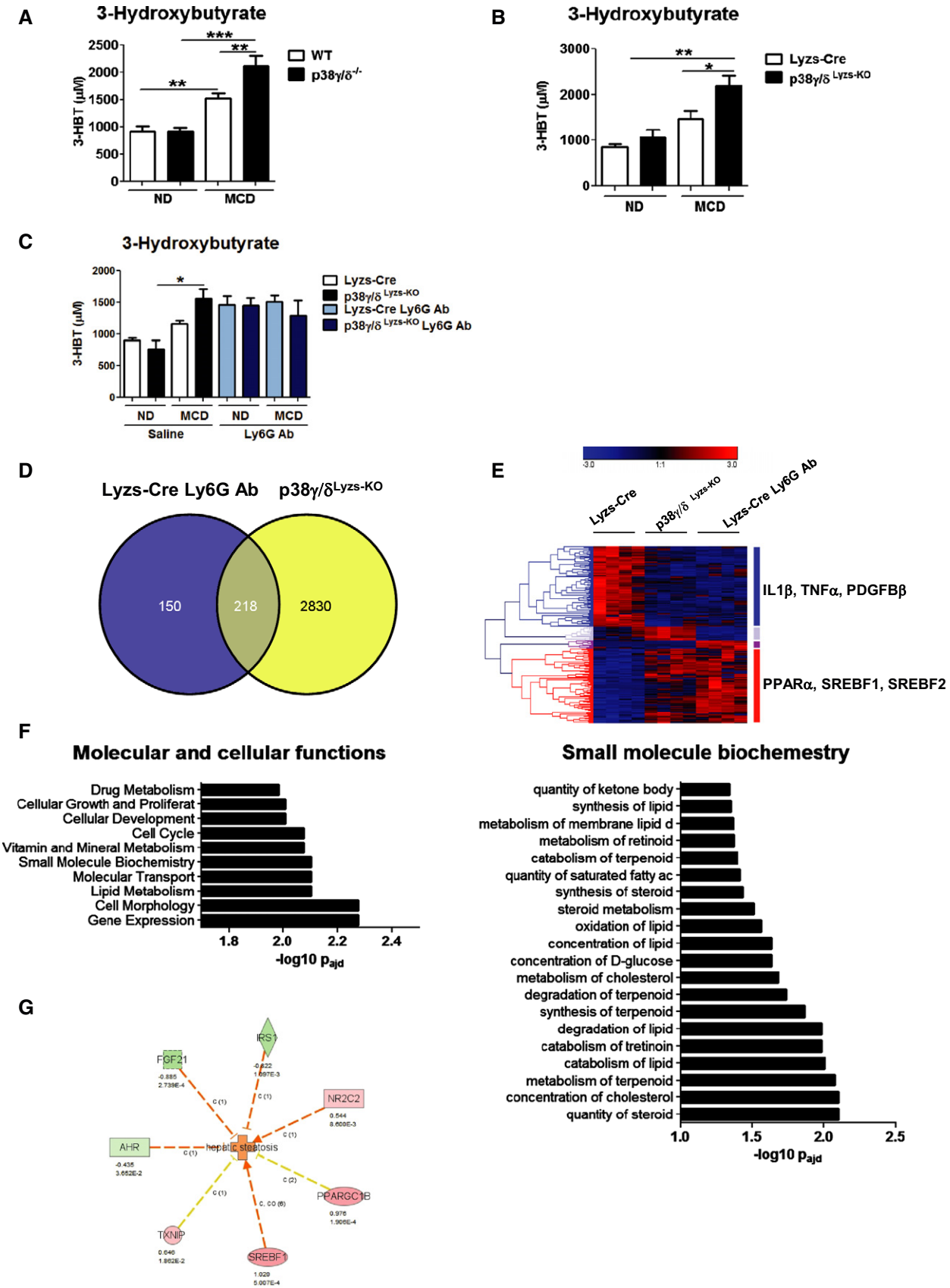

Figure 9.

neutrophil infiltration of the liver compared with MCD-diet-fed Mrp8-Cre mice (Appendix Fig S9D). These results indicate that the protection against steatosis is at least partially due to the expression of p38δ in neutrophils.

Neutrophil depletion protects against steatosis development

Early neutrophil accumulation triggers monocyte migration and inflammation (Savill *et al*, 1989), and diminished neutrophil accumulation can ameliorate NAFLD (Nathan, 2006). To clarify whether defective neutrophil migration contributes to the milder hepatic steatosis in MCD-diet p38γ/δ$^{Lyzs\text{-}KO}$ mice, we depleted neutrophils in MCD-diet Lyzs-Cre mice by administering anti-Ly6G antibody. Administration of this antibody (0.4 mg/kg per day i.v. for 7 days) reduced the levels of circulating neutrophils without affecting monocytes (Fig 8A), and treatment for 21 days significantly improved liver steatosis and reduced triglyceride accumulation to an extent similar to that observed in the MCD-diet p38γ/δ$^{Lyzs\text{-}KO}$ mice; in contrast, anti-Ly6G treatment of MCD-diet p38γ/δ$^{Lyzs\text{-}KO}$ mice did not appear to provide further benefit (Fig 8B and C). Anti-Ly6G antibody treatment of MCD-diet Lyzs-Cre animals also reduced liver necrosis assessed by serum ALT levels (Fig 8D). Moreover, while liver expression of *Il6* was not affected neutrophil depletion in Lyzs-Cre mice also significantly reduced liver expression of the pro-inflammatory markers *Tnfa* and *Lyzs* (Fig 8E).

Neutrophil depletion protects against steatosis by modulating lipid metabolism

We next measured the fatty-acid oxidation metabolite β-hydroxybutyrate, to investigate whether the improvement in hepatic steatosis in MCD-diet p38γ/δ$^{-/-}$, p38γ/δ$^{Lyzs\text{-}KO}$, and Ly6G-treated mice was linked to an increase in lipid oxidation. p38γ/δ$^{-/-}$, p38γ/δ$^{Lyzs\text{-}KO}$, and Ly6G-treated mice all had higher levels of serum β-hydroxybutyrate than similarly fed WT or Lyzs-Cre mice (Fig 9A–C), and this higher lipid oxidation correlated with the higher energy expenditure observed in p38γ/δ$^{Lyzs\text{-}KO}$ mice (Fig 4E).

To confirm an effect of impaired neutrophil infiltration on liver lipid metabolism, we examined the effect of MCD-diet on hepatic gene expression in Lyzs-Cre, p38γ/δ$^{Lyzs\text{-}KO}$, and anti-Ly6G-treated Lyzs-Cre mice by RNA-seq (Fig 9D–G). Differentially regulated genes that potentially contribute to the hepatic phenotype of the neutrophil-deficient mice were identified by comparing gene expression patterns with MCD-diet-fed Lyzs-Cre mice (Fig 9D–G). Most gene alterations observed in p38γ/δ$^{Lyzs\text{-}KO}$ mice were also detected in anti-Ly6G-treated Lyzs-Cre mice (Fig 9D). Gene ontology analysis of genes that changed in the same manner in both mice identified significant (adjusted $P < 0.001$) association of neutrophil deficiency with elevated oxidative lipid metabolism and decreased inflammation (Fig 9E), including genes regulated by PPAR-α (peroxisome proliferator-activated receptor-alpha) and by IL-2β and TNF-α (Fig 9E). Neutrophil deficiency thus causes increased lipid oxidation and decreased inflammation (Fig 9E–G).

Discussion

The alternative p38 MAPKs p38γ and p38δ regulate inflammatory processes through several mechanisms. Here, we demonstrate that expression of both kinases in myeloid cells is necessary for the development of liver steatosis and inflammation in animal models of NAFLD. Further, these kinases control neutrophil migration to the liver, and hepatic neutrophils contribute to liver steatosis by promoting liver inflammation and lipogenic metabolism. Deletion of p38γ/δ expression in the myeloid compartment curtails neutrophil recruitment to the liver, protecting animals against diet-induced steatosis and associated liver damage, and effect that is also partially mediated by the lack of p38δ in neutrophils. These findings indicate a major role of p38γ/δ in controlling neutrophil recruitment during inflammation and suggest that inhibition of neutrophil trafficking is a potential treatment route for steatosis.

The analysis of NAFLD mouse models clearly demonstrates that the protection in p38γ/δ$^{-/-}$ mice is attributable to the loss of p38γ/δ expression in hematopoietic cells. The bone marrow transfer experiments and conditional KO animal results confirm that p38γ and δ expressions by hematopoietic cells drive steatosis in both diet-induced steatosis models. Neutrophils were recently shown to be important mediators of alcoholic fatty liver disease (Bertola *et al*, 2013), and p38δ is known to control neutrophil inflammatory response in lung by regulating PKD1 activity (Ittner *et al*, 2012). Our analysis shows that loss of p38γ and p38δ in neutrophils might be responsible for the protection observed in the KO animals. Livers from mice lacking p38γ and p38δ had lower neutrophil infiltration, and neutrophils lacking these kinases could not be recruited to the liver in a competition assay, indicating a cell autonomous effect. The low adhesion and higher rolling velocity detected in neutrophils lacking p38γ and p38δ are broadly consistent with previous reports using p38δ$^{-/-}$ animals (Ittner *et al*, 2012). We also observed lower

Figure 9. Neutrophils control liver metabolic changes in steatosis development.

A–C Plasma levels of 3-hydroxybutyrate in WT and p38γ/δ$^{-/-}$ (A), Lyzs-Cre and p38γ/δ$^{Lyzs\text{-}KO}$ mice (B) and Lyzs-Cre Ly6G Ab treated after MCD diet (C) (n = 5–10).

D Overlap of gene expression changes between Lyzs-Cre mice treated with anti-Ly6G and p38γ/δ$^{Lyzs\text{-}KO}$ at the end of the MCD diet period n = 4 (each n is a mix of two different animals).

E Hierarchical clustering of the expression profiles of genes differentially expressed both between p38γ/δ$^{Lyzs\text{-}KO}$ and MCD-diet-fed Lyzs-Cre and between Lyzs-Cre treated with anti-Ly6G and MCD-diet-fed Lyzs-Cre mice. Genes up-regulated in both comparisons (red cluster) were mainly regulated by PPAR-α, SREBF1, and SREBF2, while the enriched upstream regulators of genes down-regulated in both conditions versus the control group (blue cluster) were IL-1β, TNF-α, and PDGFB-β.

F IPA (http://ingenuity.com) functional categories enriched in the set of genes differentially expressed between p38γ/δ$^{Lyzs\text{-}KO}$ and MCD-diet-fed Lyzs-Cre and between Lyzs-Cre treated with anti-Ly6G and MCD-diet-fed Lyzs-Cre mice (n = 4).

G Genes differentially expressed between p38γ/δ$^{Lyzs\text{-}KO}$ and MCD-diet-fed Lyzs-Cre and between Lyzs-Cre treated with anti-Ly6G and MCD-diet-fed Lyzs-Cre mice and involved in liver steatosis according to IPA.

Data information: Data are means ± SEM. *$P < 0.05$; **$P < 0.01$; ***$P < 0.001$ (one-way ANOVA coupled to Bonferroni's post-tests).

CD11b and higher L-selectin membrane expression, which could account for these defects in adhesion and rolling observed in the neutrophils lacking p38γ and p38δ. Moreover, lack of p38δ alone is insufficient to reduce neutrophil infiltration after the MCD diet and protect against liver steatosis. The ability of p38γ to compensate for the loss of p38δ is somewhat surprising given the low expression level of p38γ in neutrophils (Gonzalez-Teran *et al*, 2013; Han *et al*, 2013). A possible explanation is that $p38\delta^{-/-}$ neutrophils might increase the activation or expression of p38γ as a compensatory mechanism. It is also possible that p38γ in another myeloid cell type (e.g. resident macrophages) contributes to neutrophil migration by controlling cytokine and chemokine production. However, the results of competition migration assays in which resident macrophages are WT, and of the parabiosis experiment, argue against this possibility. Further experiments will be needed to determine the specific roles of p38γ and p38δ in different myeloid subsets and how these two isoforms can compensate each other. However, a role of neutrophils is clear because lack of p38δ only in neutrophils is enough to protect against steatosis.

On the other hand, the fact that neutrophil-specific deletion of p38δ has a more marked effect on phenotype than the whole-body p38δ KO might indicate that p38δ has an opposing role in another tissue and thereby modulates biological actions in a tissue-specific fashion. Opposing effects in different tissues have been shown for the stress kinase JNK: deletion of this kinase in the liver induces steatosis whereas deletion in fat is protective (Sabio *et al*, 2008, 2009).

Our data point out an important role of p38γ/δ in neutrophils. The same level of protection against diet-induced steatosis observed in $p38\gamma/\delta^{Lyzs\text{-}KO}$ mice was also achieved in mice depleted of neutrophils with anti-Ly6G antibody. Moreover, deletion of p38δ in neutrophils reduces hepatic neutrophils infiltration and partially protected against steatosis. These observations strongly suggest that neutrophil recruitment to the liver is essential for the initiation and progression of NAFLD and that neutrophil p38γ/δ expression contributes to the progression of this disease. The central role for neutrophils in NAFLD is consistent with their roles in ethanol-induced liver damage (Bertola *et al*, 2013) and macrophage recruitment to damaged tissue in obesity (Mansuy-Aubert *et al*, 2013) and with the description of neutrophil elastase as an important mediator of obesity-induced diabetes (Talukdar *et al*, 2012; Mansuy-Aubert *et al*, 2013). The importance of infiltrating neutrophils in liver inflammatory responses is also indicated by the underexpression of inflammatory genes in MCD-diet-fed $p38\gamma/\delta^{Lyzs\text{-}KO}$ and neutrophil-depleted mice and by the increased lipid oxidation and reduced lipogenesis in the neutrophil-depleted mice.

The data from mouse models correlate well with the overexpression p38δ and p38γ in livers of individuals with NAFLD, regardless of BMI, which could indicate the involvement of these kinases in the development of steatosis. This elevated p38δ expression could be due to increased neutrophil influx to these livers, as neutrophils are known to express high levels of p38δ (Ittner *et al*, 2012; Gonzalez-Teran *et al*, 2013). Accordingly, we also observed elevated neutrophil activity in the livers of obese patients with NAFLD. It would be interesting to characterize the cell-type contribution to p38δ and p38γ expression in human liver. However, we cannot rule out important roles for p38δ and p38γ expressed in other cell types involved in steatosis development.

In summary, our findings indicate that neutrophil infiltration triggers the development of NAFLD and that p38γ/δ regulate this process by controlling neutrophil infiltration. Therefore, inhibition of p38γ/δ might represent a novel therapeutic target for NAFLD in humans, with the potential to limit injury and possibly prevent progression to NASH and cirrhosis.

Materials and Methods

Study population and sample collection

The study population included a group of obese adult patients with body mass index (BMI) ≥ 35 kg/m^2 and a liver biopsy compatible with NAFLD. Participants were recruited from patients undergoing elective bariatric surgery at the University Hospital of Salamanca. As controls, we included individuals with BMI < 35 kg/m^2 who underwent laparoscopic cholecystectomy for gallstones. These individuals were divided into two groups according to the presence of NAFLD: (i) controls without NALFD ($n = 11$) if they had no laboratory or histopathological evidence of NAFLD or other liver diseases; (ii) controls with NAFLD ($n = 9$) if they had a liver biopsy compatible with NAFLD. Therefore, three groups of subjects were included in the study: obese patients (BMI ≥ 35 kg/m^2) with NAFLD, controls with BMI < 35 without liver disease, and controls with BMI < 35 kg/m^2 and with NAFLD. Baseline characteristics of these groups are listed in Appendix Table S1.

Participants were excluded if they had a history of alcohol use disorders or excessive alcohol consumption (> 30 g/day in men and > 20 g/day in women), chronic hepatitis C or B, or if laboratory and/or histopathological data showed causes of liver disease other than NAFLD. The study was approved by the Ethics Committee of the University Hospital of Salamanca and all subjects provided written informed consent to undergo liver biopsy under direct vision during surgery.

Data were collected on demographic information (age, sex, and ethnicity), anthropomorphic measurements (BMI), smoking and alcohol history, coexisting medical conditions, and medication use. Before surgery, fasting venous blood samples were collected for determination of complete cell blood count, total bilirubin, aspartate aminotransferase (AST), alanine aminotransferase (ALT), total cholesterol, high-density lipoprotein, low-density lipoprotein, triglycerides, creatinine, glucose, and albumin.

A portion of each liver biopsy was fixed in 10% formalin and stained with hematoxylin–eosin and Masson's trichrome for standard histopathological analysis. The remaining portion was stored at −80°C for later protein was extraction. The presence of NAFLD was diagnosed using standard criteria, and severity of the disease was established using the NAFLD activity score (NAS) described by Kleiner (Kleiner *et al*, 2005).

Mice

Mice deficient for p38γ (B6.129-Mapk12tm1) and p38δ (B6.129-Mapk13tm1) were crossed with B6.129P2-Lyz2tm1(cre)Ifo/J mice or with B6.Cg-Tg(S100A8-cre,-EGFP)1Ilw/J mice backcrossed for 10 generations to the C57BL/6J background (Jackson Laboratory). Genotype was confirmed by PCR analysis of genomic DNA.

Radiation chimeras were generated by exposing recipient mice to 2 doses of ionizing radiation (625 Gy) and reconstituting them with 2×10^7 donor BM cells by injection into the tail vein. Proper reconstitution was checked in B6.SJL (CD45.1) control mice transplanted with CD45.2 BM mononuclear cells by immunostaining and FACS analysis of peripheral blood and liver $CD45^+$ cells. Mice were fed a standard chow diet or a methionine–choline-deficient (MCD) diet for 3 weeks (Research Diets Inc). Alternatively, mice were fed a high-fat diet (HFD) or a high-fat and high-fructose (HFF) diet (Research Diets Inc) for 10 weeks. For neutrophil depletion, mice were treated with anti-Ly6G antibody (0.4 mg/kg per day, 21 days) via subcutaneously implanted mini-osmotic pumps (Alzet); saline was administered as a control. All animal procedures conformed to EU Directive 86/609/EEC and Recommendation 2007/526/EC regarding the protection of animals used for experimental and other scientific purposes, enacted under Spanish law 1201/2005.

Hepatic peroxidation

Liver extracts were prepared by sonication (15 cycles) in cytoplasmic lysis buffer [25 mM Tris–HCl (pH 7.5), 10 mM NaCl, 1 mM EDTA, 100 mM $MgCl_2$, 1% NP-40, 0.1 mM phenylmethylsulfonyl fluoride, and 10 μg/ml aprotinin and leupeptin]. Malondialdehyde and hydrogen peroxide were assayed with the TBARS Assay kit (Cayman) and the Amplex Red Hydrogen Peroxide/Peroxidase Assay Kit (Invitrogen).

Glucose tolerance test

Glucose tolerance test was performed as described (Mora *et al*, 2005).

Isolation of liver-infiltrating mononuclear leukocytes

Mouse livers were collected, and a single-cell suspension was obtained and passed through a 70-μm strainer. Leukocytes were collected from the interphase of centrifuged Ficoll gradients.

Flow cytometry

Isolated liver-infiltrating leukocytes were counted with a CASY Cell Counter (57) and then labeled by surface staining (Streptavidin-PERCP/biotin-conjugated anti-CD11b and APC-conjugated anti-Gr-1; Invitrogen). Flow cytometry was performed with a FACScan cytofluorometer (FACS Canto BD), and data were collected and analyzed with FlowJo software.

Intravital microscopy

Intravital microscopy of the cremaster muscle after TNF-α injection (0.5 μg, intrascrotal injection) was performed as reported (Sreeramkumar *et al*, 2013) using an Axio Examiner Z.1 workstation (Zeiss, Germany). Fluorescently conjugated anti-Ly6G (1 mg/mouse) was injected immediately before acquisition to specifically identify neutrophils. Recorded videos were analyzed using Slidebook software (Intelligent Imaging Innovations). At least 30 venules were analyzed from 3 mice per group.

Competitive cell migration assay

Lyzs-Cre and $p38\gamma/\delta^{Lyzs\text{-}KO}$ neutrophils were isolated from bone marrow by labeling with biotin-conjugated anti-Ly6C/G antibody (BD Pharmigen) and magnetic streptavidin microbeads (Miltenyi Biotec) and then separating them on MACS MS columns (Miltenyi Biotec). Isolated Lyzs-Cre neutrophils were stained with DiO and $p38\gamma/\delta^{Lyzs\text{-}KO}$ neutrophils were stained with DiD (Vybrant Cell-Labeling Solution, Molecular Probes). Cell viability was checked by DAPI staining followed by FACS. The labeled cells were then mixed at a 1:1 ratio and injected (6×10^6 cells) into MCD-diet WT mice. After 1 h, liver-infiltrating mononuclear leukocytes were isolated and directly detected by FACS. Fluorescent neutrophils were also detected by confocal microscopy in OCT-cryopreserved liver sections.

Statistical analysis

Differences between experimental groups were examined for statistical significance by two-tailed Student's *t*-test or one-way ANOVA coupled to Bonferroni's and Newman–Keuls post-test. Characteristics of patients and controls were compared by means of Mann–Whitney *U*-test for quantitative variables and χ^2 or Fisher's tests for qualitative variables.

For more Materials and Methods, see the Appendix.

Expanded View for this article is available online.

Acknowledgements
We thank S. Bartlett for English editing, L. Manzanedo, A. Mateos, and O. Rozo for help with sample and data collection, and A. Molina for histological analysis. We are grateful to R.J. Davis for critical reading of the manuscript, R. González-Sarmiento for help with clinical study design. We thank the staff at the CNIC Genomics, Cellomics, and Bioinformatics units for technical support and help with data analysis. G.S. is an investigator of the Ramón y Cajal Program. B.G.T. is a fellow of FPI Severo Ochoa CNIC Program (SVP-2013-067639). I.G.N. is supported by a CNIC IPP FP7 Marie Curie Programme (PCOFUND-2012-600396). M.A.V. is a recipient of a Madrid Regional Government Fellowship. This work was funded by the following grants to G.S.: ERC 260464, EFSD 2030, MICINN SAF2010-19347, and Comunidad de Madrid S2010/BMD-2326; to M.M.: ISCIII and FEDER, PI10/01692, and I3SNS-INT12/049; to L.H.C.: Junta de Castilla y León GRS 681/A/11; to A.H.: SAF 2012-31142; to R.N.: MICINN BFU2012-35255, Xunta de Galicia EM 2012/039 and 2012-CP069; and to A.C.: MICINN SAF2010-19734. The CNIC is supported by the Ministerio de Economía y Competitividad and the Pro-CNIC Foundation.

Author contributions
BG-T, NM, IGN, and GS designed the study; BG-T, NM, IGN, MAV, VS, AM, GC, MLS, EB, LL-V, ER, VB, and GS performed experimental analysis; metabolic cages were performed by RN and SP-S; intravital microscopy was performed by VS and AH; *in vitro* neutrophil migration was performed by MLS and FS-M; MM designed and coordinated human study; MM, LH-C, JLT, and LO recruited subjects and were responsible for sample and data collection; AC provided reagents and BG-T, NM, IGN, and GS wrote the manuscript. All authors contributed to the revision of the manuscript and approved the final version.

Conflict of interest
The authors declare that they have no conflict of interest.

References

Abbassi O, Kishimoto TK, McIntire LV, Anderson DC, Smith CW (1993) E-selectin supports neutrophil rolling *in vitro* under conditions of flow. *J Clin Invest* 92: 2719 – 2730

Adams RH, Porras A, Alonso G, Jones M, Vintersten K, Panelli S, Valladares A, Perez L, Klein R, Nebreda AR (2000) Essential role of p38alpha MAP kinase in placental but not embryonic cardiovascular development. *Mol Cell* 6: 109 – 116

Allen M, Svensson L, Roach M, Hambor J, McNeish J, Gabel CA (2000) Deficiency of the stress kinase p38alpha results in embryonic lethality: characterization of the kinase dependence of stress responses of enzyme-deficient embryonic stem cells. *J Exp Med* 191: 859 – 870

Anstee QM, Goldin RD (2006) Mouse models in non-alcoholic fatty liver disease and steatohepatitis research. *Int J Exp Pathol* 87: 1 – 16

Beardmore VA, Hinton HJ, Eftychi C, Apostolaki M, Armaka M, Darragh J, McIlrath J, Carr JM, Armit LJ, Clacher C, Malone L, Kollias G, Arthur JS (2005) Generation and characterization of p38beta (MAPK11) gene-targeted mice. *Mol Cell Biol* 25: 10454 – 10464

Bertola A, Park O, Gao B (2013) Chronic plus binge ethanol feeding synergistically induces neutrophil infiltration and liver injury in mice: a critical role for E-selectin. *Hepatology* 58: 1814 – 1823

Charlton M, Krishnan A, Viker K, Sanderson S, Cazanave S, McConico A, Masuoko H, Gores G (2011) Fast food diet mouse: novel small animal model of NASH with ballooning, progressive fibrosis, and high physiological fidelity to the human condition. *Am J Physiol Gastrointest Liver Physiol* 301: G825 – G834

Criado G, Risco A, Alsina-Beauchamp D, Perez-Lorenzo MJ, Escos A, Cuenda A (2014) Alternative p38 MAPKs are essential for collagen-induced arthritis. *Arthritis Rheumatol* 66: 1208 – 1217

Fabbrini E, Sullivan S, Klein S (2010) Obesity and nonalcoholic fatty liver disease: biochemical, metabolic, and clinical implications. *Hepatology* 51: 679 – 689

Farrell GC, Larter CZ (2006) Nonalcoholic fatty liver disease: from steatosis to cirrhosis. *Hepatology* 43: S99 – S112

Gonzalez-Teran B, Cortes JR, Manieri E, Matesanz N, Verdugo A, Rodriguez ME, Gonzalez-Rodriguez A, Valverde A, Martin P, Davis RJ, Sabio G (2013) Eukaryotic elongation factor 2 controls TNF-alpha translation in LPS-induced hepatitis. *J Clin Invest* 123: 164 – 178

Han MS, Jung DY, Morel C, Lakhani SA, Kim JK, Flavell RA, Davis RJ (2013) JNK expression by macrophages promotes obesity-induced insulin resistance and inflammation. *Science* 339: 218 – 222

Ittner A, Block H, Reichel CA, Varjosalo M, Gehart H, Sumara G, Gstaiger M, Krombach F, Zarbock A, Ricci R (2012) Regulation of PTEN activity by p38delta-PKD1 signaling in neutrophils confers inflammatory responses in the lung. *J Exp Med* 209: 2229 – 2246

Kleiner DE, Brunt EM, Van Natta M, Behling C, Contos MJ, Cummings OW, Ferrell LD, Liu YC, Torbenson MS, Unalp-Arida A, Yeh M, McCullough AJ, Sanyal AJ (2005) Design and validation of a histological scoring system for nonalcoholic fatty liver disease. *Hepatology* 41: 1313 – 1321

Mansuy-Aubert V, Zhou QL, Xie X, Gong Z, Huang JY, Khan AR, Aubert G, Candelaria K, Thomas S, Shin DJ, Booth S, Baig SM, Bilal A, Hwang D, Zhang H, Lovell-Badge R, Smith SR, Awan FR, Jiang ZY (2013) Imbalance between neutrophil elastase and its inhibitor alpha1-antitrypsin in obesity alters insulin sensitivity, inflammation, and energy expenditure. *Cell Metab* 17: 534 – 548

Mantovani A, Cassatella MA, Costantini C, Jaillon S (2011) Neutrophils in the activation and regulation of innate and adaptive immunity. *Nat Rev Immunol* 11: 519 – 531

Marchesini G, Bugianesi E, Forlani G, Cerrelli F, Lenzi M, Manini R, Natale S, Vanni E, Villanova N, Melchionda N, Rizzetto M (2003) Nonalcoholic fatty liver, steatohepatitis, and the metabolic syndrome. *Hepatology* 37: 917 – 923

Mora A, Lipina C, Tronche F, Sutherland C, Alessi DR (2005) Deficiency of PDK1 in liver results in glucose intolerance, impairment of insulin-regulated gene expression and liver failure. *Biochem J* 385: 639 – 648

Nathan C (2006) Neutrophils and immunity: challenges and opportunities. *Nat Rev Immunol* 6: 173 – 182

Passegue E, Wagner EF, Weissman IL (2004) JunB deficiency leads to a myeloproliferative disorder arising from hematopoietic stem cells. *Cell* 119: 431 – 443

Risco A, del Fresno C, Mambol A, Alsina-Beauchamp D, MacKenzie KF, Yang HT, Barber DF, Morcelle C, Arthur JS, Ley SC, Ardavin C, Cuenda A (2012) p38gamma and p38delta kinases regulate the Toll-like receptor 4 (TLR4)-induced cytokine production by controlling ERK1/2 protein kinase pathway activation. *Proc Natl Acad Sci USA* 109: 11200 – 11205

Sabio G, Arthur JS, Kuma Y, Peggie M, Carr J, Murray-Tait V, Centeno F, Goedert M, Morrice NA, Cuenda A (2005) p38gamma regulates the localisation of SAP97 in the cytoskeleton by modulating its interaction with GKAP. *EMBO J* 24: 1134 – 1145

Sabio G, Das M, Mora A, Zhang Z, Jun JY, Ko HJ, Barrett T, Kim JK, Davis RJ (2008) A stress signaling pathway in adipose tissue regulates hepatic insulin resistance. *Science* 322: 1539 – 1543

Sabio G, Cavanagh-Kyros J, Ko HJ, Jung DY, Gray S, Jun JY, Barrett T, Mora A, Kim JK, Davis RJ (2009) Prevention of steatosis by hepatic JNK1. *Cell Metab* 10: 491 – 498

Sabio G, Davis RJ (2010) cJun NH2-terminal kinase 1 (JNK1): roles in metabolic regulation of insulin resistance. *Trends Biochem Sci* 35: 490 – 496

Sabio G, Kennedy NJ, Cavanagh-Kyros J, Jung DY, Ko HJ, Ong H, Barrett T, Kim JK, Davis RJ (2010) Role of muscle c-Jun NH2-terminal kinase 1 in obesity-induced insulin resistance. *Mol Cell Biol* 30: 106 – 115

Sabio G, Davis RJ (2014) TNF and MAP kinase signalling pathways. *Semin Immunol* 26: 237 – 245

Savill JS, Wyllie AH, Henson JE, Walport MJ, Henson PM, Haslett C (1989) Macrophage phagocytosis of aging neutrophils in inflammation. Programmed cell death in the neutrophil leads to its recognition by macrophages. *J Clin Invest* 83: 865 – 875

Sreeramkumar V, Leiva M, Stadtmann A, Pitaval C, Ortega-Rodriguez I, Wild MK, Lee B, Zarbock A, Hidalgo A (2013) Coordinated and unique functions of the E-selectin ligand ESL-1 during inflammatory and hematopoietic recruitment in mice. *Blood* 122: 3993 – 4001

Talukdar S, da Oh Y, Bandyopadhyay G, Li D, Xu J, McNelis J, Lu M, Li P, Yan Q, Zhu Y, Ofrecio J, Lin M, Brenner MB, Olefsky JM (2012) Neutrophils mediate insulin resistance in mice fed a high-fat diet through secreted elastase. *Nat Med* 18: 1407 – 1412

Tamura K, Sudo T, Senftleben U, Dadak AM, Johnson R, Karin M (2000) Requirement for p38alpha in erythropoietin expression: a role for stress kinases in erythropoiesis. *Cell* 102: 221 – 231

Tiniakos DG, Vos MB, Brunt EM (2010) Nonalcoholic fatty liver disease: pathology and pathogenesis. *Annu Rev Pathol* 5: 145 – 171

Vernon G, Baranova A, Younossi ZM (2011) Systematic review: the epidemiology and natural history of non-alcoholic fatty liver disease and non-alcoholic steatohepatitis in adults. *Aliment Pharmacol Ther* 34: 274 – 285

